

Development and Evaluation of Sediment and Pore-Water Toxicity Thresholds to Support Sediment Quality Assessments in the Tri-State Mining District (TSMD), Missouri, Oklahoma, and Kansas

*DRAFT FINAL TECHNICAL REPORT
Volume II: Appendices 1 through 4*

Submitted To:

Gary Baumgarten and John Meyer
U.S. Environmental Protection Agency
Region 6, 1445 Ross Avenue
Dallas, Texas 75202

Mark Doolan
U.S. Environmental Protection Agency
Region 7, 901 North 5th Street
Kansas City, Kansas 66101

David Drake
U.S. Environmental Protection Agency
Region 7, 901 North 5th Street
Kansas City, Kansas 66101

Jim Dwyer
U.S. Fish and Wildlife Service
101 Park DeVillie Drive, Suite A
Columbia, Missouri 65203-0057

Submitted – February, 2009 – by:

**Donald D. MacDonald¹, Dawn E. Smorong¹, Christopher G. Ingersoll²,
John M. Besser², William G. Brumbaugh², Nile Kemble², Thomas W. May²,
Christopher D. Ivey², Scott Irving³, and Margaret O’Hare³**

¹**MacDonald Environmental Sciences Ltd.**
#24 - 4800 Island Highway North
Nanaimo, British Columbia V9T 1W6

²**United States Geological Survey**
4200 New Haven Road
Columbia, Missouri 65201

³**CH2M Hill**
Suite 10 - 12377 Merit Drive
Dallas, Texas 75251



List of Appendices

Appendix 1	Plots Illustrating the Relationship Between Concentrations of Chemicals of Potential Concern and/or Mixtures of Potential Concern and Toxicity Test Results for the Tri-State Mining District (Plots A1-1 to A1-220).....	II
Appendix 2	Procedures for Calculating Selected Metrics for Sediment and Pore Water.....	XX
Appendix 3	Overview of the Quality of the Data Collected During the 2007 Sediment Sampling Program (as excerpted from Ingersoll <i>et al.</i> 2008).....	XXI
Appendix 4	Scatter plots showing the relationships between sediment and pore-water concentrations and survival and biomass of amphipods (<i>Hyalella azteca</i>), mussels (<i>Lampsilis siliquoidea</i>), and midges (<i>Chironomus dilutus</i>).....	XXII

Appendix 1 Plots Illustrating the Relationship Between Concentrations of Chemicals of Potential Concern and/or Mixtures of Potential Concern and Toxicity Test Results for the Tri-State Mining District

Plot A1-1	Plot illustrating the relationship between the concentration of cadmium (mg/kg DW) in sediment (<2 mm) and the control-adjusted survival of amphipods (<i>Hyalella azteca</i>) in 28-d exposures to sediment samples from the Tri-State Mining District.	A1-1
Plot A1-2	Plot illustrating the relationship between the concentration of chromium (mg/kg DW) in sediment (<2 mm) and the control-adjusted survival of amphipods (<i>Hyalella azteca</i>) in 28-d exposures to sediment samples from the Tri-State Mining District.	A1-2
Plot A1-3	Plot illustrating the relationship between the concentration of copper (mg/kg DW) in sediment (<2 mm) and the control-adjusted survival of amphipods (<i>Hyalella azteca</i>) in 28-d exposures to sediment samples from the Tri-State Mining District.	A1-3
Plot A1-4	Plot illustrating the relationship between the concentration of lead (mg/kg DW) in sediment (<2 mm) and the control-adjusted survival of amphipods (<i>Hyalella azteca</i>) in 28-d exposures to sediment samples from the Tri-State Mining District.	A1-4
Plot A1-5	Plot illustrating the relationship between the concentration of nickel (mg/kg DW) in sediment (<2 mm) and the control-adjusted survival of amphipods (<i>Hyalella azteca</i>) in 28-d exposures to sediment samples from the Tri-State Mining District.	A1-5
Plot A1-6	Plot illustrating the relationship between the concentration of zinc (mg/kg DW) in sediment (<2 mm) and the control-adjusted survival of amphipods (<i>Hyalella azteca</i>) in 28-d exposures to sediment samples from the Tri-State Mining District.	A1-6
Plot A1-7	Plot illustrating the relationship between the concentration of total PAH ($\mu\text{g/kg DW}$) in sediment (<2 mm) and the control-adjusted survival of amphipods (<i>Hyalella azteca</i>) in 28-d exposures to sediment samples from the Tri-State Mining District.	A1-7
Plot A1-8	Plot illustrating the relationship between the concentration of $\sum\text{SEM-AVS}$ ($\mu\text{mol/g DW}$) in sediment (<2 mm) and the control-adjusted survival of amphipods (<i>Hyalella azteca</i>) in 28-d exposures to sediment samples from the Tri-State Mining District.	A1-8
Plot A1-9	Plot illustrating the relationship between the concentration of $(\sum\text{SEM-AVS})/f_{\text{oc}}$ ($\mu\text{mol/g DW}$) in sediment (<2 mm) and the control-adjusted survival of amphipods (<i>Hyalella azteca</i>) in 28-d exposures to sediment samples from the Tri-State Mining District.	A1-9
Plot A1-10	Plot illustrating the relationship between the concentration of $\sum\text{ESB-TU}_{\text{FCV}}$ in sediment (<2 mm) and the control-adjusted survival of amphipods (<i>Hyalella azteca</i>) in 28-d exposures to sediment samples from the Tri-State Mining District.	A1-10

Plot A1-11	Plot illustrating the relationship between the concentration of Mean PEC-Q in sediment (<2 mm) and the control-adjusted survival of amphipods (<i>Hyalella azteca</i>) in 28-d exposures to sediment samples from the Tri-State Mining District.	A1-11
Plot A1-12	Plot illustrating the relationship between the concentration of Mean PEC-Q _{METAL} in sediment (<2 mm) and the control-adjusted survival of amphipods (<i>Hyalella azteca</i>) in 28-d exposures to sediment samples from the Tri-State Mining District.	A1-12
Plot A1-13	Plot illustrating the relationship between the concentration of Mean PEC-Q _{METAL(1%OC)} in sediment (<2 mm) and the control-adjusted survival of amphipods (<i>Hyalella azteca</i>) in 28-d exposures to sediment samples from the Tri-State Mining District.	A1-13
Plot A1-14	Plot illustrating the relationship between the concentration of \sum PEC-Q _{Cd,Pb,Zn} in sediment (<2 mm) and the control-adjusted survival of amphipods (<i>Hyalella azteca</i>) in 28-d exposures to sediment samples from the Tri-State Mining District.	A1-14
Plot A1-15	Plot illustrating the relationship between the concentration of \sum STT-Q _{Cd,Cu,Pb,Zn} in sediment (<2 mm) and the control-adjusted survival of amphipods (<i>Hyalella azteca</i>) in 28-d exposures to sediment samples from the Tri-State Mining District.	A1-15
Plot A1-16	Plot illustrating the relationship between the concentration of cadmium (mg/kg DW) in sediment (<2 mm) and the control-adjusted biomass of amphipods (<i>Hyalella azteca</i>) in 28-d exposures to sediment samples from the Tri-State Mining District.	A1-16
Plot A1-17	Plot illustrating the relationship between the concentration of chromium (mg/kg DW) in sediment (<2 mm) and the control-adjusted biomass of amphipods (<i>Hyalella azteca</i>) in 28-d exposures to sediment samples from the Tri-State Mining District.	A1-17
Plot A1-18	Plot illustrating the relationship between the concentration of copper (mg/kg DW) in sediment (<2 mm) and the control-adjusted biomass of amphipods (<i>Hyalella azteca</i>) in 28-d exposures to sediment samples from the Tri-State Mining District.	A1-18
Plot A1-19	Plot illustrating the relationship between the concentration of lead (mg/kg DW) in sediment (<2 mm) and the control-adjusted biomass of amphipods (<i>Hyalella azteca</i>) in 28-d exposures to sediment samples from the Tri-State Mining District.	A1-19
Plot A1-20	Plot illustrating the relationship between the concentration of nickel (mg/kg DW) in sediment (<2 mm) and the control-adjusted biomass of amphipods (<i>Hyalella azteca</i>) in 28-d exposures to sediment samples from the Tri-State Mining District.	A1-20
Plot A1-21	Plot illustrating the relationship between the concentration of zinc (mg/kg DW) in sediment (<2 mm) and the control-adjusted biomass of amphipods (<i>Hyalella azteca</i>) in 28-d exposures to sediment samples from the Tri-State Mining District.	A1-21

Plot A1-22	Plot illustrating the relationship between the concentration of total PAH ($\mu\text{g}/\text{kg}$ DW) in sediment (<2 mm) and the control-adjusted biomass of amphipods (<i>Hyalella azteca</i>) in 28-d exposures to sediment samples from the Tri-State Mining District.	A1-22
Plot A1-23	Plot illustrating the relationship between the concentration of $\sum\text{SEM-AVS}$ ($\mu\text{mol}/\text{g}$ DW) in sediment (<2 mm) and the control-adjusted biomass of amphipods (<i>Hyalella azteca</i>) in 28-d exposures to sediment samples from the Tri-State Mining District.	A1-23
Plot A1-24	Plot illustrating the relationship between the concentration of $(\sum\text{SEM-AVS})/f_{\text{OC}}$ ($\mu\text{mol}/\text{g}$ DW) in sediment (<2 mm) and the control-adjusted biomass of amphipods (<i>Hyalella azteca</i>) in 28-d exposures to sediment samples from the Tri-State Mining District.	A1-24
Plot A1-25	Plot illustrating the relationship between the concentration of $\sum\text{ESB-TU}_{\text{FCV}}$ in sediment (<2 mm) and the control-adjusted biomass of amphipods (<i>Hyalella azteca</i>) in 28-d exposures to sediment samples from the Tri-State Mining District.	A1-25
Plot A1-26	Plot illustrating the relationship between the concentration of Mean PEC-Q in sediment (<2 mm) and the control-adjusted biomass of amphipods (<i>Hyalella azteca</i>) in 28-d exposures to sediment samples from the Tri-State Mining District.	A1-26
Plot A1-27	Plot illustrating the relationship between the concentration of Mean $\text{PEC-Q}_{\text{METAL}}$ in sediment (<2 mm) and the control-adjusted biomass of amphipods (<i>Hyalella azteca</i>) in 28-d exposures to sediment samples from the Tri-State Mining District.	A1-27
Plot A1-28	Plot illustrating the relationship between the concentration of Mean $\text{PEC-Q}_{\text{METAL}(1\%\text{OC})}$ in sediment (<2 mm) and the control-adjusted biomass of amphipods (<i>Hyalella azteca</i>) in 28-d exposures to sediment samples from the Tri-State Mining District.	A1-28
Plot A1-29	Plot illustrating the relationship between the concentration of $\sum\text{PEC-Q}_{\text{Cd,Pb,Zn}}$ in sediment (<2 mm) and the control-adjusted biomass of amphipods (<i>Hyalella azteca</i>) in 28-d exposures to sediment samples from the Tri-State Mining District.	A1-29
Plot A1-30	Plot illustrating the relationship between the concentration of $\sum\text{STT-Q}_{\text{Cd,Cu,Pb,Zn}}$ in sediment (<2 mm) and the control-adjusted biomass of amphipods (<i>Hyalella azteca</i>) in 28-d exposures to sediment samples from the Tri-State Mining District.	A1-30
Plot A1-31	Plot illustrating the relationship between the concentration of cadmium (mg/kg DW) in sediment (<250 μm) and the control-adjusted survival of mussels (<i>Lampsilis siliquoidea</i>) in 28-d exposures to sediment samples from the Tri-State Mining District.	A1-31
Plot A1-32	Plot illustrating the relationship between the concentration of chromium (mg/kg DW) in sediment (<250 μm) and the control-adjusted survival of mussels (<i>Lampsilis siliquoidea</i>) in 28-d exposures to sediment samples from the Tri-State Mining District.	A1-32

Plot A1-33	Plot illustrating the relationship between the concentration of copper (mg/kg DW) in sediment (<250 μm) and the control-adjusted survival of mussels (<i>Lampsilis siliquoidea</i>) in 28-d exposures to sediment samples from the Tri-State Mining District.	A1-33
Plot A1-34	Plot illustrating the relationship between the concentration of lead (mg/kg DW) in sediment (<250 μm) and the control-adjusted survival of mussels (<i>Lampsilis siliquoidea</i>) in 28-d exposures to sediment samples from the Tri-State Mining District.	A1-34
Plot A1-35	Plot illustrating the relationship between the concentration of nickel (mg/kg DW) in sediment (<250 μm) and the control-adjusted survival of mussels (<i>Lampsilis siliquoidea</i>) in 28-d exposures to sediment samples from the Tri-State Mining District.	A1-35
Plot A1-36	Plot illustrating the relationship between the concentration of zinc (mg/kg DW) in sediment (<250 μm) and the control-adjusted survival of mussels (<i>Lampsilis siliquoidea</i>) in 28-d exposures to sediment samples from the Tri-State Mining District.	A1-36
Plot A1-37	Plot illustrating the relationship between the concentration of total PAH ($\mu\text{g/kg DW}$) in sediment (<250 μm) and the control-adjusted survival of mussels (<i>Lampsilis siliquoidea</i>) in 28-d exposures to sediment samples from the Tri-State Mining District.	A1-37
Plot A1-38	Plot illustrating the relationship between the concentration of $\sum\text{SEM-AVS}$ ($\mu\text{mol/g DW}$) in sediment (<250 μm) and the control-adjusted survival of mussels (<i>Lampsilis siliquoidea</i>) in 28-d exposures to sediment samples from the Tri-State Mining District.	A1-38
Plot A1-39	Plot illustrating the relationship between the concentration of $(\sum\text{SEM-AVS})/f_{\text{OC}}$ ($\mu\text{mol/g DW}$) in sediment (<250 μm) and the control-adjusted survival of mussels (<i>Lampsilis siliquoidea</i>) in 28-d exposures to sediment samples from the Tri-State Mining District.	A1-39
Plot A1-40	Plot illustrating the relationship between the concentration of $\sum\text{ESB-TU}_{\text{FCV}}$ in sediment (<250 μm) and the control-adjusted survival of mussels (<i>Lampsilis siliquoidea</i>) in 28-d exposures to sediment samples from the Tri-State Mining District.	A1-40
Plot A1-41	Plot illustrating the relationship between the concentration of Mean PEC-Q in sediment (<250 μm) and the control-adjusted survival of mussels (<i>Lampsilis siliquoidea</i>) in 28-d exposures to sediment samples from the Tri-State Mining District.	A1-41
Plot A1-42	Plot illustrating the relationship between the concentration of Mean $\text{PEC-Q}_{\text{METAL}}$ in sediment (<250 μm) and the control-adjusted survival of mussels (<i>Lampsilis siliquoidea</i>) in 28-d exposures to sediment samples from the Tri-State Mining District.	A1-42
Plot A1-43	Plot illustrating the relationship between the concentration of Mean $\text{PEC-Q}_{\text{METAL}(1\%\text{OC})}$ in sediment (<250 μm) and the control-adjusted survival of mussels (<i>Lampsilis siliquoidea</i>) in 28-d exposures to sediment samples from the Tri-State Mining District.	A1-43

Plot A1-44	Plot illustrating the relationship between the concentration of $\sum\text{PEC-Q}_{\text{Cd,Pb,Zn}}$ in sediment (<250 μm) and the control-adjusted survival of mussels (<i>Lampsilis siliquoidea</i>) in 28-d exposures to sediment samples from the Tri-State Mining District.	A1-44
Plot A1-45	Plot illustrating the relationship between the concentration of $\sum\text{STT-Q}_{\text{Cd,Cu,Pb,Zn}}$ in sediment (<250 μm) and the control-adjusted survival of mussels (<i>Lampsilis siliquoidea</i>) in 28-d exposures to sediment samples from the Tri-State Mining District.	A1-45
Plot A1-46	Plot illustrating the relationship between the concentration of cadmium (mg/kg DW) in sediment (<250 μm) and the control-adjusted biomass of mussels (<i>Lampsilis siliquoidea</i>) in 28-d exposures to sediment samples from the Tri-State Mining District.	A1-46
Plot A1-47	Plot illustrating the relationship between the concentration of chromium (mg/kg DW) in sediment (<250 μm) and the control-adjusted biomass of mussels (<i>Lampsilis siliquoidea</i>) in 28-d exposures to sediment samples from the Tri-State Mining District.	A1-47
Plot A1-48	Plot illustrating the relationship between the concentration of copper (mg/kg DW) in sediment (<250 μm) and the control-adjusted biomass of mussels (<i>Lampsilis siliquoidea</i>) in 28-d exposures to sediment samples from the Tri-State Mining District.	A1-48
Plot A1-49	Plot illustrating the relationship between the concentration of lead (mg/kg DW) in sediment (<250 μm) and the control-adjusted biomass of mussels (<i>Lampsilis siliquoidea</i>) in 28-d exposures to sediment samples from the Tri-State Mining District.	A1-49
Plot A1-50	Plot illustrating the relationship between the concentration of nickel (mg/kg DW) in sediment (<250 μm) and the control-adjusted biomass of mussels (<i>Lampsilis siliquoidea</i>) in 28-d exposures to sediment samples from the Tri-State Mining District.	A1-50
Plot A1-51	Plot illustrating the relationship between the concentration of zinc (mg/kg DW) in sediment (<250 μm) and the control-adjusted biomass of mussels (<i>Lampsilis siliquoidea</i>) in 28-d exposures to sediment samples from the Tri-State Mining District.	A1-51
Plot A1-52	Plot illustrating the relationship between the concentration of total PAH ($\mu\text{g/kg DW}$) in sediment (<250 μm) and the control-adjusted biomass of mussels (<i>Lampsilis siliquoidea</i>) in 28-d exposures to sediment samples from the Tri-State Mining District.	A1-52
Plot A1-53	Plot illustrating the relationship between the concentration of $\sum\text{SEM-AVS}$ ($\mu\text{mol/g DW}$) in sediment (<250 μm) and the control-adjusted biomass of mussels (<i>Lampsilis siliquoidea</i>) in 28-d exposures to sediment samples from the Tri-State Mining District.	A1-53
Plot A1-54	Plot illustrating the relationship between the concentration of $(\sum\text{SEM-AVS})/f_{\text{OC}}$ ($\mu\text{mol/g DW}$) in sediment (<250 μm) and the control-adjusted biomass of mussels (<i>Lampsilis siliquoidea</i>) in 28-d exposures to sediment samples from the Tri-State Mining District.	A1-54

- Plot A1- 55** Plot illustrating the relationship between the concentration of \sum ESB-TU_{FCV} in sediment (<250 μ m) and the control-adjusted biomass of mussels (*Lampsilis siliquoidea*) in 28-d exposures to sediment samples from the Tri-State Mining District. A1-55
- Plot A1- 56** Plot illustrating the relationship between the concentration of Mean PEC-Q in sediment (<250 μ m) and the control-adjusted biomass of mussels (*Lampsilis siliquoidea*) in 28-d exposures to sediment samples from the Tri-State Mining District. A1-56
- Plot A1- 57** Plot illustrating the relationship between the concentration of Mean PEC-Q_{METAL} in sediment (<250 μ m) and the control-adjusted biomass of mussels (*Lampsilis siliquoidea*) in 28-d exposures to sediment samples from the Tri-State Mining District. A1-57
- Plot A1- 58** Plot illustrating the relationship between the concentration of Mean PEC-Q_{METAL(1%OC)} in sediment (<250 μ m) and the control-adjusted biomass of mussels (*Lampsilis siliquoidea*) in 28-d exposures to sediment samples from the Tri-State Mining District. A1-58
- Plot A1-59** Plot illustrating the relationship between the concentration of \sum PEC-Q_{Cd,Pb,Zn} in sediment (<250 μ m) and the control-adjusted biomass of mussels (*Lampsilis siliquoidea*) in 28-d exposures to sediment samples from the Tri-State Mining District. A1-59
- Plot A1-60** Plot illustrating the relationship between the concentration of \sum STT-Q_{Cd,Cu,Pb,Zn} in sediment (<250 μ m) and the control-adjusted biomass of mussels (*Lampsilis siliquoidea*) in 28-d exposures to sediment samples from the Tri-State Mining District. A1-60
- Plot A1-61** Plot illustrating the relationship between the concentration of cadmium (mg/kg DW) in sediment (<2 mm) and the control-adjusted survival of midges (*Chironomus dilutus*) in 10-d exposures to sediment samples from the Tri-State Mining District. A1-61
- Plot A1-62** Plot illustrating the relationship between the concentration of chromium (mg/kg DW) in sediment (<2 mm) and the control-adjusted survival of midges (*Chironomus dilutus*) in 10-d exposures to sediment samples from the Tri-State Mining District. A1-62
- Plot A1-63** Plot illustrating the relationship between the concentration of copper (mg/kg DW) in sediment (<2 mm) and the control-adjusted survival of midges (*Chironomus dilutus*) in 10-d exposures to sediment samples from the Tri-State Mining District. A1-63
- Plot A1-64** Plot illustrating the relationship between the concentration of lead (mg/kg DW) in sediment (<2 mm) and the control-adjusted survival of midges (*Chironomus dilutus*) in 10-d exposures to sediment samples from the Tri-State Mining District. A1-64
- Plot A1-65** Plot illustrating the relationship between the concentration of nickel (mg/kg DW) in sediment (<2 mm) and the control-adjusted survival of midges (*Chironomus dilutus*) in 10-d exposures to sediment samples from the Tri-State Mining District. A1-65

Plot A1-66	Plot illustrating the relationship between the concentration of zinc (mg/kg DW) in sediment (<2 mm) and the control-adjusted survival of midges (<i>Chironomus dilutus</i>) in 10-d exposures to sediment samples from the Tri-State Mining District.	A1-66
Plot A1-67	Plot illustrating the relationship between the concentration of total PAH ($\mu\text{g/kg DW}$) in sediment (<2 mm) and the control-adjusted survival of midges (<i>Chironomus dilutus</i>) in 10-d exposures to sediment samples from the Tri-State Mining District.	A1-67
Plot A1-68	Plot illustrating the relationship between the concentration of $\sum\text{SEM-AVS}$ ($\mu\text{mol/g DW}$) in sediment (<2 mm) and the control-adjusted survival of midges (<i>Chironomus dilutus</i>) in 10-d exposures to sediment samples from the Tri-State Mining District.	A1-68
Plot A1-69	Plot illustrating the relationship between the concentration of $(\sum\text{SEM-AVS})/f_{\text{OC}}$ ($\mu\text{mol/g DW}$) in sediment (<2 mm) and the control-adjusted survival of midges (<i>Chironomus dilutus</i>) in 10-d exposures to sediment samples from the Tri-State Mining District.	A1-69
Plot A1-70	Plot illustrating the relationship between the concentration of $\sum\text{ESB-TU}_{\text{FCV}}$ in sediment (<2 mm) and the control-adjusted survival of midges (<i>Chironomus dilutus</i>) in 10-d exposures to sediment samples from the Tri-State Mining District.	A1-70
Plot A1-71	Plot illustrating the relationship between the concentration of Mean PEC-Q in sediment (<2 mm) and the control-adjusted survival of midges (<i>Chironomus dilutus</i>) in 10-d exposures to sediment samples from the Tri-State Mining District.	A1-71
Plot A1-72	Plot illustrating the relationship between the concentration of Mean $\text{PEC-Q}_{\text{METAL}}$ in sediment (<2 mm) and the control-adjusted survival of midges (<i>Chironomus dilutus</i>) in 10-d exposures to sediment samples from the Tri-State Mining District.	A1-72
Plot A1-73	Plot illustrating the relationship between the concentration of Mean $\text{PEC-Q}_{\text{METAL}(1\%\text{OC})}$ in sediment (<2 mm) and the control-adjusted survival of midges (<i>Chironomus dilutus</i>) in 10-d exposures to sediment samples from the Tri-State Mining District.	A1-73
Plot A1-74	Plot illustrating the relationship between the concentration of $\sum\text{PEC-Q}_{\text{Cd,Pb,Zn}}$ in sediment (<2 mm) and the control-adjusted survival of midges (<i>Chironomus dilutus</i>) in 10-d exposures to sediment samples from the Tri-State Mining District.	A1-74
Plot A1-75	Plot illustrating the relationship between the concentration of $\sum\text{STT-Q}_{\text{Cd,Cu,Pb,Zn}}$ in sediment (<2 mm) and the control-adjusted survival of midges (<i>Chironomus dilutus</i>) in 10-d exposures to sediment samples from the Tri-State Mining District.	A1-75
Plot A1-76	Plot illustrating the relationship between the concentration of cadmium (mg/kg DW) in sediment (<2 mm) and the control-adjusted biomass of midges (<i>Chironomus dilutus</i>) in 10-d exposures to sediment samples from the Tri-State Mining District.	A1-76

Plot A1-77	Plot illustrating the relationship between the concentration of chromium (mg/kg DW) in sediment (<2 mm) and the control-adjusted biomass of midges (<i>Chironomus dilutus</i>) in 10-d exposures to sediment samples from the Tri-State Mining District.	A1-77
Plot A1-78	Plot illustrating the relationship between the concentration of copper (mg/kg DW) in sediment (<2 mm) and the control-adjusted biomass of midges (<i>Chironomus dilutus</i>) in 10-d exposures to sediment samples from the Tri-State Mining District.	A1-78
Plot A1-79	Plot illustrating the relationship between the concentration of lead (mg/kg DW) in sediment (<2 mm) and the control-adjusted biomass of midges (<i>Chironomus dilutus</i>) in 10-d exposures to sediment samples from the Tri-State Mining District.	A1-79
Plot A1-80	Plot illustrating the relationship between the concentration of nickel (mg/kg DW) in sediment (<2 mm) and the control-adjusted biomass of midges (<i>Chironomus dilutus</i>) in 10-d exposures to sediment samples from the Tri-State Mining District.	A1-80
Plot A1-81	Plot illustrating the relationship between the concentration of zinc (mg/kg DW) in sediment (<2 mm) and the control-adjusted biomass of midges (<i>Chironomus dilutus</i>) in 10-d exposures to sediment samples from the Tri-State Mining District.	A1-81
Plot A1-82	Plot illustrating the relationship between the concentration of total PAH ($\mu\text{g/kg DW}$) in sediment (<2 mm) and the control-adjusted biomass of midges (<i>Chironomus dilutus</i>) in 10-d exposures to sediment samples from the Tri-State Mining District.	A1-82
Plot A1-83	Plot illustrating the relationship between the concentration of $\sum\text{SEM-AVS}$ ($\mu\text{mol/g DW}$) in sediment (<2 mm) and the control-adjusted biomass of midges (<i>Chironomus dilutus</i>) in 10-d exposures to sediment samples from the Tri-State Mining District.	A1-83
Plot A1-84	Plot illustrating the relationship between the concentration of $(\sum\text{SEM-AVS})/f_{\text{OC}}$ ($\mu\text{mol/g DW}$) in sediment (<2 mm) and the control-adjusted biomass of midges (<i>Chironomus dilutus</i>) in 10-d exposures to sediment samples from the Tri-State Mining District.	A1-84
Plot A1-85	Plot illustrating the relationship between the concentration of $\sum\text{ESB-TU}_{\text{FCV}}$ in sediment (<2 mm) and the control-adjusted biomass of midges (<i>Chironomus dilutus</i>) in 10-d exposures to sediment samples from the Tri-State Mining District.	A1-85
Plot A1-86	Plot illustrating the relationship between the concentration of Mean PEC-Q in sediment (<2 mm) and the control-adjusted biomass of midges (<i>Chironomus dilutus</i>) in 10-d exposures to sediment samples from the Tri-State Mining District.	A1-86
Plot A1-87	Plot illustrating the relationship between the concentration of Mean $\text{PEC-Q}_{\text{METAL}}$ in sediment (<2 mm) and the control-adjusted biomass of midges (<i>Chironomus dilutus</i>) in 10-d exposures to sediment samples from the Tri-State Mining District.	A1-87

- Plot A1-88** Plot illustrating the relationship between the concentration of Mean $\text{PEC-Q}_{\text{METAL}(1\% \text{OC})}$ in sediment (<2 mm) and the control-adjusted biomass of midges (*Chironomus dilutus*) in 10-d exposures to sediment samples from the Tri-State Mining District. A1-88
- Plot A1-89** Plot illustrating the relationship between the concentration of $\sum \text{PEC-Q}_{\text{Cd,Pb,Zn}}$ in sediment (<2 mm) and the control-adjusted biomass of midges (*Chironomus dilutus*) in 10-d exposures to sediment samples from the Tri-State Mining District. A1-89
- Plot A1-90** Plot illustrating the relationship between the concentration of $\sum \text{STT-Q}_{\text{Cd,Cu,Pb,Zn}}$ in sediment (<2 mm) and the control-adjusted biomass of midges (*Chironomus dilutus*) in 10-d exposures to sediment samples from the Tri-State Mining District. A1-90
- Plot A1-91** Plot illustrating the relationship between $\sum \text{PW-TU}_{\text{METALS}}$ and the control-adjusted survival of amphipods (*Hyalella azteca*) in 28-d exposures to sediment samples from the Tri-State Mining District. A1-91
- Plot A1-92** Plot illustrating the relationship between $\sum \text{PW-TU}_{\text{DIVALENT METALS}}$ and the control-adjusted survival of amphipods (*Hyalella azteca*) in 28-d exposures to sediment samples from the Tri-State Mining District. A1-92
- Plot A1-93** Plot illustrating the relationship between $\text{PW-TU}_{\text{ALUMINUM}}$ and the control-adjusted survival of amphipods (*Hyalella azteca*) in 28-d exposures to sediment samples from the Tri-State Mining District. A1-93
- Plot A1-94** Plot illustrating the relationship between $\text{PW-TU}_{\text{ARSENIC}}$ and the control-adjusted survival of amphipods (*Hyalella azteca*) in 28-d exposures to sediment samples from the Tri-State Mining District. A1-94
- Plot A1-95** Plot illustrating the relationship between $\text{PW-TU}_{\text{CADMIUM}}$ (7 day) and the control-adjusted survival of amphipods (*Hyalella azteca*) in 28-d exposures to sediment samples from the Tri-State Mining District. A1-95
- Plot A1-96** Plot illustrating the relationship between $\text{PW-TU}_{\text{CADMIUM}}$ (28 day) and the control-adjusted survival of amphipods (*Hyalella azteca*) in 28-d exposures to sediment samples from the Tri-State Mining District. A1-96
- Plot A1-97** Plot illustrating the relationship between $\text{PW-TU}_{\text{CADMIUM}}$ (mean) and the control-adjusted survival of amphipods (*Hyalella azteca*) in 28-d exposures to sediment samples from the Tri-State Mining District. A1-97
- Plot A1-98** Plot illustrating the relationship between $\text{PW-TU}_{\text{CHROMIUM}}$ and the control-adjusted survival of amphipods (*Hyalella azteca*) in 28-d exposures to sediment samples from the Tri-State Mining District. A1-98
- Plot A1-99** Plot illustrating the relationship between $\text{PW-TU}_{\text{COPPER}}$ (7 day) and the control-adjusted survival of amphipods (*Hyalella azteca*) in 28-d exposures to sediment samples from the Tri-State Mining District. A1-99
- Plot A1-100** Plot illustrating the relationship between $\text{PW-TU}_{\text{COPPER}}$ (28 day) and the control-adjusted survival of amphipods (*Hyalella azteca*) in 28-d exposures to sediment samples from the Tri-State Mining District. A1-100

- Plot A1-101** Plot illustrating the relationship between PW-TU_{COPPER} (mean) and the control-adjusted survival of amphipods (*Hyaella azteca*) in 28-d exposures to sediment samples from the Tri-State Mining District. A1-101
- Plot A1-102** Plot illustrating the relationship between PW-TU_{IRON} and the control-adjusted survival of amphipods (*Hyaella azteca*) in 28-d exposures to sediment samples from the Tri-State Mining District. A1-102
- Plot A1-103** Plot illustrating the relationship between PW-TU_{LEAD} (7 day) and the control-adjusted survival of amphipods (*Hyaella azteca*) in 28-d exposures to sediment samples from the Tri-State Mining District. A1-103
- Plot A1-104** Plot illustrating the relationship between PW-TU_{LEAD} (28 day) and the control-adjusted survival of amphipods (*Hyaella azteca*) in 28-d exposures to sediment samples from the Tri-State Mining District. A1-104
- Plot A1-105** Plot illustrating the relationship between PW-TU_{LEAD} (mean) and the control-adjusted survival of amphipods (*Hyaella azteca*) in 28-d exposures to sediment samples from the Tri-State Mining District. A1-105
- Plot A1-106** Plot illustrating the relationship between PW-TU_{NICKEL} (7 day) and the control-adjusted survival of amphipods (*Hyaella azteca*) in 28-d exposures to sediment samples from the Tri-State Mining District. A1-106
- Plot A1-107** Plot illustrating the relationship between PW-TU_{NICKEL} (28 day) and the control-adjusted survival of amphipods (*Hyaella azteca*) in 28-d exposures to sediment samples from the Tri-State Mining District. A1-107
- Plot A1-108** Plot illustrating the relationship between PW-TU_{TUNICKEL} (mean) and the control-adjusted survival of amphipods (*Hyaella azteca*) in 28-d exposures to sediment samples from the Tri-State Mining District. A1-108
- Plot A1-109** Plot illustrating the relationship between PW-TU_{SELENIUM} and the control-adjusted survival of amphipods (*Hyaella azteca*) in 28-d exposures to sediment samples from the Tri-State Mining District. A1-109
- Plot A1-110** Plot illustrating the relationship between PW-TU_{SILVER} and the control-adjusted survival of amphipods (*Hyaella azteca*) in 28-d exposures to sediment samples from the Tri-State Mining District. A1-110
- Plot A1-111** Plot illustrating the relationship between PW-TU_{ZINC} (7 day) and the control-adjusted survival of amphipods (*Hyaella azteca*) in 28-d exposures to sediment samples from the Tri-State Mining District. A1-111
- Plot A1-112** Plot illustrating the relationship between PW-TU_{ZINC} (28 day) and the control-adjusted survival of amphipods (*Hyaella azteca*) in 28-d exposures to sediment samples from the Tri-State Mining District. A1-112
- Plot A1-113** Plot illustrating the relationship between PW-TU_{ZINC} (mean) and the control-adjusted survival of amphipods (*Hyaella azteca*) in 28-d exposures to sediment samples from the Tri-State Mining District. A1-113
- Plot A1-114** Plot illustrating the relationship between PW-TU_{LEAD(DOC)} and the control-adjusted survival of amphipods (*Hyaella azteca*) in 28-d exposures to sediment samples from the Tri-State Mining District. A1-114

- Plot A1-115** Plot illustrating the relationship between $PW-TU_{ZINC(DOC)}$ and the control-adjusted survival of amphipods (*Hyalella azteca*) in 28-d exposures to sediment samples from the Tri-State Mining District. A1-115
- Plot A1-116** Plot illustrating the relationship between $\sum PW-TU_{METALS}$ and the control-adjusted biomass of amphipods (*Hyalella azteca*) in 28-d exposures to sediment samples from the Tri-State Mining District. A1-116
- Plot A1-117** Plot illustrating the relationship between $\sum PW-TU_{DIVALENT METALS}$ and the control-adjusted biomass of amphipods (*Hyalella azteca*) in 28-d exposures to sediment samples from the Tri-State Mining District. A1-117
- Plot A1-118** Plot illustrating the relationship between $PW-TU_{ALUMINUM}$ and the control-adjusted biomass of amphipods (*Hyalella azteca*) in 28-d exposures to sediment samples from the Tri-State Mining District. A1-118
- Plot A1-119** Plot illustrating the relationship between $PW-TU_{ARSENIC}$ and the control-adjusted biomass of amphipods (*Hyalella azteca*) in 28-d exposures to sediment samples from the Tri-State Mining District. A1-119
- Plot A1-120** Plot illustrating the relationship between $PW-TU_{CADMIUM}$ (7 day) and the control-adjusted biomass of amphipods (*Hyalella azteca*) in 28-d exposures to sediment samples from the Tri-State Mining District. A1-120
- Plot A1-121** Plot illustrating the relationship between $PW-TU_{CADMIUM}$ (28 day) and the control-adjusted biomass of amphipods (*Hyalella azteca*) in 28-d exposures to sediment samples from the Tri-State Mining District. A1-121
- Plot A1-122** Plot illustrating the relationship between $PW-TU_{CADMIUM}$ (mean) and the control-adjusted biomass of amphipods (*Hyalella azteca*) in 28-d exposures to sediment samples from the Tri-State Mining District. A1-122
- Plot A1-123** Plot illustrating the relationship between $PW-TU_{CHROMIUM}$ and the control-adjusted biomass of amphipods (*Hyalella azteca*) in 28-d exposures to sediment samples from the Tri-State Mining District. A1-123
- Plot A1-124** Plot illustrating the relationship between $PW-TU_{COPPER}$ (7 day) and the control-adjusted biomass of amphipods (*Hyalella azteca*) in 28-d exposures to sediment samples from the Tri-State Mining District. A1-124
- Plot A1-125** Plot illustrating the relationship between $PW-TU_{COPPER}$ (28 day) and the control-adjusted biomass of amphipods (*Hyalella azteca*) in 28-d exposures to sediment samples from the Tri-State Mining District. A1-125
- Plot A1-126** Plot illustrating the relationship between $PW-TU_{COPPER}$ (mean) and the control-adjusted biomass of amphipods (*Hyalella azteca*) in 28-d exposures to sediment samples from the Tri-State Mining District. A1-126
- Plot A1-127** Plot illustrating the relationship between $PW-TU_{IRON}$ and the control-adjusted biomass of amphipods (*Hyalella azteca*) in 28-d exposures to sediment samples from the Tri-State Mining District. A1-127
- Plot A1-128** Plot illustrating the relationship between $PW-TU_{LEAD}$ (7 day) and the control-adjusted biomass of amphipods (*Hyalella azteca*) in 28-d exposures to sediment samples from the Tri-State Mining District. A1-128

- Plot A1-129** Plot illustrating the relationship between $PW-TU_{LEAD}$ (28 day) and the control-adjusted biomass of amphipods (*Hyalella azteca*) in 28-d exposures to sediment samples from the Tri-State Mining District. A1-129
- Plot A1-130** Plot illustrating the relationship between $PW-TU_{LEAD}$ (mean) and the control-adjusted biomass of amphipods (*Hyalella azteca*) in 28-d exposures to sediment samples from the Tri-State Mining District. A1-130
- Plot A1-131** Plot illustrating the relationship between $PW-TU_{NICKEL}$ (7 day) and the control-adjusted biomass of amphipods (*Hyalella azteca*) in 28-d exposures to sediment samples from the Tri-State Mining District. A1-131
- Plot A1-132** Plot illustrating the relationship between $PW-TU_{NICKEL}$ (28 day) and the control-adjusted biomass of amphipods (*Hyalella azteca*) in 28-d exposures to sediment samples from the Tri-State Mining District. A1-132
- Plot A1-133** Plot illustrating the relationship between $PW-TU_{NICKEL}$ (mean) and the control-adjusted biomass of amphipods (*Hyalella azteca*) in 28-d exposures to sediment samples from the Tri-State Mining District. A1-133
- Plot A1-134** Plot illustrating the relationship between $PW-TU_{SELENIUM}$ and the control-adjusted biomass of amphipods (*Hyalella azteca*) in 28-d exposures to sediment samples from the Tri-State Mining District. A1-134
- Plot A1-135** Plot illustrating the relationship between $PW-TU_{SILVER}$ and the control-adjusted biomass of amphipods (*Hyalella azteca*) in 28-d exposures to sediment samples from the Tri-State Mining District. A1-135
- Plot A1-136** Plot illustrating the relationship between $PW-TU_{ZINC}$ (7 day) and the control-adjusted biomass of amphipods (*Hyalella azteca*) in 28-d exposures to sediment samples from the Tri-State Mining District. A1-136
- Plot A1-137** Plot illustrating the relationship between $PW-TU_{TUZINC}$ (28 day) and the control-adjusted biomass of amphipods (*Hyalella azteca*) in 28-d exposures to sediment samples from the Tri-State Mining District. A1-137
- Plot A1-138** Plot illustrating the relationship between $PW-TU_{ZINC}$ (mean) and the control-adjusted biomass of amphipods (*Hyalella azteca*) in 28-d exposures to sediment samples from the Tri-State Mining District. A1-138
- Plot A1-139** Plot illustrating the relationship between $PW-TU_{LEAD(DOC)}$ and the control-adjusted biomass of amphipods (*Hyalella azteca*) in 28-d exposures to sediment samples from the Tri-State Mining District. A1-139
- Plot A1-140** Plot illustrating the relationship between $PW-TU_{TUZINC(DOC)}$ and the control-adjusted biomass of amphipods (*Hyalella azteca*) in 28-d exposures to sediment samples from the Tri-State Mining District. A1-140
- Plot A1-141** Plot illustrating the relationship between $\sum PW-TU_{METALS}$ and the control-adjusted survival of mussels (*Lampsilis siliquoidea*) in 28-d exposures to sediment samples from the Tri-State Mining District. A1-141
- Plot A1-142** Plot illustrating the relationship between $\sum PW-TU_{DIVALENT METALS}$ and the control-adjusted survival of mussels (*Lampsilis siliquoidea*) in 28-d exposures to sediment samples from the Tri-State Mining District. A1-142

- Plot A1-143** Plot illustrating the relationship between PW-TU_{ALUMINUM} and the control-adjusted survival of mussels (*Lampsilis siliquoidea*) in 28-d exposures to sediment samples from the Tri-State Mining District. A1-143
- Plot A1-144** Plot illustrating the relationship between PW-TU_{ARSENIC} and the control-adjusted survival of mussels (*Lampsilis siliquoidea*) in 28-d exposures to sediment samples from the Tri-State Mining District. A1-144
- Plot A1-145** Plot illustrating the relationship between PW-TU_{CADMIUM} (7 day) and the control-adjusted survival of mussels (*Lampsilis siliquoidea*) in 28-d exposures to sediment samples from the Tri-State Mining District. A1-145
- Plot A1-146** Plot illustrating the relationship between PW-TU_{CADMIUM} (28 day) and the control-adjusted survival of mussels (*Lampsilis siliquoidea*) in 28-d exposures to sediment samples from the Tri-State Mining District. A1-146
- Plot A1-147** Plot illustrating the relationship between PW-TU_{CADMIUM} (mean) and the control-adjusted survival of mussels (*Lampsilis siliquoidea*) in 28-d exposures to sediment samples from the Tri-State Mining District. A1-147
- Plot A1-148** Plot illustrating the relationship between PW-TU_{CHROMIUM} and the control-adjusted survival of mussels (*Lampsilis siliquoidea*) in 28-d exposures to sediment samples from the Tri-State Mining District. A1-148
- Plot A1-149** Plot illustrating the relationship between PW-TU_{COPPER} (7 day) and the control-adjusted survival of mussels (*Lampsilis siliquoidea*) in 28-d exposures to sediment samples from the Tri-State Mining District. A1-149
- Plot A1-150** Plot illustrating the relationship between PW-TU_{COPPER} (28 day) and the control-adjusted survival of mussels (*Lampsilis siliquoidea*) in 28-d exposures to sediment samples from the Tri-State Mining District. A1-150
- Plot A1-151** Plot illustrating the relationship between PW-TU_{COPPER} (mean) and the control-adjusted survival of mussels (*Lampsilis siliquoidea*) in 28-d exposures to sediment samples from the Tri-State Mining District. A1-151
- Plot A1-152** Plot illustrating the relationship between PW-TU_{IRON} and the control-adjusted survival of mussels (*Lampsilis siliquoidea*) in 28-d exposures to sediment samples from the Tri-State Mining District. A1-152
- Plot A1-153** Plot illustrating the relationship between PW-TU_{LEAD} (7 day) and the control-adjusted survival of mussels (*Lampsilis siliquoidea*) in 28-d exposures to sediment samples from the Tri-State Mining District. A1-153
- Plot A1-154** Plot illustrating the relationship between PW-TU_{LEAD} (28 day) and the control-adjusted survival of mussels (*Lampsilis siliquoidea*) in 28-d exposures to sediment samples from the Tri-State Mining District. A1-154
- Plot A1-155** Plot illustrating the relationship between PW-TU_{LEAD} (mean) and the control-adjusted survival of mussels (*Lampsilis siliquoidea*) in 28-d exposures to sediment samples from the Tri-State Mining District. A1-155
- Plot A1-156** Plot illustrating the relationship between PW-TU_{NICKEL} (7 day) and the control-adjusted survival of mussels (*Lampsilis siliquoidea*) in 28-d exposures to sediment samples from the Tri-State Mining District. A1-156

- Plot A1-157** Plot illustrating the relationship between $PW-TU_{\text{NICKEL}}$ (28 day) and the control-adjusted survival of mussels (*Lampsilis siliquoidea*) in 28-d exposures to sediment samples from the Tri-State Mining District. A1-157
- Plot A1-158** Plot illustrating the relationship between $PW-TU_{\text{NICKEL}}$ (mean) and the control-adjusted survival of mussels (*Lampsilis siliquoidea*) in 28-d exposures to sediment samples from the Tri-State Mining District. A1-158
- Plot A1-159** Plot illustrating the relationship between $PW-TU_{\text{SELENIUM}}$ and the control-adjusted survival of mussels (*Lampsilis siliquoidea*) in 28-d exposures to sediment samples from the Tri-State Mining District. A1-159
- Plot A1-160** Plot illustrating the relationship between $PW-TU_{\text{SILVER}}$ and the control-adjusted survival of mussels (*Lampsilis siliquoidea*) in 28-d exposures to sediment samples from the Tri-State Mining District. A1-160
- Plot A1-161** Plot illustrating the relationship between $PW-TU_{\text{ZINC}}$ (7 day) and the control-adjusted survival of mussels (*Lampsilis siliquoidea*) in 28-d exposures to sediment samples from the Tri-State Mining District. A1-161
- Plot A1-162** Plot illustrating the relationship between $PW-TU_{\text{ZINC}}$ (28 day) and the control-adjusted survival of mussels (*Lampsilis siliquoidea*) in 28-d exposures to sediment samples from the Tri-State Mining District. A1-162
- Plot A1-163** Plot illustrating the relationship between $PW-TU_{\text{ZINC}}$ (mean) and the control-adjusted survival of mussels (*Lampsilis siliquoidea*) in 28-d exposures to sediment samples from the Tri-State Mining District. A1-163
- Plot A1-164** Plot illustrating the relationship between $PW-TU_{\text{LEAD(DOC)}}$ and the control-adjusted survival of mussels (*Lampsilis siliquoidea*) in 28-d exposures to sediment samples from the Tri-State Mining District. A1-164
- Plot A1-165** Plot illustrating the relationship between $PW-TU_{\text{ZINC(DOC)}}$ and the control-adjusted survival of mussels (*Lampsilis siliquoidea*) in 28-d exposures to sediment samples from the Tri-State Mining District. A1-165
- Plot A1-166** Plot illustrating the relationship between $\sum PW-TU_{\text{METALS}}$ and the control-adjusted biomass of mussels (*Lampsilis siliquoidea*) in 28-d exposures to sediment samples from the Tri-State Mining District. A1-166
- Plot A1-167** Plot illustrating the relationship between $\sum PW-TU_{\text{DIVALENT METALS}}$ and the control-adjusted biomass of mussels (*Lampsilis siliquoidea*) in 28-d exposures to sediment samples from the Tri-State Mining District. A1-167
- Plot A1-168** Plot illustrating the relationship between $PW-TU_{\text{ALUMINUM}}$ and the control-adjusted biomass of mussels (*Lampsilis siliquoidea*) in 28-d exposures to sediment samples from the Tri-State Mining District. A1-168
- Plot A1-169** Plot illustrating the relationship between $PW-TU_{\text{ARSENIC}}$ and the control-adjusted biomass of mussels (*Lampsilis siliquoidea*) in 28-d exposures to sediment samples from the Tri-State Mining District. A1-169
- Plot A1-170** Plot illustrating the relationship between $PW-TU_{\text{CADMIUM}}$ (7 day) and the control-adjusted biomass of mussels (*Lampsilis siliquoidea*) in 28-d exposures to sediment samples from the Tri-State Mining District. A1-170

- Plot A1-171** Plot illustrating the relationship between $PW-TU_{\text{CADMIUM}}$ (28 day) and the control-adjusted biomass of mussels (*Lampsilis siliquoidea*) in 28-d exposures to sediment samples from the Tri-State Mining District. A1-171
- Plot A1-172** Plot illustrating the relationship between $PW-TU_{\text{CADMIUM}}$ (mean) and the control-adjusted biomass of mussels (*Lampsilis siliquoidea*) in 28-d exposures to sediment samples from the Tri-State Mining District. A1-172
- Plot A1-173** Plot illustrating the relationship between $PW-TU_{\text{CHROMIUM}}$ and the control-adjusted biomass of mussels (*Lampsilis siliquoidea*) in 28-d exposures to sediment samples from the Tri-State Mining District. A1-173
- Plot A1-174** Plot illustrating the relationship between $PW-TU_{\text{COPPER}}$ (7 day) and the control-adjusted biomass of mussels (*Lampsilis siliquoidea*) in 28-d exposures to sediment samples from the Tri-State Mining District. A1-174
- Plot A1-175** Plot illustrating the relationship between $PW-TU_{\text{COPPER}}$ (28 day) and the control-adjusted biomass of mussels (*Lampsilis siliquoidea*) in 28-d exposures to sediment samples from the Tri-State Mining District. A1-175
- Plot A1-176** Plot illustrating the relationship between $PW-TU_{\text{COPPER}}$ (mean) and the control-adjusted biomass of mussels (*Lampsilis siliquoidea*) in 28-d exposures to sediment samples from the Tri-State Mining District. A1-176
- Plot A1-177** Plot illustrating the relationship between $PW-TU_{\text{IRON}}$ and the control-adjusted biomass of mussels (*Lampsilis siliquoidea*) in 28-d exposures to sediment samples from the Tri-State Mining District. A1-177
- Plot A1-178** Plot illustrating the relationship between $PW-TU_{\text{LEAD}}$ (7 day) and the control-adjusted biomass of mussels (*Lampsilis siliquoidea*) in 28-d exposures to sediment samples from the Tri-State Mining District. A1-178
- Plot A1-179** Plot illustrating the relationship between $PW-TU_{\text{LEAD}}$ (28 day) and the control-adjusted biomass of mussels (*Lampsilis siliquoidea*) in 28-d exposures to sediment samples from the Tri-State Mining District. A1-179
- Plot A1-180** Plot illustrating the relationship between $PW-TU_{\text{LEAD}}$ (mean) and the control-adjusted biomass of mussels (*Lampsilis siliquoidea*) in 28-d exposures to sediment samples from the Tri-State Mining District. A1-180
- Plot A1-181** Plot illustrating the relationship between $PW-TU_{\text{NICKEL}}$ (7 day) and the control-adjusted biomass of mussels (*Lampsilis siliquoidea*) in 28-d exposures to sediment samples from the Tri-State Mining District. A1-181
- Plot A1-182** Plot illustrating the relationship between $PW-TU_{\text{NICKEL}}$ (28 day) and the control-adjusted biomass of mussels (*Lampsilis siliquoidea*) in 28-d exposures to sediment samples from the Tri-State Mining District. A1-182
- Plot A1-183** Plot illustrating the relationship between $PW-TU_{\text{NICKEL}}$ (mean) and the control-adjusted biomass of mussels (*Lampsilis siliquoidea*) in 28-d exposures to sediment samples from the Tri-State Mining District. A1-183
- Plot A1-184** Plot illustrating the relationship between $PW-TU_{\text{SELENIUM}}$ and the control-adjusted biomass of mussels (*Lampsilis siliquoidea*) in 28-d exposures to sediment samples from the Tri-State Mining District. A1-184

- Plot A1-185** Plot illustrating the relationship between $PW-TU_{SILVER}$ and the control-adjusted biomass of mussels (*Lampsilis siliquoidea*) in 28-d exposures to sediment samples from the Tri-State Mining District. A1-185
- Plot A1-186** Plot illustrating the relationship between $PW-TU_{ZINC}$ (7 day) and the control-adjusted biomass of mussels (*Lampsilis siliquoidea*) in 28-d exposures to sediment samples from the Tri-State Mining District. A1-186
- Plot A1-187** Plot illustrating the relationship between $PW-TU_{ZINC}$ (28 day) and the control-adjusted biomass of mussels (*Lampsilis siliquoidea*) in 28-d exposures to sediment samples from the Tri-State Mining District. A1-187
- Plot A1-188** Plot illustrating the relationship between $PW-TU_{ZINC}$ (mean) and the control-adjusted biomass of mussels (*Lampsilis siliquoidea*) in 28-d exposures to sediment samples from the Tri-State Mining District. A1-188
- Plot A1-189** Plot illustrating the relationship between $PW-TU_{LEAD(DOC)}$ and the control-adjusted biomass of mussels (*Lampsilis siliquoidea*) in 28-d exposures to sediment samples from the Tri-State Mining District. A1-189
- Plot A1-190** Plot illustrating the relationship between $PW-TU_{ZINC(DOC)}$ and the control-adjusted biomass of mussels (*Lampsilis siliquoidea*) in 28-d exposures to sediment samples from the Tri-State Mining District. A1-190
- Plot A1-191** Plot illustrating the relationship between $\sum PW-TU_{METALS}$ and the control-adjusted survival of midges (*Chironomus dilutus*) in 10-d exposures to sediment samples from the Tri-State Mining District. A1-191
- Plot A1-192** Plot illustrating the relationship between $\sum PW-TU_{DIVALENT METALS}$ and the control-adjusted survival of midges (*Chironomus dilutus*) in 10-d exposures to sediment samples from the Tri-State Mining District. A1-192
- Plot A1-193** Plot illustrating the relationship between $PW-TU_{ALUMINUM}$ and the control-adjusted survival of midges (*Chironomus dilutus*) in 10-d exposures to sediment samples from the Tri-State Mining District. A1-193
- Plot A1-194** Plot illustrating the relationship between $PW-TU_{ARSENIC}$ and the control-adjusted survival of midges (*Chironomus dilutus*) in 10-d exposures to sediment samples from the Tri-State Mining District. A1-194
- Plot A1-195** Plot illustrating the relationship between $PW-TU_{CADMIUM}$ (7 day) and the control-adjusted survival of midges (*Chironomus dilutus*) in 10-d exposures to sediment samples from the Tri-State Mining District. A1-195
- Plot A1-196** Plot illustrating the relationship between $PW-TU_{CHROMIUM}$ and the control-adjusted survival of midges (*Chironomus dilutus*) in 10-d exposures to sediment samples from the Tri-State Mining District. A1-196
- Plot A1-197** Plot illustrating the relationship between $PW-TU_{COPPER}$ (7 day) and the control-adjusted survival of midges (*Chironomus dilutus*) in 10-d exposures to sediment samples from the Tri-State Mining District. A1-197
- Plot A1-198** Plot illustrating the relationship between $PW-TU_{IRON}$ and the control-adjusted survival of midges (*Chironomus dilutus*) in 10-d exposures to sediment samples from the Tri-State Mining District. A1-198

- Plot A1-199** Plot illustrating the relationship between PW-TU_{LEAD} (7 day) and the control-adjusted survival of midges (*Chironomus dilutus*) in 10-d exposures to sediment samples from the Tri-State Mining District. A1-199
- Plot A1-200** Plot illustrating the relationship between PW-TU_{NICKEL} (7 day) and the control-adjusted survival of midges (*Chironomus dilutus*) in 10-d exposures to sediment samples from the Tri-State Mining District. A1-200
- Plot A1-201** Plot illustrating the relationship between PW-TU_{SELENIUM} and the control-adjusted survival of midges (*Chironomus dilutus*) in 10-d exposures to sediment samples from the Tri-State Mining District. A1-201
- Plot A1-202** Plot illustrating the relationship between PW-TU_{SILVER} and the control-adjusted survival of midges (*Chironomus dilutus*) in 10-d exposures to sediment samples from the Tri-State Mining District. A1-202
- Plot A1-203** Plot illustrating the relationship between PW-TU_{ZINC} (7 day) and the control-adjusted survival of midges (*Chironomus dilutus*) in 10-d exposures to sediment samples from the Tri-State Mining District. A1-203
- Plot A1-204** Plot illustrating the relationship between PW-TU_{LEAD(DOC)} and the control-adjusted survival of midges (*Chironomus dilutus*) in 10-d exposures to sediment samples from the Tri-State Mining District. A1-204
- Plot A1-205** Plot illustrating the relationship between PW-TU_{ZINC(DOC)} and the control-adjusted survival of midges (*Chironomus dilutus*) in 10-d exposures to sediment samples from the Tri-State Mining District. A1-205
- Plot A1-206** Plot illustrating the relationship between \sum PW-TU_{METALS} and the control-adjusted biomass of midges (*Chironomus dilutus*) in 10-d exposures to sediment samples from the Tri-State Mining District. A1-206
- Plot A1-207** Plot illustrating the relationship between \sum PW-TU_{DIVALENT METALS} and the control-adjusted biomass of midges (*Chironomus dilutus*) in 10-d exposures to sediment samples from the Tri-State Mining District. A1-207
- Plot A1-208** Plot illustrating the relationship between PW-TU_{ALUMINUM} and the control-adjusted biomass of midges (*Chironomus dilutus*) in 10-d exposures to sediment samples from the Tri-State Mining District. A1-208
- Plot A1-209** Plot illustrating the relationship between PW-TU_{ARSENIC} and the control-adjusted biomass of midges (*Chironomus dilutus*) in 10-d exposures to sediment samples from the Tri-State Mining District. A1-209
- Plot A1-210** Plot illustrating the relationship between PW-TU_{CADMIUM} (7 day) and the control-adjusted biomass of midges (*Chironomus dilutus*) in 10-d exposures to sediment samples from the Tri-State Mining District. A1-210
- Plot A1-211** Plot illustrating the relationship between PW-TU_{CHROMIUM} and the control-adjusted biomass of midges (*Chironomus dilutus*) in 10-d exposures to sediment samples from the Tri-State Mining District. A1-211
- Plot A1-212** Plot illustrating the relationship between PW-TU_{COPPER} (7 day) and the control-adjusted biomass of midges (*Chironomus dilutus*) in 10-d exposures to sediment samples from the Tri-State Mining District. A1-212

-
- Plot A1-213** Plot illustrating the relationship between PW-TU_{IRON} and the control-adjusted biomass of midges (*Chironomus dilutus*) in 10-d exposures to sediment samples from the Tri-State Mining District. A1-213
- Plot A1-214** Plot illustrating the relationship between PW-TU_{LEAD} (7 day) and the control-adjusted biomass of midges (*Chironomus dilutus*) in 10-d exposures to sediment samples from the Tri-State Mining District. A1-214
- Plot A1-215** Plot illustrating the relationship between PW-TU_{NICKEL} (7 day) and the control-adjusted biomass of midges (*Chironomus dilutus*) in 10-d exposures to sediment samples from the Tri-State Mining District. A1-215
- Plot A1-216** Plot illustrating the relationship between PW-TU_{SELENIUM} and the control-adjusted biomass of midges (*Chironomus dilutus*) in 10-d exposures to sediment samples from the Tri-State Mining District. A1-216
- Plot A1-217** Plot illustrating the relationship between PW-TU_{SILVER} and the control-adjusted biomass of midges (*Chironomus dilutus*) in 10-d exposures to sediment samples from the Tri-State Mining District. A1-217
- Plot A1-218** Plot illustrating the relationship between PW-TU_{ZINC} (7 day) and the control-adjusted biomass of midges (*Chironomus dilutus*) in 10-d exposures to sediment samples from the Tri-State Mining District. A1-218
- Plot A1-219** Plot illustrating the relationship between PW-TU_{LEAD(DOC)} and the control-adjusted biomass of midges (*Chironomus dilutus*) in 10-d exposures to sediment samples from the Tri-State Mining District. A1-219
- Plot A1-220** Plot illustrating the relationship between PW-TU_{ZINC(DOC)} and the control-adjusted biomass of midges (*Chironomus dilutus*) in 10-d exposures to sediment samples from the Tri-State Mining District. A1-220

Appendix 2	Procedures for Calculating Selected Metrics for Sediment and Pore Water	A2-1
A2.1	Mean Probable Effect Concentration-Quotient Metals (PEC- Q_{METALS}).	A2-1
A2.2	Mean Probable Effect Concentration-Quotient (PEC-Q).	A2-1
A2.3	Sum Equilibrium Partitioning-Based Sediment Benchmark-Toxic Units for Polycyclic Aromatic Hydrocarbons ($\sum \text{ESB-TUs}$ for PAHs).	A2-2
A2.4	Sum Simultaneously Extracted Metals Minus Acid Volatile Sulfide ($\sum \text{SEM-AVS}$).	A2-2
A2.5	Sum Simultaneously Extracted Metals Minus Acid Volatile Sulfide Fraction Organic Carbon [$(\sum \text{SEM-AVS})/f_{\text{OC}}$].	A2-3
A2.6	Sum Probable Effect Concentration-Quotient Cadmium, Lead, Zinc ($\sum \text{PEC-Q}_{\text{Cd,Pb,Zn}}$).	A2-3
A2.7	Sum Sediment Toxicity Threshold-Quotient Cadmium, Copper, Lead, Zinc ($\sum \text{STT-Q}_{\text{Cd,Cu,Pb,Zn}}$).	A2-3
A2.8	References Cited.	A2-5

Appendix 2 Tables

Table A2-1	An example of how to calculate mean PEC- Q_{METALS}	A2-6
Table A2-2	An example of how to calculate mean PEC-Q.	A2-7
Table A2-3	An example of how to calculate $\sum \text{PEC-Q}_{\text{Cd,Pb,Zn}}$ (i.e., the Dudding Model).	A2-9
Table A2-4	An example of how to calculate $\sum \text{STT-Q}_{\text{Cd,Cu,Pb,Zn}}$	A2-9

Appendix 3 Overview of the Quality of the Data Collected During the 2007 Sediment Sampling Program (as excerpted from Ingersoll <i>et al.</i> 2008)	A3-1
A. Sediment toxicity and sediment bioaccumulation testing data	A3-1
B. Metals data for oligochaetes used in sediment bioaccumulation tests.	A3-8
C. Water quality data for centrifuged pore water.....	A3-9
D. Simultaneously extracted metals and acid-volatile sulfide data	A3-10
E. Metals data for pore water sampled by peepers.	A3-12
F. Grain size, total organic carbon (TOC), and total solids data and	
G. Polycyclic aromatic hydrocarbon (PAH) data and Semi-Volatile Organic Compounds (SVOC) in whole sediment	A3-12
H. Organochlorine pesticides and polychlorinated biphenyl data and.	
I. Total recoverable metals data in whole sediment.....	A3-13
J. Comparison of sampling methods (shovel versus scoop).....	A3-14
K. Comparison of methods for metals in pore water (peepers versus centrifugation).....	A3-14
References Cited.	A3-15

Appendix 4 Scatter plots showing the relationships between sediment and pore-water concentrations and survival and biomass of amphipods (*Hyaella azteca*), mussels (*Lampsilis siliquoidea*), and midges (*Chironomus dilutus*)

- Figure A4-1** Scatter plot showing the relationship between sediment metal concentrations (mean $PEC-Q_{METALS}$) and pore-water metal concentrations ($PW-TU_{DIVALENT METALS}$), showing samples that were designated as toxic or not toxic based on the survival of amphipods (*Hyaella azteca*) in 28-d exposures to sediment samples from the Tri-State Mining District. A4-1
- Figure A4-2** Scatter plot showing the relationship between sediment metal concentrations (mean $PEC-Q_{METALS}$) and pore-water metal concentrations ($PW-TU_{DIVALENT METALS}$), showing samples that were designated as toxic or not toxic based on the biomass of amphipods (*Hyaella azteca*) in 28-d exposures to sediment samples from the Tri-State Mining District. A4-2
- Figure A4-3** Scatter plot showing the relationship between sediment metal concentrations (mean $PEC-Q_{METALS}$) and pore-water metal concentrations ($PW-TU_{DIVALENT METALS}$), showing samples that were designated as toxic or not toxic based on the survival of mussels (*Lampsilis siliquoidea*) in 28-d exposures to sediment samples from the Tri-State Mining District. A4-3
- Figure A4-4** Scatter plot showing the relationship between sediment metal concentrations (mean $PEC-Q_{METALS}$) and pore-water metal concentrations ($PW-TU_{DIVALENT METALS}$), showing samples that were designated as toxic or not toxic based on the biomass of mussels (*Lampsilis siliquoidea*) in 28-d exposures to sediment samples from the Tri-State Mining District. A4-4
- Figure A4-5** Scatter plot showing the relationship between sediment metal concentrations (mean $PEC-Q_{METALS}$) and pore-water metal concentrations ($PW-TU_{DIVALENT METALS}$), showing samples that were designated as toxic or not toxic based on the survival of midges (*Chironomus dilutus*) in 10-d exposures to sediment samples from the Tri-State Mining District. A4-5
- Figure A4-6** Scatter plot showing the relationship between sediment metal concentrations (mean $PEC-Q_{METALS}$) and pore-water metal concentrations ($PW-TU_{DIVALENT METALS}$), showing samples that were designated as toxic or not toxic based on the biomass of midges (*Chironomus dilutus*) in 10-d exposures to sediment samples from the Tri-State Mining District. A4-6
- Figure A4-7** Scatter plot showing the relationship between pore-water lead concentrations ($PW-TU_{LEAD}$) and pore-water zinc concentrations ($PW-TU_{ZINC}$), showing samples that were designated as toxic or not toxic based on the survival of amphipods (*Hyaella azteca*) in 28-d exposures to sediment samples from the Tri-State Mining District. A4-7

- Figure A4-8** Scatter plot showing the relationship between pore-water lead concentrations (PW-TU_{LEAD}) and pore-water zinc concentrations (PW-TU_{ZINC}), showing samples that were designated as toxic or not toxic based on the biomass of amphipods (*Hyalella azteca*) in 28-d exposures to sediment samples from the Tri-State Mining District. A4-8
- Figure A4-9** Scatter plot showing the relationship between pore-water lead concentrations (PW-TU_{LEAD}) and pore-water zinc concentrations (PW-TU_{ZINC}), showing samples that were designated as toxic or not toxic based on the survival of mussels (*Lampsilis siliquoidea*) in 28-d exposures to sediment samples from the Tri-State Mining District. A4-9
- Figure A4-10** Scatter plot showing the relationship between pore-water lead concentrations (PW-TU_{LEAD}) and pore-water zinc concentrations (PW-TU_{ZINC}), showing samples that were designated as toxic or not toxic based on the biomass of mussels (*Lampsilis siliquoidea*) in 28-d exposures to sediment samples from the Tri-State Mining District. A4-10
- Figure A4-11** Scatter plot showing the relationship between pore-water lead concentrations (PW-TU_{LEAD}) and pore-water zinc concentrations (PW-TU_{ZINC}), showing samples that were designated as toxic or not toxic based on the survival of midges (*Chironomus dilutus*) in 10-d exposures to sediment samples from the Tri-State Mining District. A4-11
- Figure A4-12** Scatter plot showing the relationship between pore-water lead concentrations (PW-TU_{LEAD}) and pore-water zinc concentrations (PW-TU_{ZINC}), showing samples that were designated as toxic or not toxic based on the biomass midges (*Chironomus dilutus*) in 10-d exposures to sediment samples from the Tri-State Mining District. A4-12
- Figure A4-13** Scatter plot showing the relationship between pore-water zinc concentrations normalized to dissolved organic carbon (PW-TU_{ZINC(DOC)}) and pore-water zinc concentrations (PW-TU_{ZINC}), showing samples that were designated as toxic or not toxic based on the survival of amphipods (*Hyalella azteca*) in 28-d exposures to sediment samples from the Tri-State Mining District. A4-13
- Figure A4-14** Scatter plot showing the relationship between pore-water zinc concentrations normalized to dissolved organic carbon (PW-TU_{ZINC(DOC)}) and pore-water zinc concentrations (PW-TU_{ZINC}), showing samples that were designated as toxic or not toxic based on the biomass of amphipods (*Hyalella azteca*) in 28-d exposures to sediment samples from the Tri-State Mining District. A4-14
- Figure A4-15** Scatter plot showing the relationship between pore-water zinc concentrations normalized to dissolved organic carbon (PW-TU_{ZINC(DOC)}) and pore-water zinc concentrations (PW-TU_{ZINC}), showing samples that were designated as toxic or not toxic based on the survival of mussels (*Lampsilis siliquoidea*) in 28-d exposures to sediment samples from the Tri-State Mining District. A4-15

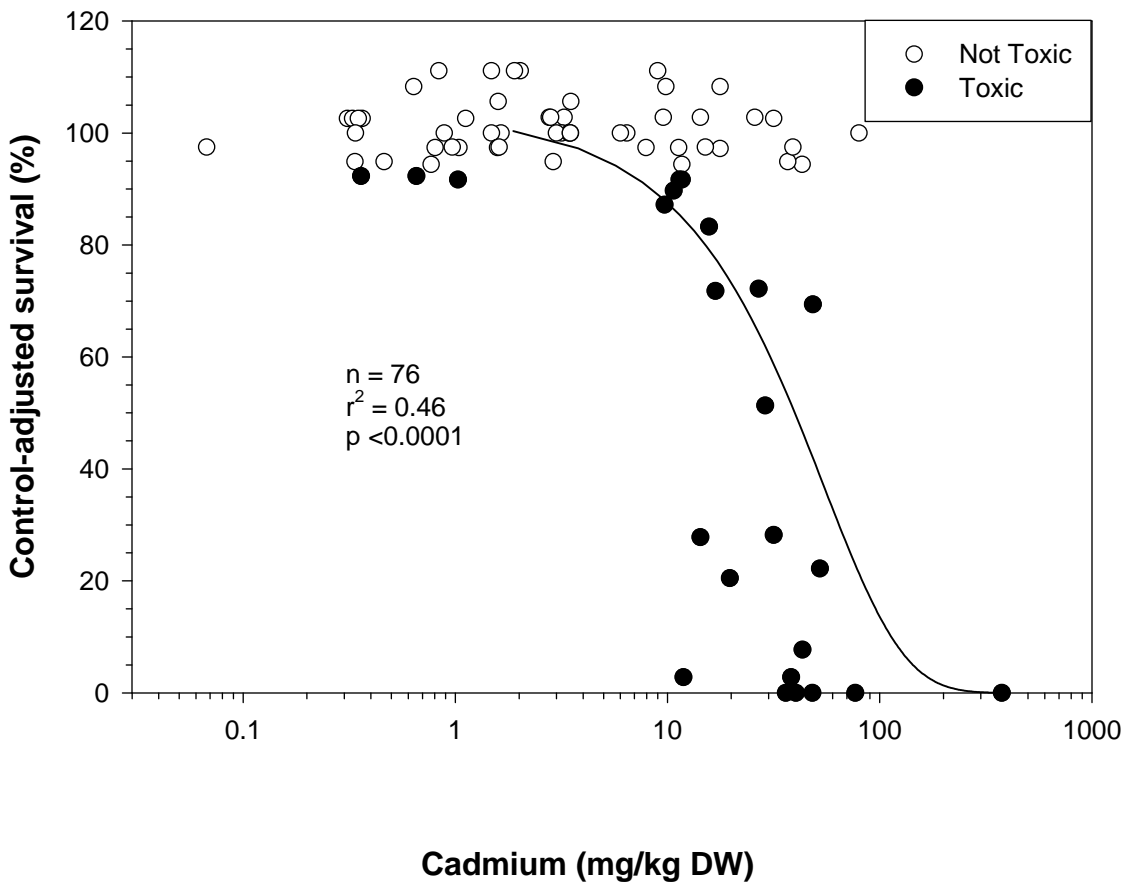
- Figure A4-16** Scatter plot showing the relationship between pore-water zinc concentrations normalized to dissolved organic carbon ($PW-TU_{ZINC(DOC)}$) and pore-water zinc concentrations ($PW-TU_{ZINC}$), showing samples that were designated as toxic or not toxic based on the biomass of mussels (*Lampsilis siliquoidea*) in 28-d exposures to sediment samples from the Tri-State Mining District. A4-16
- Figure A4-17** Scatter plot showing the relationship between pore-water zinc concentrations normalized to dissolved organic carbon ($PW-TU_{ZINC(DOC)}$) and pore-water zinc concentrations ($PW-TU_{ZINC}$), showing samples that were designated as toxic or not toxic based on the survival of midges (*Chironomus dilutus*) in 10-d exposures to sediment samples from the Tri-State Mining District. A4-17
- Figure A4-18** Scatter plot showing the relationship between pore-water zinc concentrations normalized to dissolved organic carbon ($PW-TU_{ZINC(DOC)}$) and pore-water zinc concentrations ($PW-TU_{ZINC}$), showing samples that were designated as toxic or not toxic based on the biomass of midges (*Chironomus dilutus*) in 10-d exposures to sediment samples from the Tri-State Mining District. A4-18
- Figure A4-19** Scatter plot showing the relationship between pore-water zinc concentrations ($PW-TU_{ZINC}$) and pore-water metal concentrations ($PW-TU_{DIVALENT METALS}$), showing samples that were designated as toxic or not toxic based on the survival of amphipods (*Hyaella azteca*) in 28-d exposures to sediment samples from the Tri-State Mining District. A4-19
- Figure A4-20** Scatter plot showing the relationship between pore-water zinc concentrations ($PW-TU_{ZINC}$) and pore-water metal concentrations ($PW-TU_{DIVALENT METALS}$), showing samples that were designated as toxic or not toxic based on the biomass of amphipods (*Hyaella azteca*) in 28-d exposures to sediment samples from the Tri-State Mining District. A4-20
- Figure A4-21** Scatter plot showing the relationship between pore-water zinc concentrations ($PW-TU_{ZINC}$) and pore-water metal concentrations ($PW-TU_{DIVALENT METALS}$), showing samples that were designated as toxic or not toxic based on the survival of mussels (*Lampsilis siliquoidea*) in 28-d exposures to sediment samples from the Tri-State Mining District. A4-21
- Figure A4-22** Scatter plot showing the relationship between pore-water zinc concentrations ($PW-TU_{ZINC}$) and pore-water metal concentrations ($PW-TU_{DIVALENT METALS}$), showing samples that were designated as toxic or not toxic based on the biomass of mussels (*Lampsilis siliquoidea*) in 28-d exposures to sediment samples from the Tri-State Mining District. A4-22
- Figure A4-23** Scatter plot showing the relationship between pore-water zinc concentrations ($PW-TU_{ZINC}$) and pore-water metal concentrations ($PW-TU_{DIVALENT METALS}$), showing samples that were designated as toxic or not toxic based on the survival of midges (*Chironomus dilutus*) in 10-d exposures to sediment samples from the Tri-State Mining District. A4-23

- Figure A4-24** Scatter plot showing the relationship between pore-water zinc concentrations ($PW-TU_{ZINC}$) and pore-water metal concentrations ($PW-TU_{DIVALENT METALS}$), showing samples that were designated as toxic or not toxic based on the biomass of midges (*Chironomus dilutus*) in 10-d exposures to sediment samples from the Tri-State Mining District. A4-24
- Figure A4-25** Scatter plot showing the relationship between pore-water lead concentrations normalized to dissolved organic carbon ($PW-TU_{LEAD(DOC)}$) and pore-water lead concentrations ($PW-TU_{LEAD}$), showing samples that were designated as toxic or not toxic based on the survival of amphipods (*Hyaella azteca*) in 28-d exposures to sediment samples from the Tri-State Mining District. A4-25
- Figure A4-26** Scatter plot showing the relationship between pore-water lead concentrations normalized to dissolved organic carbon ($PW-TU_{LEAD(DOC)}$) and pore-water lead concentrations ($PW-TU_{LEAD}$), showing samples that were designated as toxic or not toxic based on the biomass of amphipods (*Hyaella azteca*) in 28-d exposures to sediment samples from the Tri-State Mining District. A4-26
- Figure A4-27** Scatter plot showing the relationship between pore-water lead concentrations normalized to dissolved organic carbon ($PW-TU_{LEAD(DOC)}$) and pore-water lead concentrations ($PW-TU_{LEAD}$), showing samples that were designated as toxic or not toxic based on the survival of mussels (*Lampsilis siliquoidea*) in 28-d exposures to sediment samples from the Tri-State Mining District. A4-27
- Figure A4-28** Scatter plot showing the relationship between pore-water lead concentrations normalized to dissolved organic carbon ($PW-TU_{LEAD(DOC)}$) and pore-water lead concentrations ($PW-TU_{LEAD}$), showing samples that were designated as toxic or not toxic based on the biomass of mussels (*Lampsilis siliquoidea*) in 28-d exposures to sediment samples from the Tri-State Mining District. A4-28
- Figure A4-29** Scatter plot showing the relationship between pore-water lead concentrations normalized to dissolved organic carbon ($PW-TU_{LEAD(DOC)}$) and pore-water lead concentrations ($PW-TU_{LEAD}$), showing samples that were designated as toxic or not toxic based on the survival of midges (*Chironomus dilutus*) in 10-d exposures to sediment samples from the Tri-State Mining District. A4-29
- Figure A4-30** Scatter plot showing the relationship between pore-water lead concentrations normalized to dissolved organic carbon ($PW-TU_{LEAD(DOC)}$) and pore-water lead concentrations ($PW-TU_{LEAD}$), showing samples that were designated as toxic or not toxic based on the biomass of midges (*Chironomus dilutus*) in 10-d exposures to sediment samples from the Tri-State Mining District. A4-30
- Figure A4-31** Scatter plot showing the relationship between pore-water lead concentrations ($PW-TU_{LEAD}$) and pore-water metal concentrations ($PW-TU_{DIVALENT METALS}$), showing samples that were designated as toxic or not toxic based on the survival of amphipods (*Hyaella azteca*) in 28-d exposures to sediment samples from the Tri-State Mining District. A4-31

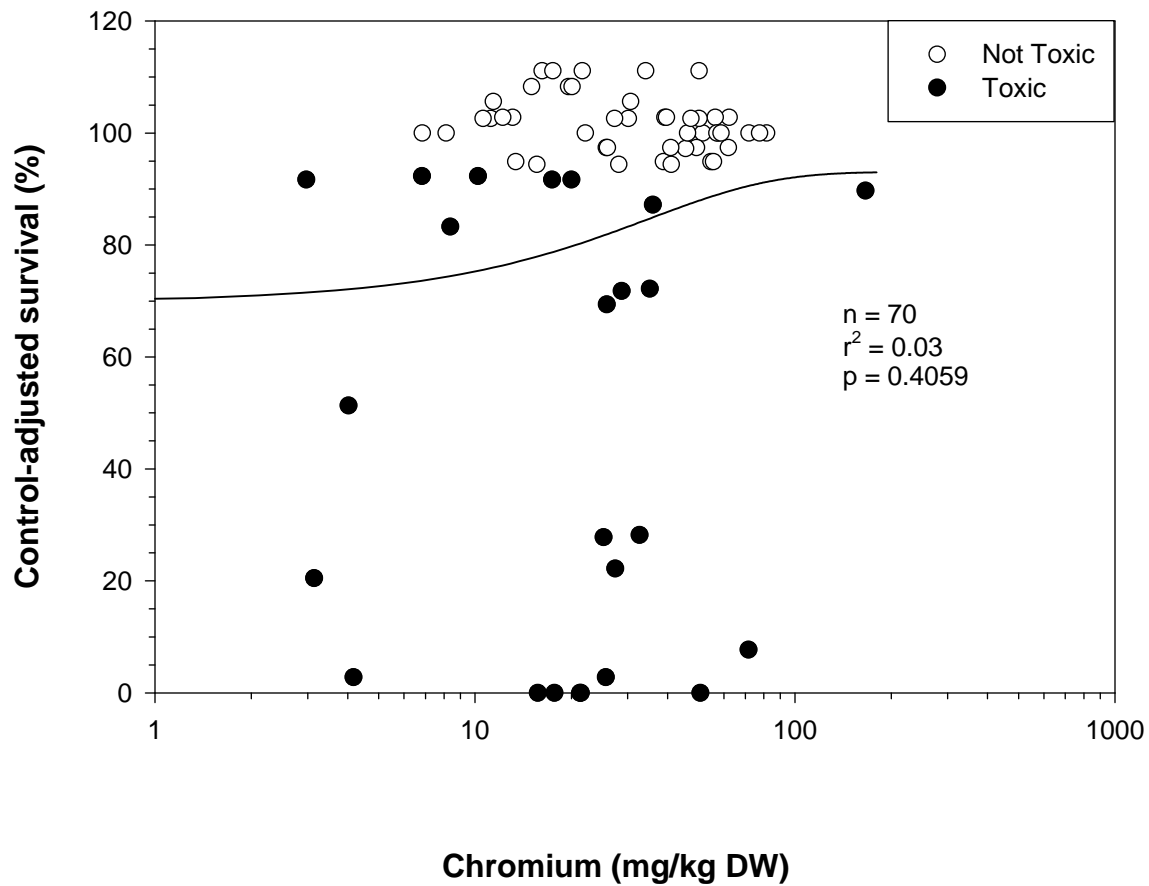
- Figure A4-32** Scatter plot showing the relationship between pore-water lead concentrations (PW-TU_{LEAD}) and pore-water metal concentrations (PW-TU_{DIVALENT METALS}), showing samples that were designated as toxic or not toxic based on the biomass of amphipods (*Hyalella azteca*) in 28-d exposures to sediment samples from the Tri-State Mining District. A4-32
- Figure A4-33** Scatter plot showing the relationship between pore-water lead concentrations (PW-TU_{LEAD}) and pore-water metal concentrations (PW-TU_{DIVALENT METALS}), showing samples that were designated as toxic or not toxic based on the survival of mussels (*Lampsilis siliquoidea*) in 28-d exposures to sediment samples from the Tri-State Mining District. A4-33
- Figure A4-34** Scatter plot showing the relationship between pore-water lead concentrations (PW-TU_{LEAD}) and pore-water metal concentrations (PW-TU_{DIVALENT METALS}), showing samples that were designated as toxic or not toxic based on the biomass of mussels (*Lampsilis siliquoidea*) in 28-d exposures to sediment samples from the Tri-State Mining District. A4-34
- Figure A4-35** Scatter plot showing the relationship between pore-water lead concentrations (PW-TU_{LEAD}) and pore-water metal concentrations (PW-TU_{DIVALENT METALS}), showing samples that were designated as toxic or not toxic based on the survival of midges (*Chironomus dilutus*) in 10-d exposures to sediment samples from the Tri-State Mining District. A4-35
- Figure A4-36** Scatter plot showing the relationship between pore-water lead concentrations (PW-TU_{LEAD}) and pore-water metal concentrations (PW-TU_{DIVALENT METALS}), showing samples that were designated as toxic or not toxic based on the biomass of midges (*Chironomus dilutus*) in 10-d exposures to sediment samples from the Tri-State Mining District. A4-36

Appendix 1

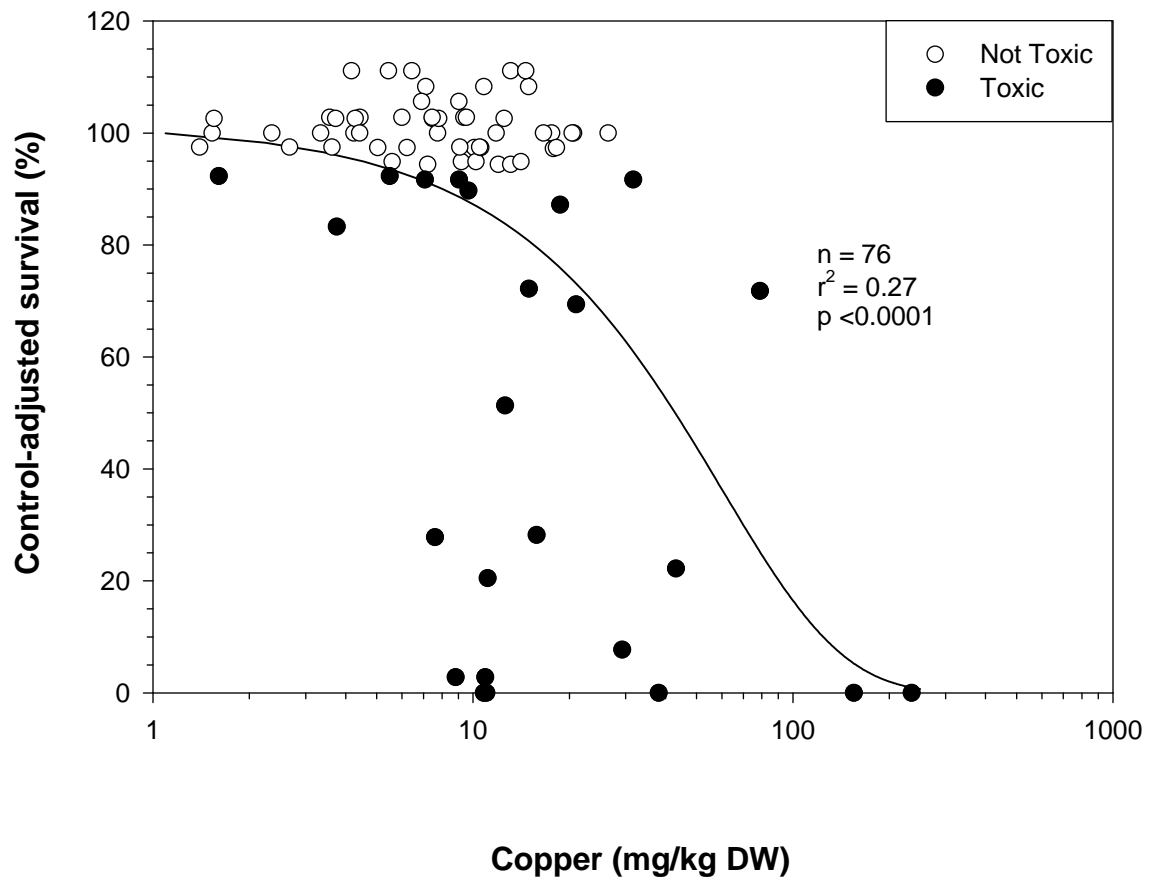
Plot A1-1. Plot illustrating the relationship between the concentration of cadmium (mg/kg DW) in sediment (<2 mm) and the control-adjusted survival of amphipods (*Hyalella azteca*) in 28-d exposures to sediment samples from the Tri-State Mining District.



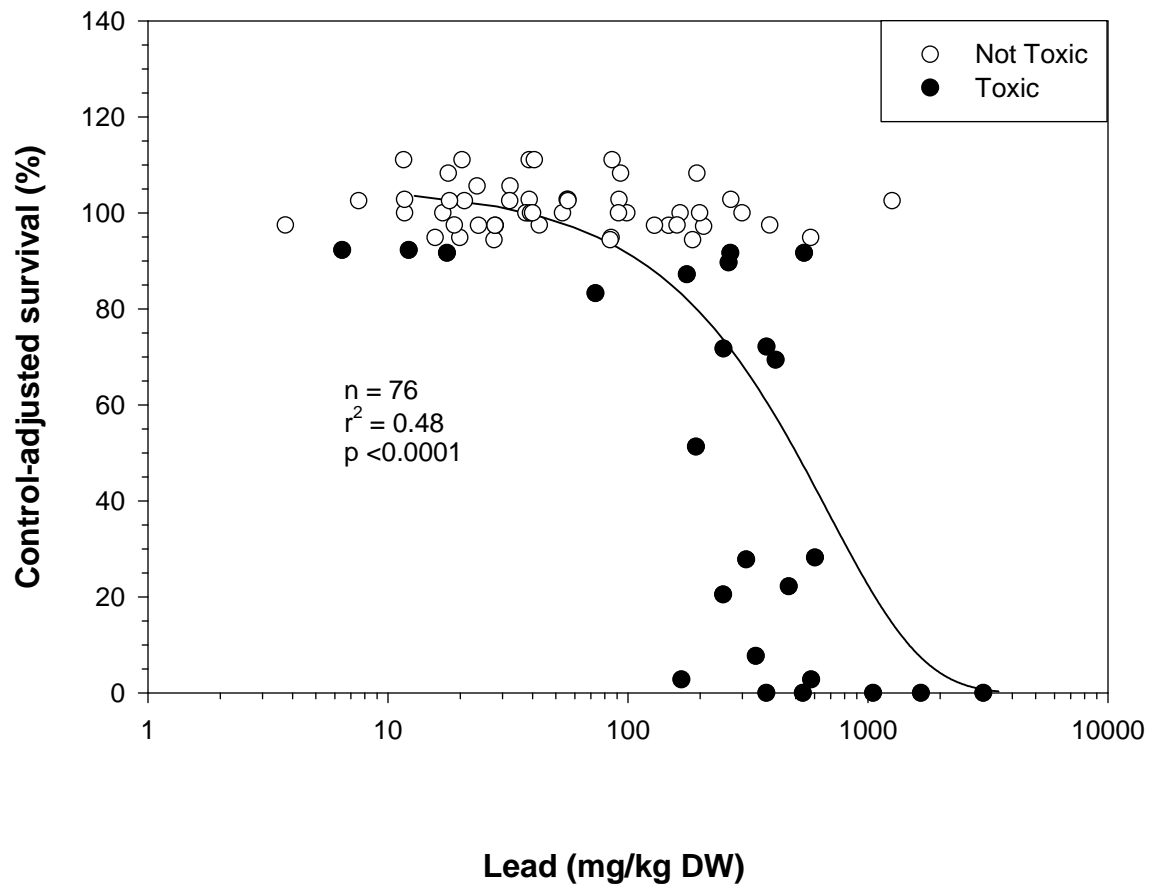
Plot A1-2. Plot illustrating the relationship between the concentration of chromium (mg/kg DW) in sediment (<2 mm) and the control-adjusted survival of amphipods (*Hyalella azteca*) in 28-d exposures to sediment samples from the Tri-State Mining District.



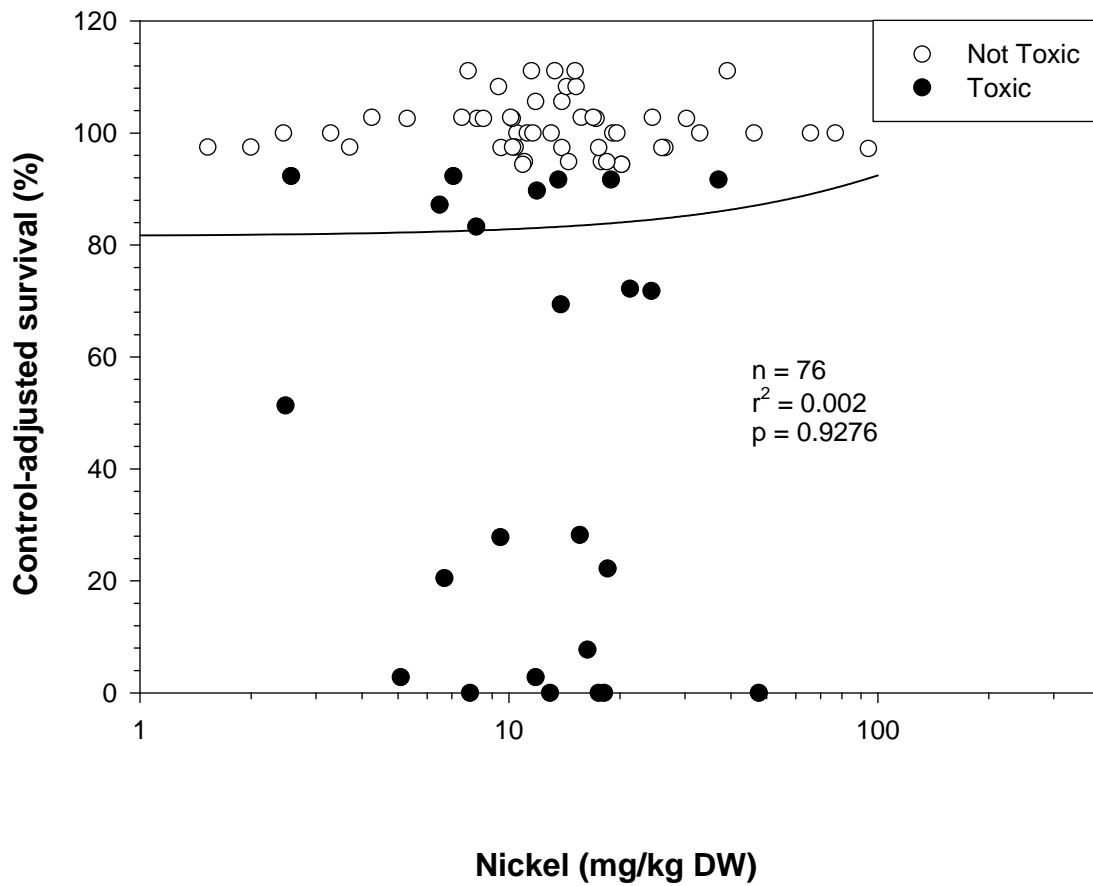
Plot A1-3. Plot illustrating the relationship between the concentration of copper (mg/kg DW) in sediment (<2 mm) and the control-adjusted survival of amphipods (*Hyalella azteca*) in 28-d exposures to sediment samples from the Tri-State Mining District.



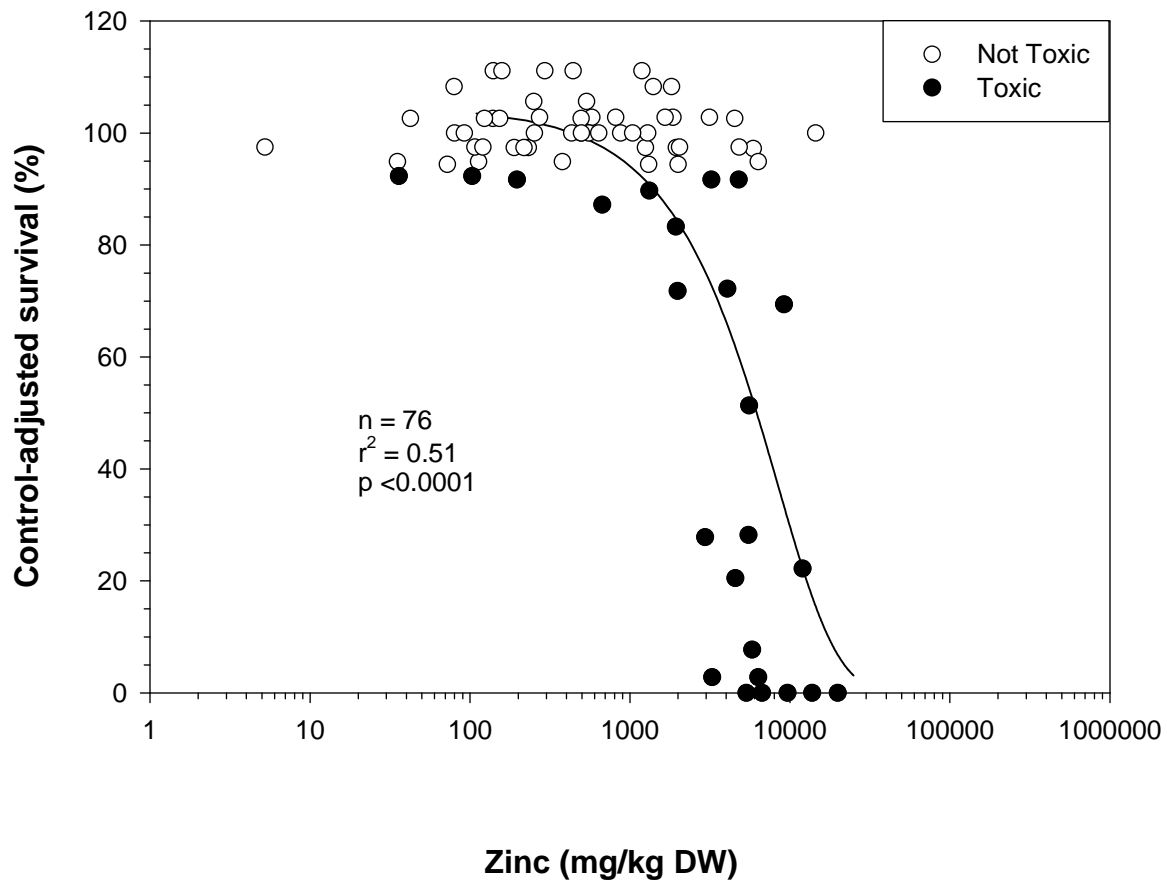
Plot A1-4. Plot illustrating the relationship between the concentration of lead (mg/kg DW) in sediment (<2 mm) and the control-adjusted survival of amphipods (*Hyalella azteca*) in 28-d exposures to sediment samples from the Tri-State Mining District.



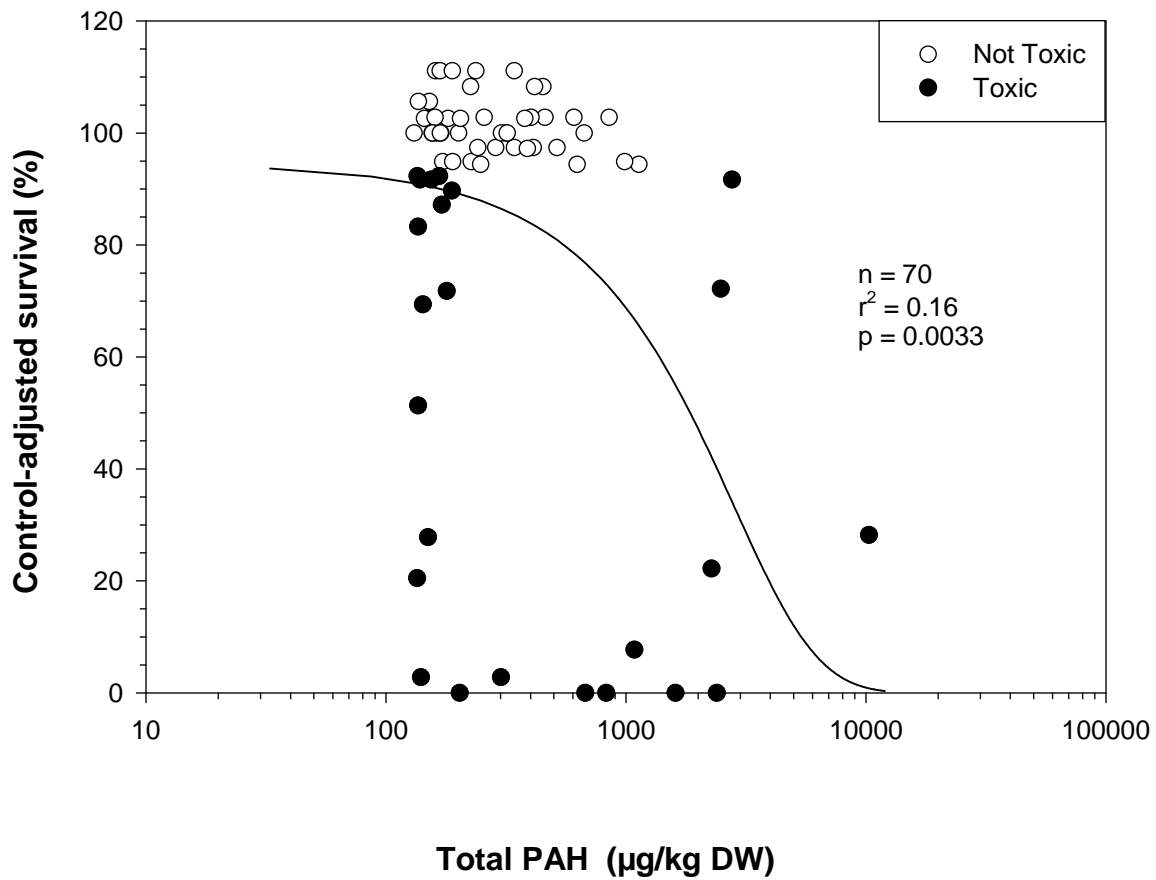
Plot A1-5. Plot illustrating the relationship between the concentration of nickel (mg/kg DW) in sediment (<2 mm) and the control-adjusted survival of amphipods (*Hyalella azteca*) in 28-d exposures to sediment samples from the Tri-State Mining District.



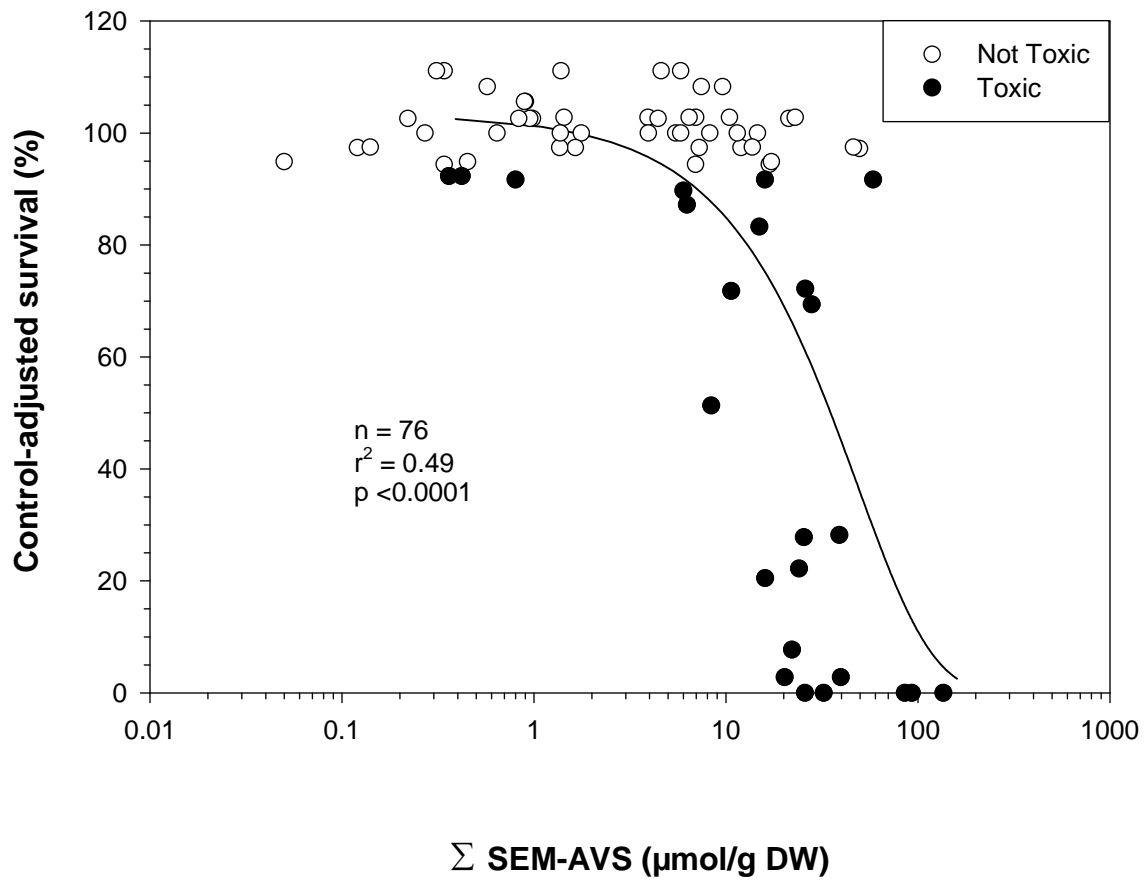
Plot A1-6. Plot illustrating the relationship between the concentration of zinc (mg/kg DW) in sediment (<2 mm) and the control-adjusted survival of amphipods (*Hyalella azteca*) in 28-d exposures to sediment samples from the Tri-State Mining District.



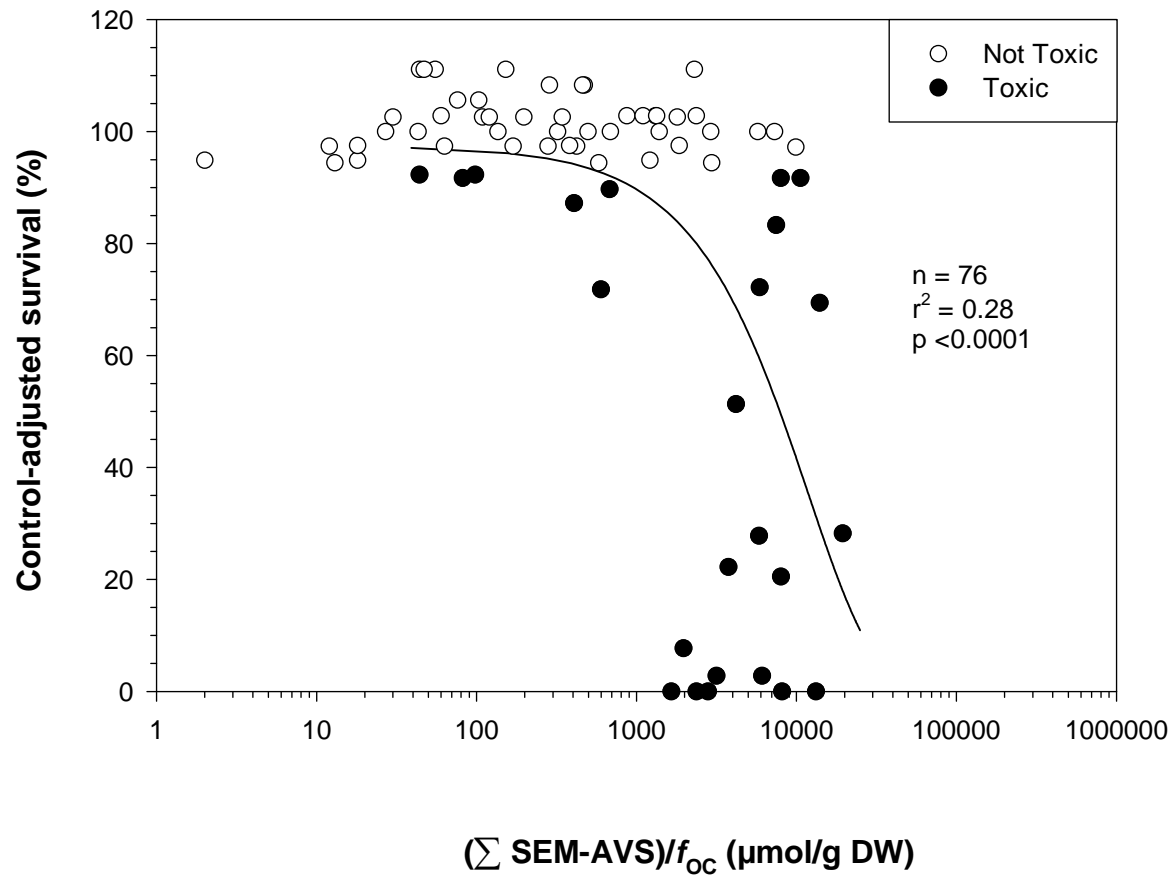
Plot A1-7. Plot illustrating the relationship between the concentration of total PAH ($\mu\text{g}/\text{kg DW}$) in sediment ($<2\text{ mm}$) and the control-adjusted survival of amphipods (*Hyalella azteca*) in 28-d exposures to sediment samples from the Tri-State Mining District.



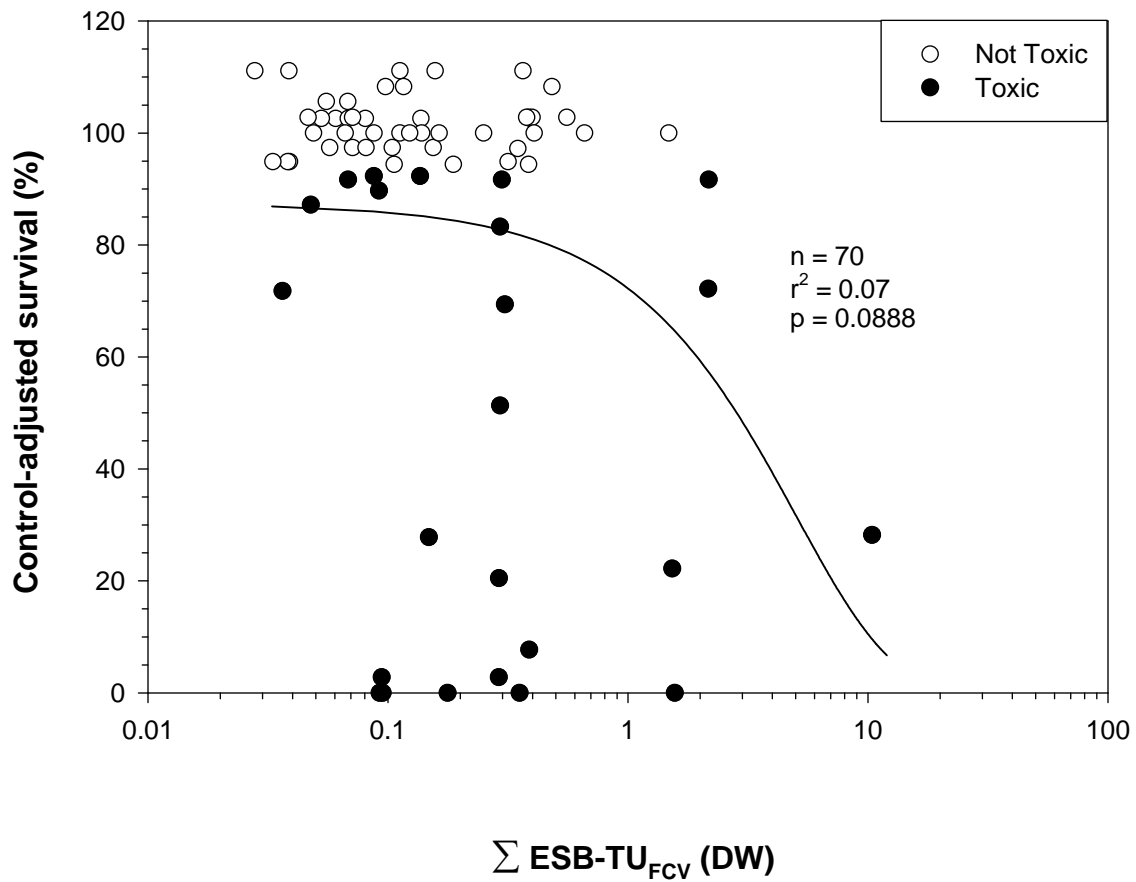
Plot A1-8. Plot illustrating the relationship between the concentration of Σ SEM-AVS ($\mu\text{mol/g DW}$) in sediment (<2 mm) and the control-adjusted survival of amphipods (*Hyalella azteca*) in 28-d exposures to sediment samples from the Tri-State Mining District.



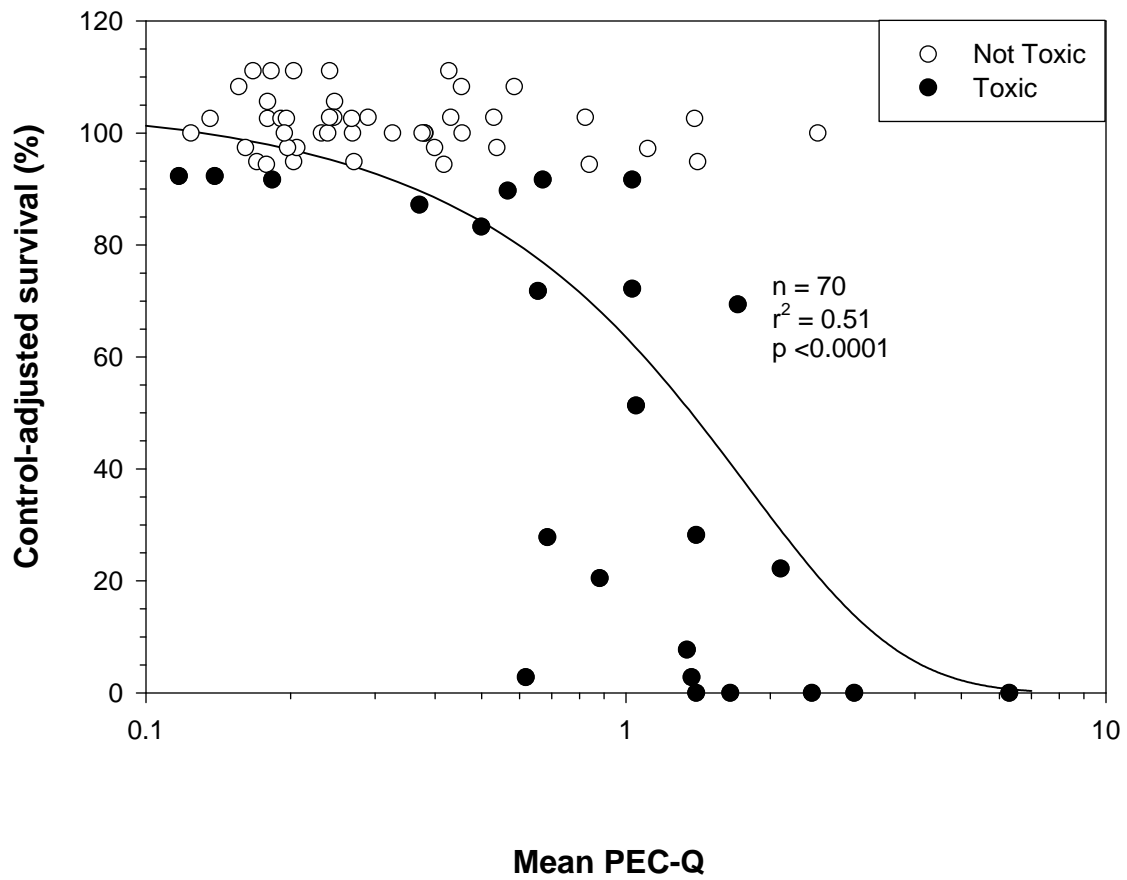
Plot A1-9. Plot illustrating the relationship between the concentration of $(\sum \text{SEM-AVS})/f_{\text{OC}}$ ($\mu\text{mol/g DW}$) in sediment (<2 mm) and the control-adjusted survival of amphipods (*Hyalella azteca*) in 28-d exposures to sediment samples from the Tri-State Mining District.



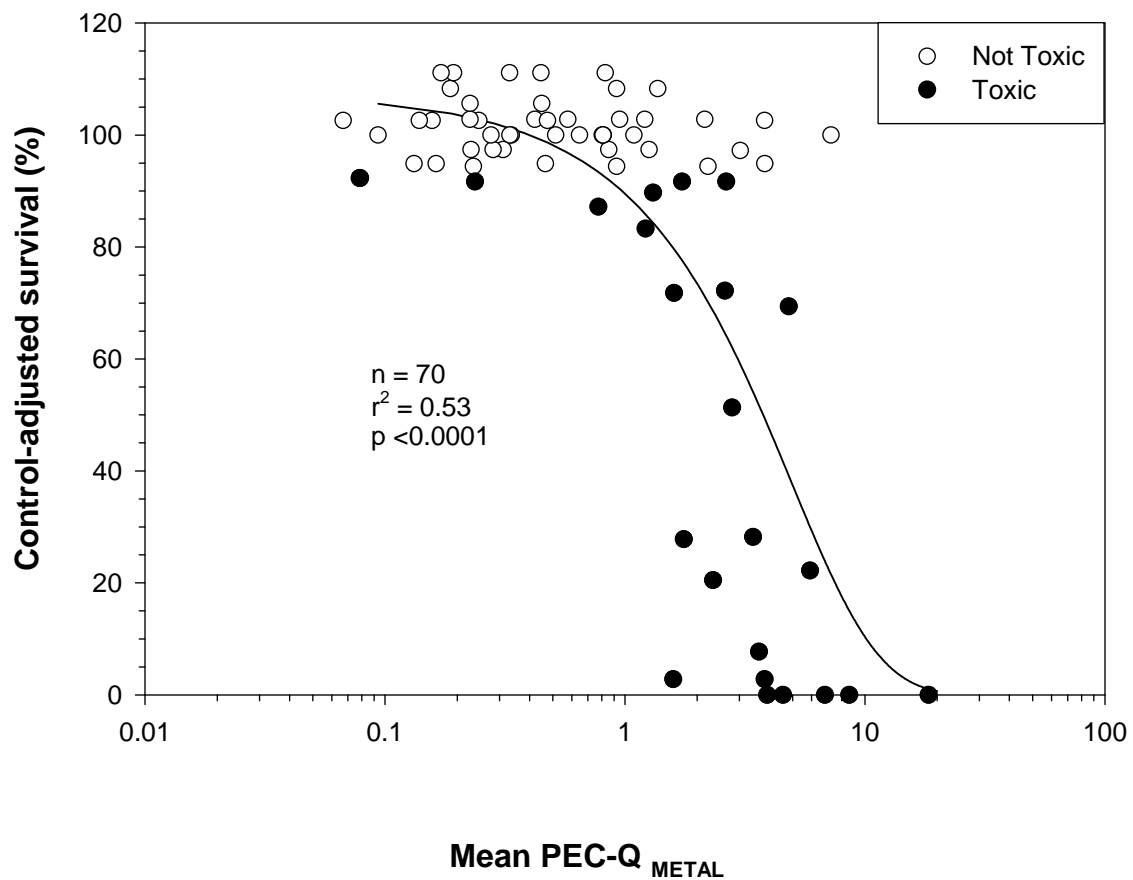
Plot A1-10. Plot illustrating the relationship between the concentration of Σ ESB-TU_{FCV} (DW) in sediment (<2 mm) and the control-adjusted survival of amphipods (*Hyalella azteca*) in 28-d exposures to sediment samples from the Tri-State Mining District.



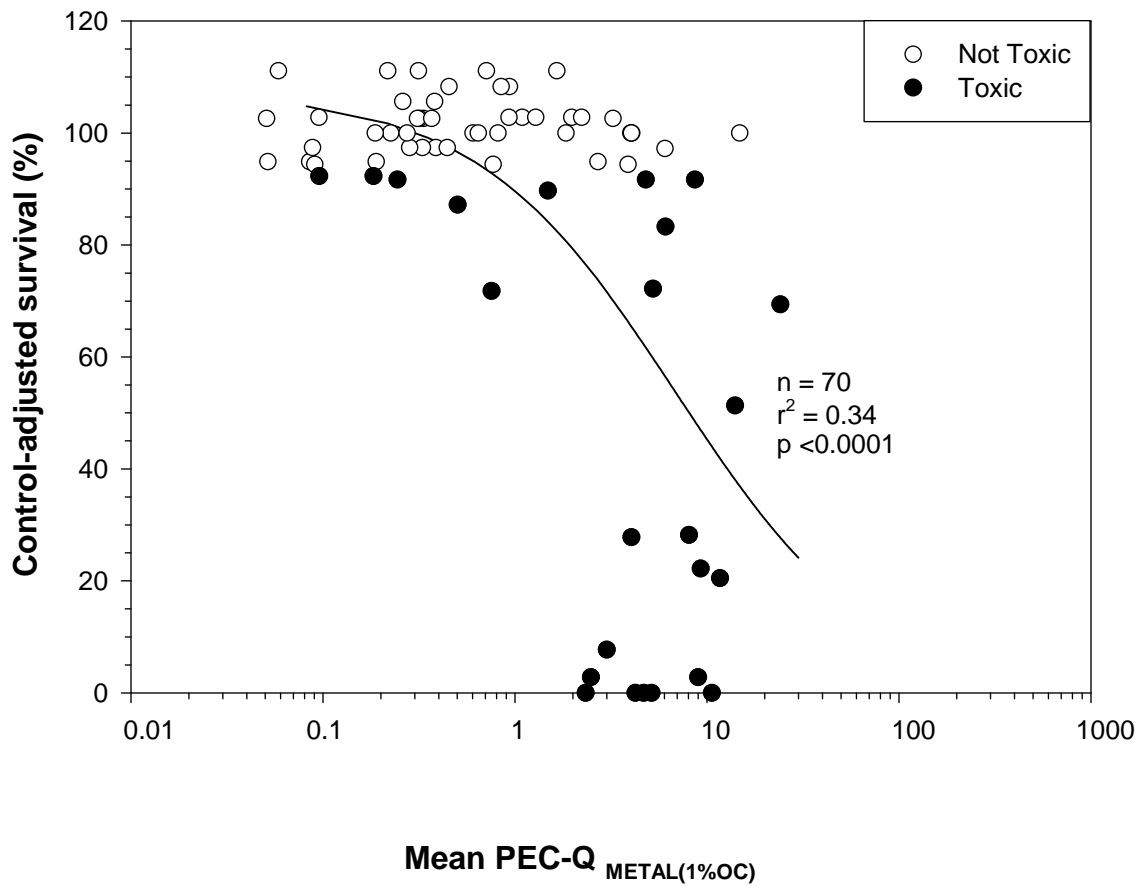
Plot A1-11. Plot illustrating the relationship between the concentration of Mean PEC-Q in sediment (<2 mm) and the control-adjusted survival of amphipods (*Hyalella azteca*) in 28-d exposures to sediment samples from the Tri-State Mining District.



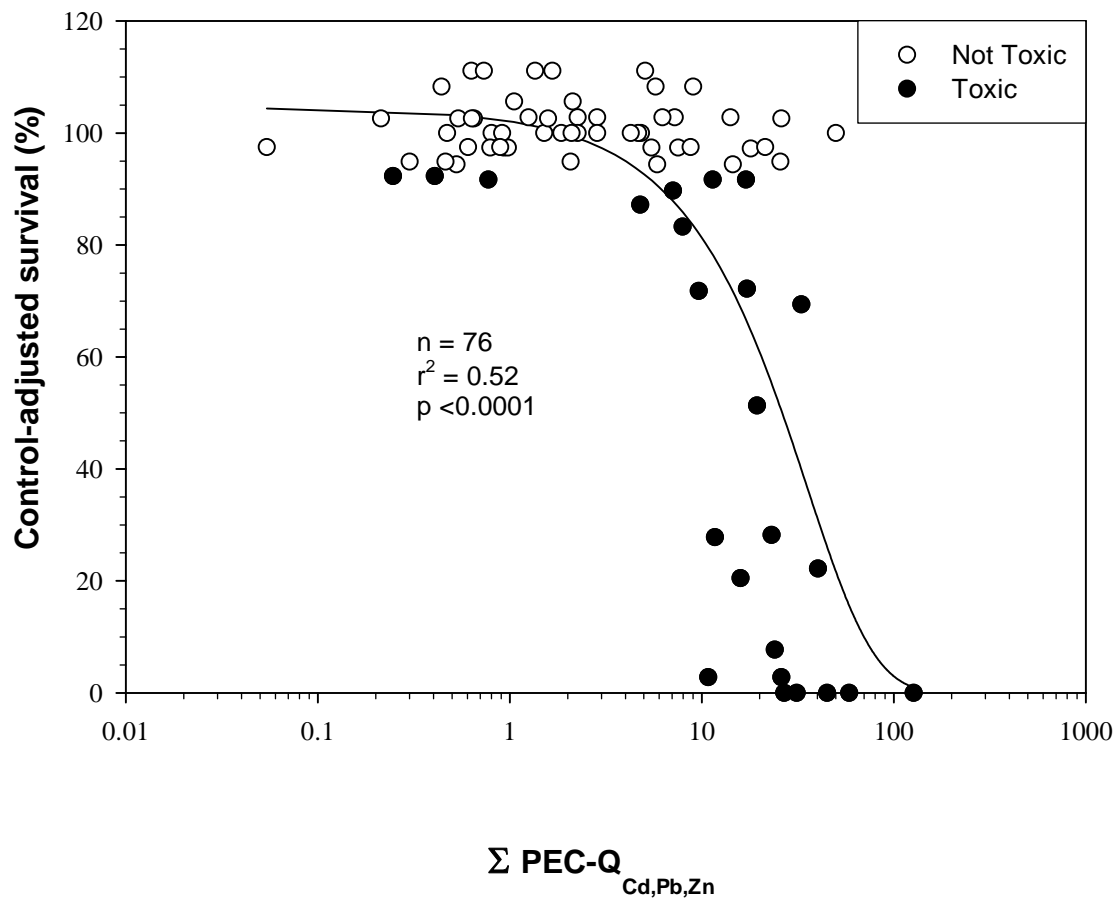
Plot A1-12. Plot illustrating the relationship between the concentration of Mean PEC-Q_{METAL} in sediment (<2 mm) and the control-adjusted survival of amphipods (*Hyalella azteca*) in 28-d exposures to sediment samples from the Tri-State Mining District.



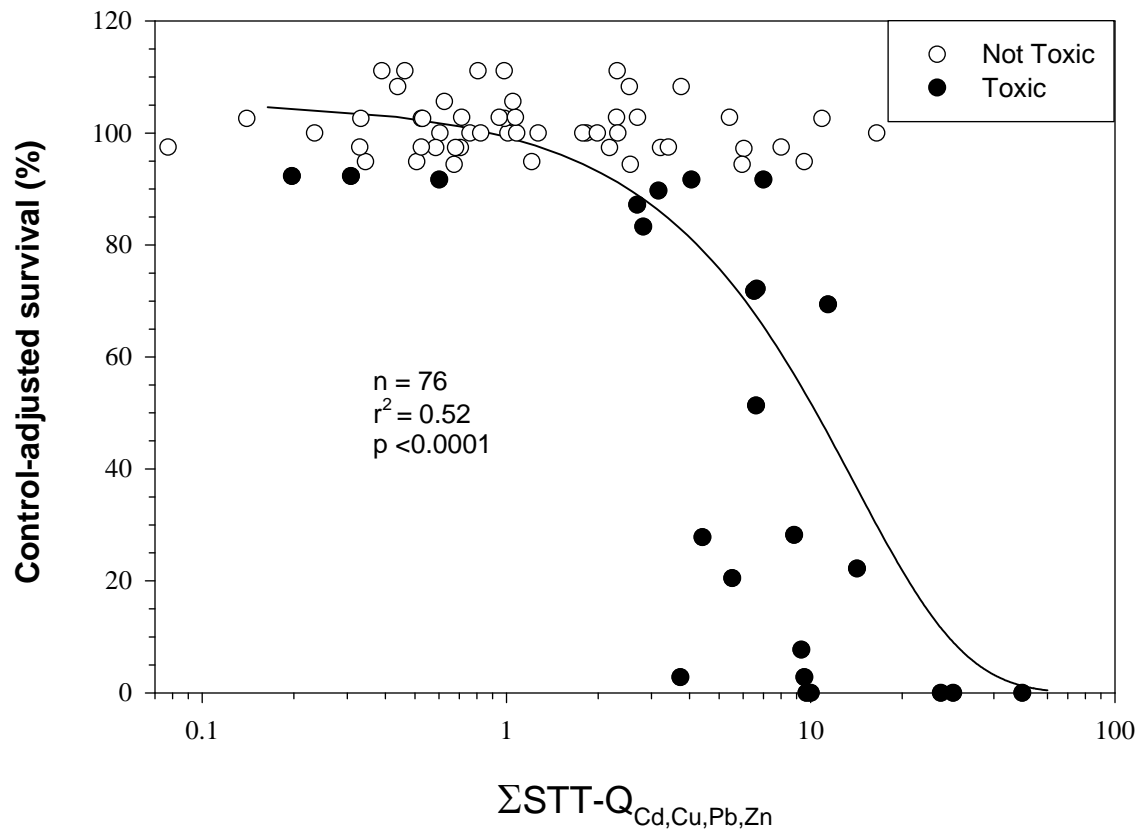
Plot A1-13. Plot illustrating the relationship between the concentration of Mean PEC-Q_{METAL(1%OC)} in sediment (<2 mm) and the control-adjusted survival of amphipods (*Hyalella azteca*) in 28-d exposures to sediment samples from the Tri-State Mining District.



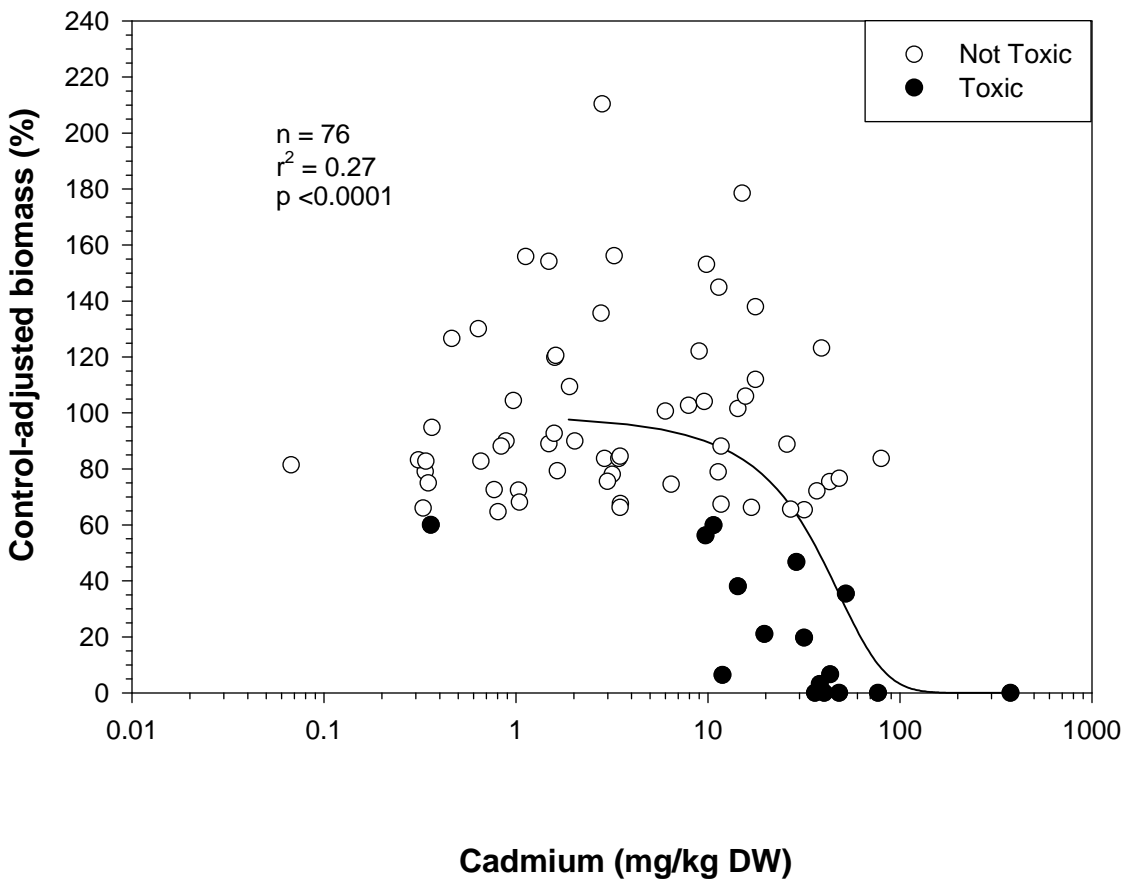
Plot A1-14. Plot illustrating the relationship between the concentration of $\Sigma \text{PEC-Q}_{\text{Cd,Pb,Zn}}$ in sediment (<2 mm) and the control-adjusted survival of amphipods (*Hyalella azteca*) in 28-d exposures to sediment samples from the Tri-State Mining District.



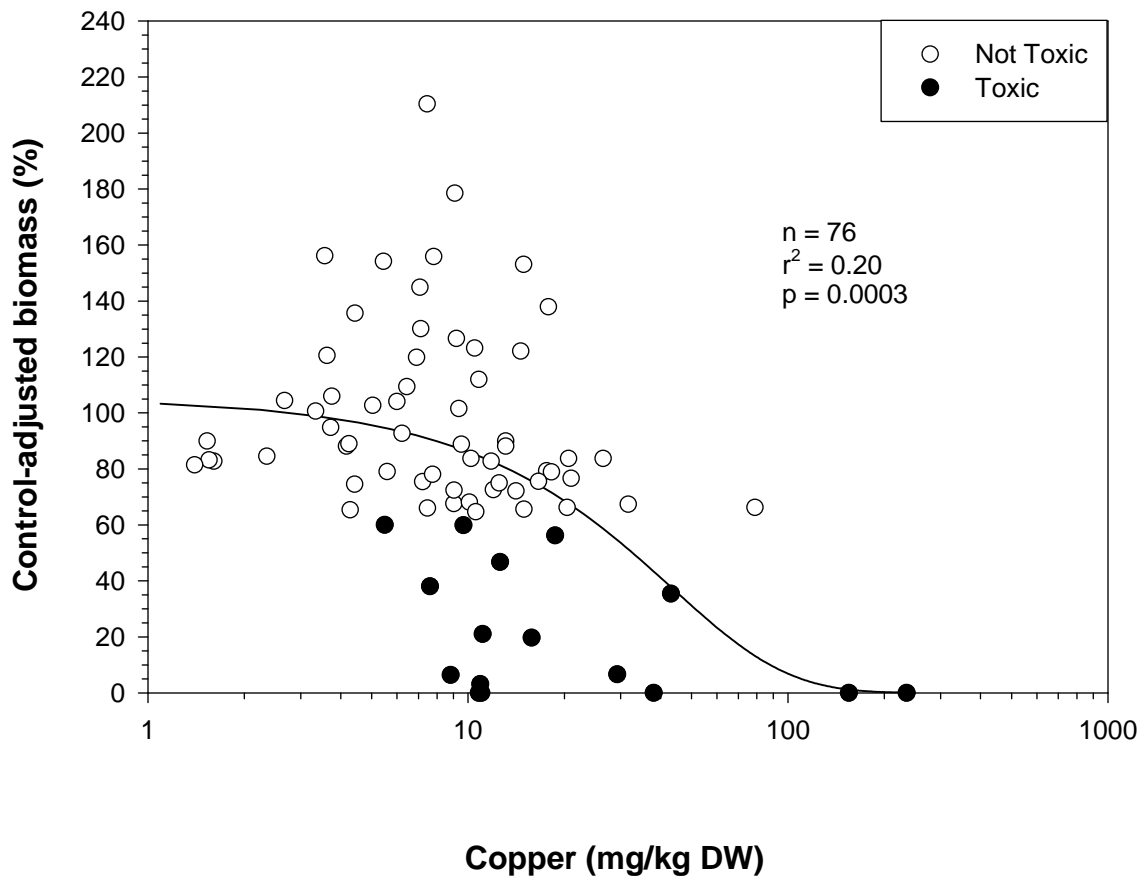
Plot A1-15. Plot illustrating the relationship between the concentration of $\Sigma\text{STT-Q}_{\text{Cd,Cu,Pb,Zn}}$ in sediment (<2 mm) and the control-adjusted survival of amphipods (*Hyalella azteca*) in 28-d exposures to sediment samples from the Tri-State Mining District.



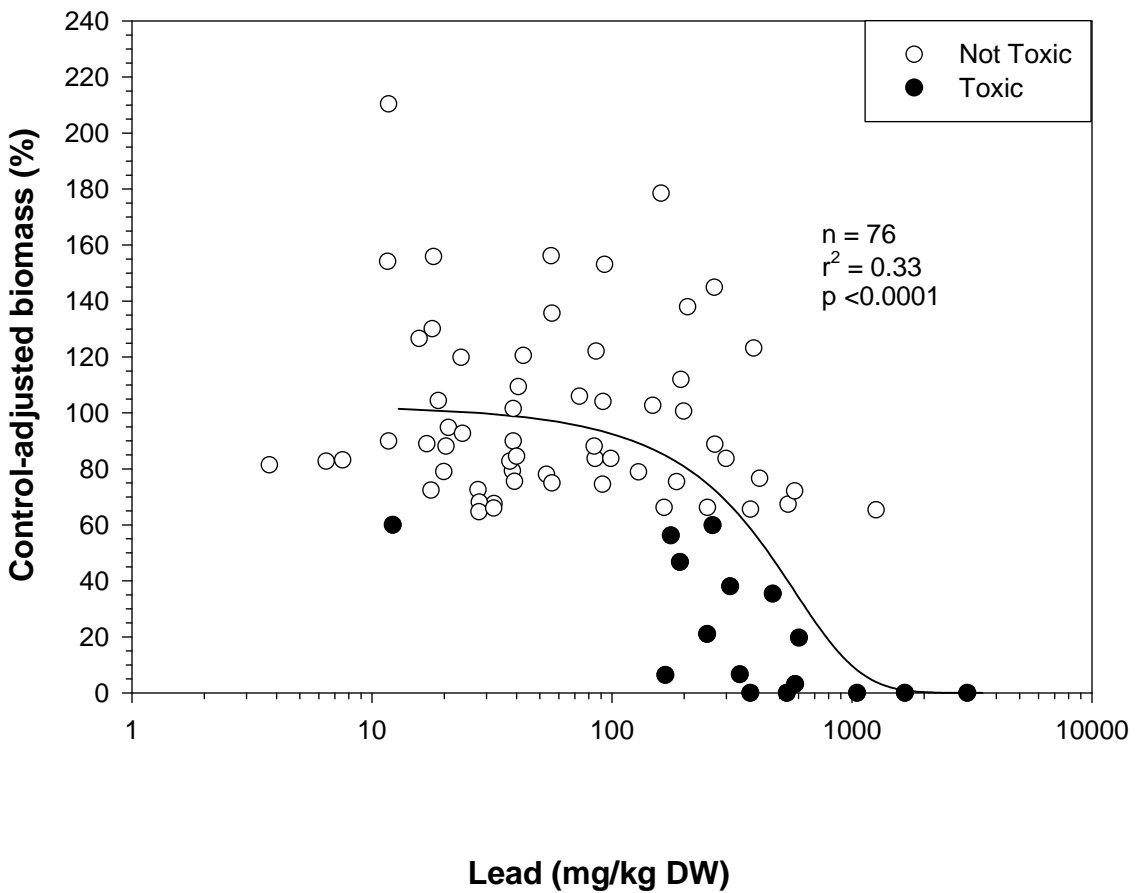
Plot A1-16. Plot illustrating the relationship between the concentration of cadmium (mg/kg DW) in sediment (<2 mm) and the control-adjusted biomass of amphipods (*Hyalella azteca*) in 28-d exposures to sediment samples from the Tri-State Mining District.



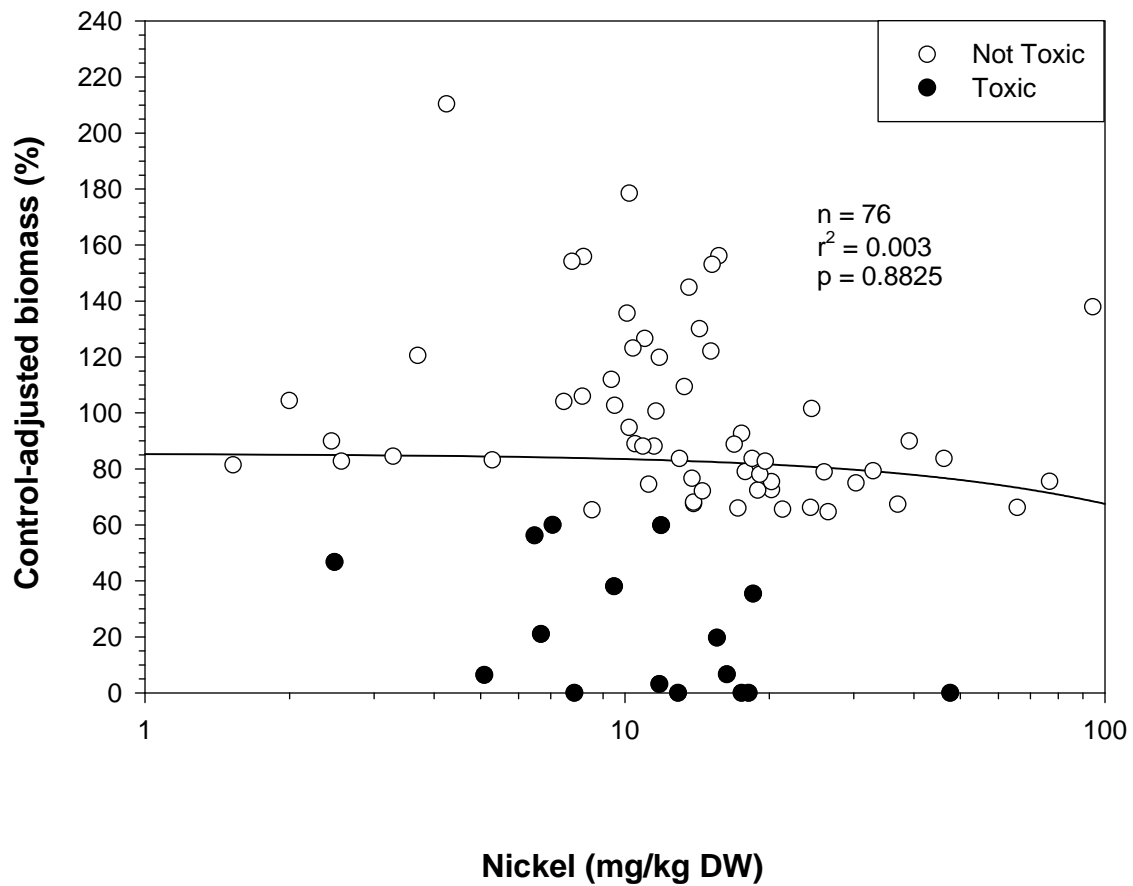
Plot A1-18. Plot illustrating the relationship between the concentration of copper (mg/kg DW) in sediment (<2 mm) and the control-adjusted biomass of amphipods (*Hyalella azteca*) in 28-d exposures to sediment samples from the Tri-State Mining District.



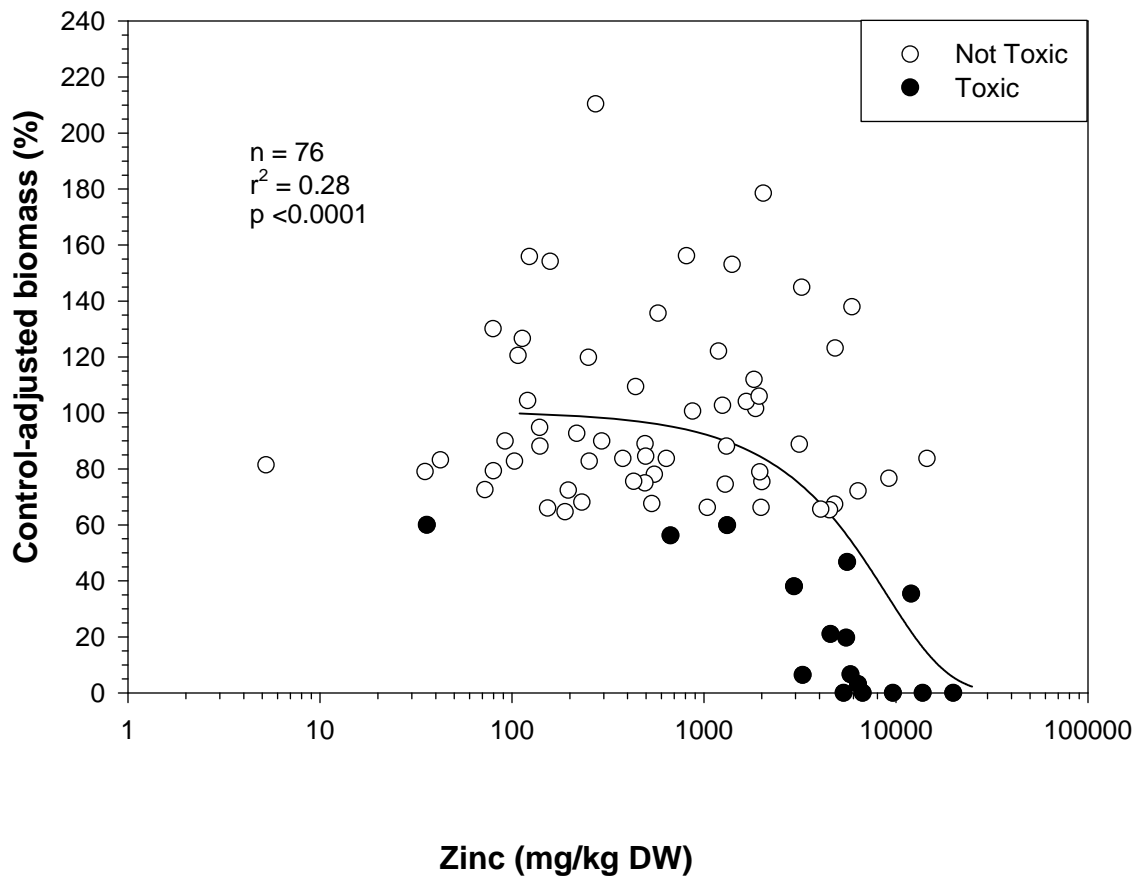
Plot A1-19. Plot illustrating the relationship between the concentration of lead (mg/kg DW) in sediment (<2 mm) and the control-adjusted biomass of amphipods (*Hyalella azteca*) in 28-d exposures to sediment samples from the Tri-State Mining District.



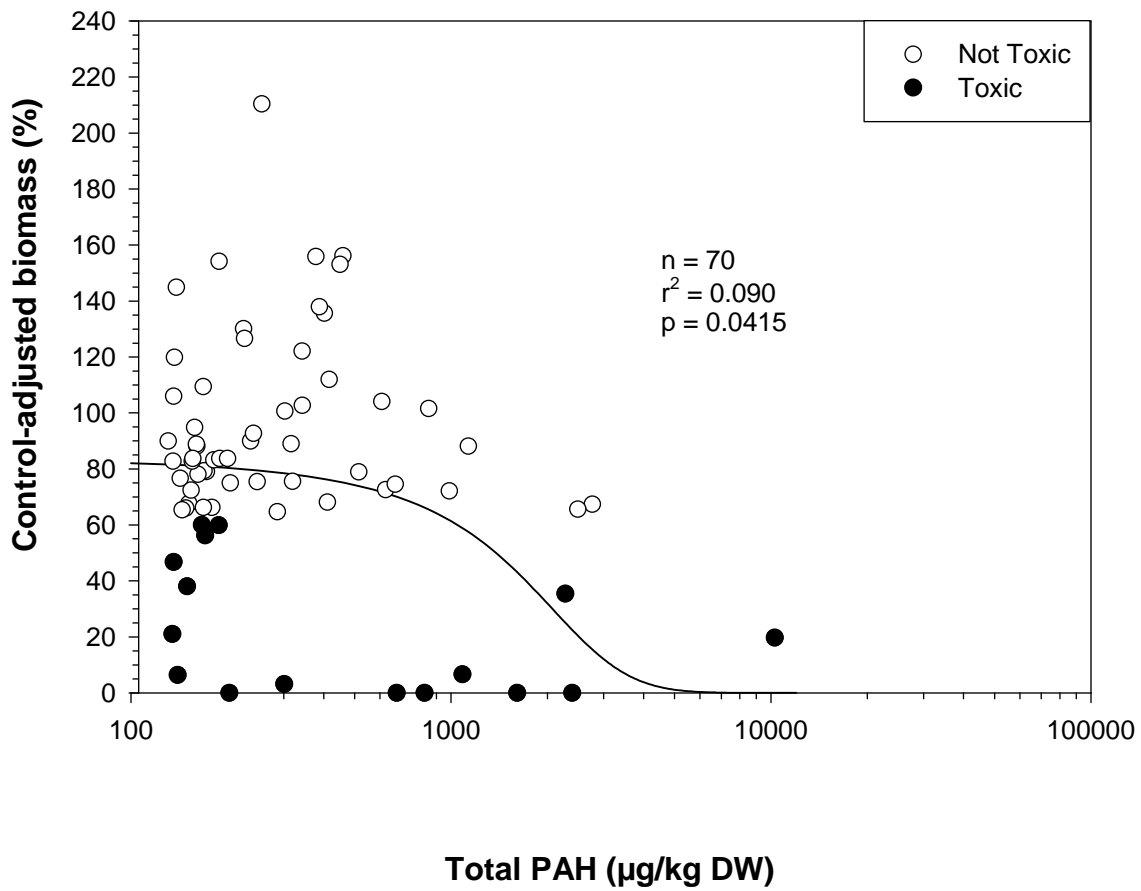
Plot A1-20. Plot illustrating the relationship between the concentration of nickel (mg/kg DW) in sediment (<2 mm) and the control-adjusted biomass of amphipods (*Hyalella azteca*) in 28-d exposures to sediment samples from the Tri-State Mining District.



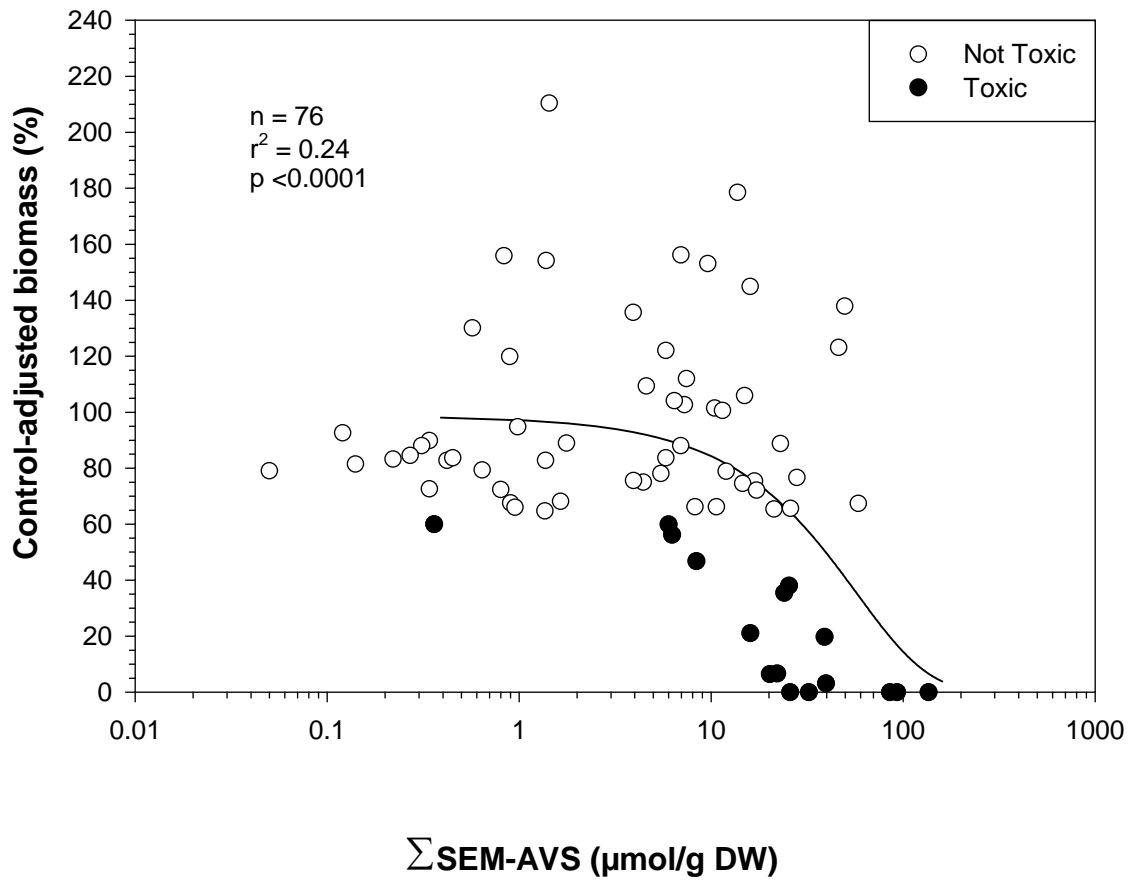
Plot A1-21. Plot illustrating the relationship between the concentration of zinc (mg/kg DW) in sediment (<2 mm) and the control-adjusted biomass of amphipods (*Hyalella azteca*) in 28-d exposures to sediment samples from the Tri-State Mining District.



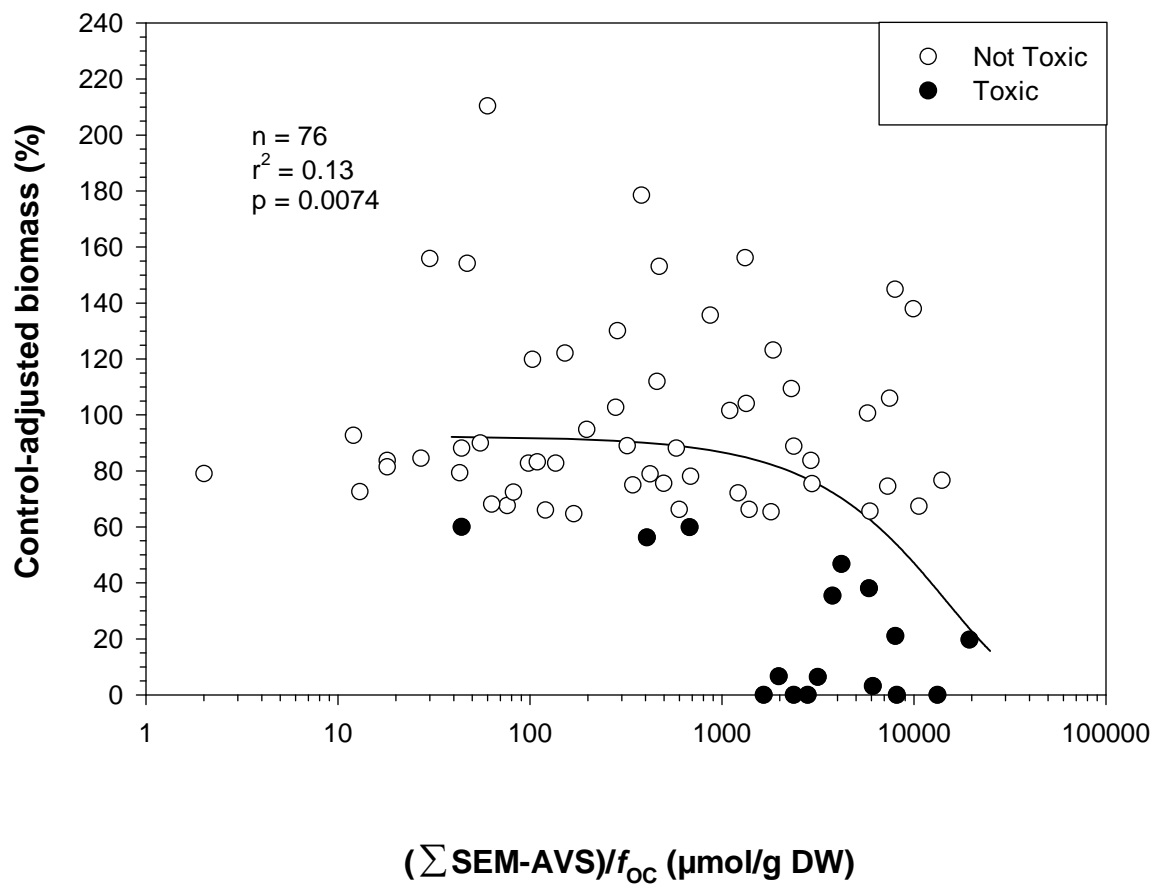
Plot A1-22. Plot illustrating the relationship between the concentration of total PAH ($\mu\text{g}/\text{kg}$ DW) in sediment (<2 mm) and the control-adjusted biomass of amphipods (*Hyalella azteca*) in 28-d exposures to sediment samples from the Tri-State Mining District.



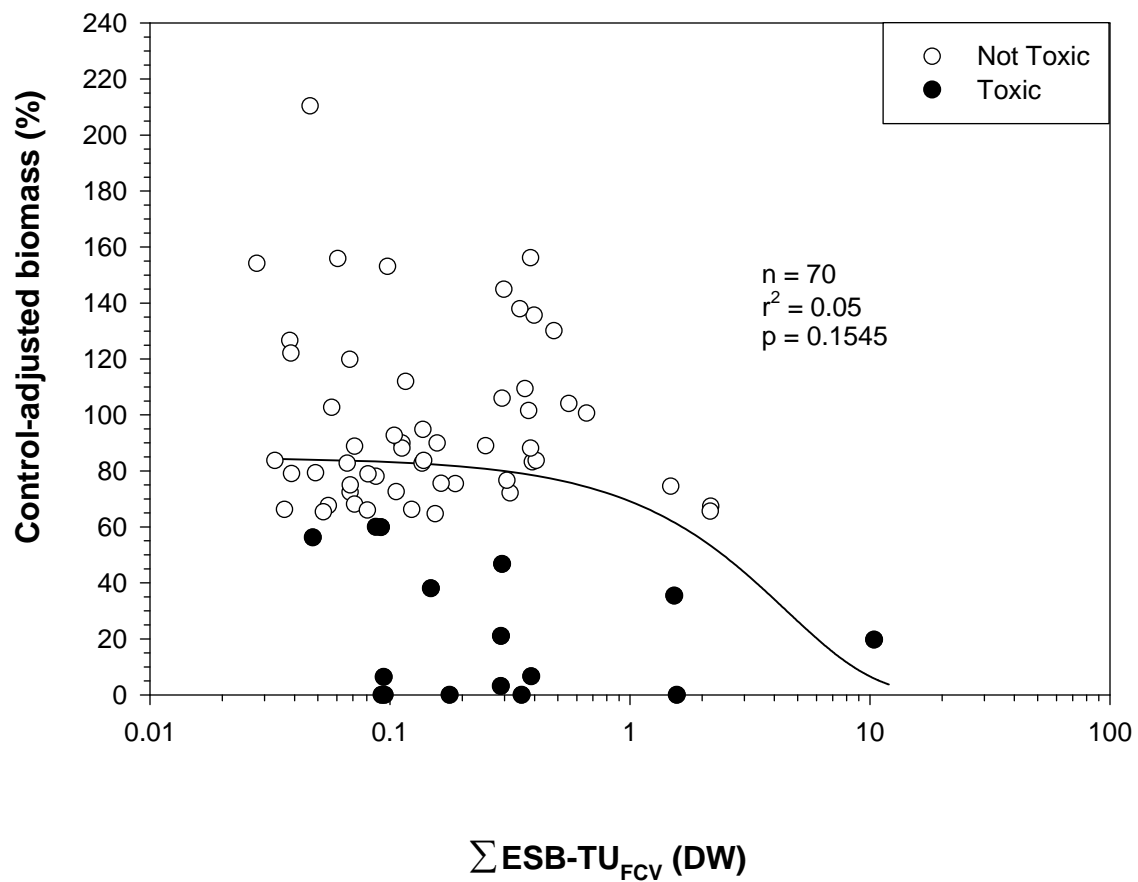
Plot A1-23. Plot illustrating the relationship between the concentration of Σ SEM-AVS ($\mu\text{mol/g DW}$) in sediment (<2 mm) and the control-adjusted biomass of amphipods (*Hyalella azteca*) in 28-d exposures to sediment samples from the Tri-State Mining District.



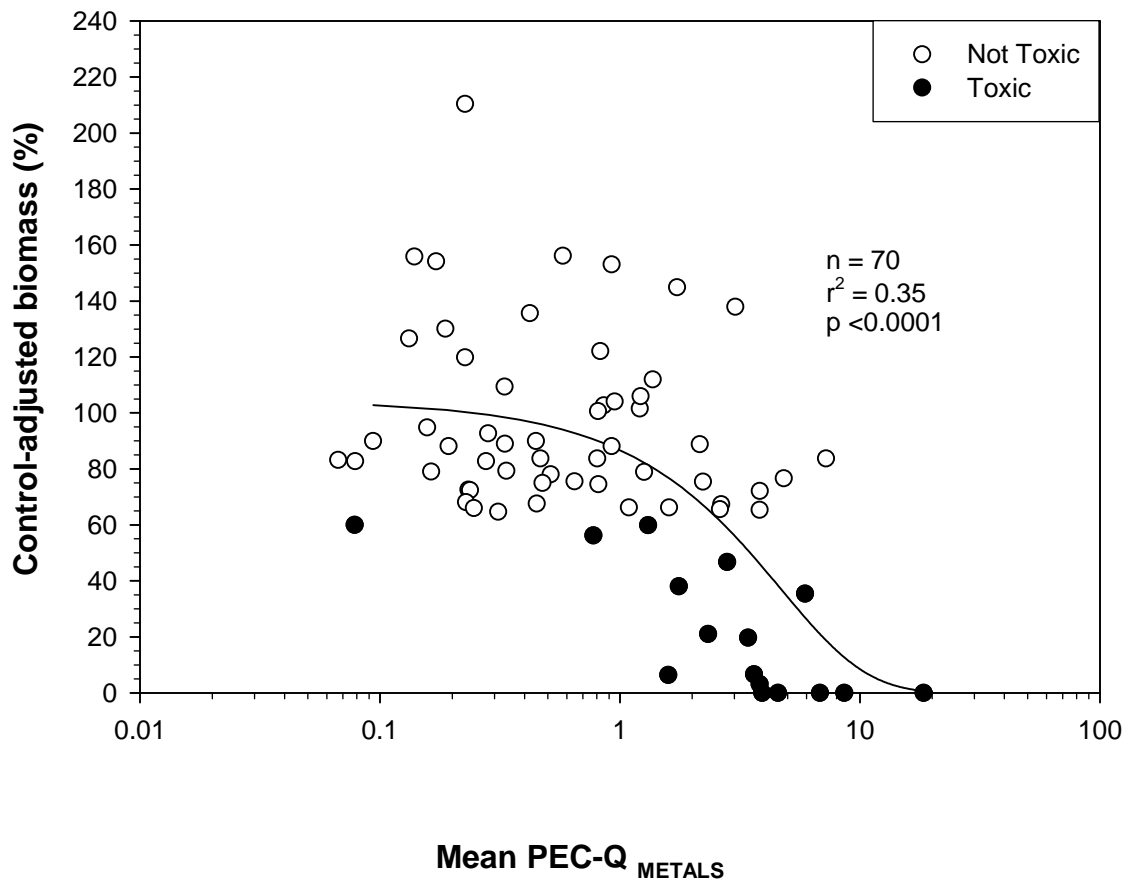
Plot A1-24. Plot illustrating the relationship between the concentration of $(\sum \text{SEM-AVS})/f_{\text{OC}}$ ($\mu\text{mol/g DW}$) in sediment (<2 mm) and the control-adjusted biomass of amphipods (*Hyalella azteca*) in 28-d exposures to sediment samples from the Tri-State Mining District.



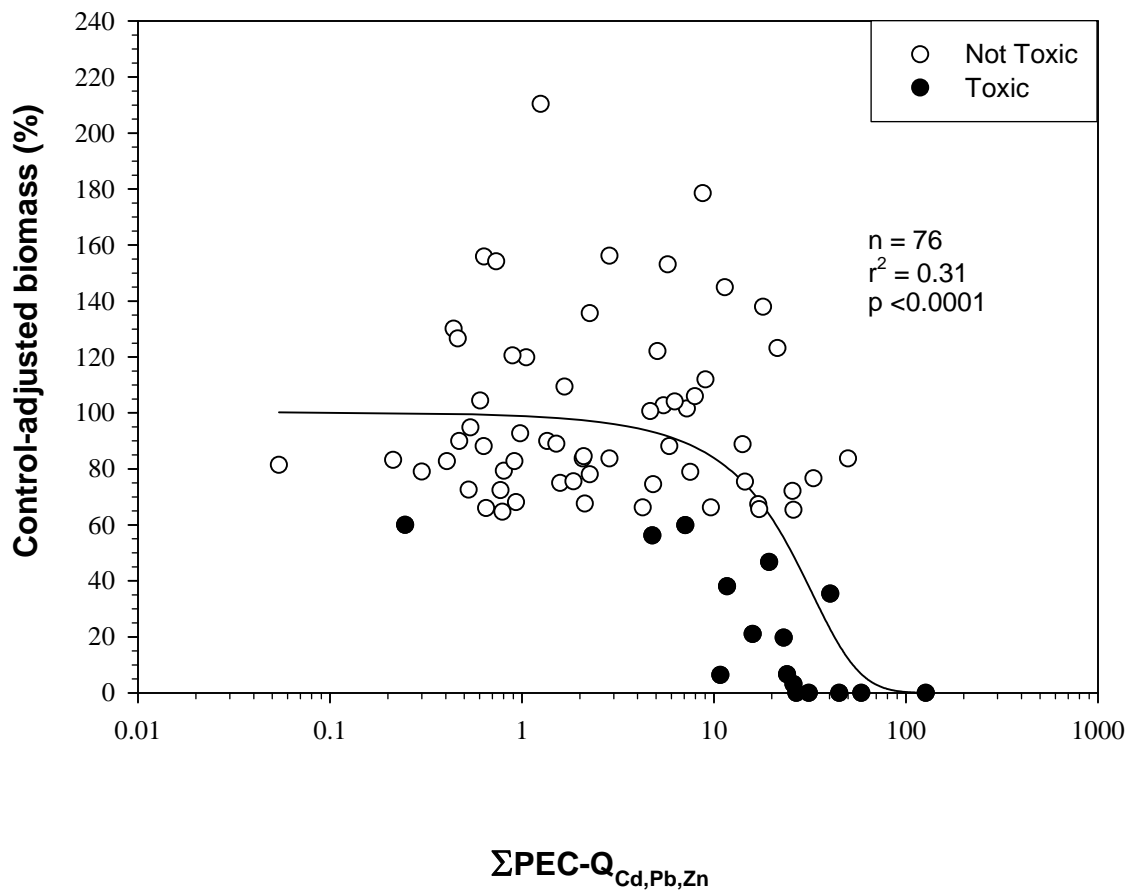
Plot A1-25. Plot illustrating the relationship between the concentration of \sum ESB-TU_{FCV} (DW) in sediment (<2 mm) and the control-adjusted biomass of amphipods (*Hyalella azteca*) in 28-d exposures to sediment samples from the Tri-State Mining District.



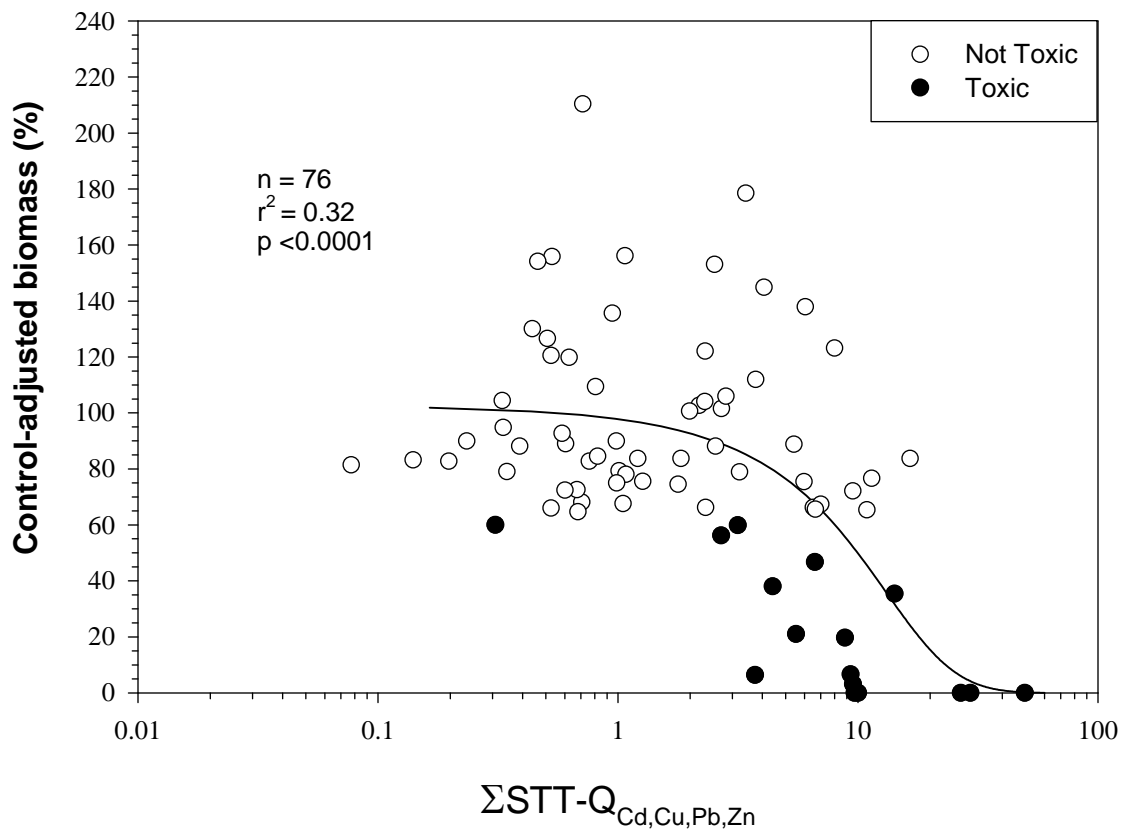
Plot A1-27. Plot illustrating the relationship between the concentration of Mean PEC-Q_{METALS} in sediment (<2 mm) and the control-adjusted biomass of amphipods (*Hyalella azteca*) in 28-d exposures to sediment samples from the Tri-State Mining District.



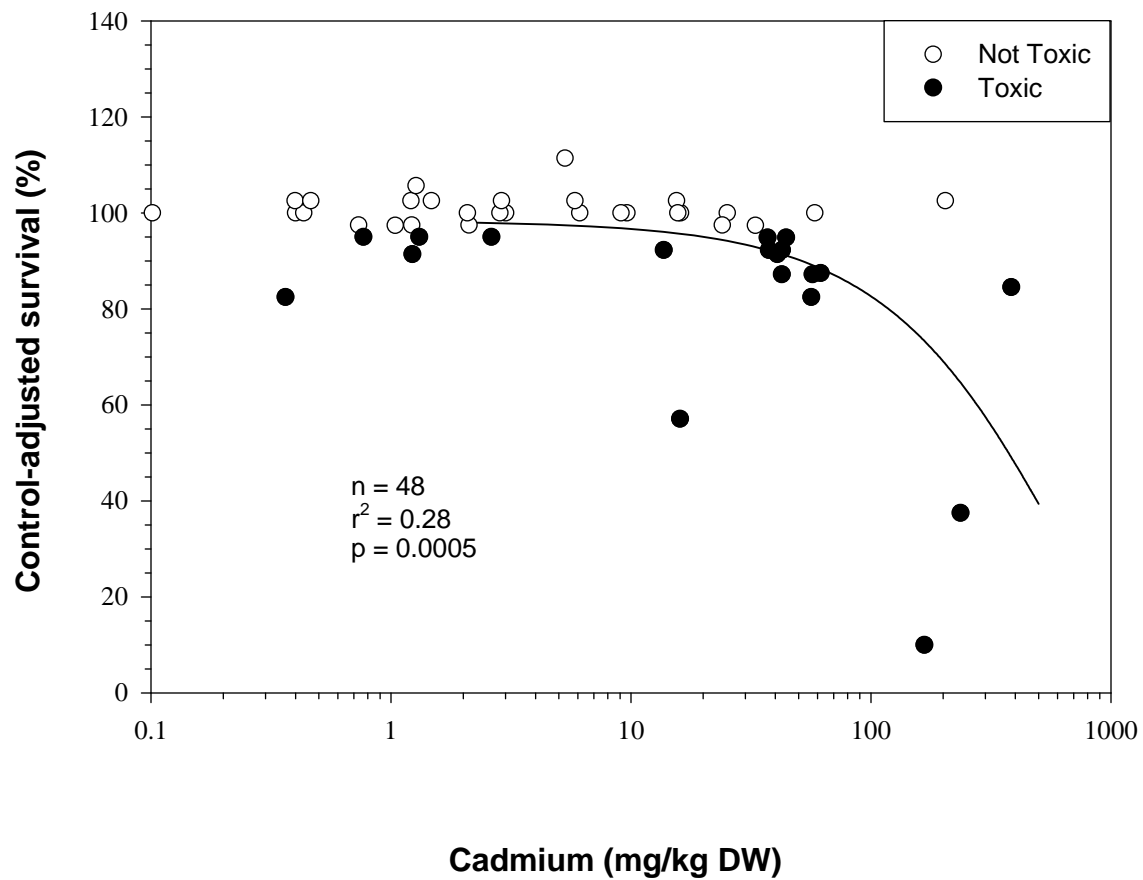
Plot A1-29. Plot illustrating the relationship between the concentration of Σ PEC-Q_{Cd,Pb,Zn} in sediment (<2 mm) and the control-adjusted biomass of amphipods (*Hyalella azteca*) in 28-d exposures to sediment samples from the Tri-State Mining District.



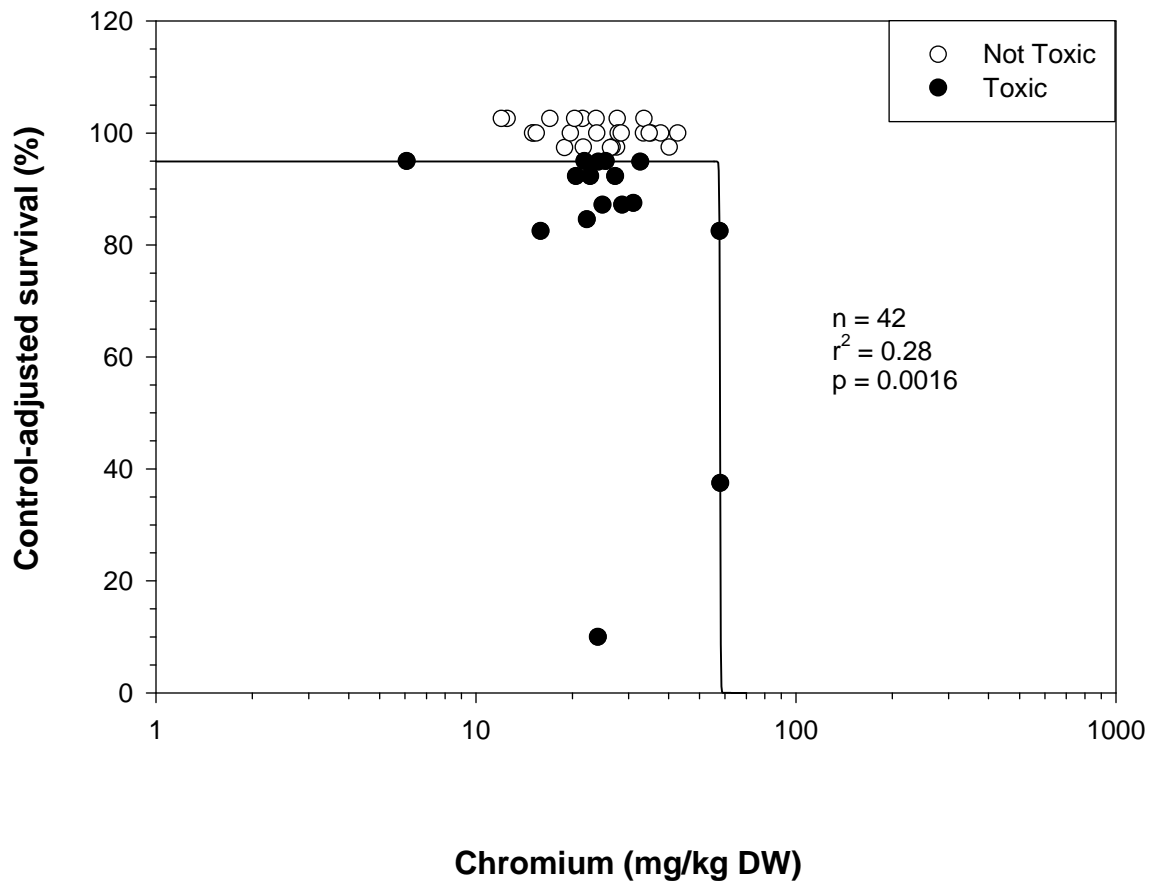
Plot A1-30. Plot illustrating the relationship between the concentration of $\Sigma\text{STT-Q}_{\text{Cd,Cu,Pb,Zn}}$ in sediment (<2 mm) and the control-adjusted biomass of amphipods (*Hyalella azteca*) in 28-d exposures to sediment samples from the Tri-State Mining District.



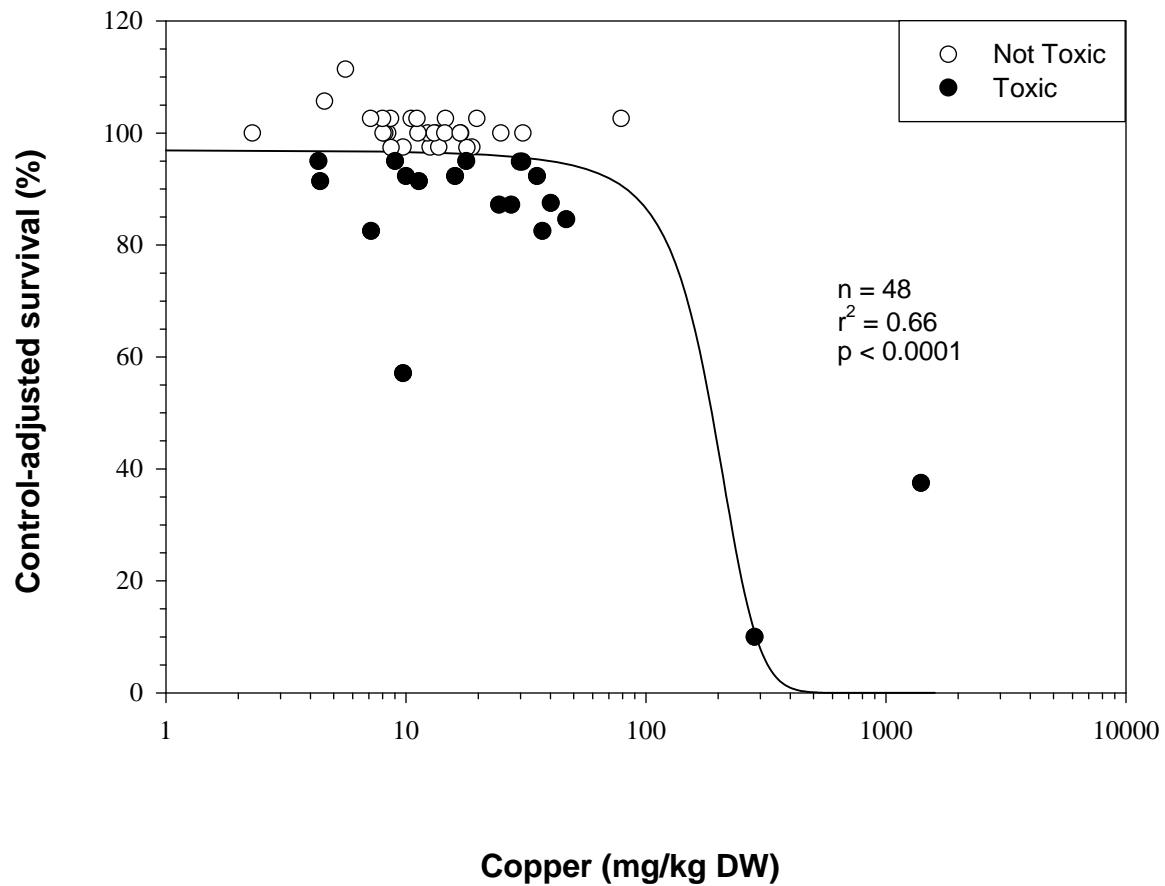
Plot A1-31. Plot illustrating the relationship between the concentration of cadmium (mg/kg DW) in sediment (<250 μm) and the control-adjusted survival of mussels (*Lampsilis siliquoidea*) in 28-d exposures to sediment samples from the Tri-State Mining District.



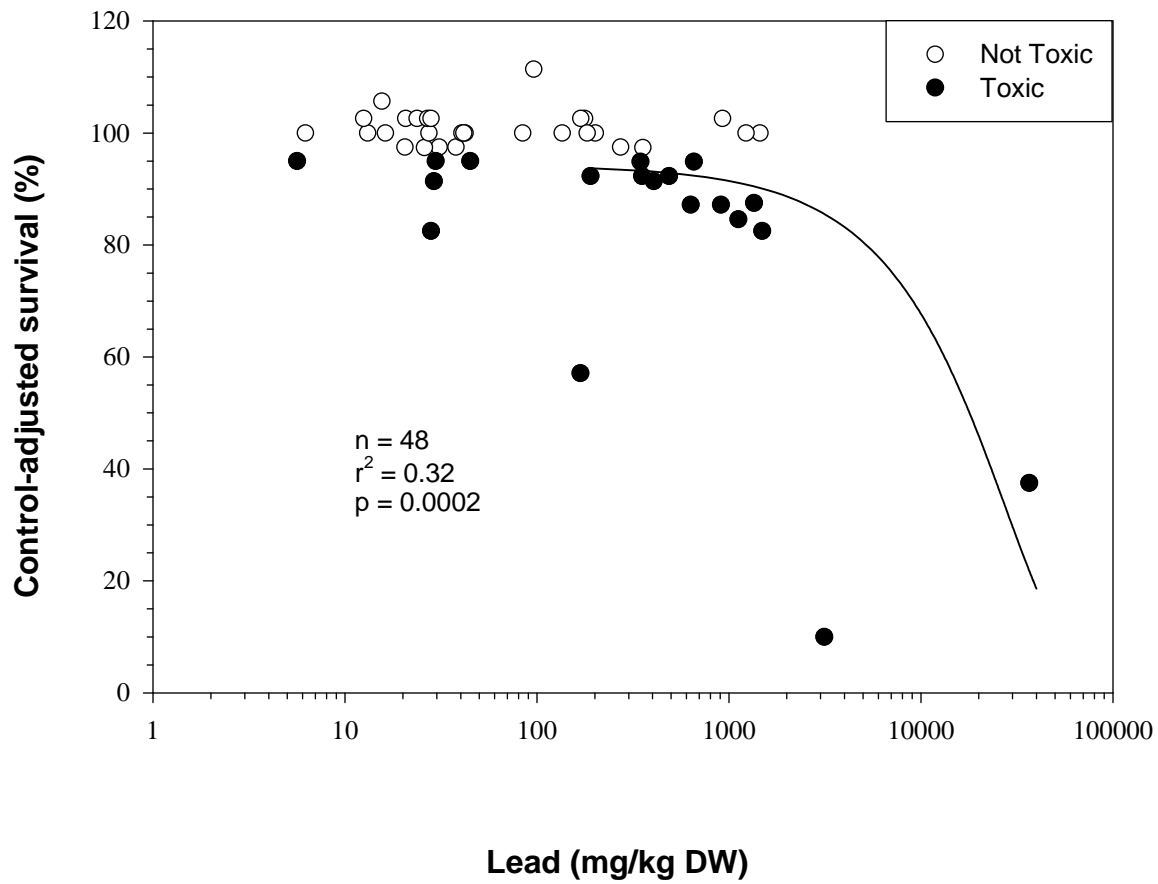
Plot A1-32. Plot illustrating the relationship between the concentration of chromium (mg/kg DW) in sediment (<250 μm) and the control-adjusted survival of mussels (*Lampsilis siliquoidea*) in 28-d exposures to sediment samples from the Tri-State Mining District.



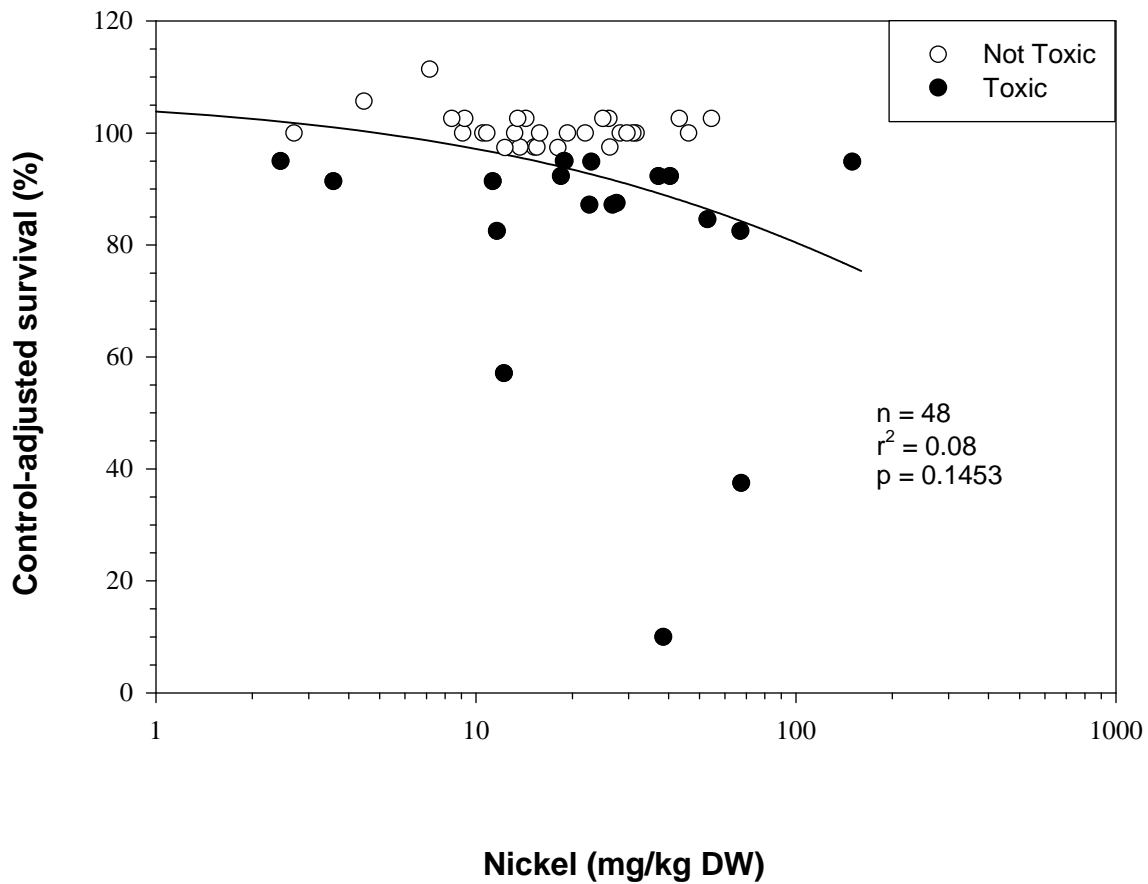
Plot A1-33. Plot illustrating the relationship between the concentration of copper (mg/kg DW) in sediment (<250 μ m) and the control-adjusted survival of mussels (*Lampsilis siliquoidea*) in 28-d exposures to sediment samples from the Tri-State Mining District.



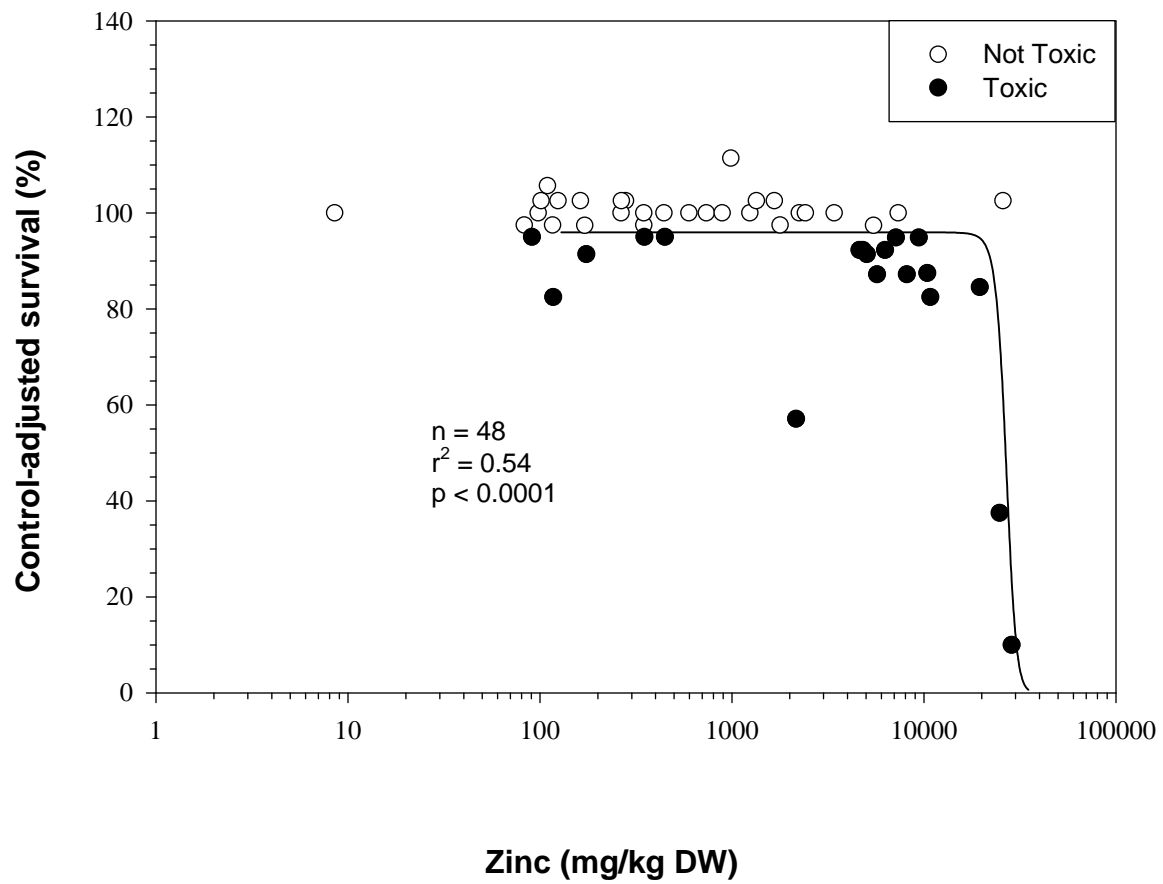
Plot A1-34. Plot illustrating the relationship between the concentration of lead (mg/kg DW) in sediment (<250 μm) and the control-adjusted survival of mussels (*Lampsilis siliquoidea*) in 28-d exposures to sediment samples from the Tri-State Mining District.



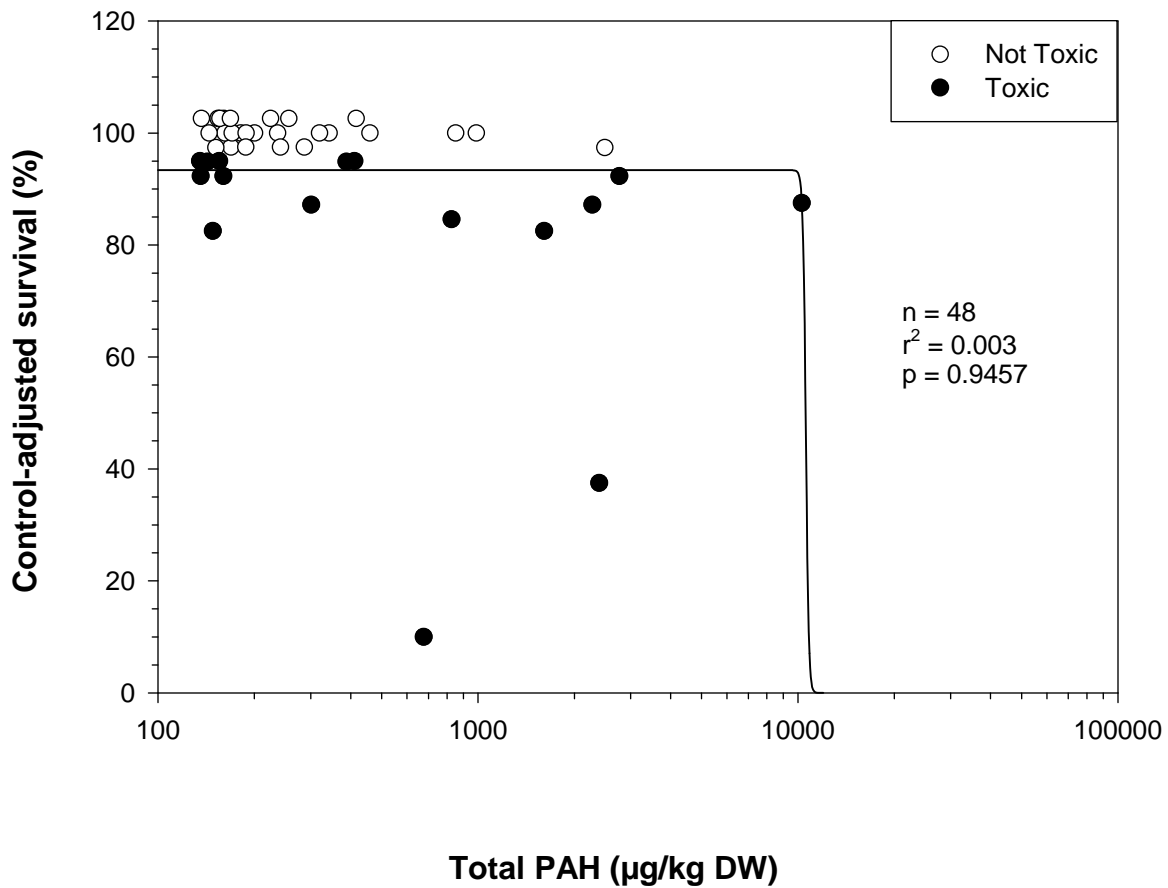
Plot A1-35. Plot illustrating the relationship between the concentration of nickel (mg/kg DW) in sediment (<250 μm) and the control-adjusted survival of mussels (*Lampsilis siliquoidea*) in 28-d exposures to sediment samples from the Tri-State Mining District.



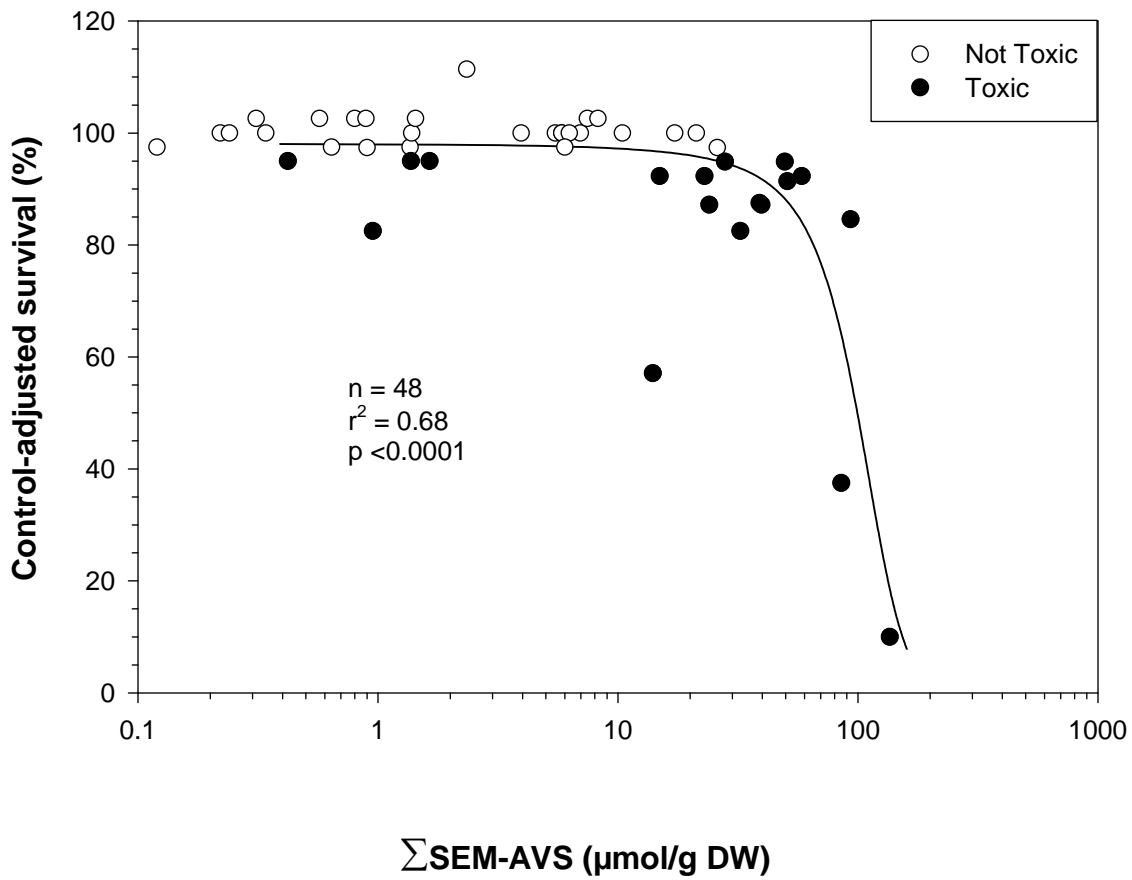
Plot A1-36. Plot illustrating the relationship between the concentration of zinc (mg/kg DW) in sediment (<250 μm) and the control-adjusted survival of mussels (*Lampsilis siliquoidea*) in 28-d exposures to sediment samples from the Tri-State Mining District.



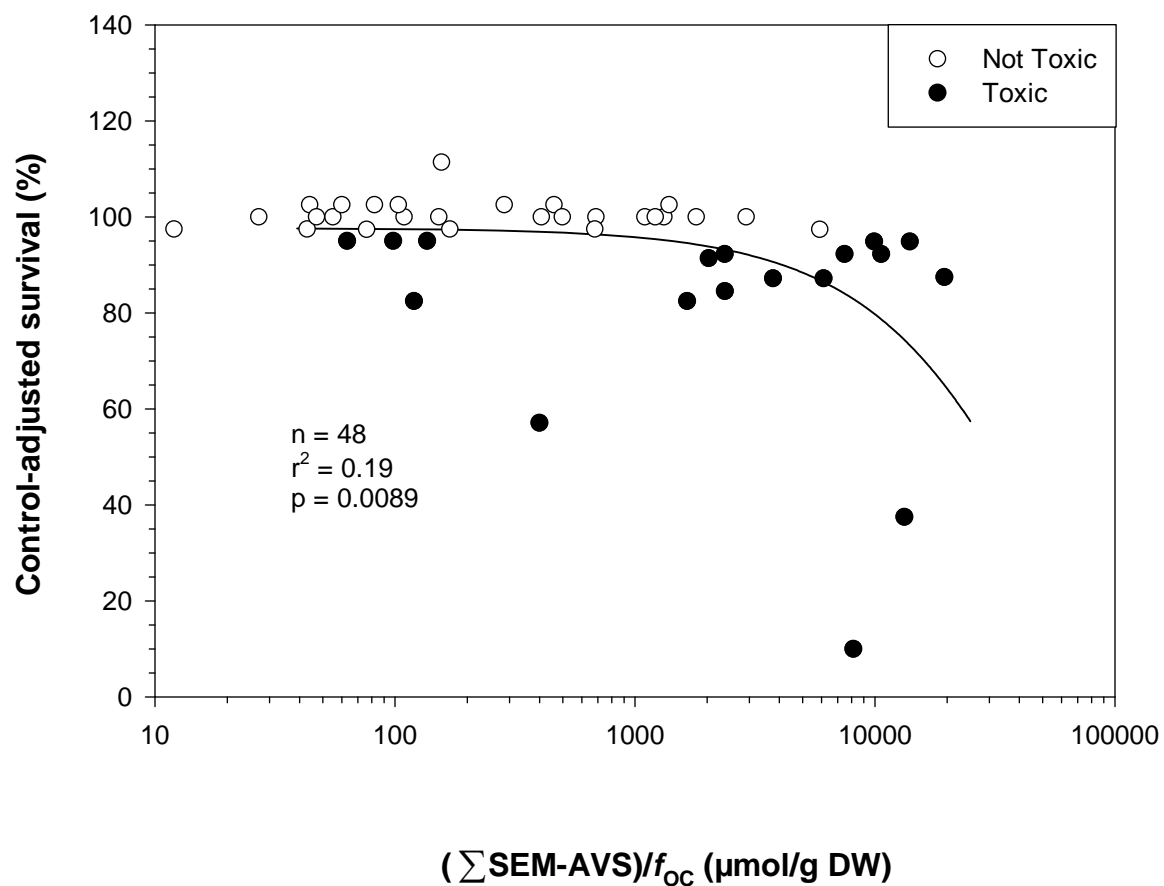
Plot A1-37. Plot illustrating the relationship between the concentration of total PAH ($\mu\text{g}/\text{kg DW}$) in sediment ($<250 \mu\text{m}$) and the control-adjusted survival of mussels (*Lampsilis siliquoidea*) in 28-d exposures to sediment samples from the Tri-State Mining District.



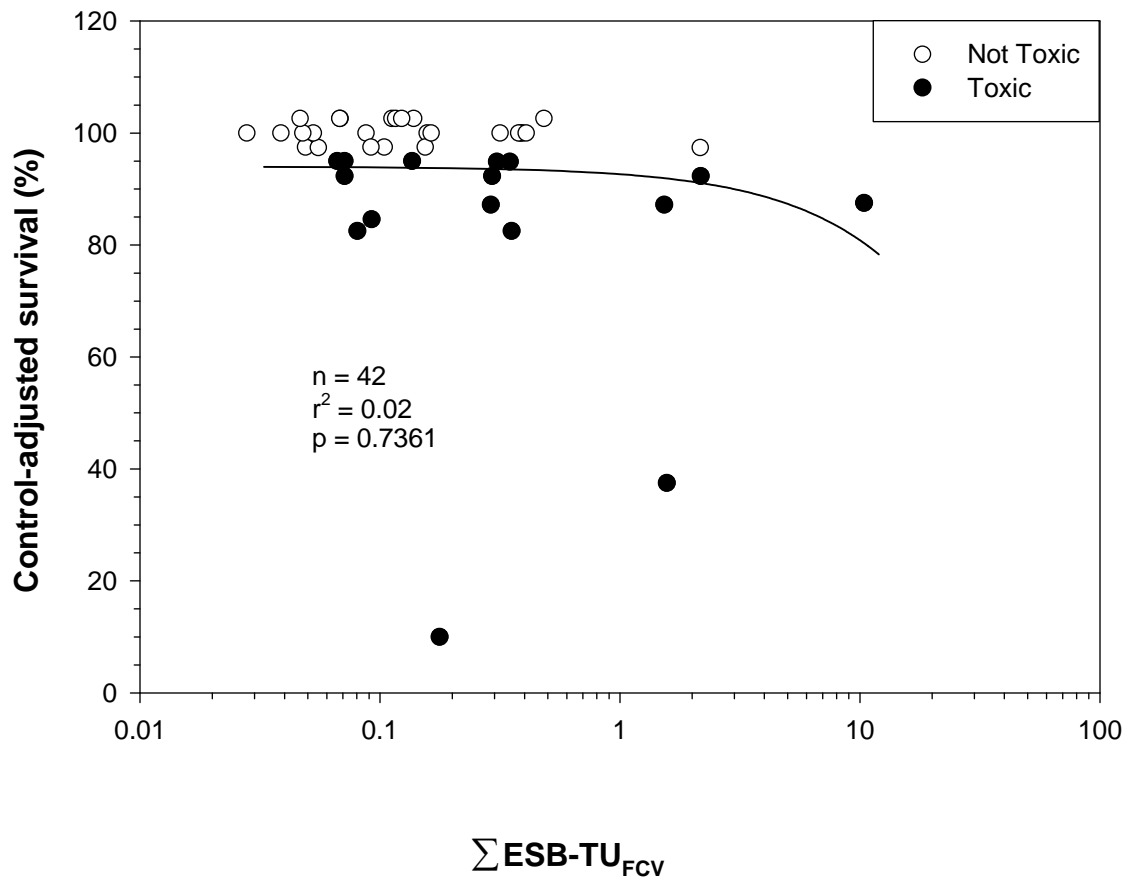
Plot A1-38. Plot illustrating the relationship between the concentration of Σ SEM-AVS ($\mu\text{mol/g DW}$) in sediment (<250 μm) and the control-adjusted survival of mussels (*Lampsilis siliquoidea*) in 28-d exposures to sediment samples from the Tri-State Mining District.



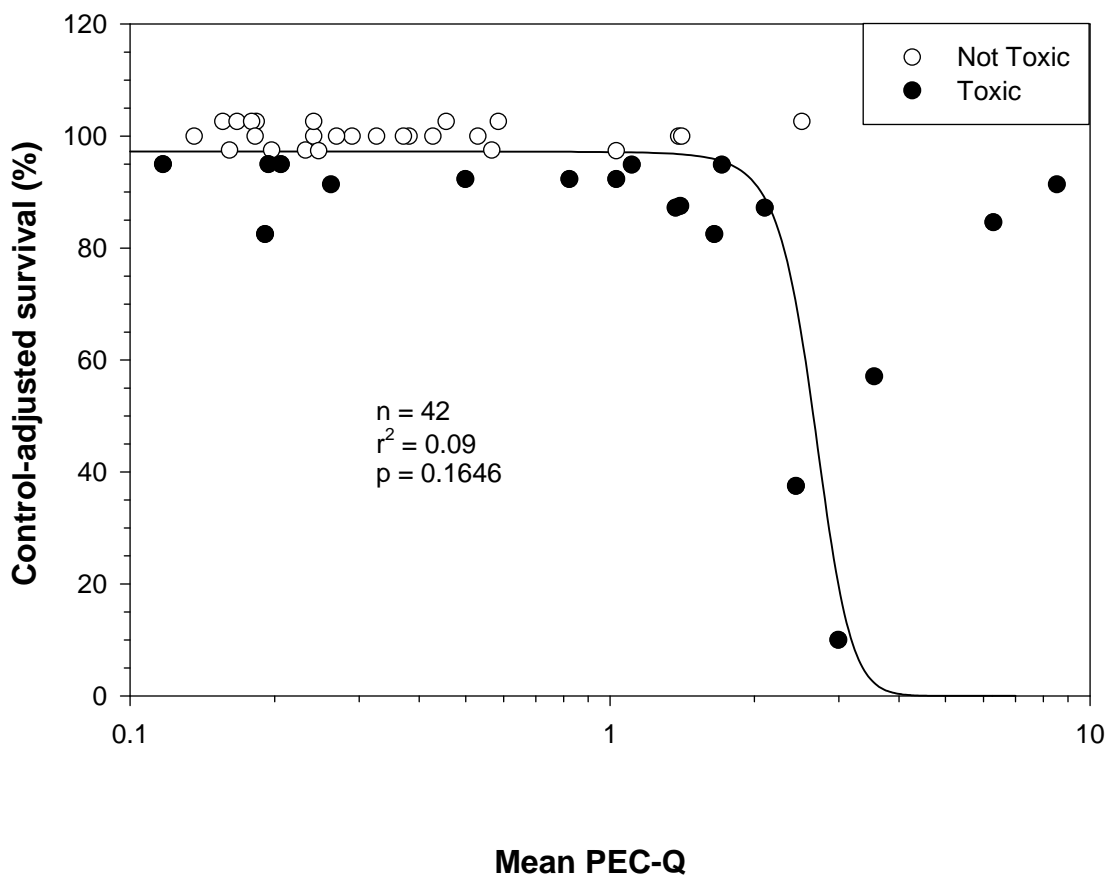
Plot A1-39. Plot illustrating the relationship between the concentration of $(\sum \text{SEM-AVS})/f_{\text{OC}}$ ($\mu\text{mol/g DW}$) in sediment ($<250 \mu\text{m}$) and the control-adjusted survival of mussels (*Lampsilis siliquoidea*) in 28-d exposures to sediment samples from the Tri-State Mining District.



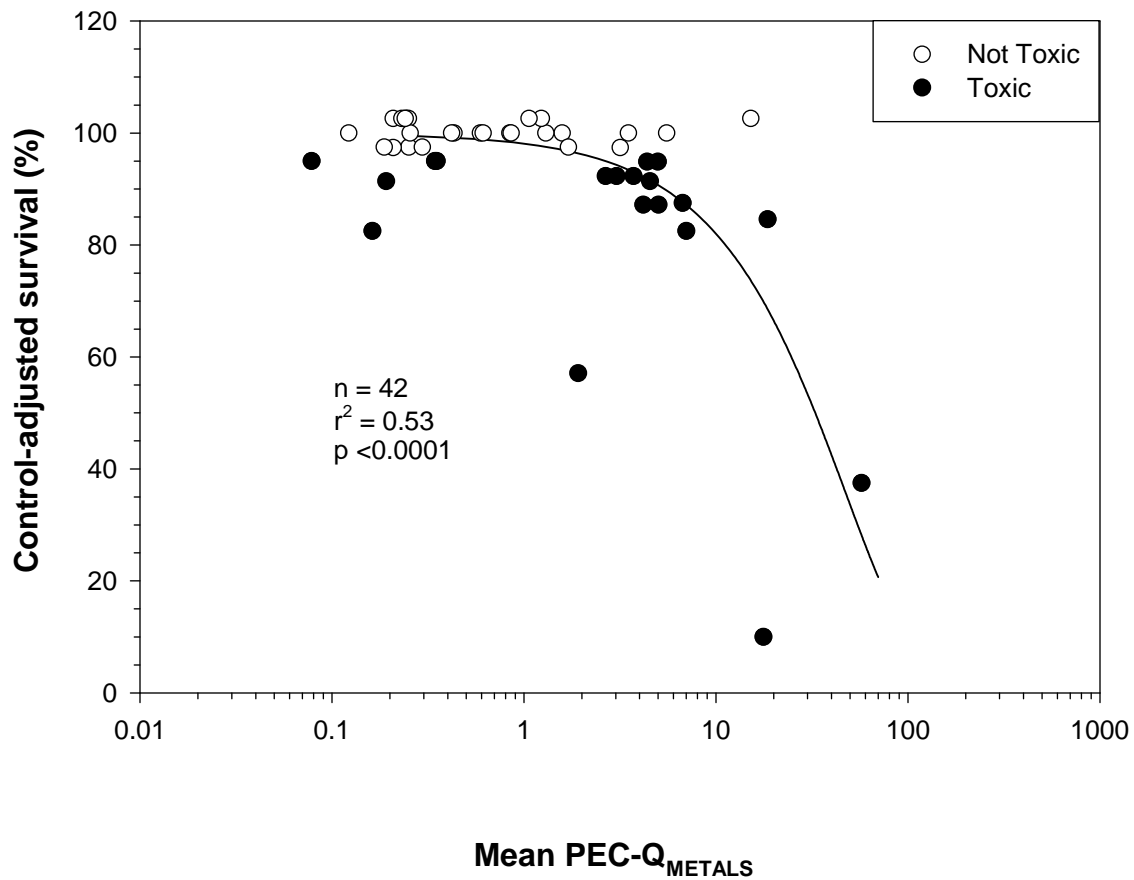
Plot A1-40. Plot illustrating the relationship between the concentration of $\sum \text{ESB-TU}_{\text{FCV}}$ in sediment (<250 μm) and the control-adjusted survival of mussels (*Lampsilis siliquoidea*) in 28-d exposures to sediment samples from the Tri-State Mining District.



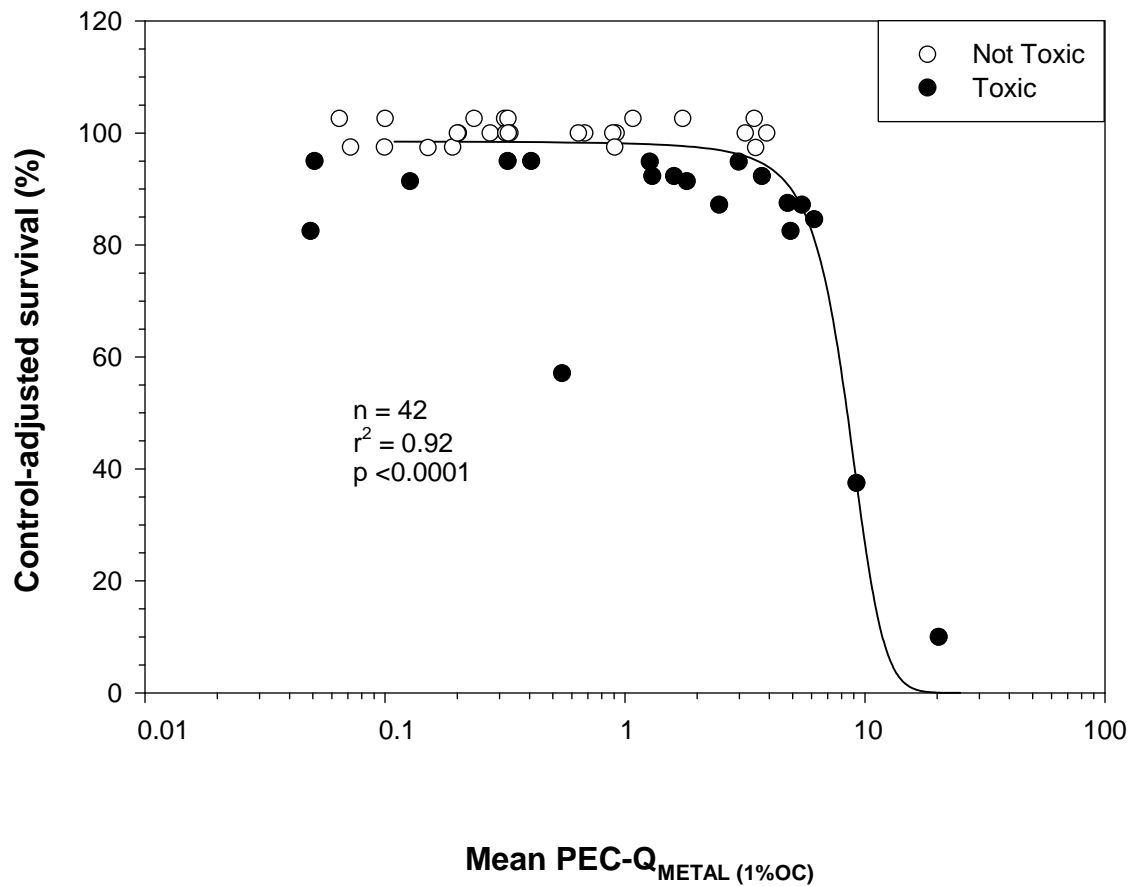
Plot A1-41. Plot illustrating the relationship between the concentration of Mean PEC-Q in sediment (<250 μm) and the control-adjusted survival of mussels (*Lampsilis siliquoidea*) in 28-d exposures to sediment samples from the Tri-State Mining District.



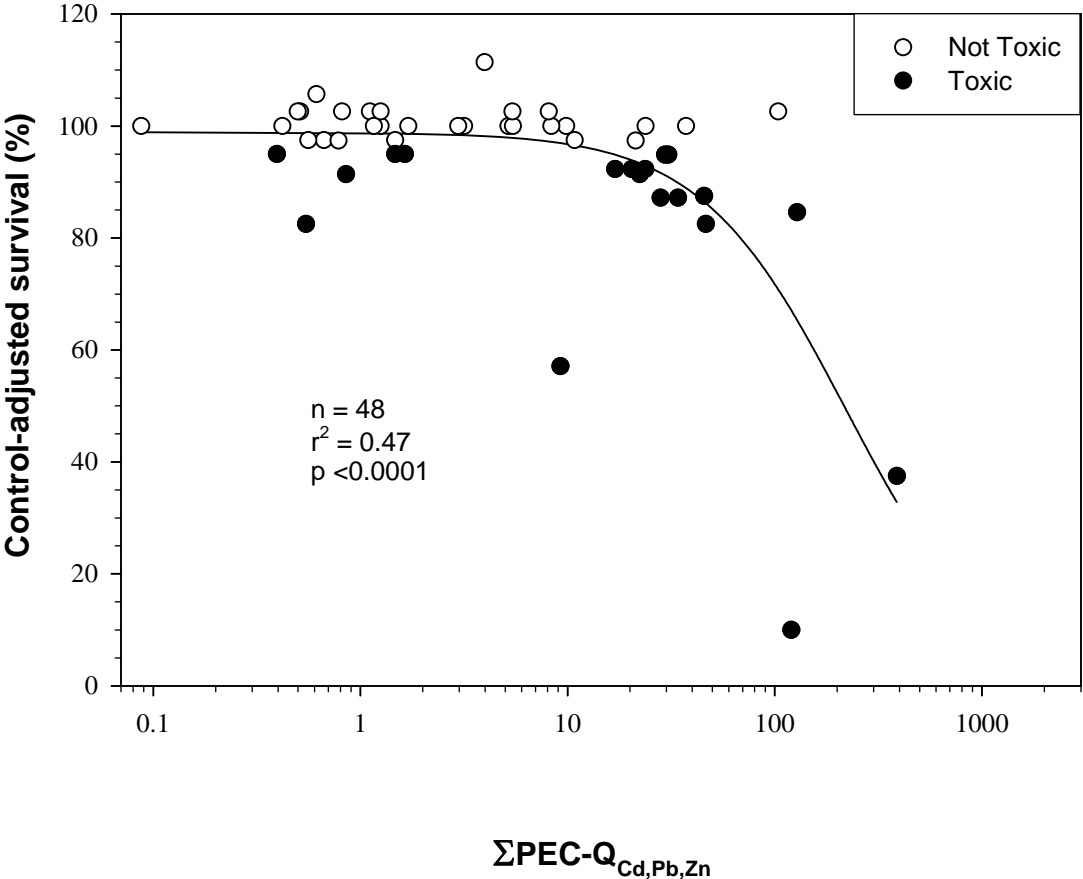
Plot A1-42. Plot illustrating the relationship between the concentration of Mean PEC-Q_{METALS} in sediment (<250 μm) and the control-adjusted survival of mussels (*Lampsilis siliquoidea*) in 28-d exposures to sediment samples from the Tri-State Mining District.



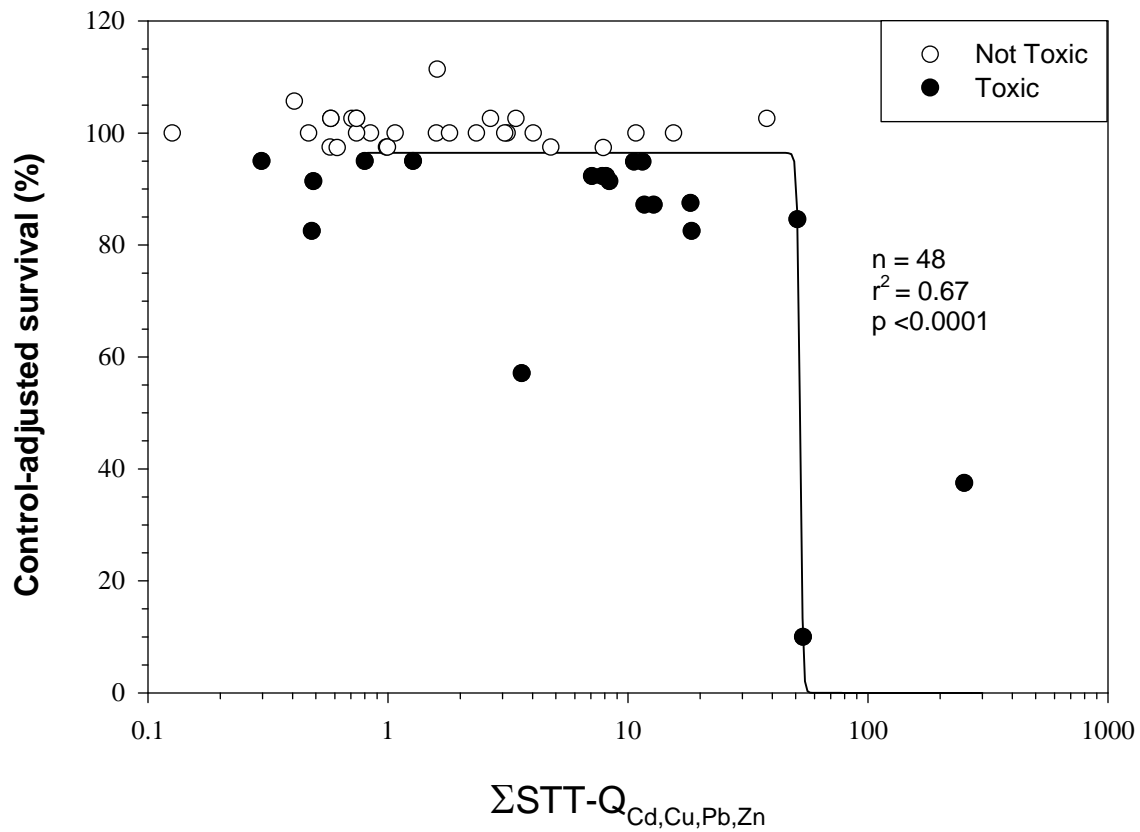
Plot A1-43. Plot illustrating the relationship between the concentration of Mean PEC-Q_{METAL(1%OC)} in sediment (<250 μm) and the control-adjusted survival of mussels (*Lampsilis siliquoidea*) in 28-d exposures to sediment samples from the Tri-State Mining District.



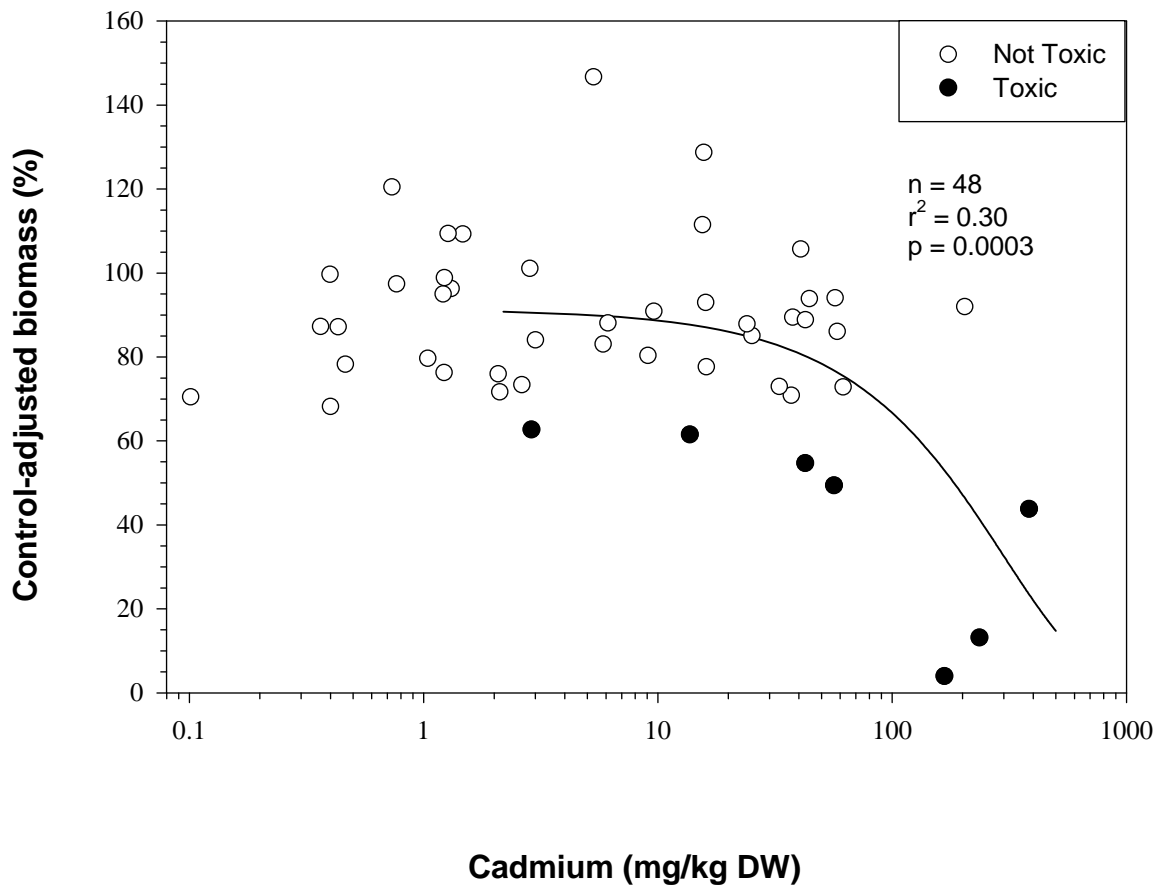
Plot A1-44. Plot illustrating the relationship between the concentration of $\sum \text{PEC-Q}_{\text{Cd,Pb,Zn}}$ in sediment (<250 μm) and the control-adjusted survival of mussels (*Lampsilis siliquoidea*) in 28-d exposures to sediment samples from the Tri-State Mining District.



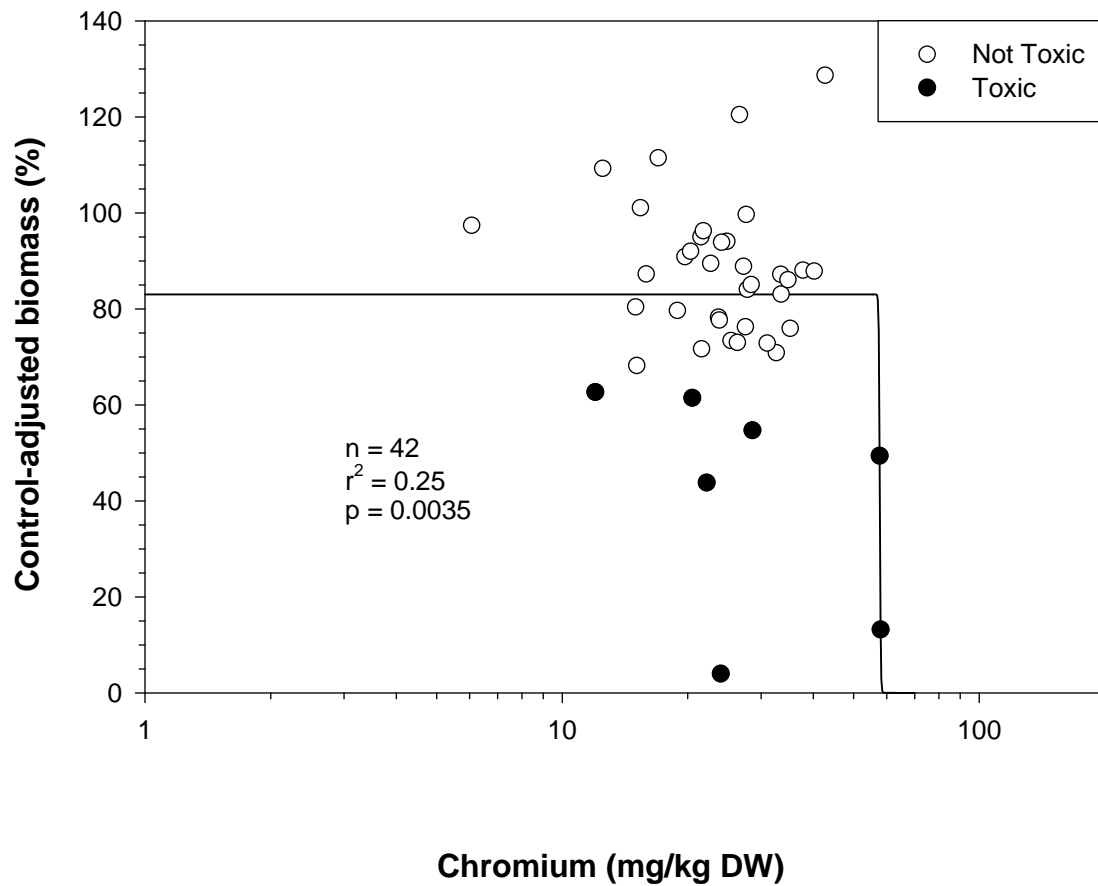
Plot A1-45. Plot illustrating the relationship between the concentration of $\Sigma \text{STT-Q}_{\text{Cd,Cu,Pb,Zn}}$ in sediment (<250 μm) and the control-adjusted survival of mussels (*Lampsilis siliquoidea*) in 28-d exposures to sediment samples from the Tri-State Mining District.



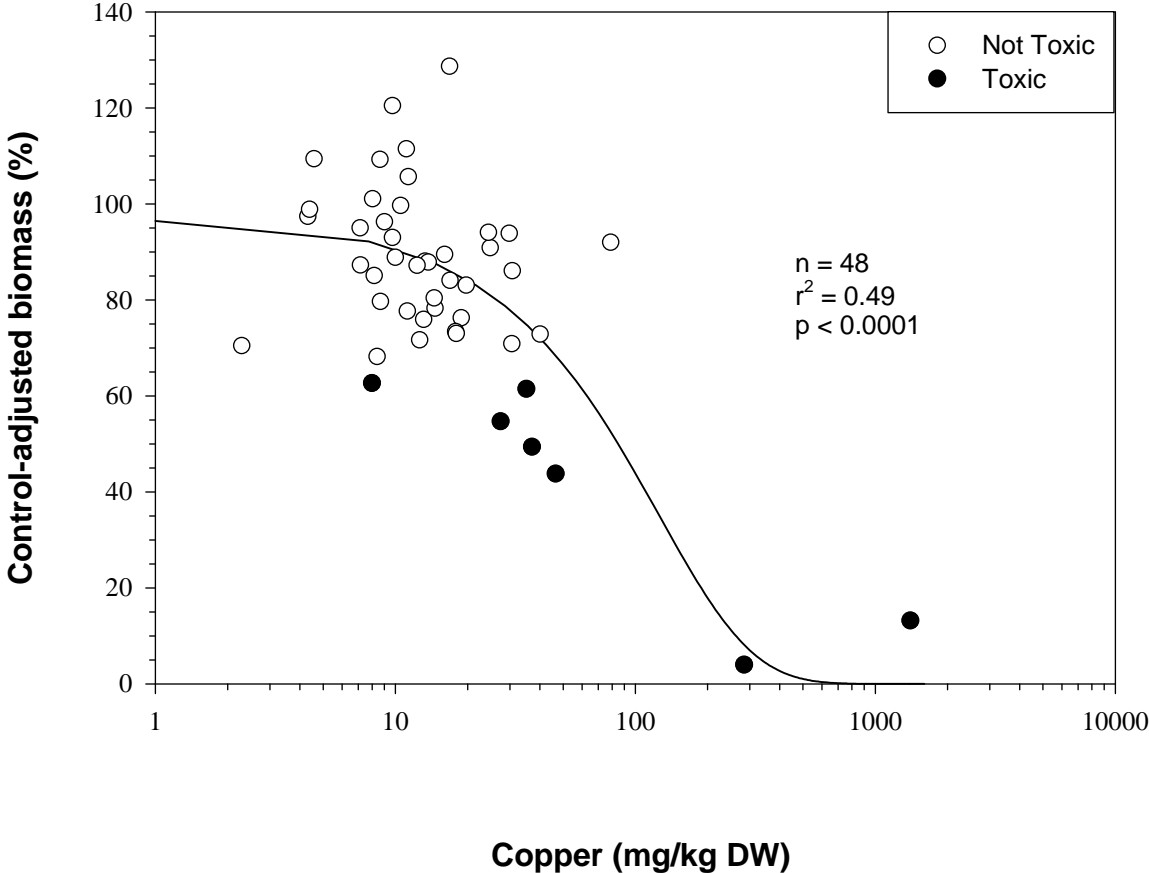
Plot A1-46. Plot illustrating the relationship between the concentration of cadmium (mg/kg DW) in sediment (<250 μm) and the control-adjusted biomass of mussels (*Lampsilis siliquoidea*) in 28-d exposures to sediment samples from the Tri-State Mining District.



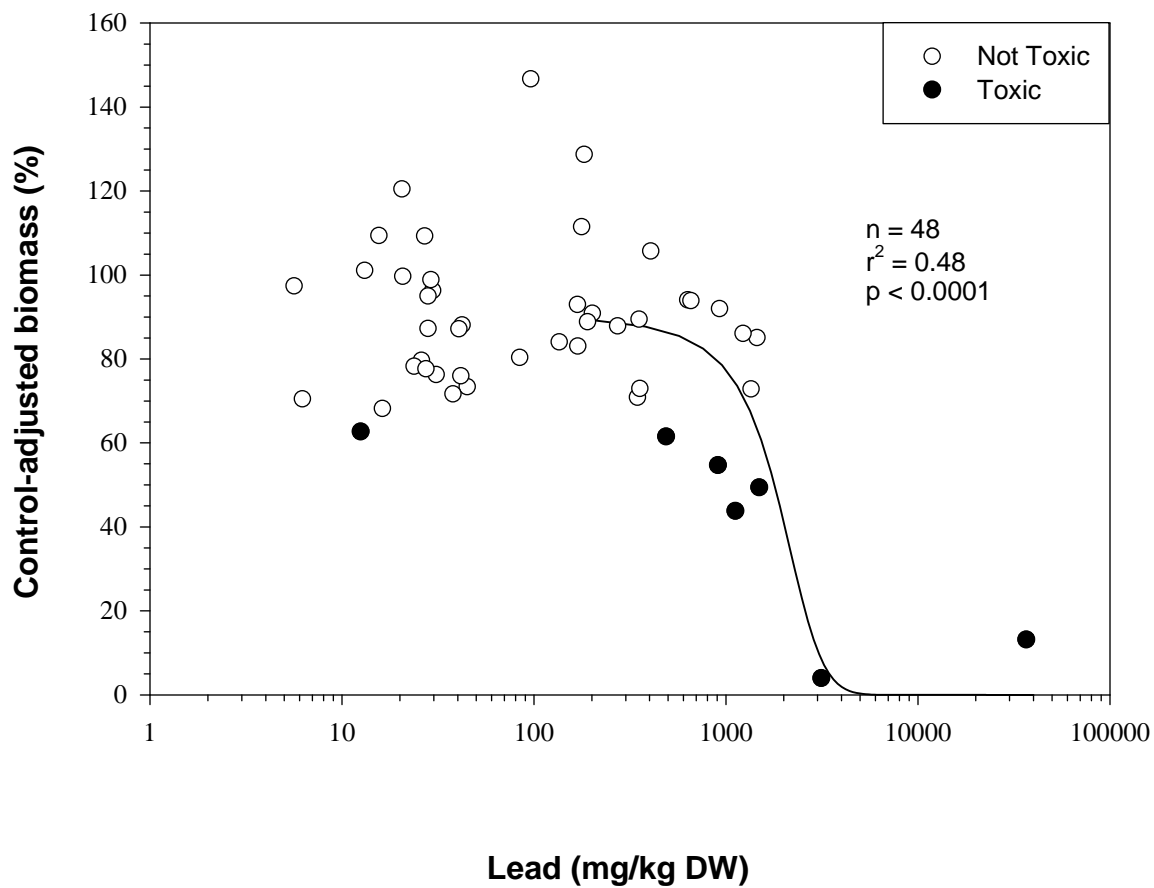
Plot A1-47. Plot illustrating the relationship between the concentration of chromium (mg/kg DW) in sediment (<250 μm) and the control-adjusted biomass of mussels (*Lampsilis siliquoidea*) in 28-d exposures to sediment samples from the Tri-State Mining District.



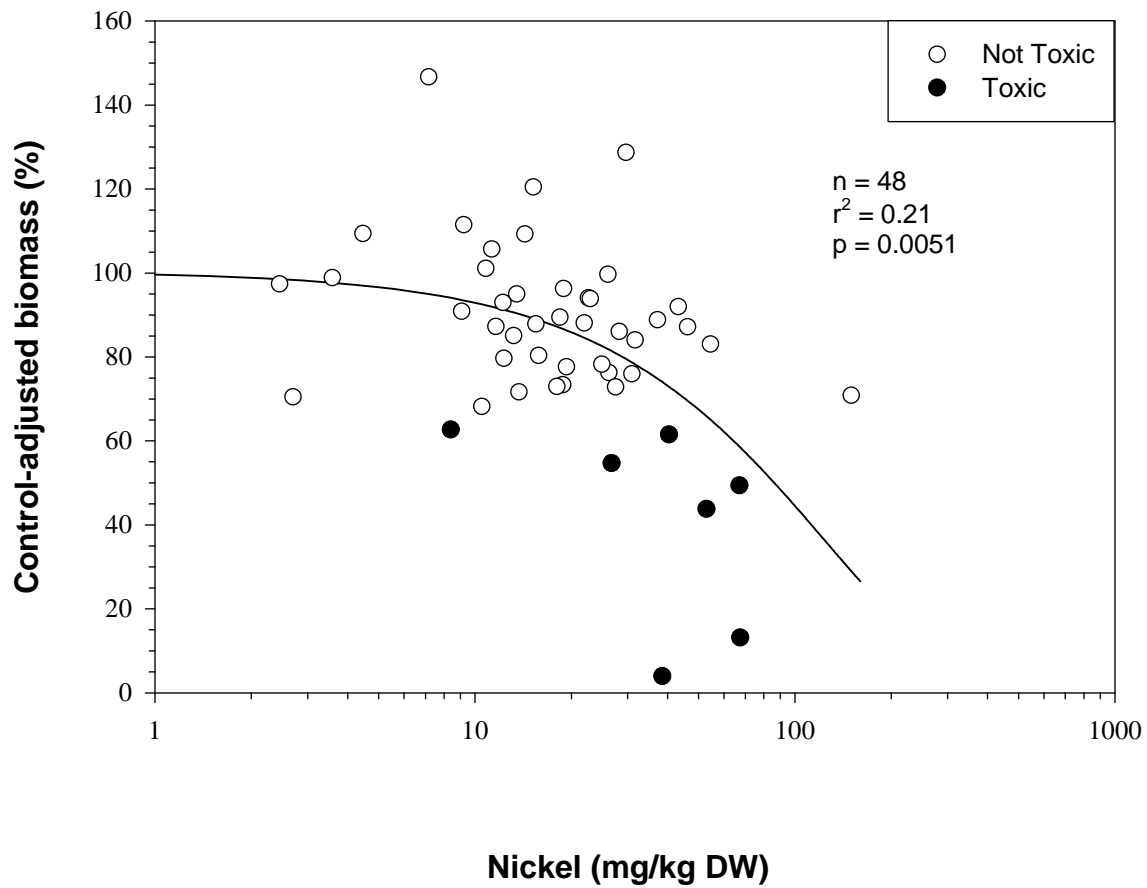
Plot A1-48. Plot illustrating the relationship between the concentration of copper (mg/kg DW) in sediment (<250 μm) and the control-adjusted biomass of mussels (*Lampsilis siliquoidea*) in 28-d exposures to sediment samples from the Tri-State Mining District.



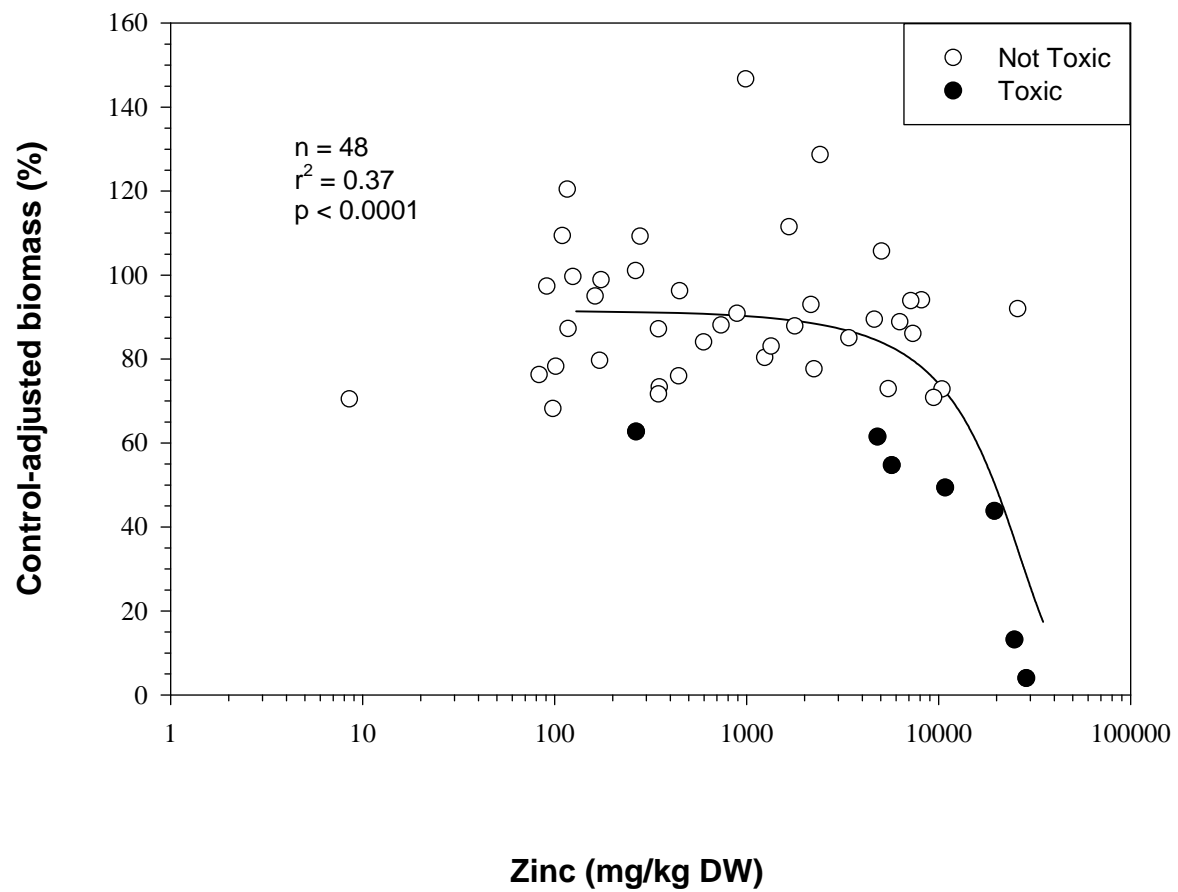
Plot A1-49. Plot illustrating the relationship between the concentration of lead (mg/kg DW) in sediment (<250 μm) and the control-adjusted biomass of mussels (*Lampsilis siliquoidea*) in 28-d exposures to sediment samples from the Tri-State Mining District.



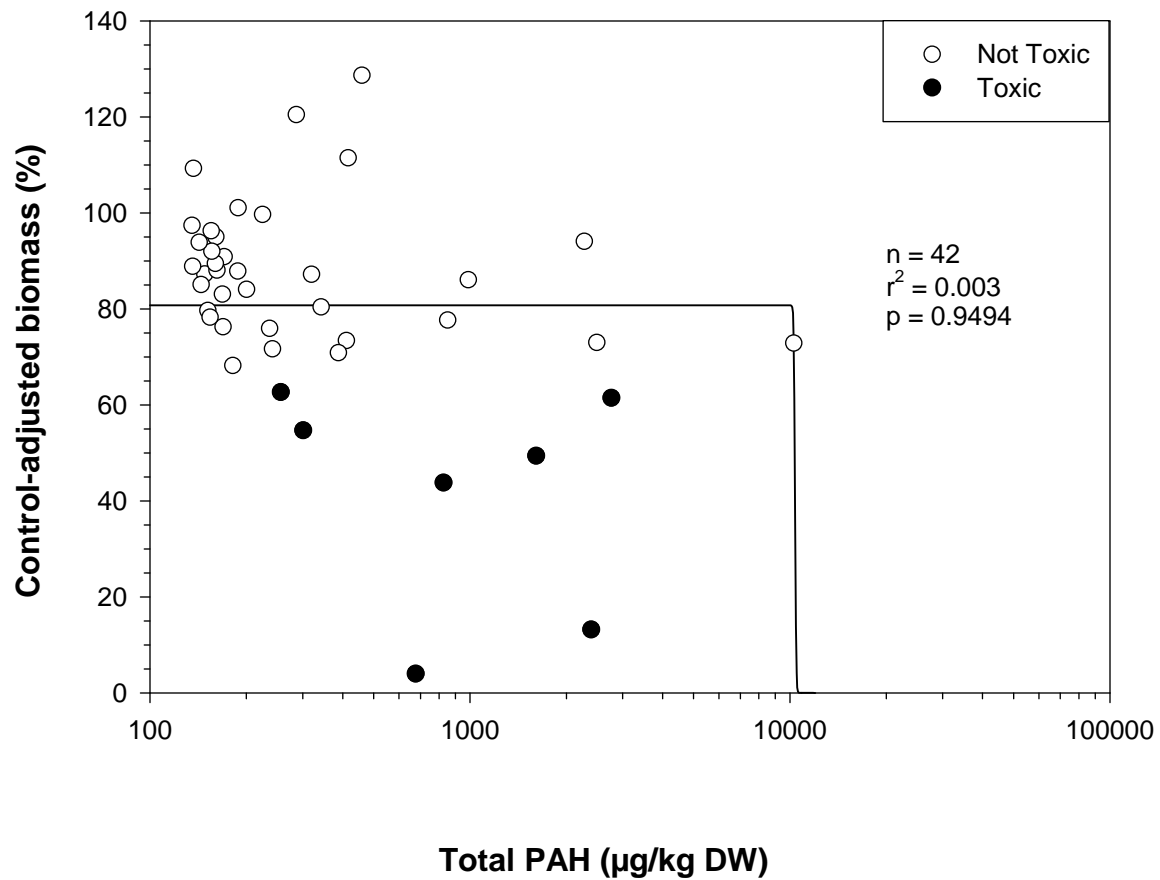
Plot A1-50. Plot illustrating the relationship between the concentration of nickel (mg/kg DW) in sediment (<250 μm) and the control-adjusted biomass of mussels (*Lampsilis siliquoidea*) in 28-d exposures to sediment samples from the Tri-State Mining District.



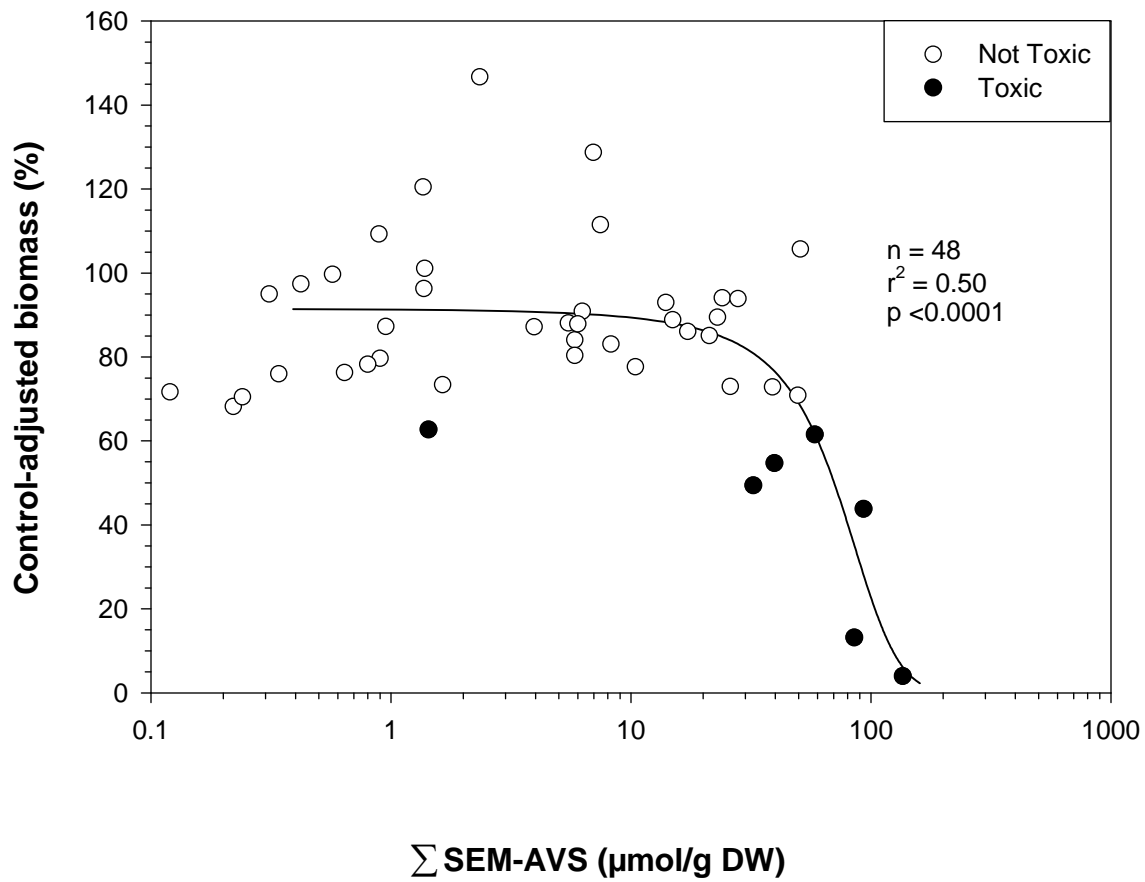
Plot A1-51. Plot illustrating the relationship between the concentration of zinc (mg/kg DW) in sediment (<250 μm) and the control-adjusted biomass of mussels (*Lampsilis siliquoidea*) in 28-d exposures to sediment samples from the Tri-State Mining District.



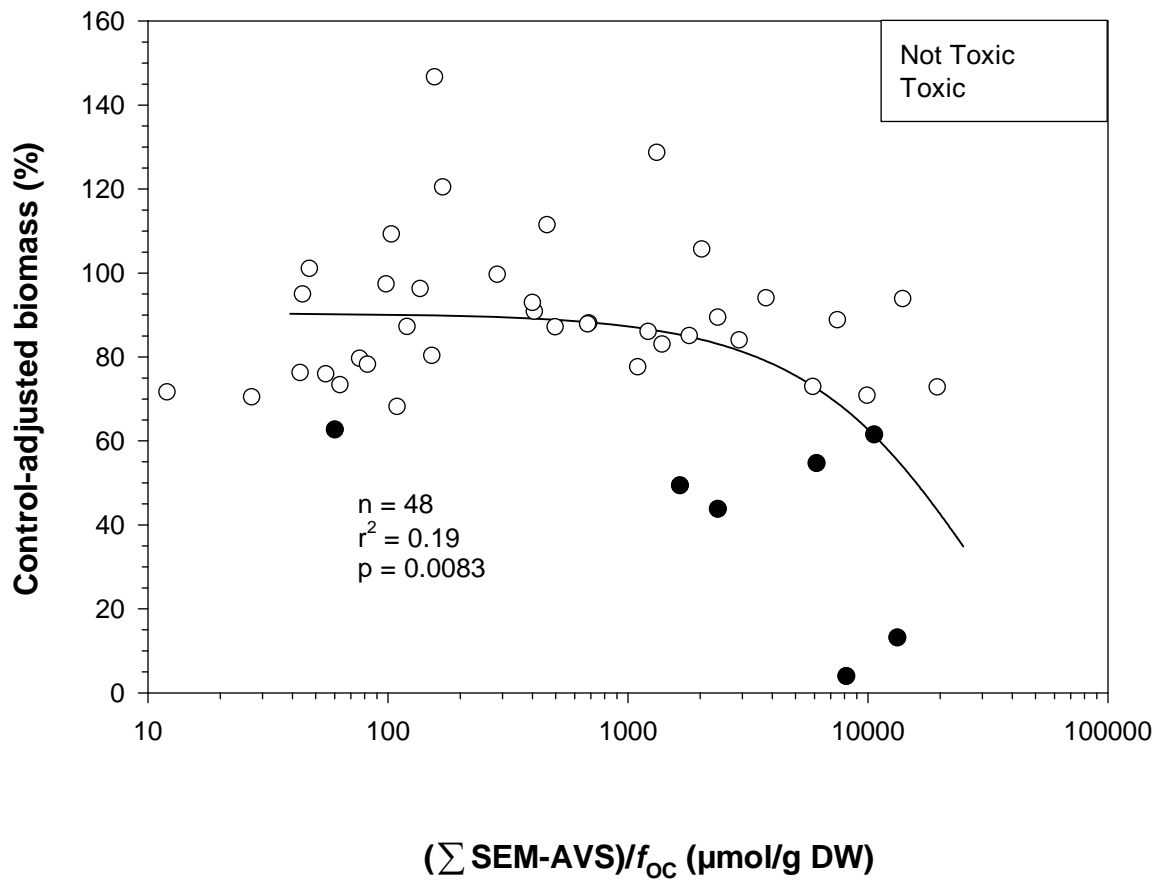
Plot A1-52. Plot illustrating the relationship between the concentration of total PAH ($\mu\text{g}/\text{kg DW}$) in sediment ($<250 \mu\text{m}$) and the control-adjusted biomass of mussels (*Lampsilis siliquoidea*) in 28-d exposures to sediment samples from the Tri-State Mining District.



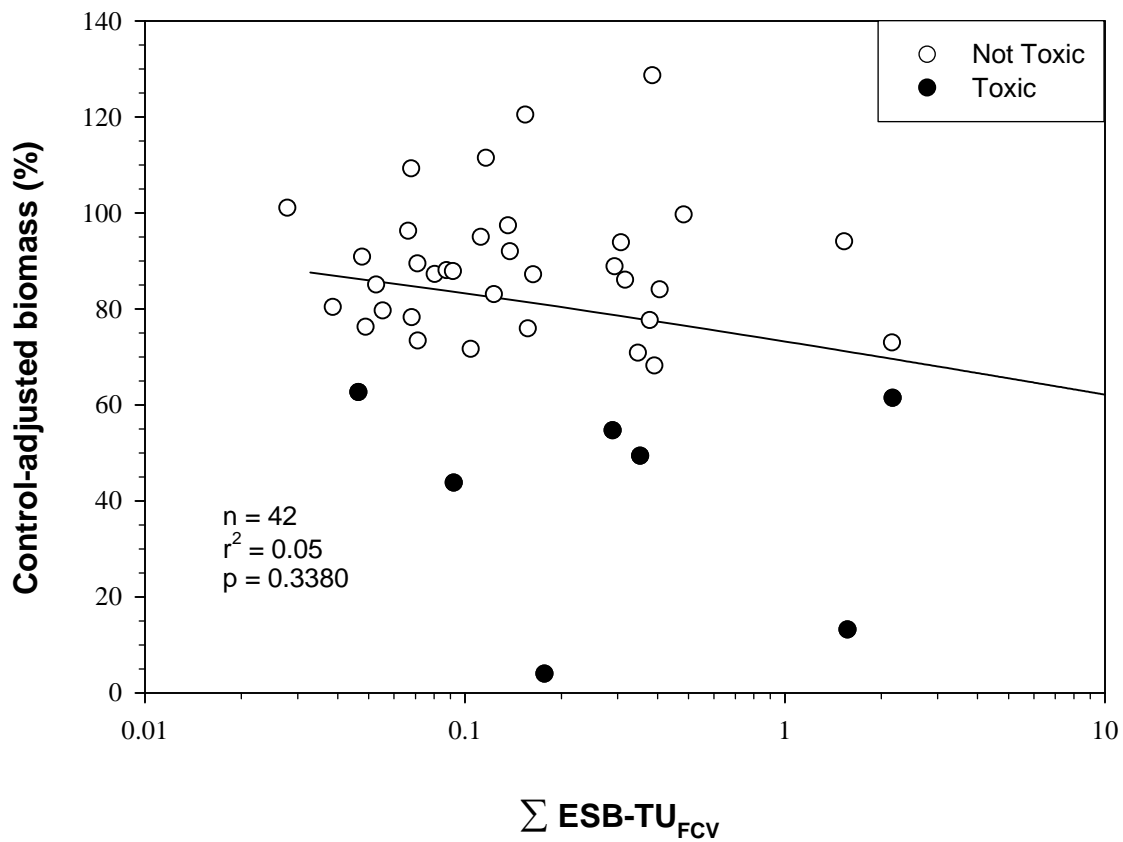
Plot A1-53. Plot illustrating the relationship between the concentration of Σ SEM-AVS ($\mu\text{mol/g DW}$) in sediment ($<250 \mu\text{m}$) and the control-adjusted biomass of mussels (*Lampsilis siliquoidea*) in 28-d exposures to sediment samples from the Tri-State Mining District.



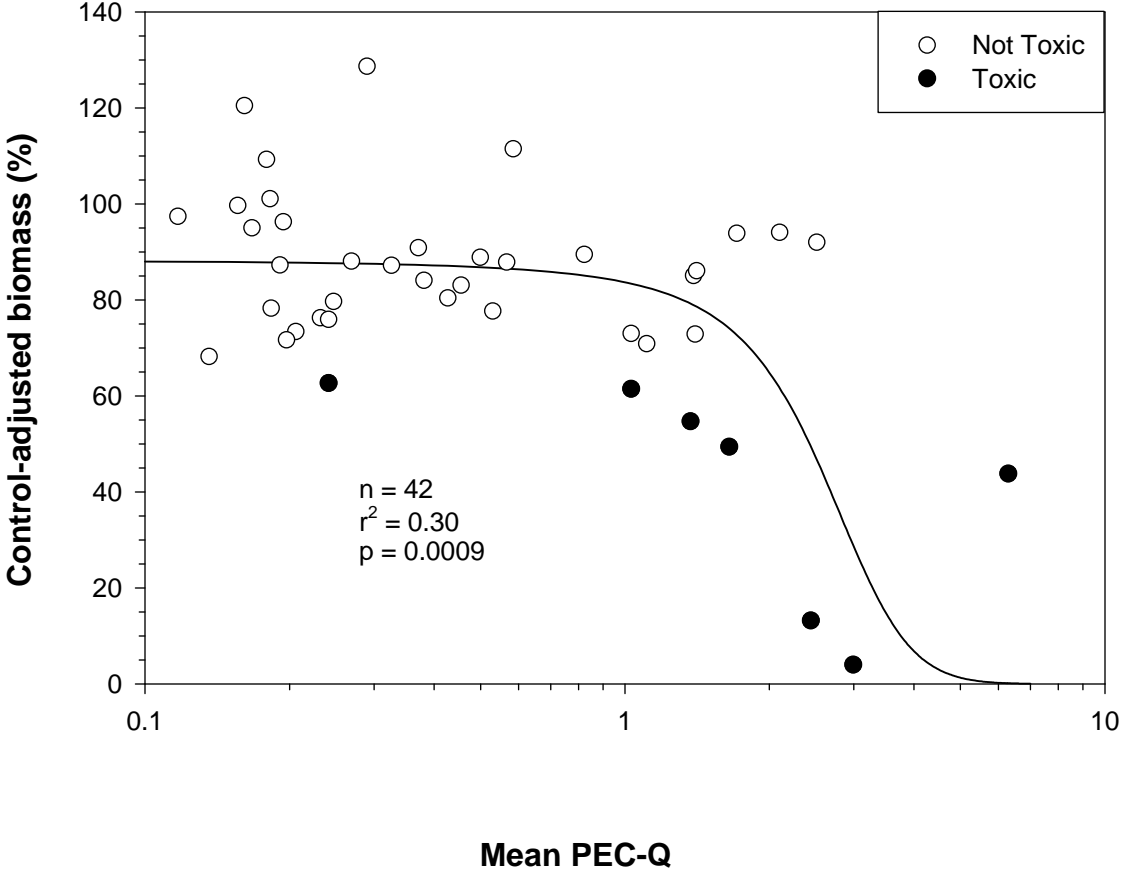
Plot A1-54. Plot illustrating the relationship between the concentration of (Σ SEM-AVS/ f_{OC} ($\mu\text{mol/g DW}$) in sediment (<250 μm) and the control-adjusted biomass of mussels (*Lampsilis siliquoidea*) in 28-d exposures to sediment samples from the Tri-State Mining District.



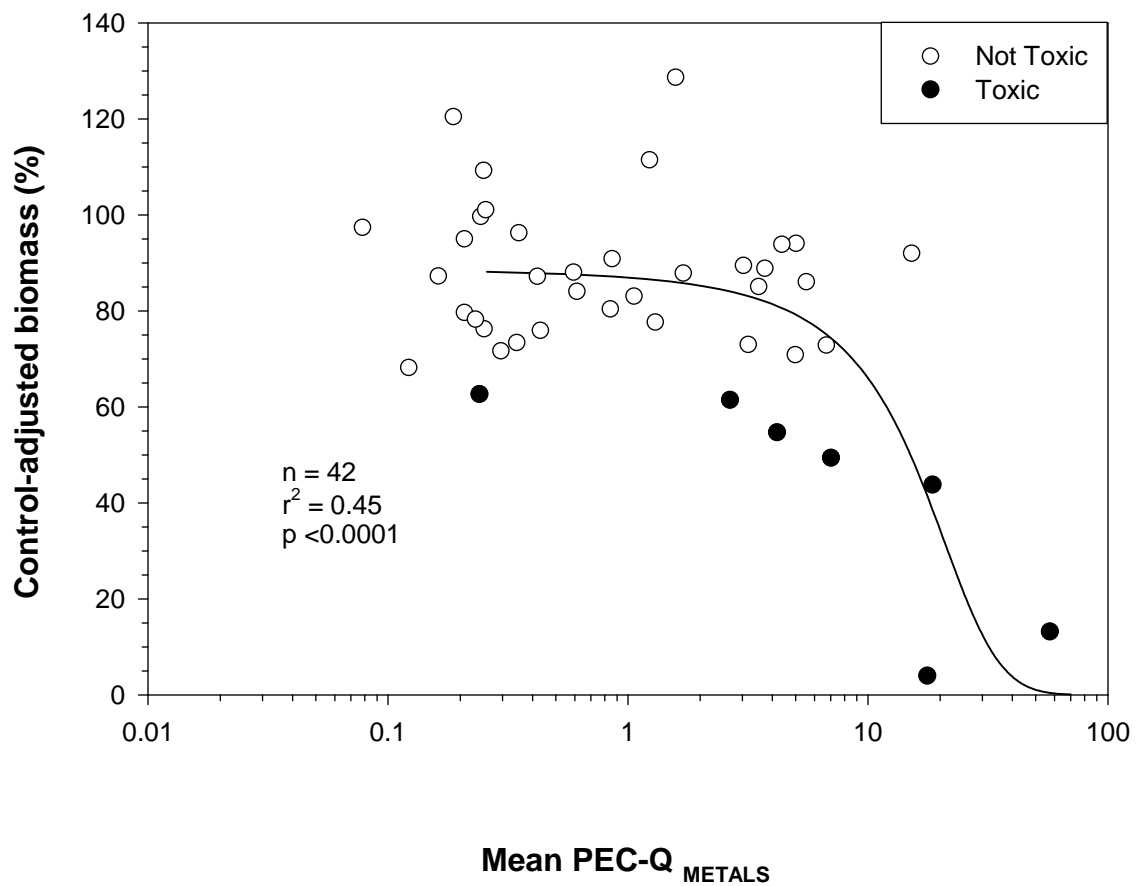
Plot A1-55. Plot illustrating the relationship between the concentration of Σ ESB-TU_{FCV} in sediment (<250 μ m) and the control-adjusted biomass of mussels (*Lampsilis siliquoidea*) in 28-d exposures to sediment samples from the Tri-State Mining District.



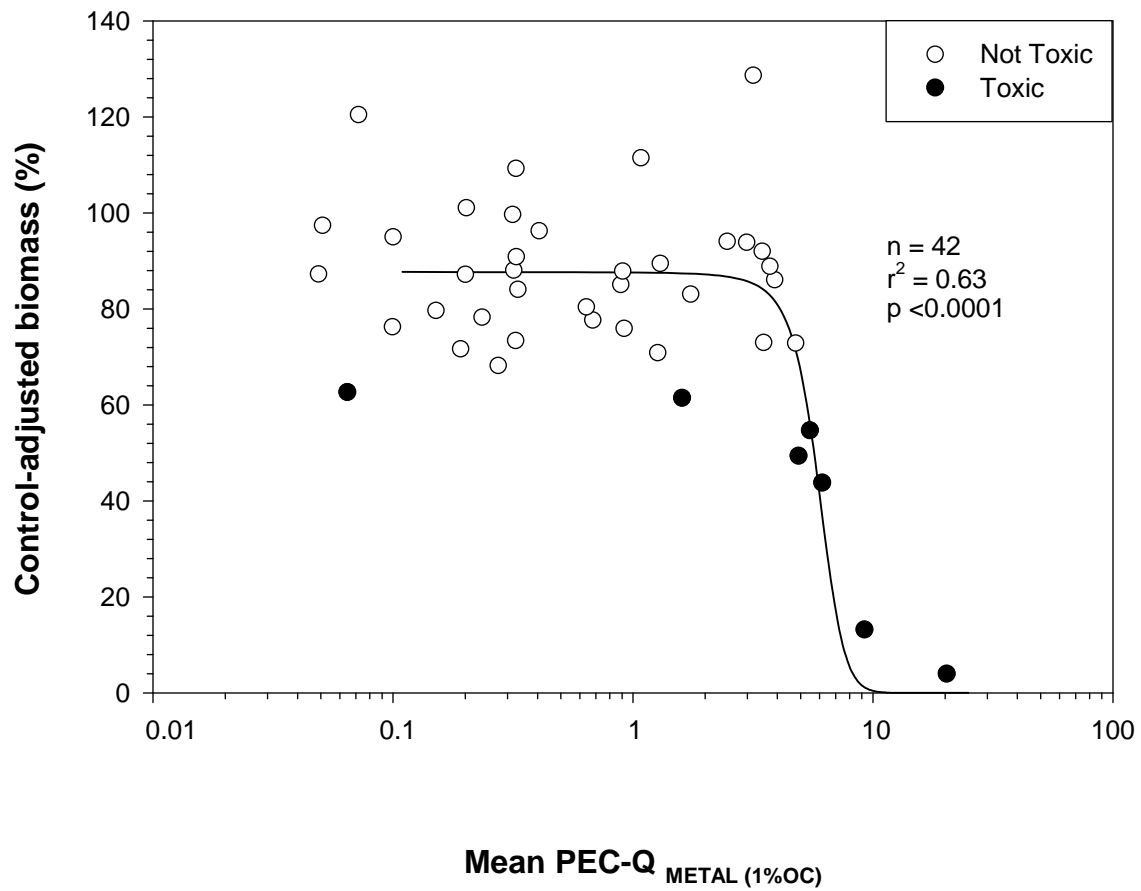
Plot A1-56. Plot illustrating the relationship between the concentration of Mean PEC-Q in sediment (<250 μm) and the control-adjusted biomass of mussels (*Lampsilis siliquoidea*) in 28-d exposures to sediment samples from the Tri-State Mining District.



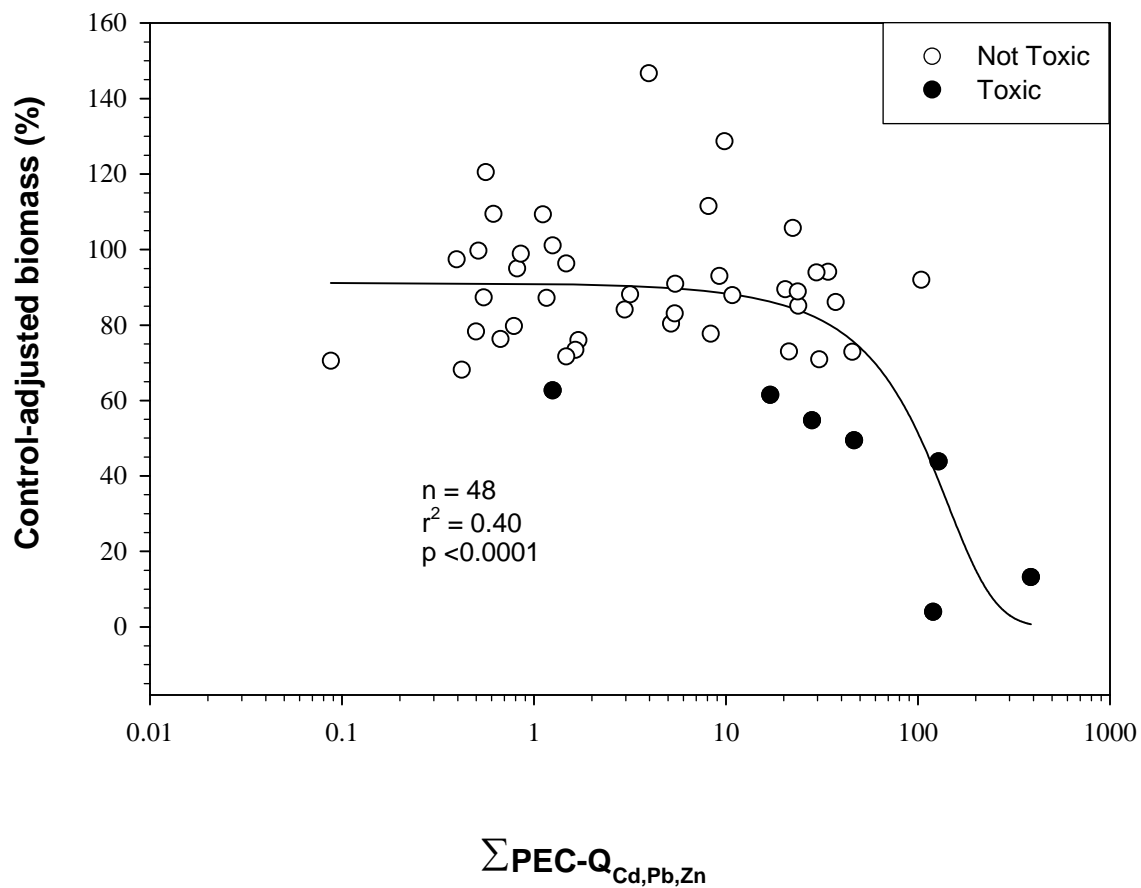
Plot A1-57. Plot illustrating the relationship between the concentration of Mean PEC-Q_{METALS} in sediment (<250 μm) and the control-adjusted biomass of mussels (*Lampsilis siliquoidea*) in 28-d exposures to sediment samples from the Tri-State Mining District.



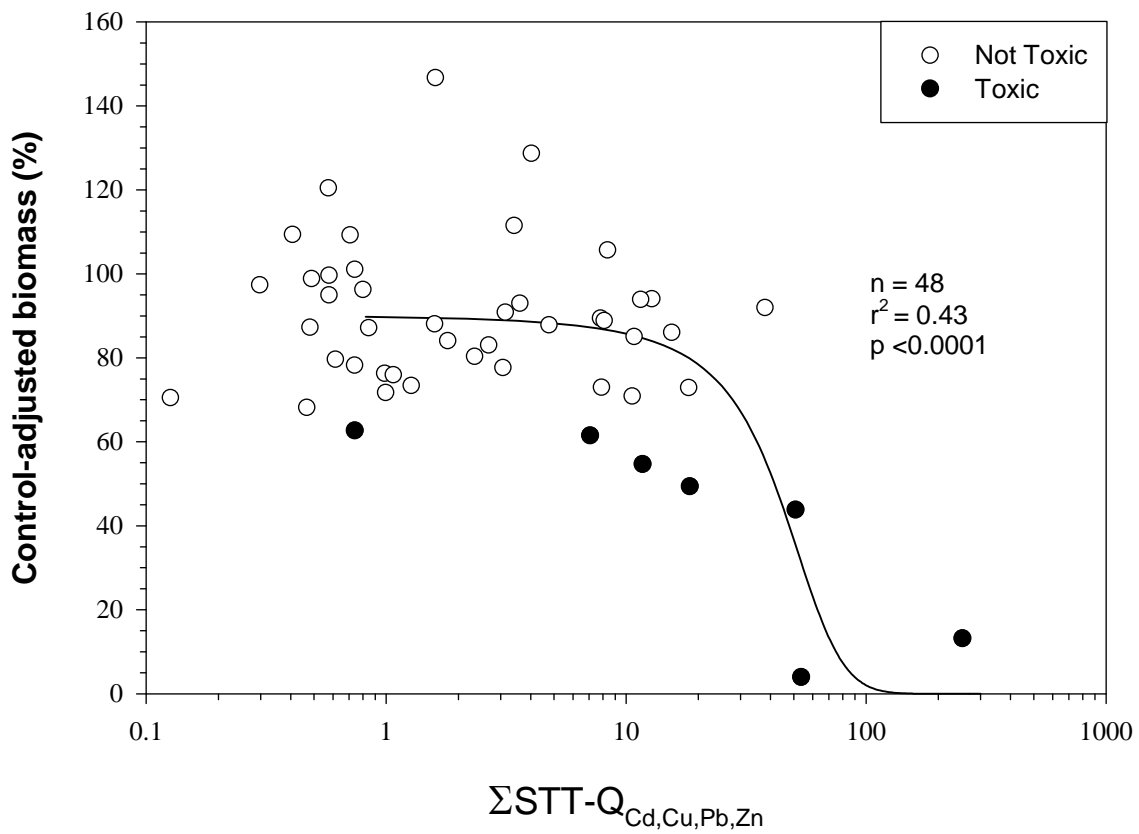
Plot A1-58. Plot illustrating the relationship between the concentration of Mean PEC-Q_{METAL(1%OC)} in sediment (<250 μm) and the control-adjusted biomass of mussels (*Lampsilis siliquoidea*) in 28-d exposures to sediment samples from the Tri-State Mining District.



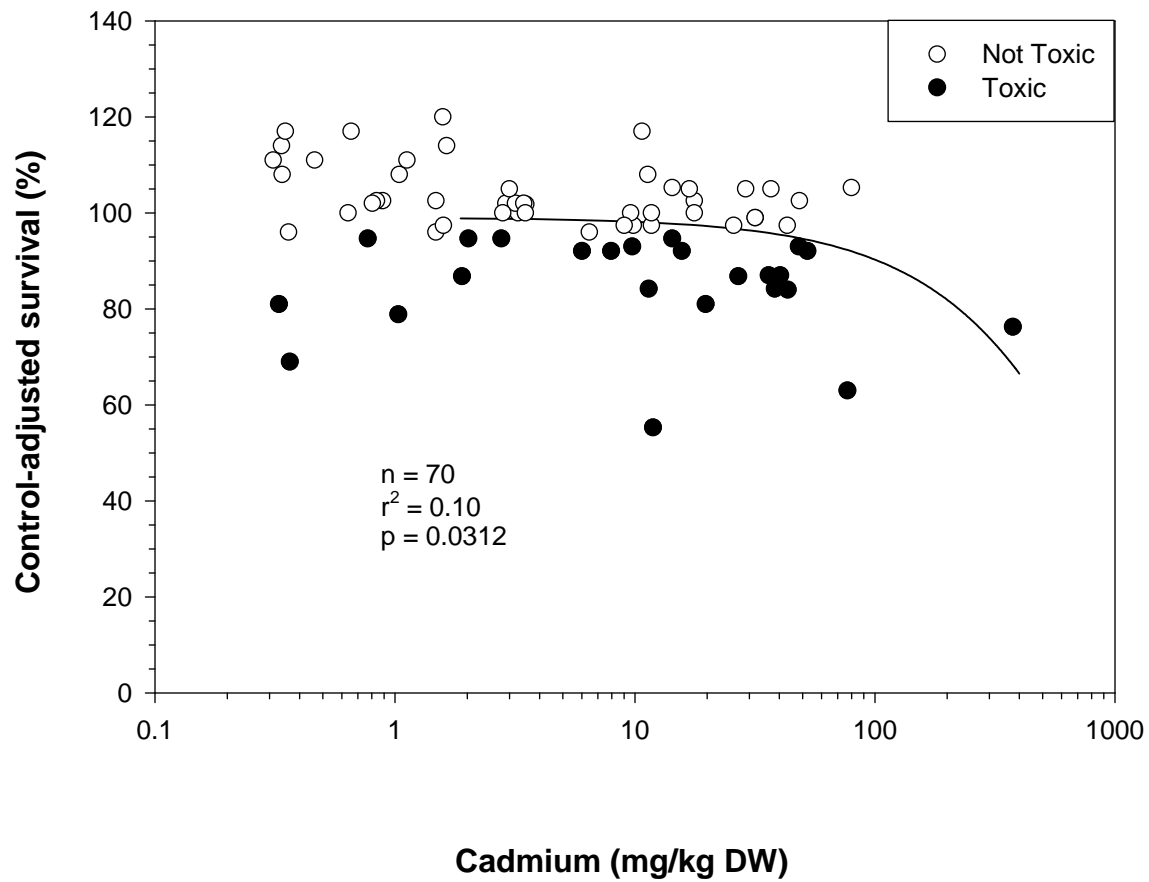
Plot A1-59. Plot illustrating the relationship between the concentration of $\sum\text{PEC-Q}_{\text{Cd,Pb,Zn}}$ in sediment (<250 μm) and the control-adjusted biomass of mussels (*Lampsilis siliquoidea*) in 28-d exposures to sediment samples from the Tri-State Mining District.



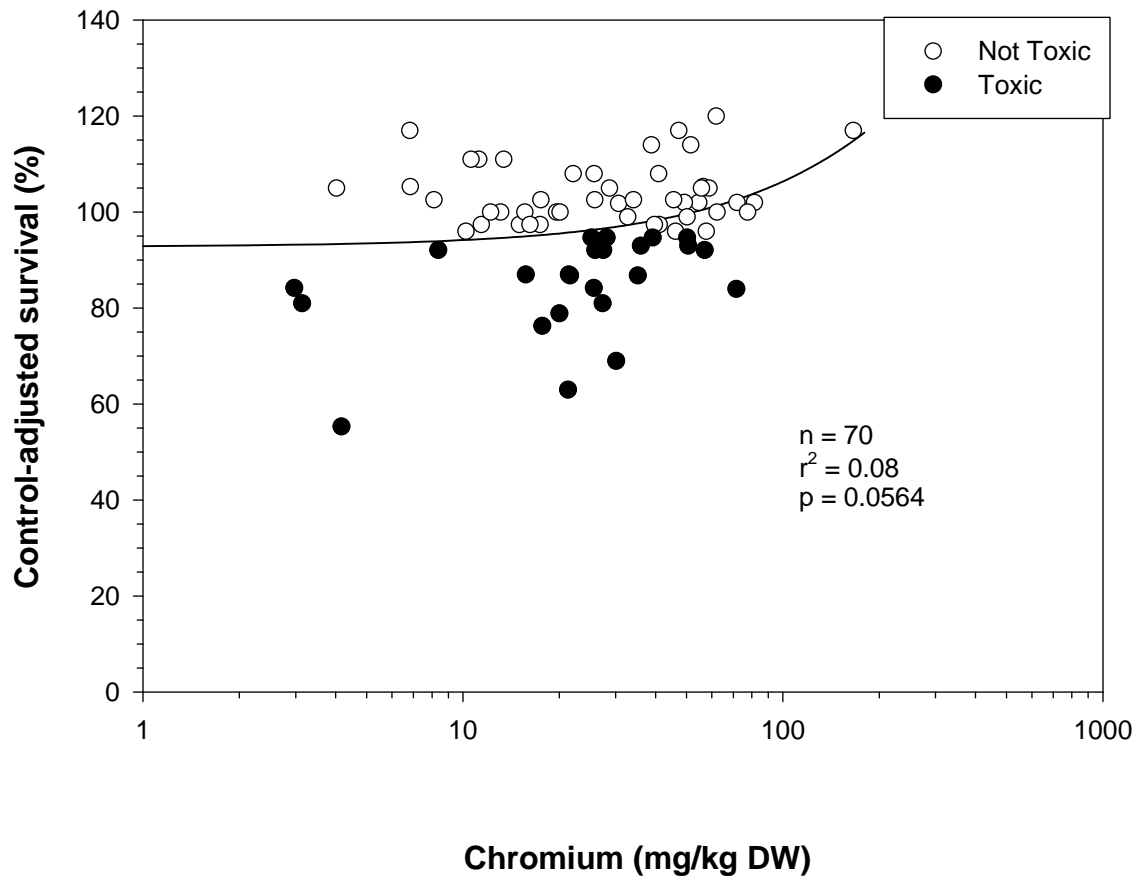
Plot A1-60. Plot illustrating the relationship between the concentration of Σ STT-Q_{Cd,Cu,Pb,Zn} in sediment (<250 μ m) and the control-adjusted biomass of mussels (*Lampsilis siliquoidea*) in 28-d exposures to sediment samples from the Tri-State Mining District.



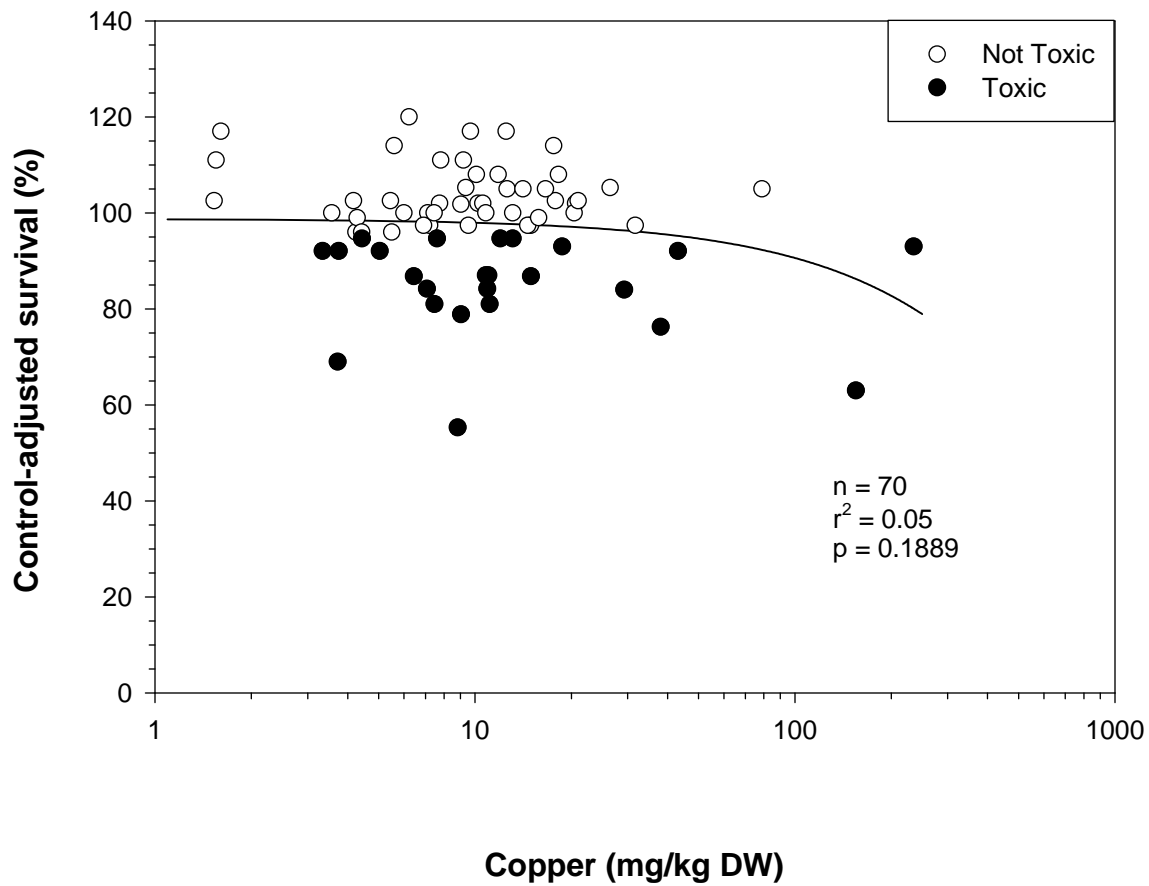
Plot A1-61. Plot illustrating the relationship between the concentration of cadmium (mg/kg DW) in sediment (<2 mm) and the control-adjusted survival of midges (*Chironomus dilutus*) in 10-d exposures to sediment samples from the Tri-State Mining District.



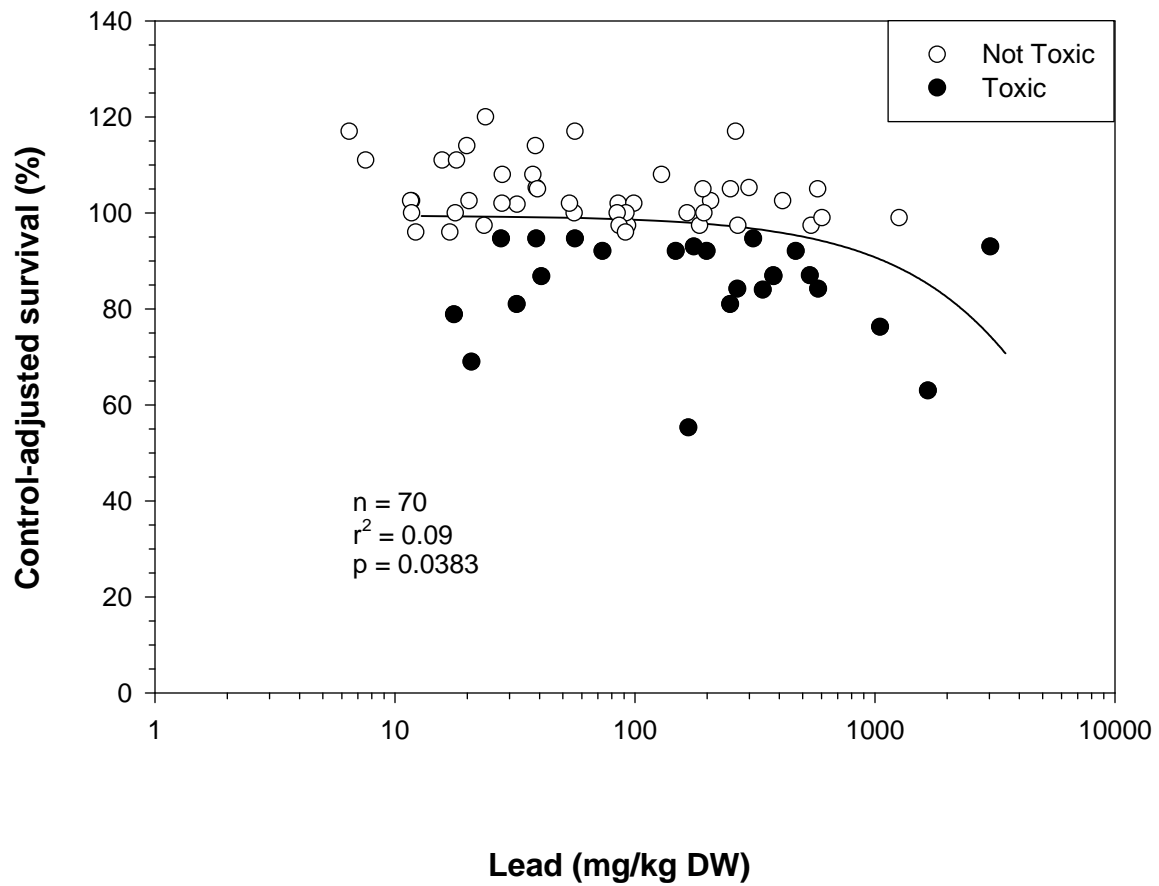
Plot A1-62. Plot illustrating the relationship between the concentration of chromium (mg/kg DW) in sediment (<2 mm) and the control-adjusted survival of midges (*Chironomus dilutus*) in 10-d exposures to sediment samples from the Tri-State Mining District.



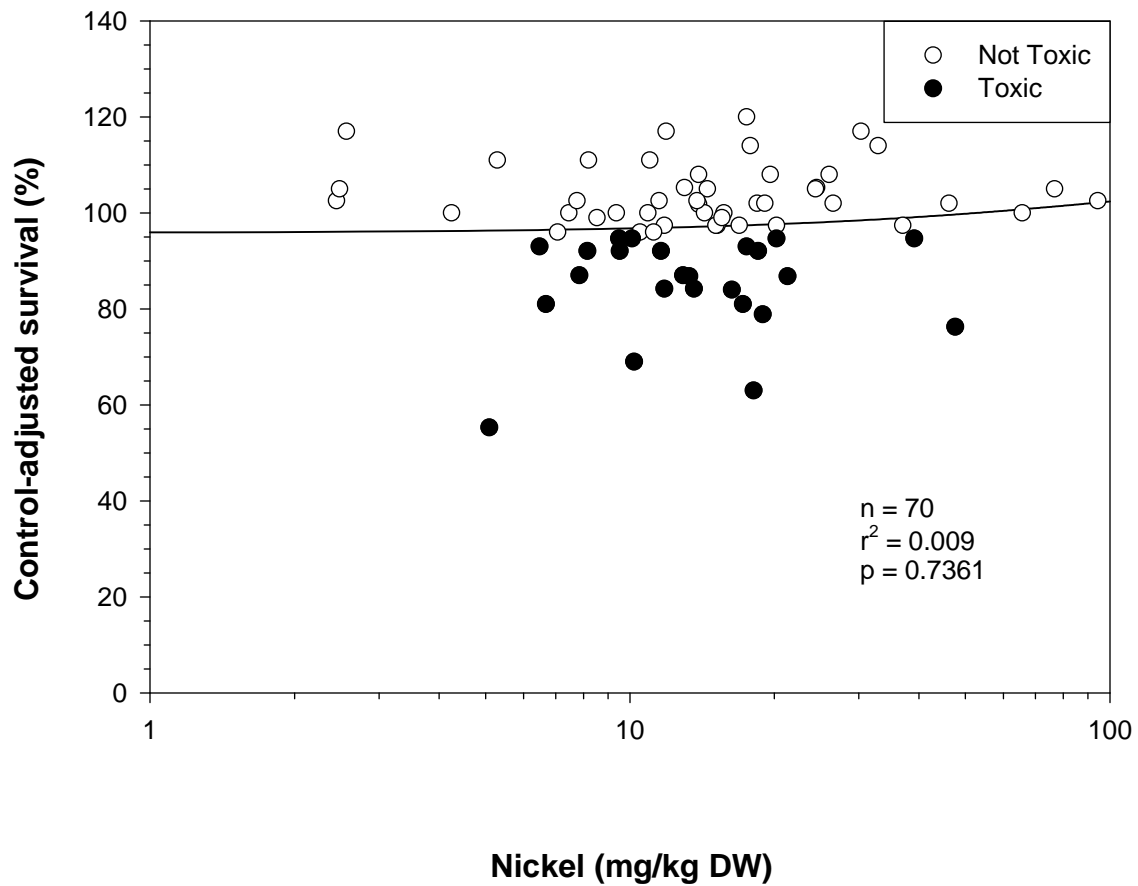
Plot A1-63. Plot illustrating the relationship between the concentration of copper (mg/kg DW) in sediment (<2 mm) and the control-adjusted survival of midges (*Chironomus dilutus*) in 10-d exposures to sediment samples from the Tri-State Mining District.



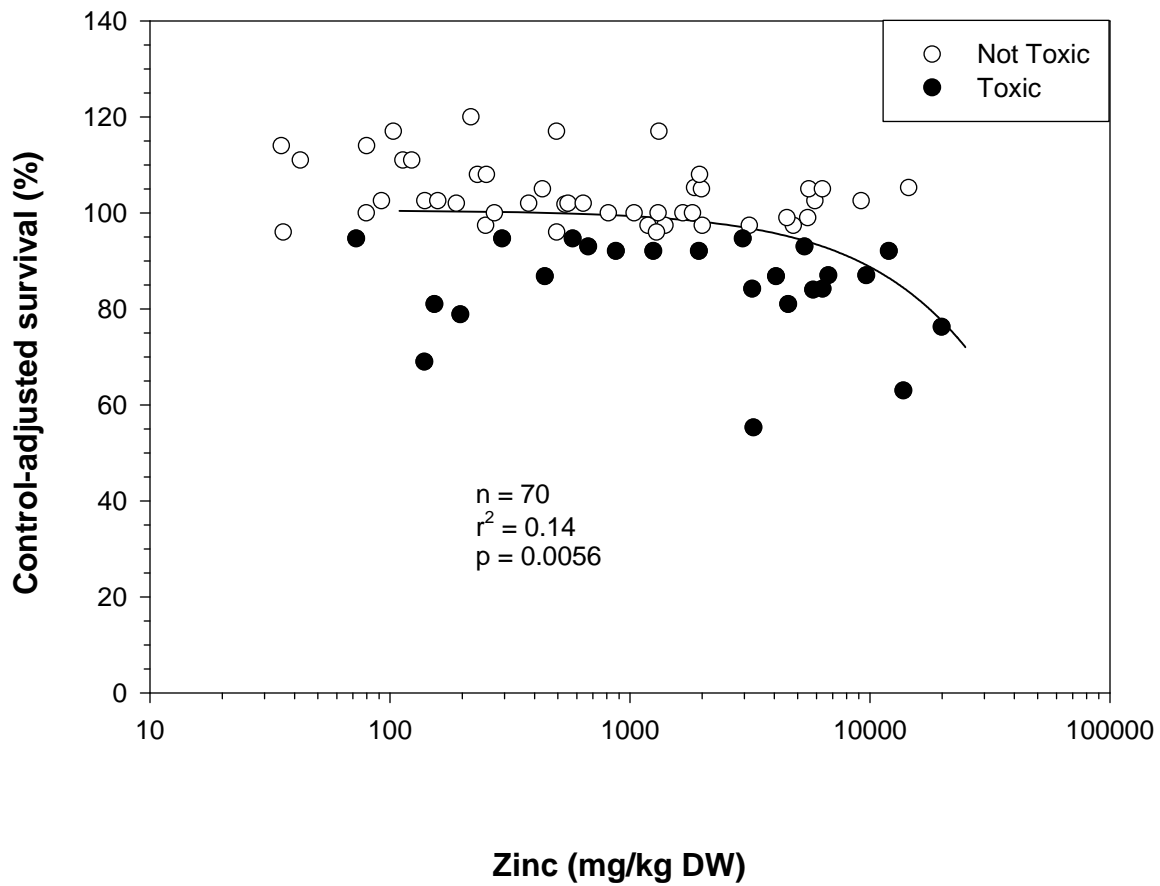
Plot A1-64. Plot illustrating the relationship between the concentration of lead (mg/kg DW) in sediment (<2 mm) and the control-adjusted survival of midges (*Chironomus dilutus*) in 10-d exposures to sediment samples from the Tri-State Mining District.



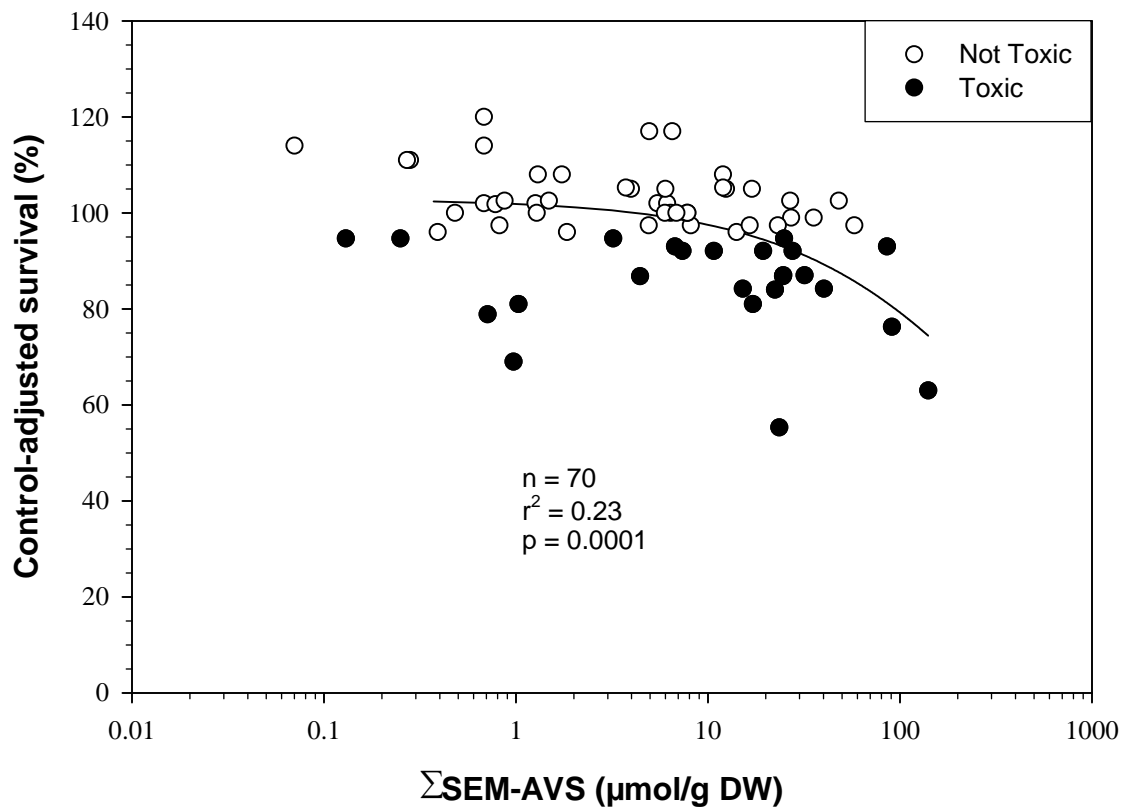
Plot A1-65. Plot illustrating the relationship between the concentration of nickel (mg/kg DW) in sediment (<2 mm) and the control-adjusted survival of midges (*Chironomus dilutus*) in 10-d exposures to sediment samples from the Tri-State Mining District.



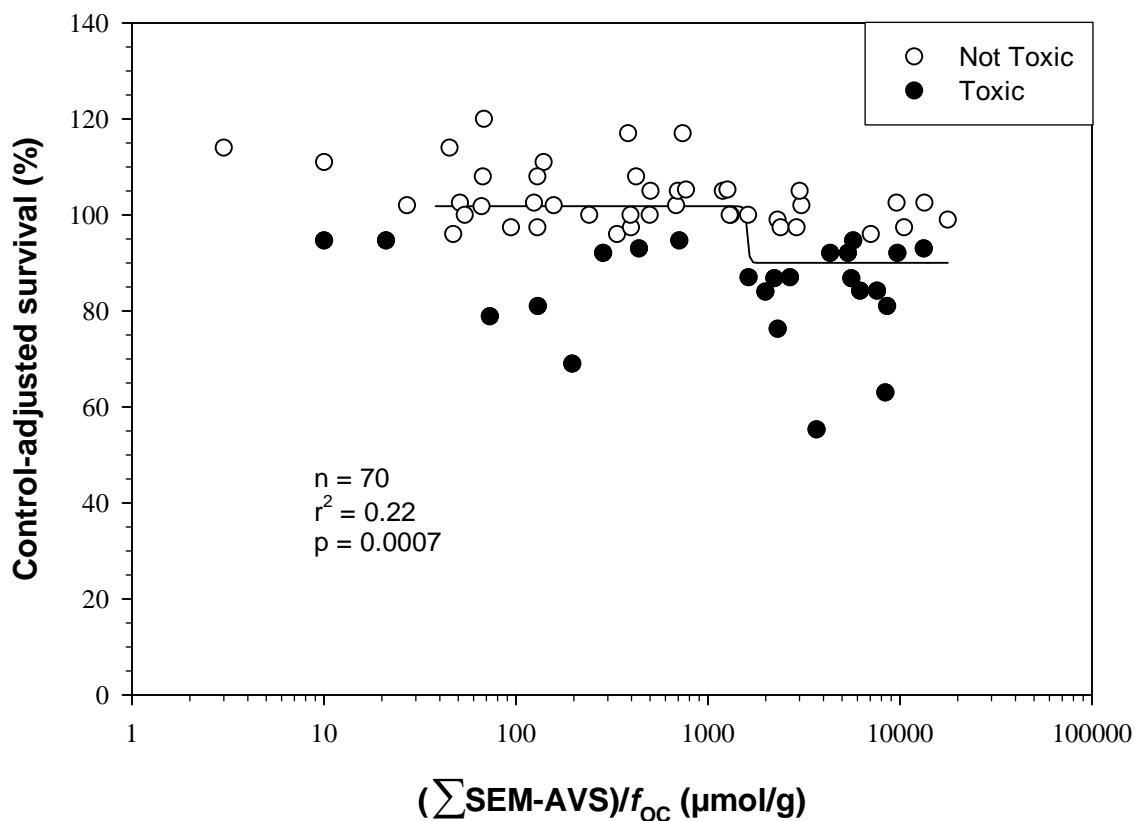
Plot A1-66. Plot illustrating the relationship between the concentration of zinc (mg/kg DW) in sediment (<2 mm) and the control-adjusted survival of midges (*Chironomus dilutus*) in 10-d exposures to sediment samples from the Tri-State Mining District.



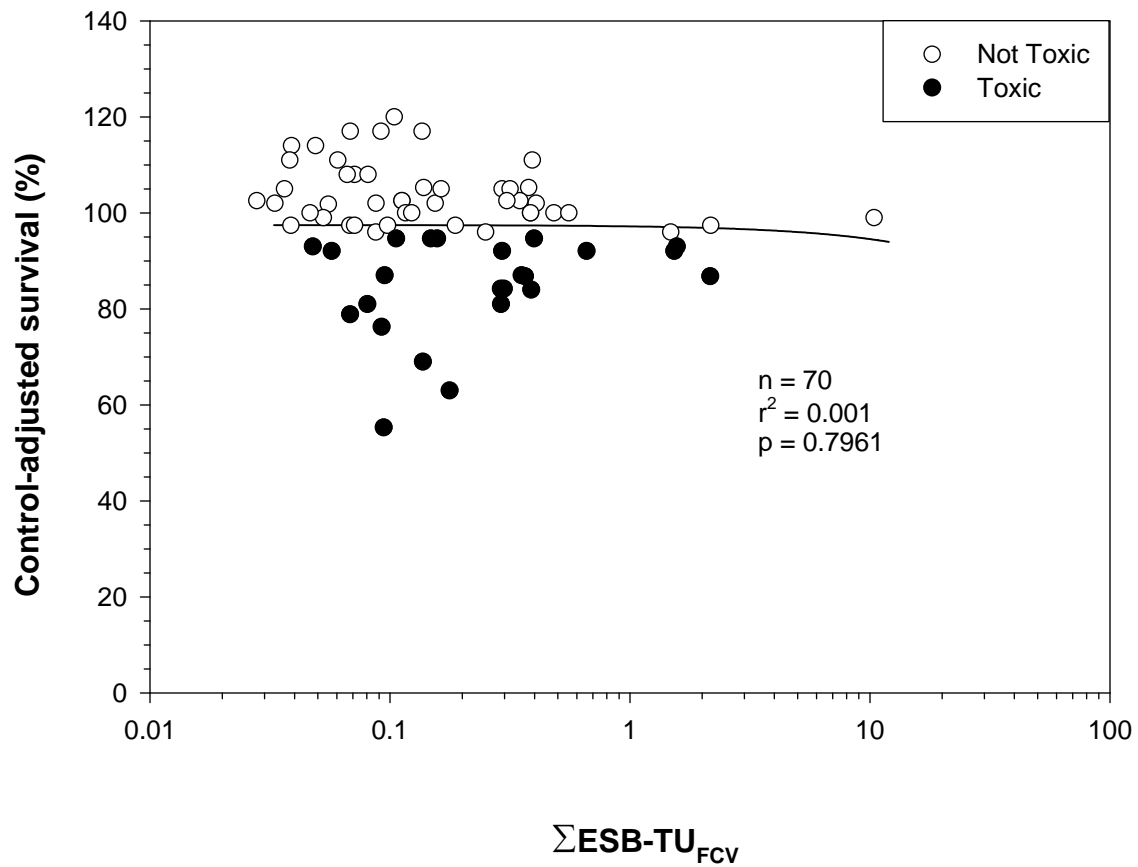
Plot A1-68. Plot illustrating the relationship between the concentration of Σ SEM-AVS ($\mu\text{mol/g DW}$) in sediment (<2 mm) and the control-adjusted survival of midges (*Chironomus dilutus*) in 10-d exposures to sediment samples from the Tri-State Mining District.



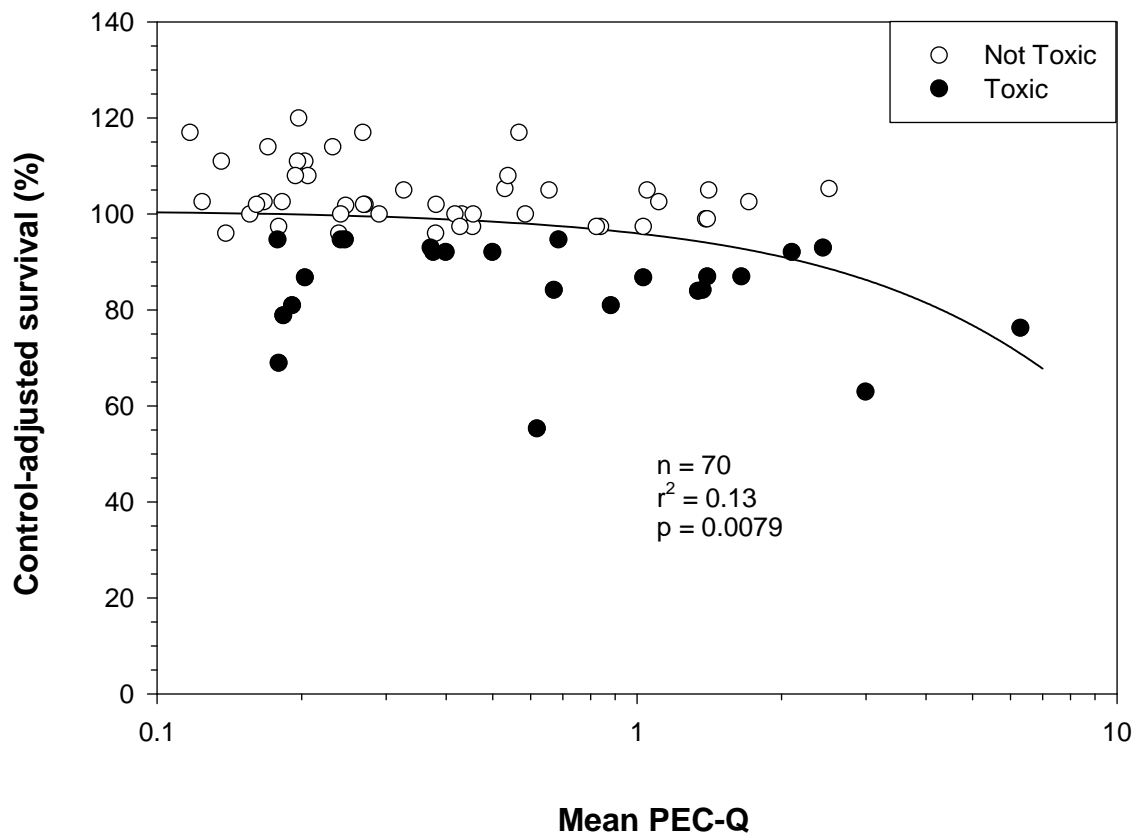
Plot A1-69. Plot illustrating the relationship between the concentration of $(\sum \text{SEM-AVS})/f_{\text{OC}}$ ($\mu\text{mol/g}$) in sediment (<2 mm) and the control-adjusted survival of midges (*Chironomus dilutus*) in 10-d exposures to sediment samples from the Tri-State Mining District.



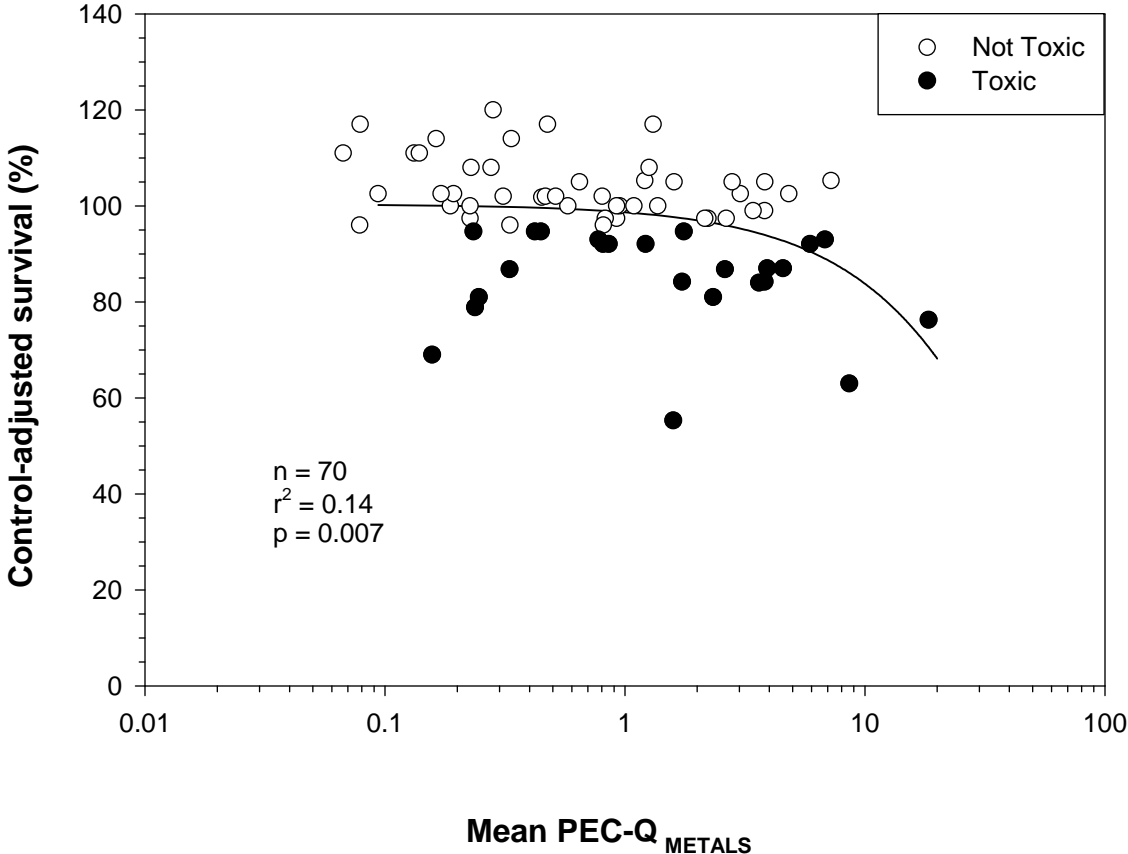
Plot A1-70. Plot illustrating the relationship between the concentration of $\Sigma\text{ESB-TU}_{\text{FCV}}$ in sediment (<2 mm) and the control-adjusted survival of midges (*Chironomus dilutus*) in 10-d exposures to sediment samples from the Tri-State Mining District.



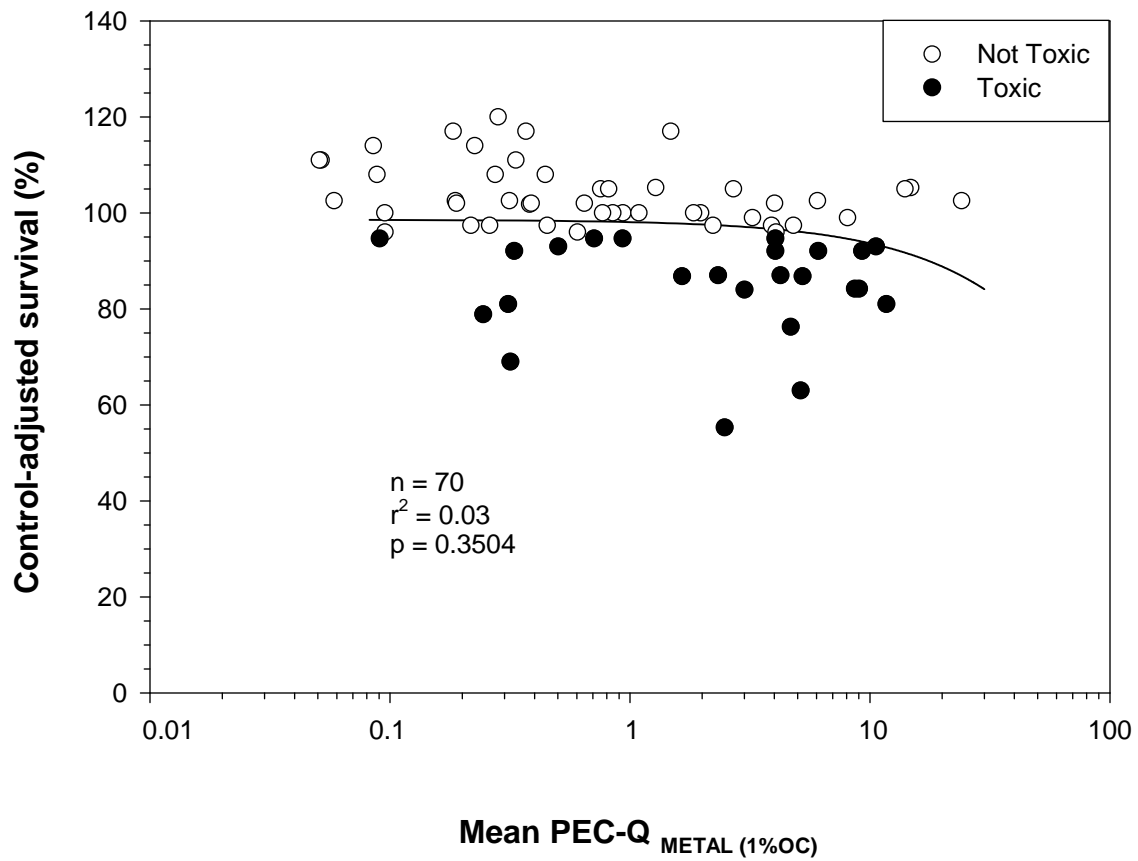
Plot A1-71. Plot illustrating the relationship between the concentration of Mean PEC-Q in sediment (<2 mm) and the control-adjusted survival of midges (*Chironomus dilutus*) in 10-d exposures to sediment samples from the Tri-State Mining District.



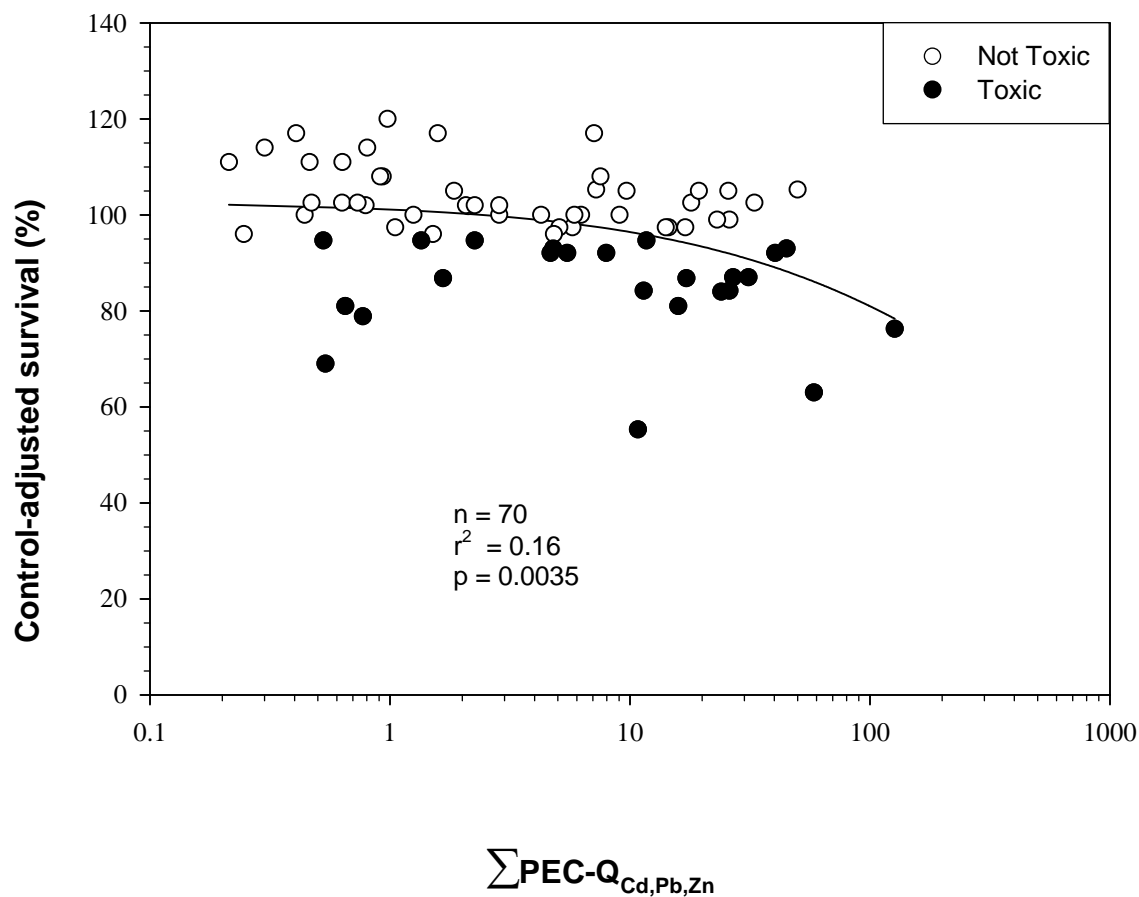
Plot A1-72. Plot illustrating the relationship between the concentration of Mean PEC-Q_{METALS} in sediment (<2 mm) and the control-adjusted survival of midges (*Chironomus dilutus*) in 10-d exposures to sediment samples from the Tri-State Mining District.



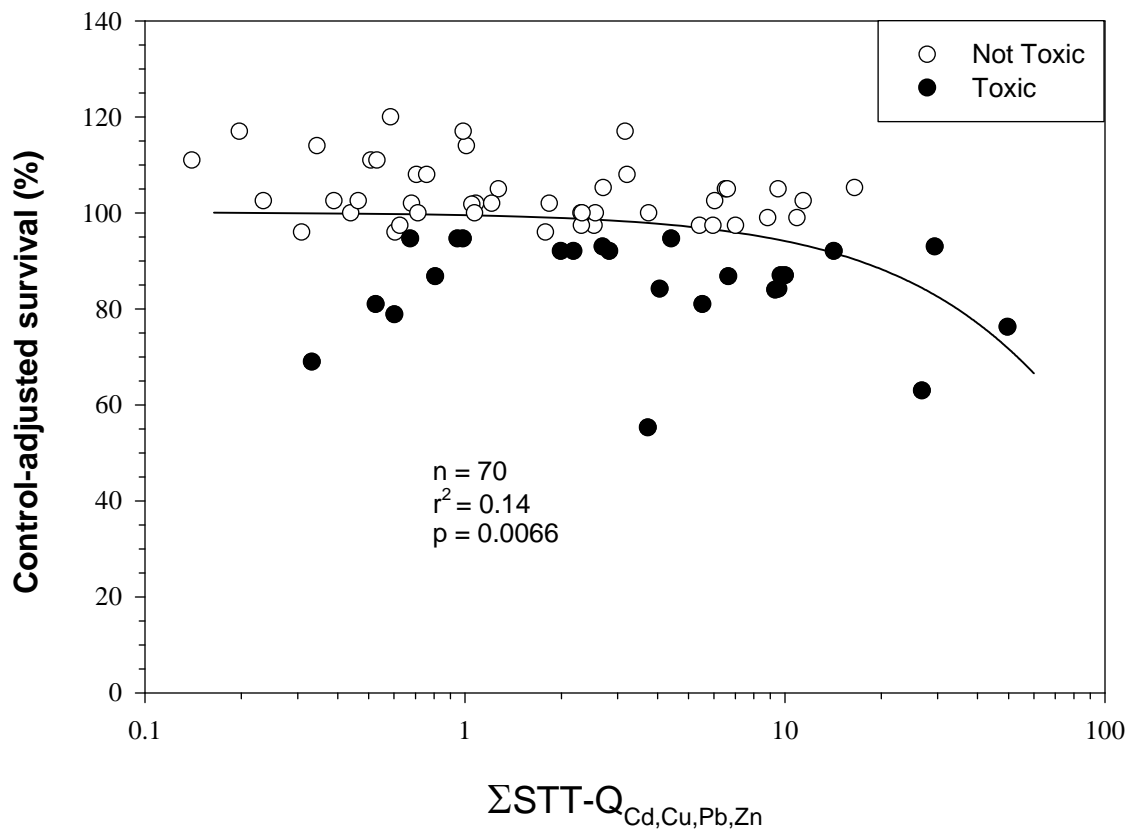
Plot A1-73. Plot illustrating the relationship between the concentration of Mean PEC-Q_{METAL(1%OC)} in sediment (<2 mm) and the control-adjusted survival of midges (*Chironomus dilutus*) in 10-d exposures to sediment samples from the Tri-State Mining District.



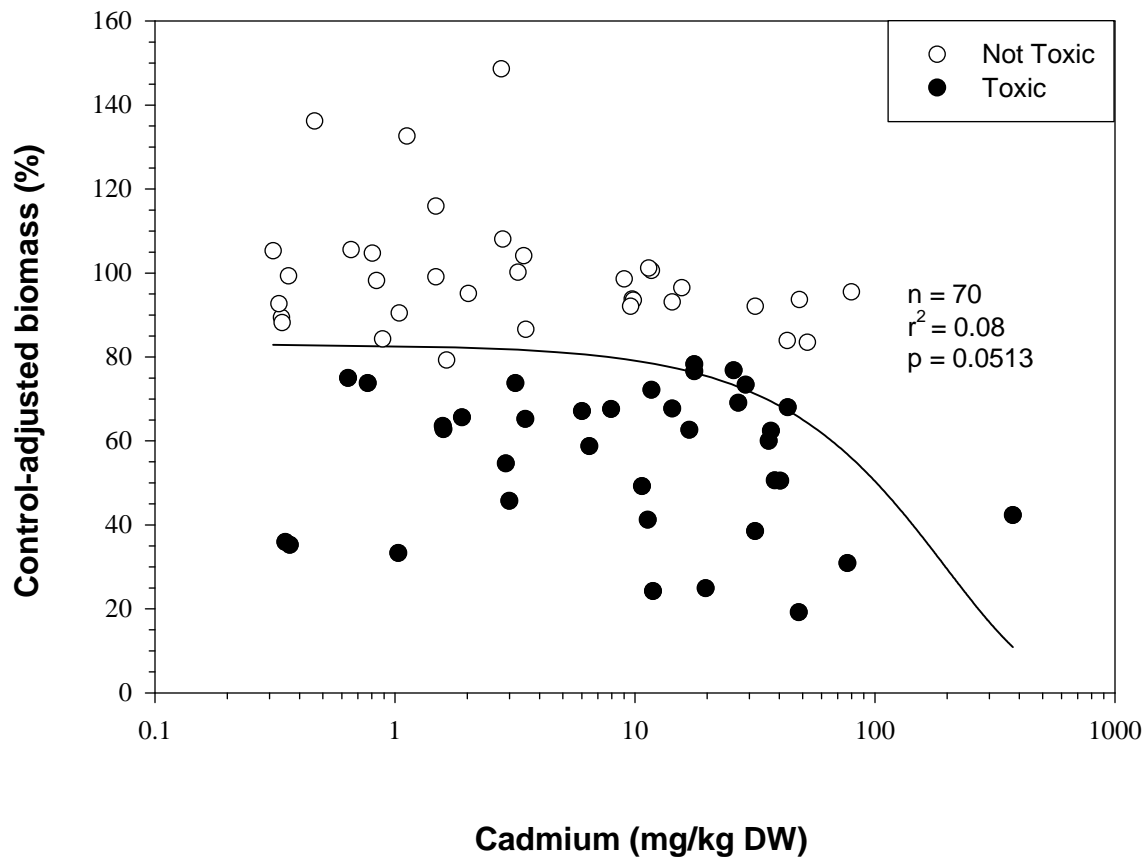
Plot A1-74. Plot illustrating the relationship between the concentration of $\sum\text{PEC-Q}_{\text{Cd,Pb,Zn}}$ in sediment (<2 mm) and the control-adjusted survival of midges (*Chironomus dilutus*) in 10-d exposures to sediment samples from the Tri-State Mining District.



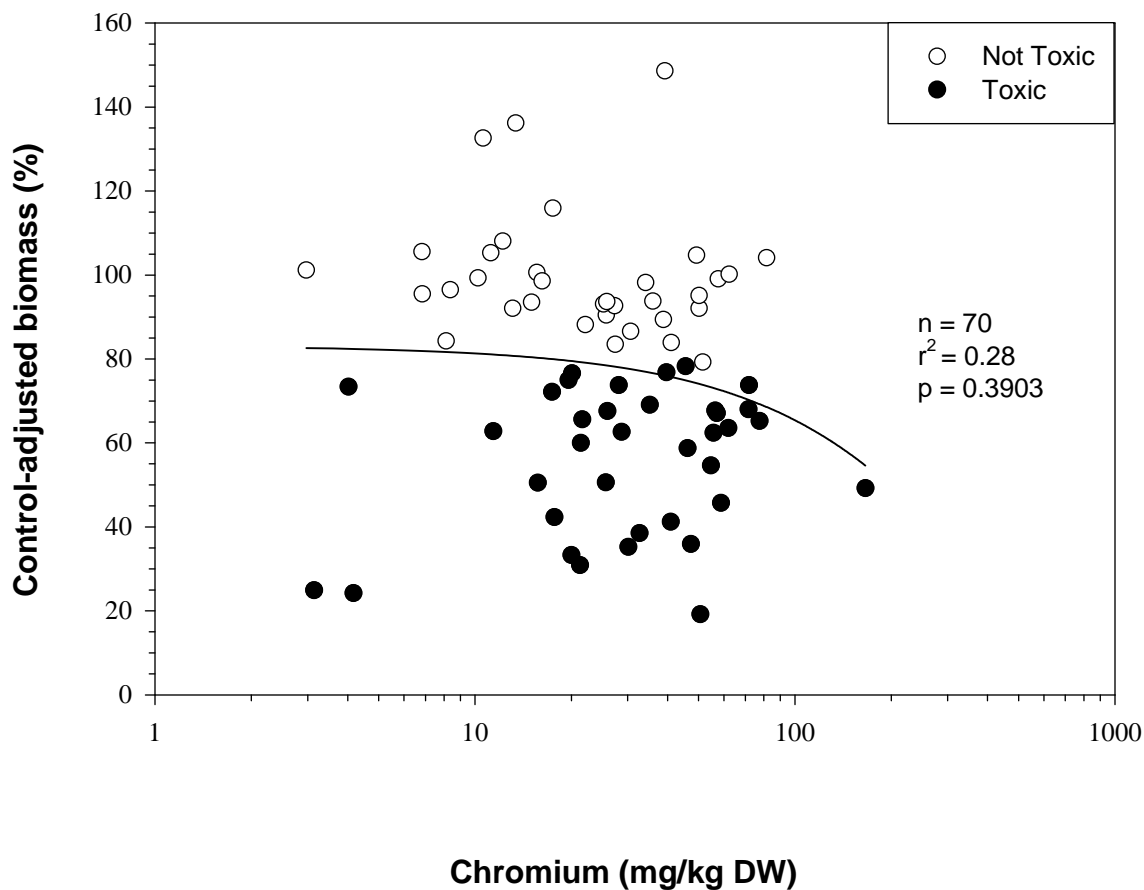
Plot A1-75. Plot illustrating the relationship between the concentration of $\Sigma\text{STT-Q}_{\text{Cd,Cu,Pb,Zn}}$ in sediment (<2 mm) and the control-adjusted survival of midges (*Chironomus dilutus*) in 28-d exposures to sediment samples from the Tri-State Mining District.



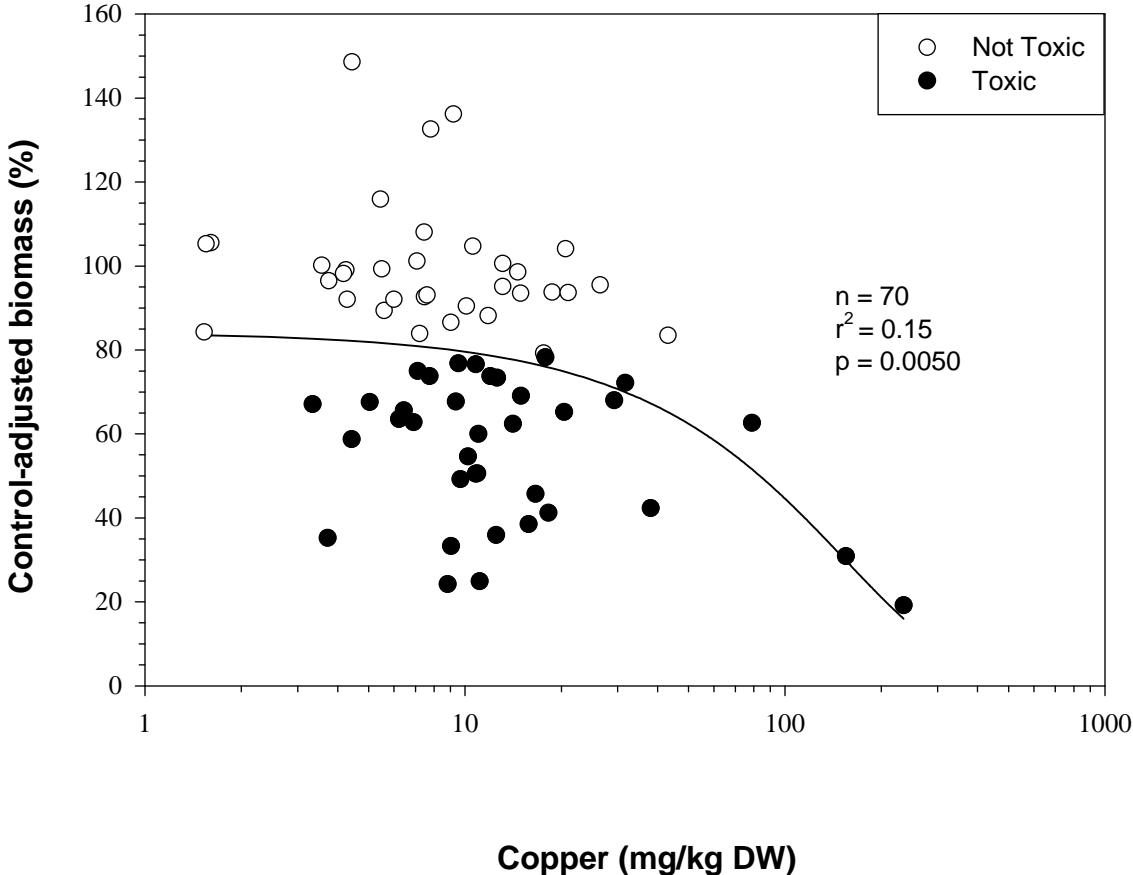
Plot A1-76. Plot illustrating the relationship between the concentration of cadmium (mg/kg DW) in sediment (<2 mm) and the control-adjusted biomass of midges (*Chironomus dilutus*) in 10-d exposures to sediment samples from the Tri-State Mining District.



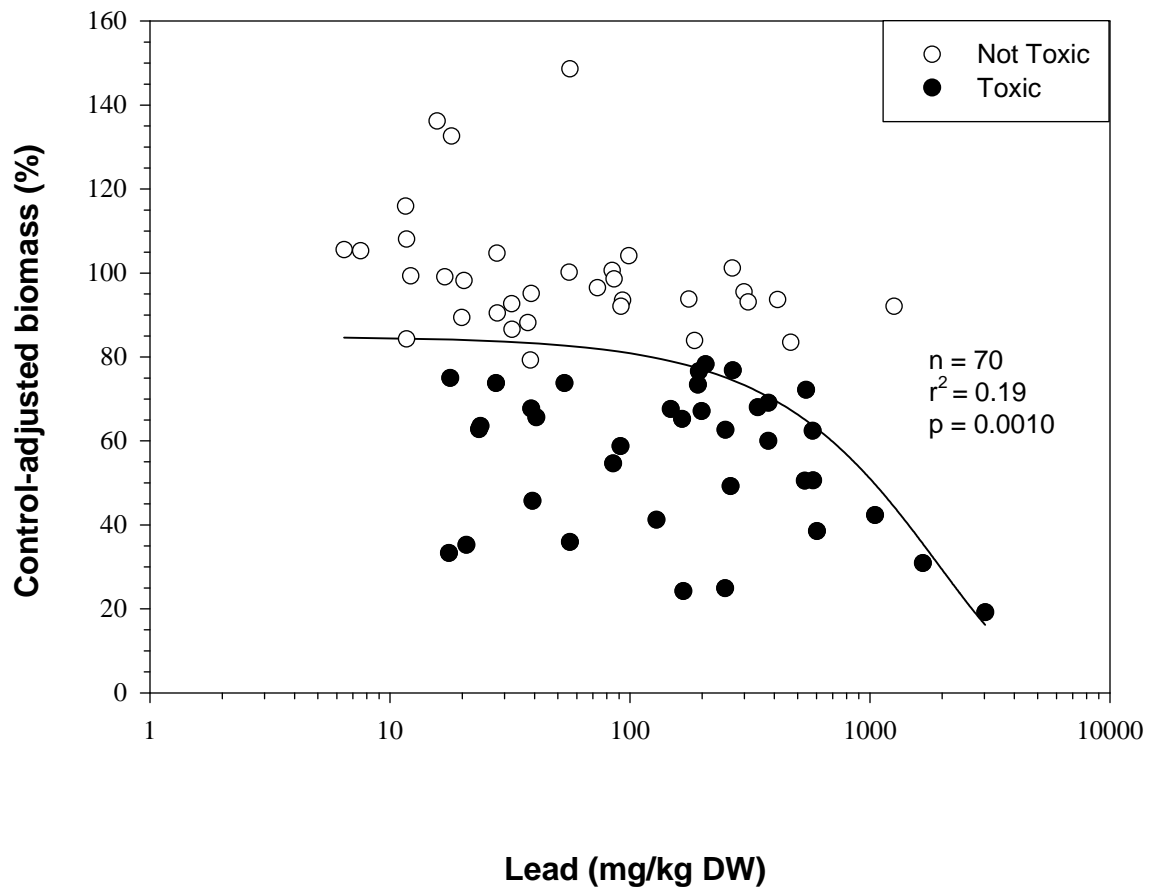
Plot A1-77. Plot illustrating the relationship between the concentration of chromium (mg/kg DW) in sediment (<2 mm) and the control-adjusted biomass of midges (*Chironomus dilutus*) in 10-d exposures to sediment samples from the Tri-State Mining District.



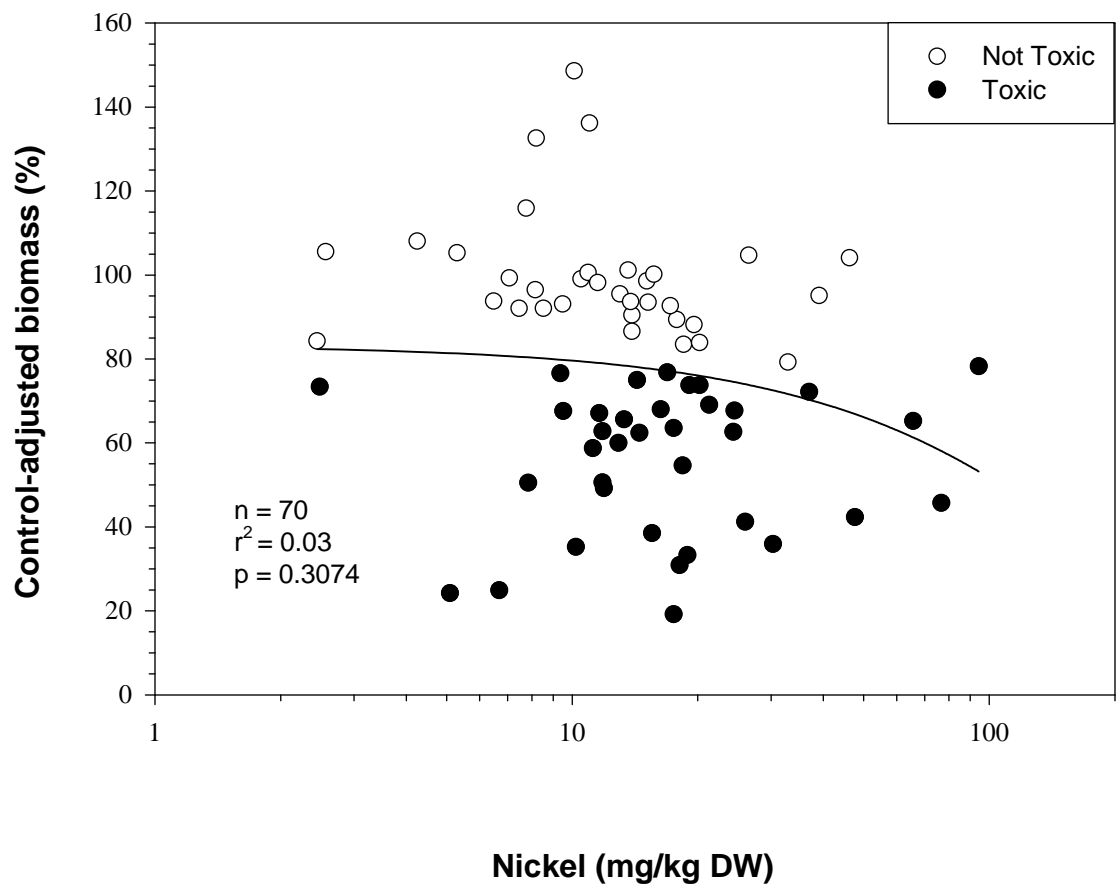
Plot A1-78. Plot illustrating the relationship between the concentration of copper (mg/kg DW) in sediment (<2 mm) and the control-adjusted biomass of midges (*Chironomus dilutus*) in 10-d exposures to sediment samples from the Tri-State Mining District.



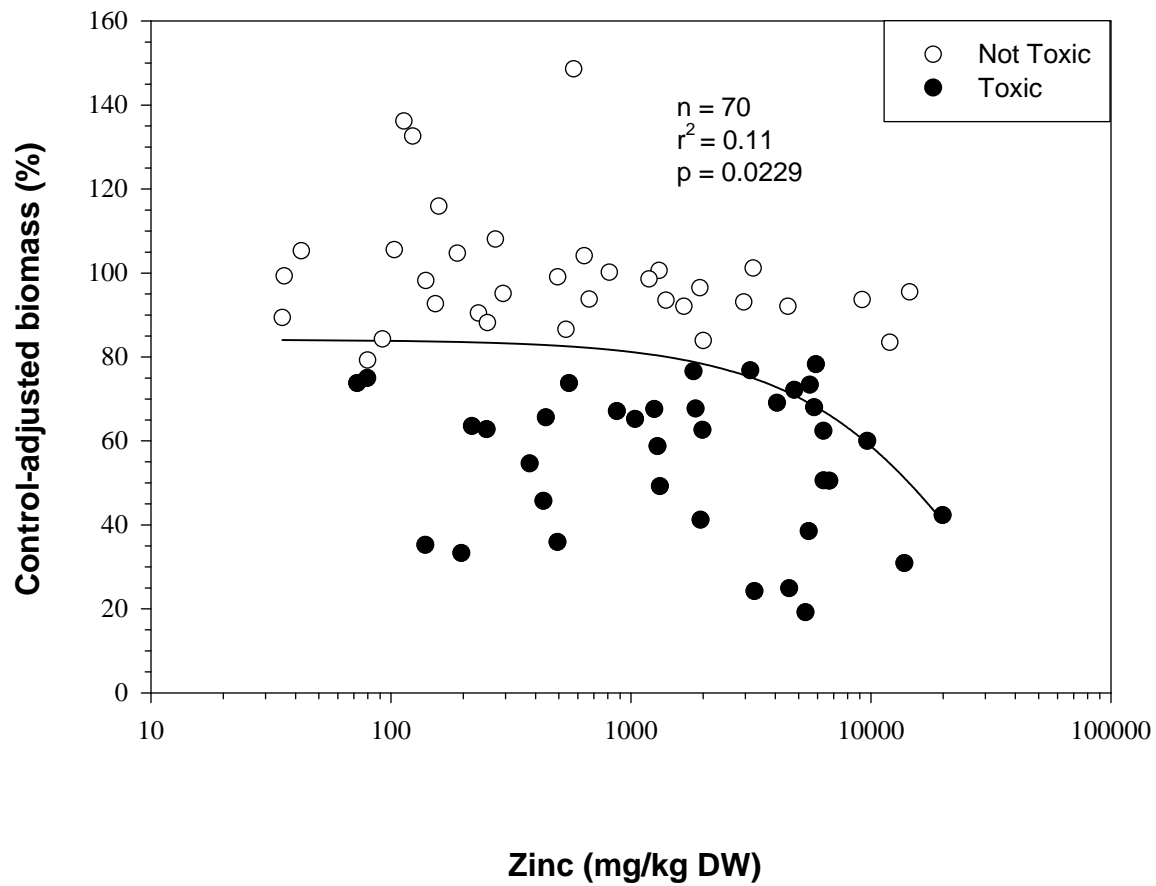
Plot A1-79. Plot illustrating the relationship between the concentration of lead (mg/kg DW) in sediment (<2 mm) and the control-adjusted biomass of midges (*Chironomus dilutus*) in 10-d exposures to sediment samples from the Tri-State Mining District.



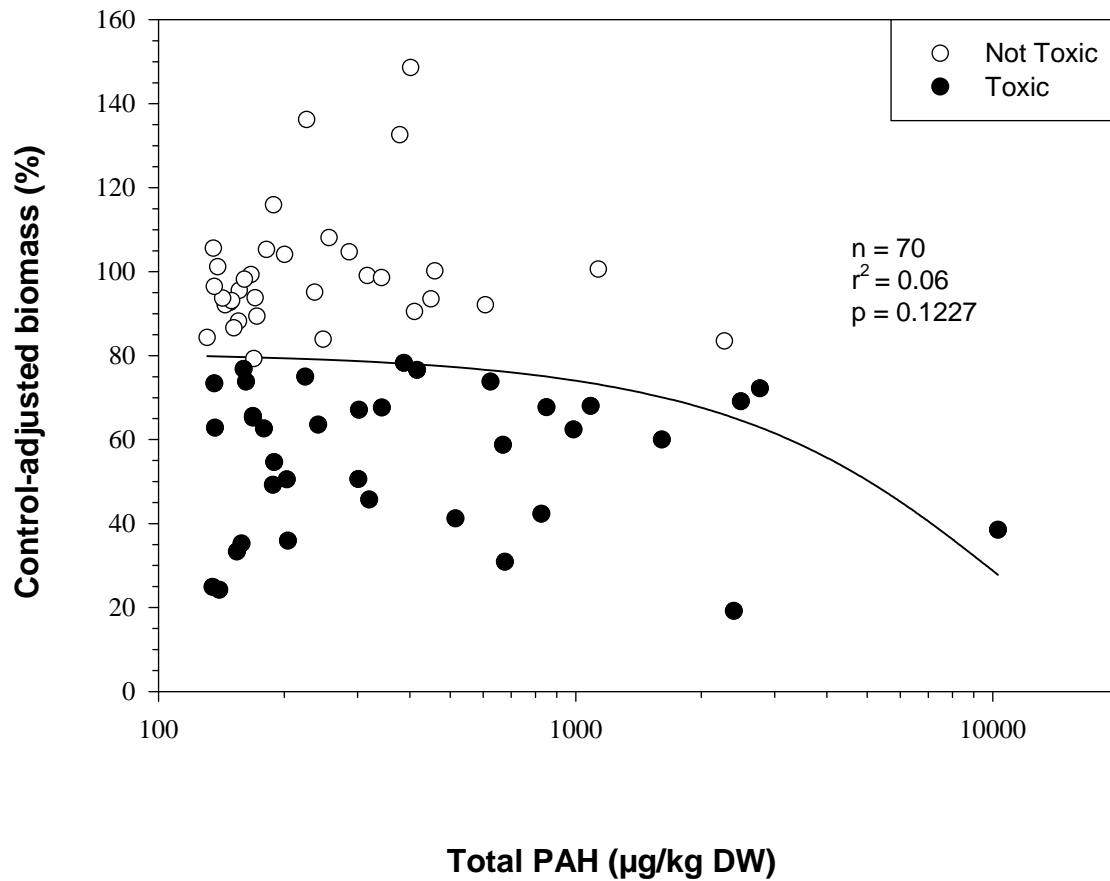
Plot A1-80. Plot illustrating the relationship between the concentration of nickel (mg/kg DW) in sediment (<2 mm) and the control-adjusted biomass of midges (*Chironomus dilutus*) in 10-d exposures to sediment samples from the Tri-State Mining District.



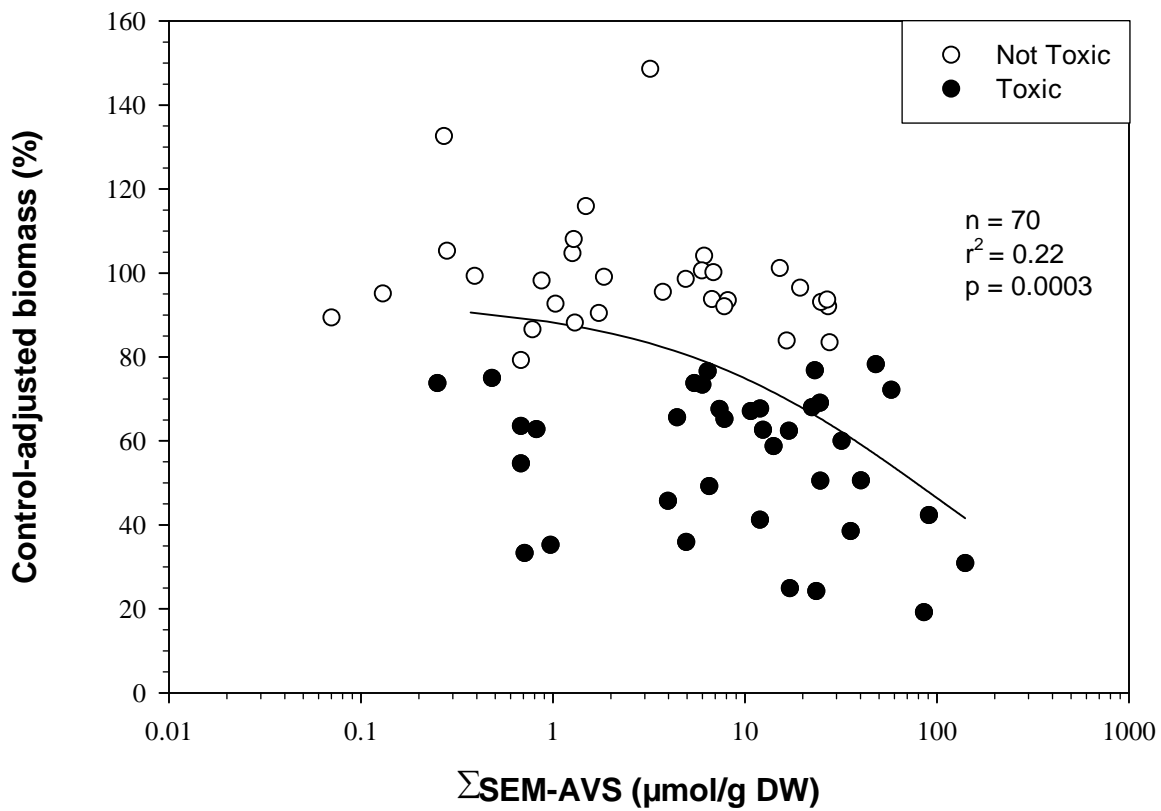
Plot A1-81. Plot illustrating the relationship between the concentration of zinc (mg/kg DW) in sediment (<2 mm) and the control-adjusted biomass of midges (*Chironomus dilutus*) in 10-d exposures to sediment samples from the Tri-State Mining District.



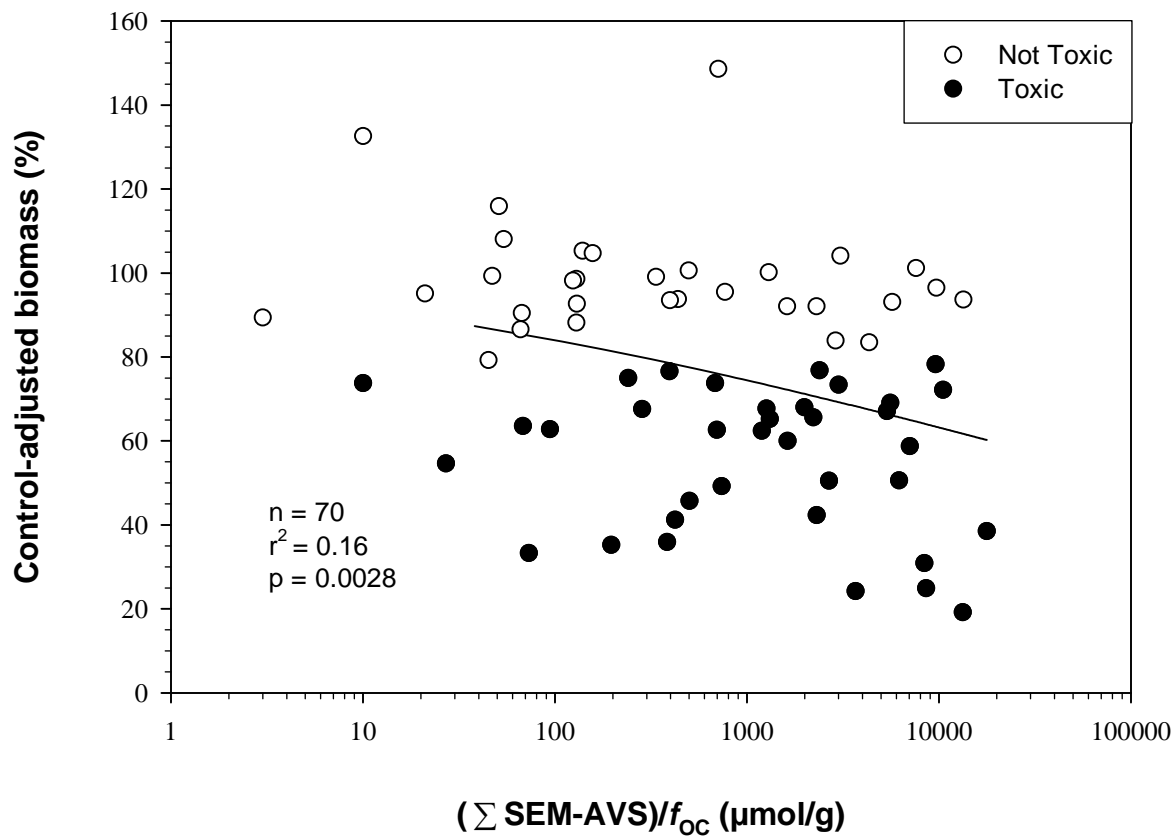
Plot A1-82. Plot illustrating the relationship between the concentration of total PAH ($\mu\text{g}/\text{kg DW}$) in sediment (<2 mm) and the control-adjusted biomass of midges (*Chironomus dilutus*) in 10-d exposures to sediment samples from the Tri-State Mining District.



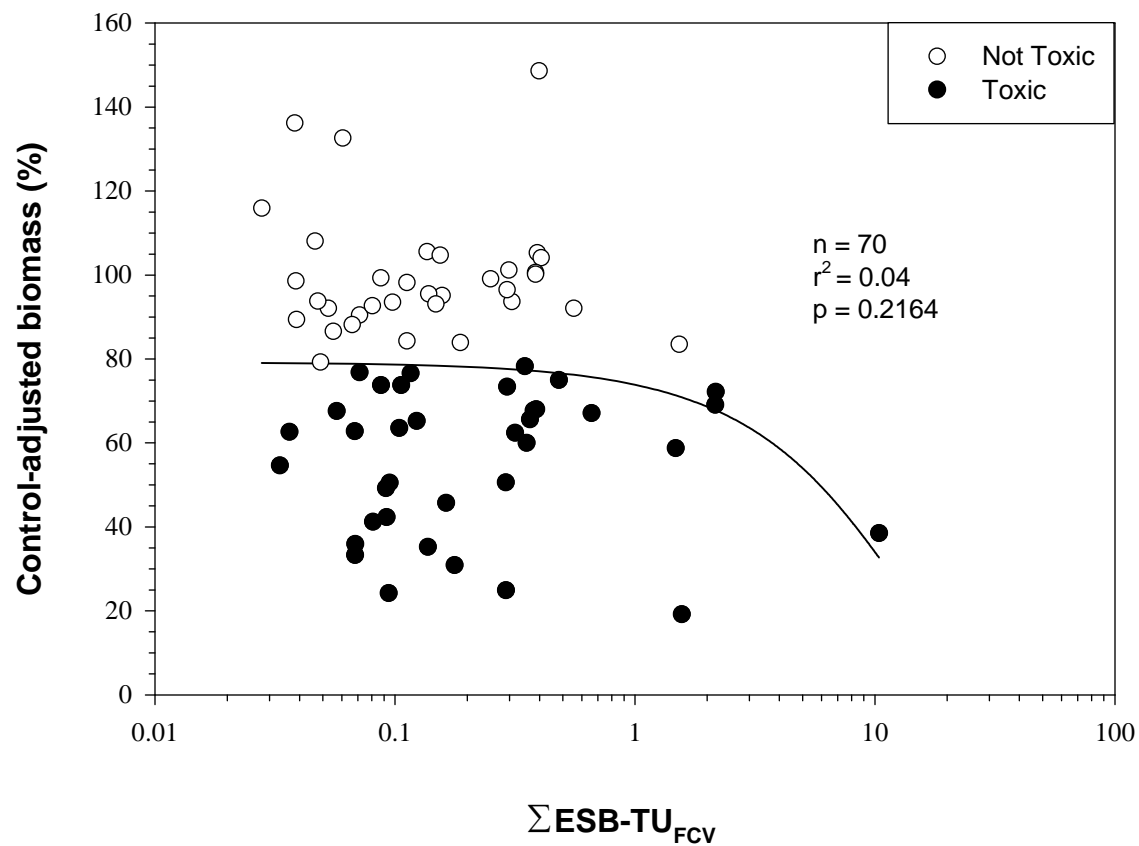
Plot A1-83. Plot illustrating the relationship between the concentration of Σ SEM-AVS ($\mu\text{mol/g DW}$) in sediment (<2 mm) and the control-adjusted biomass of midges (*Chironomus dilutus*) in 10-d exposures to sediment samples from the Tri-State Mining District.



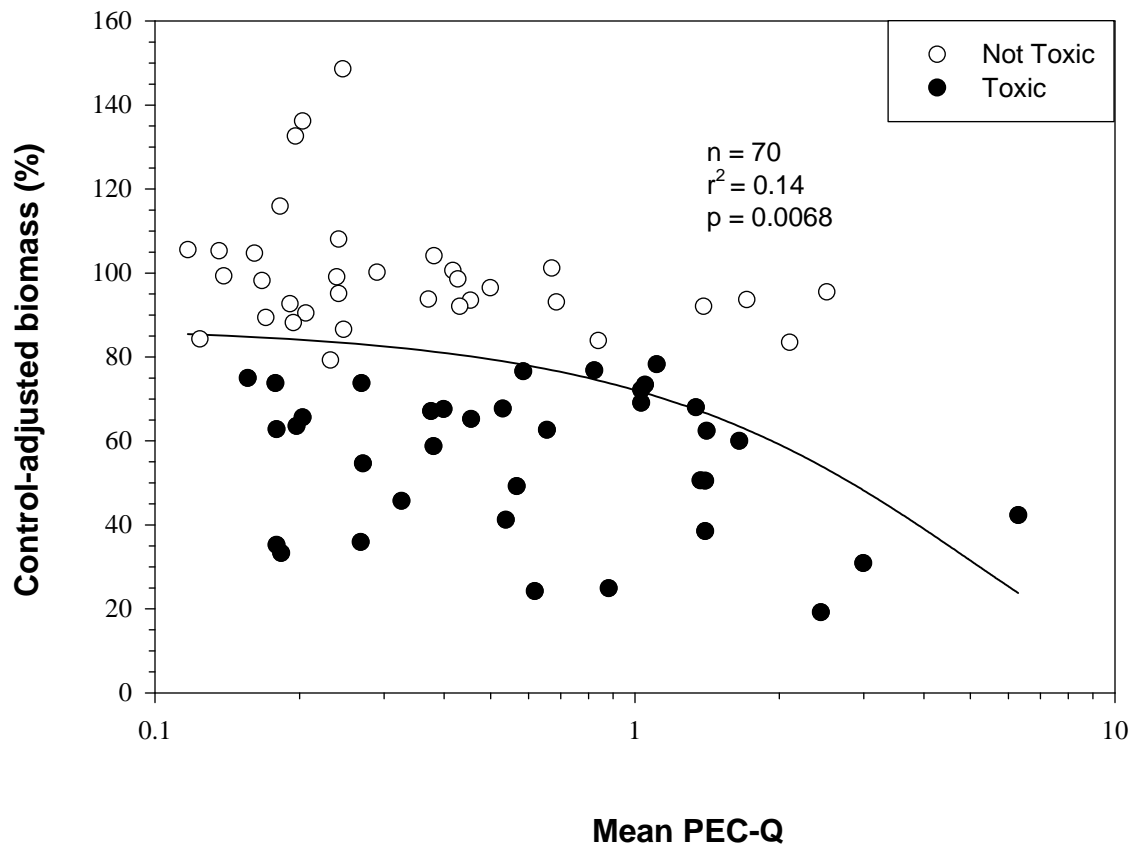
Plot A1-84. Plot illustrating the relationship between the concentration of $(\sum \text{SEM-AVS})/f_{\text{OC}}$ ($\mu\text{mol/g}$) in sediment (<2 mm) and the control-adjusted biomass of midges (*Chironomus dilutus*) in 10-d exposures to sediment samples from the Tri-State Mining District.



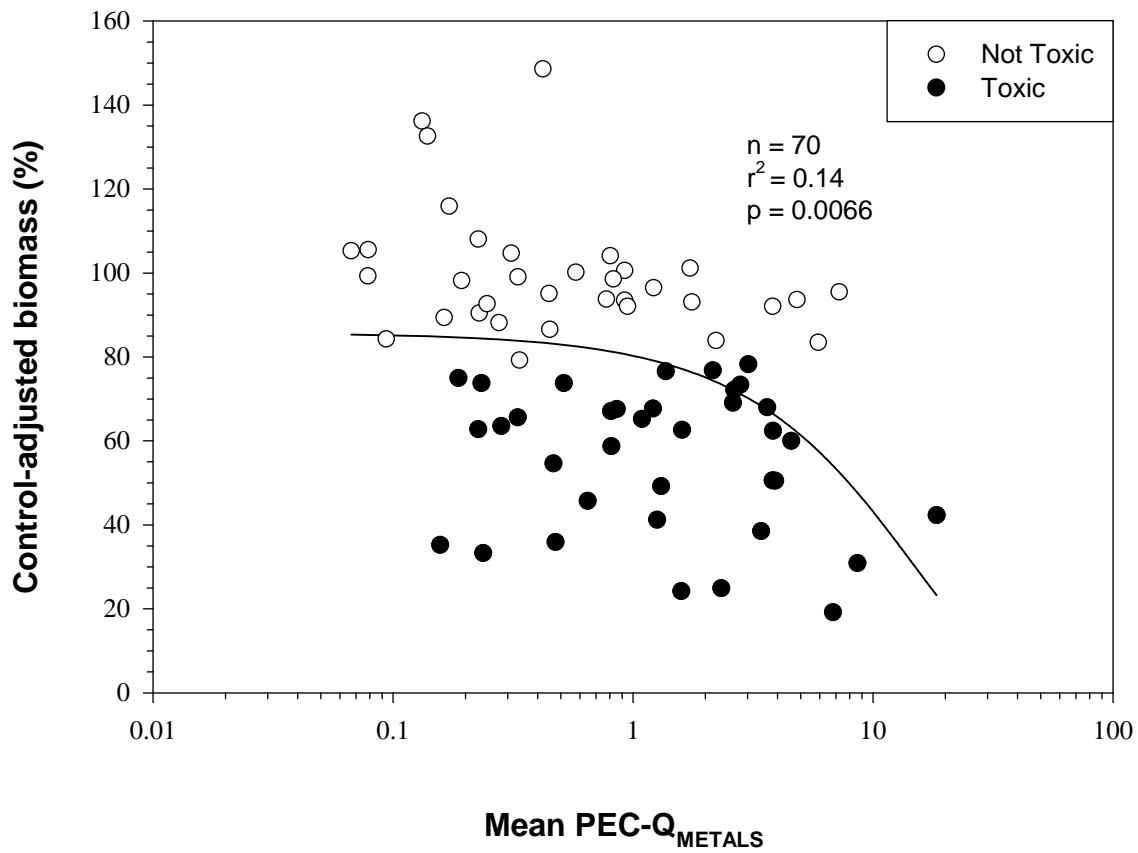
Plot A1-85. Plot illustrating the relationship between the concentration of $\Sigma\text{ESB-TU}_{\text{FCV}}$ in sediment (<2 mm) and the control-adjusted biomass of midges (*Chironomus dilutus*) in 10-d exposures to sediment samples from the Tri-State Mining District.



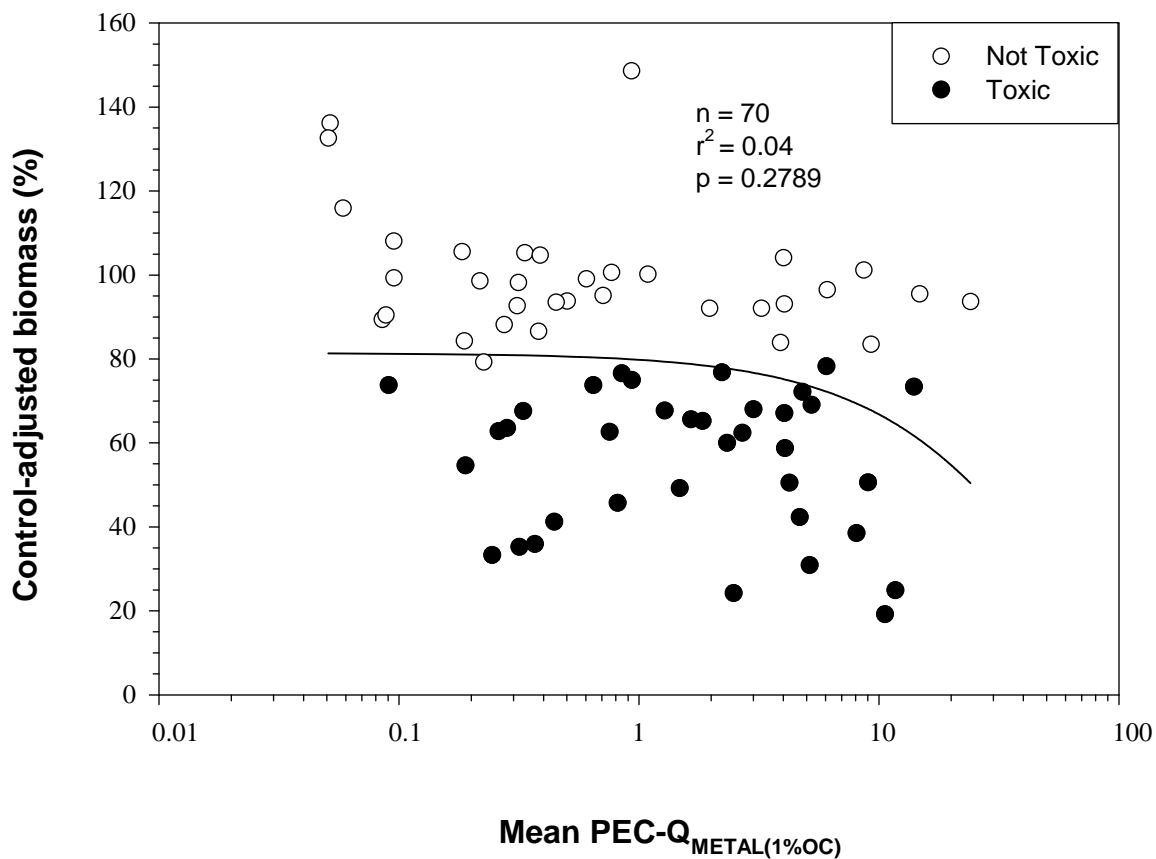
Plot A1-86. Plot illustrating the relationship between the concentration of Mean PEC-Q in sediment (<2 mm) and the control-adjusted biomass of midges (*Chironomus dilutus*) in 10-d exposures to sediment samples from the Tri-State Mining District.



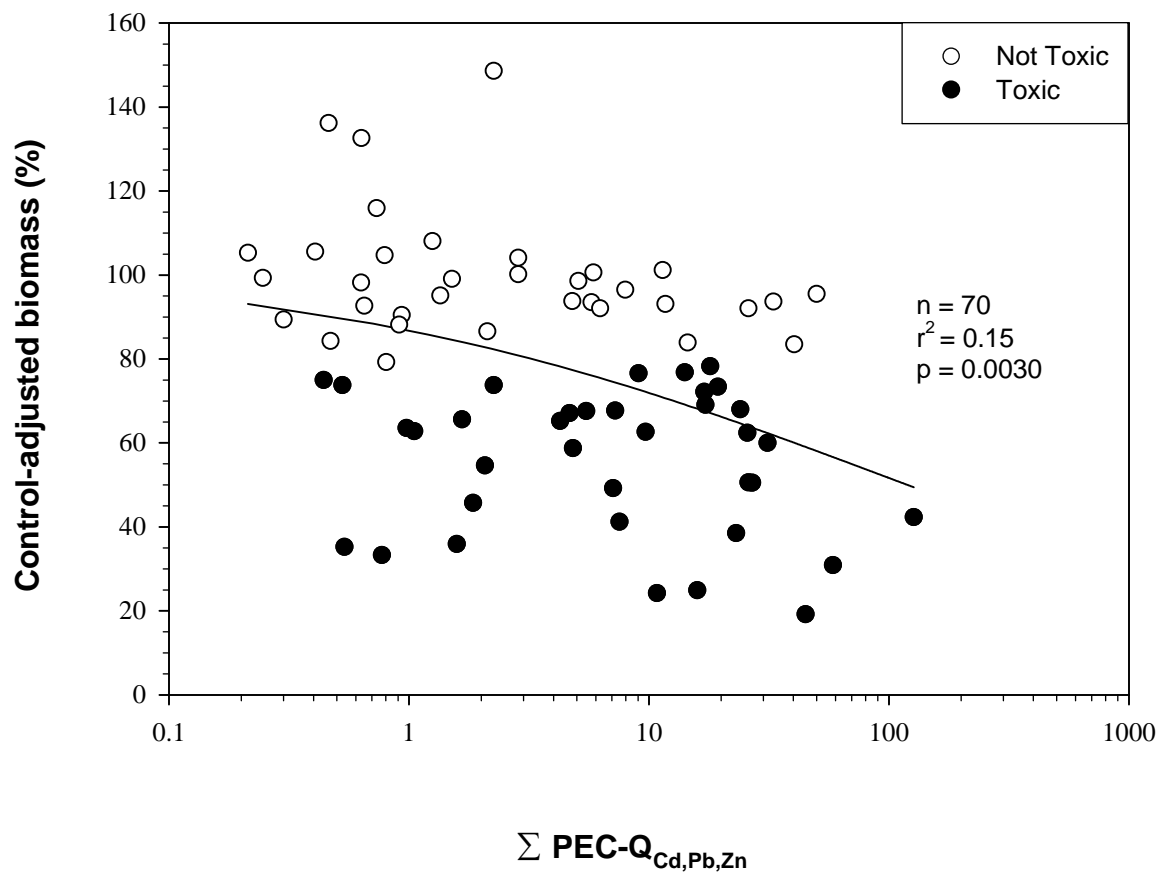
Plot A1-87. Plot illustrating the relationship between the concentration of Mean PEC-Q_{METALS} in sediment (<2 mm) and the control-adjusted biomass of midges (*Chironomus dilutus*) in 10-d exposures to sediment samples from the Tri-State Mining District.



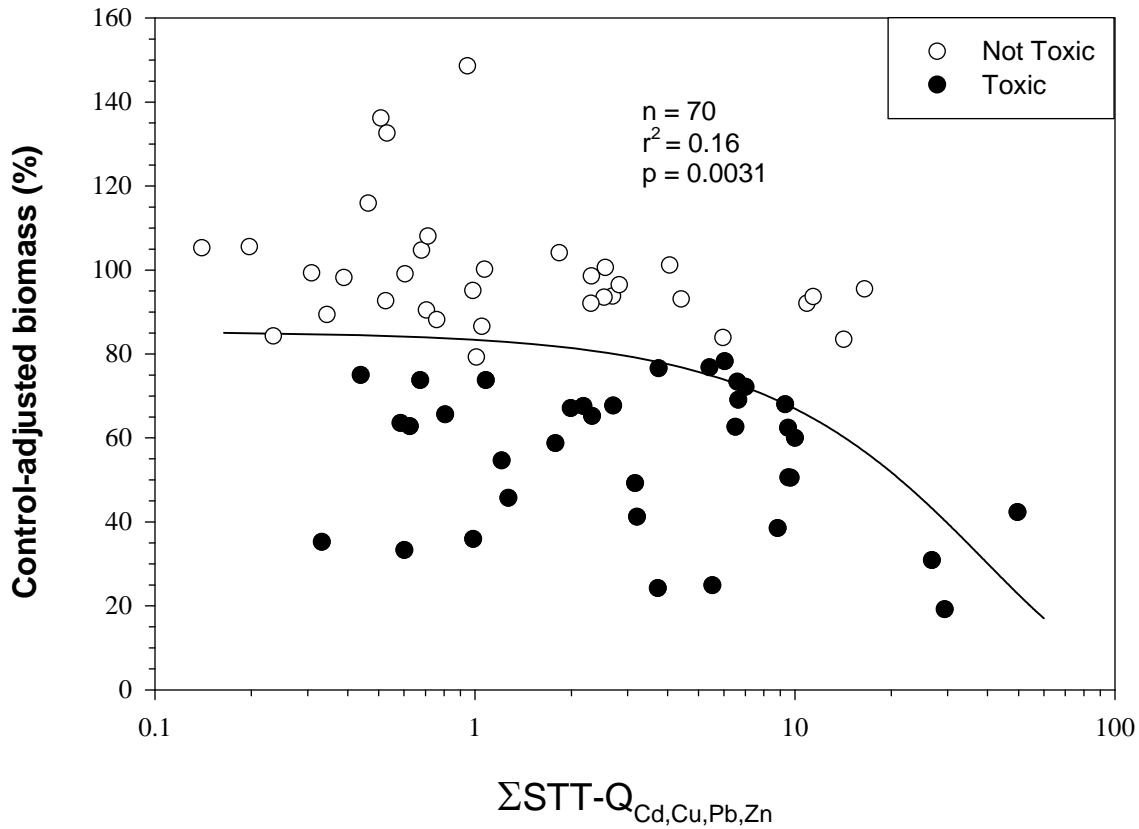
Plot A1-88. Plot illustrating the relationship between the concentration of Mean PEC-Q_{METAL(1%OC)} in sediment (<2 mm) and the control-adjusted biomass of midges (*Chironomus dilutus*) in 10-d exposures to sediment samples from the Tri-State Mining District.



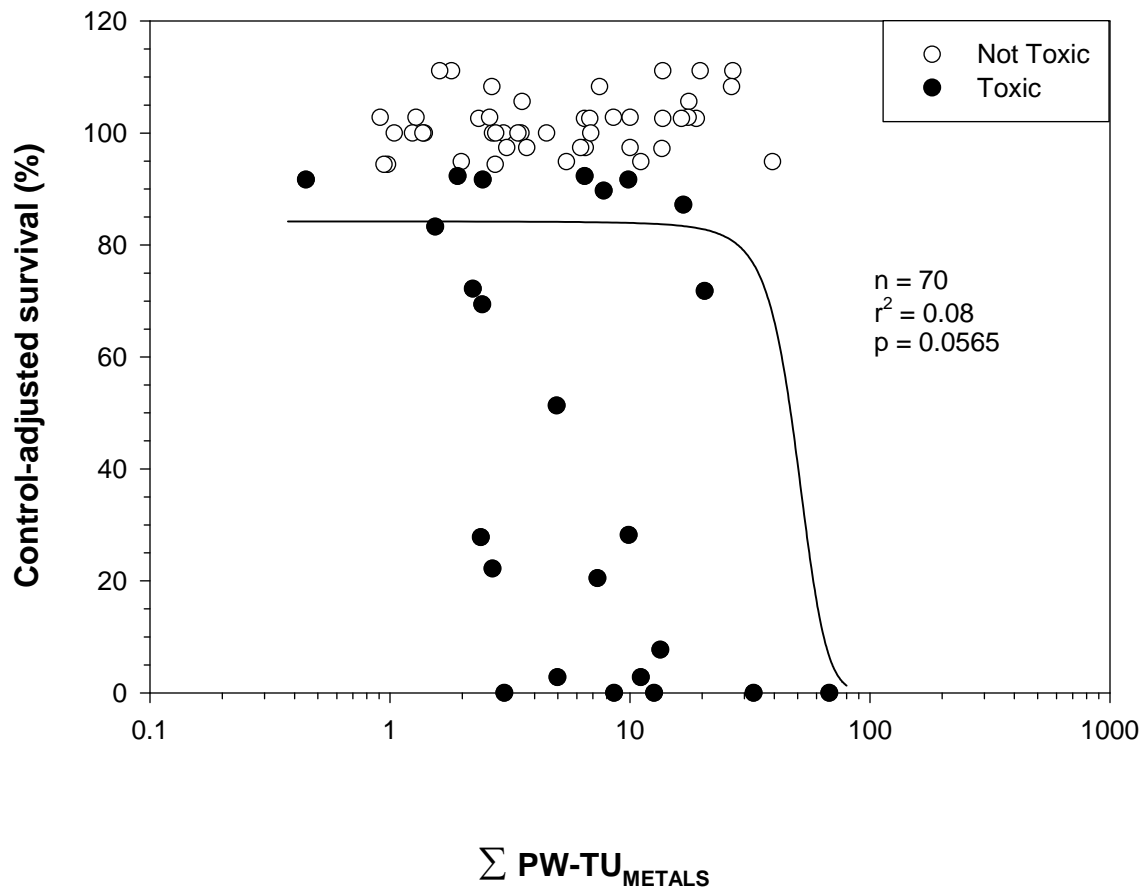
Plot A1-89. Plot illustrating the relationship between the concentration of $\Sigma\text{PEC-Q}_{\text{Cd,Pb,Zn}}$ in sediment (<2 mm) and the control-adjusted biomass of midges (*Chironomus dilutus*) in 10-d exposures to sediment samples from the Tri-State Mining District.



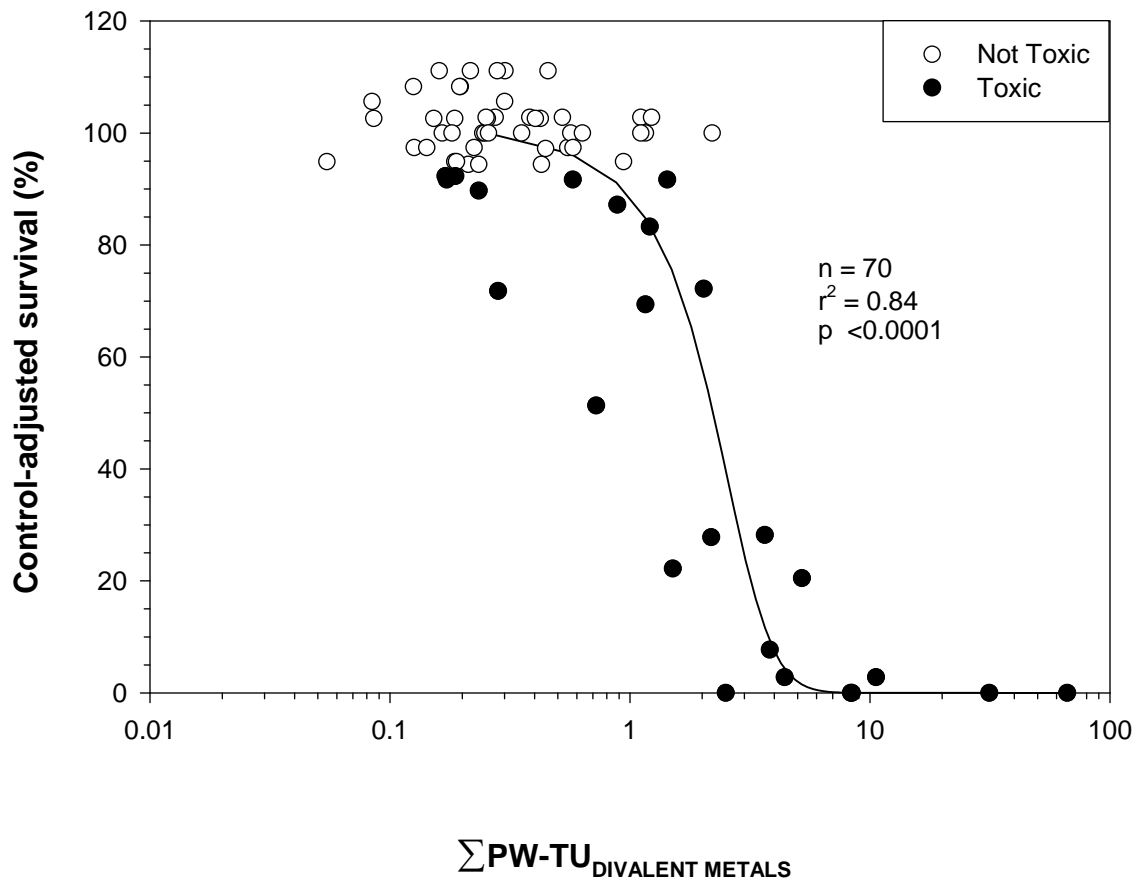
Plot A1-90. Plot illustrating the relationship between the concentration of $\Sigma\text{STT-Q}_{\text{Cd,Cu,Pb,Zn}}$ in sediment (<2 mm) and the control-adjusted biomass of midges (*Chironomus dilutus*) in 10-d exposures to sediment samples from the Tri-State Mining District.



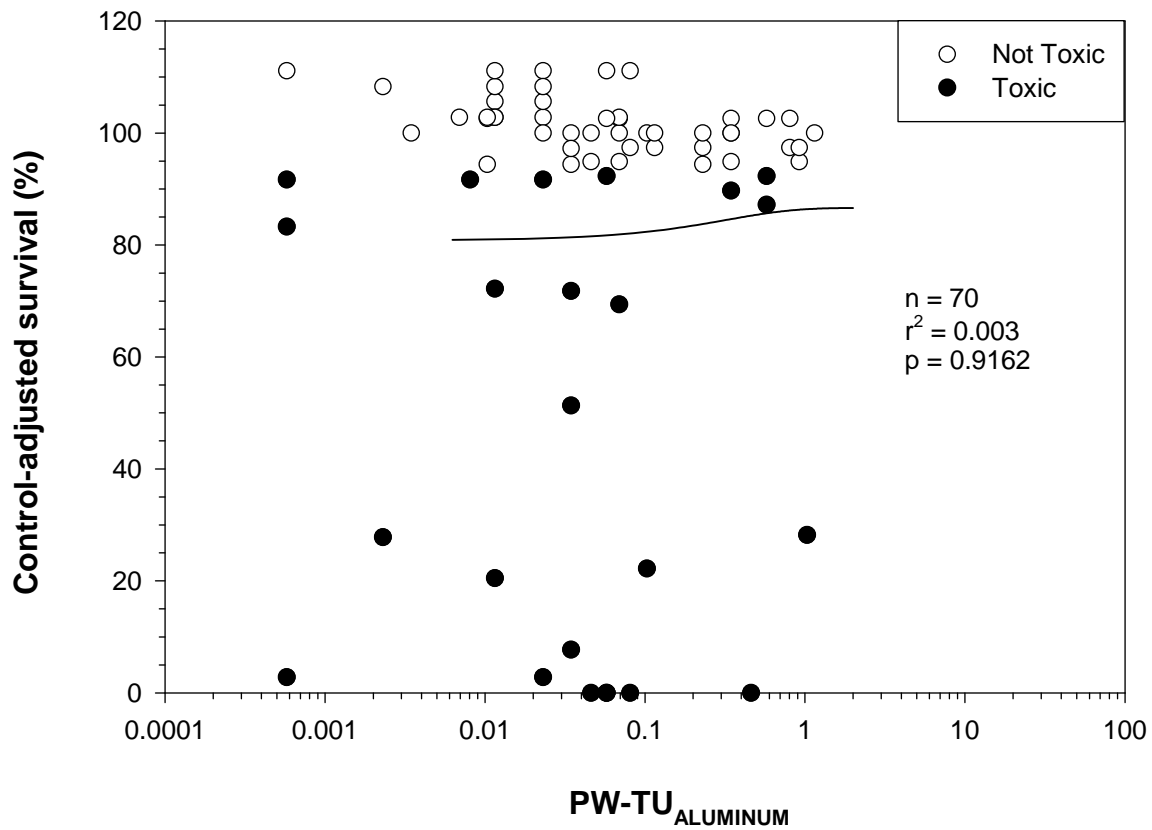
Plot A1-91. Plot illustrating the relationship between the concentration of $\sum PW-TU_{METALS}$ and the control-adjusted survival of amphipods (*Hyalella azteca*) in 28-d exposures to sediment samples from the Tri-State Mining District.



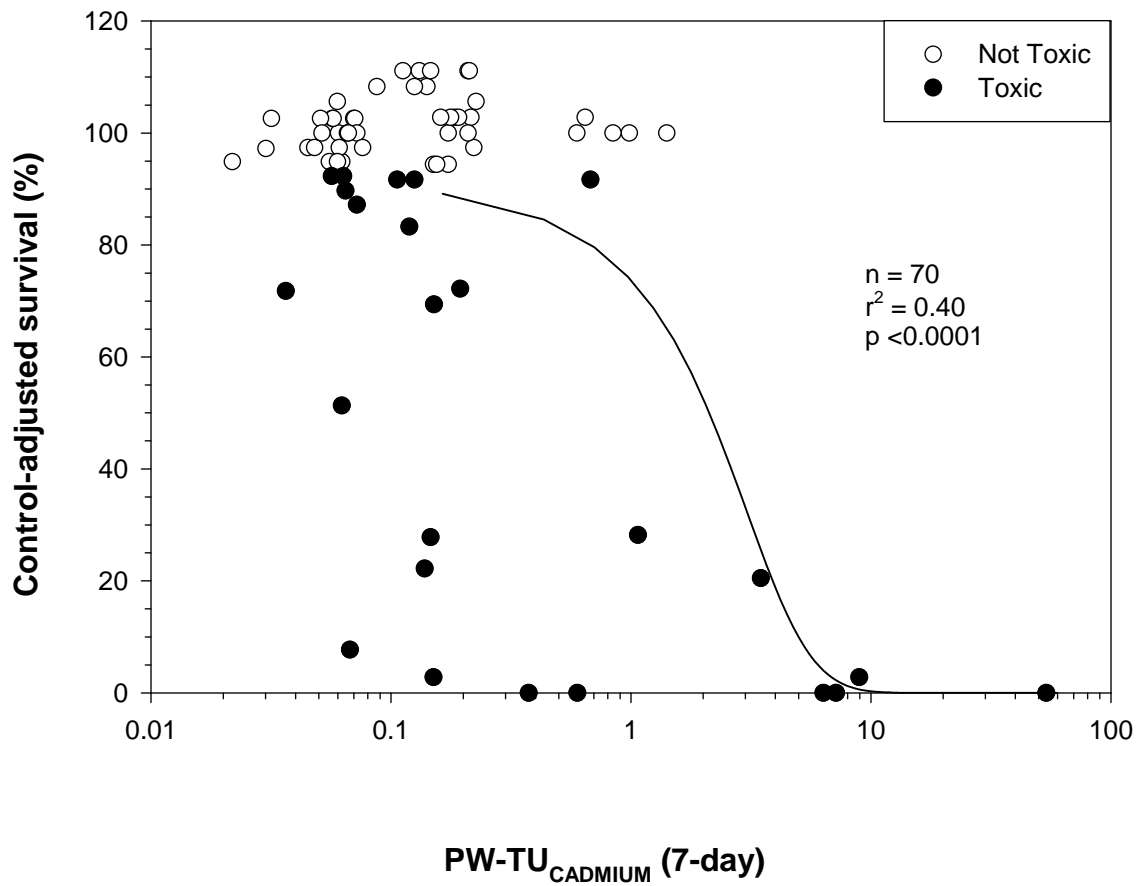
Plot A1-92. Plot illustrating the relationship between the concentration of $\sum \text{PW-TU}_{\text{Divalent Metals}}$ and the control-adjusted survival of amphipods (*Hyalella azteca*) in 28-d exposures to sediment samples from the Tri-State Mining District.



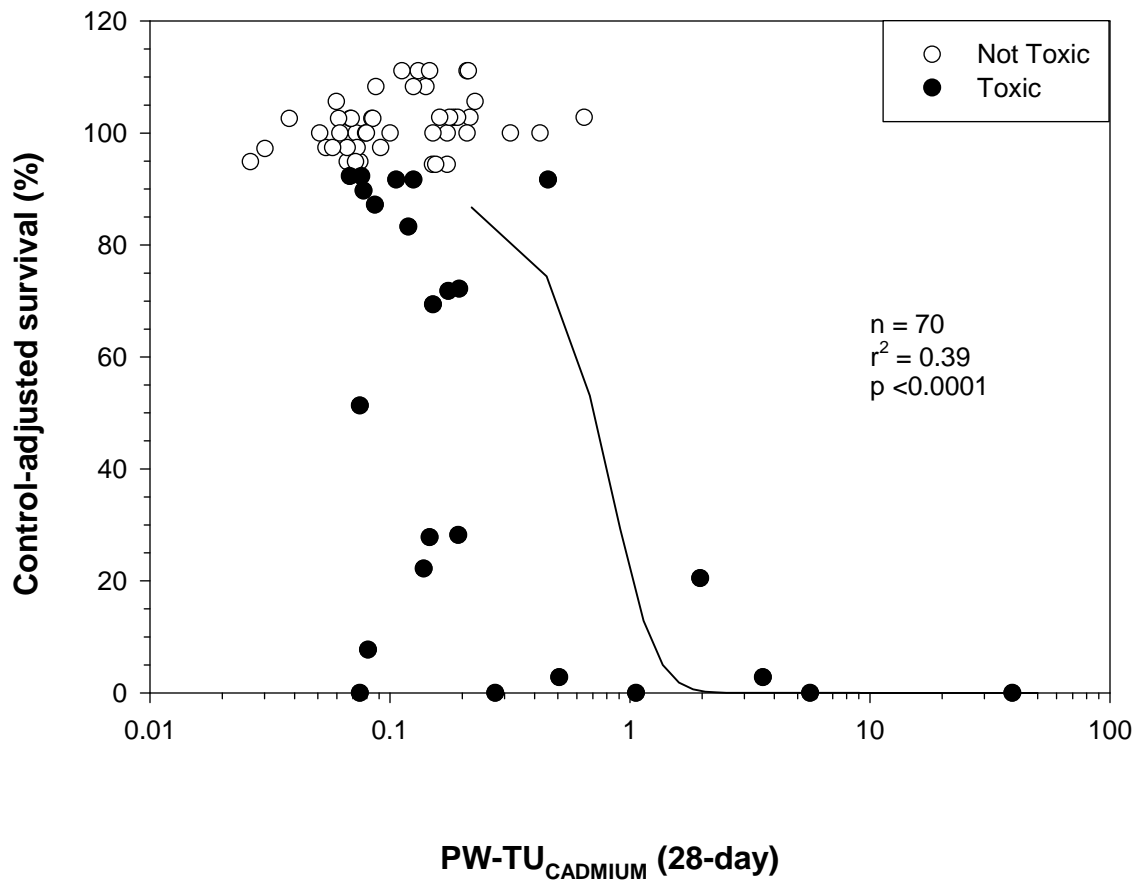
Plot A1-93. Plot illustrating the relationship between the concentration of PW-TU_{ALUMINUM} and the control-adjusted survival of amphipods (*Hyalella azteca*) in 28-d exposures to sediment samples from the Tri-State Mining District.



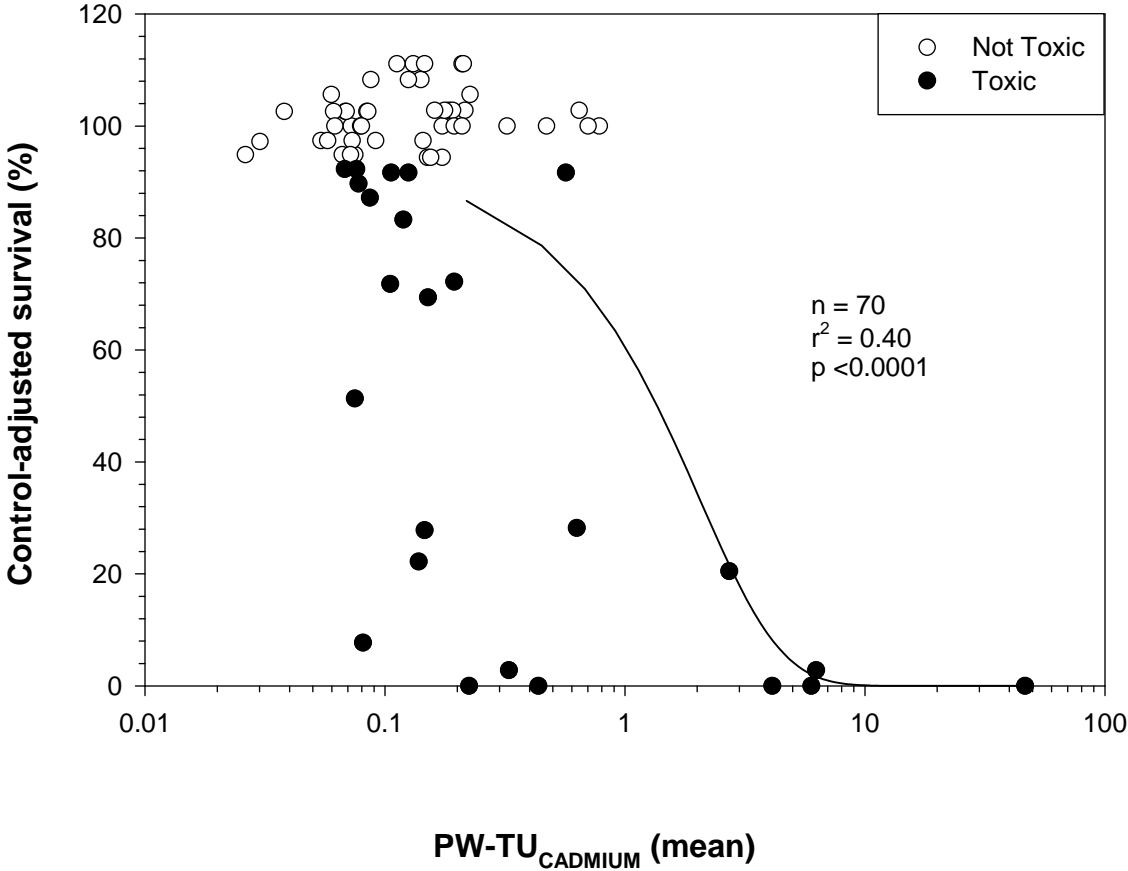
Plot A1-95. Plot illustrating the relationship between the concentration of PW-TU_{CADMIUM} (7-day) and the control-adjusted survival of amphipods (*Hyalella azteca*) in 28-d exposures to sediment samples from the Tri-State Mining District.



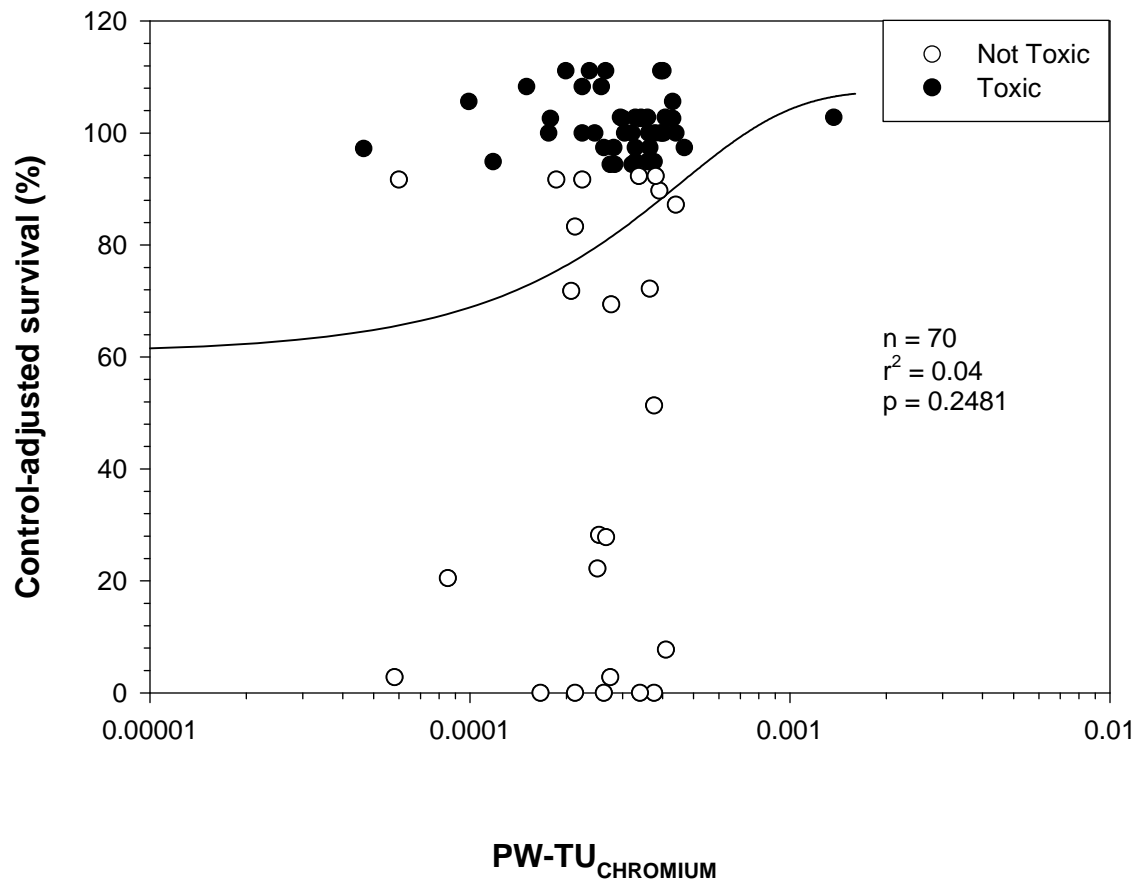
Plot A1-96. Plot illustrating the relationship between the concentration of PW-TU_{CADMIUM} (28-day) and the control-adjusted survival of amphipods (*Hyalella azteca*) in 28-d exposures to sediment samples from the Tri-State Mining District.



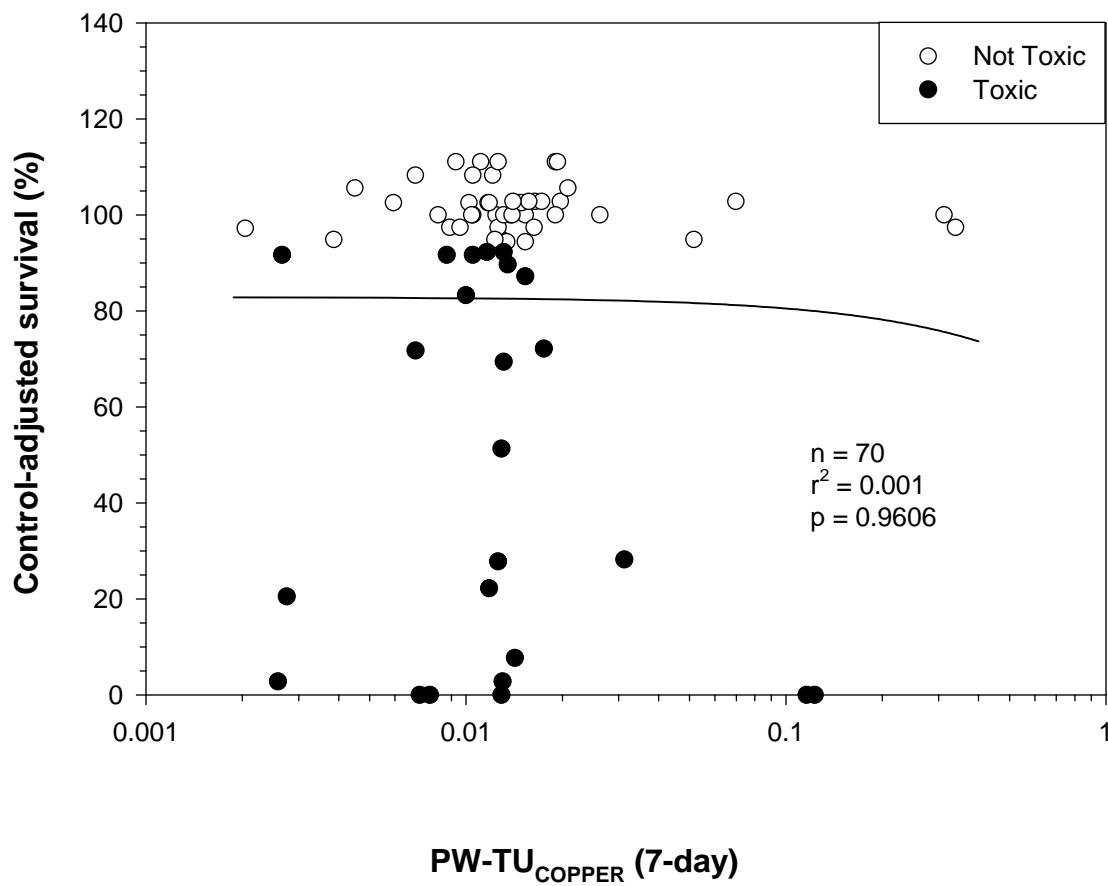
Plot A1-97. Plot illustrating the relationship between the concentration of PW-TU_{CADMIUM} (mean) and the control-adjusted survival of amphipods (*Hyalella azteca*) in 28-d exposures to sediment samples from the Tri-State Mining District.



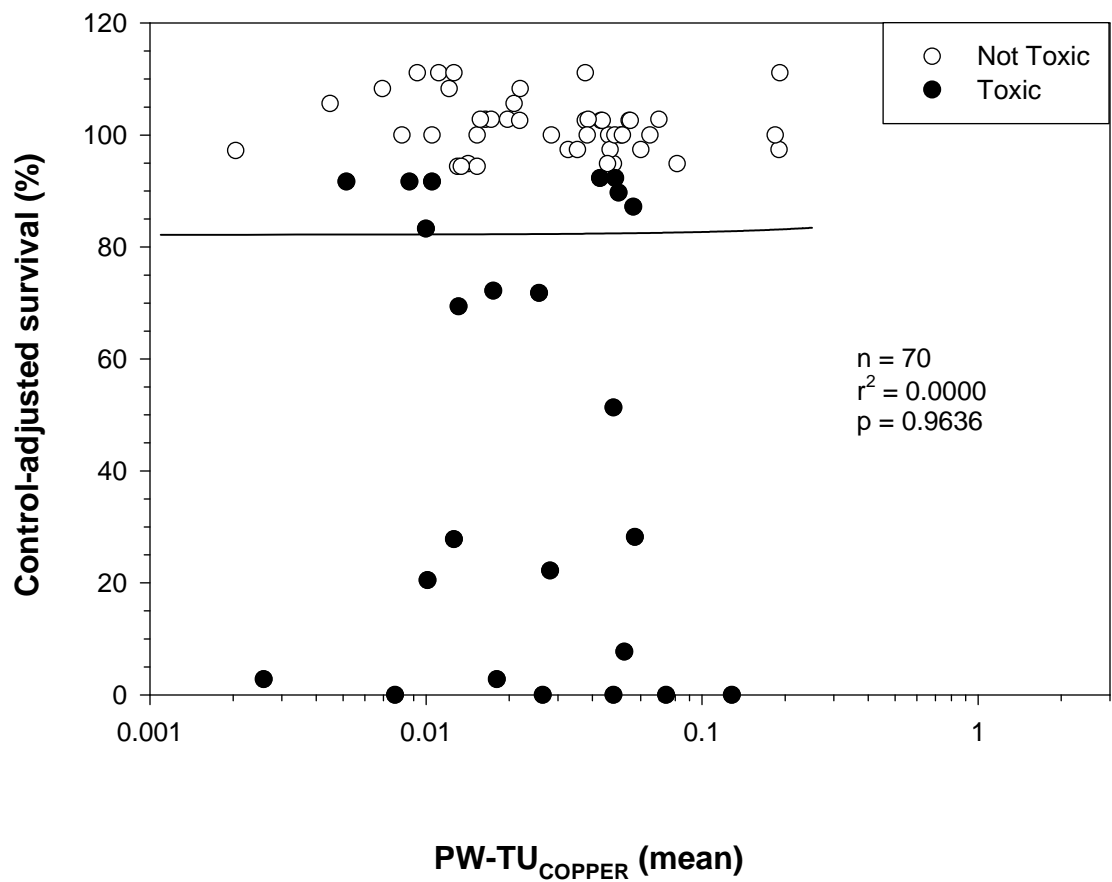
Plot A1-98. Plot illustrating the relationship between the concentration of PW-TU_{CHROMIUM} and the control-adjusted survival of amphipods (*Hyalella azteca*) in 28-d exposures to sediment samples from the Tri-State Mining District.



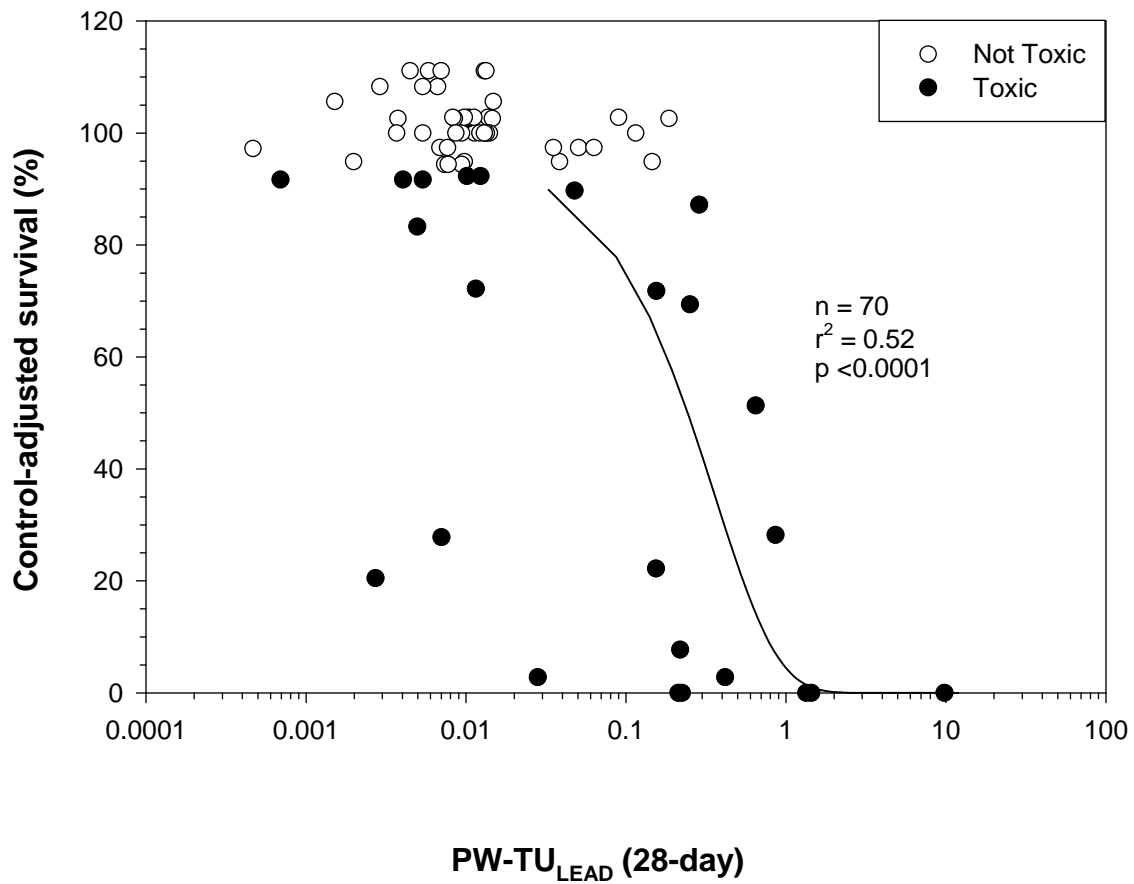
Plot A1-99. Plot illustrating the relationship between the concentration of PW-TU_{COPPER} (7-day) and the control-adjusted survival of amphipods (*Hyalella azteca*) in 28-d exposures to sediment samples from the Tri-State Mining District.



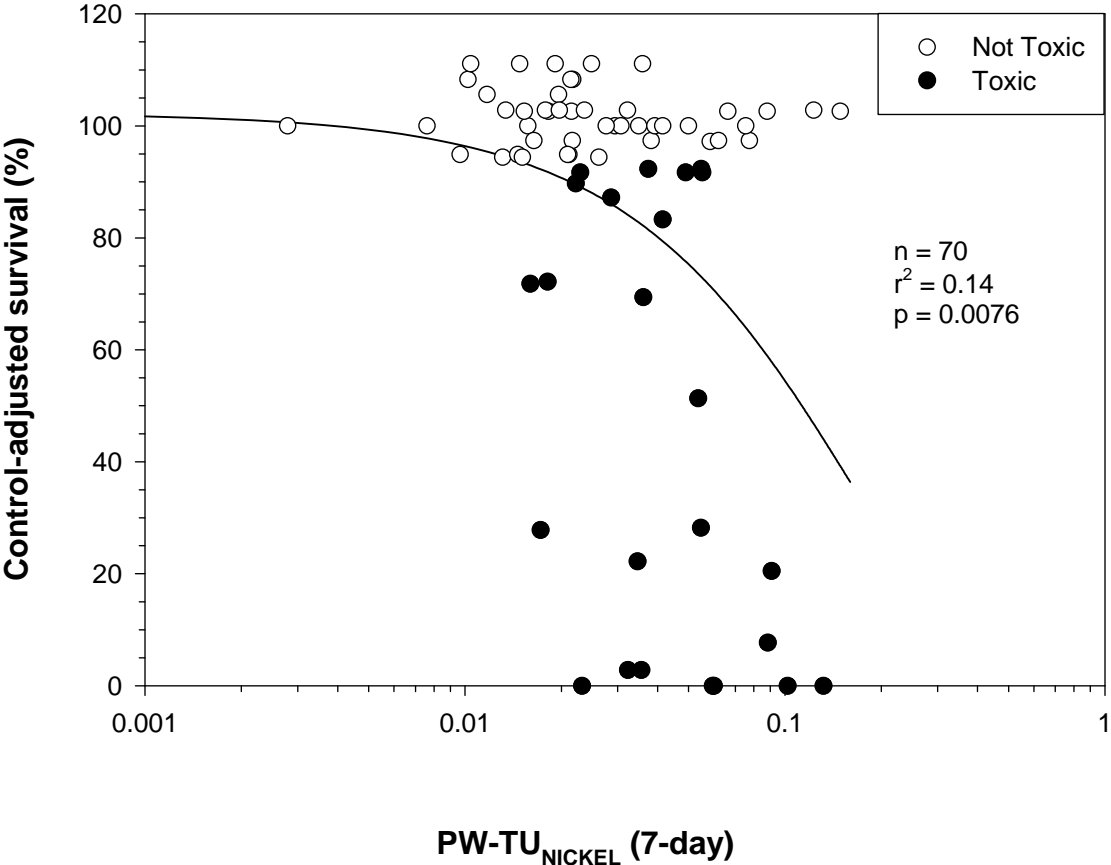
Plot A1-101. Plot illustrating the relationship between the concentration of PW-TU_{COPPER} (mean) and the control-adjusted survival of amphipods (*Hyalella azteca*) in 28-d exposures to sediment samples from the Tri-State Mining District.



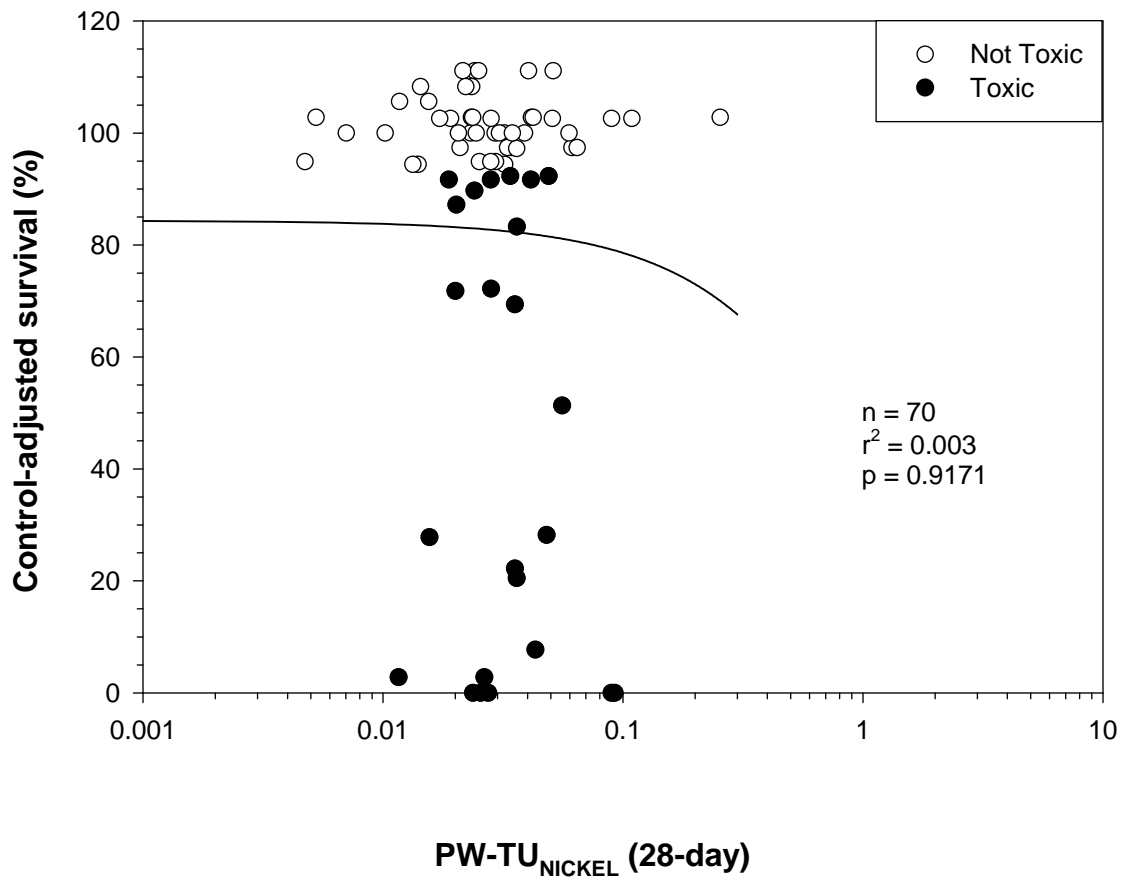
Plot A1-104. Plot illustrating the relationship between the concentration of PW-TU_{LEAD} (28-day) and the control-adjusted survival of amphipods (*Hyalella azteca*) in 28-d exposures to sediment samples from the Tri-State Mining District.



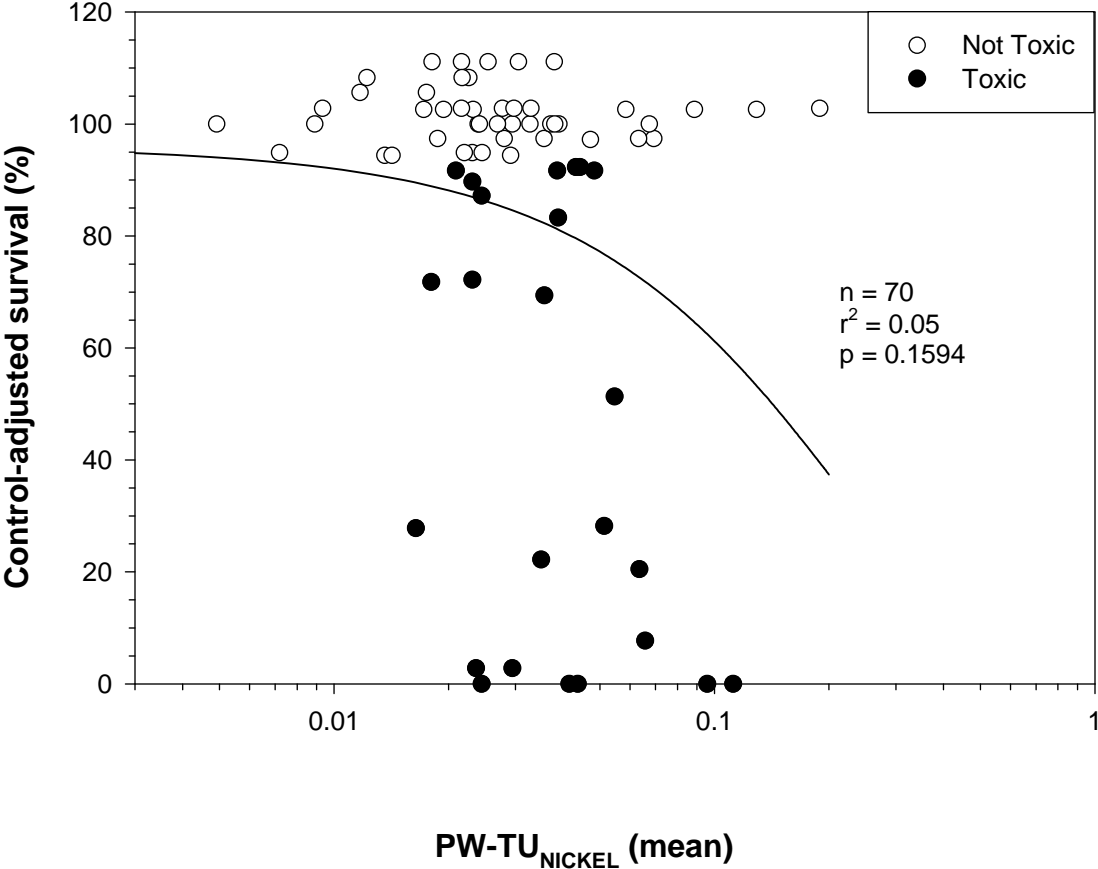
Plot A1-106. Plot illustrating the relationship between the concentration of PW-TU_{NICKEL} (7-day) and the control-adjusted survival of amphipods (*Hyalella azteca*) in 28-d exposures to sediment samples from the Tri-State Mining District.



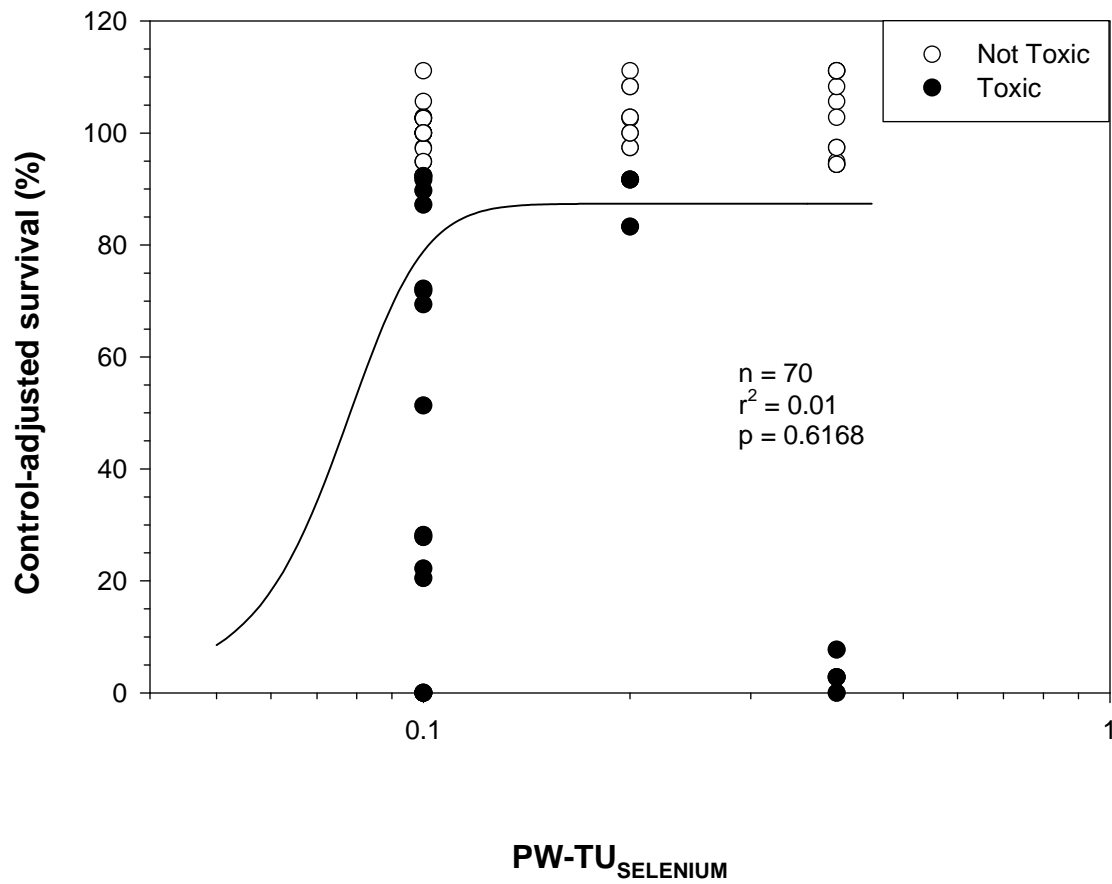
Plot A1-107. Plot illustrating the relationship between the concentration of $PW-TU_{NICKEL}$ (28-day) and the control-adjusted survival of amphipods (*Hyalella azteca*) in 28-d exposures to sediment samples from the Tri-State Mining District.



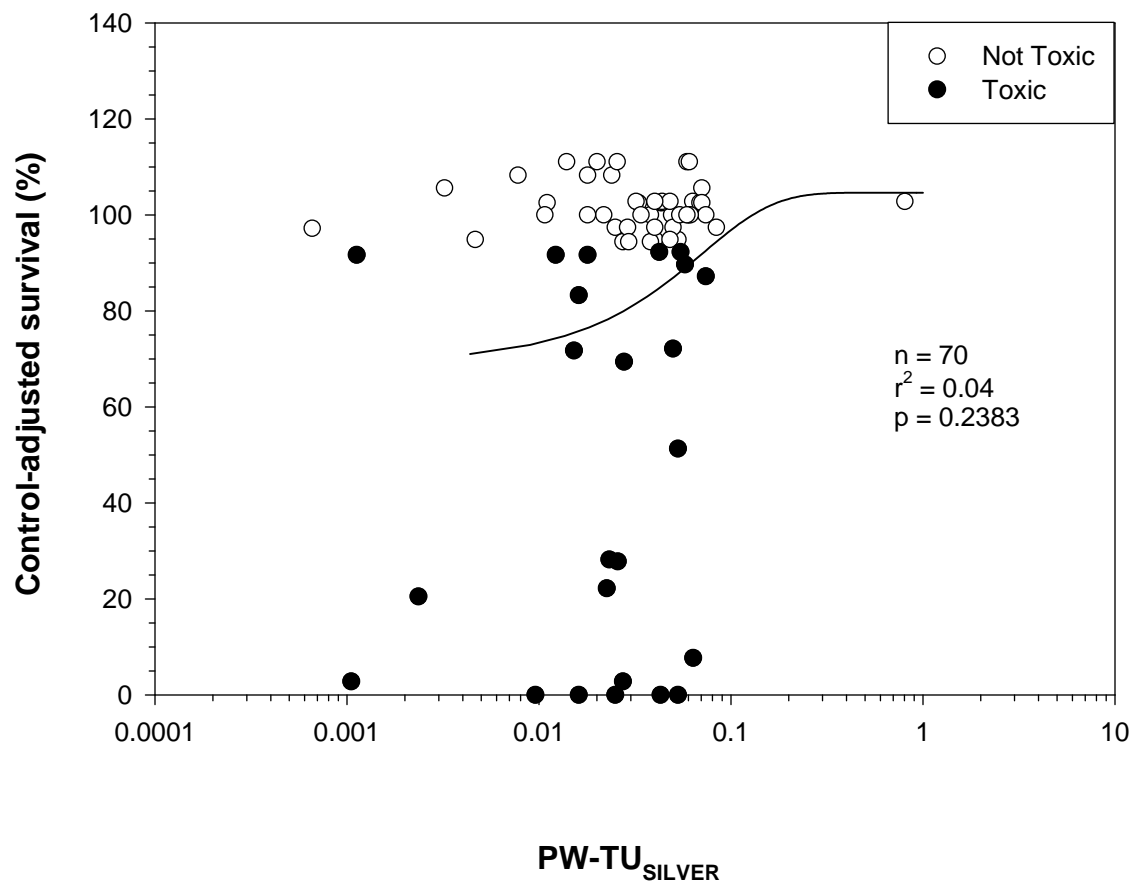
Plot A1-108. Plot illustrating the relationship between the concentration of PW-TU_{NICKEL} (mean) and the control-adjusted survival of amphipods (*Hyalella azteca*) in 28-d exposures to sediment samples from the Tri-State Mining District.



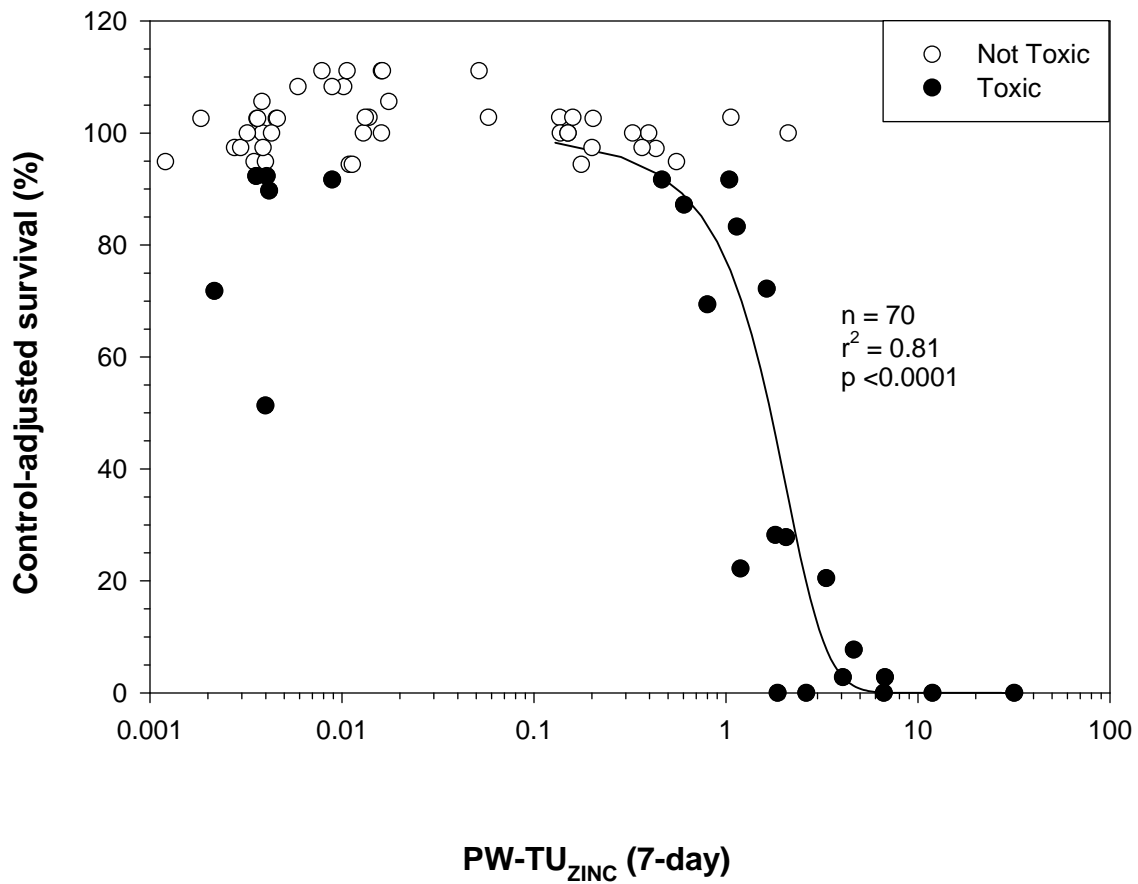
Plot A1-109. Plot illustrating the relationship between the concentration of PW-TU_{SELENIUM} and the control-adjusted survival of amphipods (*Hyalella azteca*) in 28-d exposures to sediment samples from the Tri-State Mining District.



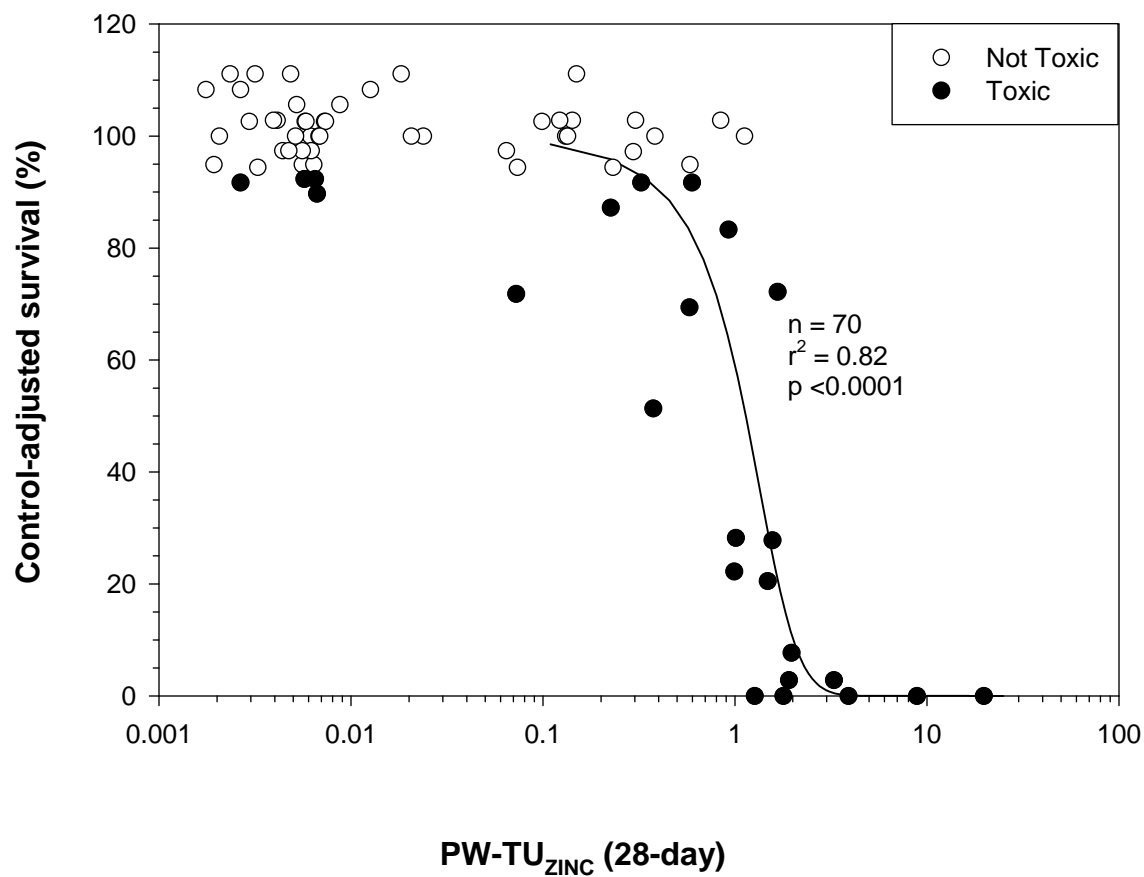
Plot A1-110. Plot illustrating the relationship between the concentration of PW-TU_{SILVER} and the control-adjusted survival of amphipods (*Hyalella azteca*) in 28-d exposures to sediment samples from the Tri-State Mining District.



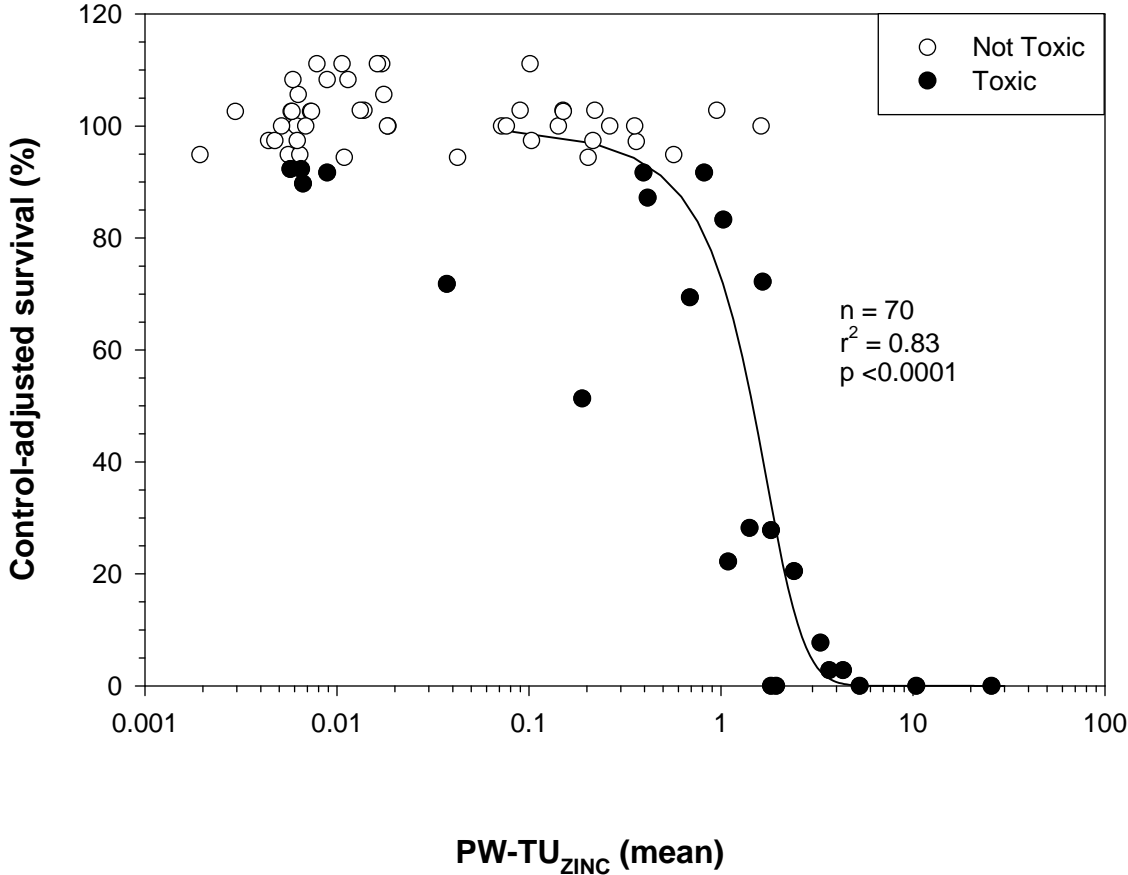
Plot A1-111. Plot illustrating the relationship between the concentration of PW-TU_{ZINC} (7-day) and the control-adjusted survival of amphipods (*Hyalella azteca*) in 28-d exposures to sediment samples from the Tri-State Mining District.



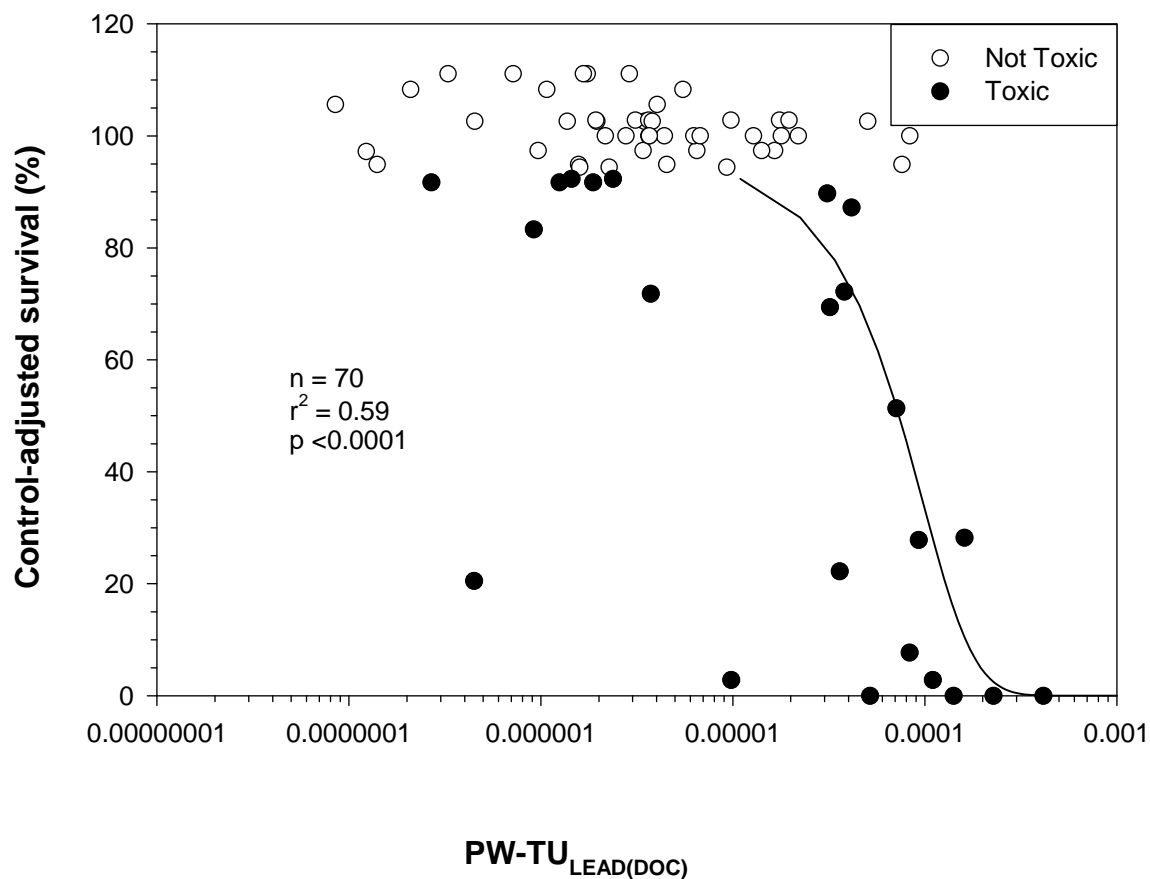
Plot A1-112. Plot illustrating the relationship between the concentration of PW-TU_{ZINC} (28-day) and the control-adjusted survival of amphipods (*Hyalella azteca*) in 28-d exposures to sediment samples from the Tri-State Mining District.



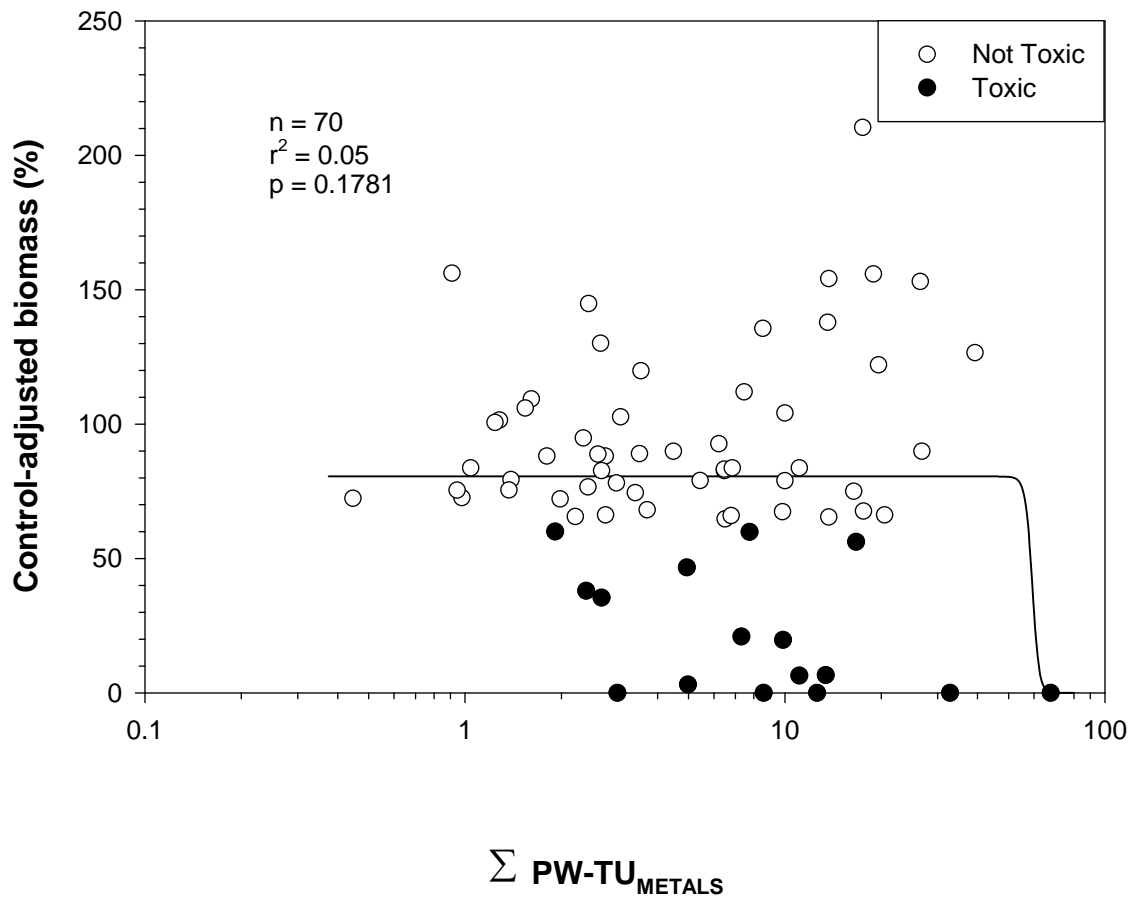
Plot A1-113. Plot illustrating the relationship between the concentration of PW-TU_{ZINC} (mean) and the control-adjusted survival of amphipods (*Hyalella azteca*) in 28-d exposures to sediment samples from the Tri-State Mining District.



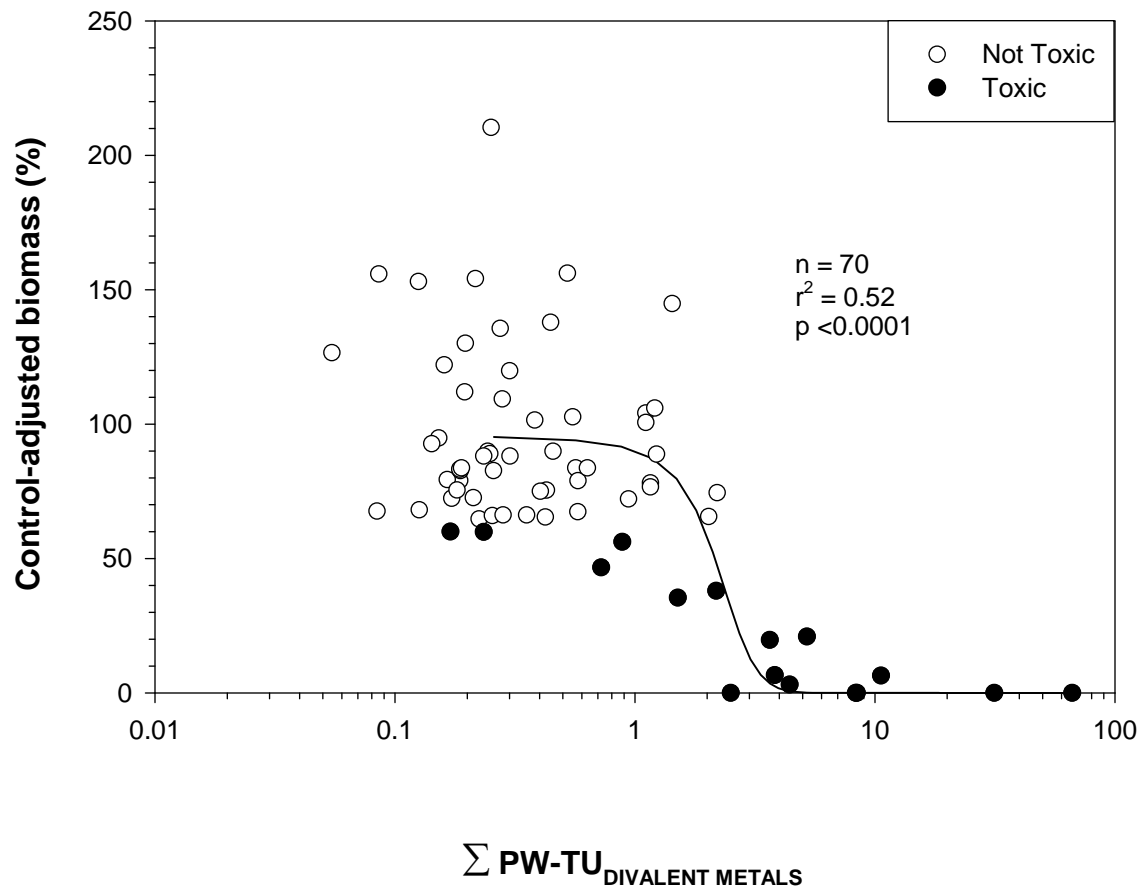
Plot A1-114. Plot illustrating the relationship between the concentration of $PW-TU_{LEAD(DOC)}$ and the control-adjusted survival of amphipods (*Hyalella azteca*) in 28-d exposures to sediment samples from the Tri-State Mining District.



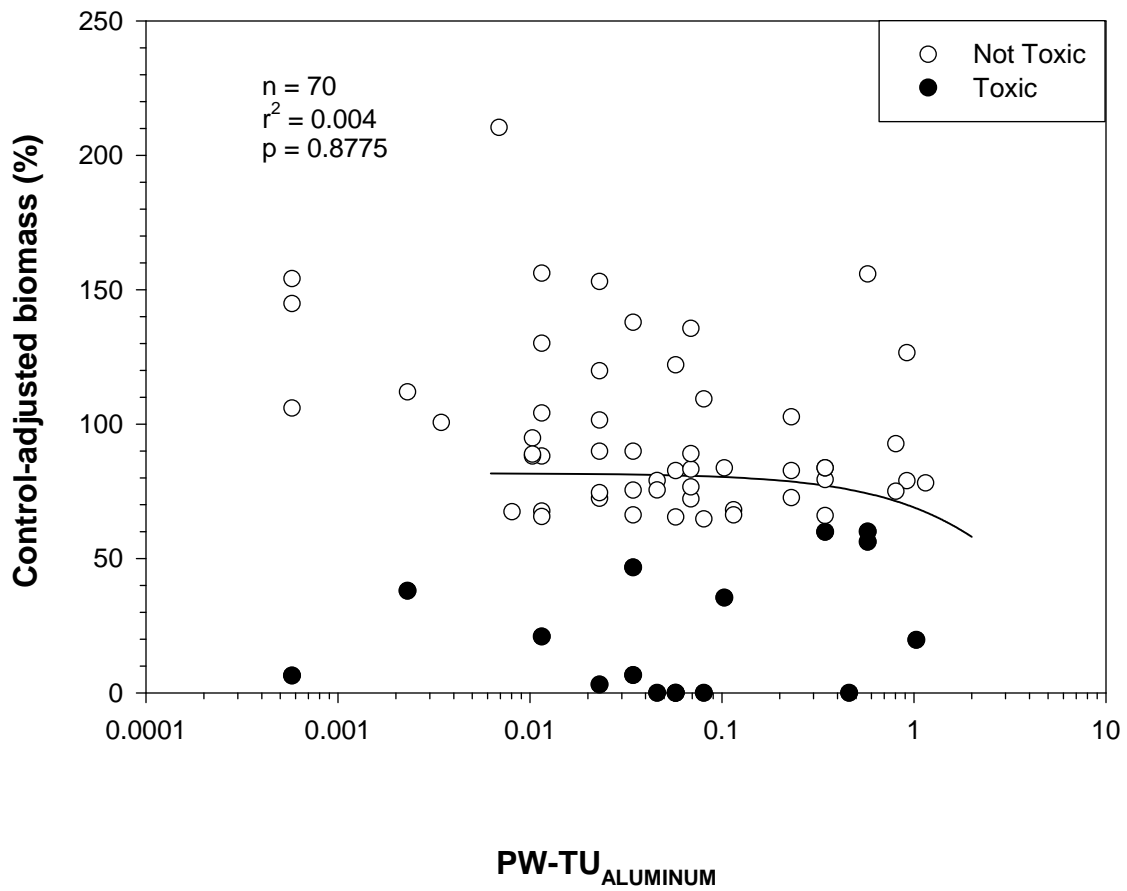
Plot A1-116. Plot illustrating the relationship between the concentration of $\Sigma \text{PW-TU}_{\text{METALS}}$ and the control-adjusted biomass of amphipods (*Hyalella azteca*) in 28-d exposures to sediment samples from the Tri-State Mining District.



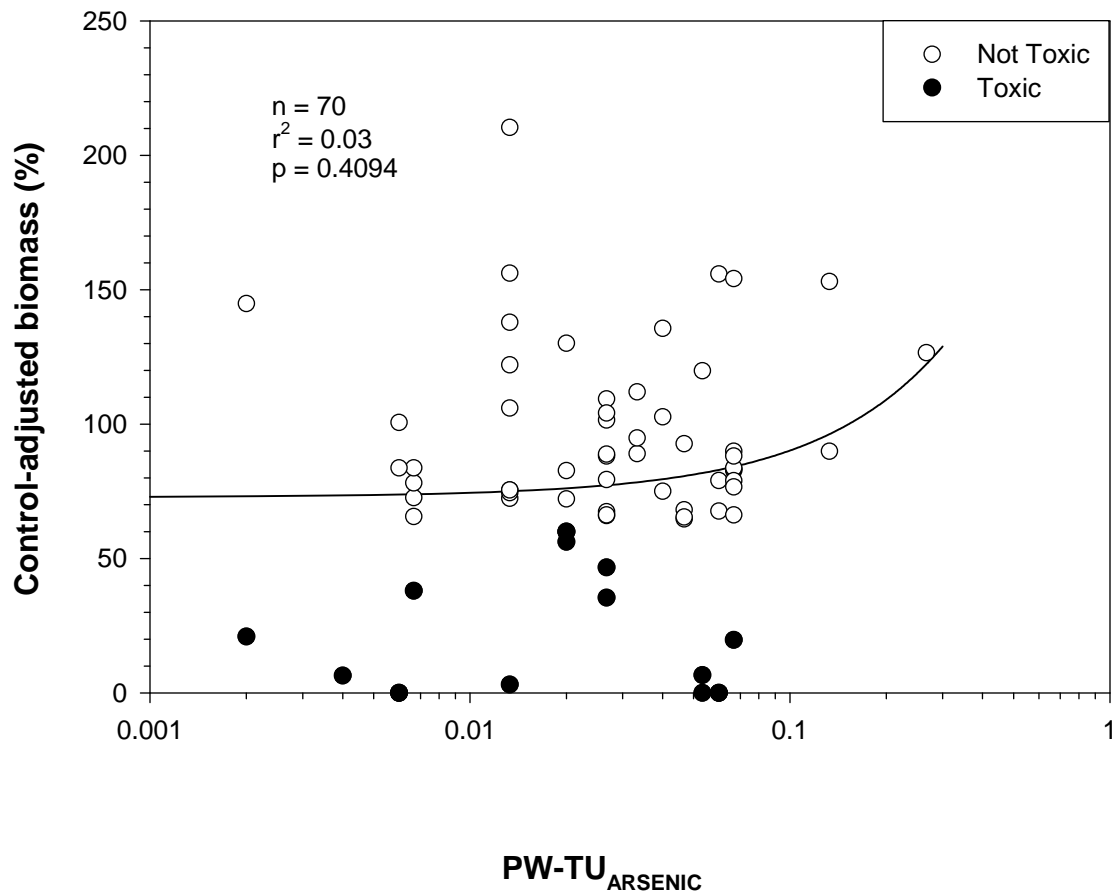
Plot A1-117. Plot illustrating the relationship between the concentration of $\Sigma\text{PW-TU}_{\text{Divalent Metals}}$ and the control-adjusted biomass of amphipods (*Hyalella azteca*) in 28-d exposures to sediment samples from the Tri-State Mining District.



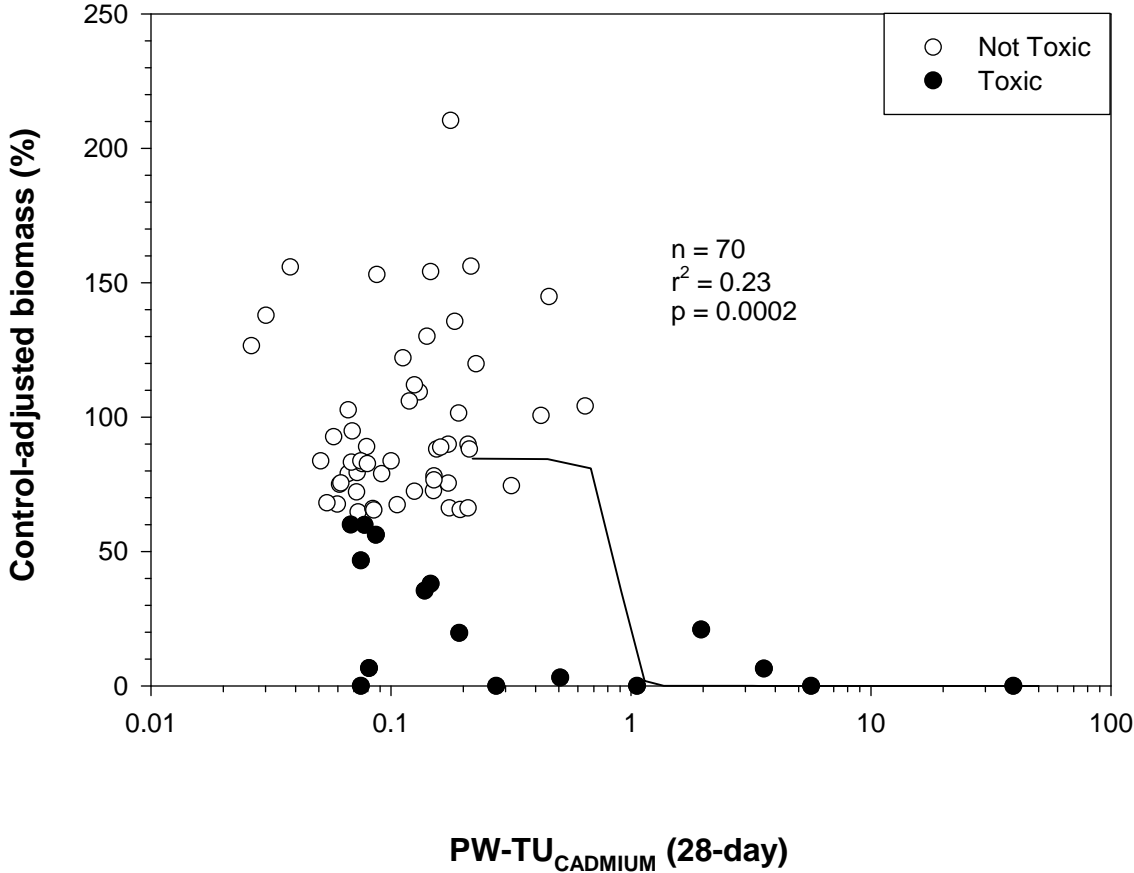
Plot A1-118. Plot illustrating the relationship between the concentration of PW-TU_{ALUMINUM} and the control-adjusted biomass of amphipods (*Hyalella azteca*) in 28-d exposures to sediment samples from the Tri-State Mining District.



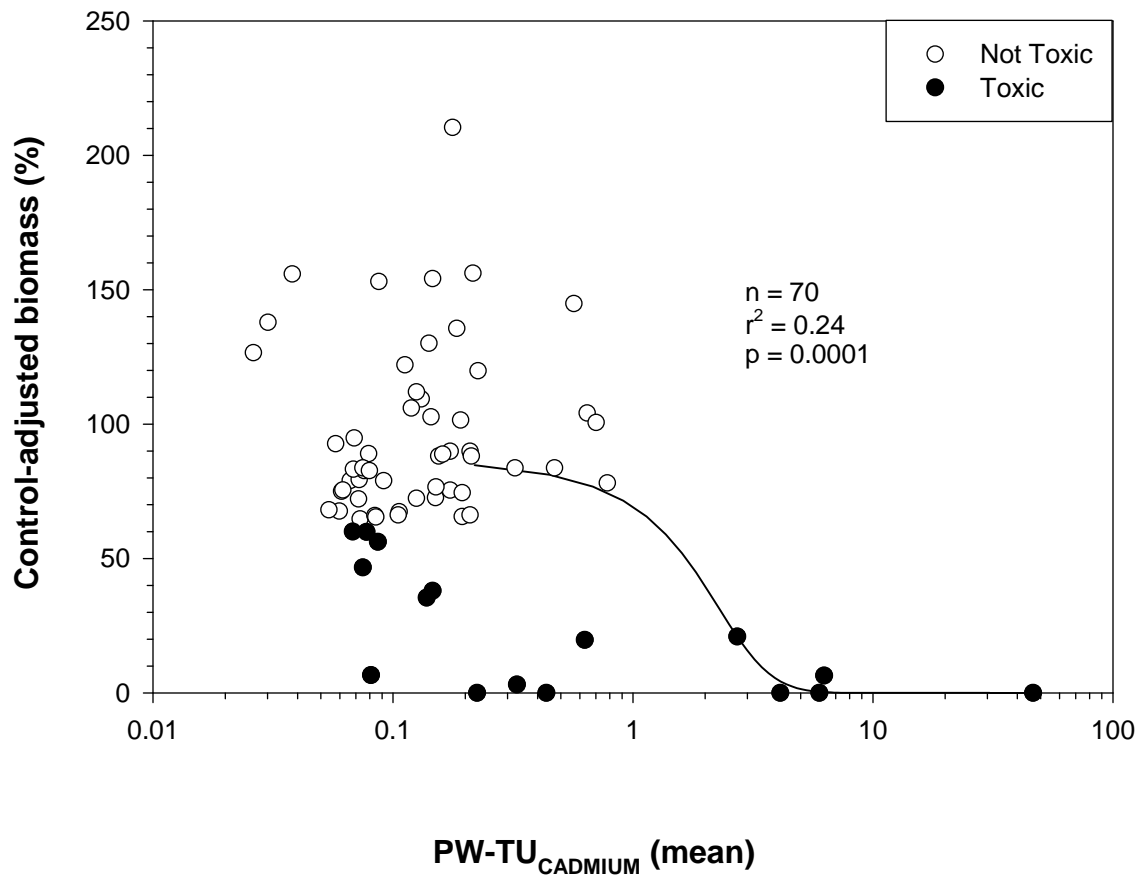
Plot A1-119. Plot illustrating the relationship between the concentration of $PW-TU_{ARSENIC}$ and the control-adjusted biomass of amphipods (*Hyalella azteca*) in 28-d exposures to sediment samples from the Tri-State Mining District.



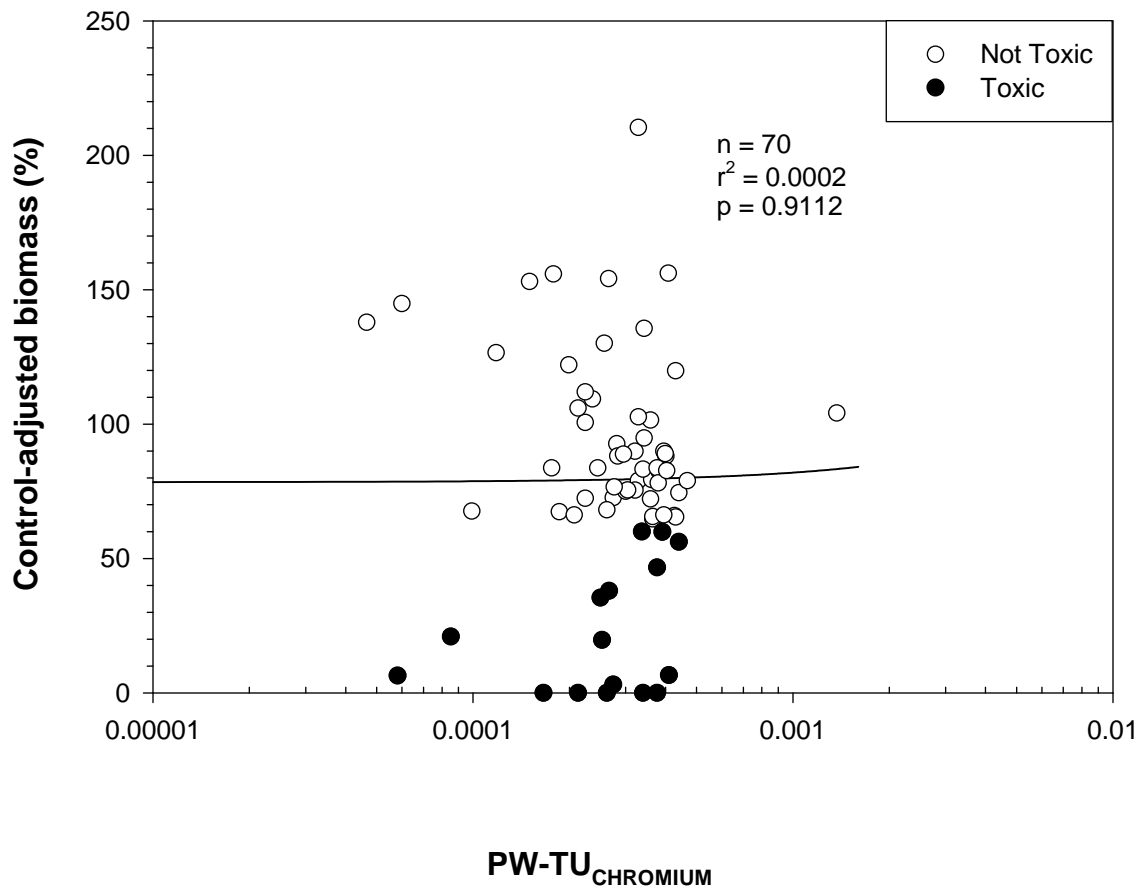
Plot A1-121. Plot illustrating the relationship between the concentration of PW-TU_{CADMIUM} (28-day) and the control-adjusted biomass of amphipods (*Hyalella azteca*) in 28-d exposures to sediment samples from the Tri-State Mining District.



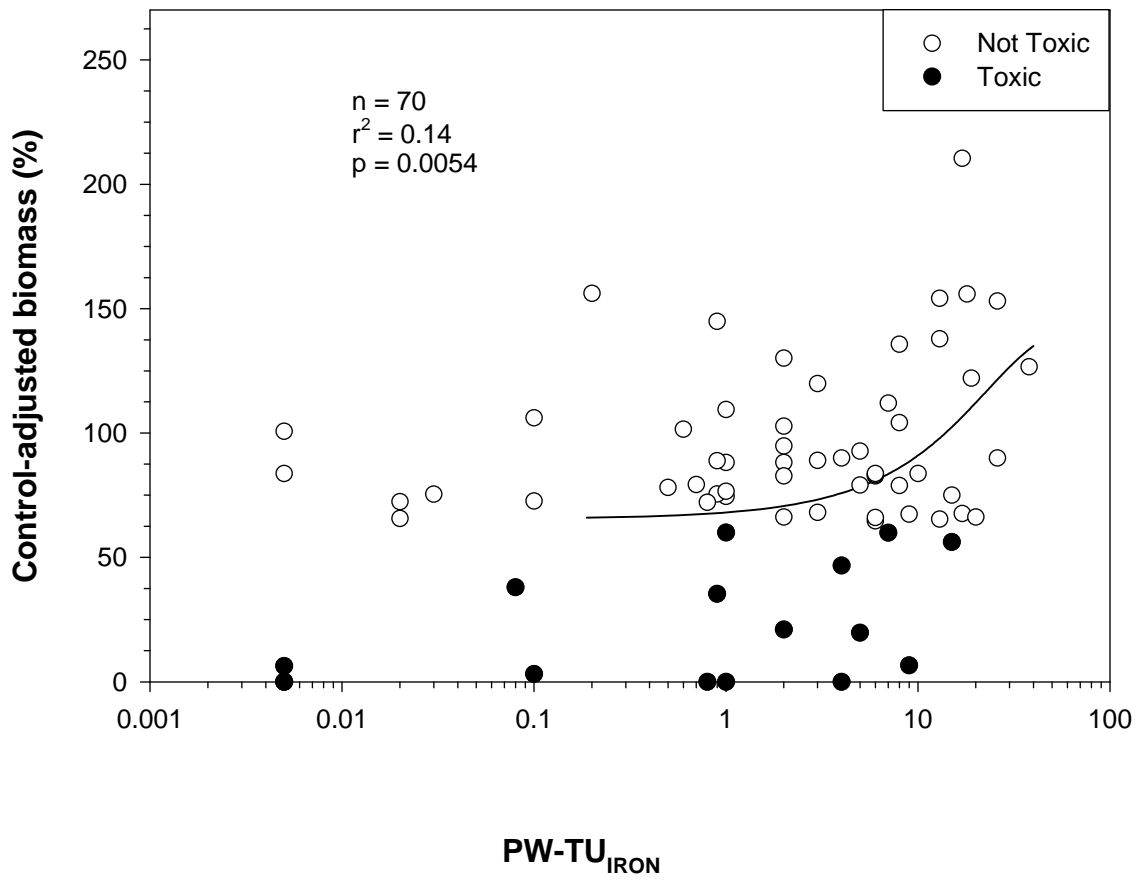
Plot A1-122. Plot illustrating the relationship between the concentration of $PW-TU_{CADMIUM}$ (mean) and the control-adjusted biomass of amphipods (*Hyalella azteca*) in 28-d exposures to sediment samples from the Tri-State Mining District.



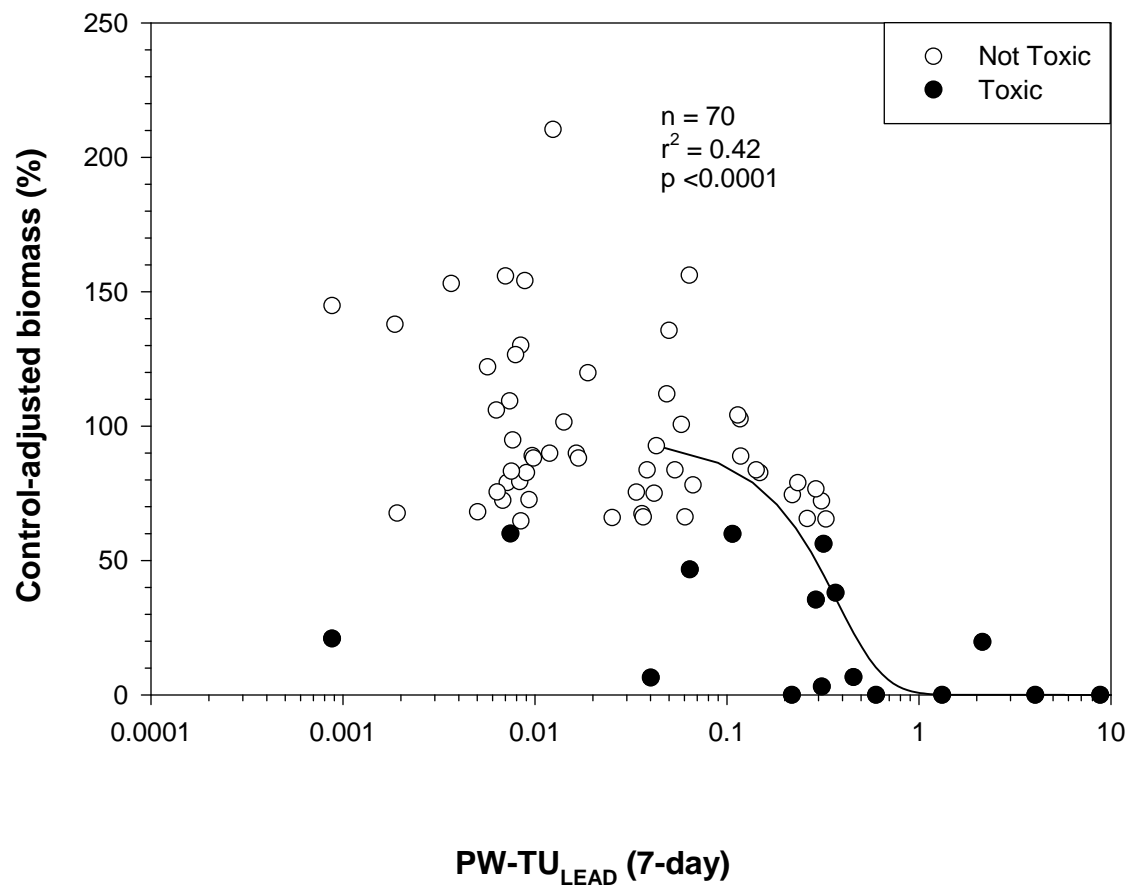
Plot A1-123. Plot illustrating the relationship between the concentration of $PW-TU_{CHROMIUM}$ and the control-adjusted biomass of amphipods (*Hyalella azteca*) in 28-d exposures to sediment samples from the Tri-State Mining District.



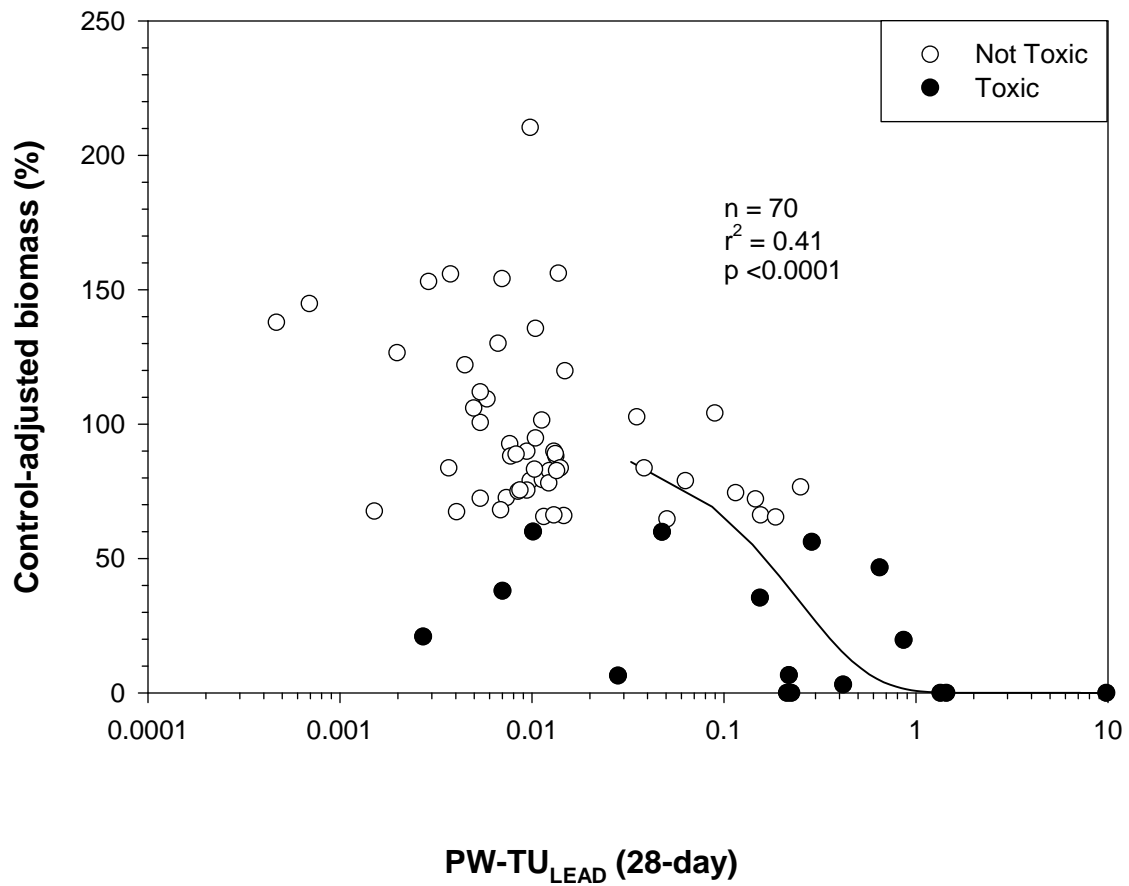
Plot A1-127. Plot illustrating the relationship between the concentration of PW-TU_{IRON} and the control-adjusted biomass of amphipods (*Hyalella azteca*) in 28-d exposures to sediment samples from the Tri-State Mining District.



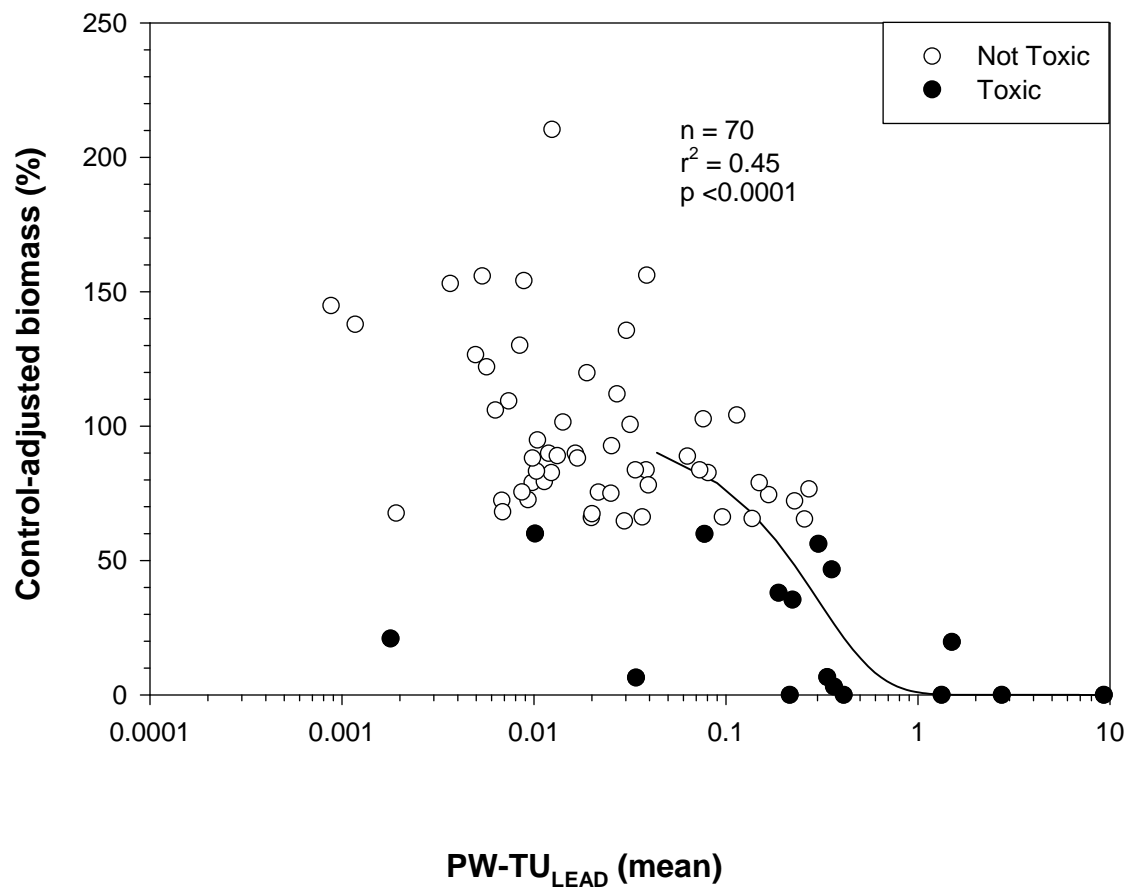
Plot A1-128. Plot illustrating the relationship between the concentration of PW-TU_{LEAD} (7-day) and the control-adjusted biomass of amphipods (*Hyalella azteca*) in 28-d exposures to sediment samples from the Tri-State Mining District.



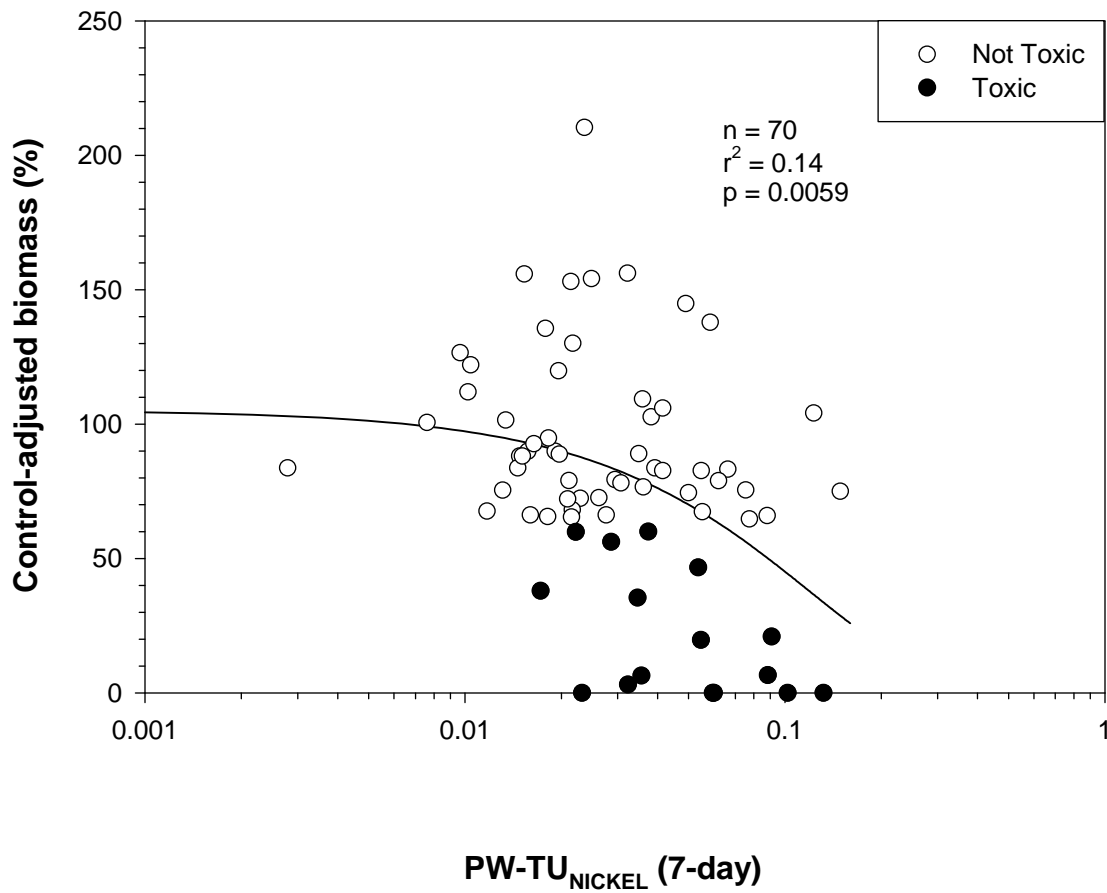
Plot A1-129. Plot illustrating the relationship between the concentration of PW-TU_{LEAD} (28-day) and the control-adjusted biomass of amphipods (*Hyalella azteca*) in 28-d exposures to sediment samples from the Tri-State Mining District.



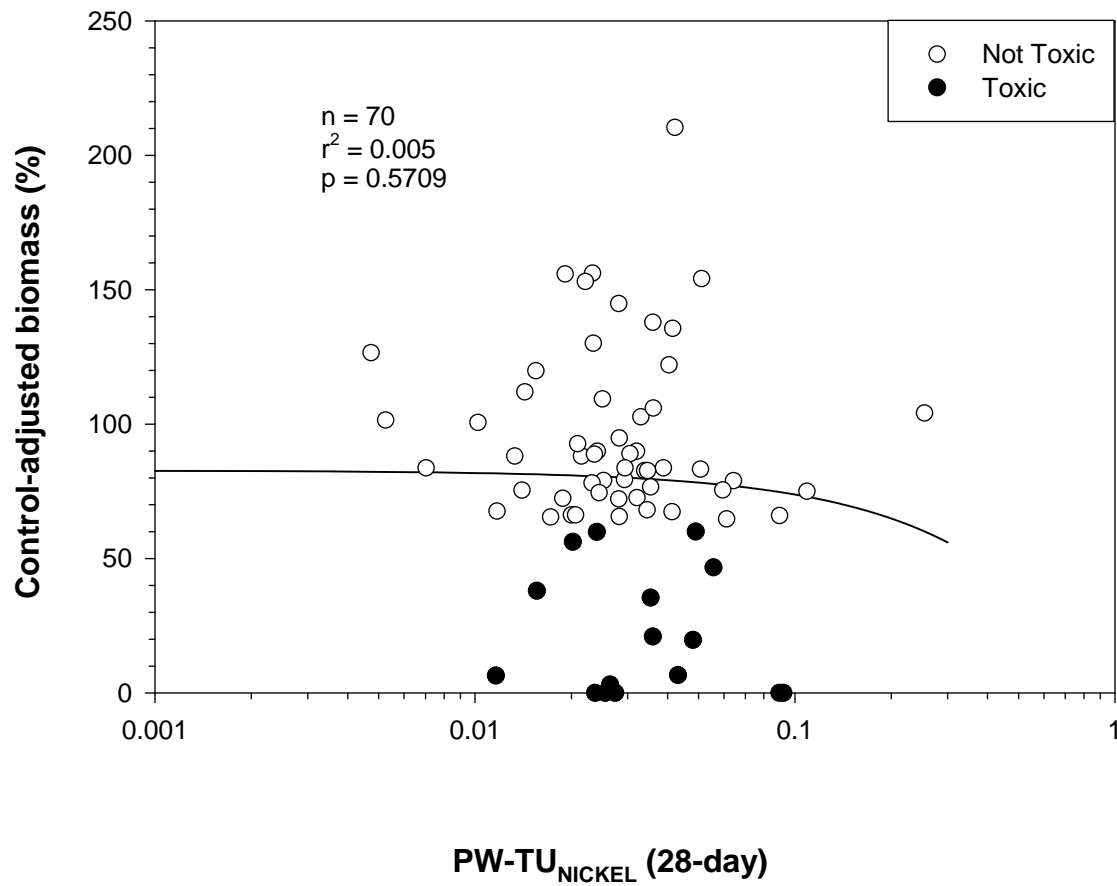
Plot A1-130. Plot illustrating the relationship between the concentration of $PW-TU_{LEAD}$ (mean) and the control-adjusted biomass of amphipods (*Hyalella azteca*) in 28-d exposures to sediment samples from the Tri-State Mining District.



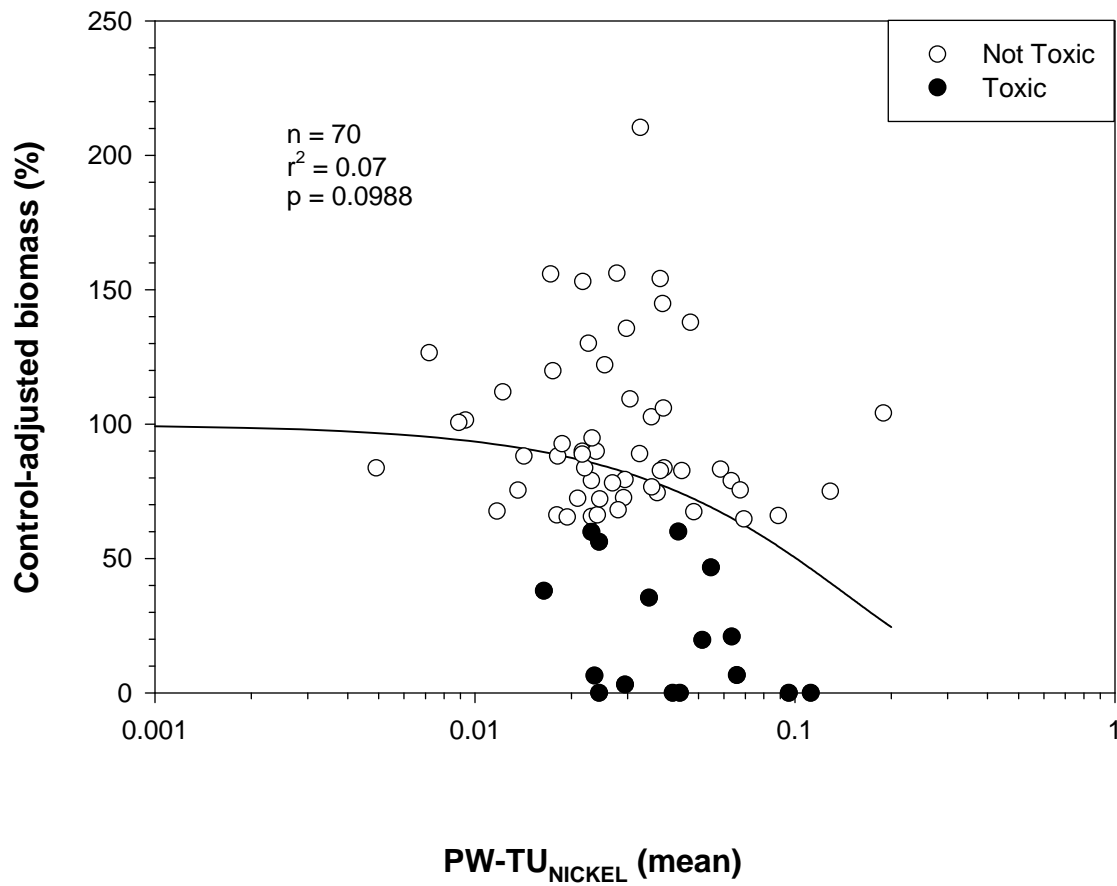
Plot A1-131. Plot illustrating the relationship between the concentration of PW-TU_{NICKEL} (7-day) and the control-adjusted biomass of amphipods (*Hyalella azteca*) in 28-d exposures to sediment samples from the Tri-State Mining District.



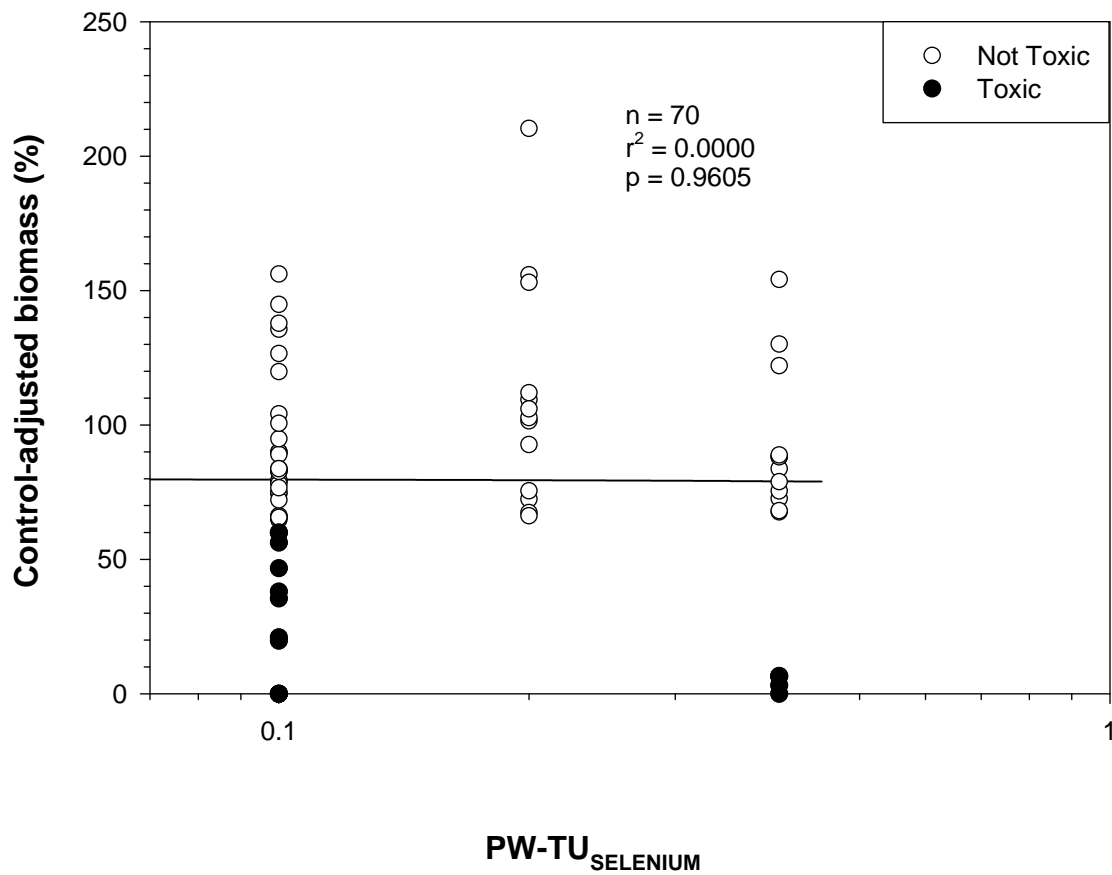
Plot A1-132. Plot illustrating the relationship between the concentration of PW-TU_{NICKEL} (28-day) and the control-adjusted biomass of amphipods (*Hyalella azteca*) in 28-d exposures to sediment samples from the Tri-State Mining District.



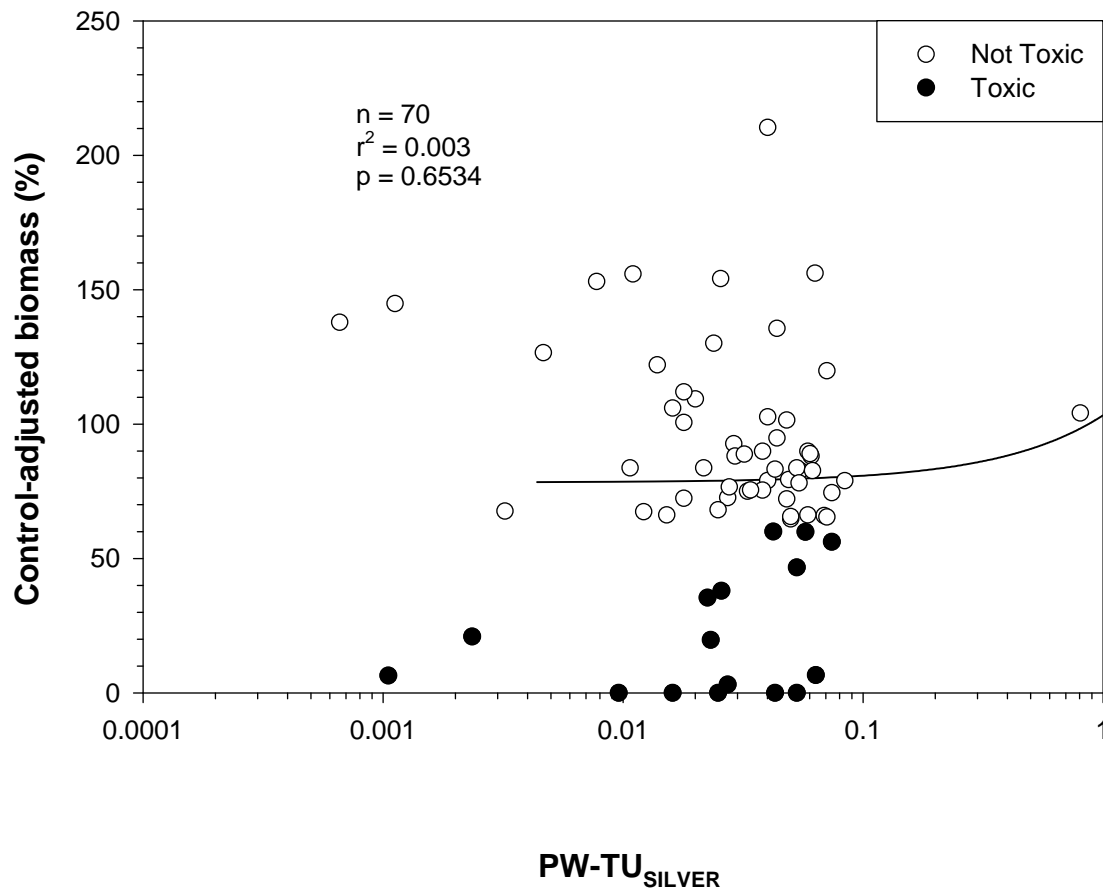
Plot A1-133. Plot illustrating the relationship between the concentration of PW-TU_{NICKEL} (mean) and the control-adjusted biomass of amphipods (*Hyalella azteca*) in 28-d exposures to sediment samples from the Tri-State Mining District.



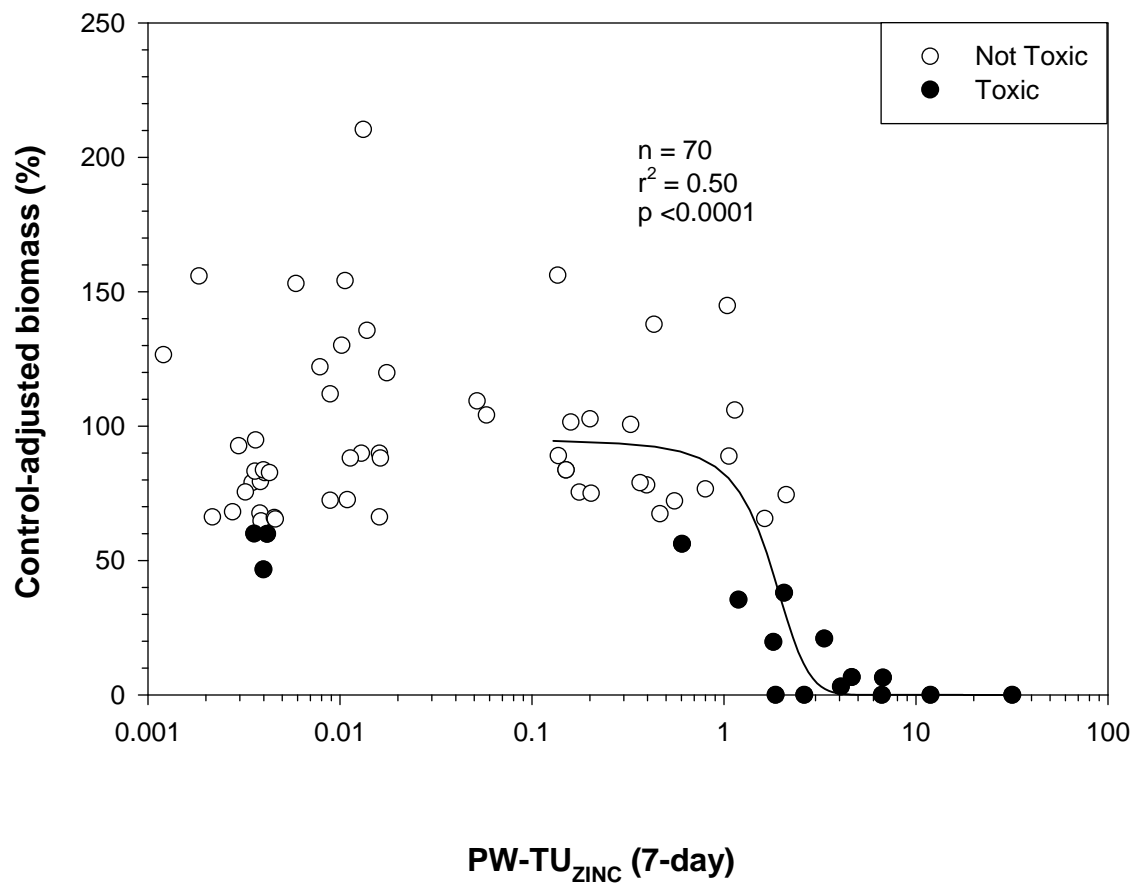
Plot A1-134. Plot illustrating the relationship between the concentration of PW-TU_{SELENIUM} and the control-adjusted biomass of amphipods (*Hyalella azteca*) in 28-d exposures to sediment samples from the Tri-State Mining District.



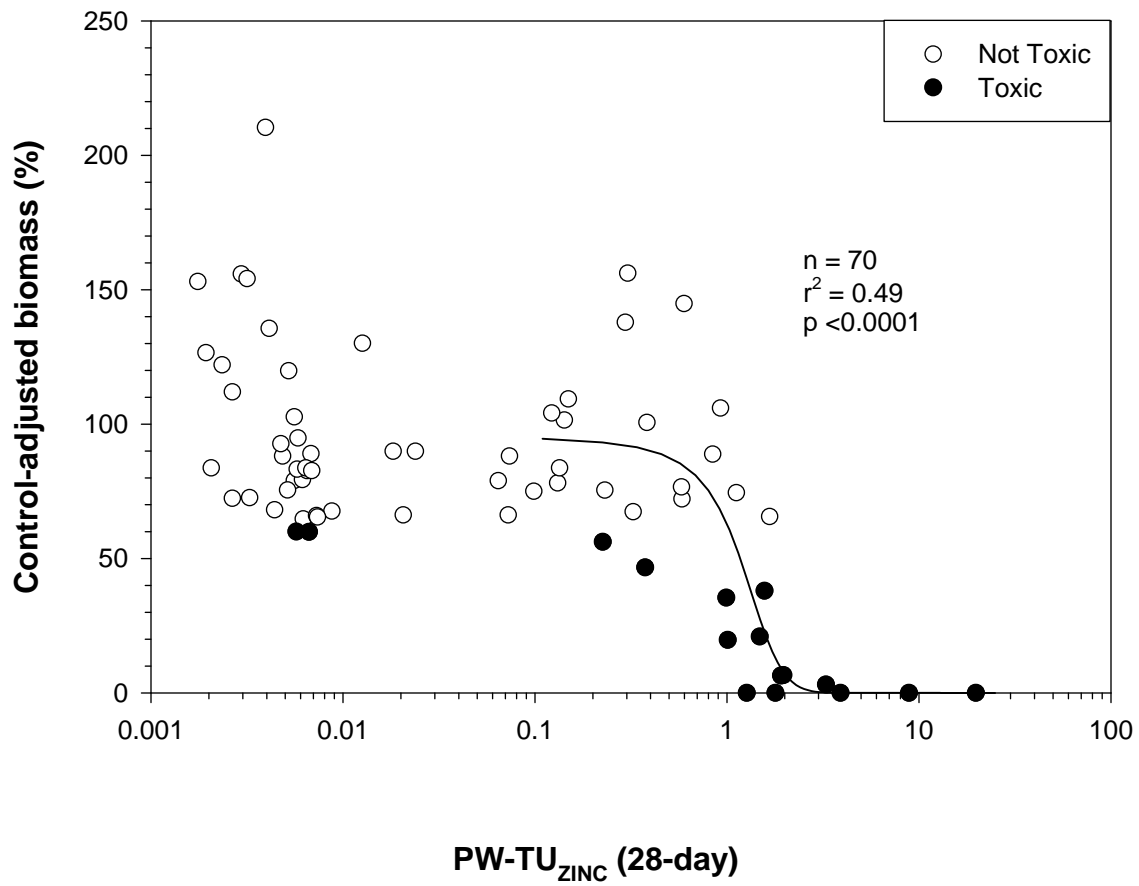
Plot A1-135. Plot illustrating the relationship between the concentration of $PW-TU_{SILVER}$ and the control-adjusted biomass of amphipods (*Hyalella azteca*) in 28-d exposures to sediment samples from the Tri-State Mining District.



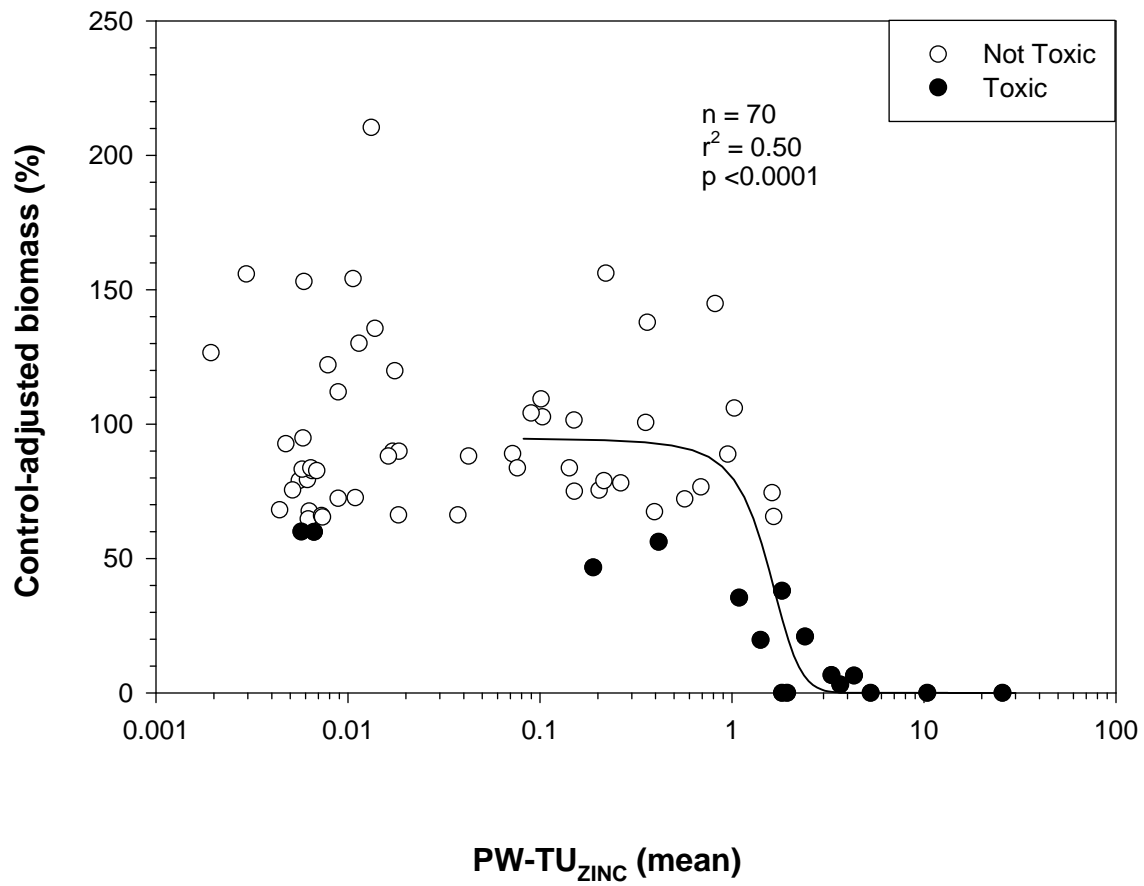
Plot A1-136. Plot illustrating the relationship between the concentration of PW-TU_{ZINC} (7-day) and the control-adjusted biomass of amphipods (*Hyalella azteca*) in 28-d exposures to sediment samples from the Tri-State Mining District.



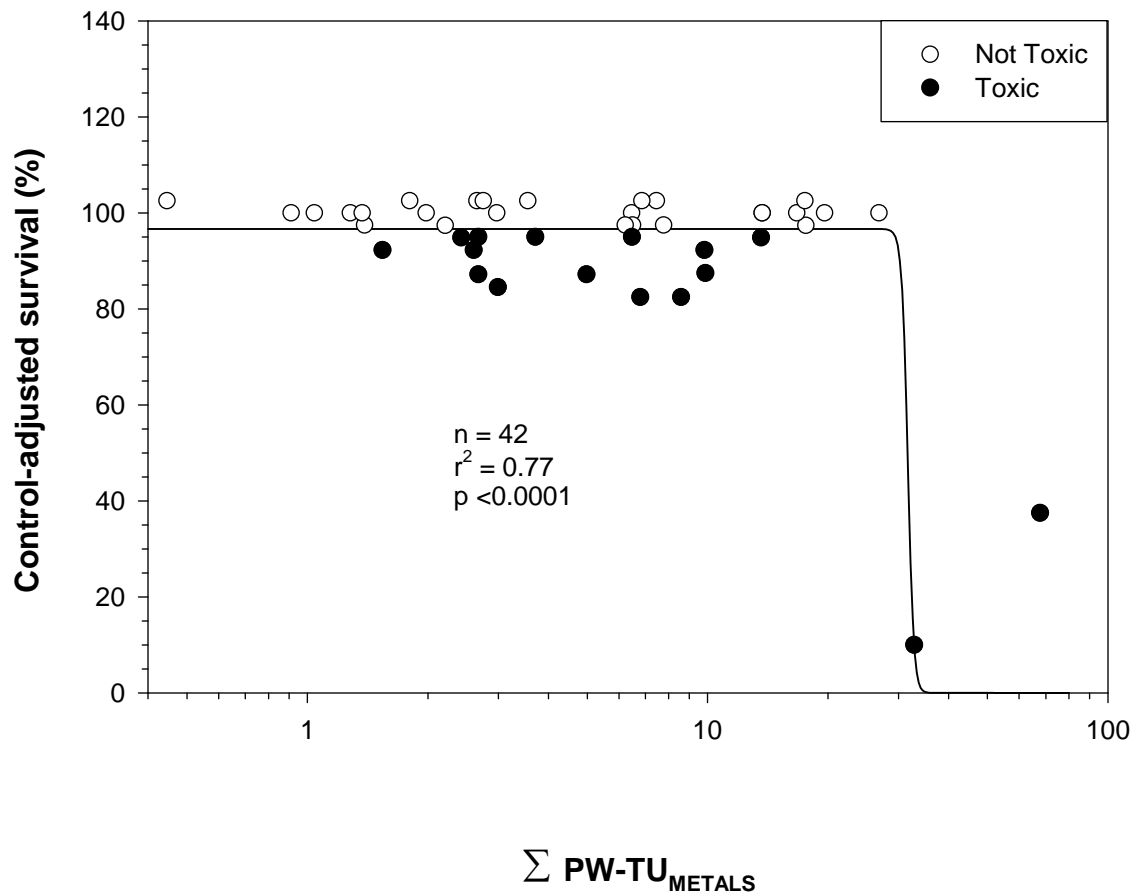
Plot A1-137. Plot illustrating the relationship between the concentration of PW-TU_{ZINC} (28-day) and the control-adjusted biomass of amphipods (*Hyalella azteca*) in 28-d exposures to sediment samples from the Tri-State Mining District.



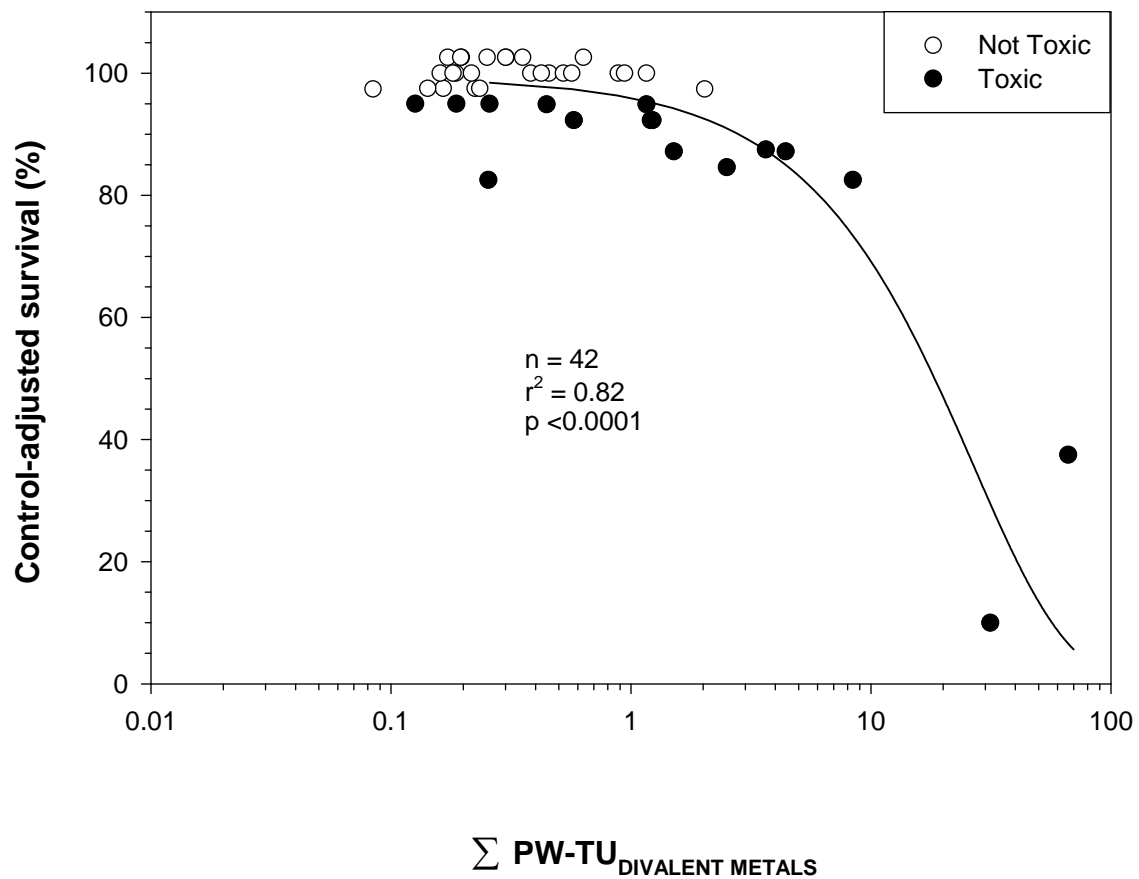
Plot A1-138. Plot illustrating the relationship between the concentration of PW-TU_{ZINC} (mean) and the control-adjusted biomass of amphipods (*Hyalella azteca*) in 28-d exposures to sediment samples from the Tri-State Mining District.



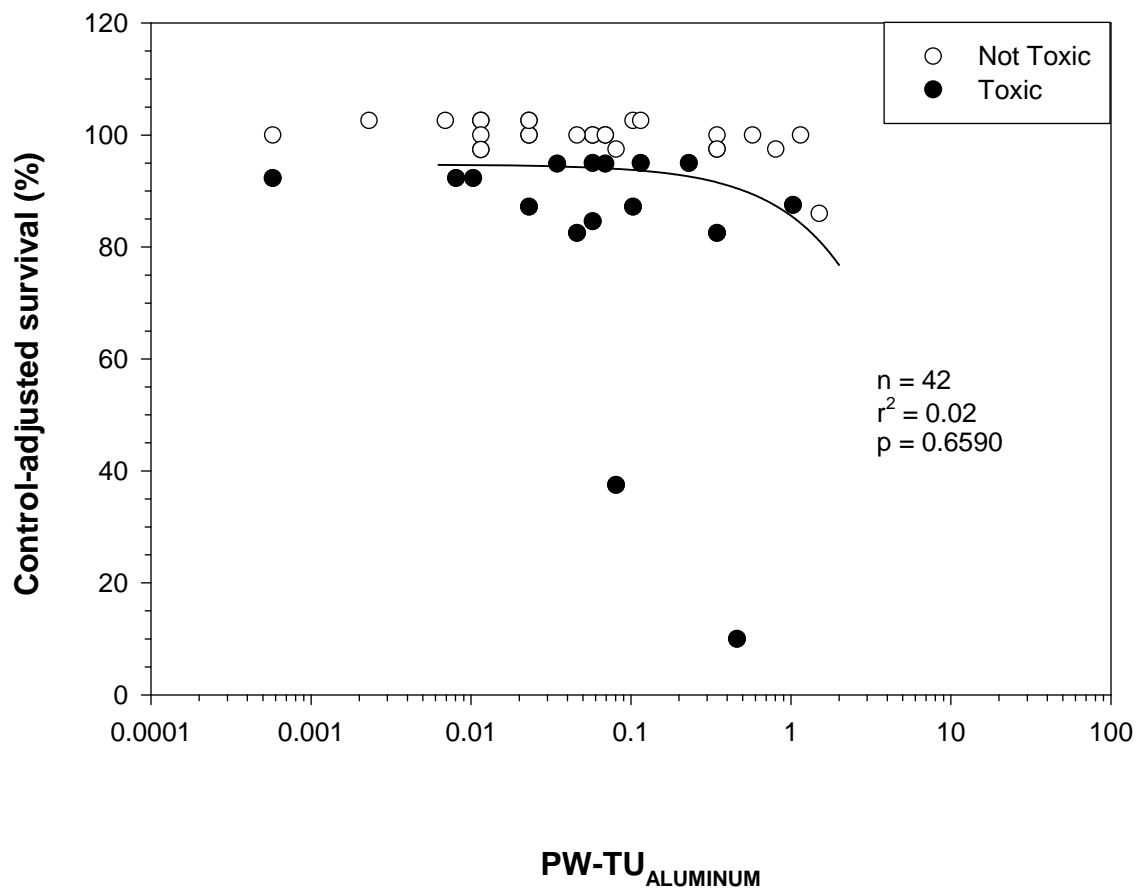
Plot A1-141. Plot illustrating the relationship between the concentration of $\sum \text{PW-TU}_{\text{METALS}}$ and the control-adjusted survival of mussels (*Lampsilis siliquoidea*) in 28-d exposures to sediment samples from the Tri-State Mining District.



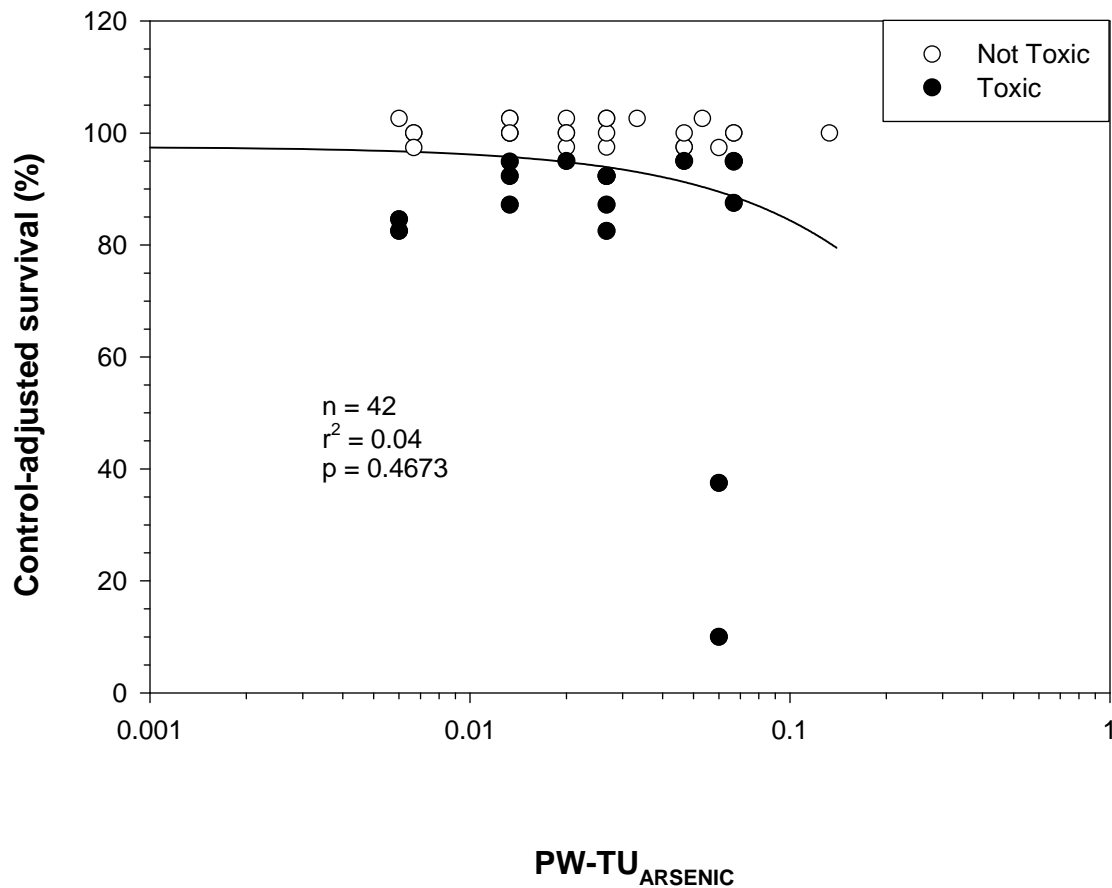
Plot A1-142. Plot illustrating the relationship between the concentration of $\sum \text{PW-TU}_{\text{Divalent Metals}}$ and the control-adjusted survival of mussels (*Lampsilis siliquoidea*) in 28-d exposures to sediment samples from the Tri-State Mining District.



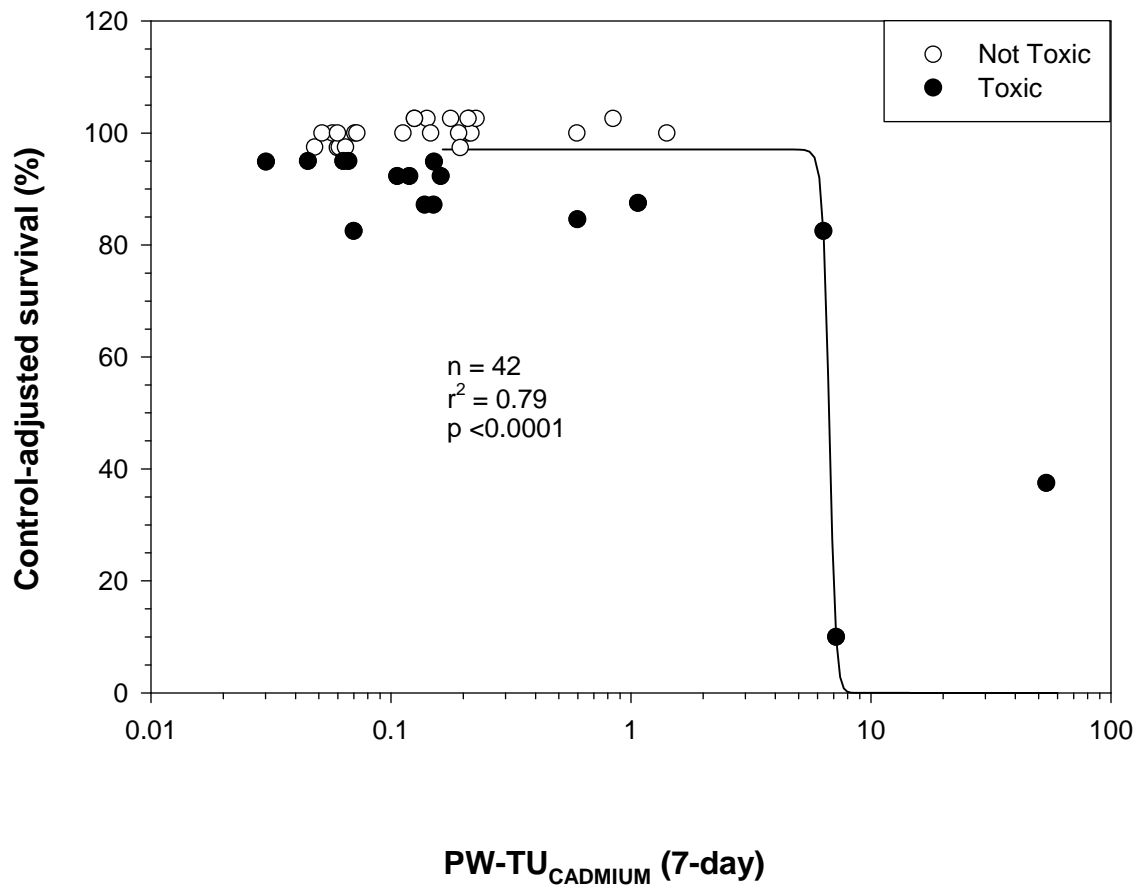
Plot A1-143. Plot illustrating the relationship between the concentration of $PW-TU_{ALUMINUM}$ and the control-adjusted survival of mussels (*Lampsilis siliquoidea*) in 28-d exposures to sediment samples from the Tri-State Mining District.



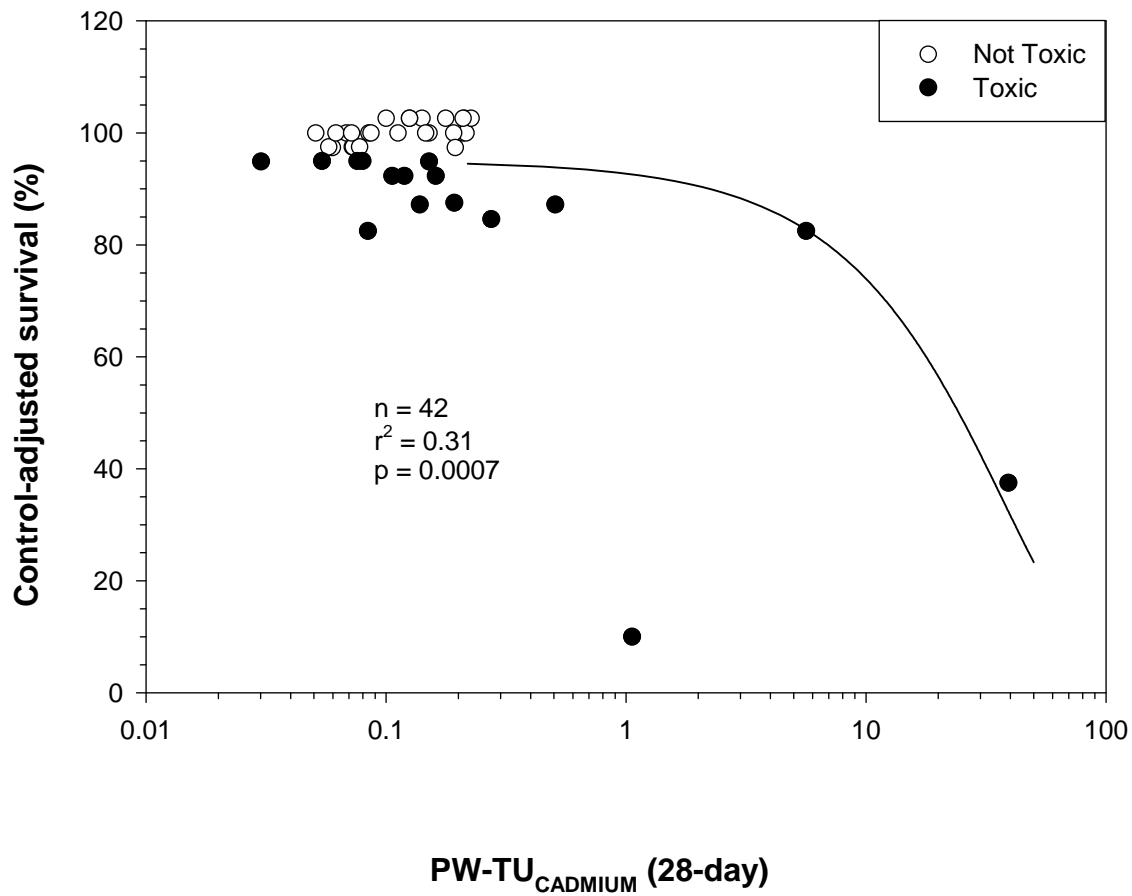
Plot A1-144. Plot illustrating the relationship between the concentration of $PW-TU_{ARSENIC}$ and the control-adjusted survival of mussels (*Lampsilis siliquoidea*) in 28-d exposures to sediment samples from the Tri-State Mining District.



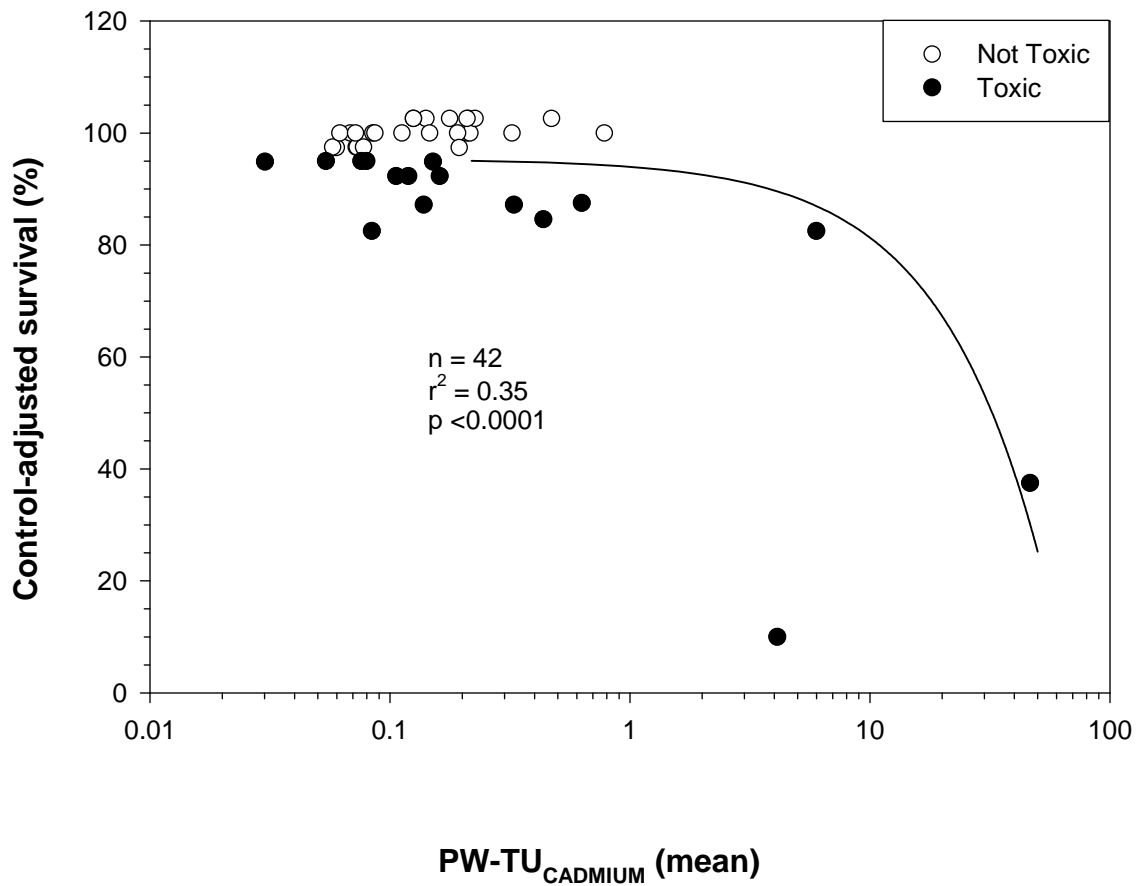
Plot A1-145. Plot illustrating the relationship between the concentration of $PW-TU_{CADMIUM}$ (7-day) and the control-adjusted survival of mussels (*Lampsilis siliquoidea*) in 28-d exposures to sediment samples from the Tri-State Mining District.



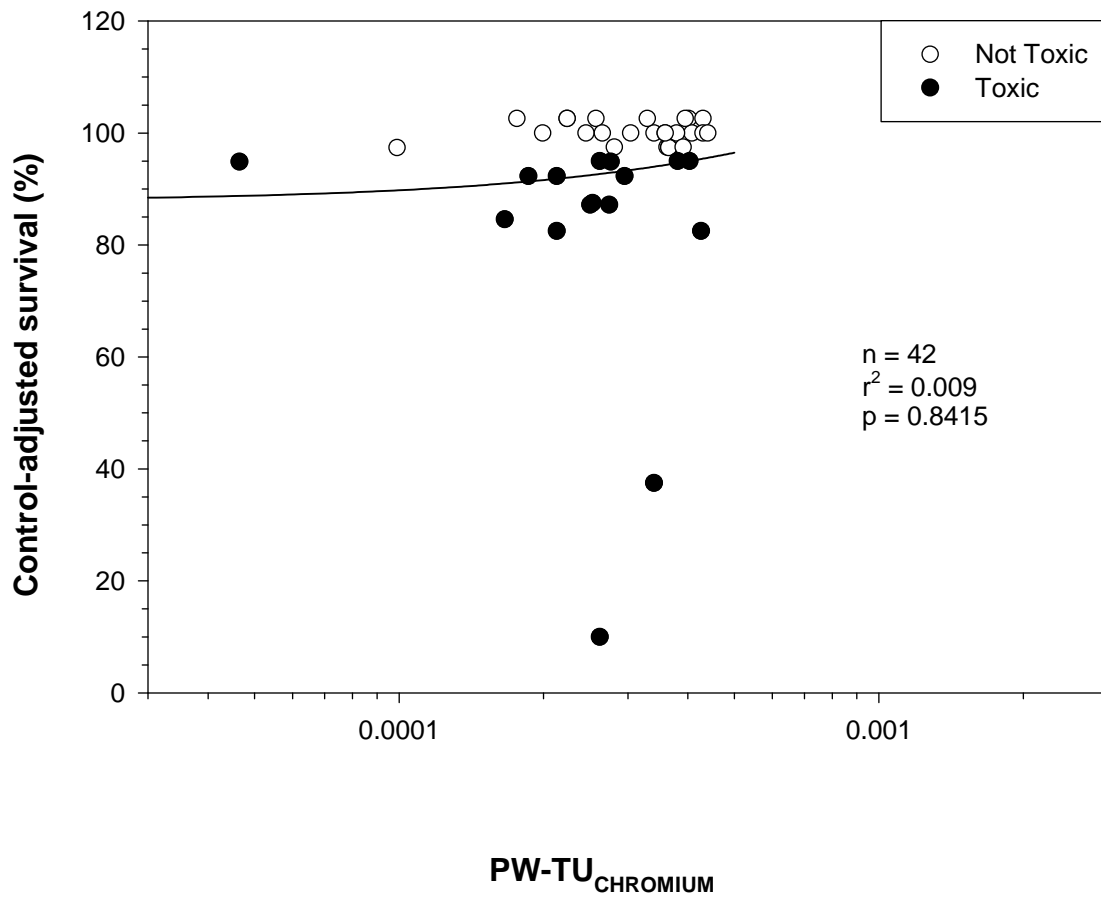
Plot A1-146. Plot illustrating the relationship between the concentration of $PW-TU_{CADMIUM}$ (28-day) and the control-adjusted survival of mussels (*Lampsilis siliquoidea*) in 28-d exposures to sediment samples from the Tri-State Mining District.



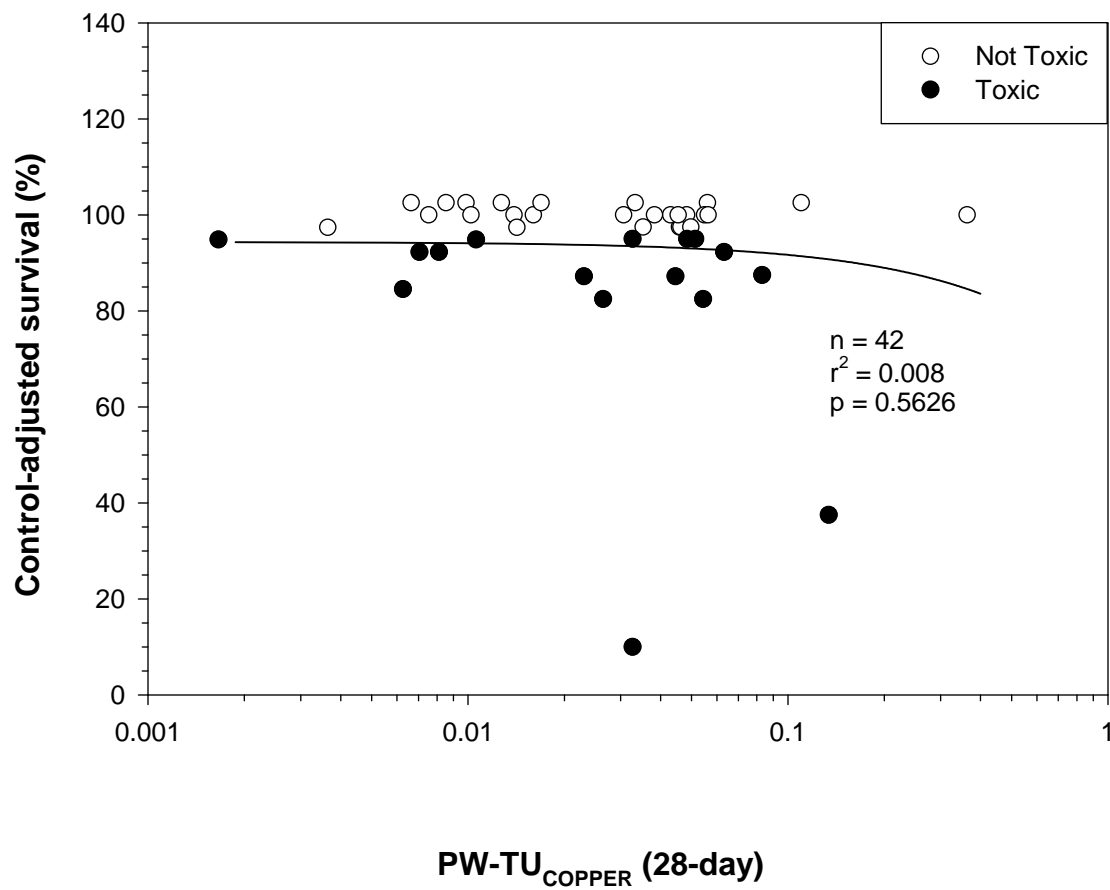
Plot A1-147. Plot illustrating the relationship between the concentration of PW-TU_{CADMIUM} (mean) and the control-adjusted survival of mussels (*Lampsilis siliquoidea*) in 28-d exposures to sediment samples from the Tri-State Mining District.



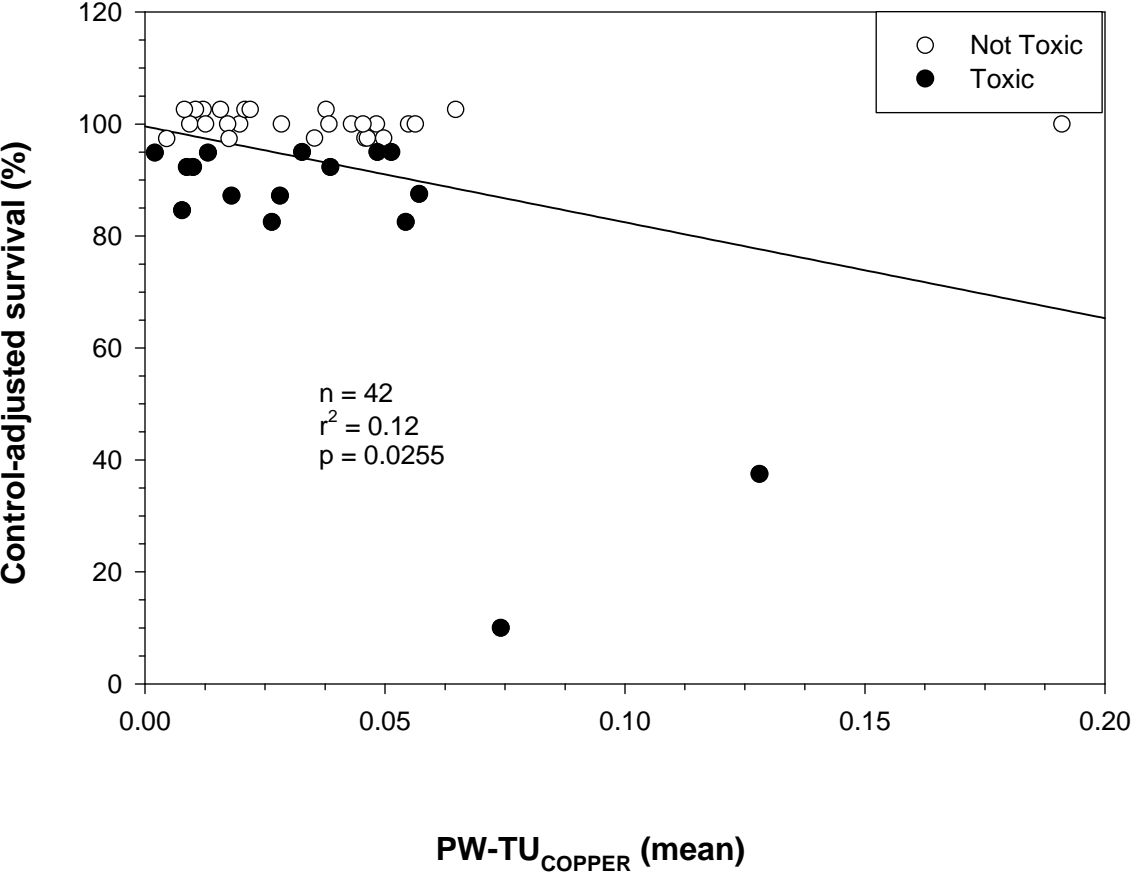
Plot A1-148. Plot illustrating the relationship between the concentration of $PW-TU_{CHROMIUM}$ and the control-adjusted survival of mussels (*Lampsilis siliquoidea*) in 28-d exposures to sediment samples from the Tri-State Mining District.



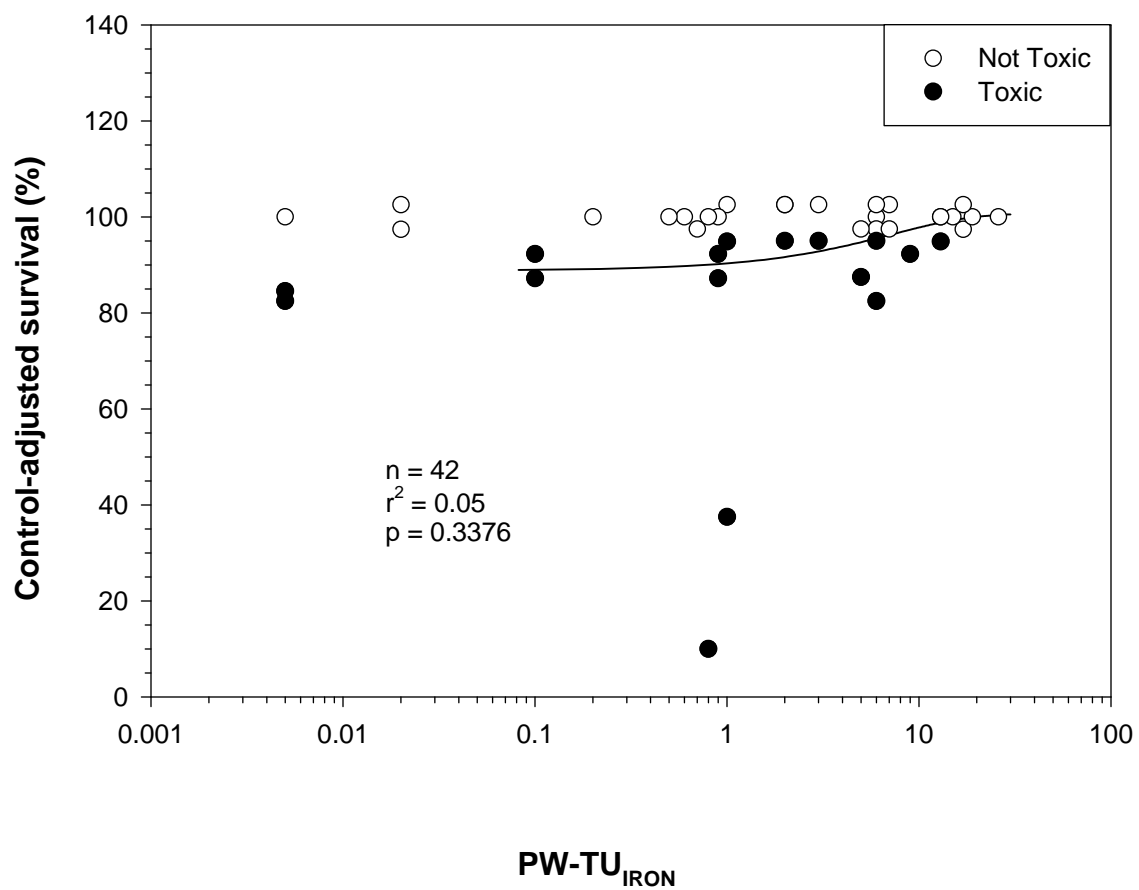
Plot A1-150. Plot illustrating the relationship between the concentration of PW-TU_{COPPER} (28-day) and the control-adjusted survival of mussels (*Lampsilis siliquoidea*) in 28-d exposures to sediment samples from the Tri-State Mining District.



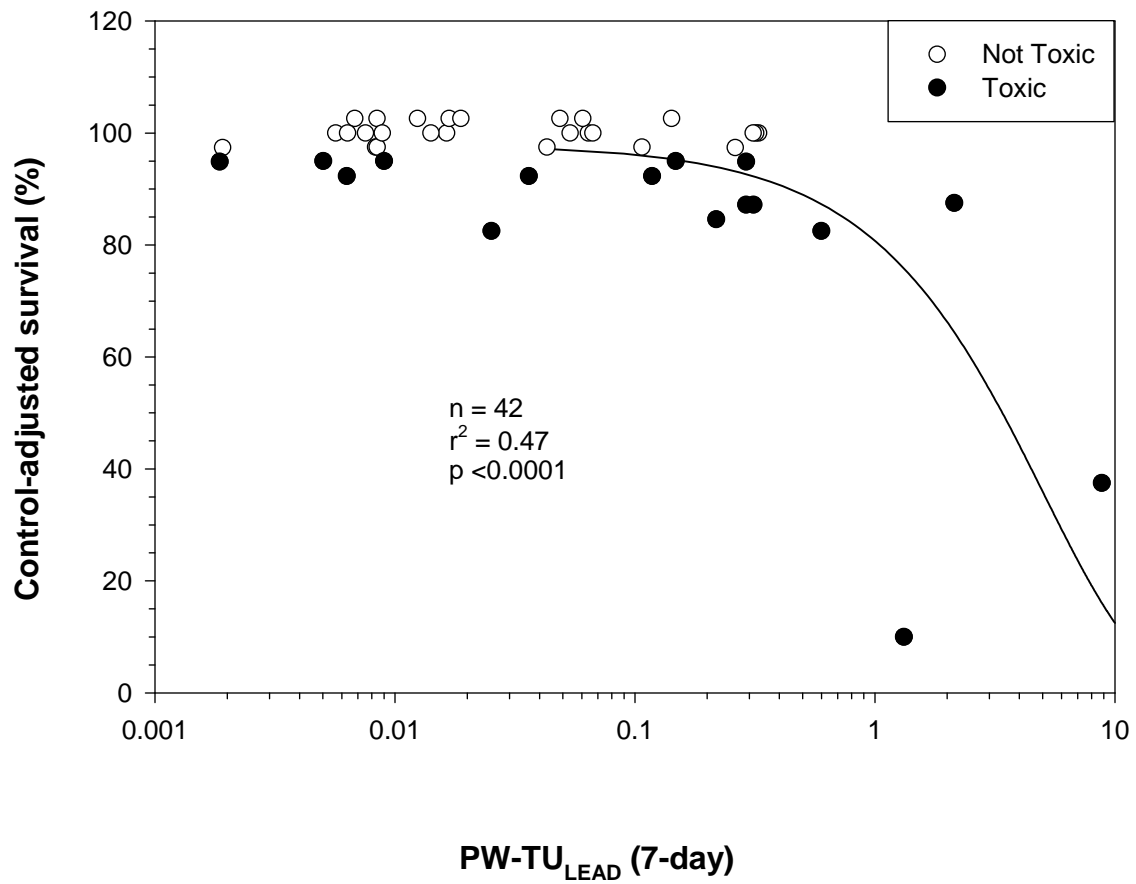
Plot A1-151. Plot illustrating the relationship between the concentration of PW-TU_{COPPER} (mean) and the control-adjusted survival of mussels (*Lampsilis siliquoidea*) in 28-d exposures to sediment samples from the Tri-State Mining District.



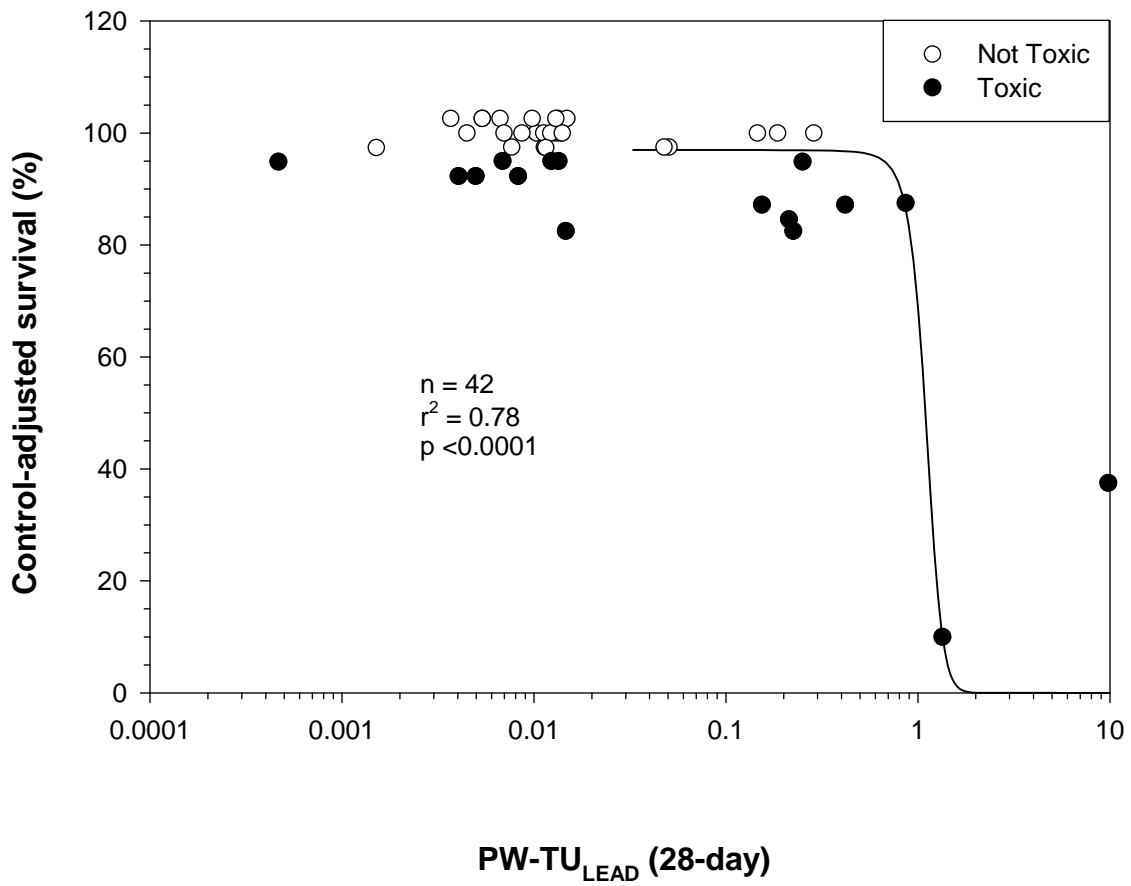
Plot A1-152. Plot illustrating the relationship between the concentration of $PW-TU_{IRON}$ and the control-adjusted survival of mussels (*Lampsilis siliquoidea*) in 28-d exposures to sediment samples from the Tri-State Mining District.



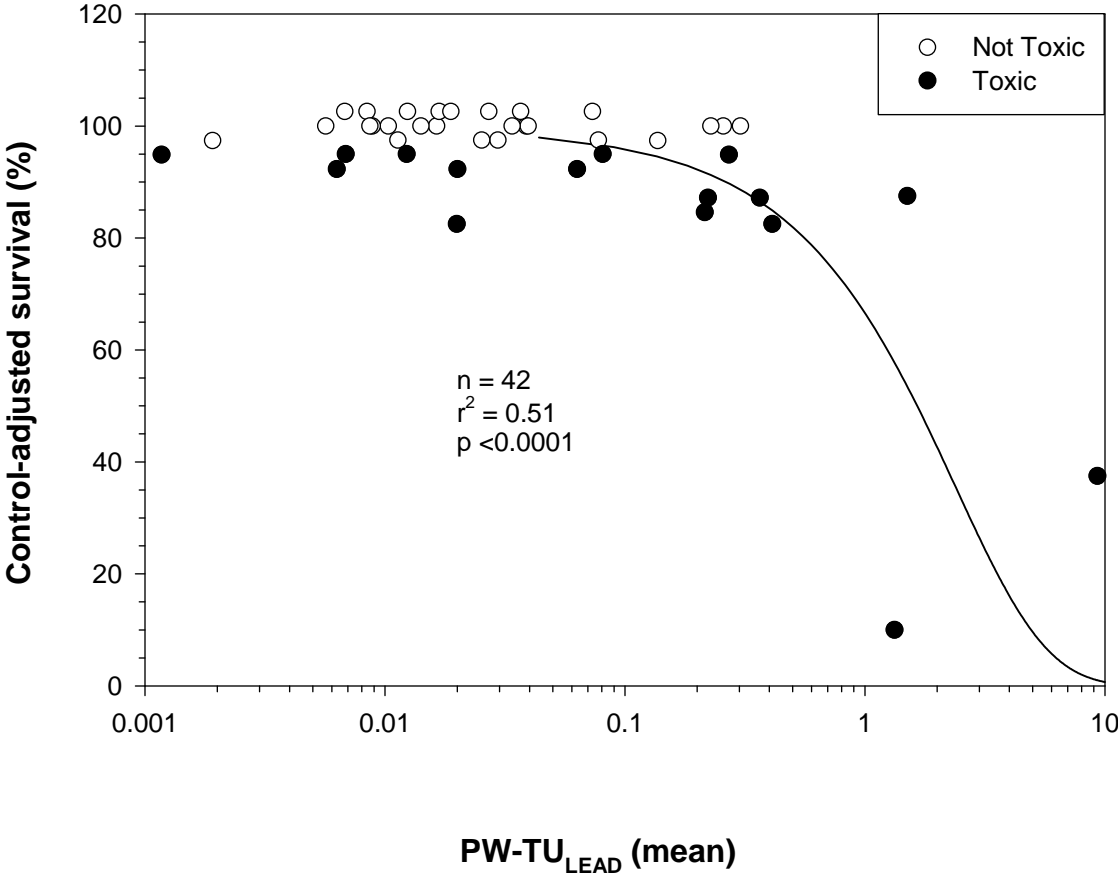
Plot A1-153. Plot illustrating the relationship between the concentration of PW-TU_{LEAD} (7-day) and the control-adjusted survival of mussels (*Lampsilis siliquoidea*) in 28-d exposures to sediment samples from the Tri-State Mining District.



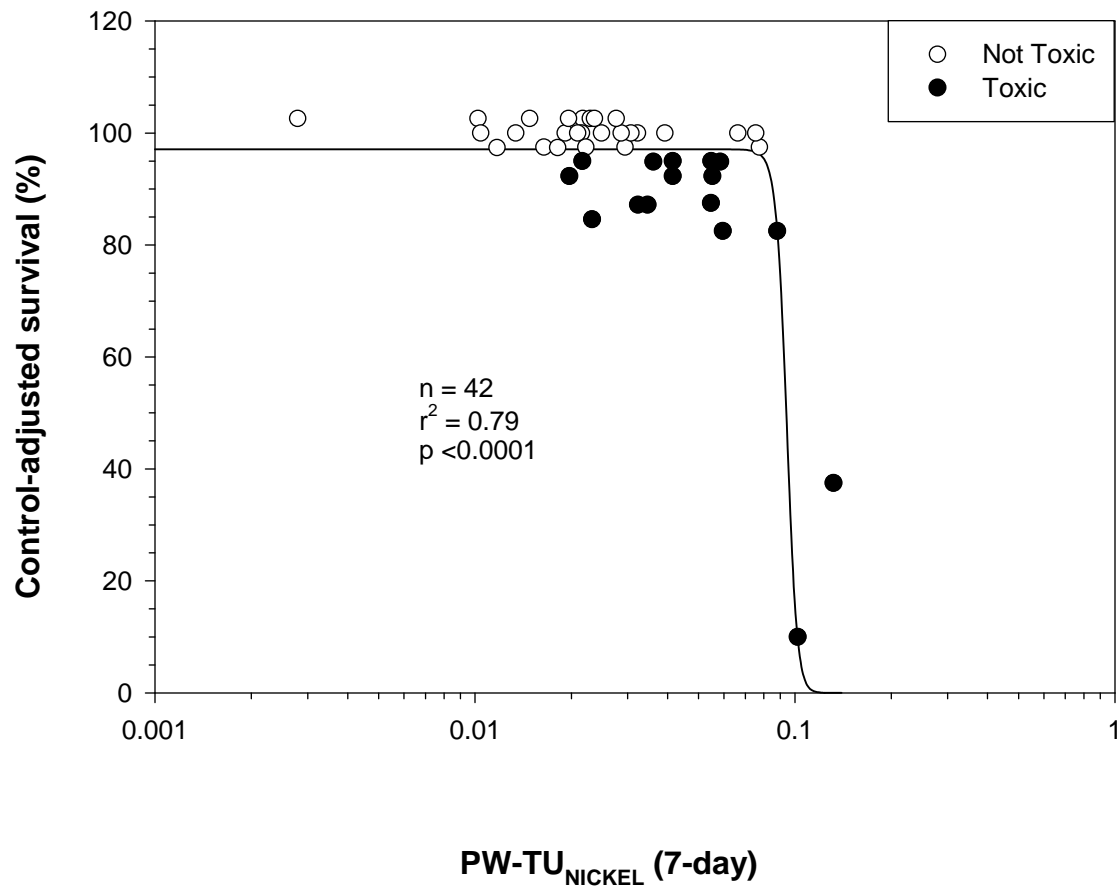
Plot A1-154. Plot illustrating the relationship between the concentration of PW-TU_{LEAD} (28-day) and the control-adjusted survival of mussels (*Lampsilis siliquoidea*) in 28-d exposures to sediment samples from the Tri-State Mining District.



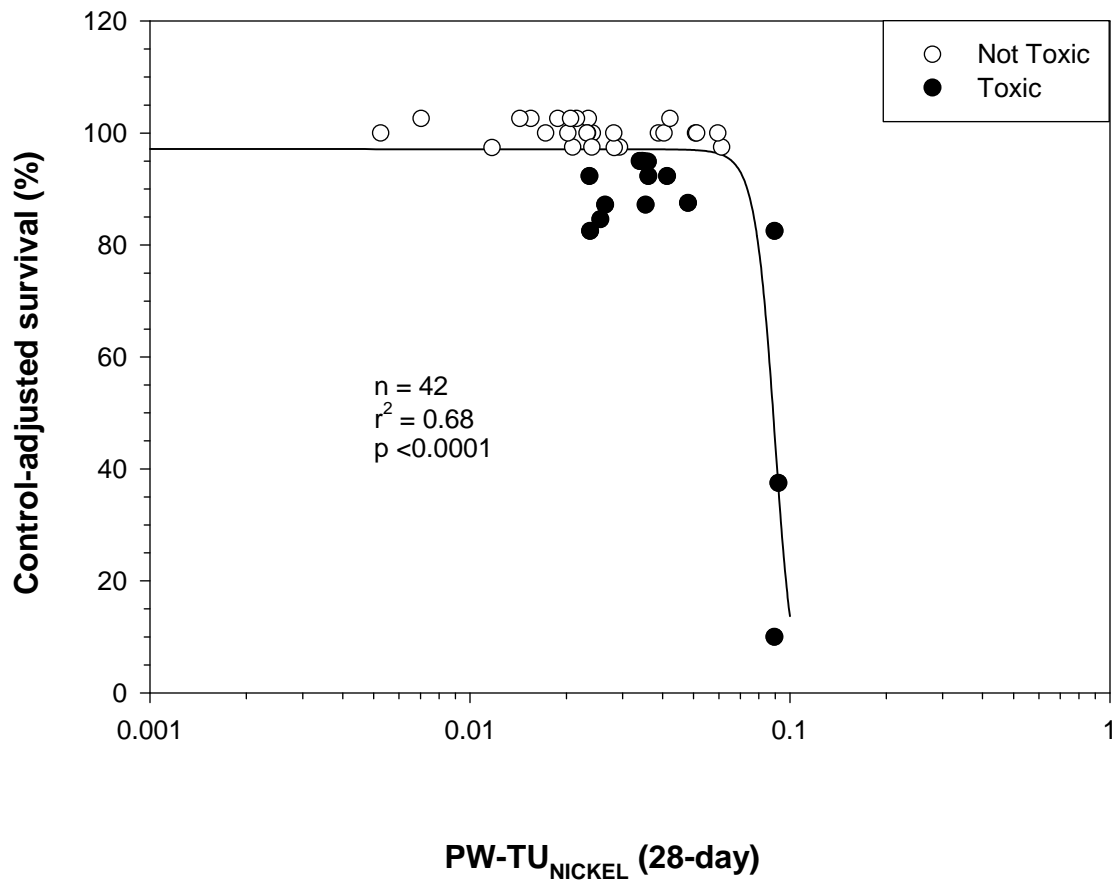
Plot A1-155. Plot illustrating the relationship between the concentration of PW-TU_{LEAD} (mean) and the control-adjusted survival of mussels (*Lampsilis siliquoidea*) in 28-d exposures to sediment samples from the Tri-State Mining District.



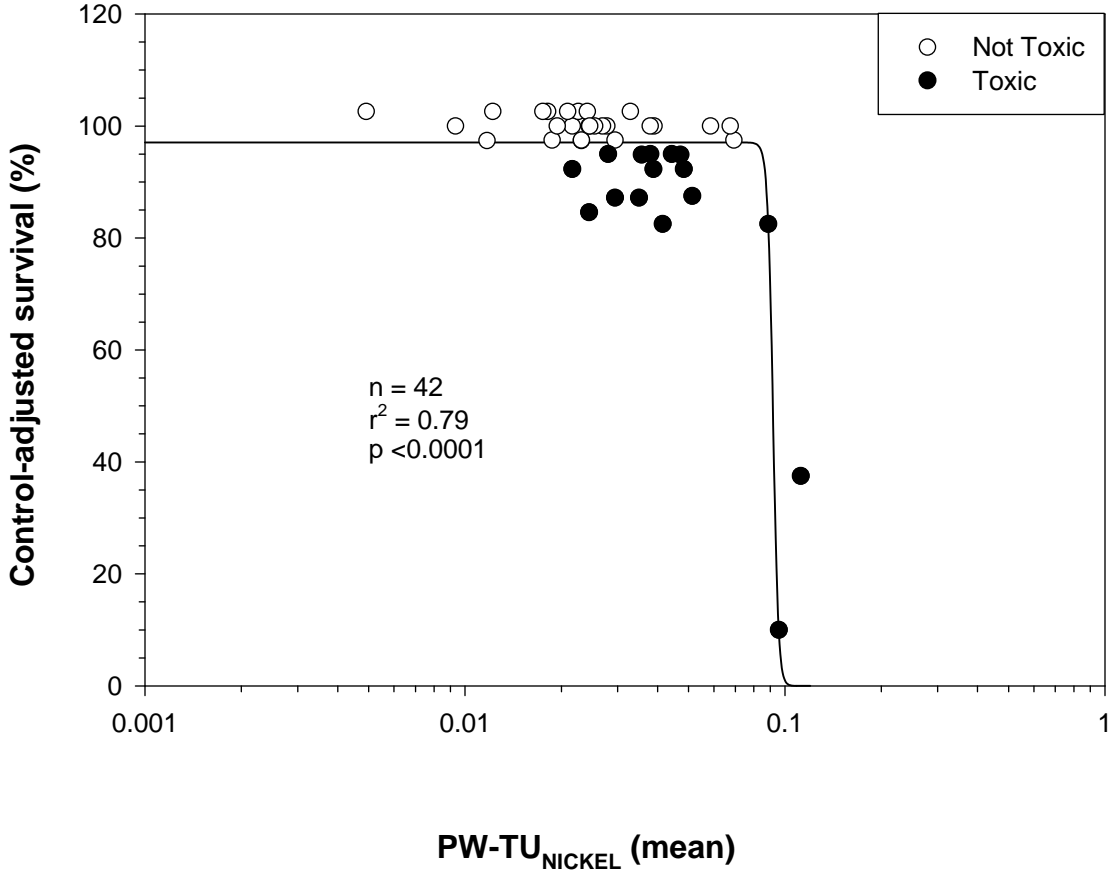
Plot A1-156. Plot illustrating the relationship between the concentration of $PW-TU_{NICKEL}$ (7-day) and the control-adjusted survival of mussels (*Lampsilis siliquoidea*) in 28-d exposures to sediment samples from the Tri-State Mining District.



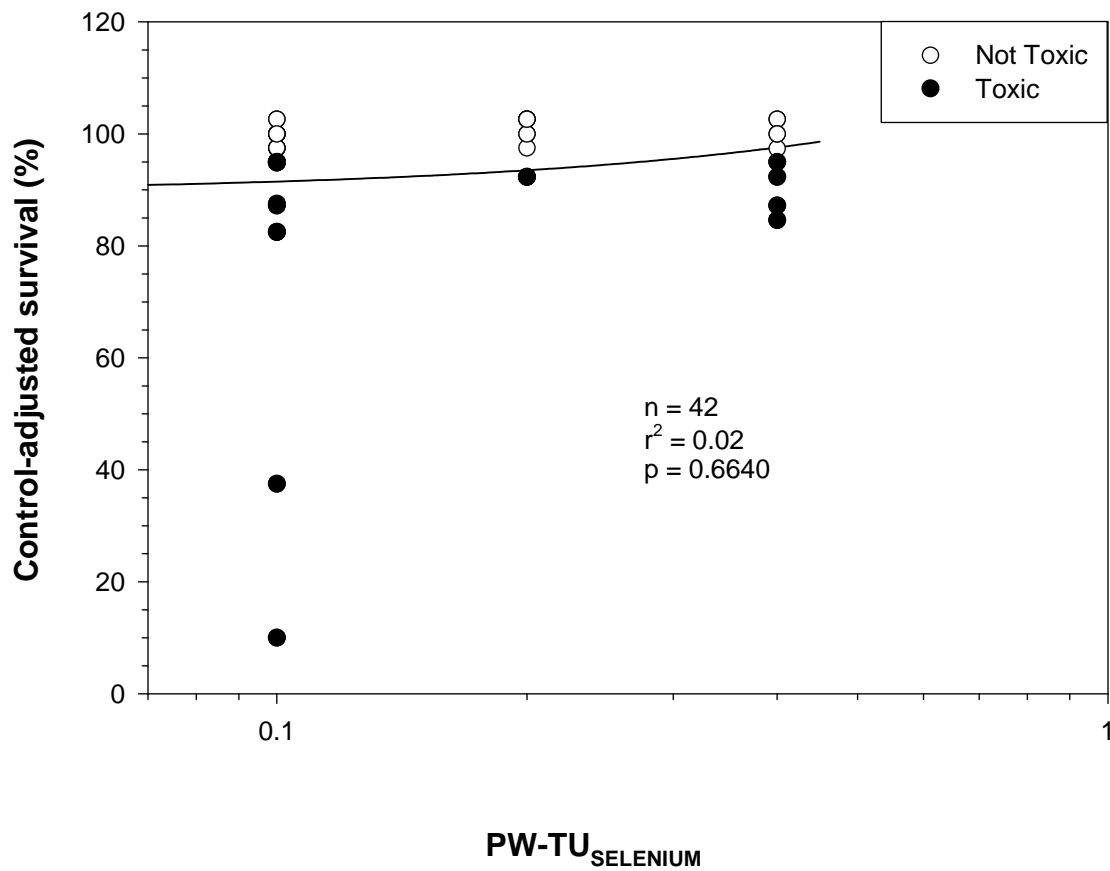
Plot A1-157. Plot illustrating the relationship between the concentration of PW-TU_{NICKEL} (28-day) and the control-adjusted survival of mussels (*Lampsilis siliquoidea*) in 28-d exposures to sediment samples from the Tri-State Mining District.



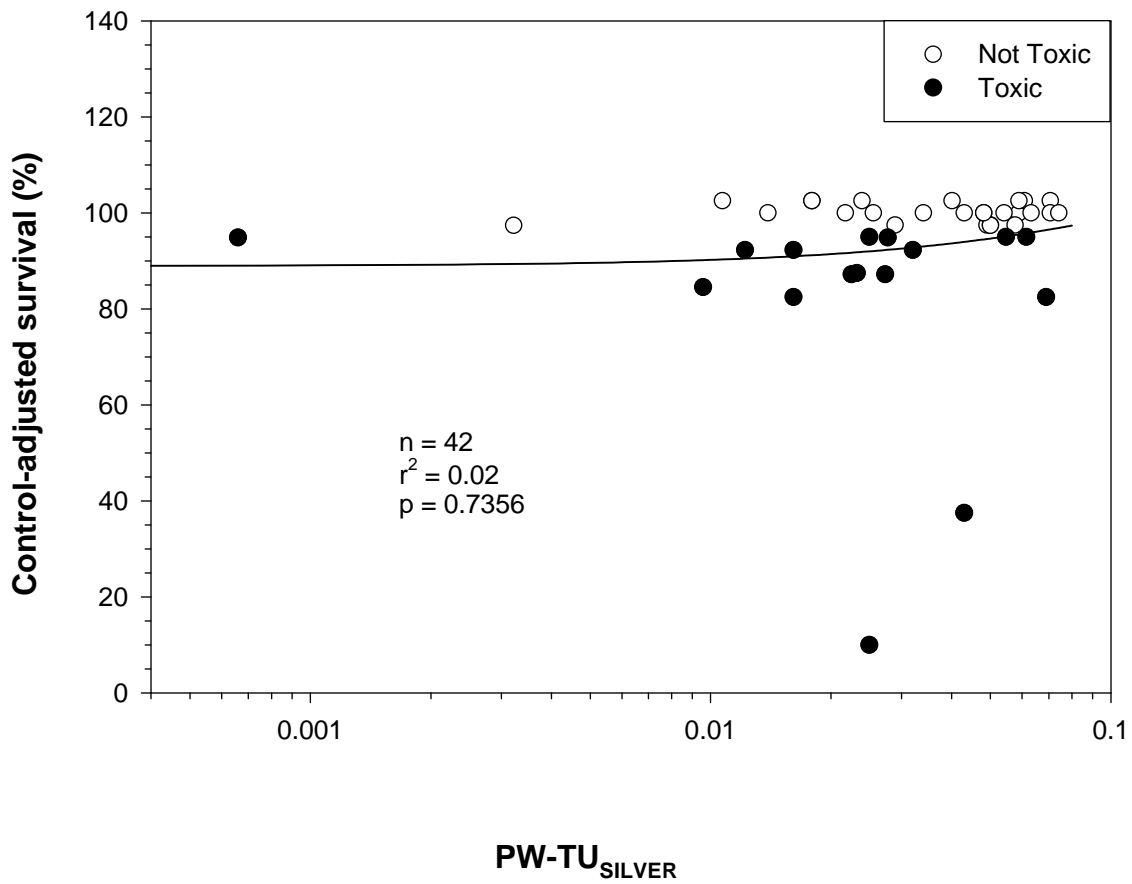
Plot A1-158. Plot illustrating the relationship between the concentration of PW-TU_{NICKEL} (mean) and the control-adjusted survival of mussels (*Lampsilis siliquoidea*) in 28-d exposures to sediment samples from the Tri-State Mining District.



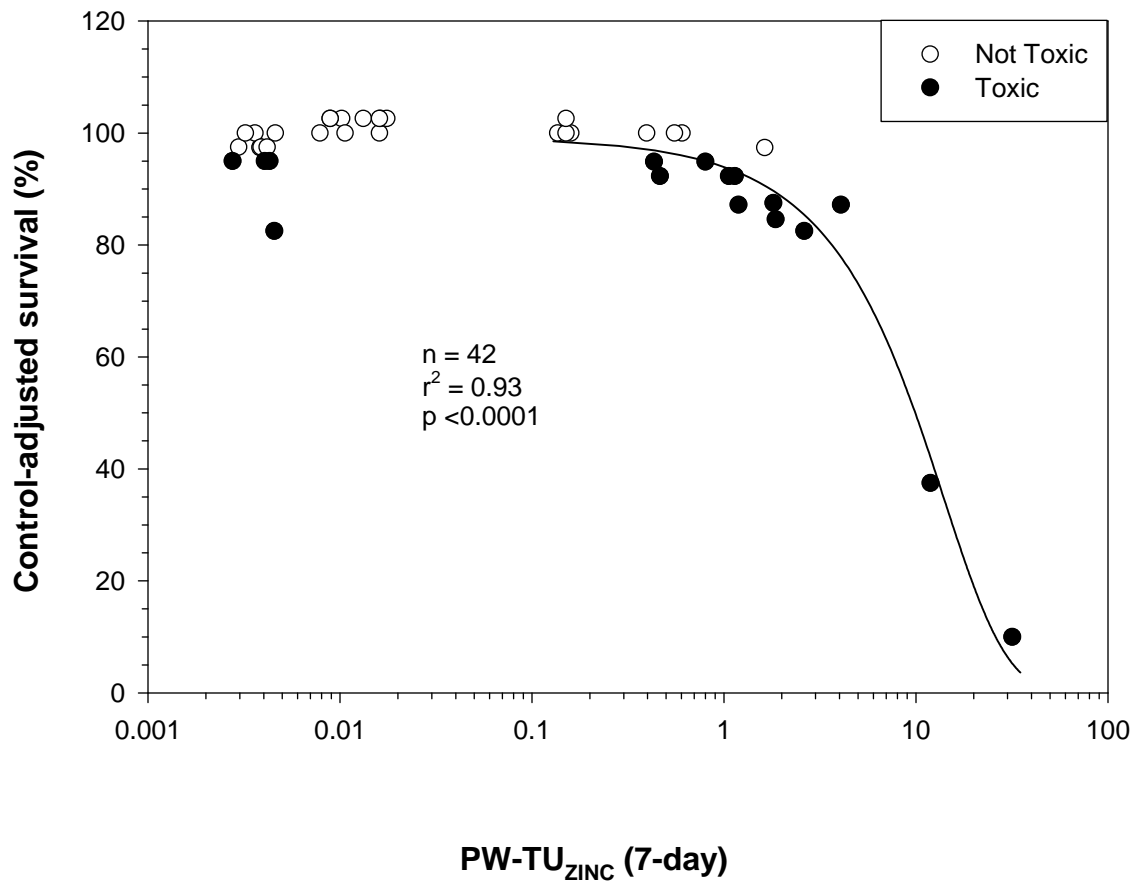
Plot A1-159. Plot illustrating the relationship between the concentration of $PW-TU_{SELENIUM}$ and the control-adjusted survival of mussels (*Lampsilis siliquoidea*) in 28-d exposures to sediment samples from the Tri-State Mining District.



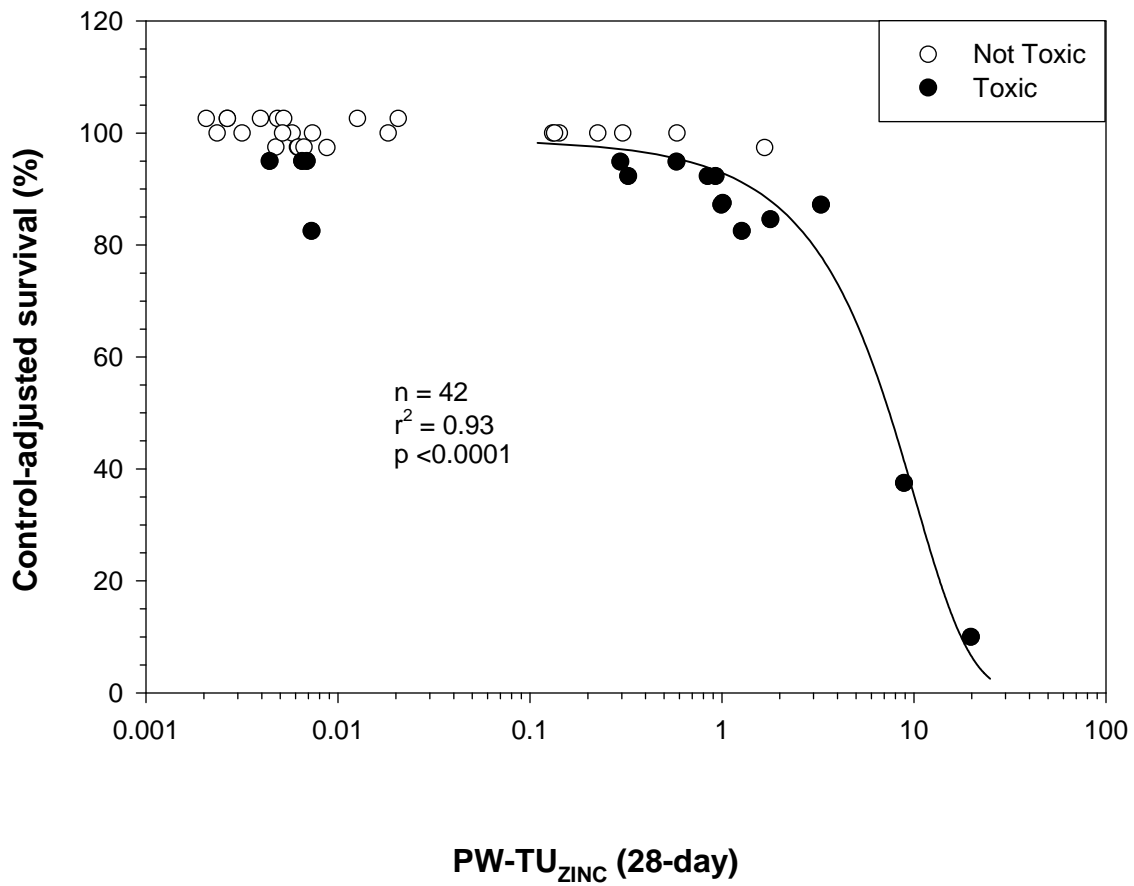
Plot A1-160. Plot illustrating the relationship between the concentration of $PW-TU_{SILVER}$ and the control-adjusted survival of mussels (*Lampsilis siliquoidea*) in 28-d exposures to sediment samples from the Tri-State Mining District.



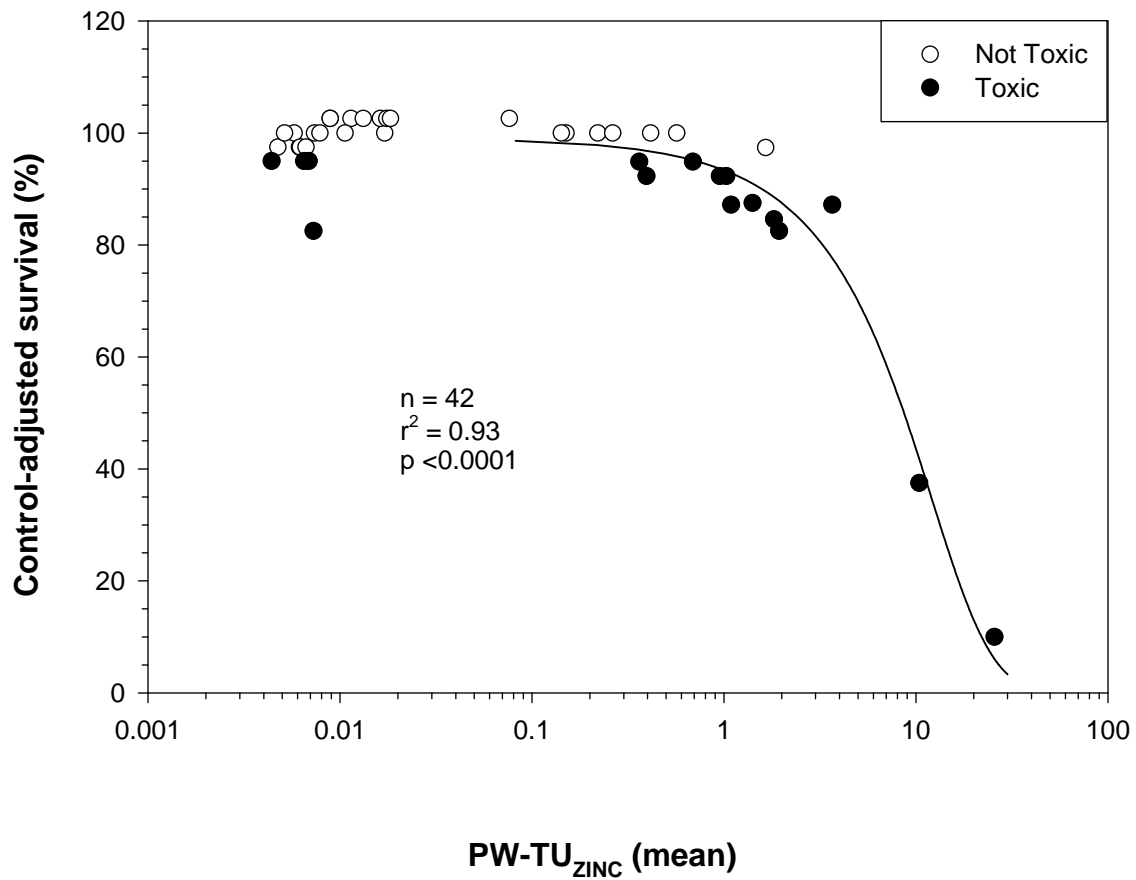
Plot A1-161. Plot illustrating the relationship between the concentration of PW-TU_{ZINC} (7-day) and the control-adjusted survival of mussels (*Lampsilis siliquoidea*) in 28-d exposures to sediment samples from the Tri-State Mining District.



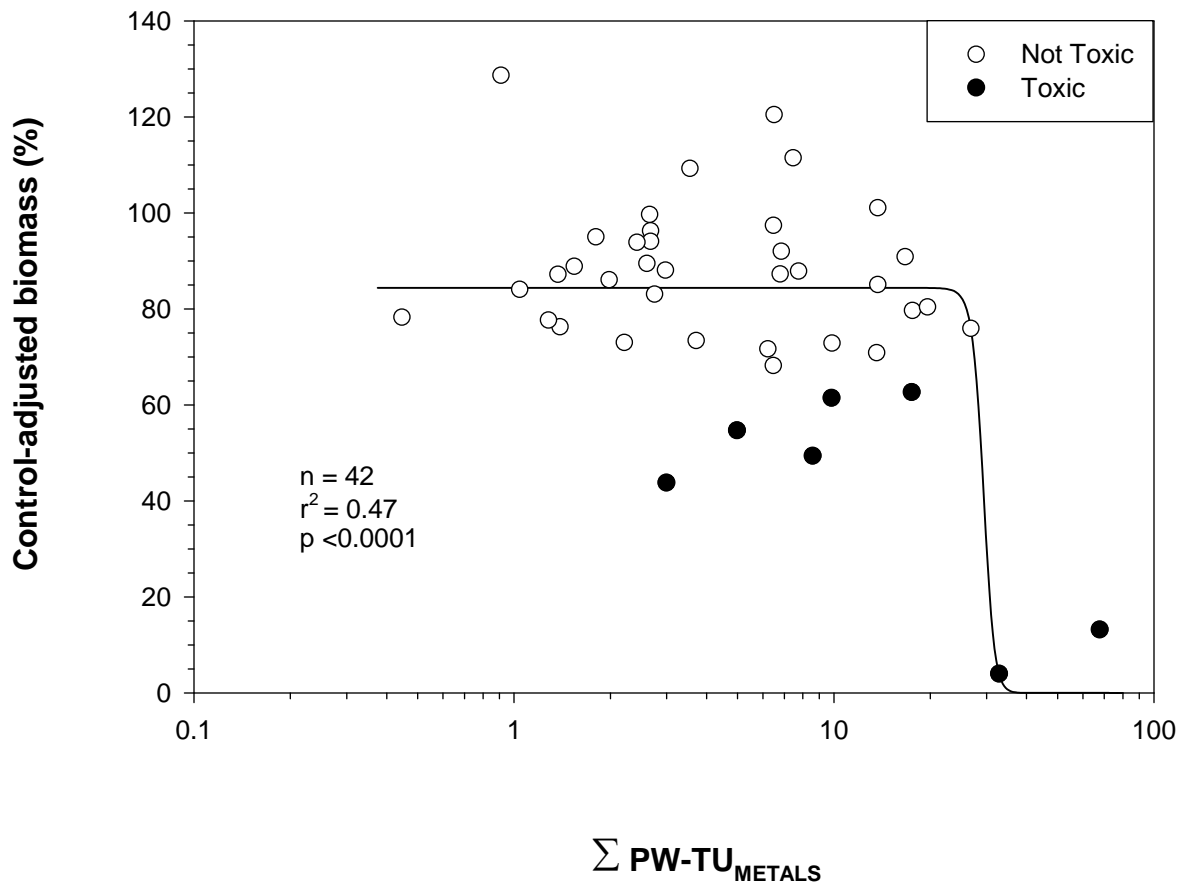
Plot A1-162. Plot illustrating the relationship between the concentration of PW-TU_{ZINC} (28-day) and the control-adjusted survival of mussels (*Lampsilis siliquoidea*) in 28-d exposures to sediment samples from the Tri-State Mining District.



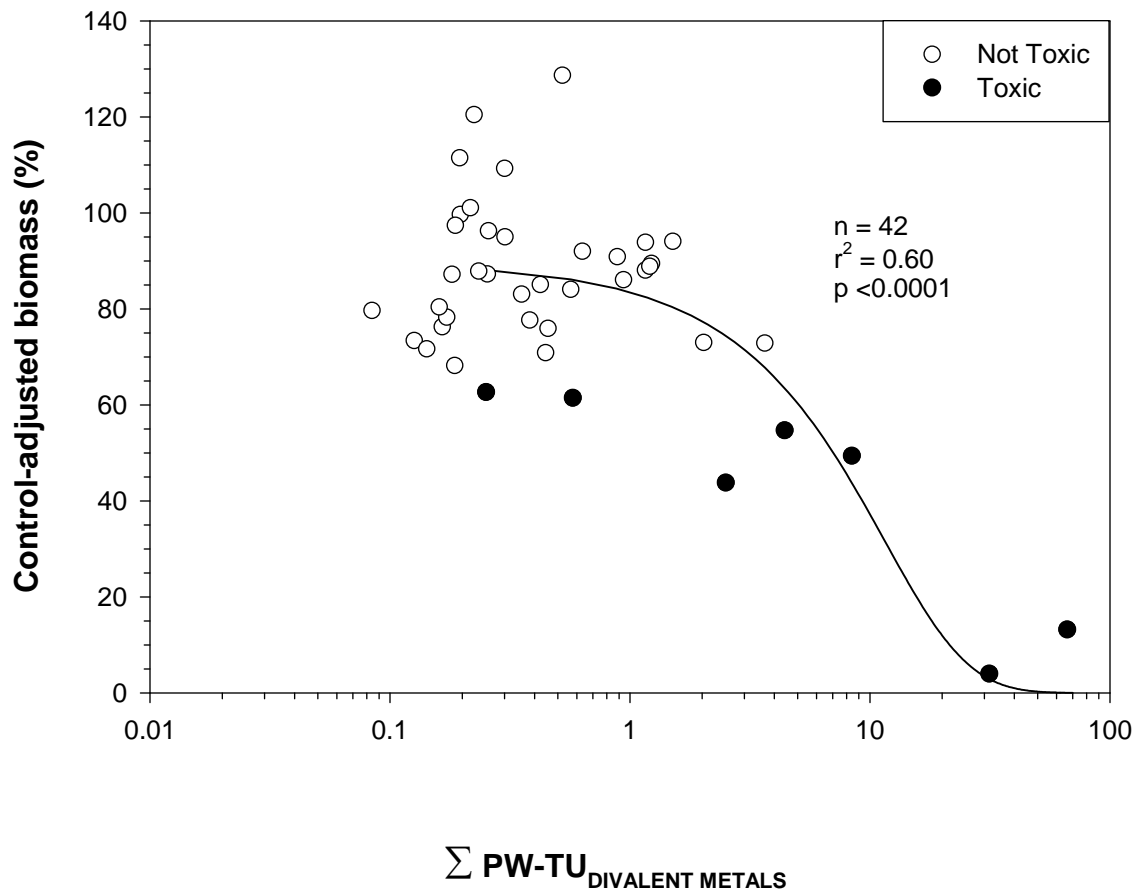
Plot A1-163. Plot illustrating the relationship between the concentration of PW-TU_{ZINC} (mean) and the control-adjusted survival of mussels (*Lampsilis siliquoidea*) in 28-d exposures to sediment samples from the Tri-State Mining District.



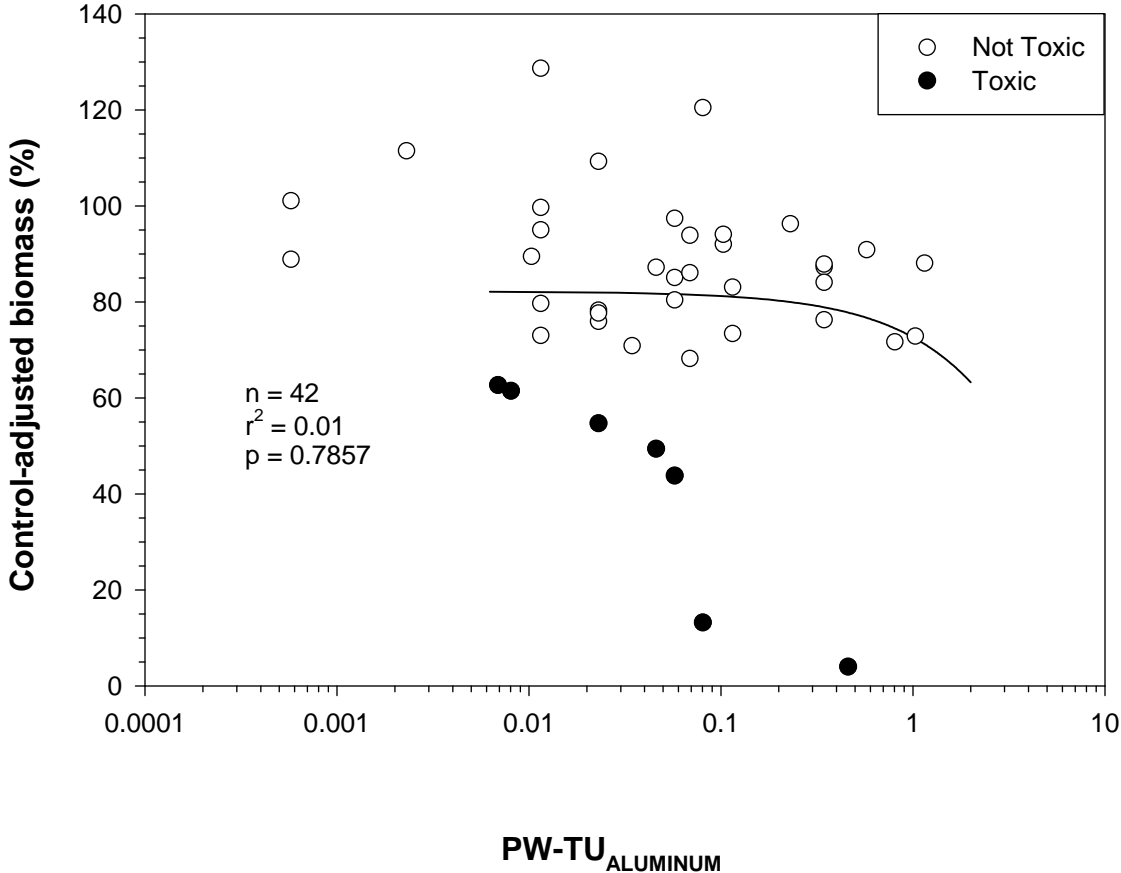
Plot A1-166. Plot illustrating the relationship between the concentration of $\Sigma PW-TU_{METALS}$ and the control-adjusted biomass of mussels (*Lampsilis siliquoidea*) in 28-d exposures to sediment samples from the Tri-State Mining District.



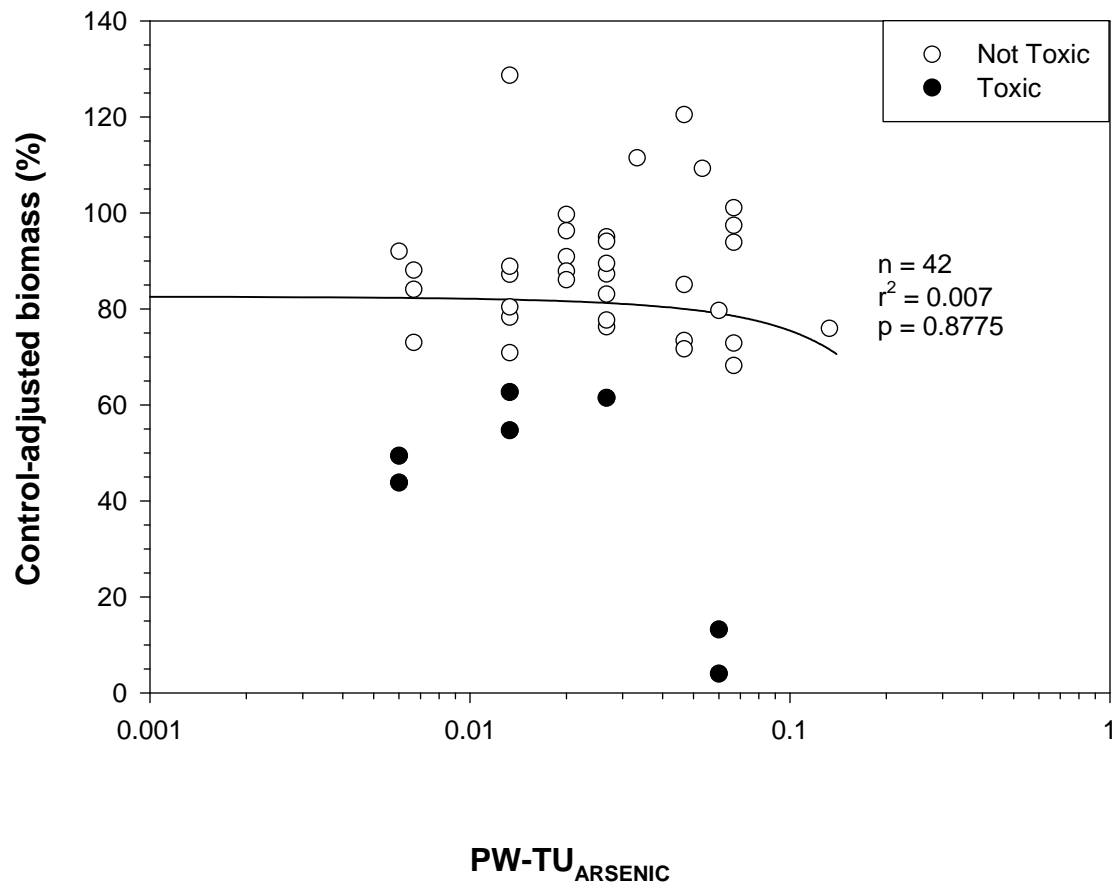
Plot A1-167. Plot illustrating the relationship between the concentration of $\sum \text{PW-TU}_{\text{Divalent Metals}}$ and the control-adjusted biomass of mussels (*Lampsilis siliquoidea*) in 28-d exposures to sediment samples from the Tri-State Mining District.



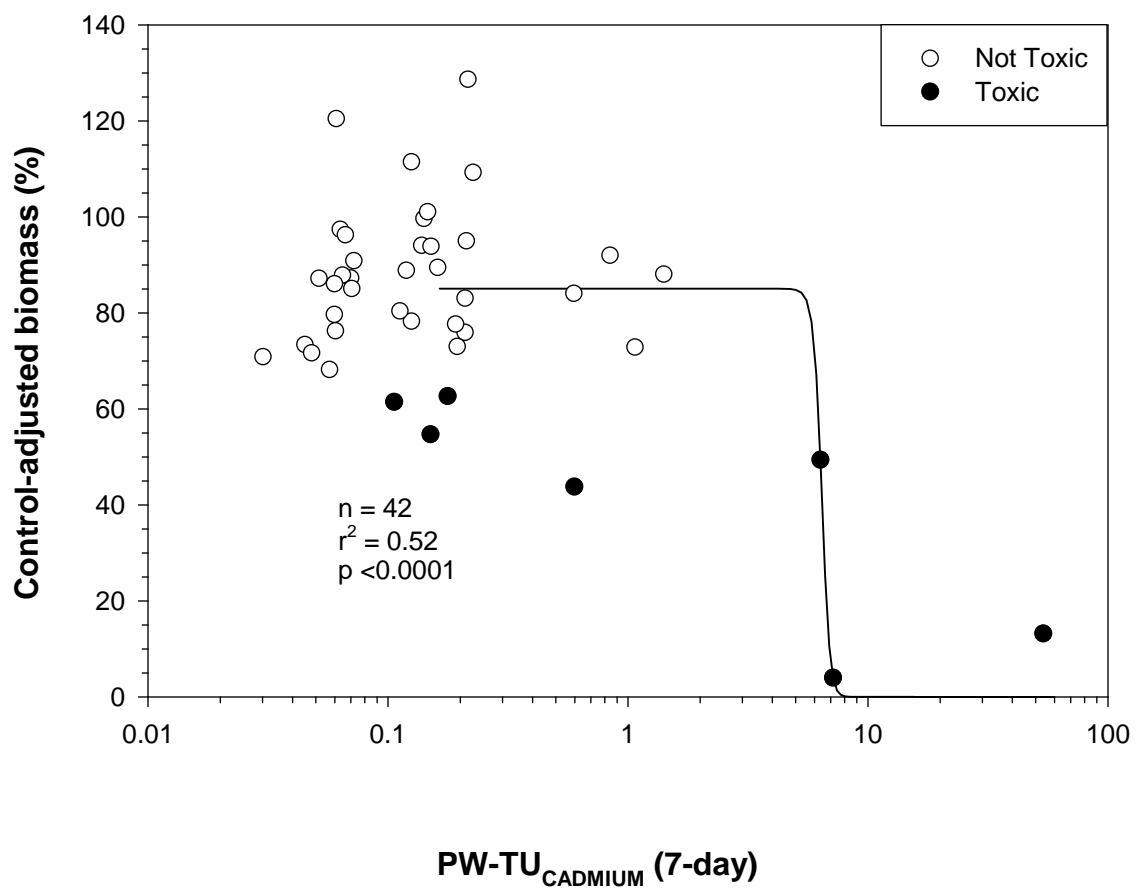
Plot A1-168. Plot illustrating the relationship between the concentration of $PW-TU_{ALUMINUM}$ and the control-adjusted biomass of mussels (*Lampsilis siliquoidea*) in 28-d exposures to sediment samples from the Tri-State Mining District.



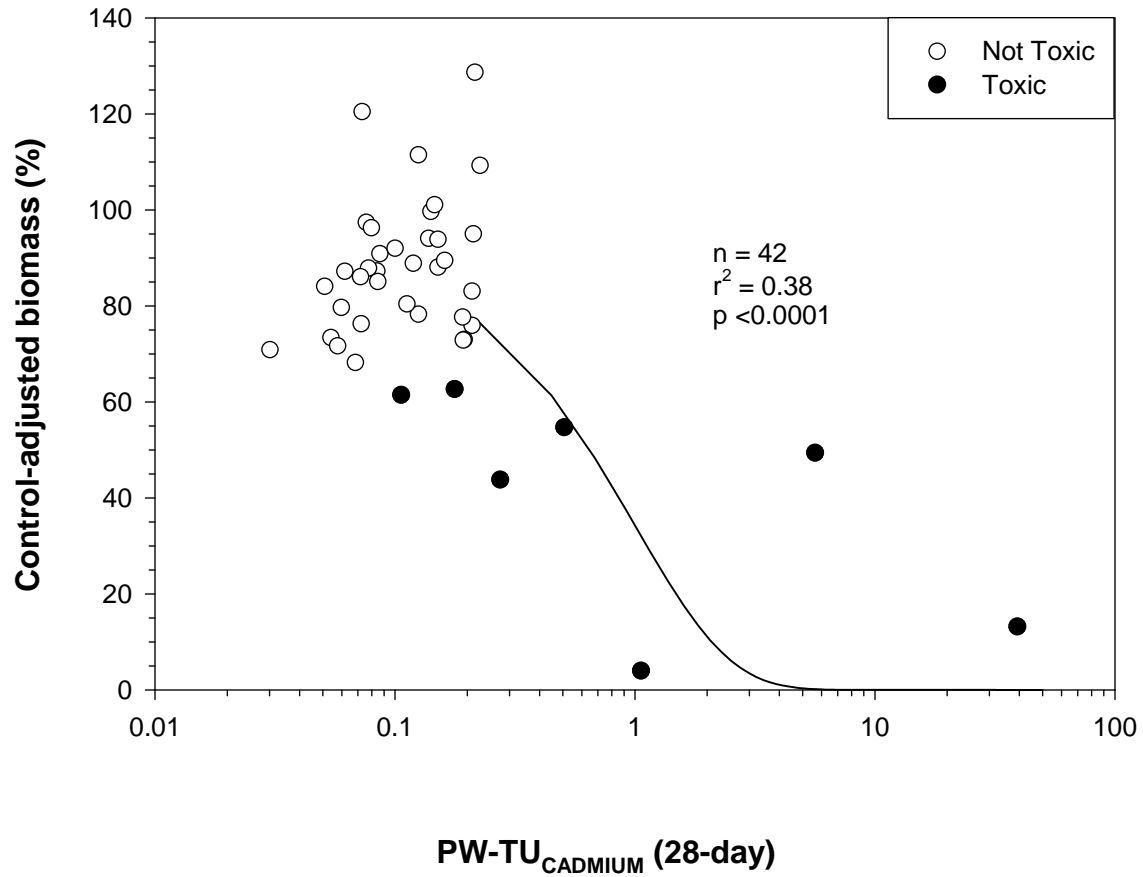
Plot A1-169. Plot illustrating the relationship between the concentration of $PW-TU_{ARSENIC}$ and the control-adjusted biomass of mussels (*Lampsilis siliquoidea*) in 28-d exposures to sediment samples from the Tri-State Mining District.



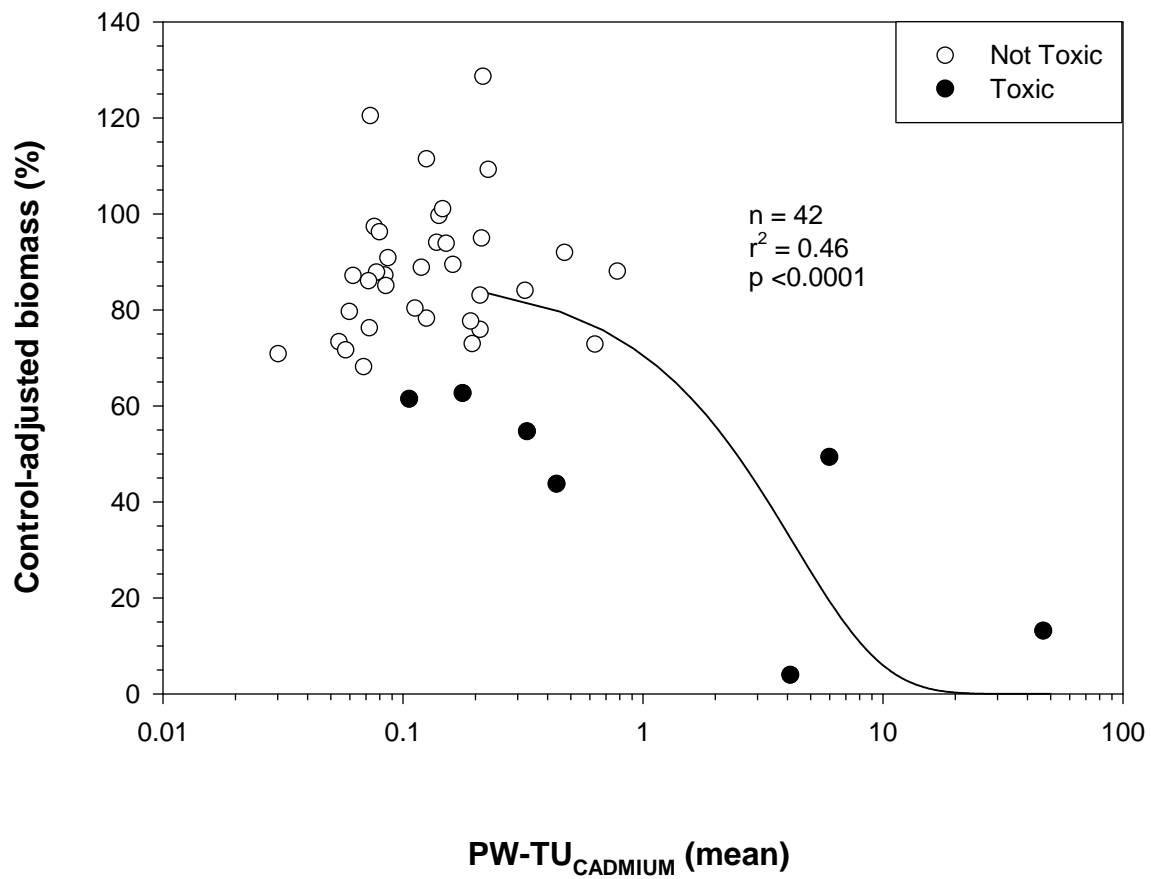
Plot A1-170. Plot illustrating the relationship between the concentration of $PW-TU_{CADMIUM}$ (7-day) and the control-adjusted biomass of mussels (*Lampsilis siliquoidea*) in 28-d exposures to sediment samples from the Tri-State Mining District.



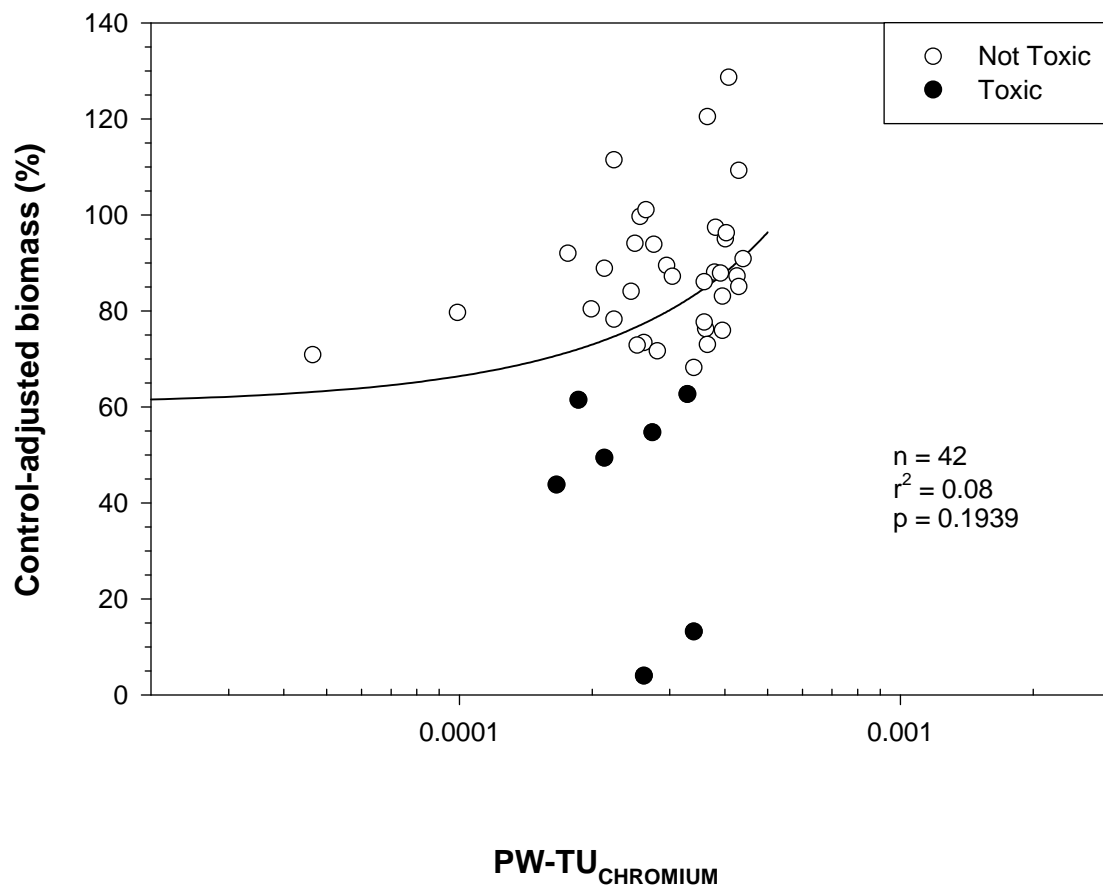
Plot A1-171. Plot illustrating the relationship between the concentration of PW-TU_{CADMIUM} (28-day) and the control-adjusted biomass of mussels (*Lampsilis siliquoidea*) in 28-d exposures to sediment samples from the Tri-State Mining District.



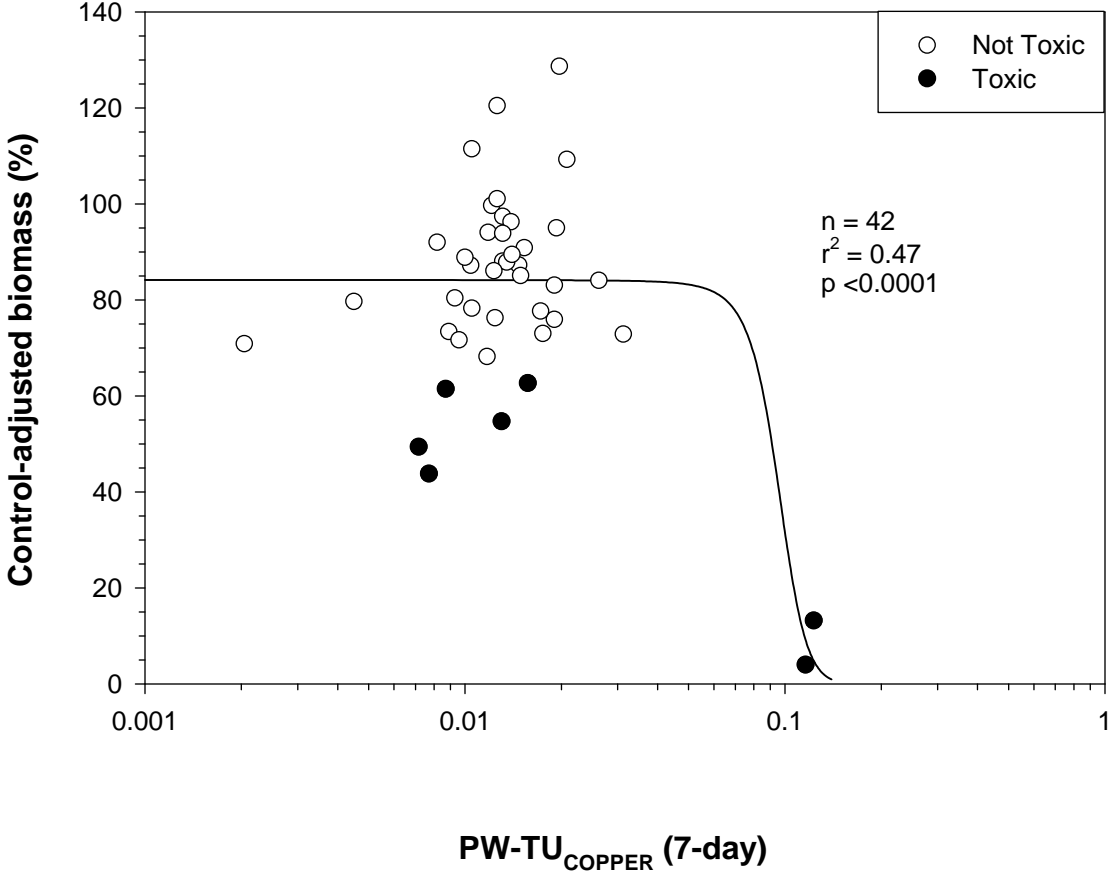
Plot A1-172. Plot illustrating the relationship between the concentration of PW-TU_{CADMIUM} (mean) and the control-adjusted biomass of mussels (*Lampsilis siliquoidea*) in 28-d exposures to sediment samples from the Tri-State Mining District.



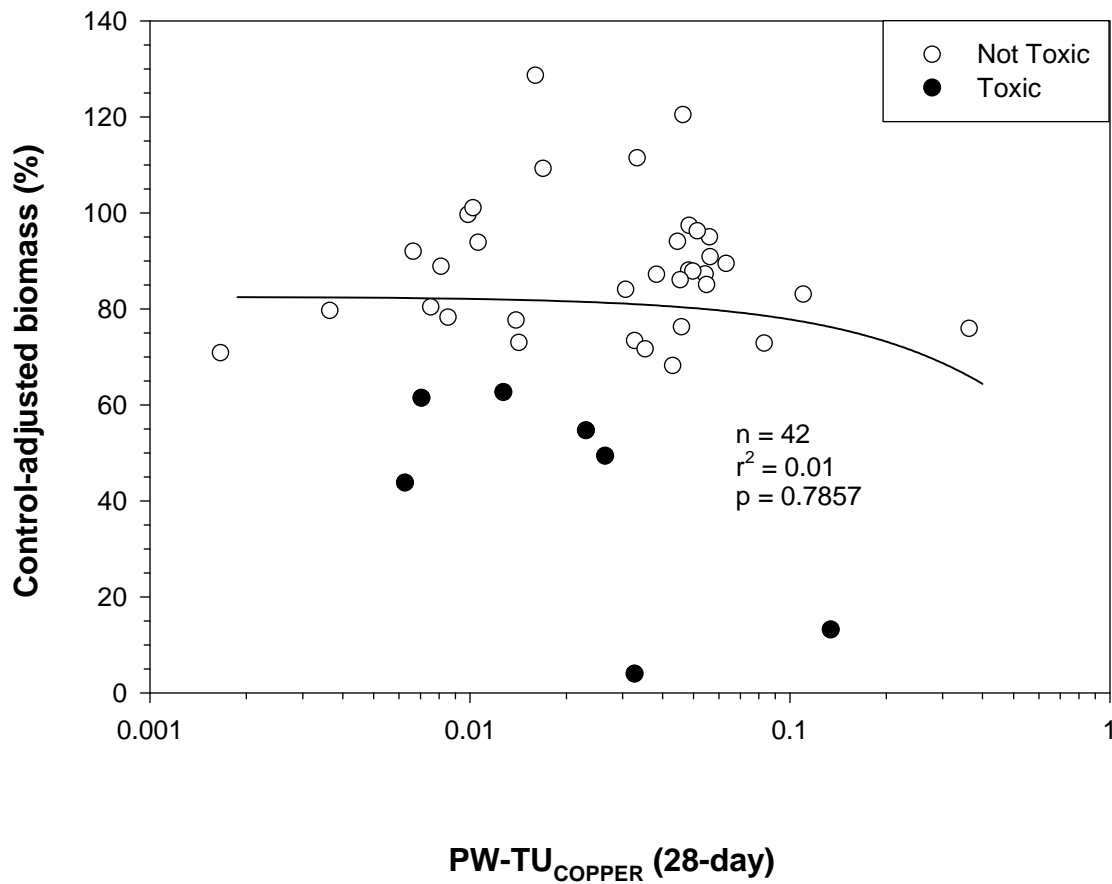
Plot A1-173. Plot illustrating the relationship between the concentration of $PW-TU_{CHROMIUM}$ and the control-adjusted biomass of mussels (*Lampsilis siliquoidea*) in 28-d exposures to sediment samples from the Tri-State Mining District.



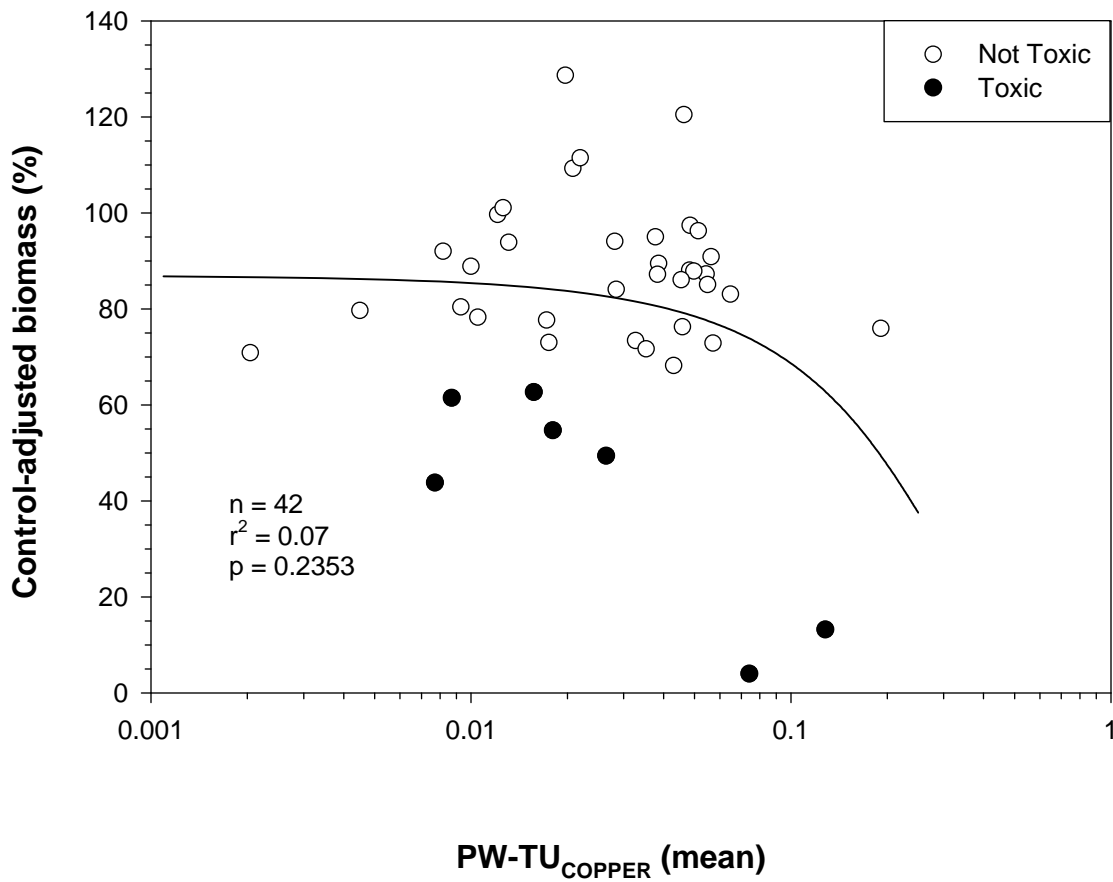
Plot A1-174. Plot illustrating the relationship between the concentration of PW-TU_{COPPER} (7-day) and the control-adjusted biomass of mussels (*Lampsilis siliquoidea*) in 28-d exposures to sediment samples from the Tri-State Mining District.



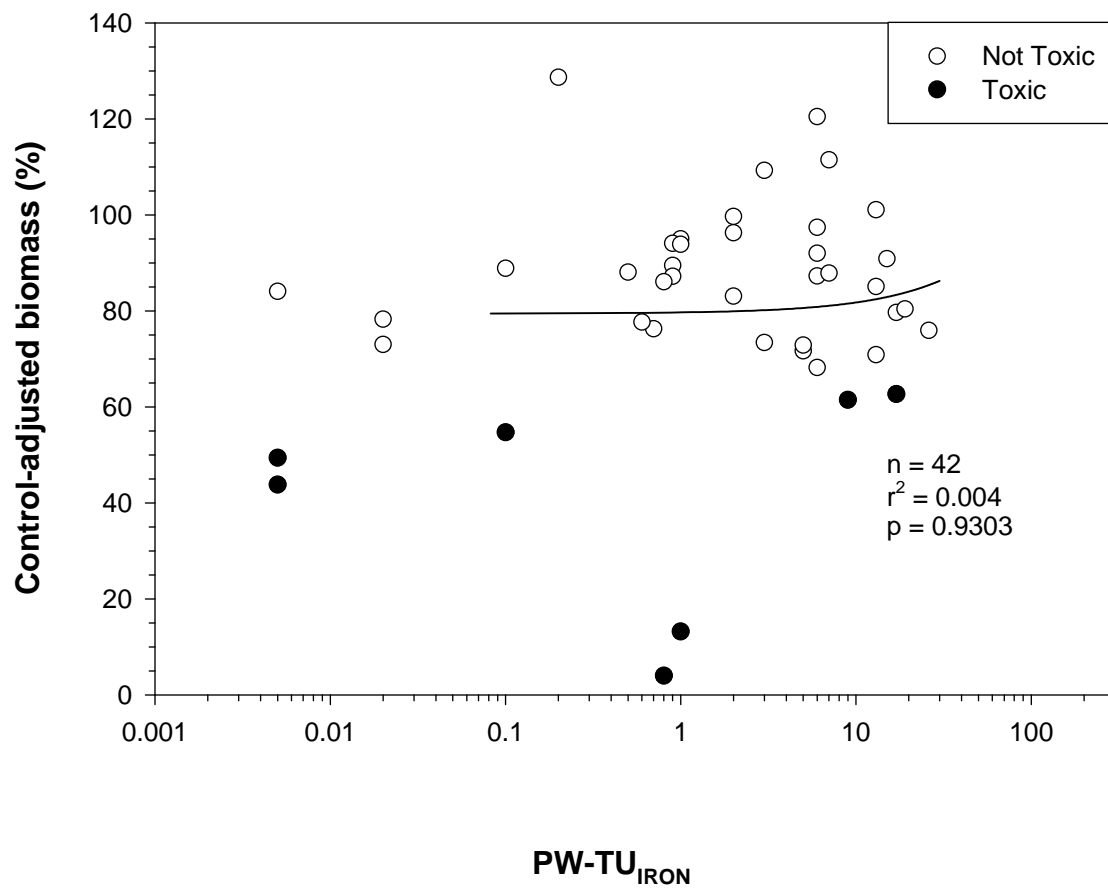
Plot A1-175. Plot illustrating the relationship between the concentration of $PW-TU_{COPPER}$ (28-day) and the control-adjusted biomass of mussels (*Lampsilis siliquoidea*) in 28-d exposures to sediment samples from the Tri-State Mining District.



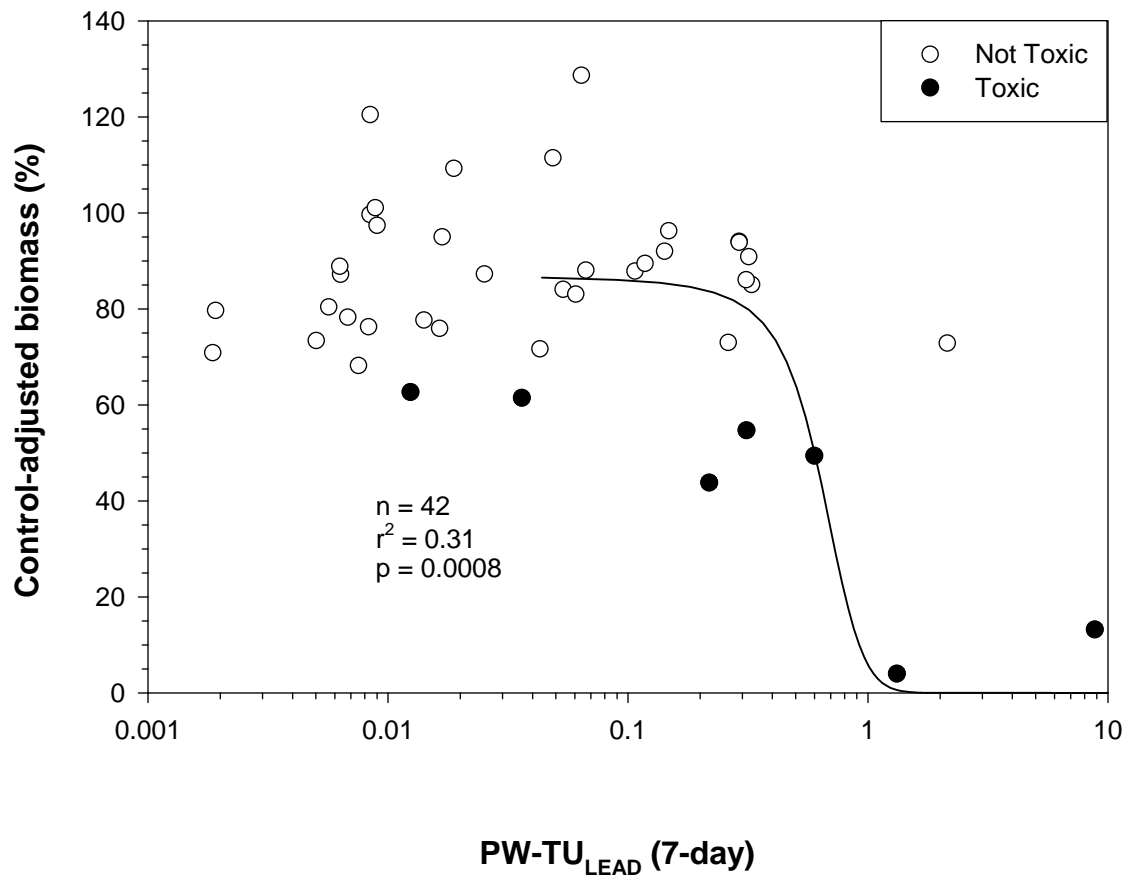
Plot A1-176. Plot illustrating the relationship between the concentration of $PW-TU_{COPPER}$ (mean) and the control-adjusted biomass of mussels (*Lampsilis siliquoidea*) in 28-d exposures to sediment samples from the Tri-State Mining District.



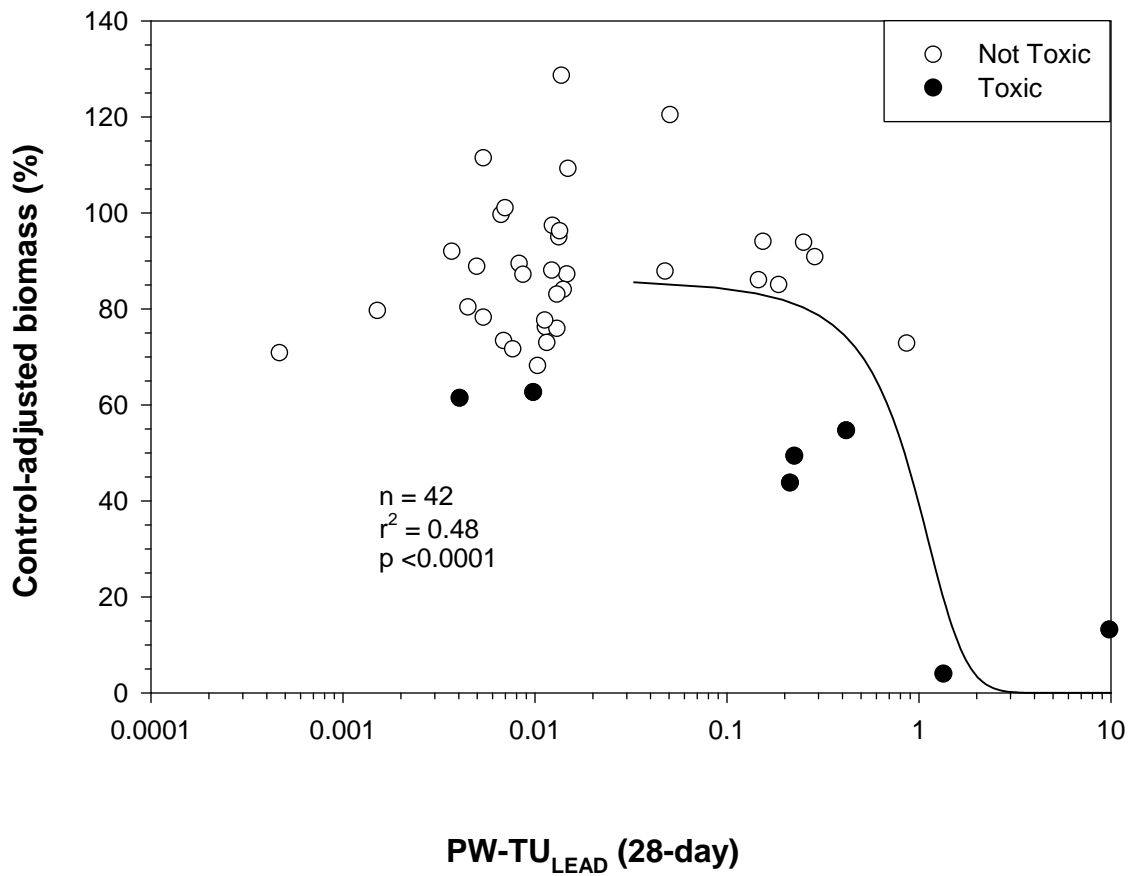
Plot A1-177. Plot illustrating the relationship between the concentration of $PW-TU_{IRON}$ and the control-adjusted biomass of mussels (*Lampsilis siliquoidea*) in 28-d exposures to sediment samples from the Tri-State Mining District.



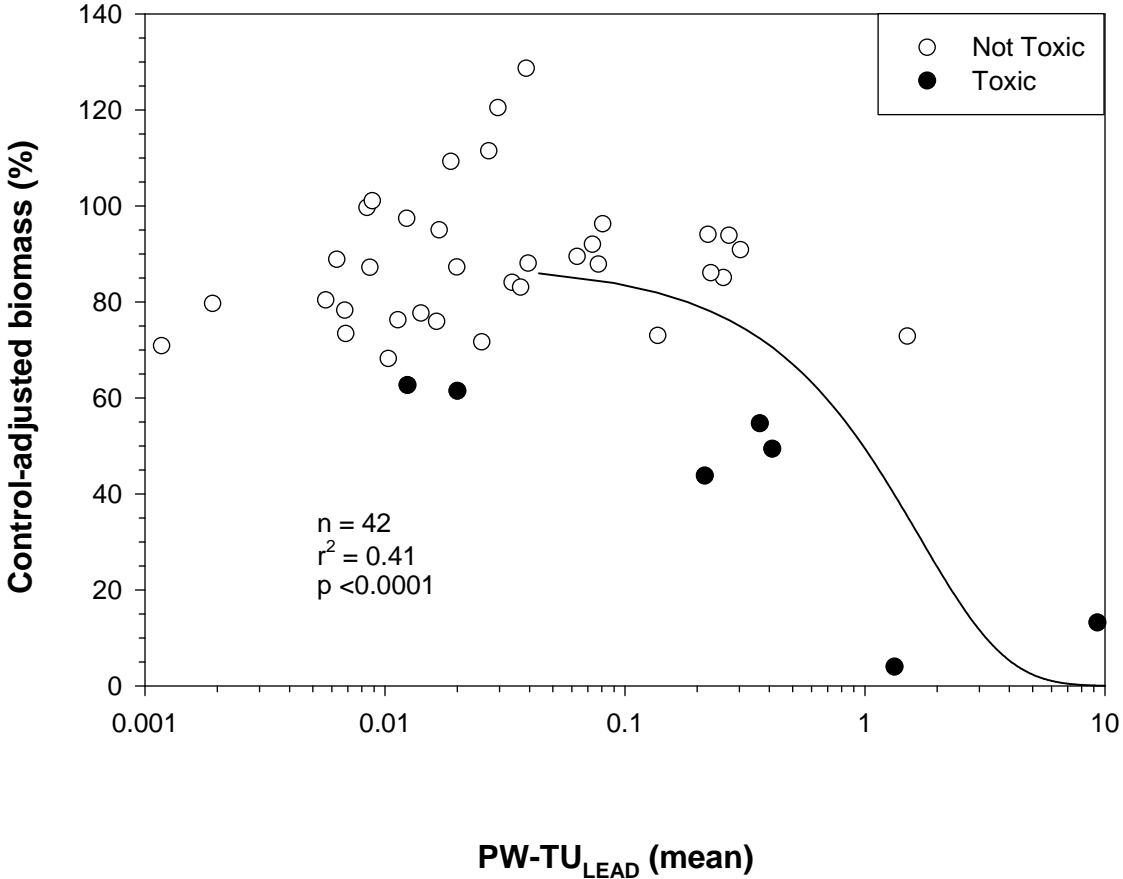
Plot A1-178. Plot illustrating the relationship between the concentration of PW-TU_{LEAD} (7-day) and the control-adjusted biomass of mussels (*Lampsilis siliquoidea*) in 28-d exposures to sediment samples from the Tri-State Mining District.



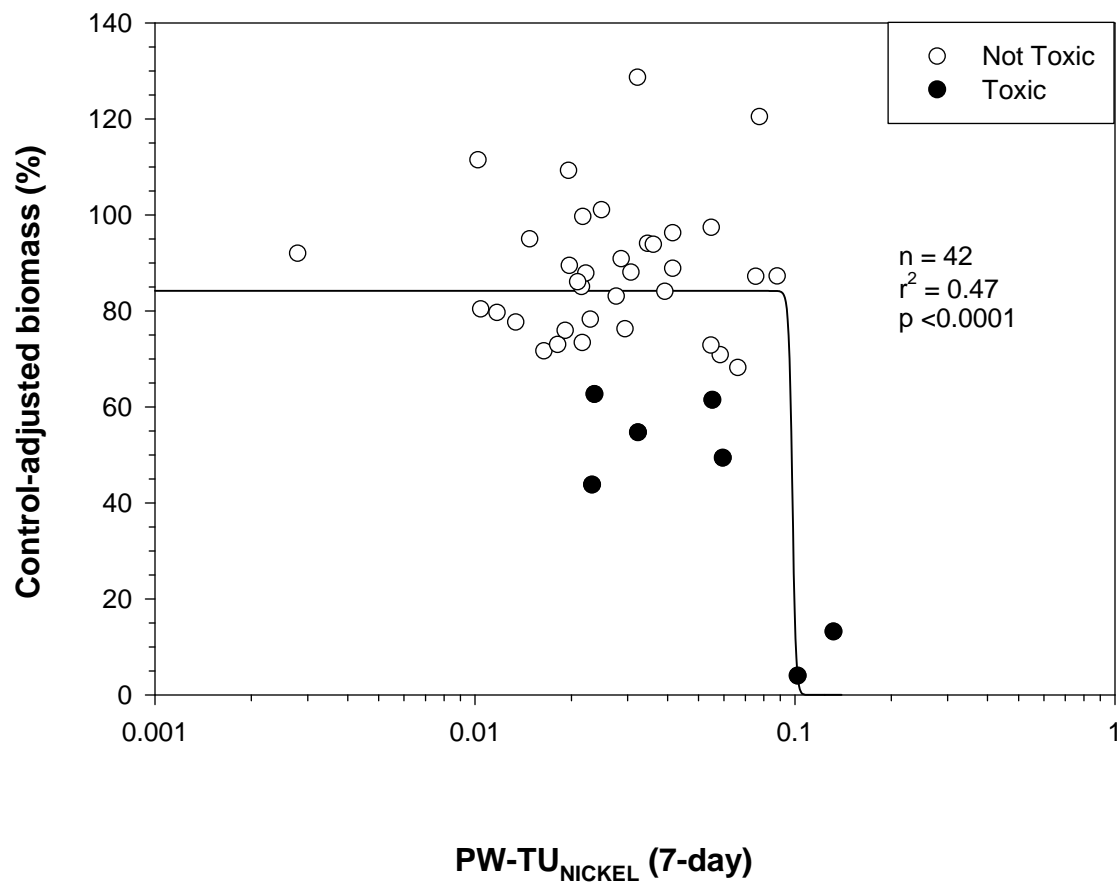
Plot A1-179. Plot illustrating the relationship between the concentration of PW-TU_{LEAD} (28-day) and the control-adjusted biomass of mussels (*Lampsilis siliquoidea*) in 28-d exposures to sediment samples from the Tri-State Mining District.



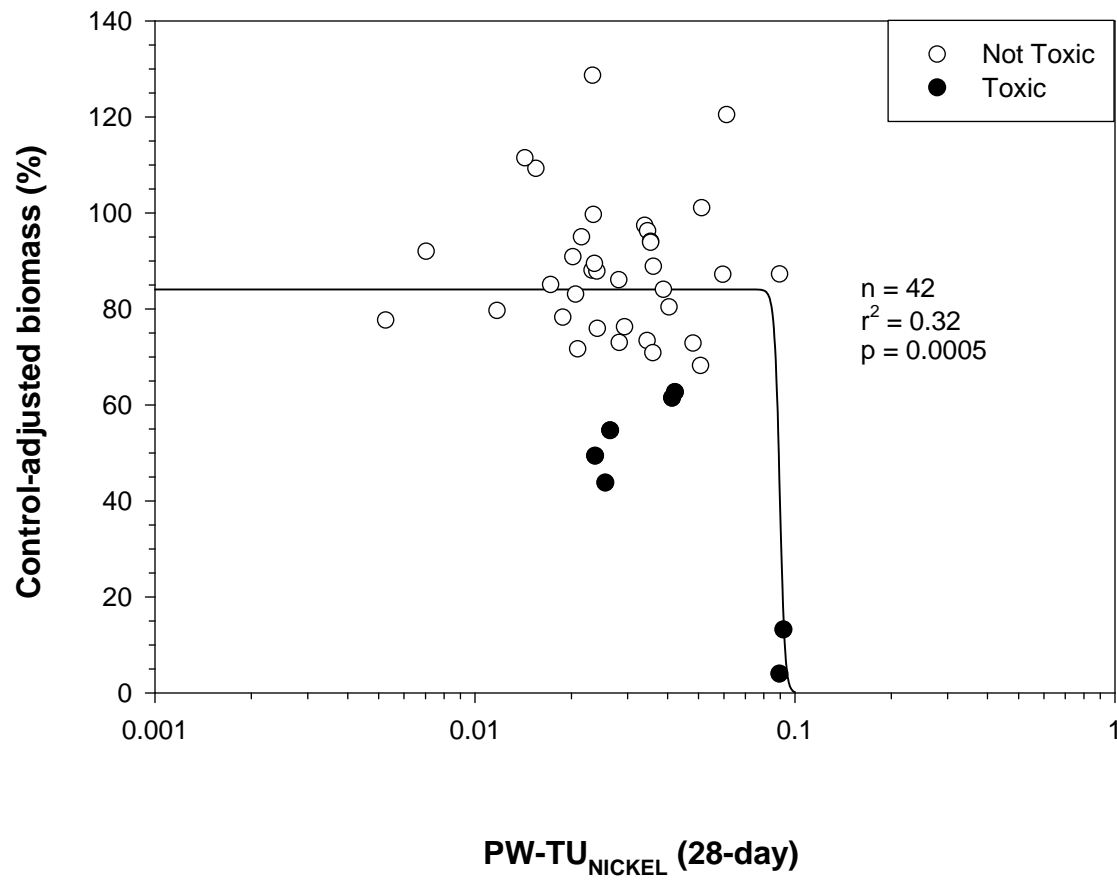
Plot A1-180. Plot illustrating the relationship between the concentration of PW-TU_{LEAD} (mean) and the control-adjusted biomass of mussels (*Lampsilis siliquoidea*) in 28-d exposures to sediment samples from the Tri-State Mining District.



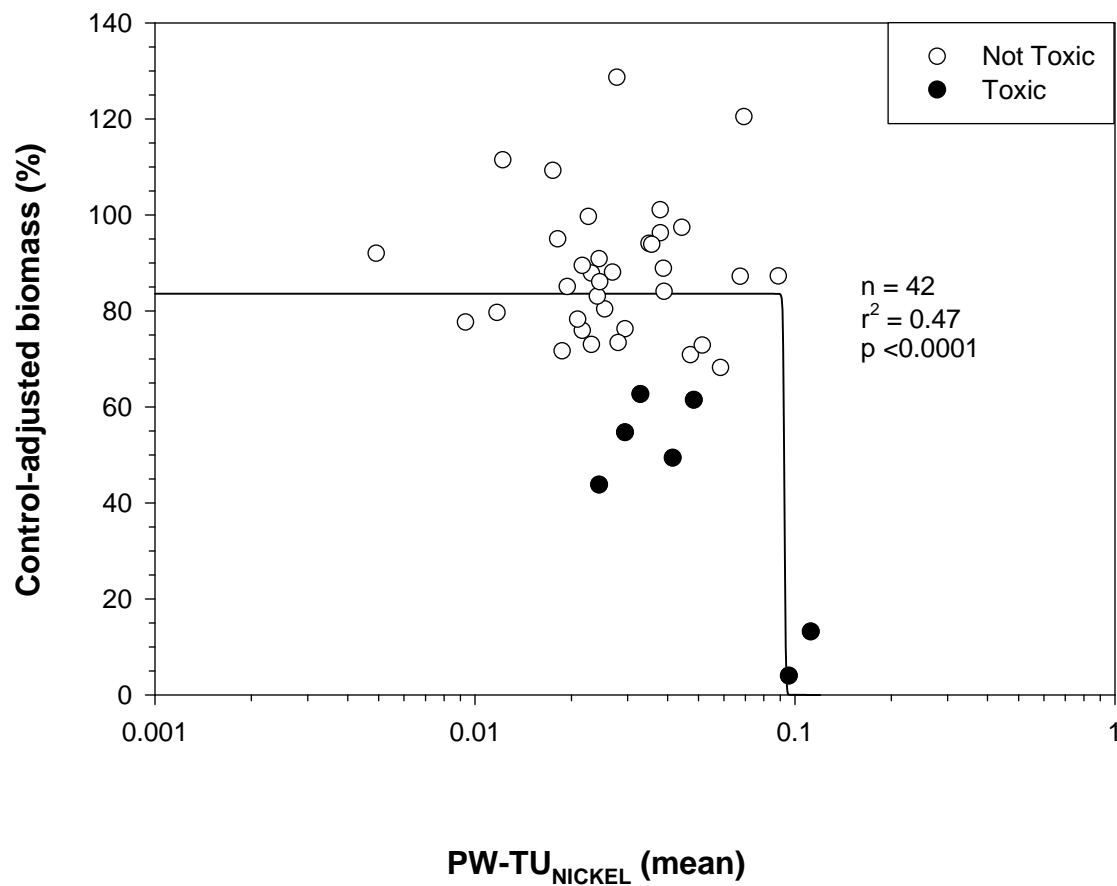
Plot A1-181. Plot illustrating the relationship between the concentration of $PW-TU_{NICKEL}$ (7-day) and the control-adjusted biomass of mussels (*Lampsilis siliquoidea*) in 28-d exposures to sediment samples from the Tri-State Mining District.



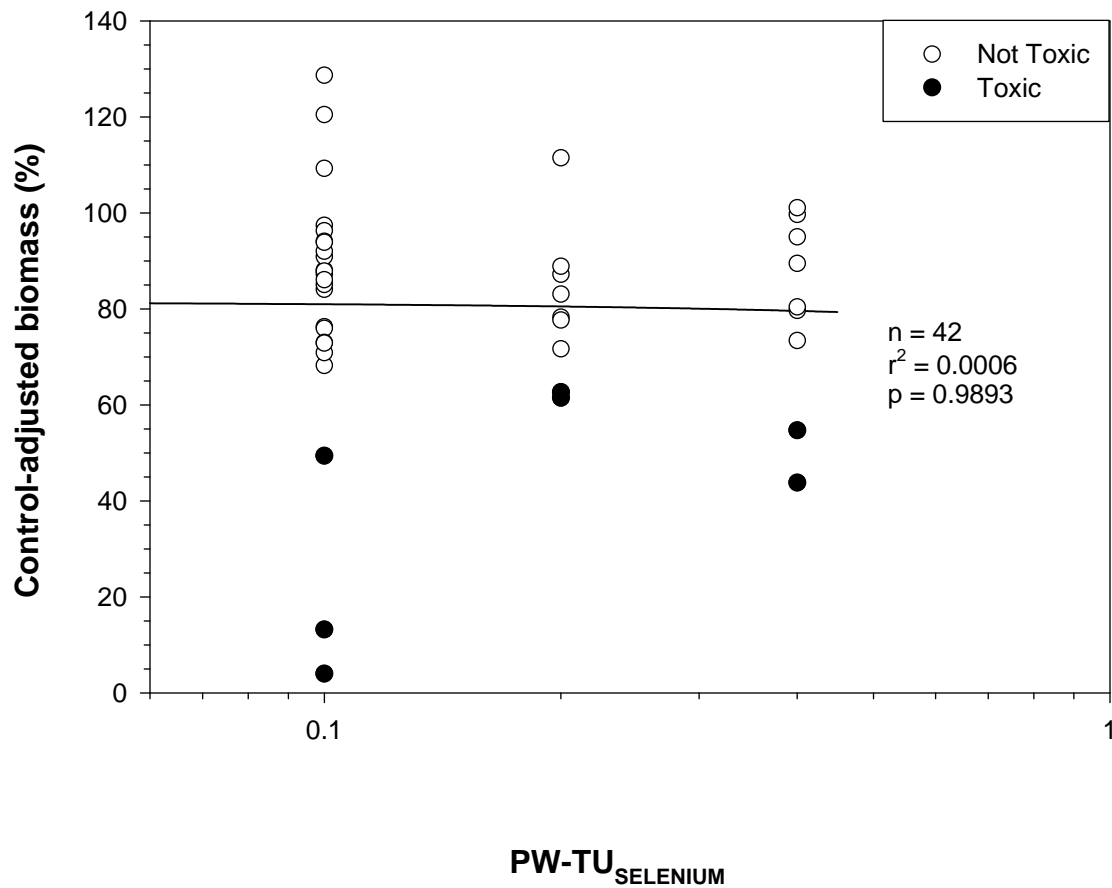
Plot A1-182. Plot illustrating the relationship between the concentration of $PW-TU_{NICKEL}$ (28-day) and the control-adjusted biomass of mussels (*Lampsilis siliquoidea*) in 28-d exposures to sediment samples from the Tri-State Mining District.



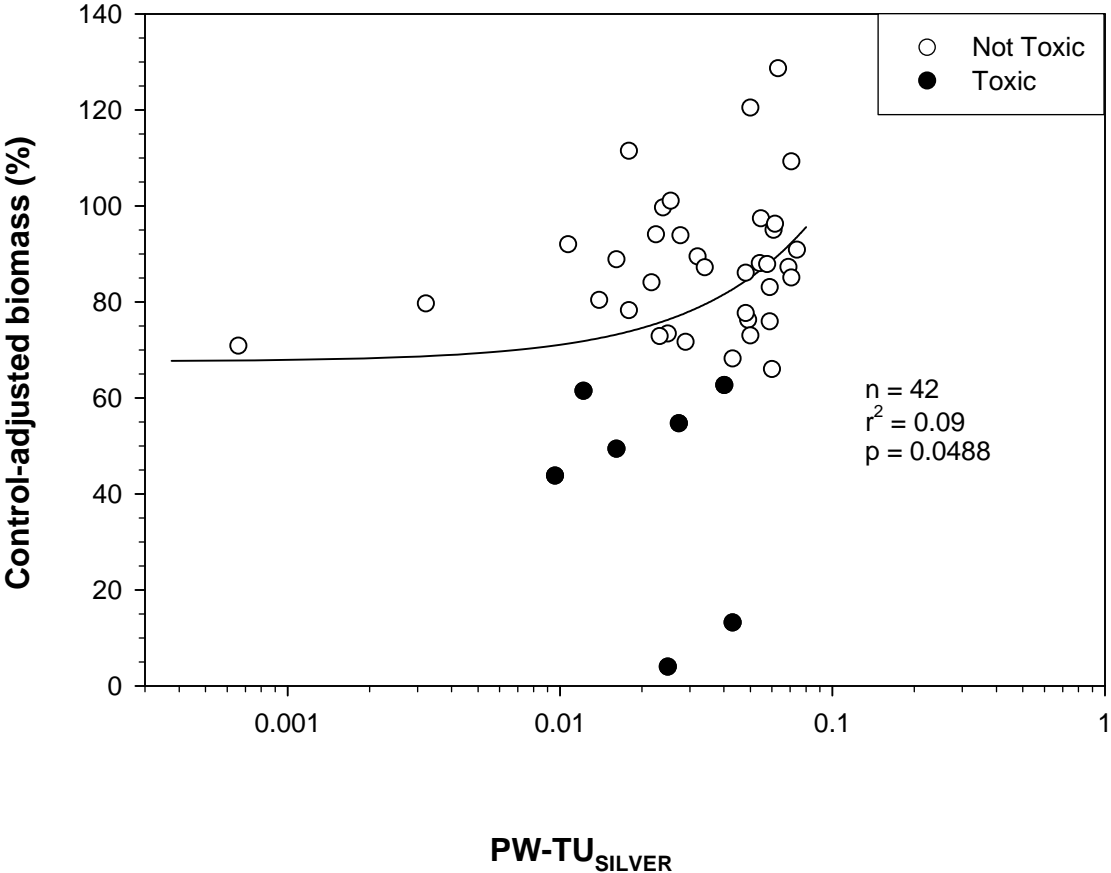
Plot A1-183. Plot illustrating the relationship between the concentration of PW-TU_{NICKEL} (mean) and the control-adjusted biomass of mussels (*Lampsilis siliquoidea*) in 28-d exposures to sediment samples from the Tri-State Mining District.



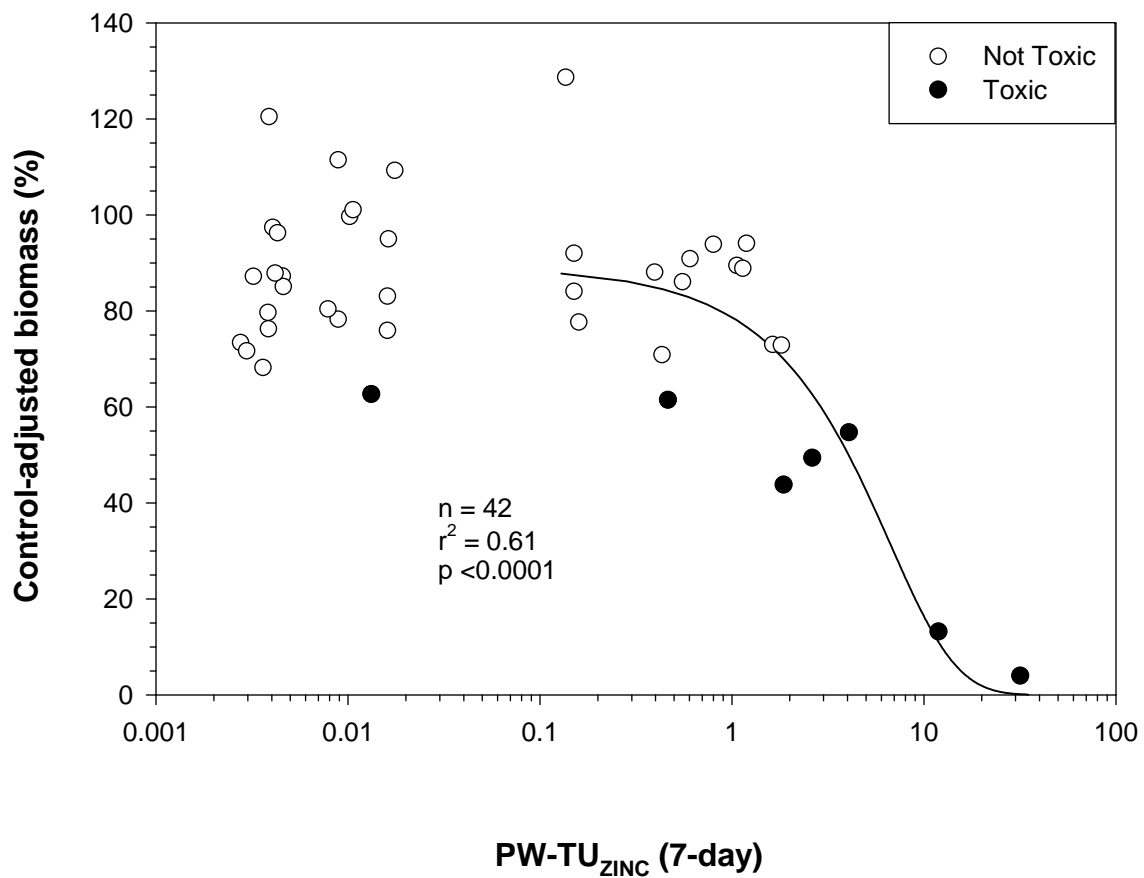
Plot A1-184. Plot illustrating the relationship between the concentration of $PW-TU_{SELENIUM}$ and the control-adjusted biomass of mussels (*Lampsilis siliquoidea*) in 28-d exposures to sediment samples from the Tri-State Mining District.



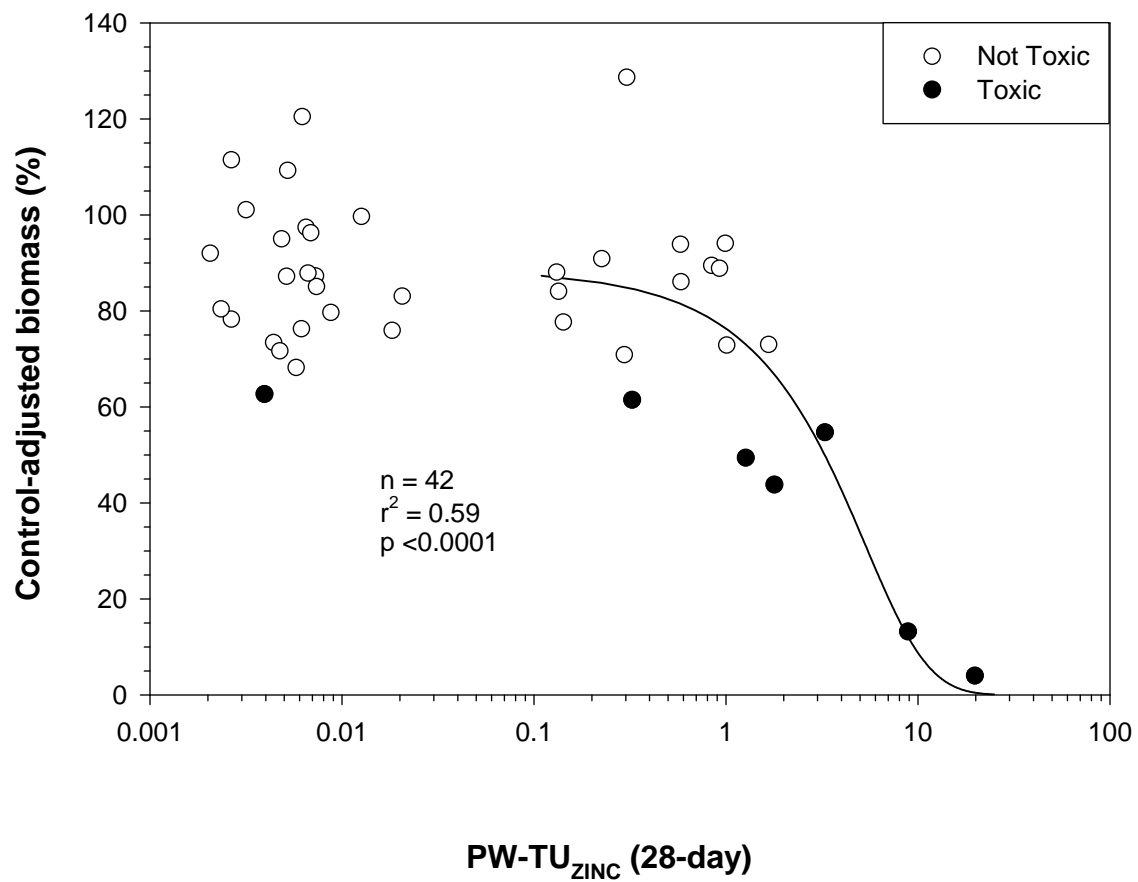
Plot A1-185. Plot illustrating the relationship between the concentration of PW-TU_{SILVER} and the control-adjusted biomass of mussels (*Lampsilis siliquoidea*) in 28-d exposures to sediment samples from the Tri-State Mining District.



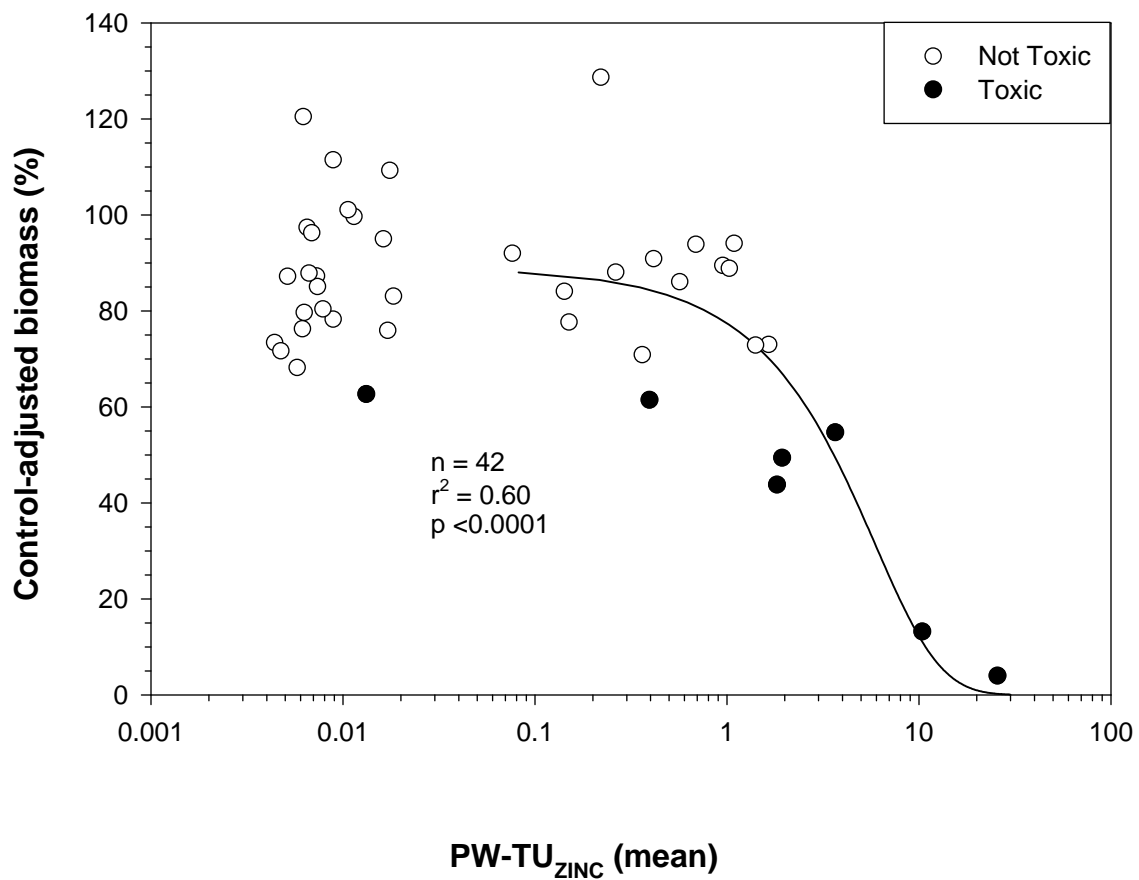
Plot A1-186. Plot illustrating the relationship between the concentration of PW-TU_{ZINC} (7-day) and the control-adjusted biomass of mussels (*Lampsilis siliquoidea*) in 28-d exposures to sediment samples from the Tri-State Mining District.



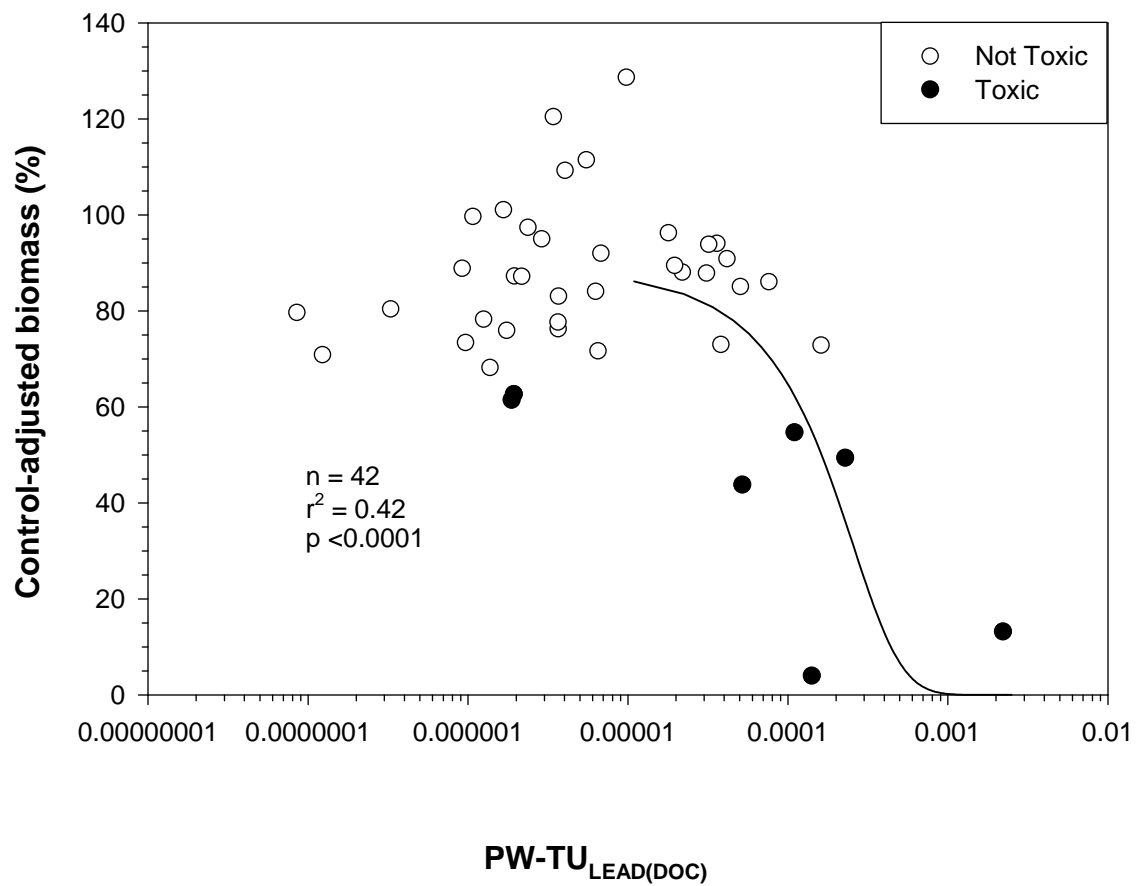
Plot A1-187. Plot illustrating the relationship between the concentration of PW-TU_{ZINC} (28-day) and the control-adjusted biomass of mussels (*Lampsilis siliquoidea*) in 28-d exposures to sediment samples from the Tri-State Mining District.



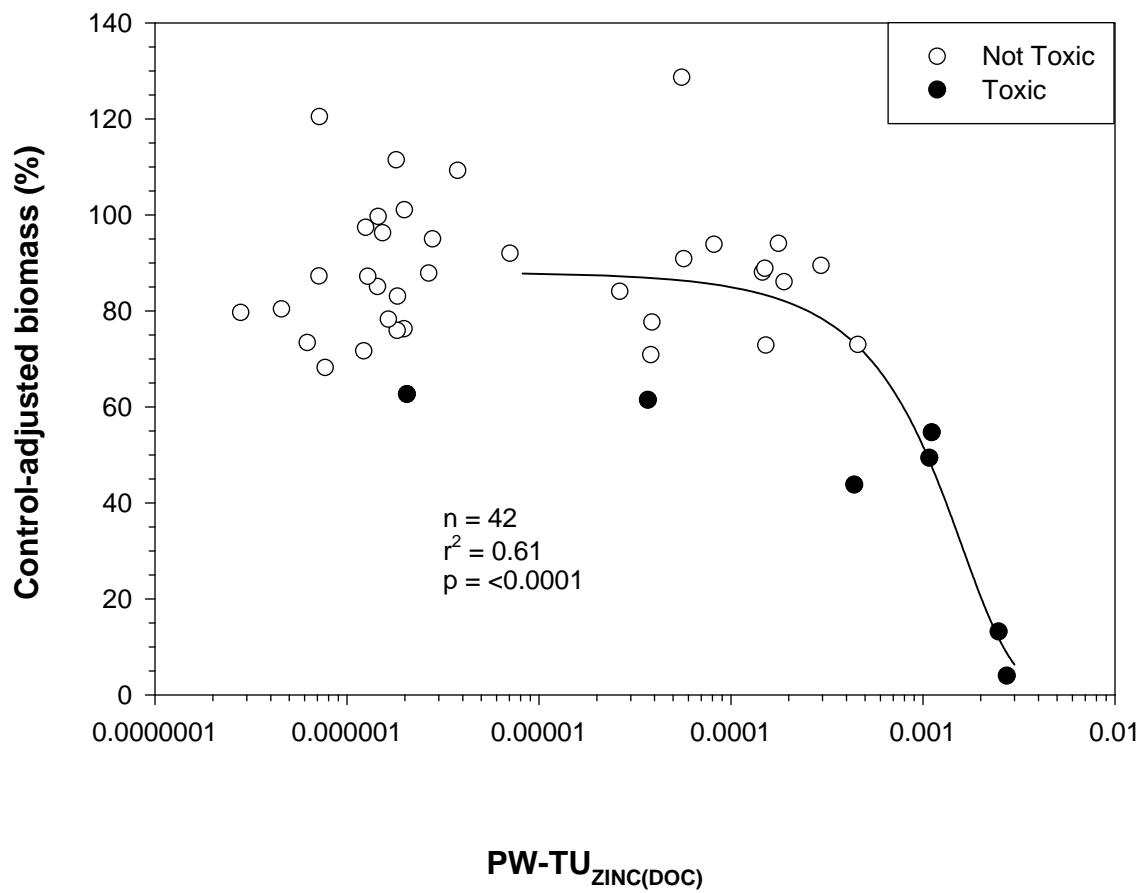
Plot A1-188. Plot illustrating the relationship between the concentration of PW-TU_{ZINC} (mean) and the control-adjusted biomass of mussels (*Lampsilis siliquoidea*) in 28-d exposures to sediment samples from the Tri-State Mining District.



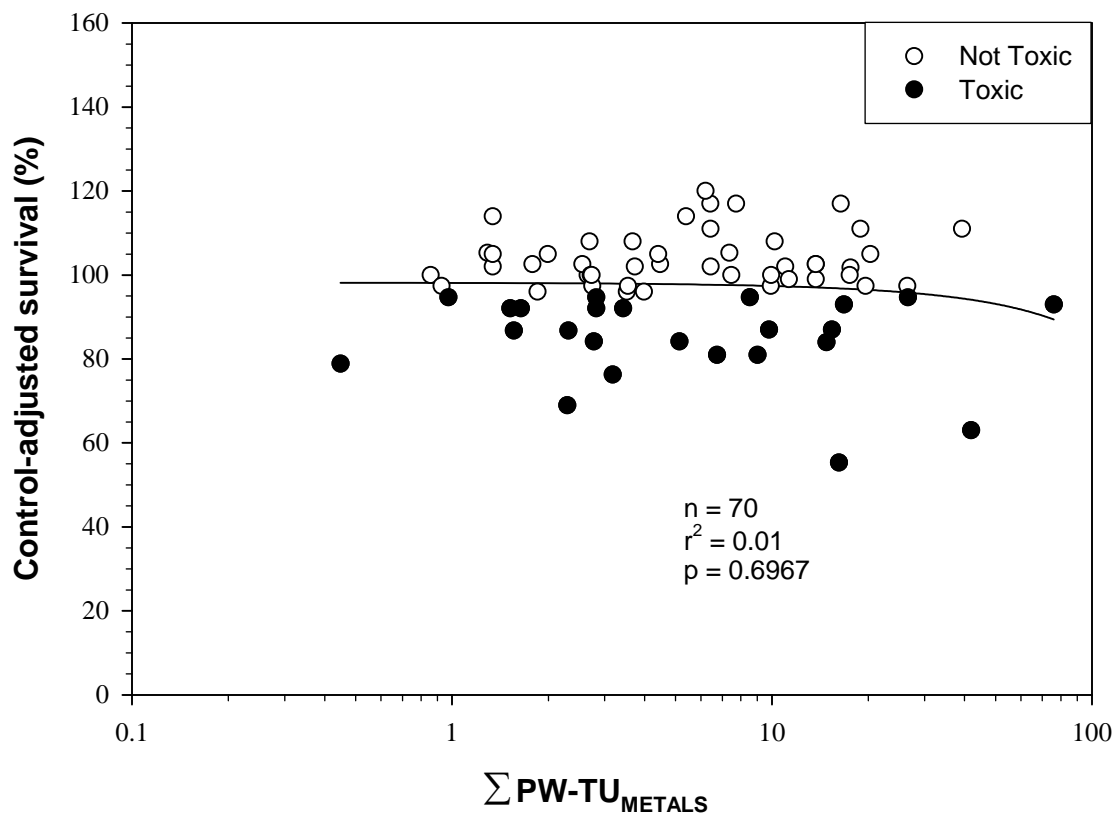
Plot A1-189. Plot illustrating the relationship between the concentration of $PW-TU_{LEAD(DOC)}$ and the control-adjusted biomass of mussels (*Lampsilis siliquoidea*) in 28-d exposures to sediment samples from the Tri-State Mining District.



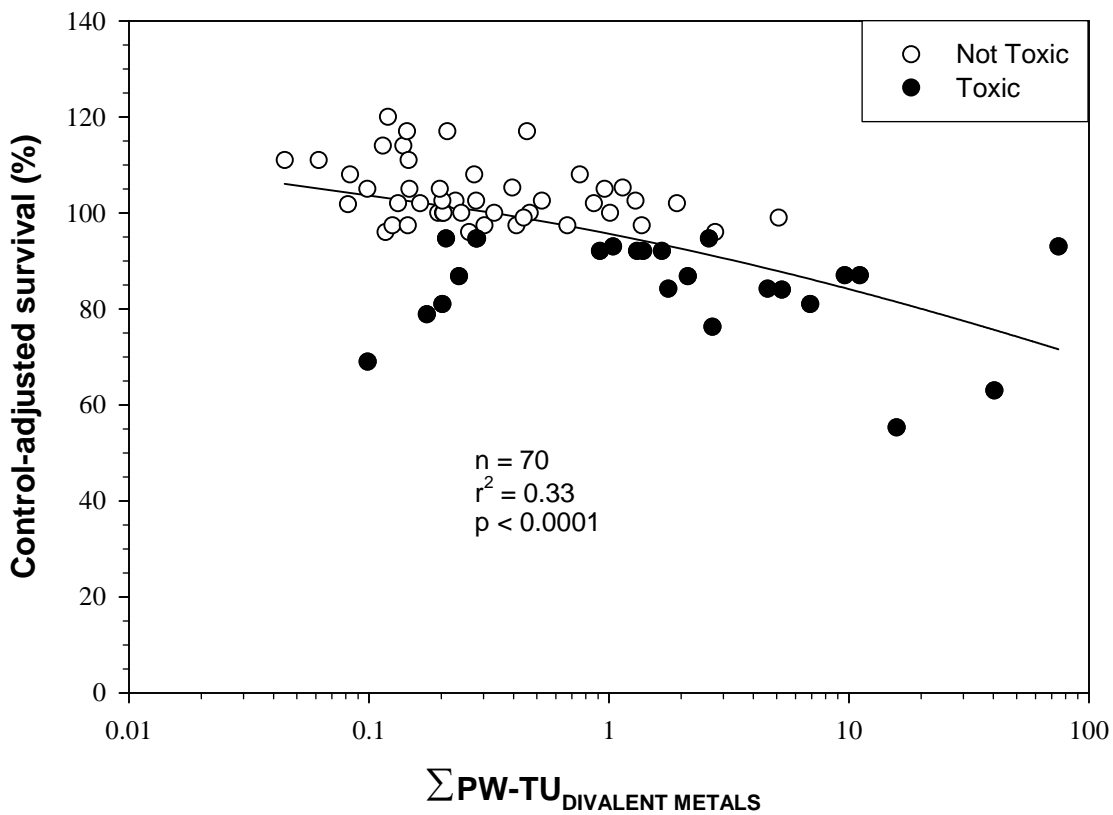
Plot A1-190. Plot illustrating the relationship between the concentration of $PW-TU_{ZINC(DOC)}$ and the control-adjusted biomass of mussels (*Lampsilis siliquoidea*) in 28-d exposures to sediment samples from the Tri-State Mining District.



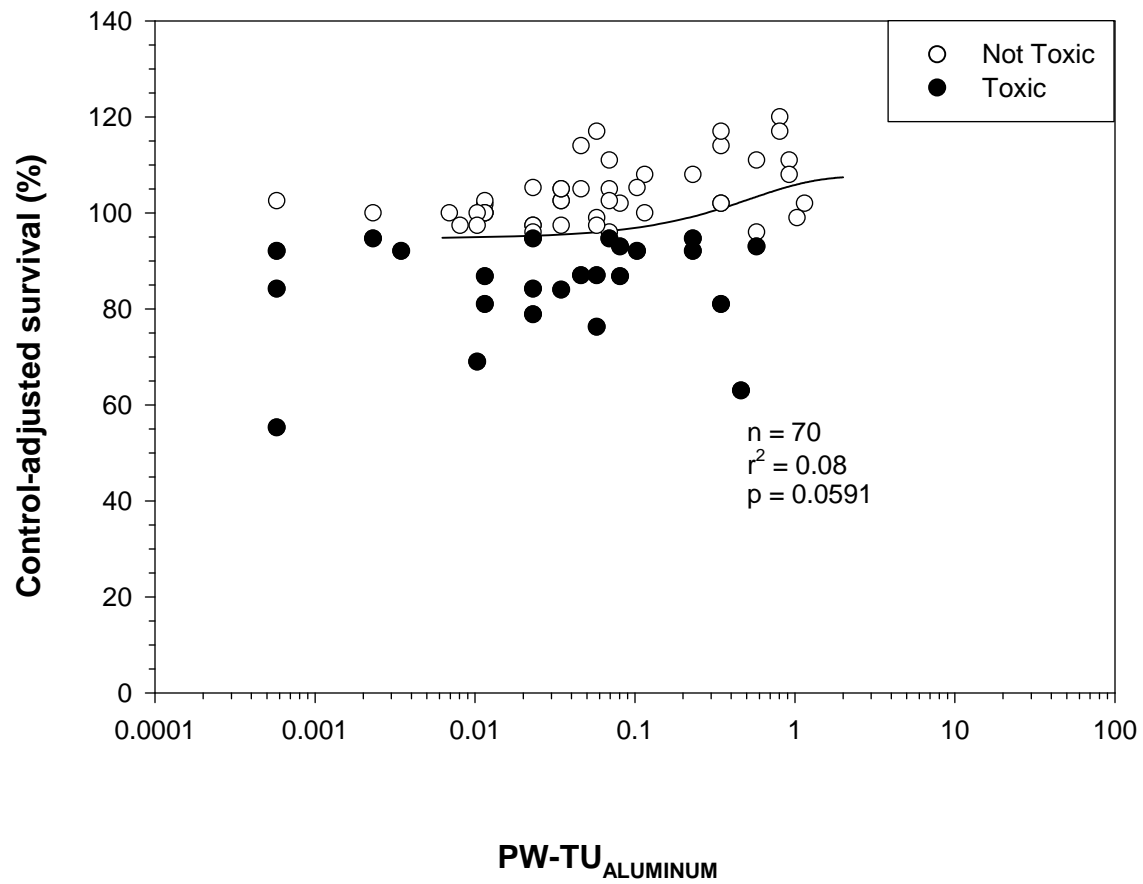
Plot A1-191. Plot illustrating the relationship between the concentration of $\sum \text{PW-TU}_{\text{METALS}}$ and the control-adjusted survival of midges (*Chironomus dilutus*) in 10-d exposures to sediment samples from the Tri-State Mining District.



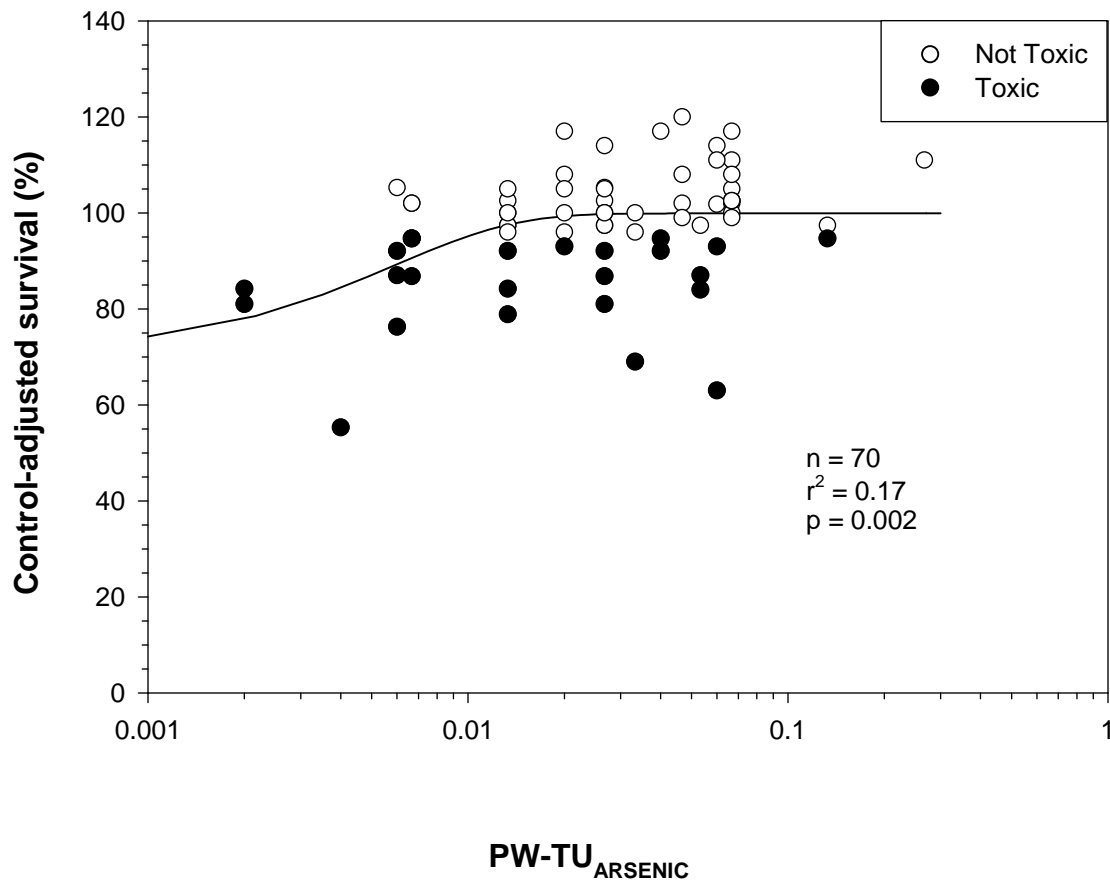
Plot A1-192. Plot illustrating the relationship between the concentration of $\sum \text{PW-TU}_{\text{DIVALENT METALS}}$ and the control-adjusted survival of midges (*Chironomus dilutus*) in 10-d exposures to sediment samples from the Tri-State Mining District.



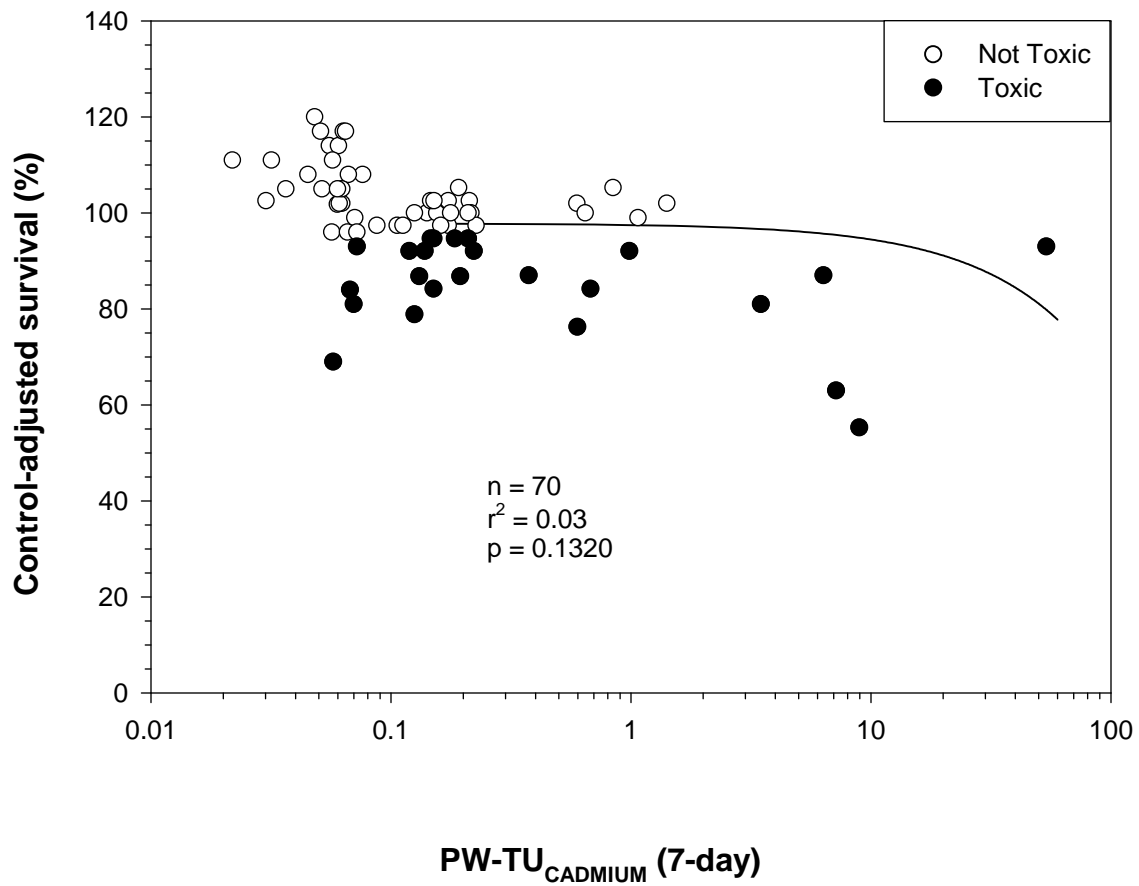
Plot A1-193. Plot illustrating the relationship between the concentration of $PW-TU_{ALUMINUM}$ and the control-adjusted survival of midges (*Chironomus dilutus*) in 10-d exposures to sediment samples from the Tri-State Mining District.



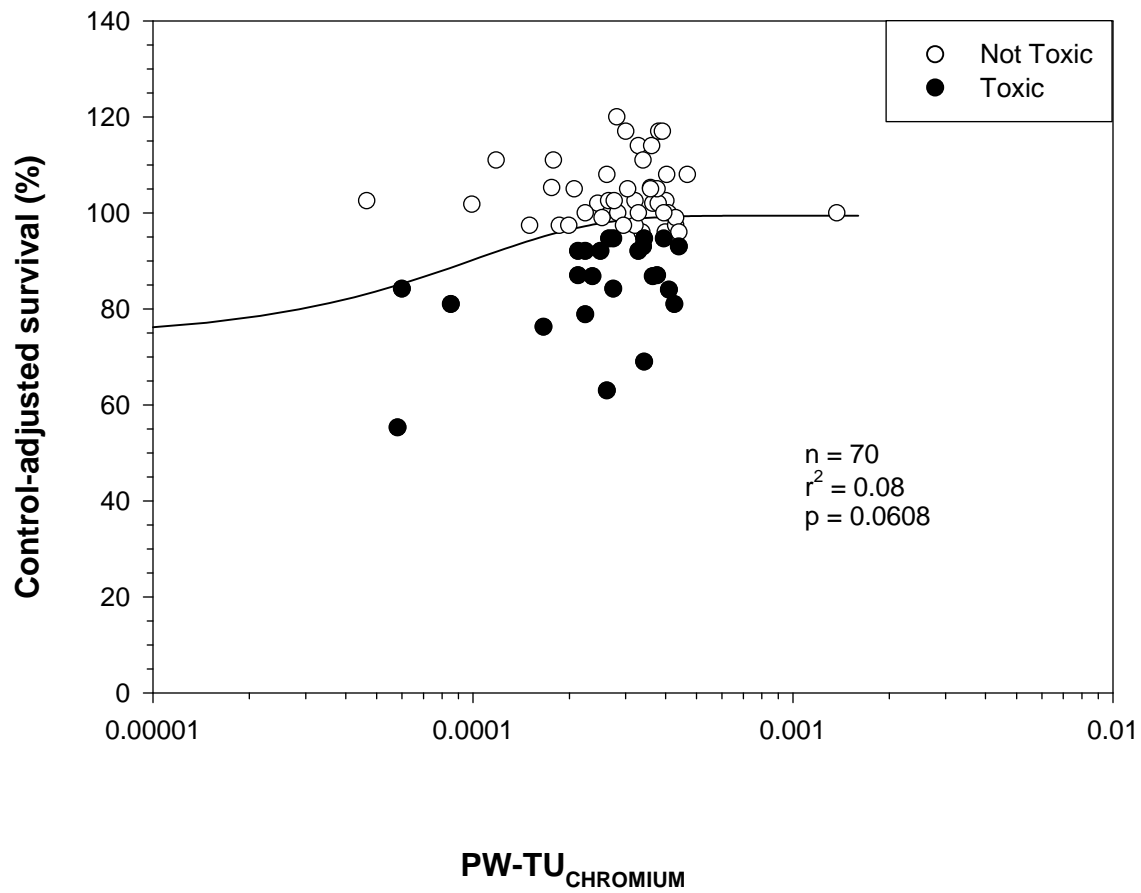
Plot A1-194. Plot illustrating the relationship between the concentration of $PW-TU_{ARSENIC}$ and the control-adjusted survival of midges (*Chironomus dilutus*) in 10-d exposures to sediment samples from the Tri-State Mining District.



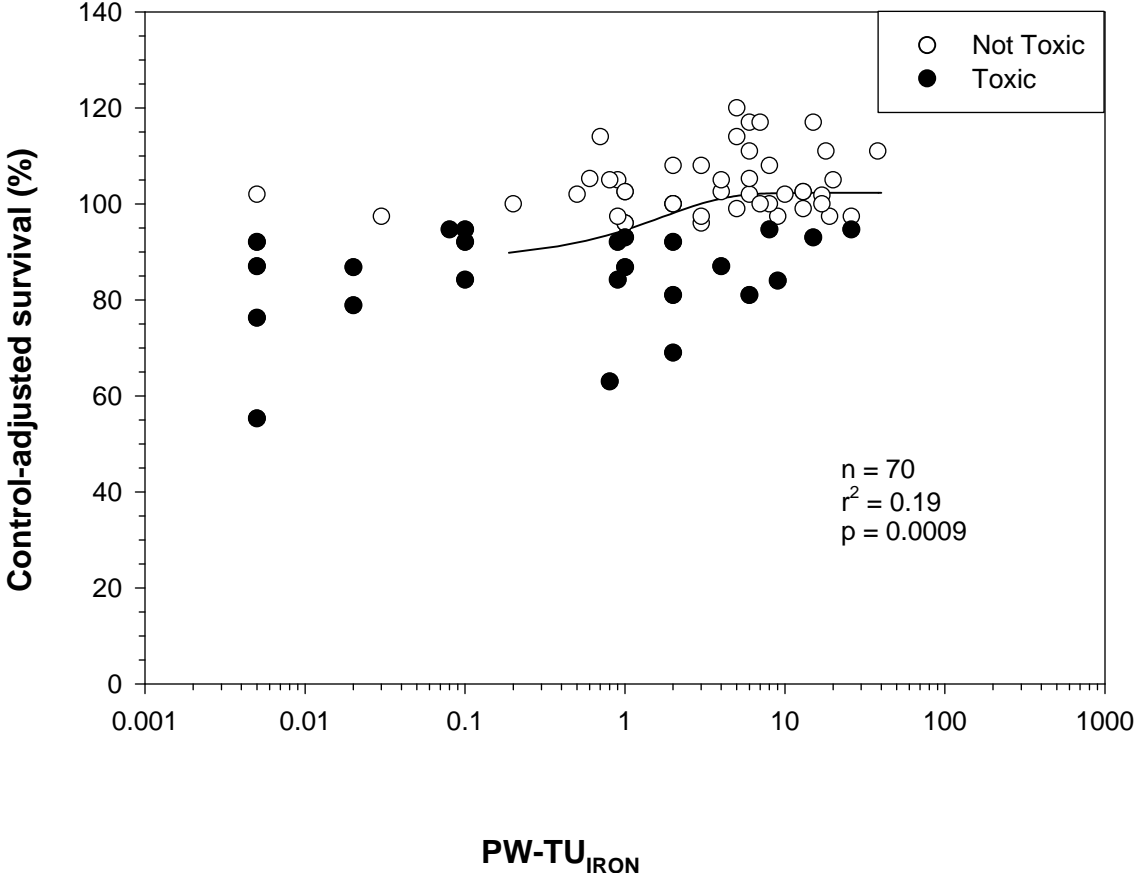
Plot A1-195. Plot illustrating the relationship between the concentration of PW-TU_{CADMIUM} (7-day) and the control-adjusted survival of midges (*Chironomus dilutus*) in 10-d exposures to sediment samples from the Tri-State Mining District.



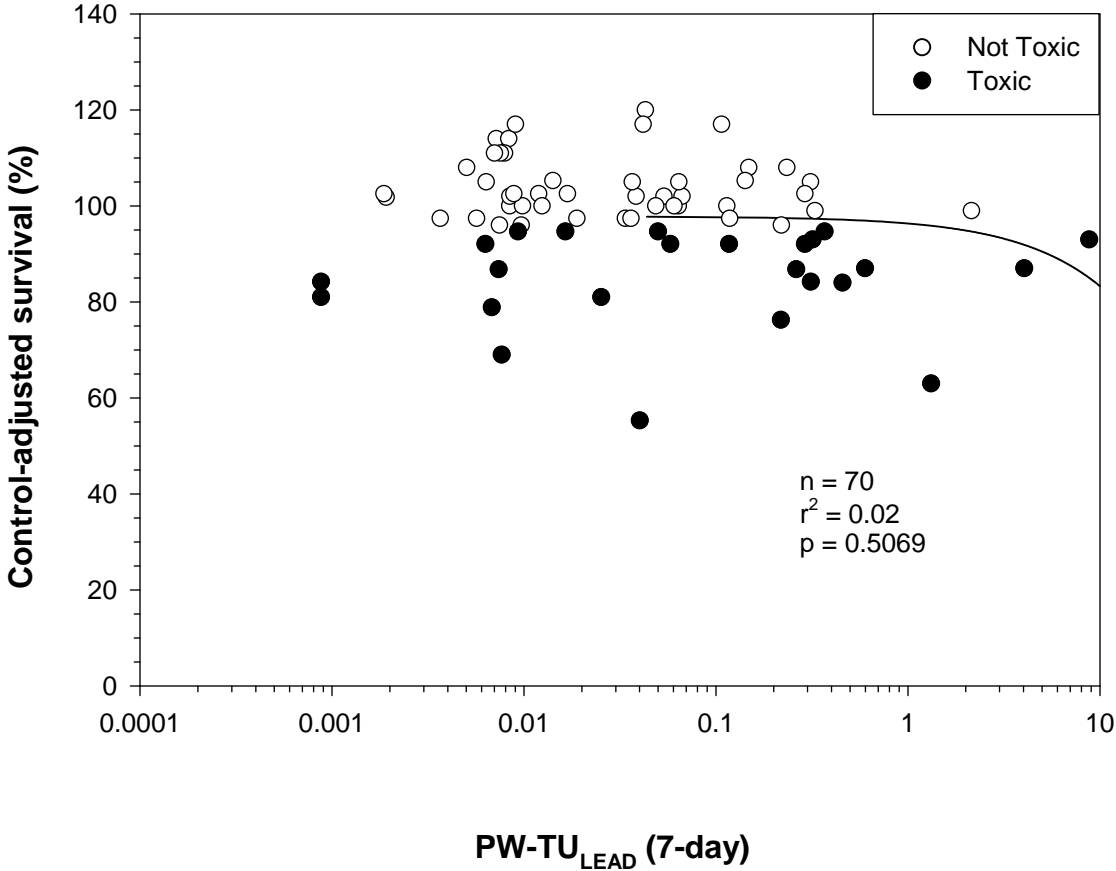
Plot A1-196. Plot illustrating the relationship between the concentration of $PW-TU_{CHROMIUM}$ and the control-adjusted survival of midges (*Chironomus dilutus*) in 10-d exposures to sediment samples from the Tri-State Mining District.



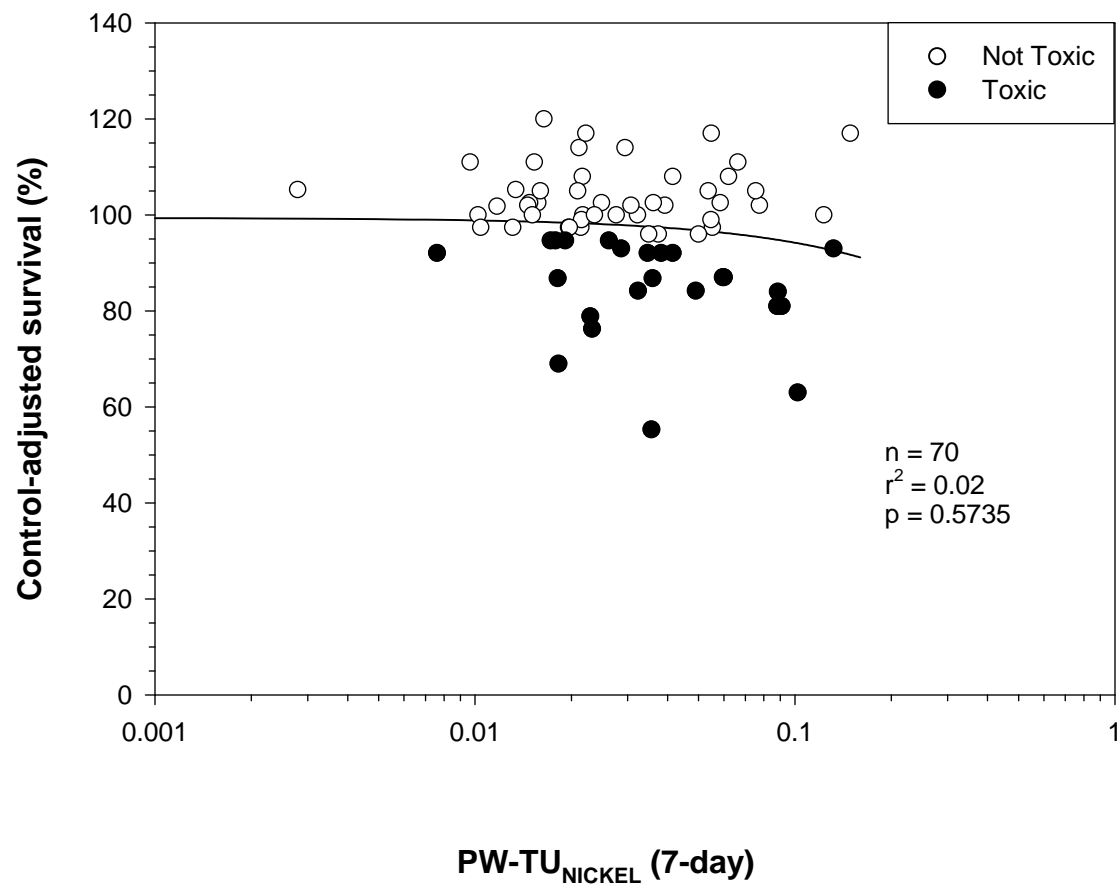
Plot A1-198. Plot illustrating the relationship between the concentration of $PW-TU_{IRON}$ and the control-adjusted survival of midges (*Chironomus dilutus*) in 10-d exposures to sediment samples from the Tri-State Mining District.



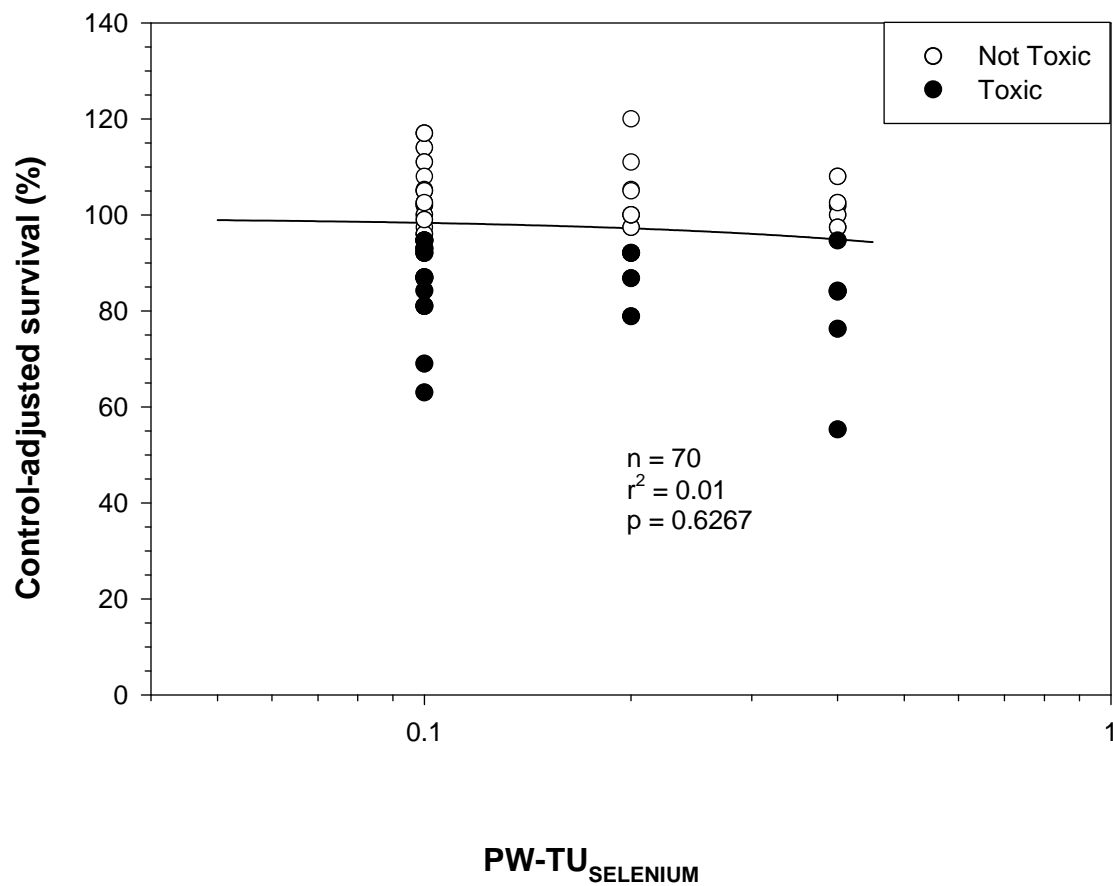
Plot A1-199. Plot illustrating the relationship between the concentration of PW-TU_{LEAD} (7-day) and the control-adjusted survival of midges (*Chironomus dilutus*) in 10-d exposures to sediment samples from the Tri-State Mining District.



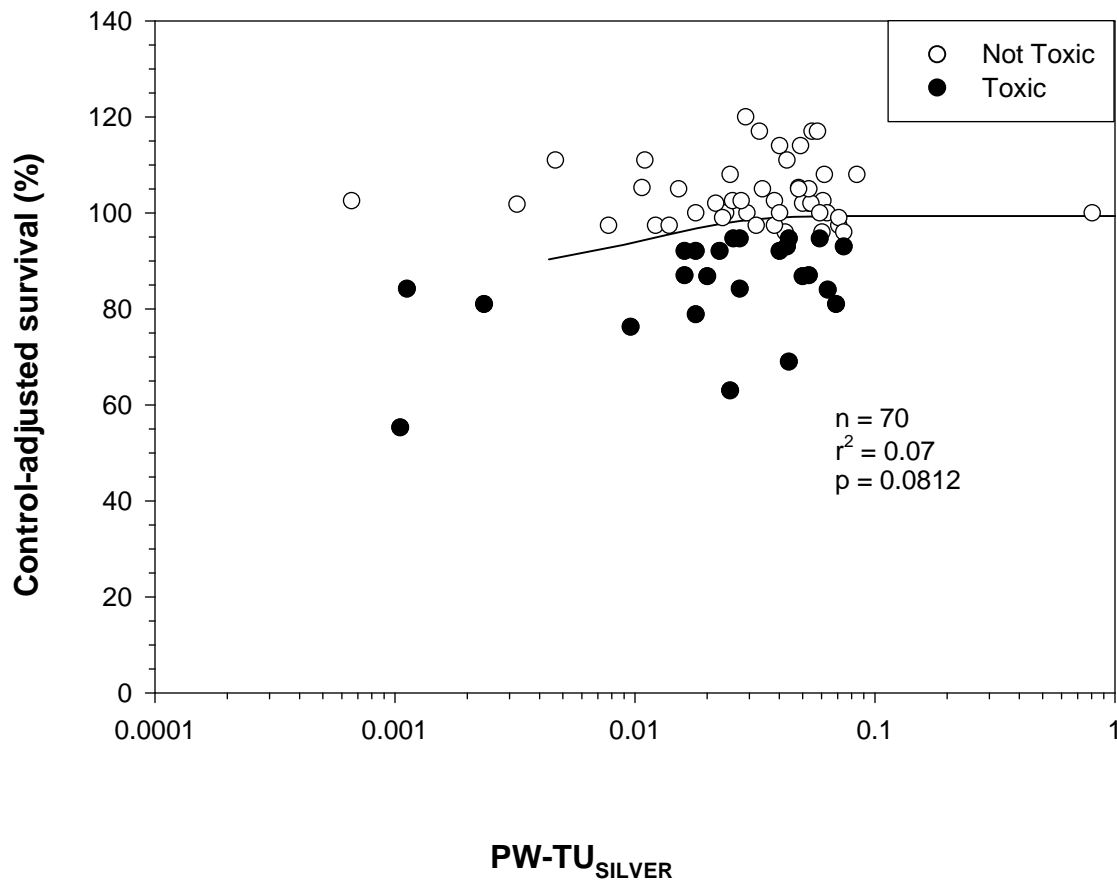
Plot A1-200. Plot illustrating the relationship between the concentration of PW-TU_{NICKEL} (7-day) and the control-adjusted survival of midges (*Chironomus dilutus*) in 10-d exposures to sediment samples from the Tri-State Mining District.



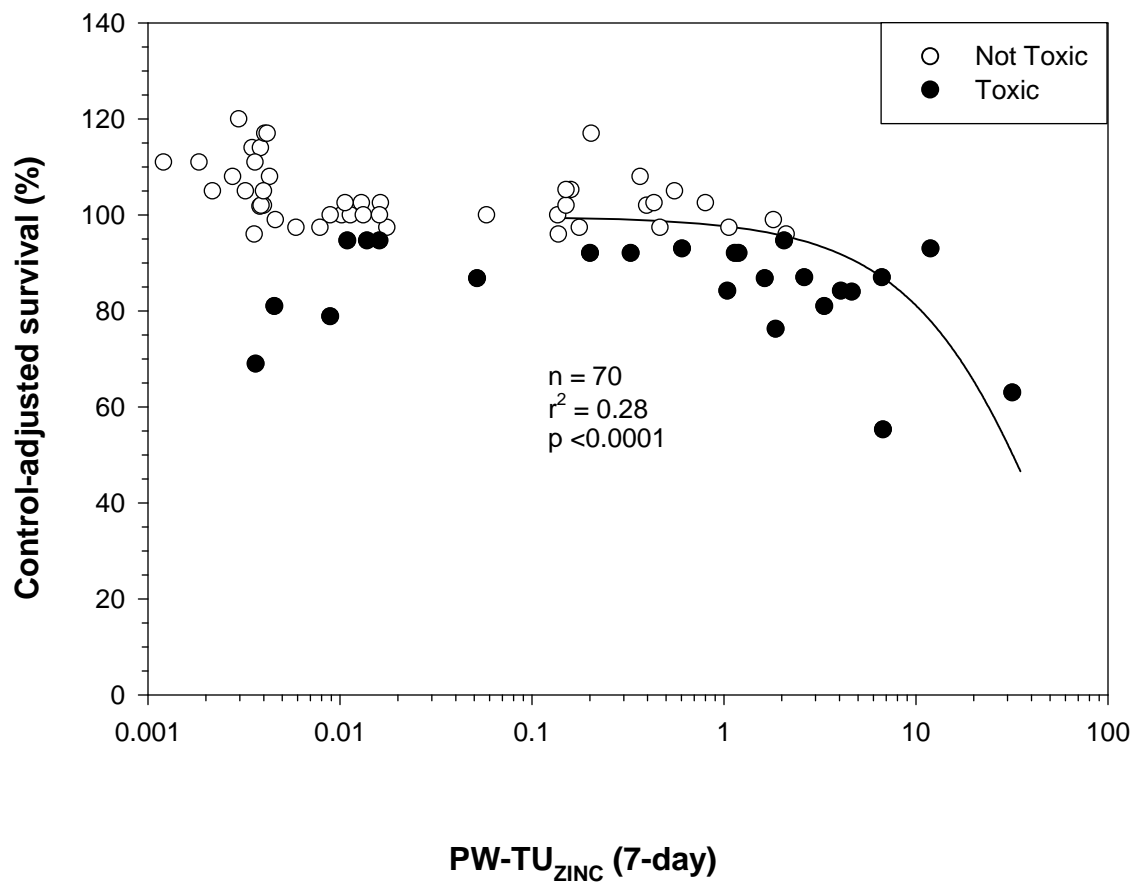
Plot A1-201. Plot illustrating the relationship between the concentration of $PW-TU_{SELENIUM}$ and the control-adjusted survival of midges (*Chironomus dilutus*) in 10-d exposures to sediment samples from the Tri-State Mining District.



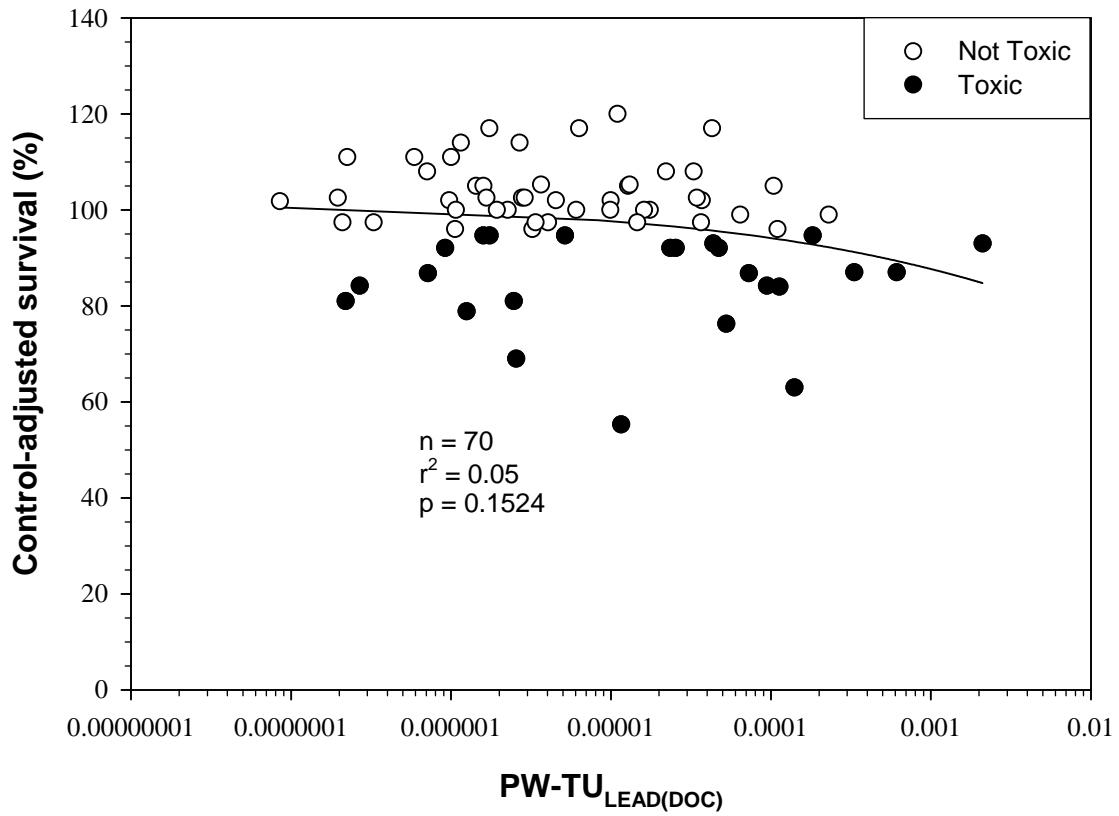
Plot A1-202. Plot illustrating the relationship between the concentration of $PW-TU_{SILVER}$ and the control-adjusted survival of midges (*Chironomus dilutus*) in 10-d exposures to sediment samples from the Tri-State Mining District.



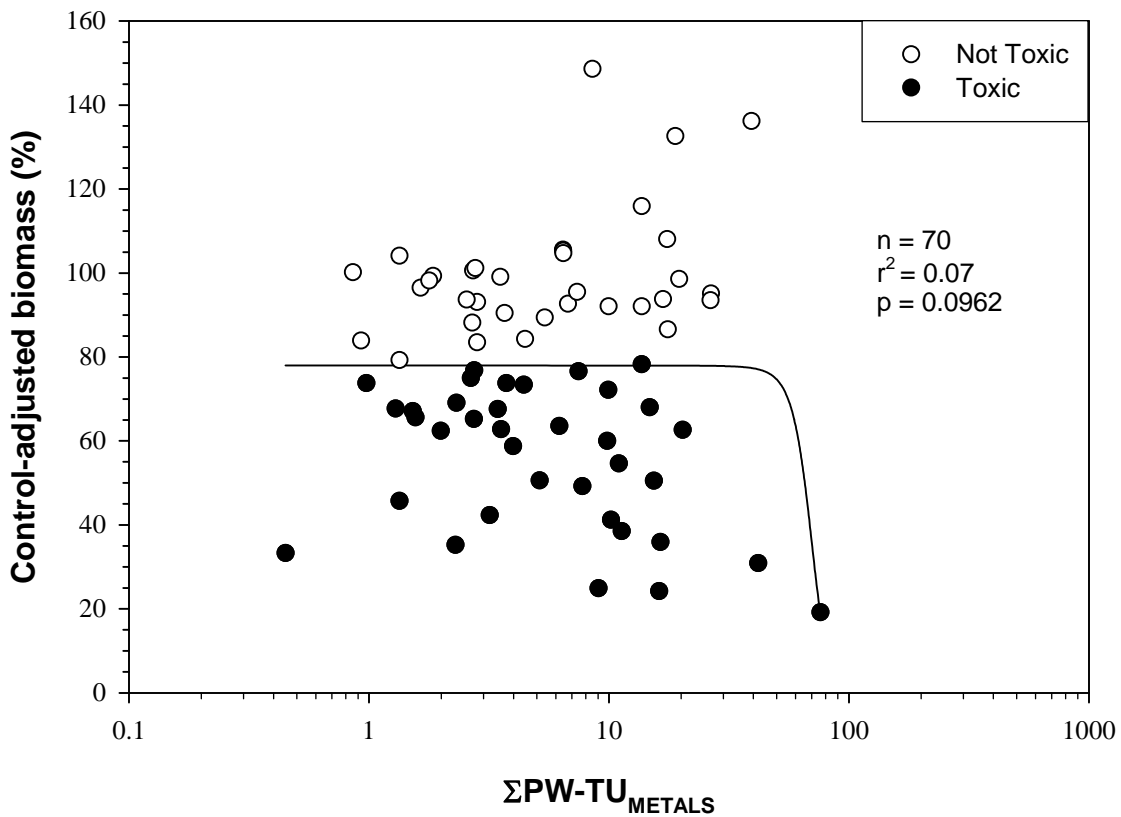
Plot A1-203. Plot illustrating the relationship between the concentration of PW-TU_{ZINC} (7-day) and the control-adjusted survival of midges (*Chironomus dilutus*) in 10-d exposures to sediment samples from the Tri-State Mining District.



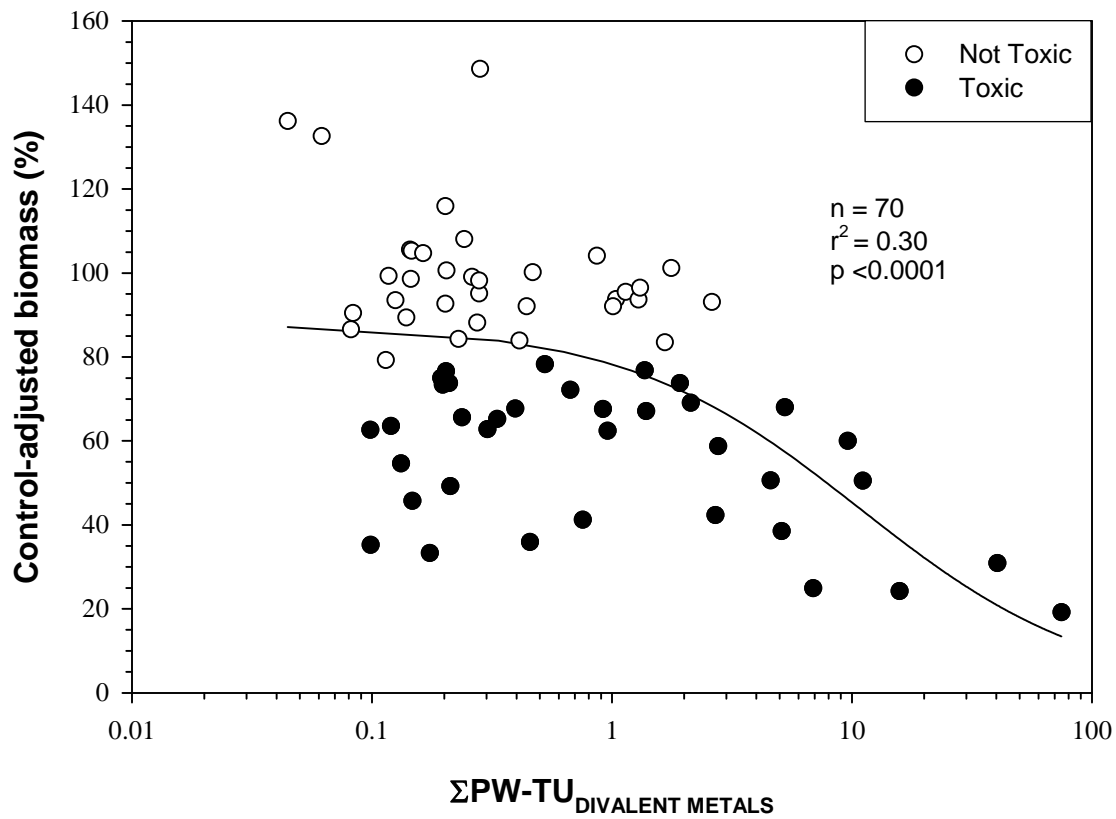
Plot A1-204. Plot illustrating the relationship between the concentration of $PW-TU_{LEAD(DOC)}$ and the control-adjusted survival of midges (*Chironomus dilutus*) in 10-d exposures to sediment samples from the Tri-State Mining District.



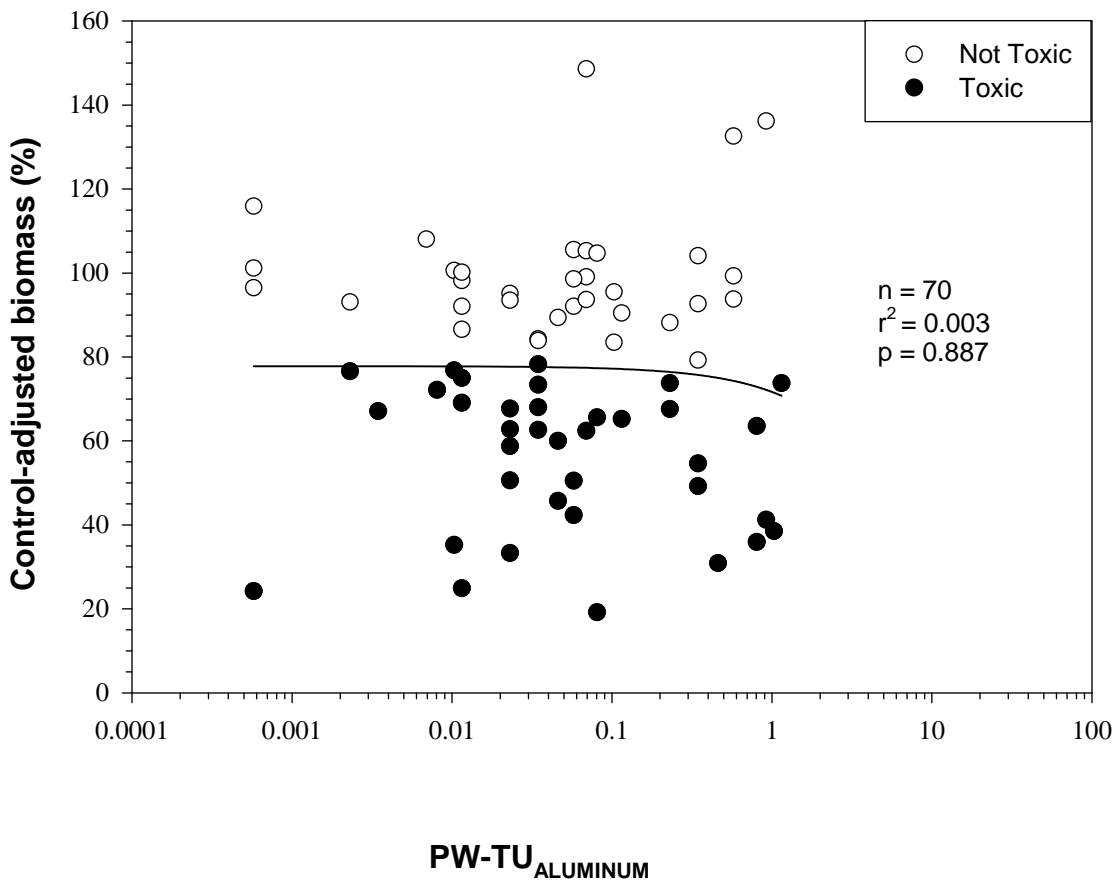
Plot A1-206. Plot illustrating the relationship between the concentration of $\Sigma\text{PW-TU}_{\text{METALS}}$ and the control-adjusted biomass of midges (*Chironomus dilutus*) in 10-d exposures to sediment samples from the Tri-State Mining District.



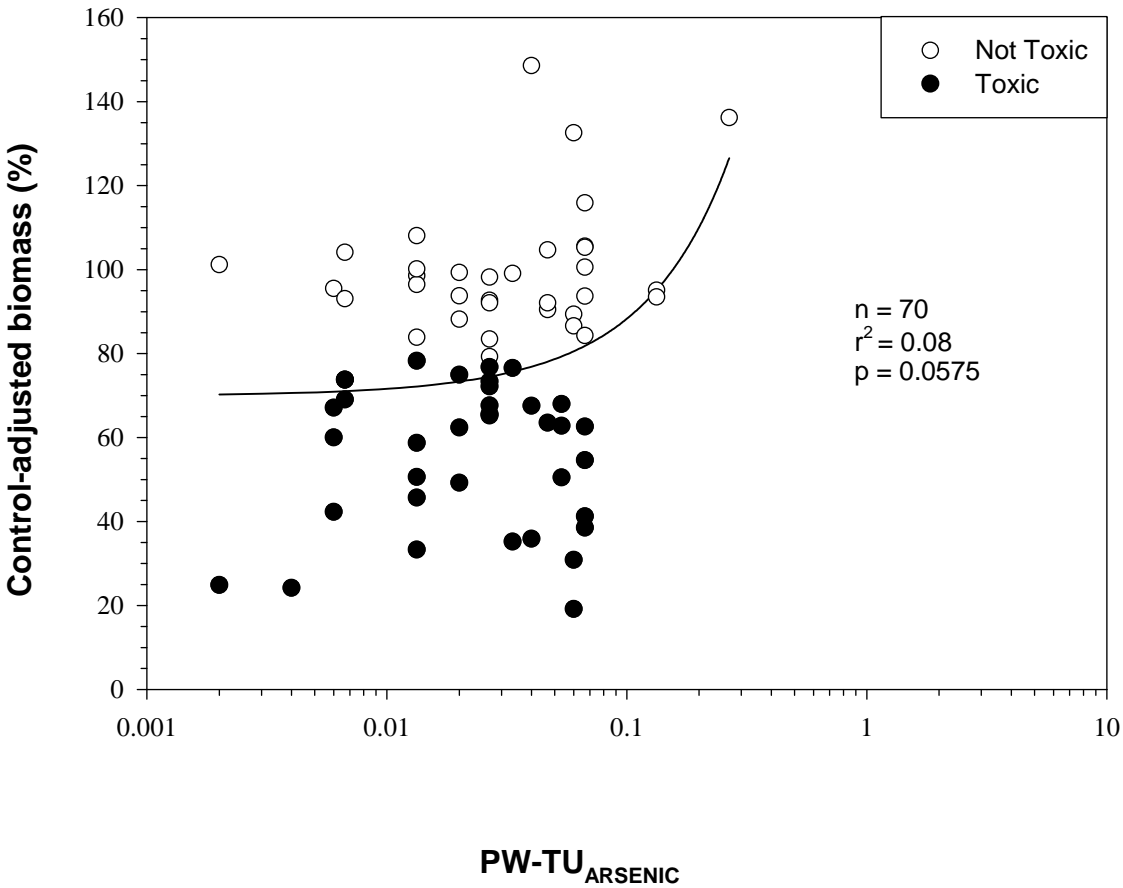
Plot A1-207. Plot illustrating the relationship between the concentration of $\Sigma\text{PW-TU}_{\text{Divalent Metals}}$ and the control-adjusted biomass of midges (*Chironomus dilutus*) in 10-d exposures to sediment samples from the Tri-State Mining District.



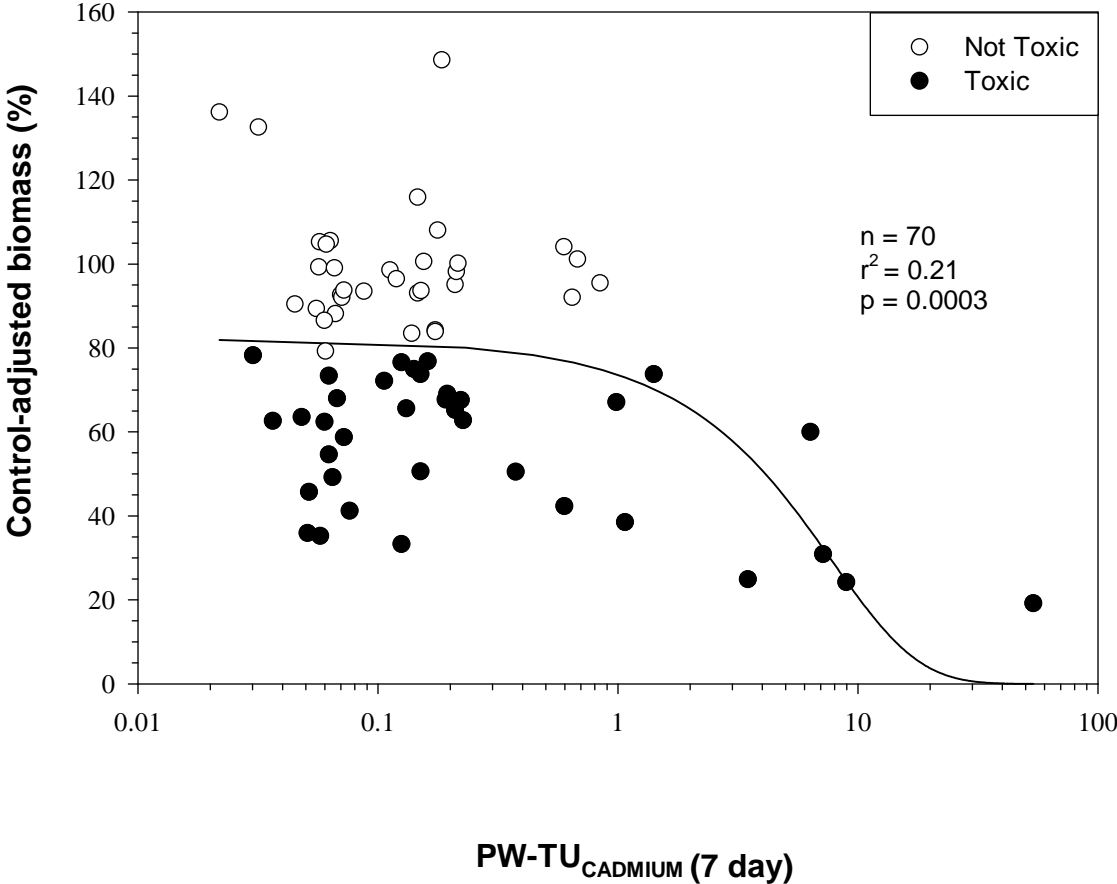
Plot A1-208. Plot illustrating the relationship between the concentration of $PW-TU_{ALUMINUM}$ and the control-adjusted biomass of midges (*Chironomus dilutus*) in 10-d exposures to sediment samples from the Tri-State Mining District.



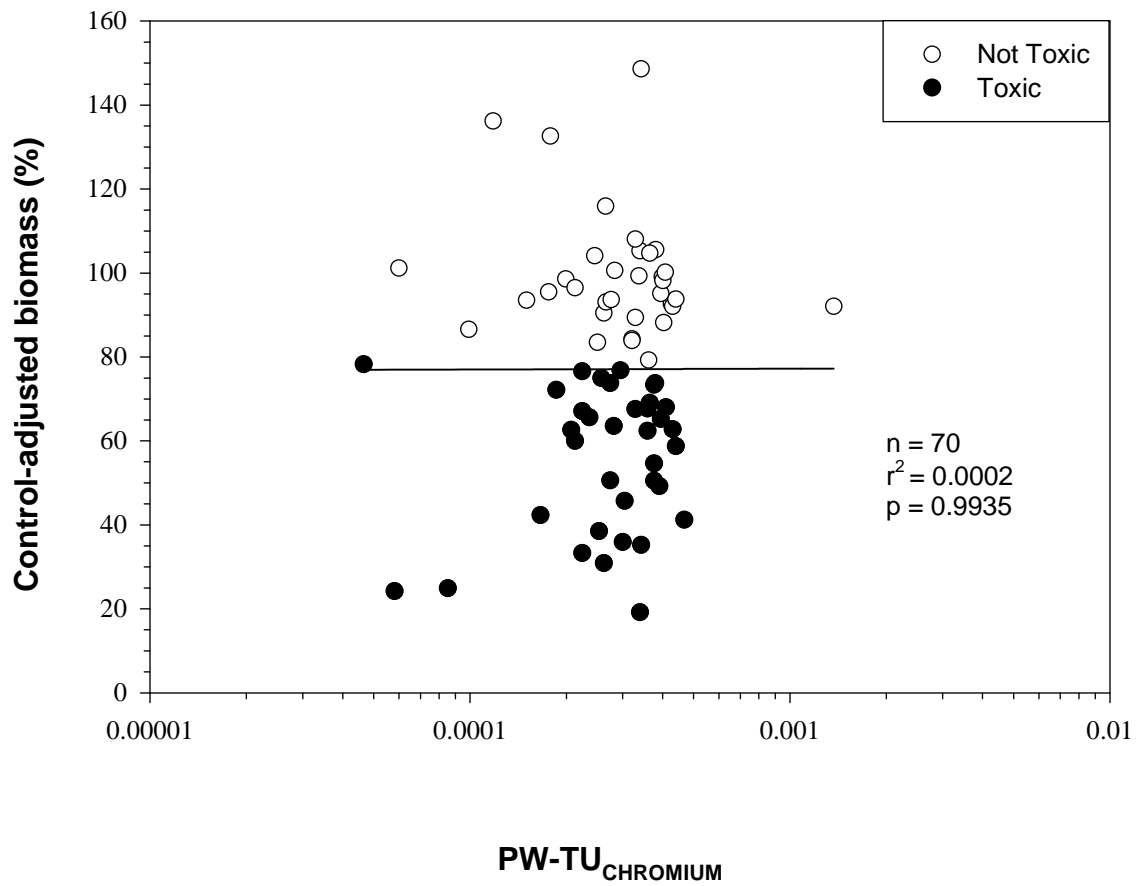
Plot A1-209. Plot illustrating the relationship between the concentration of $PW-TU_{ARSENIC}$ and the control-adjusted biomass of midges (*Chironomus dilutus*) in 10-d exposures to sediment samples from the Tri-State Mining District.



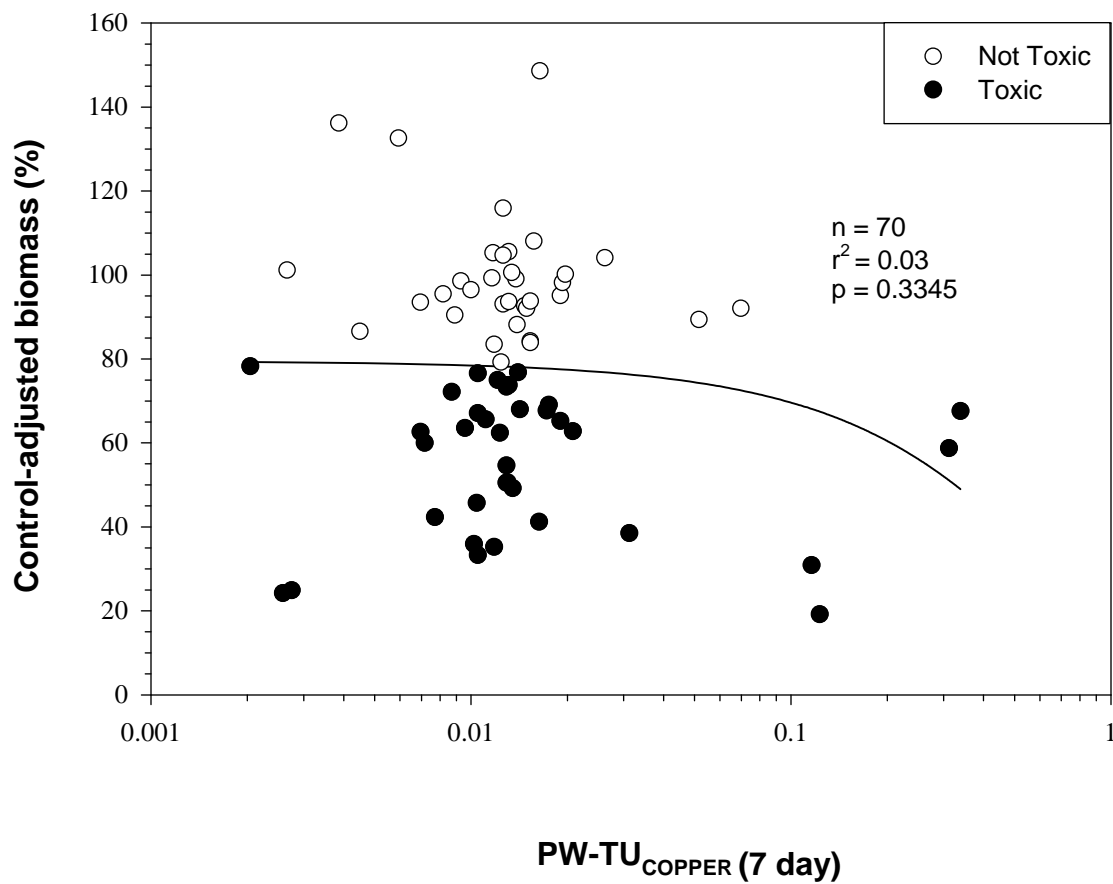
Plot A1-210. Plot illustrating the relationship between the concentration of PW-TU_{CADMIUM} (7-day) and the control-adjusted biomass of midges (*Chironomus dilutus*) in 10-d exposures to sediment samples from the Tri-State Mining District.



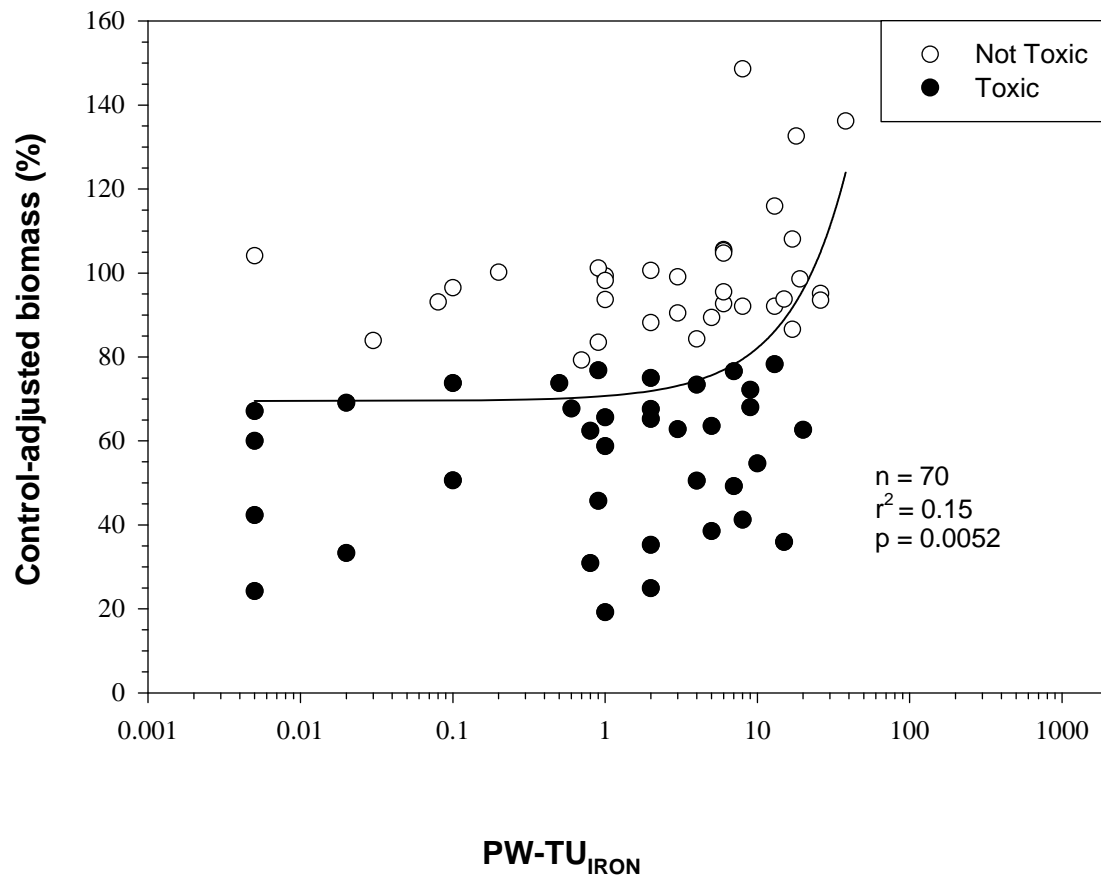
Plot A1-211. Plot illustrating the relationship between the concentration of PW-TU_{CHROMIUM} and the control-adjusted biomass of midges (*Chironomus dilutus*) in 10-d exposures to sediment samples from the Tri-State Mining District.



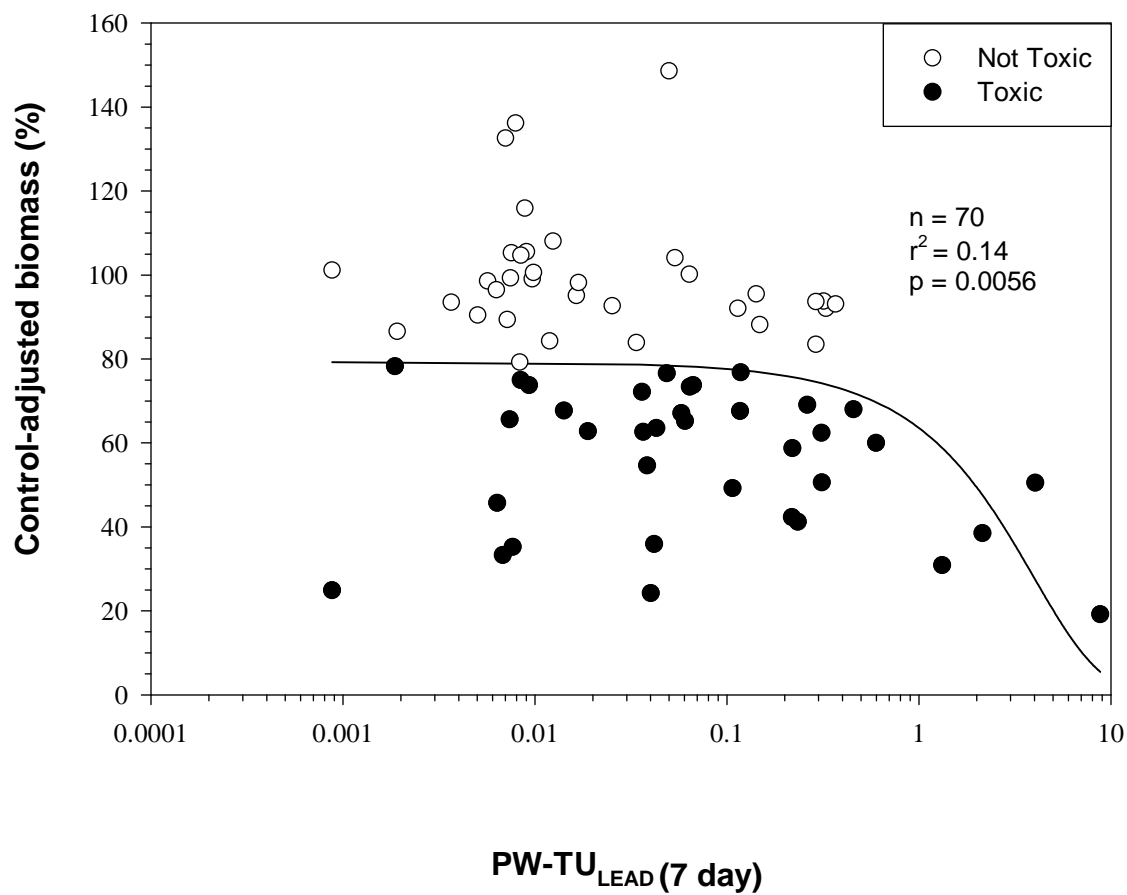
Plot A1-212. Plot illustrating the relationship between the concentration of $PW-TU_{COPPER}$ (7-day) and the control-adjusted biomass of midges (*Chironomus dilutus*) in 10-d exposures to sediment samples from the Tri-State Mining District.



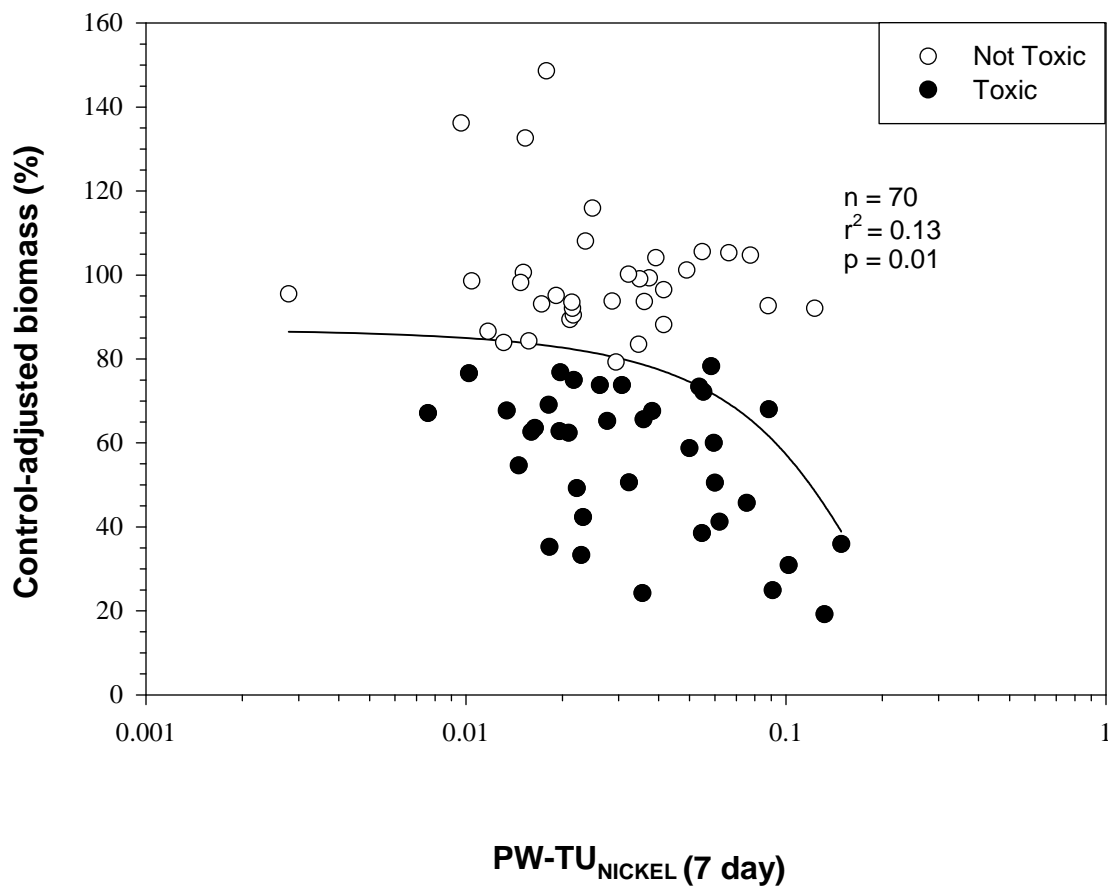
Plot A1-213. Plot illustrating the relationship between the concentration of $PW-TU_{IRON}$ and the control-adjusted biomass of midges (*Chironomus dilutus*) in 10-d exposures to sediment samples from the Tri-State Mining District.



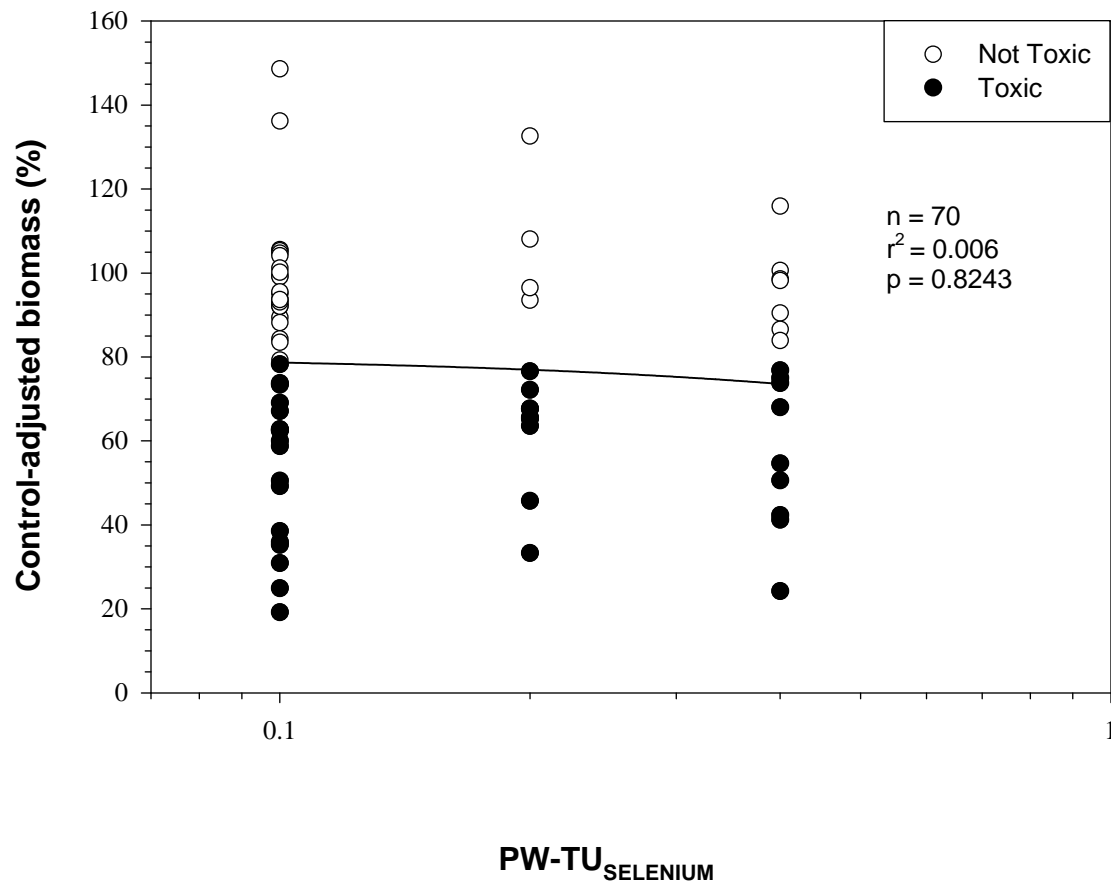
Plot A1-214. Plot illustrating the relationship between the concentration of $PW-TU_{LEAD}$ (7-day) and the control-adjusted biomass of midges (*Chironomus dilutus*) in 10-d exposures to sediment samples from the Tri-State Mining District.



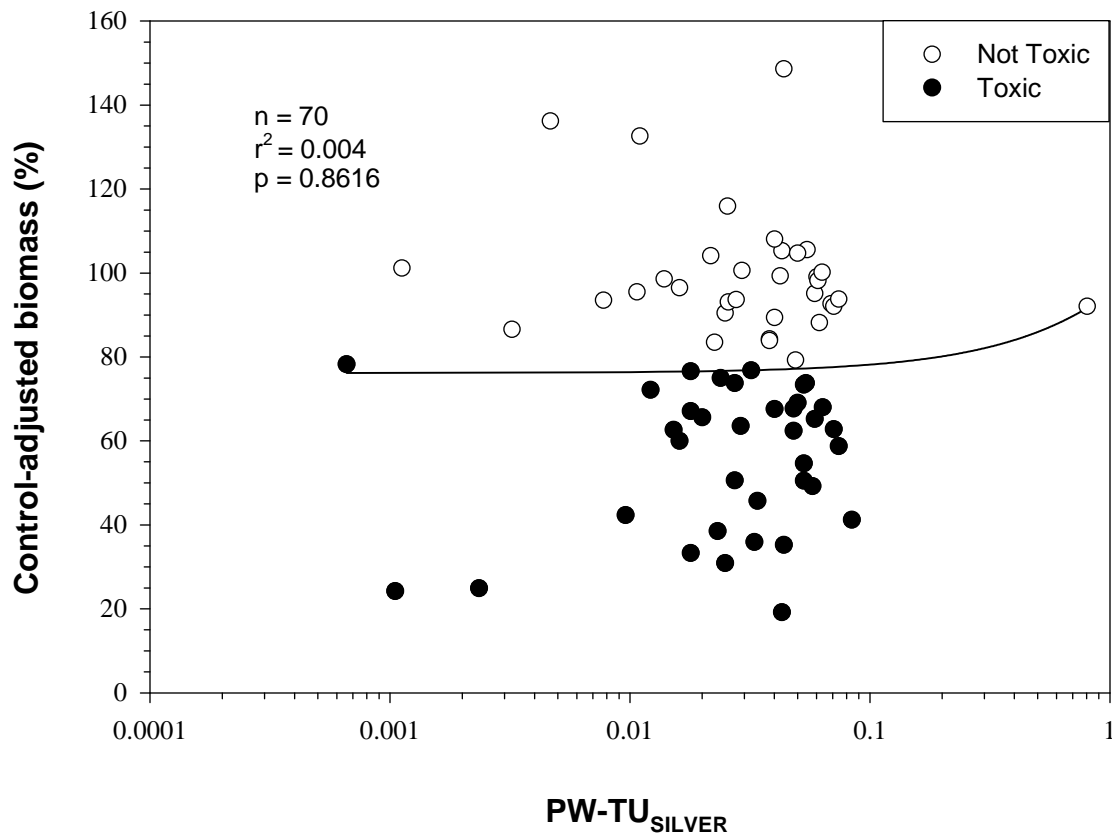
Plot A1-215. Plot illustrating the relationship between the concentration of $PW-TU_{NICKEL}$ (7-day) and the control-adjusted biomass of midges (*Chironomus dilutus*) in 10-d exposures to sediment samples from the Tri-State Mining District.



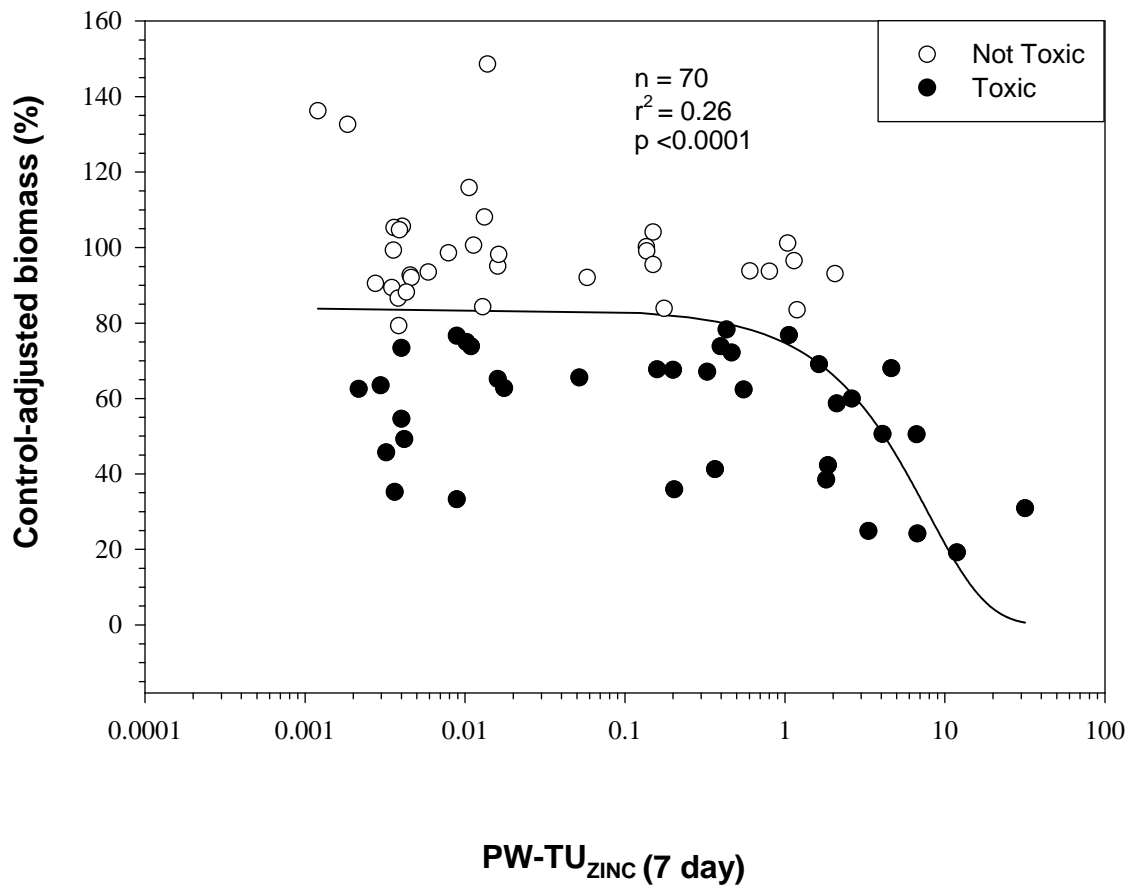
Plot A1-216. Plot illustrating the relationship between the concentration of $PW-TU_{SELENIUM}$ and the control-adjusted biomass of midges (*Chironomus dilutus*) in 10-d exposures to sediment samples from the Tri-State Mining District.



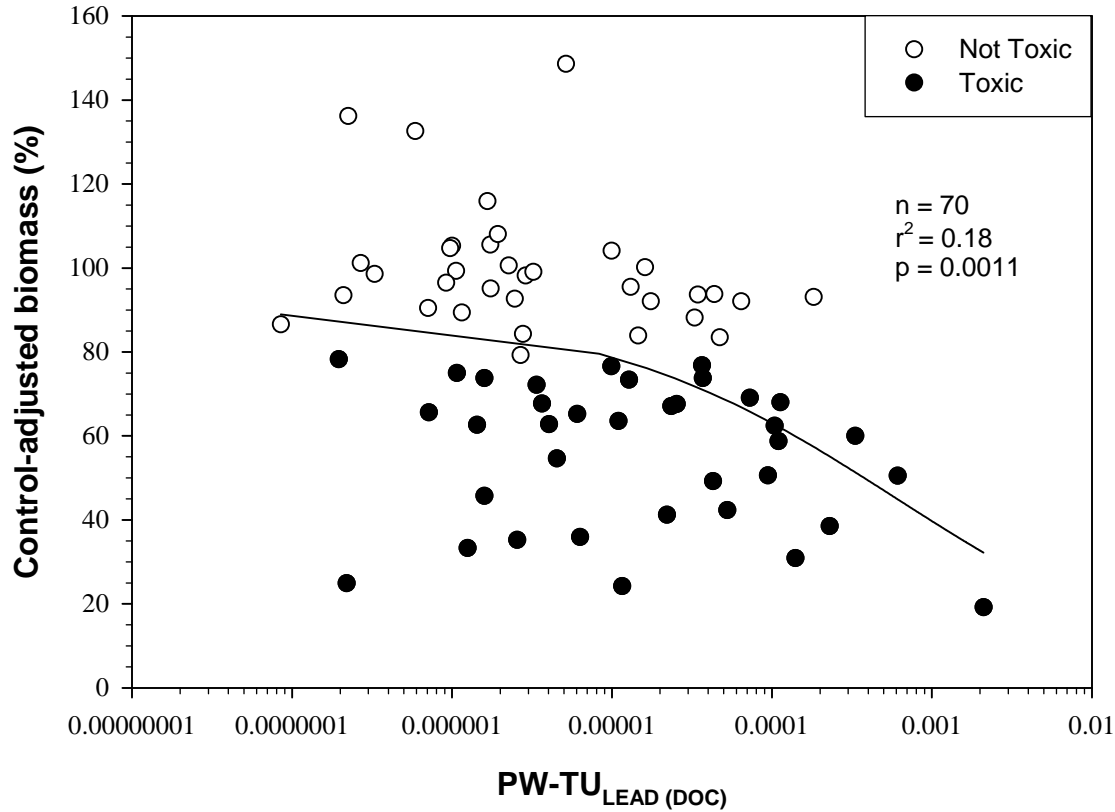
Plot A1-217. Plot illustrating the relationship between the concentration of $PW-TU_{SILVER}$ and the control-adjusted biomass of midges (*Chironomus dilutus*) in 10-d exposures to sediment samples from the Tri-State Mining District.



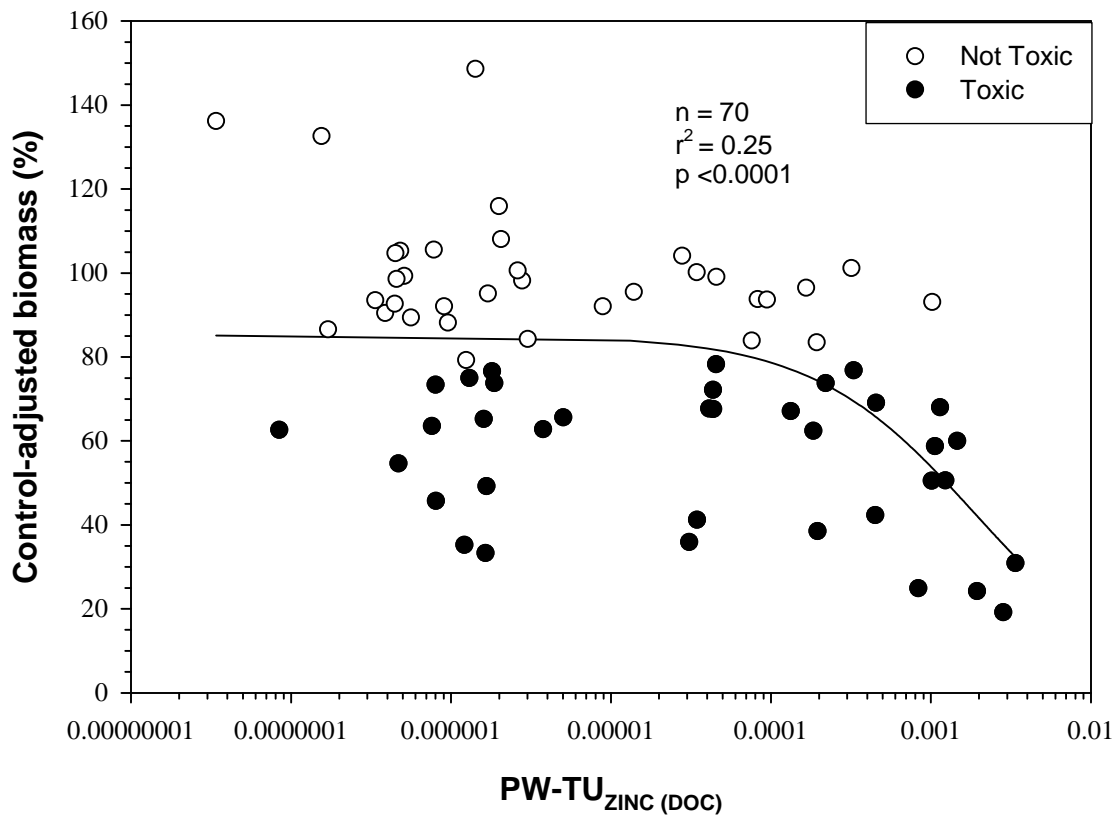
Plot A1-218. Plot illustrating the relationship between the concentration of PW-TU_{ZINC} (7-day) and the control-adjusted biomass of midges (*Chironomus dilutus*) in 10-d exposures to sediment samples from the Tri-State Mining District.



Plot A1-219. Plot illustrating the relationship between the concentration of $PW-TU_{LEAD(DOC)}$ and the control-adjusted biomass of midges (*Chironomus dilutus*) in 10-d exposures to sediment samples from the Tri-State Mining District.



Plot A1-220. Plot illustrating the relationship between the concentration of PW-TU_{ZINC(DOC)} and the control-adjusted biomass of midges (*Chironomus dilutus*) in 10-d exposures to sediment samples from the Tri-State Mining District.



Appendix 2

Appendix 2 Procedures for Calculating Selected Metrics for Sediment and Pore Water

A variety of metrics were used in this study to describe the concentrations of COPC mixtures in TSMD sediment and pore-water samples. These selected metrics were described in Section 2 of this document. The procedures for calculating each of these metrics are further described in this appendix.

A2.1 Mean Probable Effect Concentration-Quotient Metals (mean PEC-Q_{METALS})

The mean PEC-Q_{METALS} mixture model is calculated using the measured concentrations of seven metals in each sediment sample and the corresponding PECs for those metals. The following equation is used (MacDonald *et al.* 2000a):

$$\text{Mean PEC-Q}_{\text{METALS}} = \left[\frac{[\text{As}]}{\text{PEC}_{\text{As}}} + \frac{[\text{Cd}]}{\text{PEC}_{\text{Cd}}} + \frac{[\text{Cu}]}{\text{PEC}_{\text{Cu}}} + \frac{[\text{Cr}]}{\text{PEC}_{\text{Cr}}} + \frac{[\text{Pb}]}{\text{PEC}_{\text{Pb}}} + \frac{[\text{Hg}]}{\text{PEC}_{\text{Hg}}} + \frac{[\text{Zn}]}{\text{PEC}_{\text{Zn}}} \right] \div 7$$

If data are available on fewer than seven metals, then the sum of the PEC-Qs is divided by the number of metals for which data are available. In these calculations (and those for the other metrics), less than detection limit results are assigned a value of one-half of the detection limit. However, the data for a metal is not used in the calculation if the detection limit is greater than the PEC. Table A2-1 illustrates this procedure.

A2.2 Mean Probable Effect Concentration-Quotient (mean PEC-Q)

The mean PEC-Q is calculated using data on the concentrations of metals, total polycyclic aromatic hydrocarbons (tPAHs), and total polychlorinated biphenyls (tPCBs) in sediment samples, along with the corresponding PECs:

$$\text{Mean PEC-Q} = \left[\text{mean PEC-Q}_{\text{METALS}} + \frac{[\text{tPAHs}]}{\text{PEC}_{\text{tPAHs}}} + \frac{[\text{tPCBs}]}{\text{PEC}_{\text{tPCBs}}} \right] \div 3$$

The procedure for calculating mean PEC- Q_{METALS} is described in Section A2.1. The PEC- Q_{tPAH} is calculated by dividing the concentration of tPAHs by the PEC for tPAHs (22.8 mg/kg DW). In this procedure, tPAHs is calculated as the sum of the concentrations of 13 parent PAHs. Total PCBs is calculated as the sum of the 209 congeners, the sum of homologs, the sum of Aroclors, or other procedures (see MacDonald *et al.* 2000b for more information).

A2.3 Sum Equilibrium Partitioning-Based Sediment Benchmark-Toxic Units for Polycyclic Aromatic Hydrocarbons (\sum ESB-TU_{FCV} for PAHs)

The procedures for calculating \sum ESB-TU_{FCV} for PAHs are described in USEPA (2005). The reader is directed to that document for detailed information on the methods that are used to calculate this metric and specific examples of such calculations. Toxicity to benthic invertebrates due to PAHs is not predicted when \sum ESB-TU_{FCV} < 1.0 (USEPA 2005).

A2.4 Sum Simultaneously Extracted Metals Minus Acid Volatile Sulfide (\sum SEM-AVS)

The procedures for calculating \sum SEM-AVS are described in detail in USEPA (2003). Briefly, this metric is calculated by summing the molar concentrations of SE divalent metals (in $\mu\text{moles/g}$) using the following equation:

$$\sum\text{SEM} = [\text{SEM}_{\text{Cd}}] + [\text{SEM}_{\text{Cu}}] + [\text{SEM}_{\text{Pb}}] + [\text{SEM}_{\text{Ni}}] + [\text{SEM}_{\text{Zn}}] + \frac{1}{2} [\text{SEM}_{\text{Ag}}]$$

The \sum SEM-AVS metric is then calculated by subtracting the molar concentration of AVS from the \sum SEM that was determined (see USEPA 2003 for example calculations). Toxicity to benthic invertebrates due to metals is not predicted when \sum SEM-AVS < 0.0 (USEPA 2003).

A2.5 Sum Simultaneously Extracted Metals Minus Acid Volatile Sulfide Fraction Organic Carbon $[(\sum \text{SEM-AVS})/f_{\text{OC}}]$

The procedures for calculating $(\sum \text{SEM-AVS})/f_{\text{OC}}$ are described in USEPA (2003). Briefly, this metric is calculated by dividing $\sum \text{SEM-AVS}$ (see Section A2.4 above) by the fraction of organic carbon (f_{OC}) in the sediment, which is determined by dividing the percent organic carbon in a sediment sample by 100 (i.e., if a sample has 4.5% OC, then $f_{\text{OC}} = 0.045$; see USEPA 2003 for example calculations). Toxicity due to the presence of divalent metals is not expected when $(\sum \text{SEM-AVS})/f_{\text{OC}} < 130 \mu\text{mol/g}$. In contrast, toxicity to benthic invertebrates is expected to be observed when $(\sum \text{SEM-AVS})/f_{\text{OC}} > 3000 \mu\text{mol/g}$ (USEPA 2003).

A2.6 Sum Probable Effect Concentration-Quotient Cadmium, Lead, Zinc $(\sum \text{PEC-Q}_{\text{Cd,Pb,Zn}})$

The Dudding Model for evaluating the joint toxicity of cadmium, lead, and zinc to benthic invertebrates is calculated using the following equation:

$$\sum \text{PEC-Q}_{\text{Cd,Pb,Zn}} = \frac{[\text{Cd}]}{[\text{PEC}_{\text{Cd}}]} + \frac{[\text{Pb}]}{[\text{PEC}_{\text{Pb}}]} + \frac{[\text{Zn}]}{[\text{PEC}_{\text{Zn}}]}$$

For each metal, the dry weight concentration is used in the calculation, along with the PEC reported in MacDonald *et al.* (2000a). An example calculation is provided in Table A2-3.

A2.7 Sum Sediment Toxicity Threshold-Quotient Cadmium, Copper, Lead, Zinc $(\sum \text{STT-Q}_{\text{Cd,Cu,Pb,Zn}})$

Calculation of this metric relies on the selection of site-specific STTs for each of the four metals from among the various STTs that were derived for the Tri-State Mining District (TSMD). Accordingly, the information on the reliability of the various STTs

was reviewed and evaluated to support selection of the most reliable STTs for use in model development. Based on the results of this evaluation, the following STTs were selected: 11.1 mg/kg DW for cadmium; 27.1 mg/kg DW for copper; 219 mg/kg DW for lead; and 2083 mg/kg DW for zinc. This metric is calculated using the following equation:

$$\sum \text{STT-Q}_{\text{Cd,Cu,Pb,Zn}} = \frac{[\text{Cd}]}{\text{STT}_{\text{Cd}}} + \frac{[\text{Cu}]}{\text{STT}_{\text{Cu}}} + \frac{[\text{Pb}]}{\text{STT}_{\text{Pb}}} + \frac{[\text{Zn}]}{\text{STT}_{\text{Zn}}}$$

An example calculation for this metric is provide in Table A2.4.

A2.8 References Cited

MacDonald, D.D., C.G. Ingersoll, and T.A. Berger. 2000a. Development and evaluation of consensus-based sediment quality guidelines for freshwater ecosystems. *Archives of Environmental Contamination and Toxicology* 39:20-31.

MacDonald, D.D., L.M. DiPinto, J. Field, C.G. Ingersoll, E.R. Long, and R.C. Swartz. 2000b. Development and evaluation of consensus-based sediment effect concentrations for polychlorinated biphenyls (PCBs). *Environmental Toxicology and Chemistry* 19:1403-1413.

USEPA (United States Environmental Protection Agency). 2003. Procedures for the derivation of equilibrium partitioning sediment benchmarks (ESBs) for the protection of benthic organisms: PAH mixtures. EPA-600-R-02-013. Office of Research and Development. Washington, District of Columbia.

USEPA (United States Environmental Protection Agency). 2005. Procedures for the derivation of equilibrium partitioning sediment benchmarks (ESBs) for the protection of benthic organisms: Metal mixtures (cadmium, copper, lead, nickel, silver, and zinc). EPA-600-R-02-11. Office of Research and Development. Washington, District of Columbia.

Table A2-1. An example of how to calculate mean PEC-Q_{METALS}.

Metal COPC	Concentration (mg/kg DW)	PEC (mg/kg DW)	PEC-Q (= concentration x PEC)	Mean PEC-Q_{METALS} (= average of individual PEC-Qs)
Arsenic	40	33.0	1.2	
Cadmium	12.6	4.98	2.5	
Chromium	55	111	0.50	
Copper	120	149	0.81	
Lead	220	128	1.7	
Nickel	1.74	48.6	0.0	
Zinc	190	459	0.41	

COPC = chemical of potential concern; PEC = probable effect concentration-quotient; DW = dry weight.

It is important to note that the mean PEC-Q_{METALS} is calculated by taking the average of the PEC-Qs for up to seven metals (in this example, n=7).

Table A2-2. An example of how to calculate mean PEC-Q.

Metal COPC	Concentration (mg/kg DW)	PEC (mg/kg DW)	PEC-Q (= concentration x PEC)	Mean PEC-Q _{METALS} (= average of individual PEC-Qs)	Mean PEC-Q (= average of Mean PEC-Q _{METALS} , PEC-Q _{tPAH} , PEC-Q _{tPCB})
Arsenic	40	33.0	1.2		
Cadmium	12.6	4.98	2.5		
Chromium	55	111	0.50		
Copper	120	149	0.81		
Lead	220	128	1.7		
Nickel	1.74	48.6	0.04		
Zinc	190	459	0.41		
Total PAHs (tPAH)	16	20.8	0.769		
Total PCBs (tPCB)	0.69	0.676	1.02		

COPC = chemical of potential concern; PEC = probable effect concentration-quotient; DW = dry weight; PAH = polycyclic aromatic hydrocarbons.
 PCBs = polychlorinated biphenyls.

It is important to note that the mean PEC-Q is calculated by taking the average of up to three classes of COPCs (in this example, n=3). This procedure for calculating the mean PEC-Q was selected from a total of 11 methods that were investigated by Ingersoll *et al.* (2001). Although there are additional classes of COPCs for which PECs are available, procedures for calculating mean PEC-Qs using more than the three principal classes of COPCs have not been developed.

Table A2-3. An example of how to calculate $\Sigma\text{PEC-Q}_{\text{Cd,Pb,Zn}}$ (i.e., the Dudding Model).

Metal COPC	Concentration (mg/kg DW)	PEC (mg/kg DW)	PEC-Q (= concentration x PEC)	$\Sigma\text{PEC-Q}_{\text{Cd,Pb,Zn}}$ (= sum of individual PEC-Qs)
Cadmium	12.6	4.98	2.5	
Lead	220	128	1.7	
Zinc	190	459	0.4	

COPC = chemical of potential concern; PEC = probable effect concentration-quotient; DW = dry weight.

Table A2-4. An example of how to calculate $\Sigma\text{STT-Q}_{\text{Cd,Cu,Pb,Zn}}$

Metal COPC	Concentration (mg/kg DW)	PEC (mg/kg DW)	PEC-Q (= concentration x PEC)	$\Sigma\text{STT-Q}_{\text{Cd,Cu,Pb,Zn}}$ (= sum of individual PEC-Qs)
Cadmium	12.6	11.1	1.1	
Copper	120	27.1	4.4	
Lead	220	219	1.0	
Zinc	190	2083	0.1	

COPC = chemical of potential concern; PEC = probable effect concentration-quotient; STT = sediment toxicity threshold; DW = dry weight.
 Cd = cadmium; Cu = copper; Pb = lead; Zn = zinc.

Appendix 3

Appendix 3 Overview of the Quality of the Data Collected During the 2007 Sediment Sampling Program (as excerpted from Ingersoll *et al.* 2008)

A. Sediment toxicity and sediment bioaccumulation testing data

Appendix A of Ingersoll *et al.* (2008) provides a summary of the data for the toxicity tests and bioaccumulation tests conducted with samples from the TSMD (n=76 sediment toxicity samples for amphipods and midges, n=48 sediment toxicity samples for mussels, and n=21 sediment bioaccumulation samples for oligochaetes across the three sediment sampling events; Table 1, of Ingersoll *et al.* 2008). Table A1 of Ingersoll *et al.* (2008) summarizes the water quality characteristics of the pore-water samples isolated by centrifugation at the start of the sediment toxicity and sediment bioaccumulation tests. Table A2 of Ingersoll *et al.* (2008) summarizes the mean water quality characteristics of the overlying water sampled during the sediment toxicity and sediment bioaccumulation tests. Table A3 of Ingersoll *et al.* (2008) summarizes the mean treatment responses of test organisms in each sediment toxicity treatment. Table A4 of Ingersoll *et al.* (2008) summarizes the treatment responses of test organisms in each replicate beaker within each sediment toxicity treatment. Table A5 of Ingersoll *et al.* (2008) summarizes the body length measurements of individual amphipods (and the associated estimated weight of individual amphipods) and shell length measurements of individual mussels within each beaker within each sediment treatment. Appendix B of Ingersoll *et al.* (2008) provides a summary of the bioaccumulation of metals by oligochaetes within each replicate beaker and as treatment mean responses. Table 6 of Ingersoll *et al.* (2008) provides a summary of the response of test organisms in the control sediment and a summary of the size or age of test organisms at the start of the sediment toxicity and sediment bioaccumulation tests. Table 6 of Ingersoll *et al.* (2008) also provides a summary of the response of test organisms in 48- to 96-hour water-only NaCl reference toxicant

tests conducted in conjunction with the sediment toxicity and sediment bioaccumulation tests.

The Quality Assurance Project Plan (of I) for the project established acceptable levels of precision, accuracy, completeness and sensitivity for the chemical, physical, or biological data measured in the sediment toxicity and sediment bioaccumulation tests (Table 5 in the QAPP, Ingersoll 2007). Precision in the sediment toxicity and sediment bioaccumulation tests was established based on analyses of laboratory duplicates of pore-water samples (Table A1 of Ingersoll *et al.* 2008). Relative percent deviation between duplicate measures of water quality characteristics of pore water were typically less than 20%; however wider ranges were observed for ammonia for some duplicate samples (e.g., sample CERC-19; Table A1 of Ingersoll *et al.* 2008).

For biological data measured in sediment toxicity or sediment bioaccumulation tests, no true accuracy estimates are possible because of the lack of available standard sediment(s) (Ingersoll 2007). Instead, accuracy was established for sediment toxicity testing based on test acceptability for test organisms in the negative control sediment [without the addition of the test chemical; American Society for Testing and Materials (ASTM) 2008a, USEPA 2000].

Completeness was established as the amount of valid data obtained from a measurement system compared to the amount that was expected to be obtained under normal conditions. Target completeness was established as 90% for chemical analyses of pore water, overlying water, toxicity tests, and bioaccumulation tests (Ingersoll 2007). Sensitivity of toxicity test organisms was evaluated using 48- to 96-hour reference toxicant water-only exposures with NaCl (Table 6 of Ingersoll *et al.* 2008, described below).

Amphipod toxicity tests: Mean 28-d survival of amphipods in control sediment ranged from 90 to 100% across the three sets of sediment tests (Set 1, 2, and 3; Table 6 of Ingersoll *et al.* 2008). Mean 28-d body length of amphipods in control sediment ranged from 3.41 to 4.35 mm, with increases ranging from 2.2 to 3.6X (Table 6 of

Ingersoll *et al.* 2008). Both control mean survival and growth exceeded the test acceptability criteria (ASTM 2008a, USEPA 2000; Table 6 of Ingersoll *et al.* 2008). Hence, the data quality objectives (DQOs) were met for all of the amphipod toxicity tests (as identified in Table A1.1 of the QAPP, Ingersoll 2007). Specifically, completeness was 100% for the 76 sediment samples evaluated in sediment toxicity tests conducted with amphipods (based on performance of amphipods in control sediment; Table 6 of Ingersoll *et al.* 2008). More than 11 test organisms were recovered from CERC-41, replicate 2 (Table A4 of Ingersoll *et al.* 2008), so this replicate was not included in the calculation of the mean response of test organisms in this treatment (Table A3 of Ingersoll *et al.* 2008).

Mean starting lengths of amphipods (range from 1.21 to 1.54 mm) were consistent with the starting length of about 7-d-old amphipods historically used to start sediment toxicity tests at the USGS laboratory in Columbia, MO (Table 6 of Ingersoll *et al.* 2008). Because of the difference in mean length of amphipods in the control sediment on Day 28 (3.41 mm for Set 2 to 4.35 mm for Set 1; Table 6 of Ingersoll *et al.* 2008) amphipod lengths in the test sediment were normalized to the percent of control response (Table A3 of Ingersoll *et al.* 2008). Estimated mean weight of amphipods in the control sediment at Day 28 ranged from 0.20 to 0.41 mg/individual and estimated mean biomass of amphipods in control sediment at Day 28 ranged from 1.7 to 3.9 mg/treatment (Table 6 of Ingersoll *et al.* 2008). No guidance is provided in USEPA (2000) or in ASTM (2008a) regarding acceptable growth of control organisms (other than the statement that amphipods in the control sediment should grow during the 28-d exposure). The response of amphipods in the two 48-hour water-only NaCl reference toxicant tests (LC50s) was 5.7 and 6.1 g/L (Table 6 of Ingersoll *et al.* 2008) and is representative of historic reference toxicant tests for amphipods conducted at the CERC laboratory in ASTM hard water (ASTM 2008d). No reference toxicant tests were conducted with amphipods associated with the Set 3 samples conducted in 2006.

Midge toxicity tests: For the Set 1 and Set 2 sediment samples tested in 2007, mean survival of midges in the control sediment was 83% in Set 1 to 95% in Set 2 (Table

6 of Ingersoll *et al.* 2008) and exceeded the test acceptability criterion (ASTM 2008a, USEPA 2000, Table 6 of Ingersoll *et al.* 2008). For the Set 3 sediment samples tested in 2006, mean 10-d survival of midges in the control sediment was 53% (n=6 TSMD samples; Table 6 of Ingersoll *et al.* 2008) which was less than the test acceptability criterion of 70% mean control survival (USEPA 2000, ASTM 2008a).

Before the start of the sediment toxicity tests conducted with the Set 1 and Set 2 samples evaluated in 2007, personnel at the USEPA laboratory in Duluth, Minnesota (MN) were contacted to discuss the poor control performance of the midge associated with the Set 3 samples (and in other studies conducted at the CERC laboratory). Two changes to the ASTM (2008a) and USEPA (2000) method were suggested for conducting 10-d sediment toxicity tests with *C. dilutus* to improve performance of midges in control sediment. The changes included: (1) starting toxicity tests with larvae less than 10-d old (to reduce the possibility of larvae emerging by the end of a 10-d sediment exposure) and (2) starting the exposures with larvae isolated from cultures still in their surrounding tubes rather than with larvae that have left (or have been removed from) their culture tubes (Dave Mount, USEPA, Duluth MN; personal communication). Larvae outside of their culture tubes may not be as healthy as larvae still inside their culture tubes. Once in the sediment exposures, larvae will typically rebuild their tubes with material in the beakers within 24 hours (Dave Mount, personal communication).

In 2007, the CERC laboratory implemented these two revisions to the ASTM (2008a) and USEPA (2000) method for conducting 10-d sediment toxicity tests with *C. dilutus* and improved control survival of midges was observed in the Set 1 and Set 2 sediments evaluated in 2007 and improved control survival has been observed in other subsequent midge sediment toxicity tests conducted at the CERC laboratory (>80% and typically >90% survival of midges in control sediment).

Mean 10-d ash-free-dry weight of midges in the control sediment was 1.51 mg/individual in Set 1, 1.33 mg/individual in Set 2, and 1.41 mg/individual in Set 3 (Table 6 of Ingersoll *et al.* 2008). Mean weight of midges in controls at Day 10 for

all three sets of sediment tests met the test acceptability criterion of 0.48 mg/individual [Table 6 of Ingersoll *et al.* (2008); ASTM 2008a, USEPA 2000]. Mean biomass of midges in control sediment at Day 10 ranged from 9.71 to 12.7 mg/treatment (Table 6 of Ingersoll *et al.* 2008). No guidance is provided in USEPA (2000) or in ASTM (2008a) regarding acceptable mean biomass of control organisms at Day 10. The DQOs were met for all of the sediments evaluated with midges in 2007; however, the 6 samples evaluated with midges in 2006 did not meet test acceptability requirements (as identified in Table A1.1 of the QAPP, Ingersoll 2007). Specifically, completeness was 92% (70 of the 76 sediment samples) in the sediment toxicity tests conducted with midges (the six Set 3 midge samples did not meet acceptability requirements based on poor control survival in this test; Table 6 of Ingersoll *et al.* 2008). An error was made in weighing two replicate chambers of midges at the end of the exposure to CERC-55 sediment (negative weight for these two replicates, Table A4 of Ingersoll *et al.* 2008), so these two replicates were not included in the calculation of the mean response of midges in Table A3. If more than 11 test organisms were recovered from a replicate, this replicate was not included in the calculation of the mean test organism response for that treatment in Table A3 (i.e., [CERC-4, replicate 3]; [CERC-25, replicate 4]; [CERC-27, replicate 2]; [CERC-41, replicate 2]; [CERC-S6, replicate 3]; [CERC-WB, Set 1, replicate 3]; and [CERC-WB, Set 3, replicate 4]; Table A4 of Ingersoll *et al.* 2008). Extra midge larvae in these treatments may have resulted from inadvertently transferring two midge larvae at a time with some of the individual tubes from the cultures.

Average ash-free-dry weight of midge larvae at the start of the tests was 0.08 mg/individual in Set 1, 0.31 mg/individual in Set 2, and 0.25 mg/individual in Set 3 (Table 6 of Ingersoll *et al.* 2008). This wide range may have resulted from only weighing two replicates of 10 organisms each at the start of the sediment exposures. The proportional increase in mean weight of midges at Day 10 in the control sediment ranged from 4.3 to 19X (which may reflect high variance in the two replicate weight measurements at the start of the exposures). The CERC laboratory is now measuring at least 4 replicates of 10 organisms each at the start of midge exposures, with lower variance observed in starting weight of midge larvae. Control survival of midges in

the 96-hour water only reference toxicant test conducted in conjunction with the first set of sediment samples was 85%, which is below the acceptability criterion of 90% [Table 6 of Ingersoll *et al.* (2008); ASTM 2008a, USEPA 2000). Even with the low control survival, the response of midges in the two water-only NaCl reference toxicant tests (LC50s) was 7.0 and 9.1 g/L, and is representative of historic reference toxicant tests for midges conducted at the CERC laboratory in ASTM hard water (ASTM 2008d; no reference toxicant tests were conducted with midges associated with the Set 3 samples).

Mussel toxicity tests: Mean 28-d survival of mussels in control sediment ranged from 88 to 100% across the three sets of sediment tests (Table 6 of Ingersoll *et al.* 2008). Mean survival of mussels in the control sediment exceeded a test acceptability criterion of 80% established for this study based the test acceptability criterion for water-only 28-d mussel toxicity tests (ASTM 2008b; Table 6 of Ingersoll *et al.* 2008). Mean shell length of mussels in control sediment on Day 28 was 2.56 mm/individual in Set 1, 3.18 mm/individual in Set 2, and 1.66 mm/individual in Set 3 with increases from Day 0 shell lengths ranging from 1.4 to 1.7X (Table 6 of Ingersoll *et al.* 2008). Mean weight of mussels in the control sediment at Day 28 ranged from 0.29 to 2.2 mg/individual and mean biomass of mussels in control sediment at Day 28 ranged from 2.5 to 21 mg/treatment (Table 6 of Ingersoll *et al.* 2008). The wide range in mean length, mean weight and mean biomass reflects the wide range in age and size of the mussels at the start of the exposures (Set 1: 3-months old, Set 2: about 4-months old, and Set 3: about 2 months old at the start of the exposures). No guidance is provided by ASTM (2008b) regarding acceptability of mussel growth in 28-d water-only or sediment exposures. The DQOs were met for all of the mussel toxicity tests (as identified in Table A1.1 of the QAPP, Ingersoll 2007) and specifically, completeness was 100% for the 48 sediment samples evaluated in sediment toxicity tests conducted with mussels (based on performance of mussels in control sediment; Table 6 of Ingersoll *et al.* 2008). The response of mussels in the two 96-hour water-only NaCl reference toxicant tests (LC50s) was 3.1 and 3.3 g/L (Table 6 of Ingersoll *et al.* 2008) and is representative of historic reference toxicant tests for juvenile mussels conducted at the CERC laboratory in ASTM hard water (ASTM 2008d; no

reference toxicant tests were conducted with mussels associated with the Set 3 samples).

Oligochaete sediment bioaccumulation tests: About 2 g of oligochaetes tissue was obtained from each replicate beaker at the end of the 28-d sediment exposures. No overt mortality or avoidance of sediment was observed in any of the sediment exposures. Appendix B of Ingersoll *et al.* (2008) provides a summary of the metal analyses of oligochaetes that were isolated from sediment on Day 28. Despite the 6-hour depuration period recommended by USEPA (2000) and by ASTM (2008c), some sediment was visible in some of the oligochaetes samples after digestion, which likely contributed to increased variability and greater than anticipated concentrations of some metals (additional discussion follows). The DQOs were met for all of the oligochaete sediment bioaccumulation tests (as identified in Table A1.1 of the QAPP, Ingersoll 2007) and specifically, completeness was 100% for the 21 sediment samples evaluated in sediment bioaccumulation tests conducted with oligochaetes. The response of oligochaetes in the two 96-hour water-only NaCl reference toxicant tests (LC50s) were 6.0 and 11 g/L (Table 6 of Ingersoll *et al.* 2008); however, the CERC laboratory does not have historic reference toxicant tests for oligochaetes, given that reference toxicant tests are not typically conducted for test organisms used in bioaccumulation exposures.

In summary, the response of amphipods, mussels, and oligochaetes in the sediment exposures for all three sets of samples met the DQOs identified in Table A1.1 of the QAPP (Ingersoll 2007). The response of the midges in the sediment exposures for the Set 1 and Set 2 samples also met the DQOs indentified in Table A1.1 of the QAPP (Ingersoll 2007). While the lower control survival of midges in the reference toxicant test conducted in conjunction with the Set 1 samples was 85%, this deviation should not compromise the subsequent use of the data for this set of samples. However, control survival of midges in the Set 3 samples (n=6) did not meet the DQOs identified in Table A1.1 of the QAPP, so these data should be used with caution.

B. Metals data for oligochaetes used in sediment bioaccumulation tests

The concentrations of metals in oligochaetes used in bioaccumulation testing are presented in Appendix B-1 of Ingersoll *et al.* (2008). A sample of each of the four oligochaete replicates was analyzed for nickel (Ni), copper (Cu), zinc (Zn), cadmium (Cd), and lead (Pb) using a quantitative method, and the first replicate sample for each treatment also was analyzed for a total of 52 elements using a semi-quantitative method. Only results for 14 of those 52 elements are reported, because concentrations of the remaining elements (excluding the 5 elements run by quantitative analysis) were at or less than the reporting limits for all samples. Individual recoveries of Ni, Cu, Zn, Cd, and Pb obtained from analysis of 3 replicates of each of two certified mussel reference tissues were between 100 and 114% of certified ranges, with the exception of one Cu result (132%). Recoveries of all 13 certified elements analyzed by semi-quantitative method were between 79 and 140% of certified ranges (Appendix B-2 of Ingersoll *et al.* 2008), indicating that the selected analytical methods provided acceptable levels of accuracy.

Six oligochaete samples were prepared in duplicate for analysis of Ni, Cu, Zn, Cd, and Pb by the quantitative method. The mean relative percent differences (RPDs) between the duplicates ranged from 12.3 to 18.4% for Ni, Cu, Zn, and Pb, which were within the target of $\pm 20\%$, but the mean RPD for Cd was 41.6% (Appendix B-3 of Ingersoll *et al.* 2008). Although the oligochaetes were depurated in clean water for 6 hours before sampling so as to allow them to eliminate ingested sediment particles (as is recommended by USEPA 2000 and by ASTM 2008c), sediment was still evident in most of the digested samples, and this probably contributed to greater than expected variability between duplicates. Aluminum, which is usually present at percent levels in sediments or soils, but only at a few parts per million in biological tissues, can be used to qualitatively indicate the presence sediment particles in the guts of the oligochaetes. In this study, the aluminum concentration in replicate-1 of the oligochaetes at the start of the exposures (not yet placed into sediments) was only 18 $\mu\text{g/g}$, whereas concentrations in oligochaetes following the sediment exposures ranged in the hundreds to thousands of $\mu\text{g/g}$ for all other samples analyzed (Appendix

B-1 of Ingersoll *et al.* 2008). Oligochaete tissues were assumed to be reasonably homogeneous, and therefore were not physically homogenized before sub-sampling for digestion. Coupled with the fact that only 0.05-g subsamples were used for each analysis, sediment particles (which could be enriched with metals relative to the oligochaete tissue) that were non-uniformly distributed in the tissues could account for the large differences measured between some of the duplicates for Cd and other elements.

Six oligochaete samples were spiked with Ni, Cu, Zn, Cd, and Pb before digestion and analysis by the quantitative method. Mean recoveries of these spikes ranged from 97.3% (Cu) to 102.5% (Zn); only one individual result (for Zn) exceeded the target recovery of $100 \pm 20\%$ (Appendix B-4 of Ingersoll *et al.* 2008). Overall, recoveries of pre-digestion spikes were considered acceptable. Blank equivalent concentrations and method detection limits for the 3 sample preparation sets are presented in Appendix B-5. Mean blank equivalent concentrations were less than the corresponding method detection limits for all but 1 instance each for Cu ($0.08 \mu\text{g/g}$), Pb ($0.05 \mu\text{g/g}$), and Zn ($0.38 \mu\text{g/g}$); however, each of those values was many-fold less than the corresponding concentrations of all oligochaete samples except for Pb in 2 of the 4 replicates of oligochaetes at the start of the exposures (Appendix B-1 of Ingersoll *et al.* 2008). Therefore, laboratory-induced contamination was not considered to be a significant source of error in the measurement of metals in any of the oligochaete samples.

C. Water quality data for centrifuged pore water

Results of selected water quality parameters in filtered samples of centrifuged pore water are presented in Appendix C of Ingersoll *et al.* (2008). These measurements were performed by USGS contractors who conducted internal quality control checks during the analyses, but did not provide summaries of those results. Consequently, only results for 8 “field” duplicates and 2 filtration blanks (Appendix C-2 of Ingersoll *et al.* 2008) are discussed herein. For DOC, relative percent differences (RPDs) between duplicates averaged 10.4%. The RPDs for sulfide averaged 85%, but all

duplicate sample results were near method detection limits, so variation this large was not unusual. For anions, mean RPDs ranged from 7.0% (chloride) to 20.9% (sulfate); however, the mean RPD for sulfate was affected by one result for sample duplicates of pore water isolated from the control sediment (WB-1 and WB-2). Excluding aluminum (78%) and iron (77.7%), the mean RPDs for major cations ranged from 1.8% (sodium) to 13.6% (manganese). In many of the duplicate samples, aluminum and iron concentrations were near detection limits, which probably was a reason why the mean variation was large for those elements. In addition, iron was probably present as ferrous ion in most of the digested samples, which might have been partly lost in some samples as a result of oxidation and precipitation during sample processing. Overall, the variation between duplicate samples was not considered unusual for these measurements.

D. Simultaneously extracted metals and acid-volatile sulfide data

Concentrations of acid-volatile sulfide and simultaneously extracted metals (1N HCl) in sediments are presented in Appendix D-1 (Sets 1 and 2, collected in 2007, Ingersoll *et al.* 2008) and in Appendix D-1A (Set 3, collected in August 2006, Ingersoll *et al.* 2008). A single subsample, obtained at the start of toxicity testing, was analyzed for each of the 2006 sediments. For 2007 sediments, subsamples were obtained for analysis from simulated toxicity test beakers on Day 7 and Day 28 of the tests (from additional replicate chemistry beakers containing amphipods that were fed during the exposures). Calculations of the difference between SEM and AVS, and the difference divided by the fraction of organic carbon (USEPA 2005) are presented for each of the two samples individually, and for the mean of the two (Appendix D-1 and Appendix D-1A of Ingersoll *et al.* 2008). Results for 1N HCl extractable elements and AVS obtained from NIST 1645 river sediment are presented in Appendix D-2 of Ingersoll *et al.* (2008). Results are shown in chart form, and include CERC historical results because reference sediments having certified concentrations of AVS or extractable metals do not exist. Results obtained during analyses of TSMD sediments are indicated by open symbols, all which fell within the usual range for each respective analyte (Appendix D-2 of Ingersoll *et al.* 2008). Compared to the certified total metal

concentrations, the percentage of each metal recovered by the 1N HCl procedure was about 40% for Ni, 50% for Cu, 78% for Zn, 66% for Cd, and 72% for Pb. Duplicate preparations of eight 2007 sediment samples produced mean relative percent differences (RPDs) of 9.6% for AVS (Appendix D-3 of Ingersoll *et al.* 2008) and between 2.6% and 15.8% for simultaneously extracted metals (Appendix D-4 of Ingersoll *et al.* 2008). Similarly, RPDs were between 4.6% and 18% for duplicate preparation of a 2006 sample (Appendix D-8 of Ingersoll *et al.* 2008). The mean recovery of AVS for pre-extraction blank spikes (as sodium sulfide) was 96% (Appendix D-5 of Ingersoll *et al.* 2008), and was between 99% and 111% for metals (Appendix D-6 of Ingersoll *et al.* 2008). Recoveries of pre-extraction spikes prepared with the 2006 samples were between 93% and 107% (Appendix D-9 of Ingersoll *et al.* 2008). Blank equivalent concentrations (BECs), method detection limits (MDLs), and method quantitation limits (MQLs) are presented in Appendix D-7 and in Appendix D-10 of Ingersoll *et al.* (2008). There were some instances in which BECs were greater than the corresponding MDLs, particularly for Cd, Zn, and Pb in the first sample set prepared on August 7, 2007. Consequently, all of the samples prepared in the first set were re-prepared on December 4, 2007 and re-analyzed for those 3 elements (12/04/07 BECs; Appendix D-7 of Ingersoll *et al.* 2008). All of the results from the re-analysis were in close agreement with those obtained from the first preparation and analysis (data not shown), indicating that the metal levels detected in the first blank were largely absent during subsequent preparations. Based on results from the re-preparation of the first set combined with the other preparation sets, none of the BECs were significant compared to the sample concentrations. Overall, QC results indicated acceptable precision and accuracy for these measurements and generally met targeted values.

E. Metals data for pore water sampled by peepers

Results for metals in peeper samples are indicated in Appendices E-1 (quantitative analyses of Ingersoll *et al.* 2008) and E-2 (semi-quantitative analyses of Ingersoll *et al.* 2008). Recoveries of various elements from reference water solutions analyzed with peeper samples are indicated in Appendix E-3 of Ingersoll *et al.* (2008).

Recoveries of Ni, Cu, Zn, Cd, and Pb ranged from 88 to 102% using the quantitative analysis mode and, with the exception of potassium (158%), ranged from 79 to 125% for 26 elements determined in the semi-quantitative mode. Duplicate analyses of selected diluted and spiked peeper samples using the quantitative analysis mode for Ni, Cu, Zn, Cd, and Pb produced relative percent differences ranging from 0.0 to 2.7%, and averaged less than 1% for Ni, Cu, Zn, Cd, and Pb (Appendix E-4 of Ingersoll *et al.* 2008). Recoveries of analysis spikes added to 12 different peeper solutions ranged from 96.4% to 106.4% for Ni, Cu, Zn, Cd, and Pb (Appendix E-5 of Ingersoll *et al.* 2008). Blank equivalent concentrations for peepers were at or below method detection limits in most instances except for Zn, which ranged from 8 to 22 µg/L in the first set of peeper samples (Set 1 samples; Appendix E-6 of Ingersoll *et al.* 2008). Overall, QC results indicated acceptable precision and accuracy for peeper measurements.

F. Grain size, total organic carbon (TOC), and total solids data

G. Polycyclic aromatic hydrocarbon (PAH) data and Semi-Volatile Organic Compounds (SVOC) in whole sediment

Results for analyses of grain size, TOC, and water, are presented in Appendix F of Ingersoll *et al.* (2008). Results for PAH and SVOC analyses are presented in Appendix G of Ingersoll *et al.* (2008). Data quality review of these data by USEPA Region 6 is provided in Appendix L of Ingersoll *et al.* (2008). Based on the USEPA Region 6 Laboratory's review, the overall quality of the analytical data was found to satisfy the QC requirements established by the analytical methods and the USEPA Region 6 Laboratory (Appendix L of Ingersoll *et al.* 2008). Concentrations of hexachlorocyclopentadiene was not recovered in one laboratory control sample and well below acceptance criteria in spiked samples which resulted in the rejection of the hexachlorocyclopentadiene results for six samples (indicated by the letter "R" in Appendix G of Ingersoll *et al.* 2008). No TOC results were rejected; however, multiple recovery failures resulted in several TOC results being qualified as estimated. A total of 73 of the TOC samples were analyzed outside holding time with

some analyzed as late as six months past the holding time expiration. Quality control issues were encountered with grain size determinations for nine sediment samples. More specifically, clay or silt settled out with the sand which resulted in underestimating the fine fractions and overestimating the sand fraction. This resulted in negative results for clay in some instances. In the SLERA, these data will be adjusted by setting negative values to 0 and apportioning the amount of the negative value to the other grain-size fractions.

H. Organochlorine pesticides and polychlorinated biphenyl data

I. Total recoverable metals data in whole sediment

Results for analyses of pesticides and PCBs are presented in Appendix H of Ingersoll *et al.* (2008). Results for analyses of total recoverable metals are presented in Appendix I-1 of Ingersoll *et al.* (2008; <2-mm sediment samples) and in Appendix I-2 of Ingersoll *et al.* (2008; <0.25-mm sediment samples). Data quality review of these data by USEPA Region 7 is provided in Appendix M of Ingersoll *et al.* (2008). Based on the USEPA Region 7 Laboratory's review, the overall quality of the analytical data was found to satisfy the QC requirements established by the analytical methods and the USEPA Region 7 Laboratory. All of the pesticide and PCB samples were analyzed after the required holding time and all results were qualified in Appendix M of Ingersoll *et al.* (2008). All analytical results, with the exception of 14 rejected results for barium (indicated by the letter "R") and the poor precision of mercury in samples CERC-42 and -42_9 (values followed by the letter "J") may be used to support project decisions.

J. Comparison of sampling methods (shovel versus scoop)

Results from comparisons between shovel and scoop sampling performed at 3 locations are presented in Appendix J-1 (grain size comparison, see Ingersoll *et al.* 2008) and in Appendix J-2 (metal concentrations in equipment rinses, see Ingersoll *et al.* 2008). No QC results are presently included with these data because the analyses were performed by USEPA (grain size) or a contract laboratory (metals in

equipment rinseates). Based on these data, there were minimal and insignificant differences between the two sampling methods with respect to grain size sampled or to metals contamination from use of a shovel to collect some of the Set 1 sediment samples (iron and sodium were slightly elevated in samples collected with a shovel compared to samples collected with the PVC sediment scoop; Appendix J-2 of Ingersoll *et al.* 2008).

K. Comparison of methods for metals in pore water (peepers versus centrifugation)

Six samples of centrifuged pore water isolated on Day -7 (before the start of the exposures) were subsampled for ICPMS analyses so that comparisons could be made to peeper samples isolated on Day 7 of the exposures which were also measured by ICPMS. In addition, all of the centrifuged pore-water samples were analyzed for “major cations and metals” using ICPAES (which has marginal sensitivity for some of the metals of interest), but never-the-less, these six samples could also be used to compare analysis methods directly. Results for Cu, Ni, Zn, Cd, and Pb obtained by the ICPMS and ICPAES methods are compared in Appendix K-1 of Ingersoll *et al.* (2008). Trace metal results obtained by the ICP-AES method for all centrifuged pore-water samples are indicated in Appendix K-2 of Ingersoll *et al.* (2008). Also included in Appendix K-1 of Ingersoll *et al.* (2008) are pore-water results for 12 sediments in which pore-water Zn concentrations were $>500 \mu\text{g/L}$, obtained either by ICPAES for centrifuged pore waters prepared 7 days before the addition of test animals to sediment samples (Day -7), or by ICPMS for peepers retrieved 7 days after the addition of test organisms (Day 7). Results from these 12 samples were selected for comparing pore-water preparation methods because the Zn concentrations were well above the method quantitation limit for ICPAES, thereby avoiding large analytical variability which is expected at concentrations near the detection limit. For comparison of the first six samples, there was close agreement between ICPMS and ICPAES results (considering that many of the results were near detection limits for the ICPAES method), except for Zn in sample CERC-35 ($148 \mu\text{g/L}$ versus $65 \mu\text{g/L}$). Concentrations obtained by peeper sampling on Day 7 of the test tended to be lower than those obtained by centrifugation (on Day -7), except for Zn in samples CERC-

53, -67, and -69. A similar trend, in which most peeper samples had lower concentrations, was apparent for the 12 additional samples which contained high concentrations of Zn. Lower concentrations obtained by peeper sampling was not unexpected because dissolved metals are prone to partial losses over time caused by co-precipitation with iron as pore waters become more oxidic, or by diffusion into overlying water which is periodically renewed during toxicity testing. Moreover, centrifugation may result in the release of insoluble metals from sediment particles compared to the measurement of dissolved metal concentrations in the peeper samples. Overall, the agreement between sampling and analysis methods was quite reasonable, indicating that sampling and analysis precision was acceptable.

References Cited

American Society for Testing and Materials International (ASTM) 2008a. Standard test method for measuring the toxicity of sediment-associated contaminants with freshwater invertebrates (ASTM E1706-05). Annual Book of ASTM Standards Volume 11.06, West Conshohocken, PA.

ASTM. 2008b. Standard guide for conducting laboratory toxicity tests with freshwater mussels (ASTM E2455-06). Annual Book of ASTM Standards Volume 11.06. West Conshohocken, PA.

ASTM 2008c. Standard guide for determination of the bioaccumulation of sediment-associated contaminants by benthic invertebrates (ASTM E1688-00a). Annual Book of ASTM Standards Volume 11.06, West Conshohocken, PA.

ASTM. 2008d. Standard guide for conducting acute toxicity tests on test materials with fishes, macroinvertebrates, and amphibians. (ASTM E729-96 (2002)). Annual Book of ASTM Standards Volume 11.06. West Conshohocken, PA.

Ingersoll CG. 2007. Quality assurance project plan (QAPP) for the sediment toxicity testing associated with implementation of the Spring River/Tar Creek Watershed Management Framework, Phase I, Interagency Agreement #DW 14-95225601-1.

Prepared for John Meyer and Mark Doolan, USEPA, Kansas City, MO and Dallas, TX and Jim Dwyer, USFWS, Columbia, MO. Prepared by the USGS, Columbia, MO, July 3, 2007.

Ingersoll, C.G., D.D. MacDonald, J.M. Besser, W.G. Brumbaugh, C.D. Ivey, N.E. Kemble, J.L. Kunz, T.W. May, N. Wang, and D. Smorong. 2008. Sediment chemistry, toxicity, and bioaccumulation data report for the US Environmental Protection Agency - Department of the Interior sampling of metal-contaminated sediment in the Tri-state Mining District in Missouri, Oklahoma, and Kansas. Report prepared by MacDonald Environmental Sciences Ltd and USGS Columbia Missouri for USEPA, Kansas City, Missouri and Dallas, Texas and for USFWS, Columbia, Missouri.

USEPA. 2005. Procedures for the derivation of equilibrium partitioning sediment benchmarks (ESBs) for the protection of benthic organisms: Metal mixtures (cadmium, copper, lead, nickel, silver, and zinc). EPA-600-R-02-11, Office of Research and Development, Washington DC.

Wang N, Ingersoll CG, Greer IE, Hardesty DK, Ivey CD, Kunz JL, Brumbaugh WG, Dwyer FJ, Roberts AD, Augspurger T, Kane CM, Neves RJ, Barnhart MC. 2007. Chronic toxicity of copper and ammonia to juvenile freshwater mussels (Unionidae).

Appendix 4

Figure A4-1. Scatter plot showing the relationship between sediment metal concentrations (mean PEC- Q_{METALS}) and pore-water metal concentrations ($\Sigma\text{PW-TU}_{\text{DIVALENT METALS}}$), showing samples that were designated as toxic or not toxic based on the survival of amphipods (*Hyaella azteca*) in 28-d exposures to sediment samples from the Tri-State Mining District.

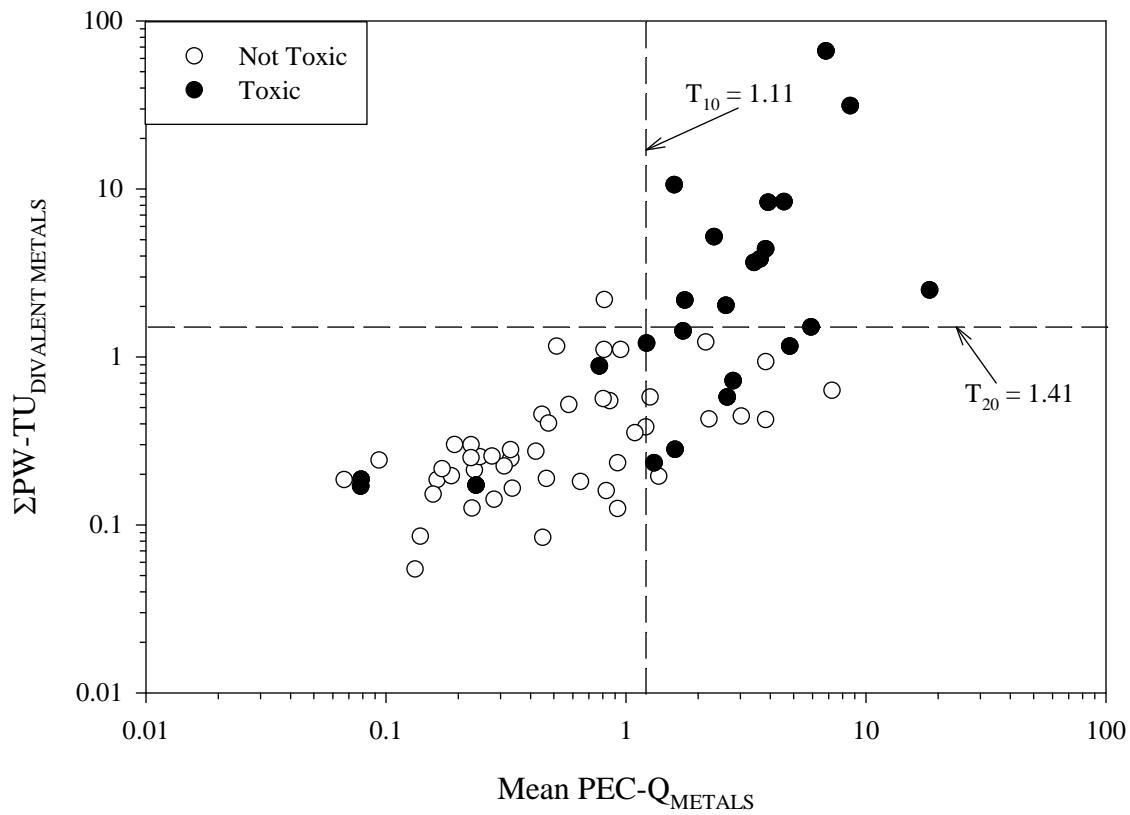
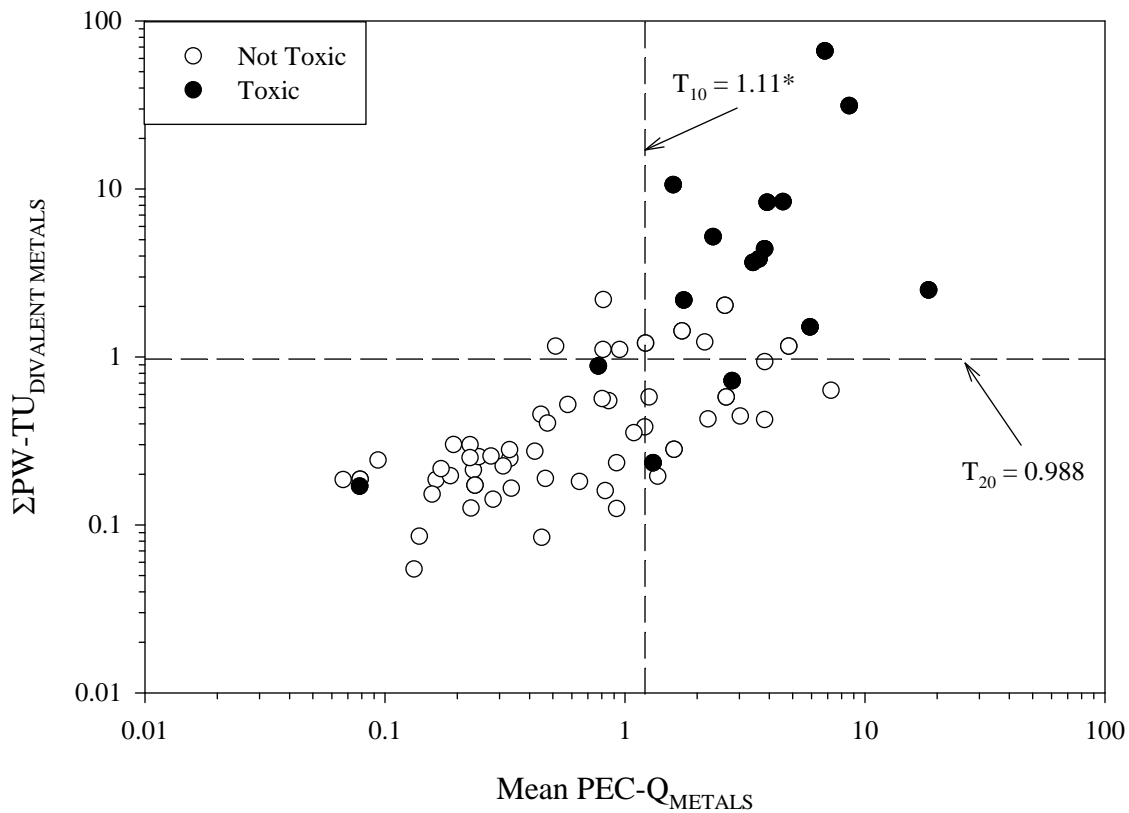


Figure A4-2. Scatter plot showing the relationship between sediment metal concentrations (mean PEC-Q_{METALS}) and pore-water metal concentrations (Σ PW-TU_{DIVALENT METALS}), showing samples that were designated as toxic or not toxic based on the biomass of amphipods (*Hyaella azteca*) in 28-d exposures to sediment samples from the Tri-State Mining District.



*Toxicity threshold was derived using 28-d *H. azteca* toxicity test results (Endpoint: Survival).

Figure A4-3. Scatter plot showing the relationship between sediment metal concentrations (mean $PEC-Q_{METALS}$) and pore-water metal concentrations ($\Sigma PW-TU_{DIVALENT METALS}$), showing samples that were designated as toxic or not toxic based on the survival of mussels (*Lampsilis siliquoidea*) in 28-d exposures to sediment samples from the Tri-State Mining District.

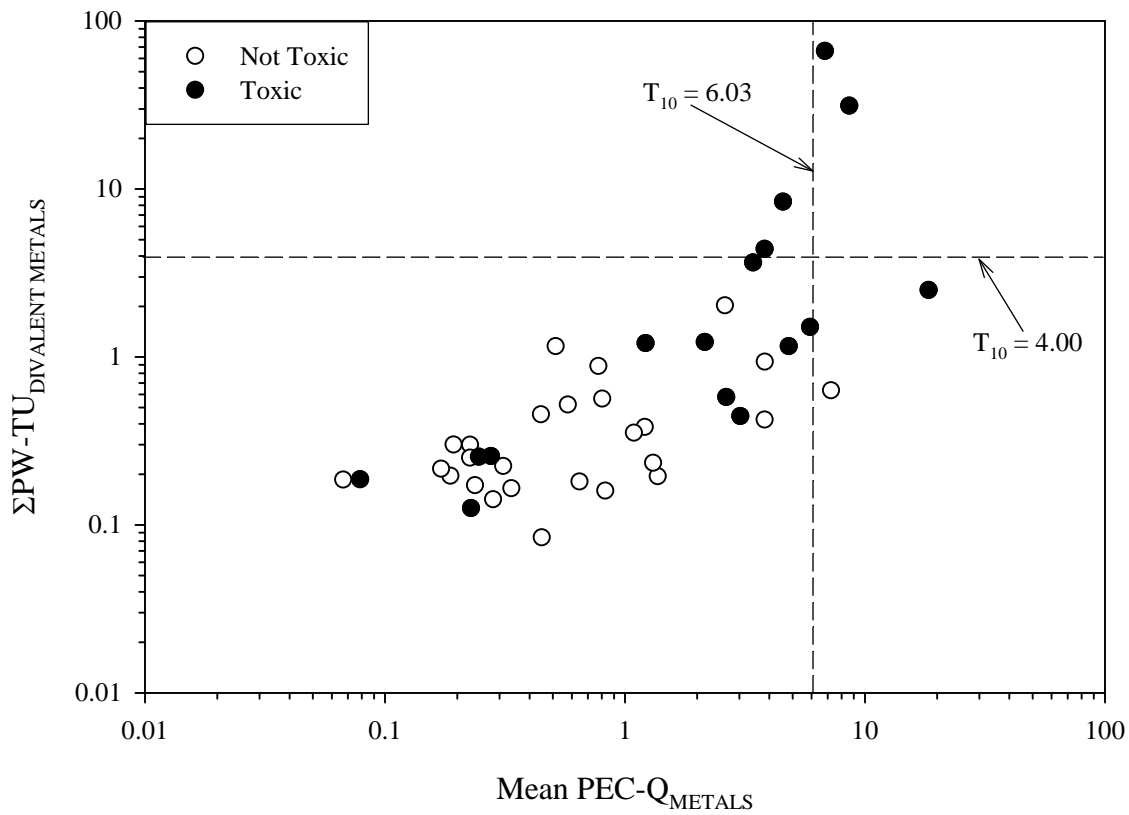


Figure A4-4. Scatter plot showing the relationship between sediment metal concentrations (mean PEC-Q_{METALS}) and pore-water metal concentrations (Σ PW-TU_{DIVALENT METALS}), showing samples that were designated as toxic or not toxic based on the biomass of mussels (*Lampsilis siliquoidea*) in 28-d exposures to sediment samples from the Tri-State Mining District.

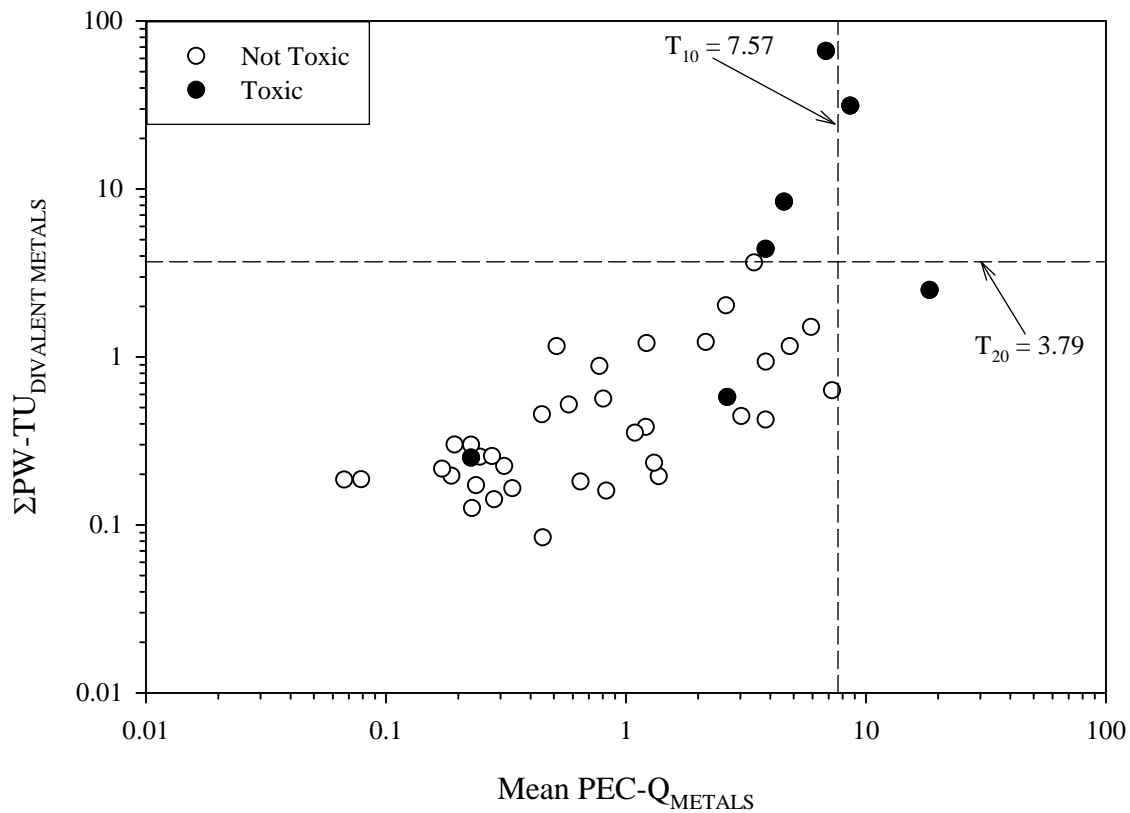
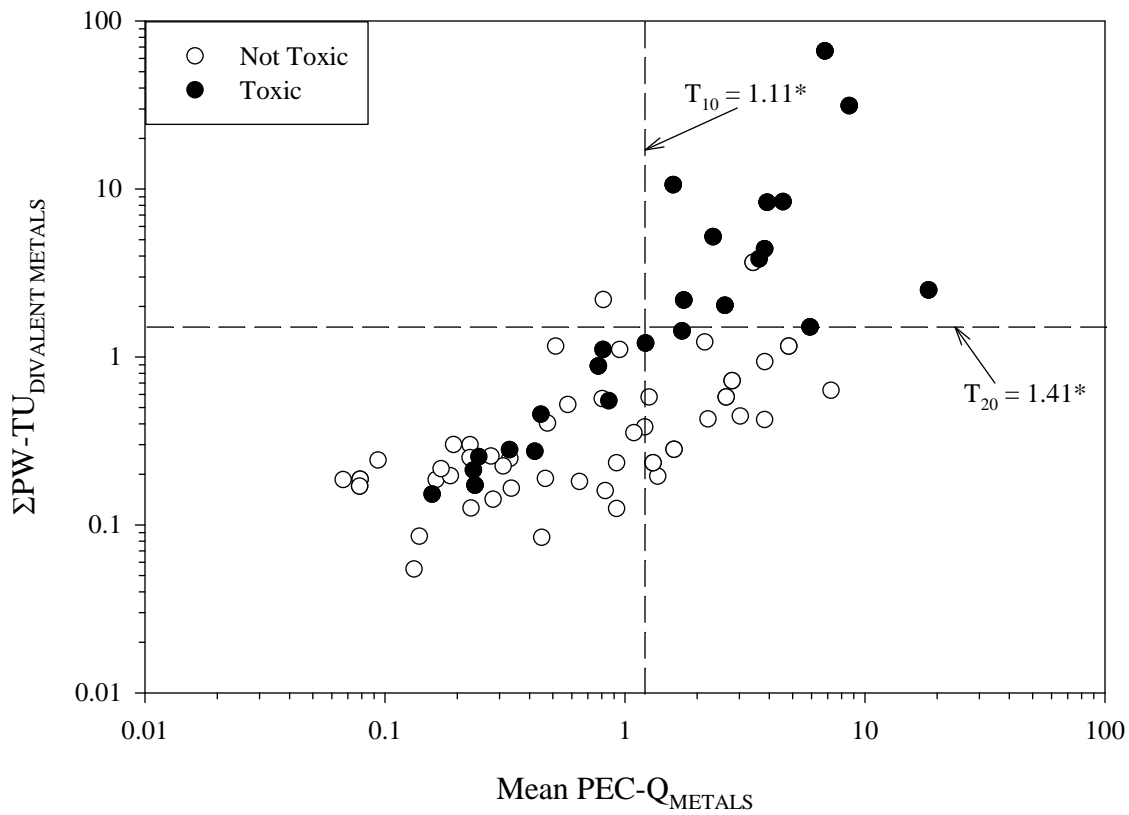
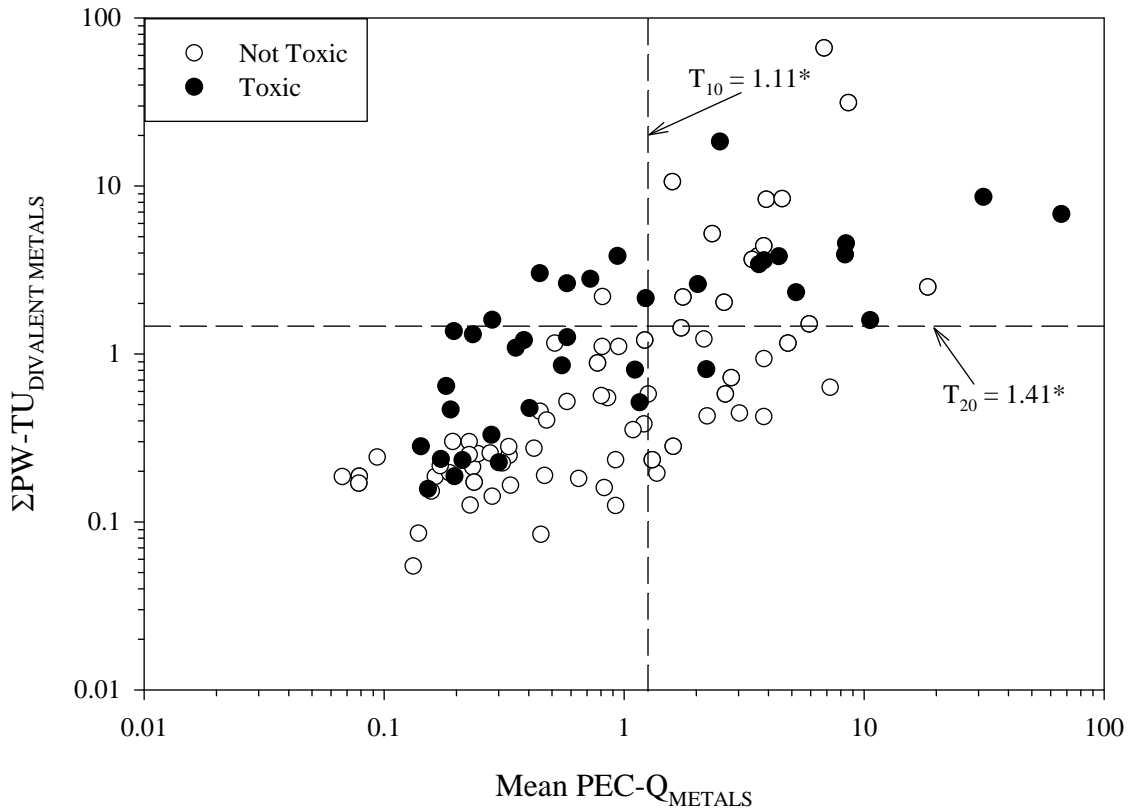


Figure A4-5. Scatter plot showing the relationship between sediment metal concentrations (mean PEC-Q_{METALS}) and pore-water metal concentrations (Σ PW-TU_{DIVALENT METALS}), showing samples that were designated as toxic or not toxic based on the survival of midges (*Chironomus dilutus*) in 10-d exposures to sediment samples from the Tri-State Mining District.



*Toxicity threshold was derived using 28-d *H. azteca* toxicity test results (Endpoint: Survival).

Figure A4-6. Scatter plot showing the relationship between sediment metal concentrations (mean PEC-Q_{METALS}) and pore-water metal concentrations (Σ PW-TU_{DIVALENT METALS}), showing samples that were designated as toxic or not toxic based on the biomass of midges (*Chironomus dilutus*) in 10-d exposures to sediment samples from the Tri-State Mining District.



*Toxicity threshold was derived using 28-d *H. azteca* toxicity test results (Endpoint: Survival).

Figure A4-7. Scatter plot showing the relationship between pore-water lead concentrations ($PW-TU_{LEAD}$) and pore-water zinc concentrations ($PW-TU_{ZINC}$), showing samples that were designated as toxic or not toxic based on the survival of amphipods (*Hyaella azteca*) in 28-d exposures to sediment samples from the Tri-State Mining District.

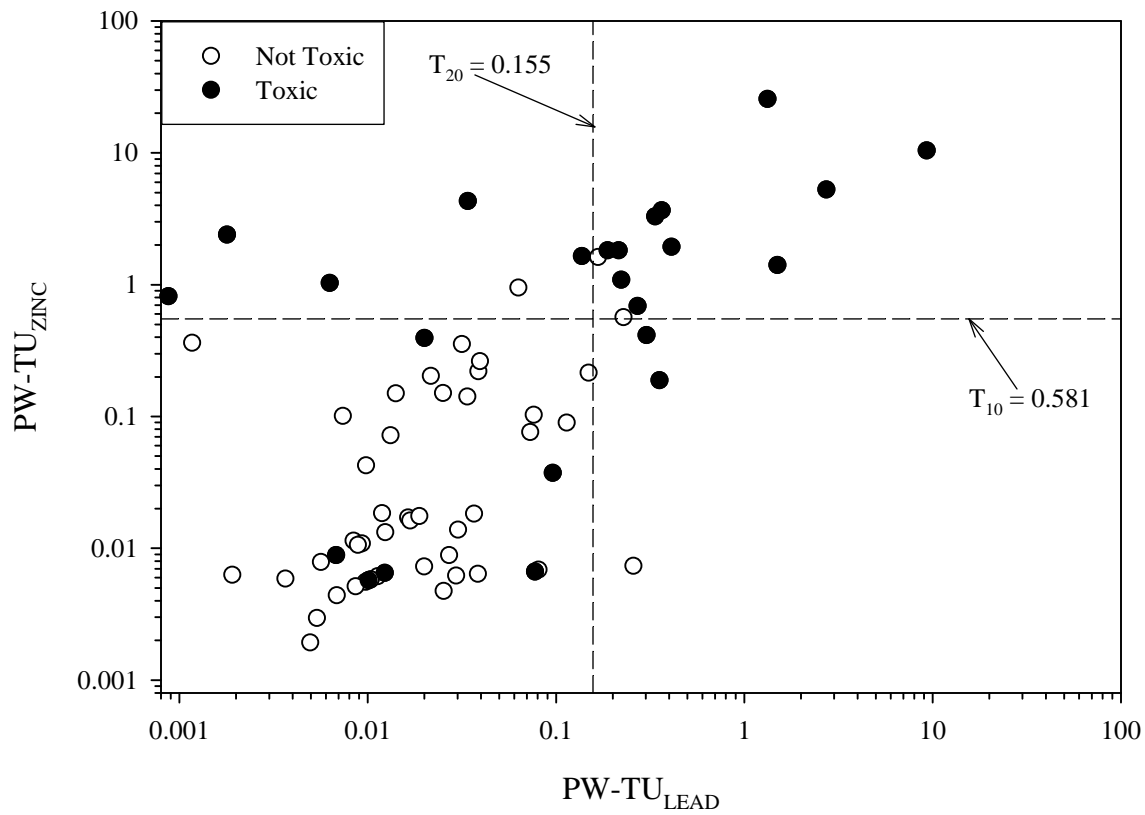


Figure A4-8. Scatter plot showing the relationship between pore-water lead concentrations ($PW-TU_{LEAD}$) and pore-water zinc concentrations ($PW-TU_{ZINC}$), showing samples that were designated as toxic or not toxic based on the biomass of amphipods (*Hyaella azteca*) in 28-d exposures to sediment samples from the Tri-State Mining District.

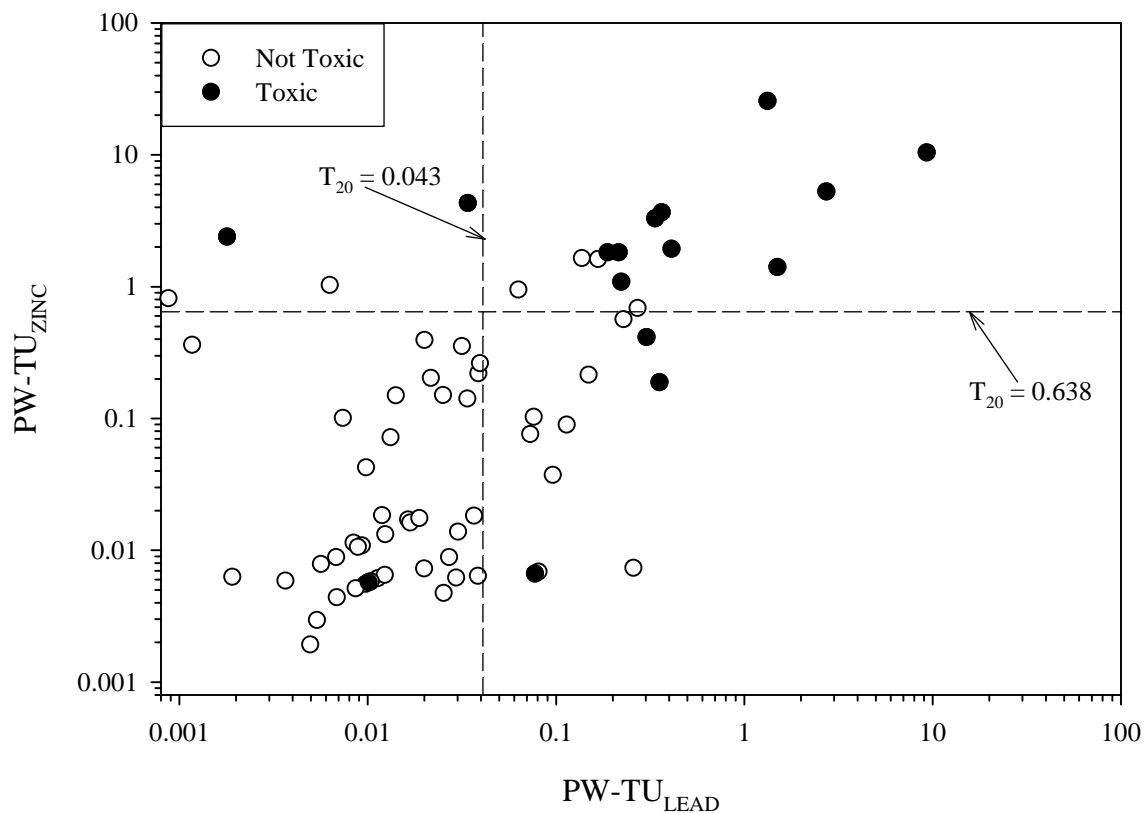


Figure A4-10. Scatter plot showing the relationship between pore-water lead concentrations ($PW-TU_{LEAD}$) and pore-water zinc concentrations ($PW-TU_{ZINC}$), showing samples that were designated as toxic or not toxic based on the biomass of mussels (*Lampsilis siliquoidea*) in 28-d exposures to sediment samples from the Tri-State Mining District.

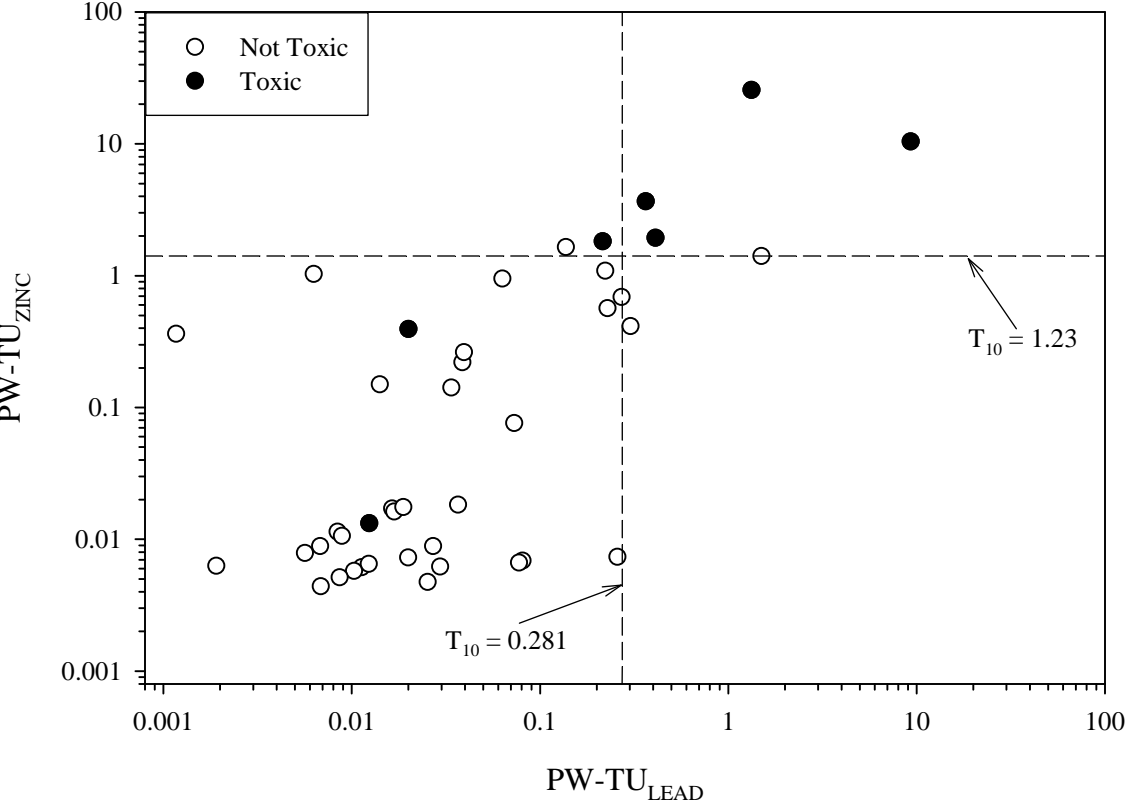
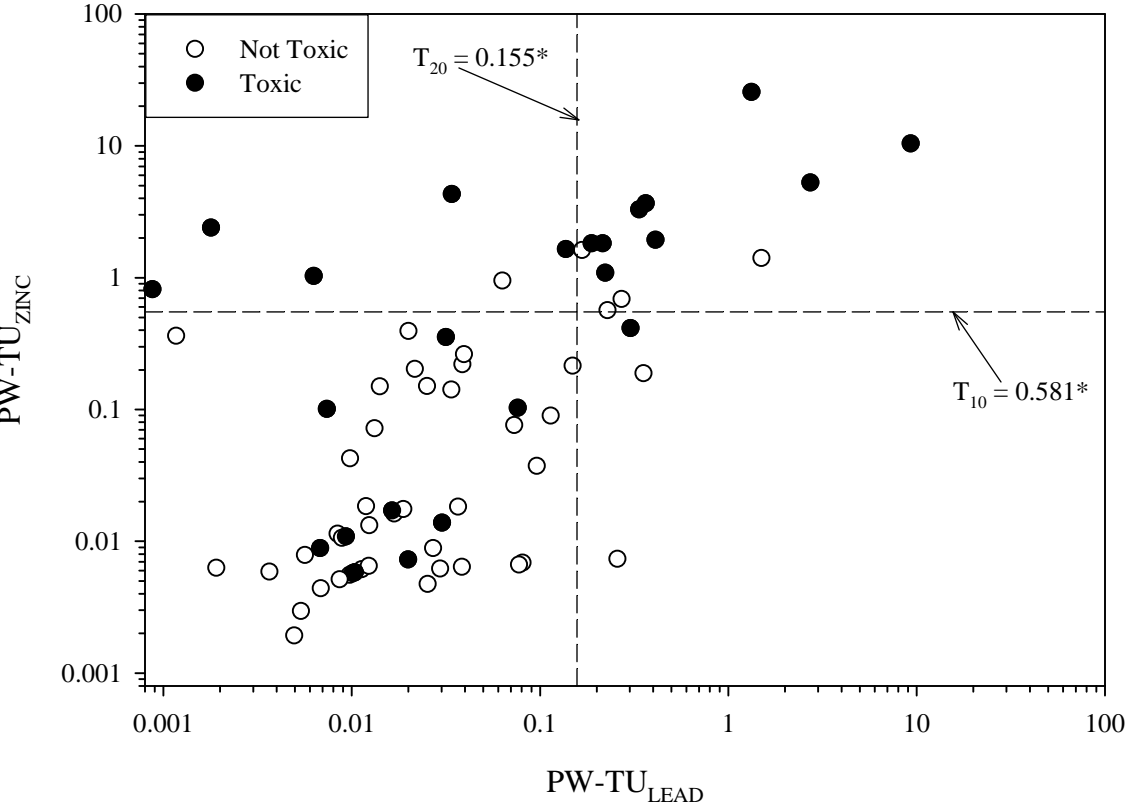
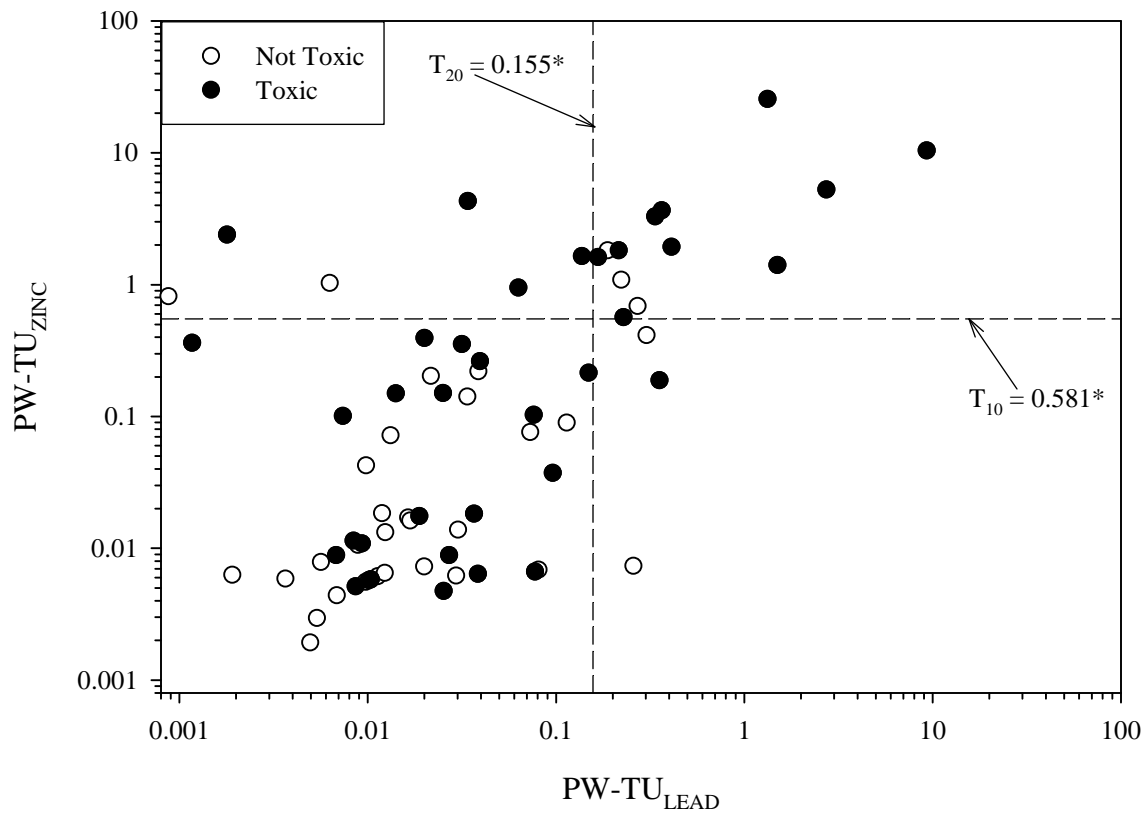


Figure A4-11. Scatter plot showing the relationship between pore-water lead concentrations (PW-TU_{LEAD}) and pore-water zinc concentrations (PW-TU_{ZINC}), showing samples that were designated as toxic or not toxic based on the survival of midges (*Chironomus dilutus*) in 10-d exposures to sediment samples from the Tri-State Mining District.



*Toxicity threshold was derived using 28-d *H. azteca* toxicity test results (Endpoint: Survival).

Figure A4-12. Scatter plot showing the relationship between pore-water lead concentrations ($PW-TU_{LEAD}$) and pore-water zinc concentrations ($PW-TU_{ZINC}$), showing samples that were designated as toxic or not toxic based on the biomass of midges (*Chironomus dilutus*) in 10-d exposures to sediment samples from the Tri-State Mining District.



*Toxicity threshold was derived using 28-d *H. azteca* toxicity test results (Endpoint: Survival).

Figure A4-13. Scatter plot showing the relationship between pore-water zinc concentrations normalized to dissolved organic carbon ($PW-TU_{ZINC(DOC)}$) and pore-water zinc concentrations ($PW-TU_{ZINC}$), showing samples that were designated as toxic or not toxic based on the survival of amphipods (*Hyaella azteca*) in 28-d exposures to sediment samples from the Tri-State Mining District.

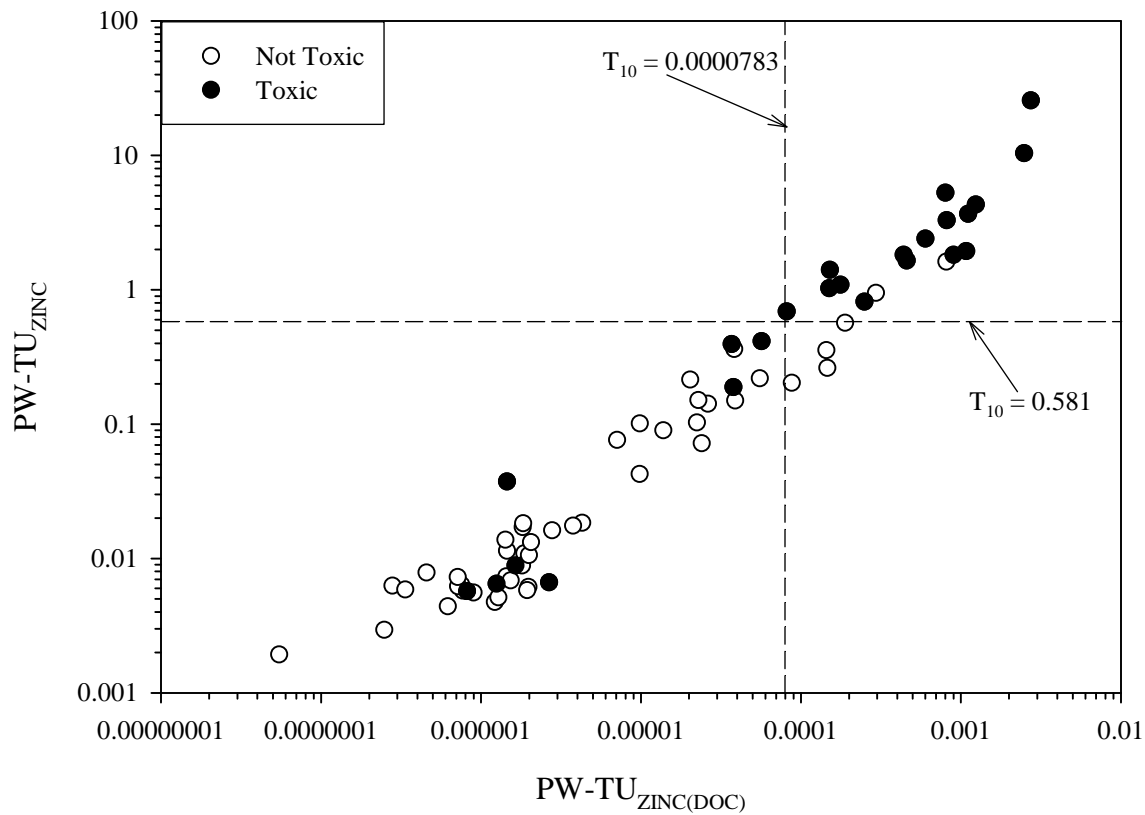


Figure A4-14. Scatter plot showing the relationship between pore-water zinc concentrations normalized to dissolved organic carbon ($PW-TU_{ZINC(DOC)}$) and pore-water zinc concentrations ($PW-TU_{ZINC}$), showing samples that were designated as toxic or not toxic based on the biomass of amphipods (*Hyaella azteca*) in 28-d exposures to sediment samples from the Tri-State Mining District.

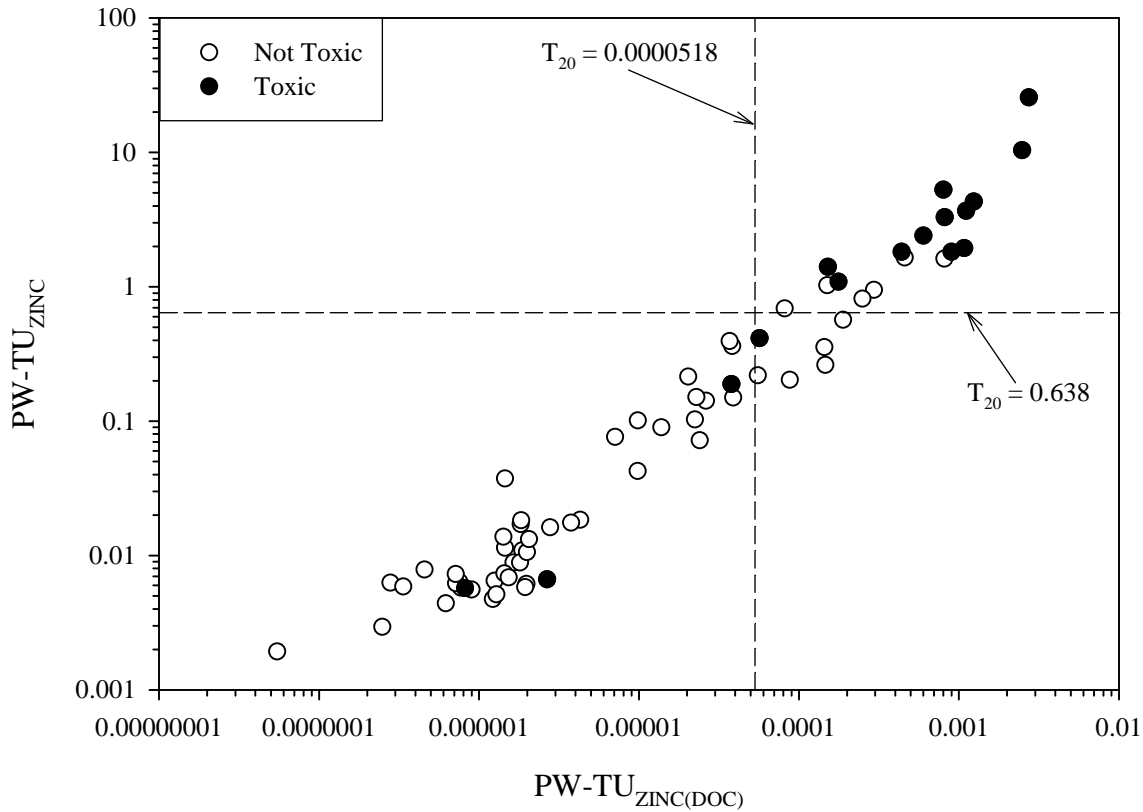


Figure A4-15. Scatter plot showing the relationship between pore-water zinc concentrations normalized to dissolved organic carbon ($PW-TU_{ZINC(DOC)}$) and pore-water zinc concentrations ($PW-TU_{ZINC}$), showing samples that were designated as toxic or not toxic based on the survival of mussels (*Lampsilis siliquoidea*) in 28-d exposures to sediment samples from the Tri-State Mining District.

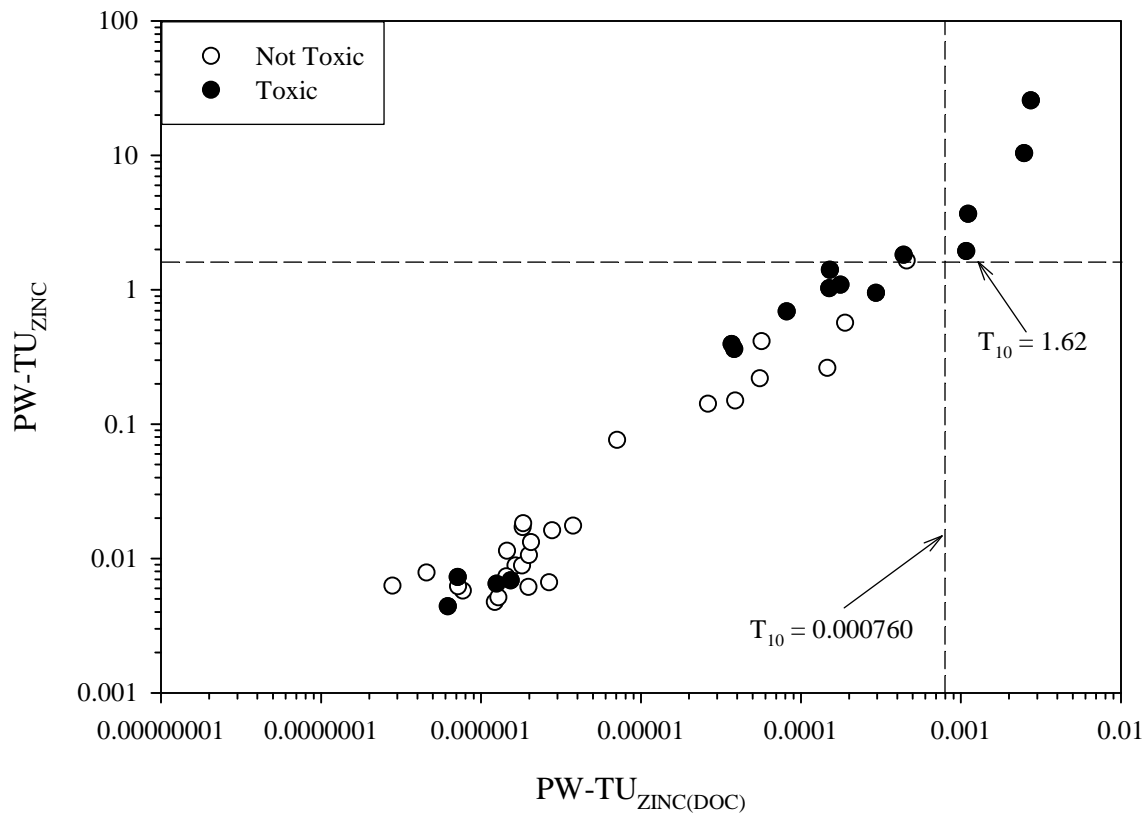


Figure A4-16. Scatter plot showing the relationship between pore-water zinc concentrations normalized to dissolved organic carbon ($PW-TU_{ZINC(DOC)}$) and pore-water zinc concentrations ($PW-TU_{ZINC}$), showing samples that were designated as toxic or not toxic based on the biomass of mussels (*Lampsilis siliquoidea*) in 28-d exposures to sediment samples from the Tri-State Mining District.

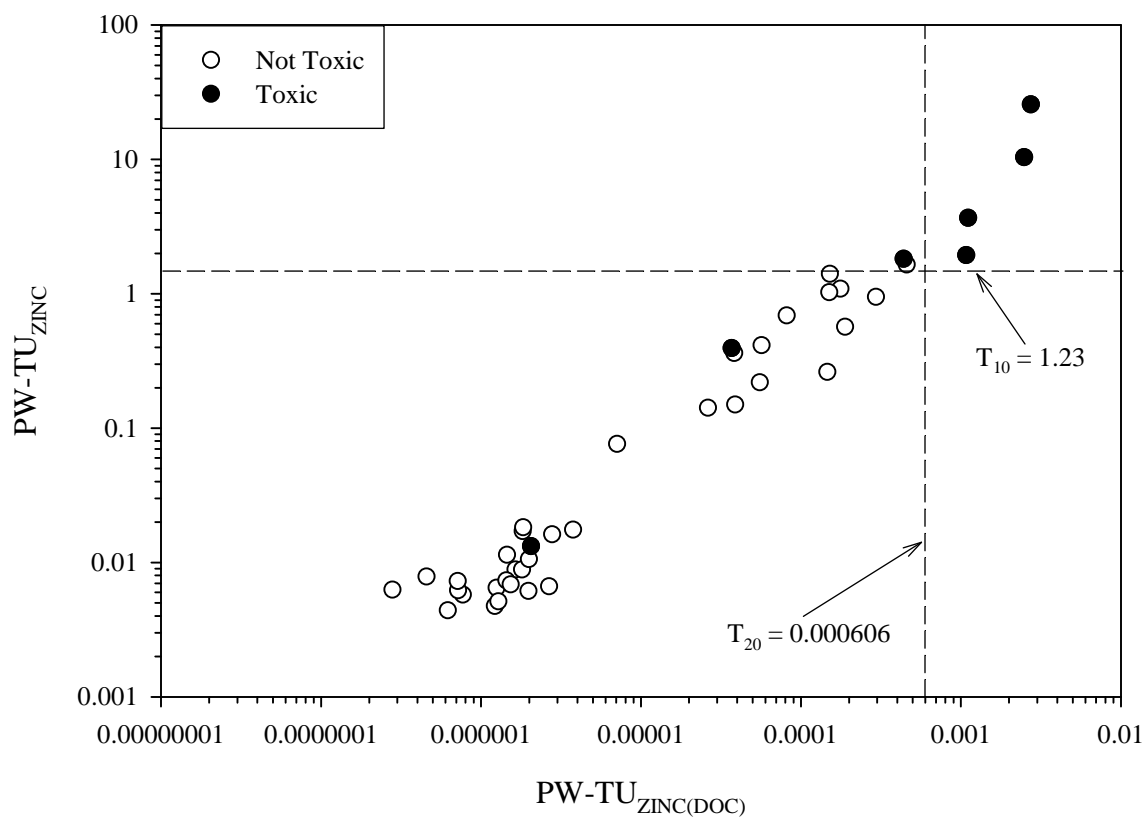
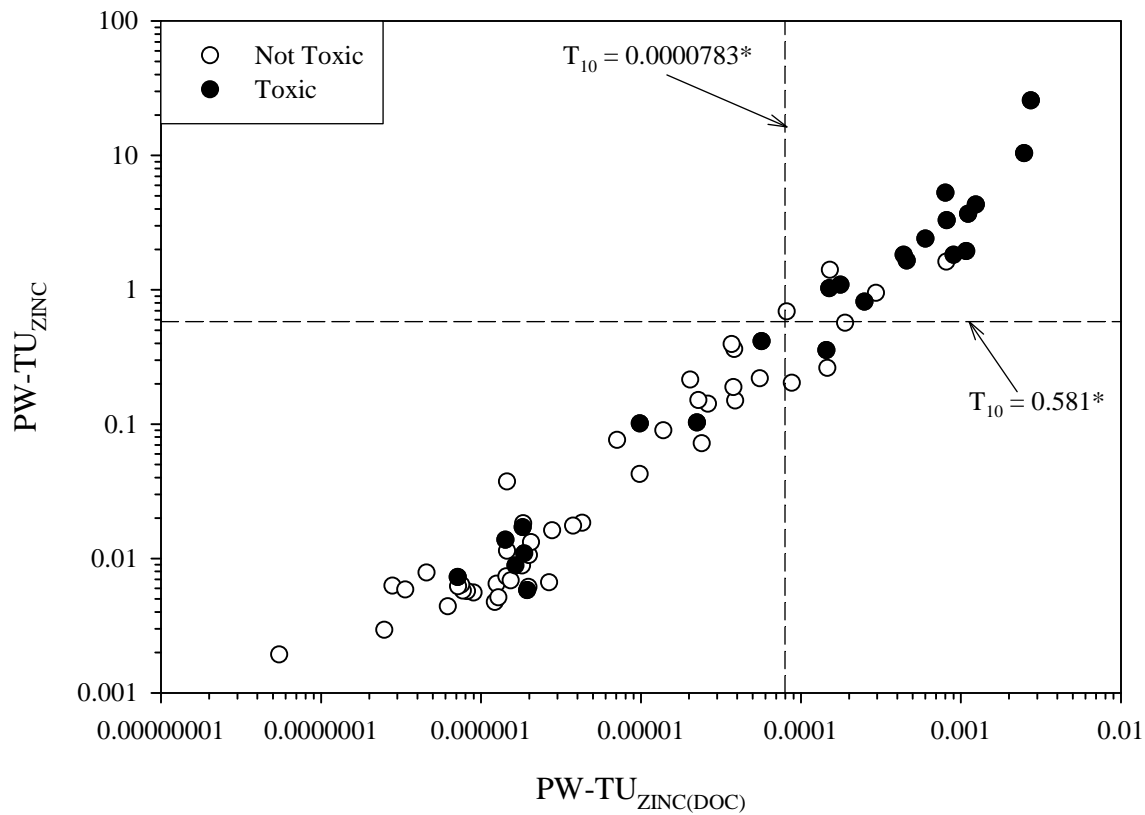
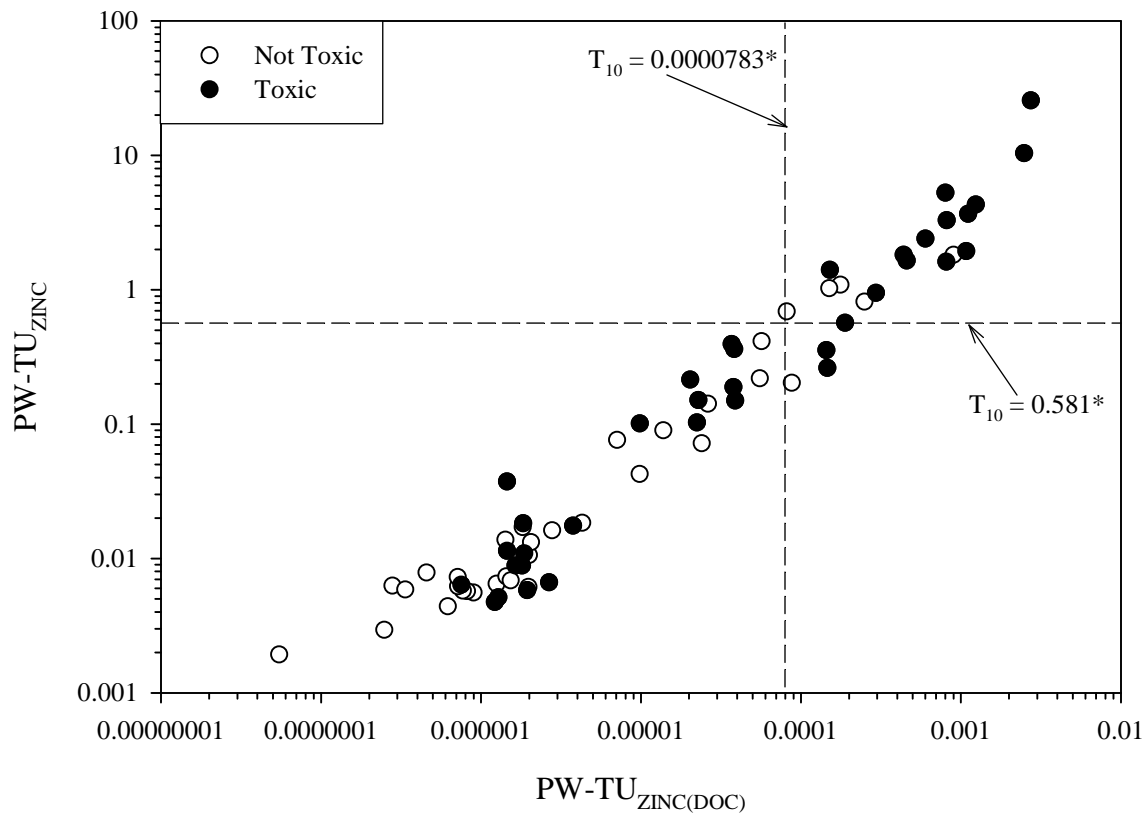


Figure A4-17. Scatter plot showing the relationship between pore-water zinc concentrations normalized to dissolved organic carbon ($PW-TU_{ZINC(DOC)}$) and pore-water zinc concentrations ($PW-TU_{ZINC}$), showing samples that were designated as toxic or not toxic based on the survival of midges (*Chironomus dilutus*) in 10-d exposures to sediment samples from the Tri-State Mining District.



*Toxicity threshold was derived using 28-d *H. azteca* toxicity test results (Endpoint: Survival).

Figure A4-18. Scatter plot showing the relationship between pore-water zinc concentrations normalized to dissolved organic carbon ($PW-TU_{ZINC(DOC)}$) and pore-water zinc concentrations ($PW-TU_{ZINC}$), showing samples that were designated as toxic or not toxic based on the biomass of midges (*Chironomus dilutus*) in 10-d exposures to sediment samples from the Tri-State Mining District.



*Toxicity threshold was derived using 28-d *H. azteca* toxicity test results (Endpoint: Survival).

Figure A4-19. Scatter plot showing the relationship between pore-water zinc concentrations ($PW-TU_{ZINC}$) and pore-water metal concentrations ($\Sigma PW-TU_{DIVALENT METALS}$), showing samples that were designated as toxic or not toxic based on the survival of amphipods (*Hyaella azteca*) in 28-d exposures to sediment samples from the Tri-State Mining District.

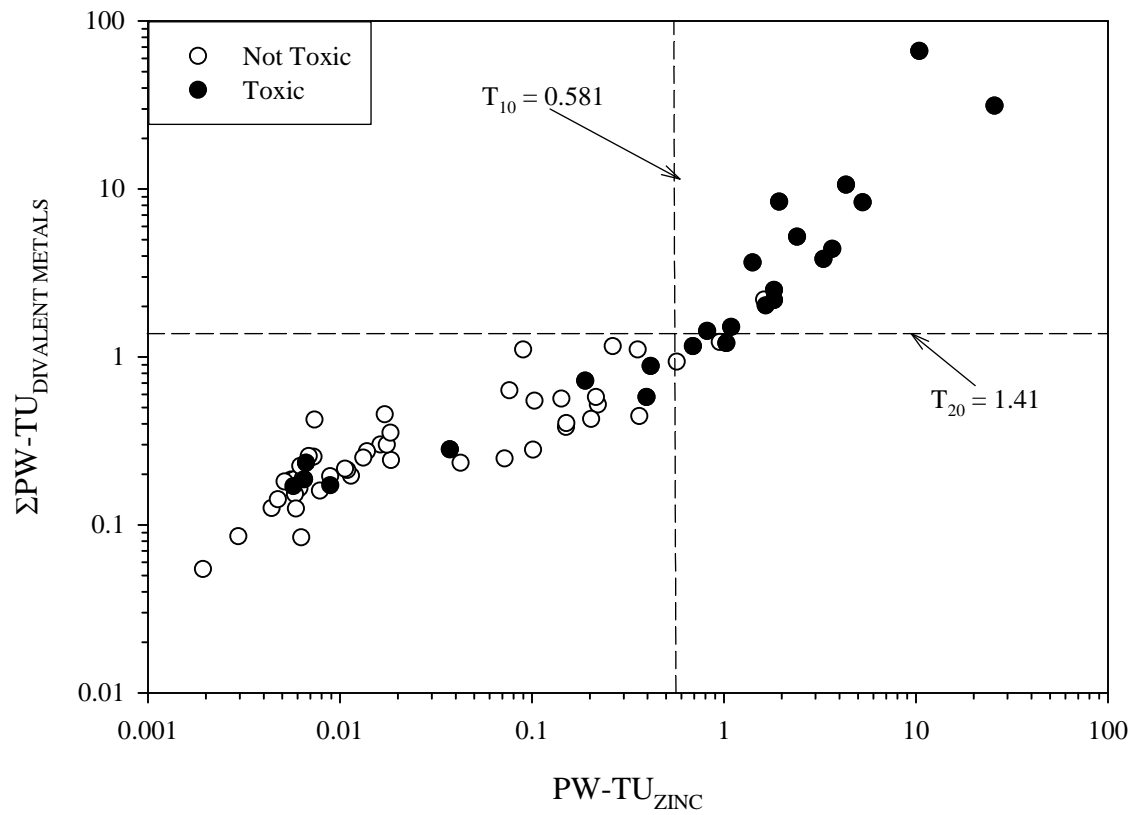


Figure A4-20. Scatter plot showing the relationship between pore-water zinc concentrations ($PW-TU_{ZINC}$) and pore-water metal concentrations ($\Sigma PW-TU_{DIVALENT METALS}$), showing samples that were designated as toxic or not toxic based on the biomass of amphipods (*Hyaella azteca*) in 28-d exposures to sediment samples from the Tri-State Mining District.

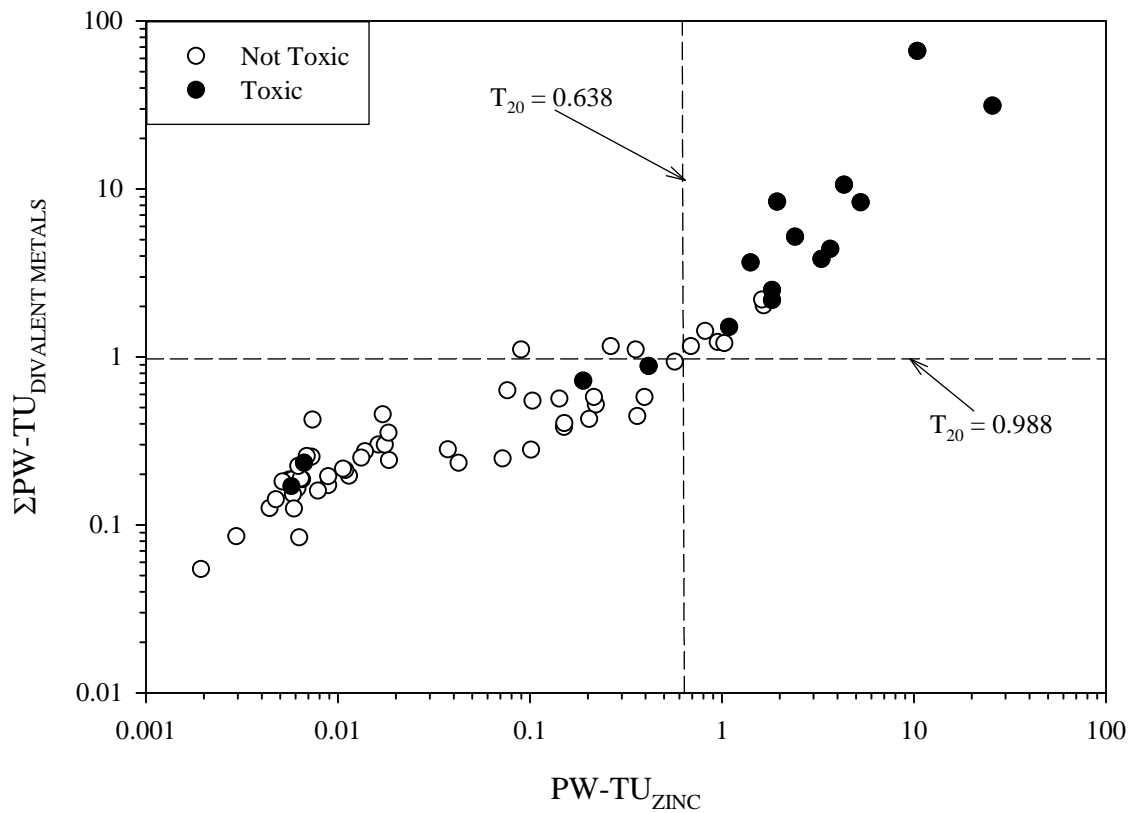


Figure A4-21. Scatter plot showing the relationship between pore-water zinc concentrations ($PW-TU_{ZINC}$) and pore-water metal concentrations ($\Sigma PW-TU_{DIVALENT METALS}$), showing samples that were designated as toxic or not toxic based on the survival of mussels (*Lampsilis siliquoidea*) in 28-d exposures to sediment samples from the Tri-State Mining District.

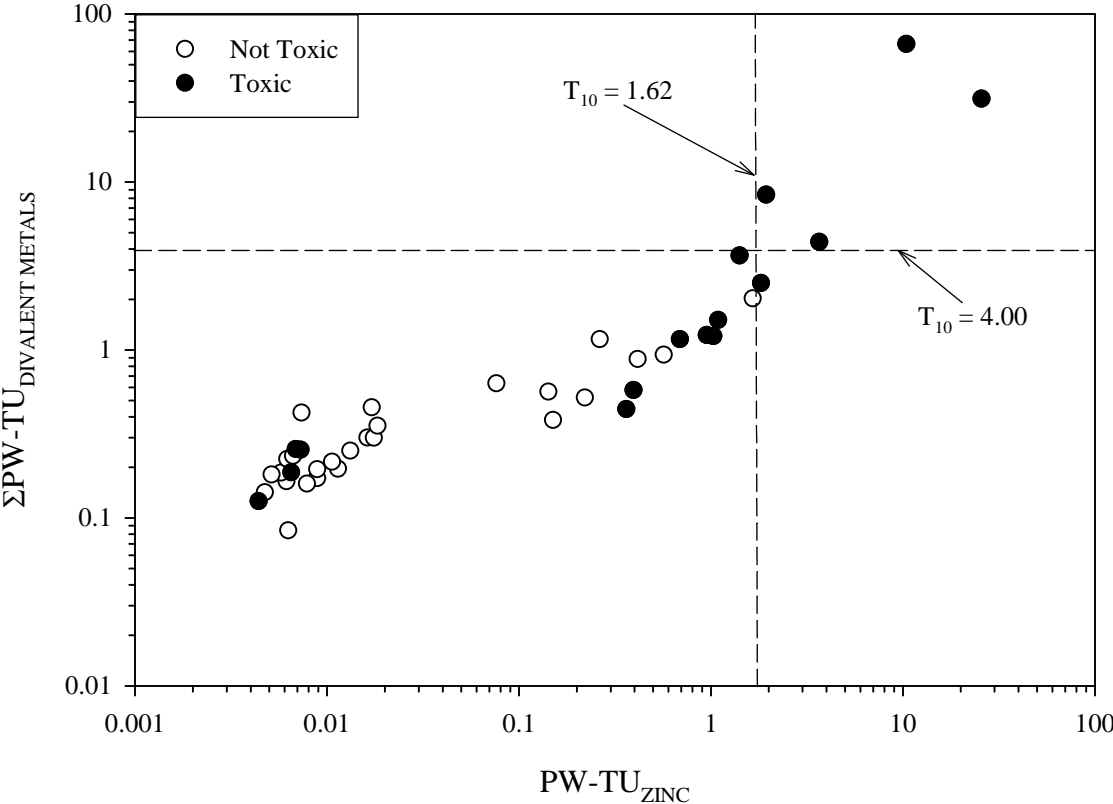


Figure A4-22. Scatter plot showing the relationship between pore-water zinc concentrations ($PW-TU_{ZINC}$) and pore-water metal concentrations ($\Sigma PW-TU_{DIVALENT METALS}$), showing samples that were designated as toxic or not toxic based on the biomass of mussels (*Lampsilis siliquoidea*) in 28-d exposures to sediment samples from the Tri-State Mining District.

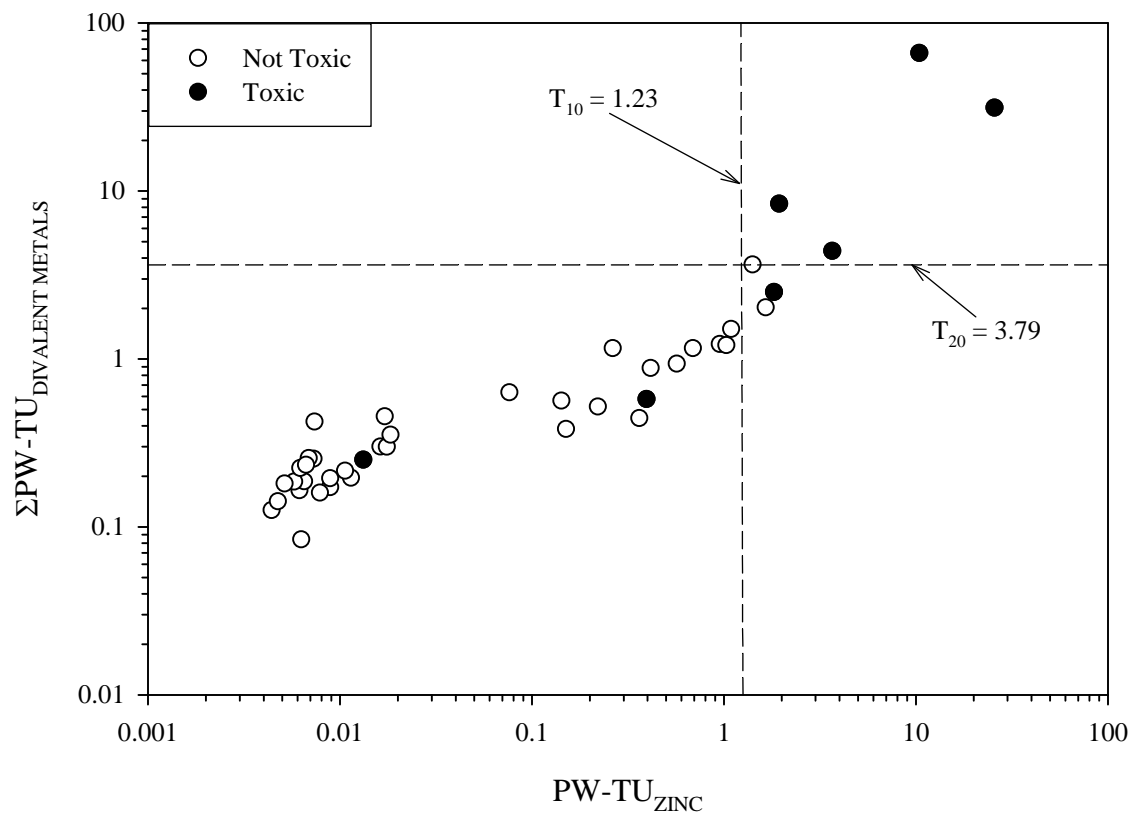
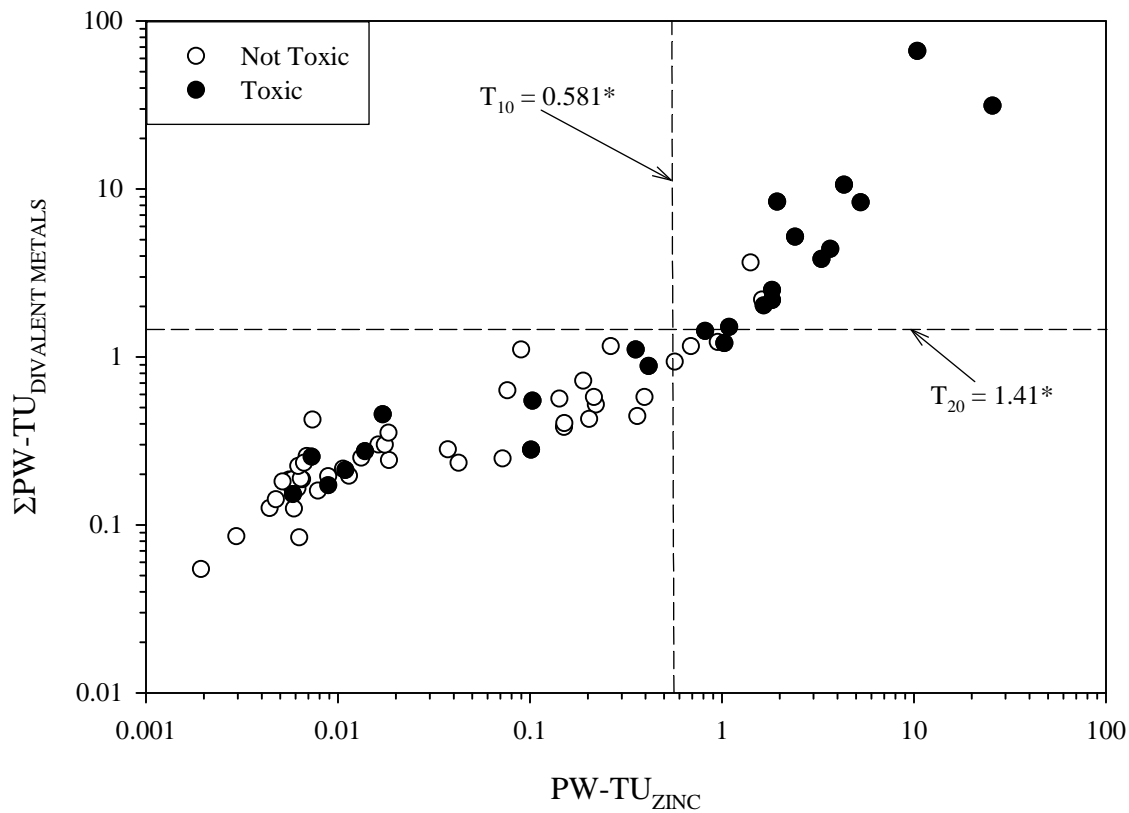
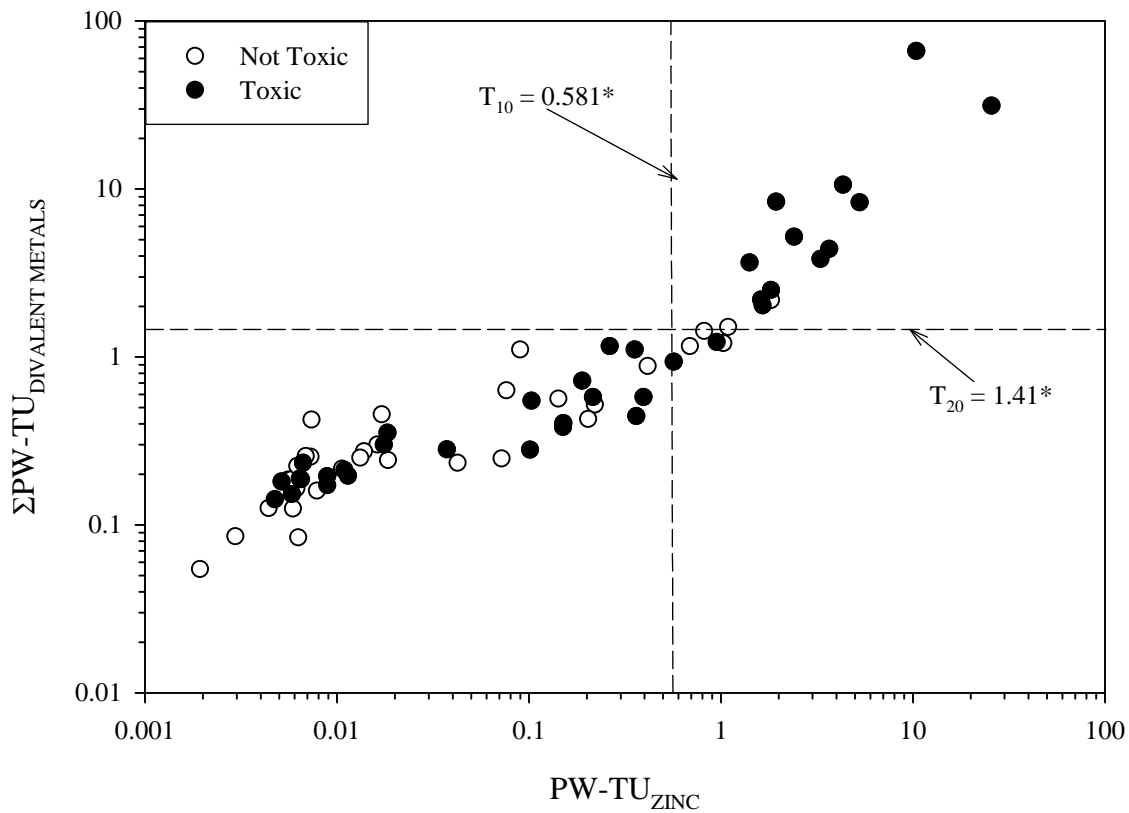


Figure A4-23. Scatter plot showing the relationship between pore-water zinc concentrations ($PW-TU_{ZINC}$) and pore-water metal concentrations ($\Sigma PW-TU_{DIVALENT METALS}$), showing samples that were designated as toxic or not toxic based on the survival of midges (*Chironomus dilutus*) in 10-d exposures to sediment samples from the Tri-State Mining District.



*Toxicity threshold was derived using 28-d *H. azteca* toxicity test results (Endpoint: Survival).

Figure A4-24. Scatter plot showing the relationship between pore-water zinc concentrations ($PW-TU_{ZINC}$) and pore-water metal concentrations ($\Sigma PW-TU_{DIVALENT METALS}$), showing samples that were designated as toxic or not toxic based on the biomass of midges (*Chironomus dilutus*) in 10-d exposures to sediment samples from the Tri-State Mining District.



*Toxicity threshold was derived using 28-d *H. azteca* toxicity test results (Endpoint: Survival).

Figure A4-25. Scatter plot showing the relationship between pore-water lead concentrations normalized to dissolved organic carbon ($PW-TU_{LEAD(DOC)}$) and pore-water lead concentrations ($PW-TU_{LEAD}$), showing samples that were designated as toxic or not toxic based on the survival of amphipods (*Hyaella azteca*) in 28-d exposures to sediment samples from the Tri-State Mining District.

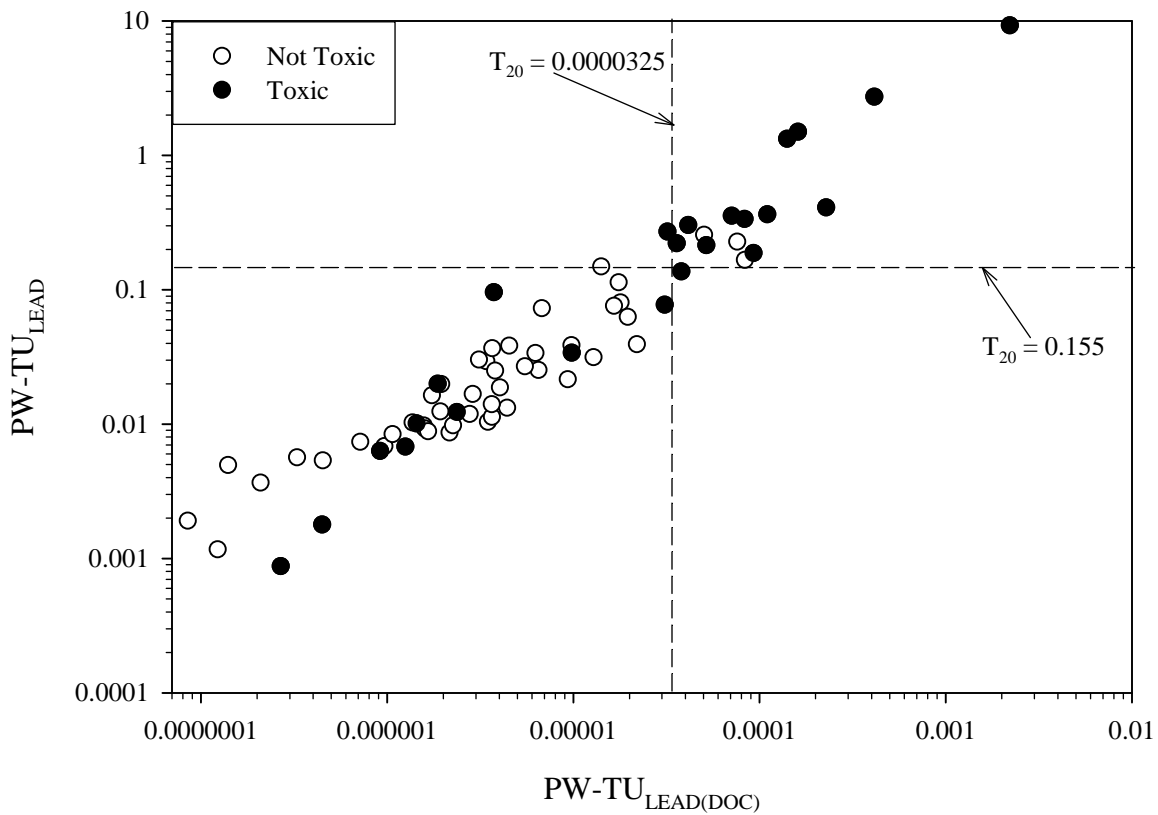


Figure A4-26. Scatter plot showing the relationship between pore-water lead concentrations normalized to dissolved organic carbon ($PW-TU_{LEAD(DOC)}$) and pore-water lead concentrations ($PW-TU_{LEAD}$), showing samples that were designated as toxic or not toxic based on the biomass of amphipods (*Hyalella azteca*) in 28-d exposures to sediment samples from the Tri-State Mining District.

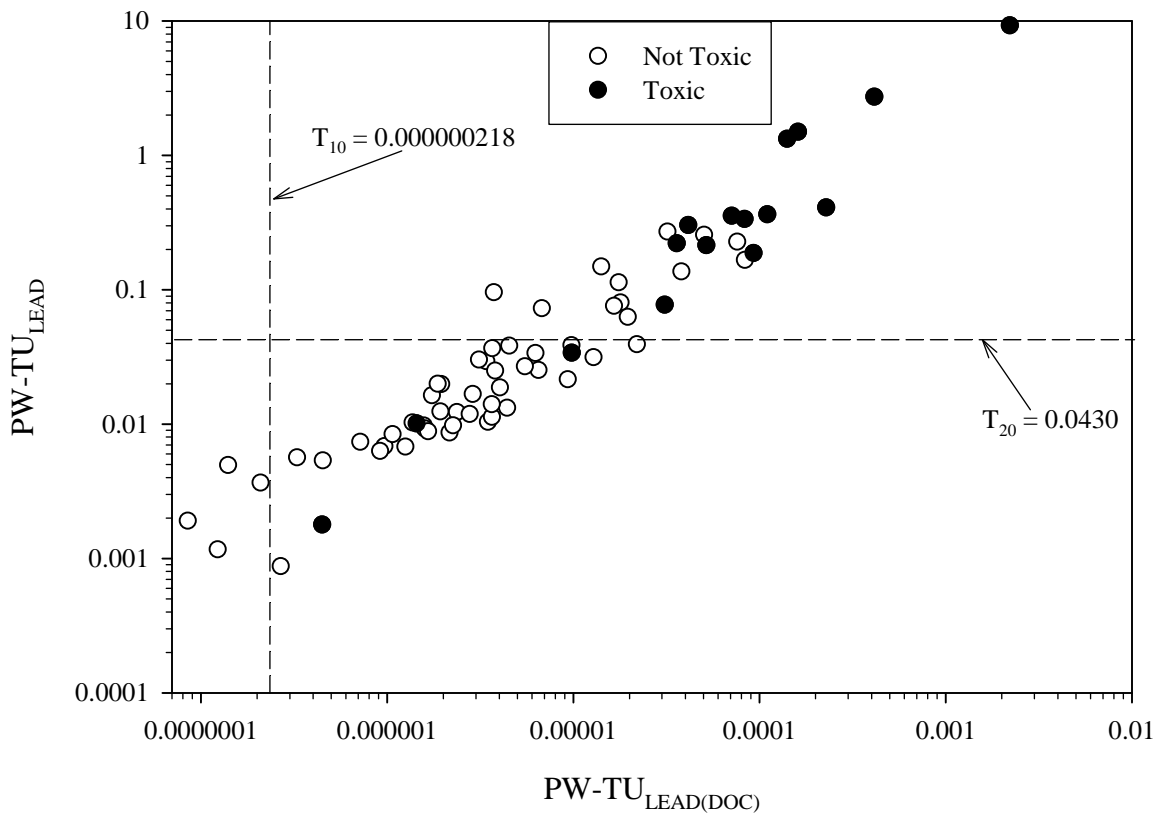
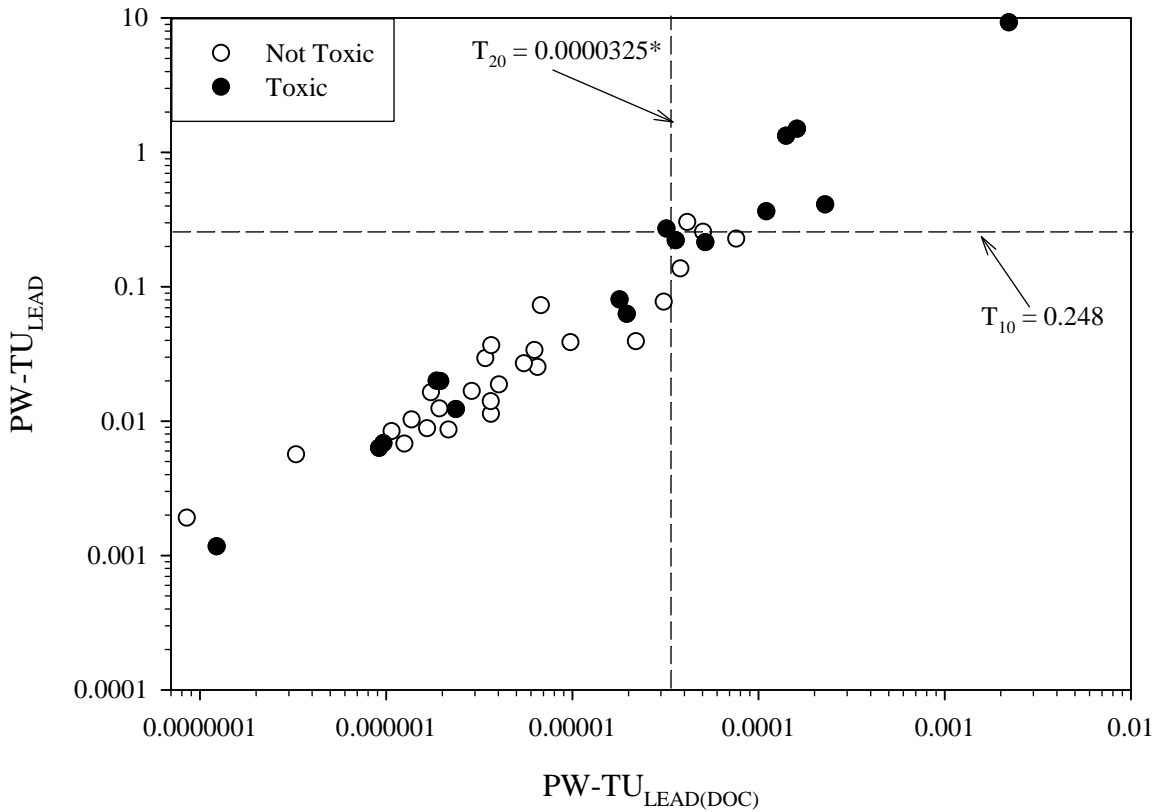


Figure A4-27. Scatter plot showing the relationship between pore-water lead concentrations normalized to dissolved organic carbon ($PW-TU_{LEAD(DOC)}$) and pore-water lead concentrations ($PW-TU_{LEAD}$), showing samples that were designated as toxic or not toxic based on the survival of mussels (*Lampsilis siliquoidea*) in 28-d exposures to sediment samples from the Tri-State Mining District.



*Toxicity threshold was derived using 28-d *H. azteca* toxicity test results (Endpoint: Survival).

Figure A4-28. Scatter plot showing the relationship between pore-water lead concentrations normalized to dissolved organic carbon ($PW-TU_{LEAD(DOC)}$) and pore-water lead concentrations ($PW-TU_{LEAD}$), showing samples that were designated as toxic or not toxic based on the biomass of mussels (*Lampsilis siliquoidea*) in 28-d exposures to sediment samples from the Tri-State Mining District.

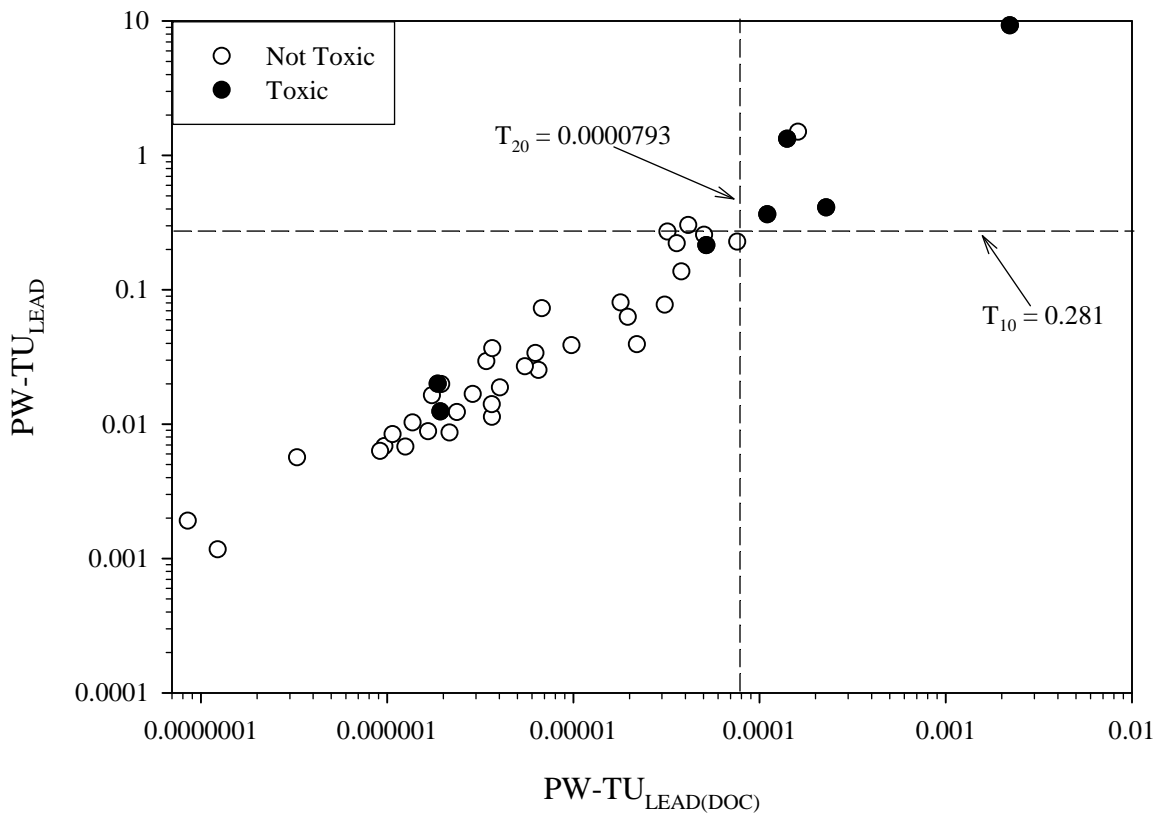
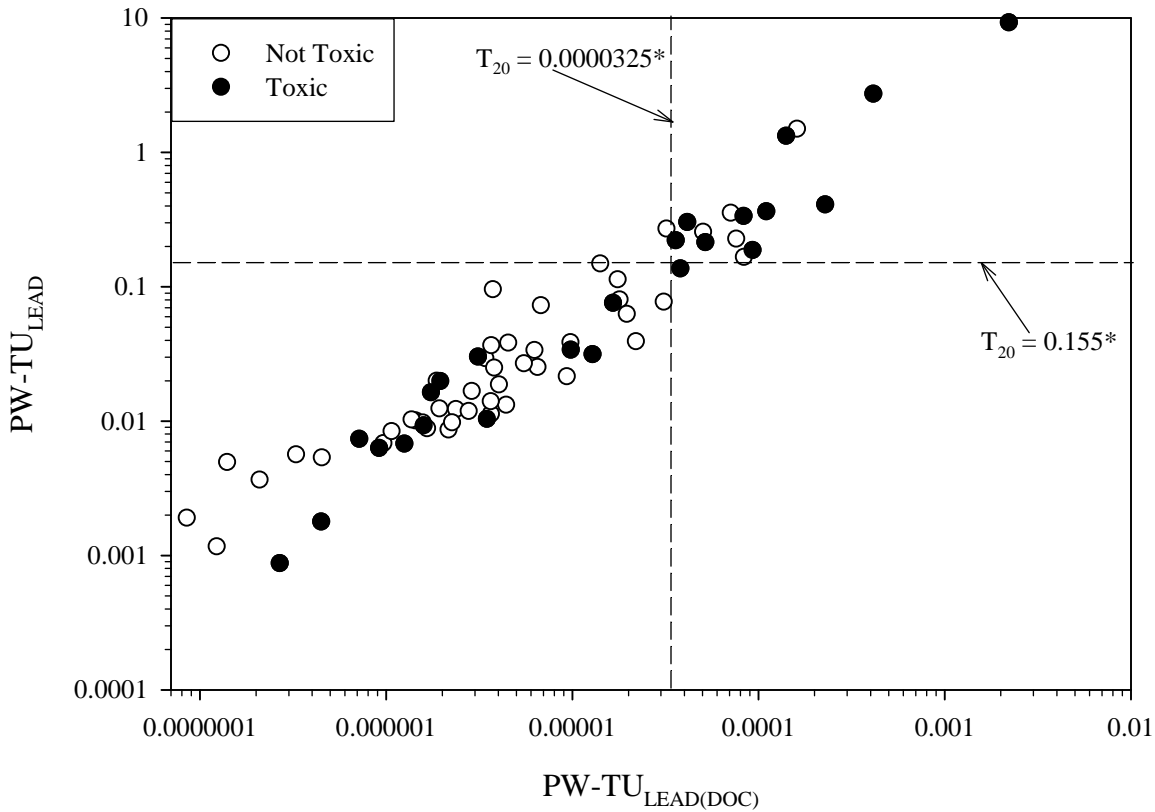
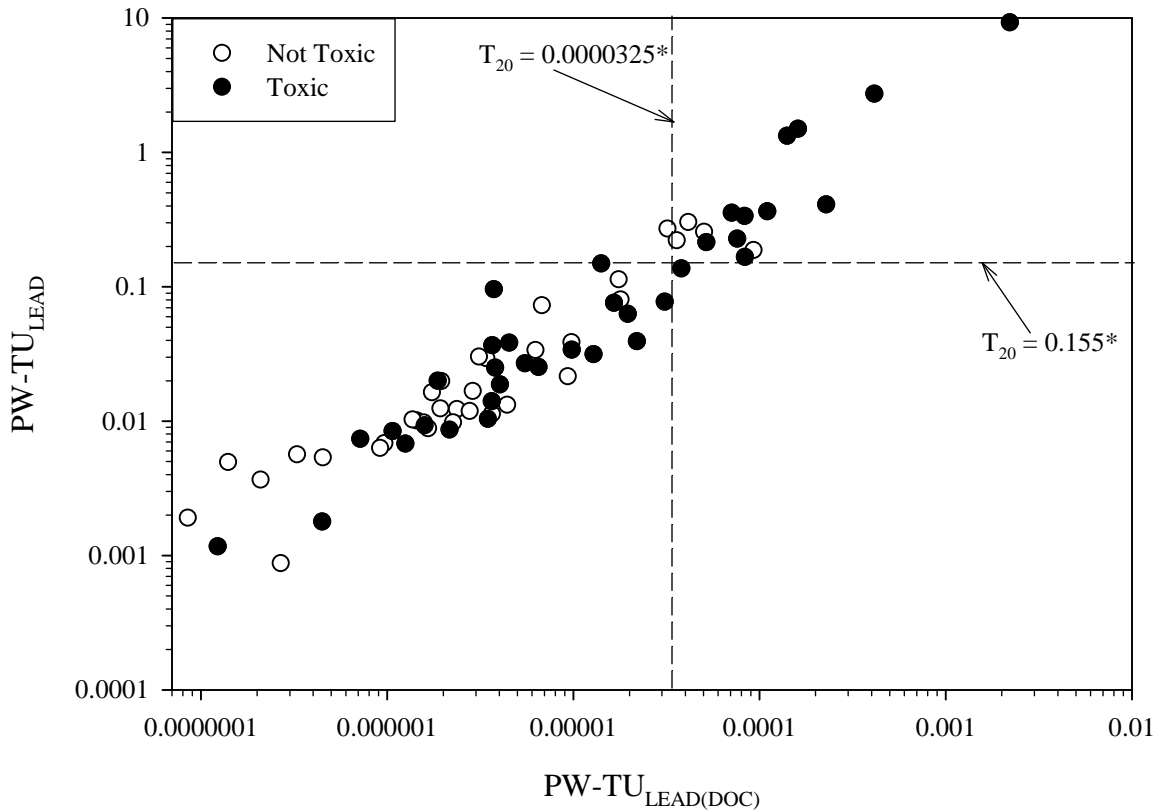


Figure A4-29. Scatter plot showing the relationship between pore-water lead concentrations normalized to dissolved organic carbon ($PW-TU_{LEAD(DOC)}$) and pore-water lead concentrations ($PW-TU_{LEAD}$), showing samples that were designated as toxic or not toxic based on the survival of midges (*Chironomus dilutus*) in 10-d exposures to sediment samples from the Tri-State Mining District.



*Toxicity threshold was derived using 28-d *H. azteca* toxicity test results (Endpoint: Survival).

Figure A4-30. Scatter plot showing the relationship between pore-water lead concentrations normalized to dissolved organic carbon ($PW-TU_{LEAD(DOC)}$) and pore-water lead concentrations ($PW-TU_{LEAD}$), showing samples that were designated as toxic or not toxic based on the biomass of midges (*Chironomus dilutus*) in 10-d exposures to sediment samples from the Tri-State Mining District.



*Toxicity threshold was derived using 28-d *H. azteca* toxicity test results (Endpoint: Survival).

Figure A4-31. Scatter plot showing the relationship between pore-water lead concentrations ($PW-TU_{LEAD}$) and pore-water metal concentrations ($\Sigma PW-TU_{DIVERGENT METALS}$), showing samples that were designated as toxic or not toxic based on the survival of amphipods (*Hyaella azteca*) in 28-d exposures to sediment samples from the Tri-State Mining District.

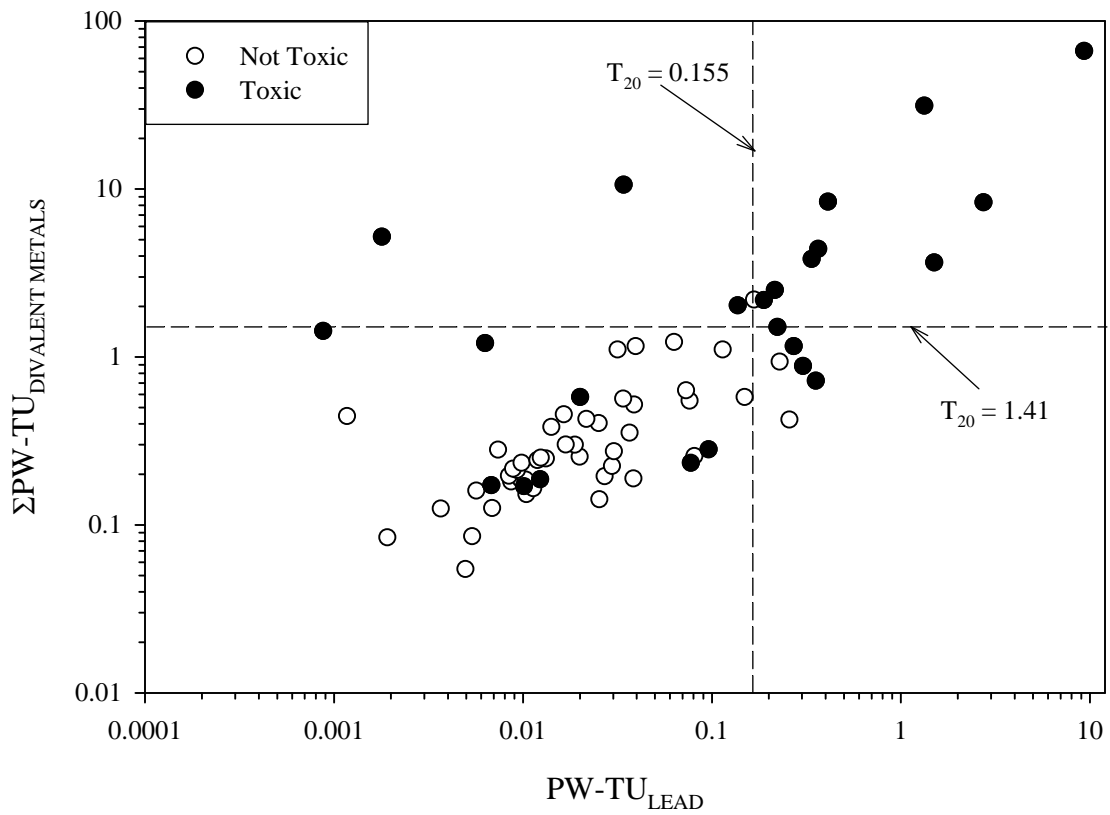


Figure A4-32. Scatter plot showing the relationship between pore-water lead concentrations ($PW-TU_{LEAD}$) and pore-water metal concentrations ($\Sigma PW-TU_{DIVERGENT METALS}$), showing samples that were designated as toxic or not toxic based on the biomass of amphipods (*Hyaletta azteca*) in 28-d exposures to sediment samples from the Tri-State Mining District.

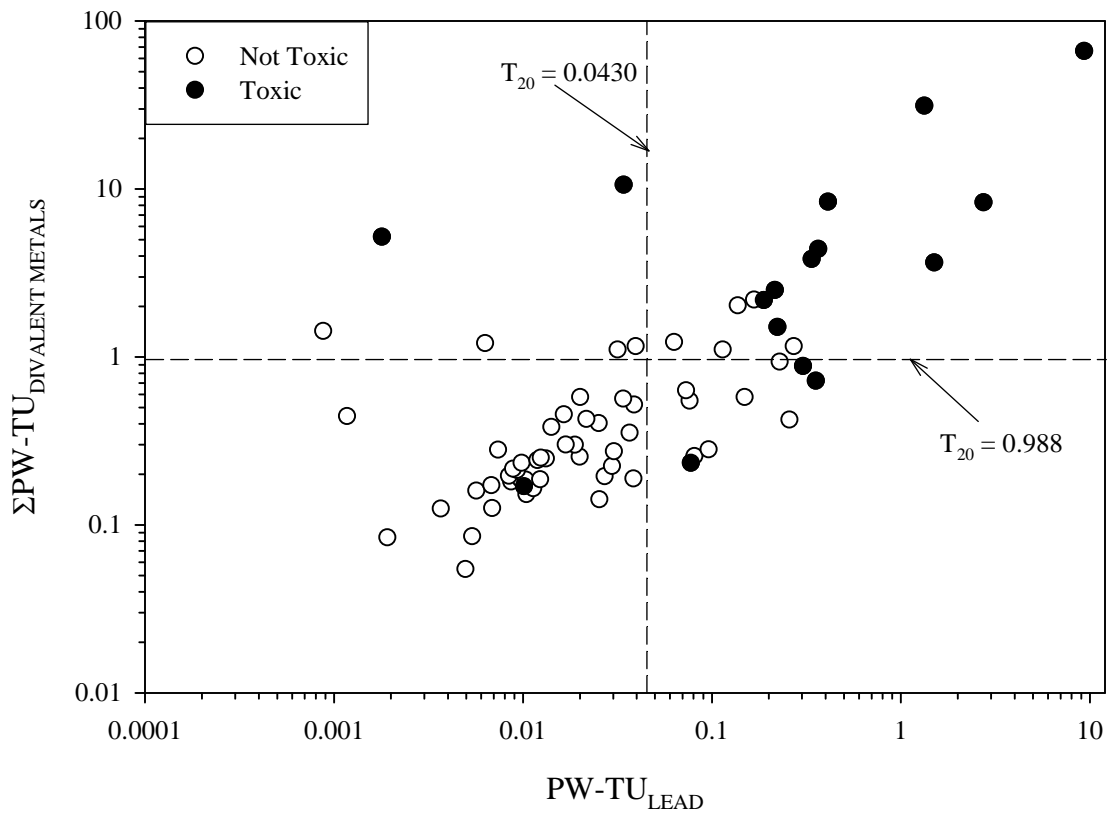


Figure A4-33. Scatter plot showing the relationship between pore-water lead concentrations ($PW-TU_{LEAD}$) and pore-water metal concentrations ($\Sigma PW-TU_{DIVERGENT METALS}$), showing samples that were designated as toxic or not toxic based on the survival of mussels (*Lampsilis siliquoidea*) in 28-d exposures to sediment samples from the Tri-State Mining District.

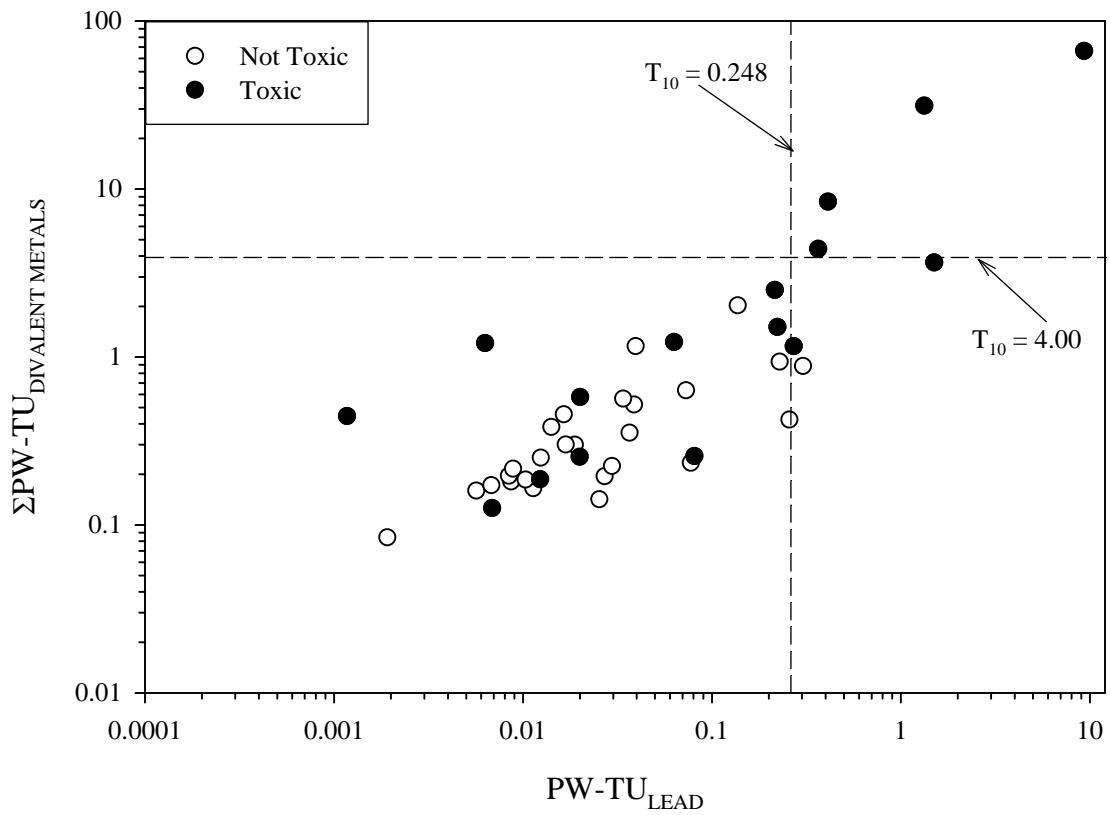


Figure A4-34. Scatter plot showing the relationship between pore-water lead concentrations ($PW-TU_{LEAD}$) and pore-water metal concentrations ($\Sigma PW-TU_{DIVERGENT METALS}$), showing samples that were designated as toxic or not toxic based on the biomass of mussels (*Lampsilis siliquoidea*) in 28-d exposures to sediment samples from the Tri-State Mining District.

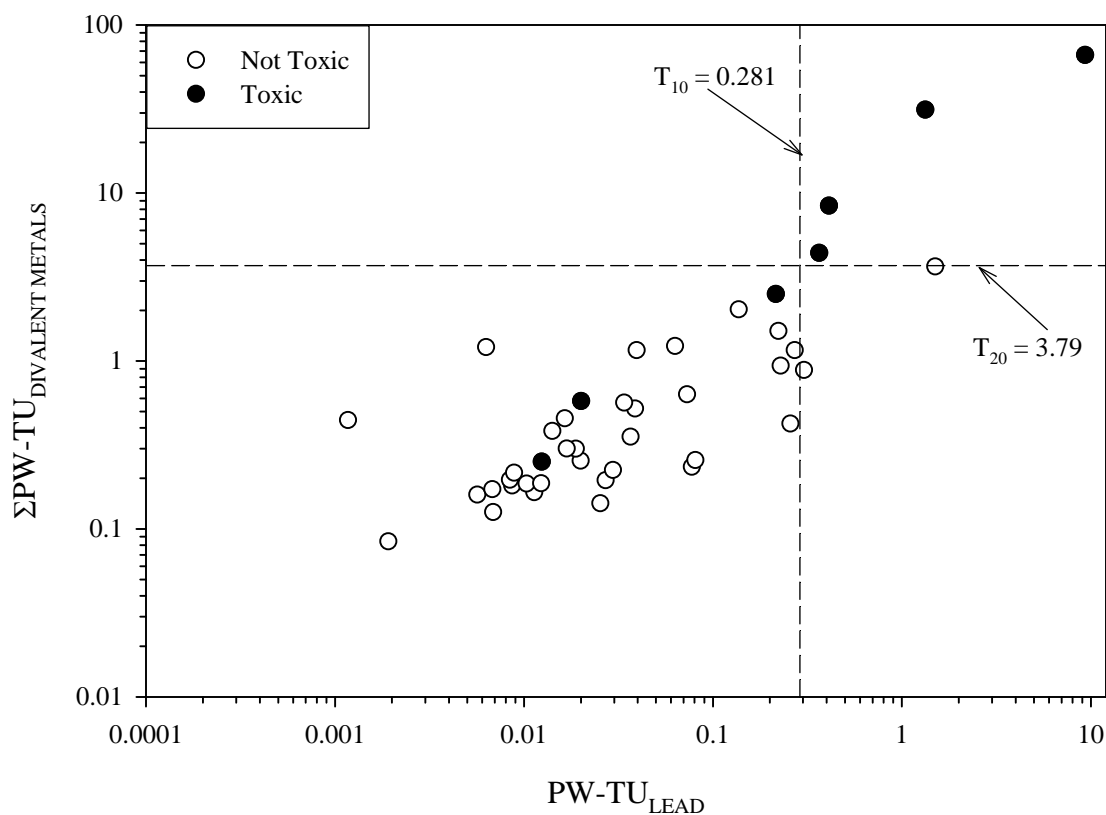
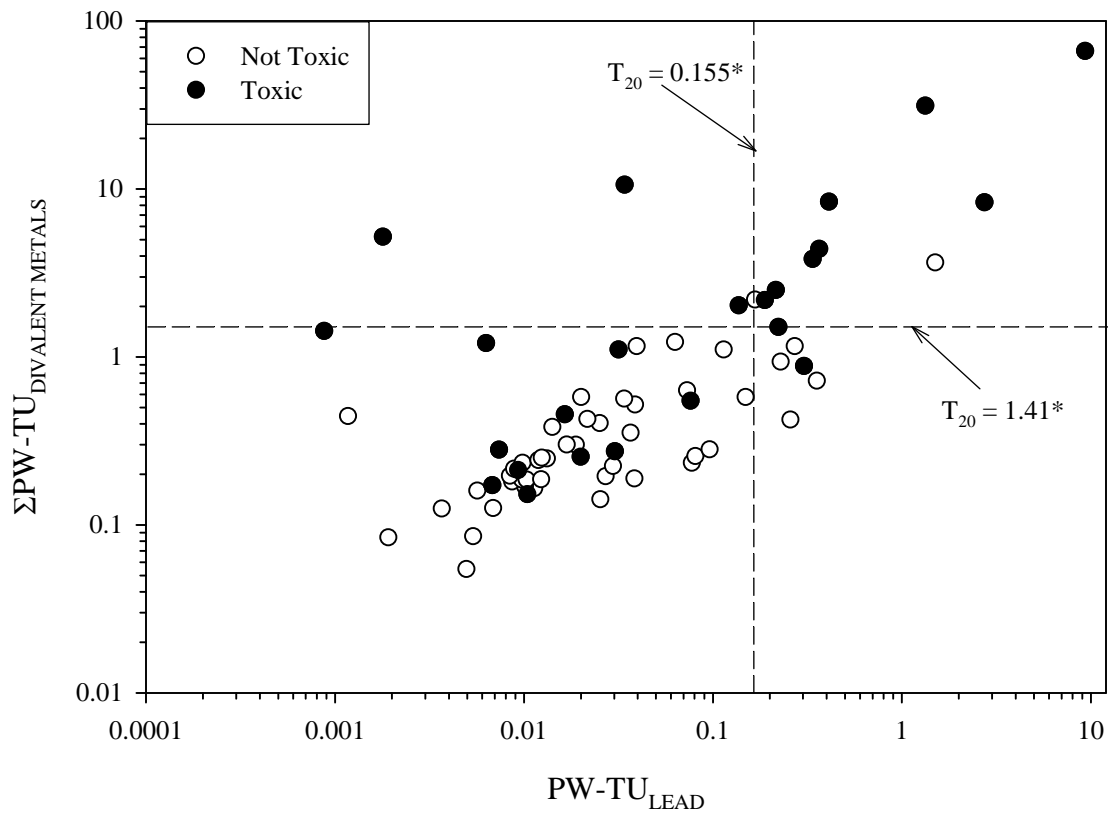
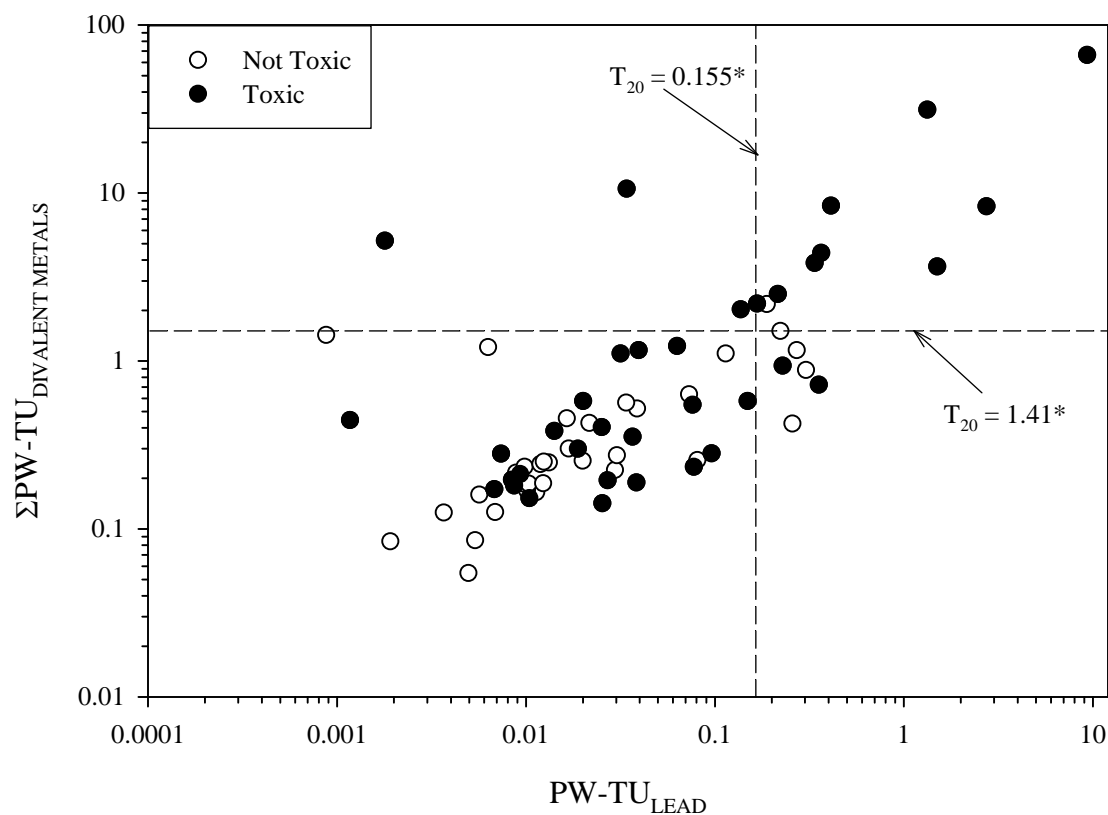


Figure A4-35. Scatter plot showing the relationship between pore-water lead concentrations ($PW-TU_{LEAD}$) and pore-water metal concentrations ($\Sigma PW-TU_{DIVERGENT METALS}$), showing samples that were designated as toxic or not toxic based on the survival of midges (*Chironomus dilutus*) in 10-d exposures to sediment samples from the Tri-State Mining District.



*Toxicity threshold was derived using 28-d *H. azteca* toxicity test results (Endpoint: Survival).

Figure A4-36. Scatter plot showing the relationship between pore-water lead concentrations ($PW-TU_{LEAD}$) and pore-water metal concentrations ($\Sigma PW-TU_{DIVERGENT METALS}$), showing samples that were designated as toxic or not toxic based on the biomass of midges (*Chironomus dilutus*) in 10-d exposures to sediment samples from the Tri-State Mining District.



*Toxicity threshold was derived using 28-d *H. azteca* toxicity test results (Endpoint: Survival).